

Animal Cell Technology: Basic & Applied Aspects

Proceedings of the 17th Annual Meeting of the
Japanese Association for Animal Cell Technology
(JAACT), Nagoya, Japan, November 15-18, 2004

VOLUME 14



Edited by
Shinji Iijima and
Ken-ichi Nishijima

ANIMAL CELL TECHNOLOGY: BASIC & APPLIED ASPECTS

JAACT 2004 Organizing Committee

Meeting Chairperson

S. Iijima (Japan)

Vice Chairperson

T. Matsuda (Japan)

Meeting Secretaries

M. Kamihira (Japan) K. Miyake (Japan) K. Nishijima (Japan) M. Goto (Japan)

Organizing Boards

H. Anazawa (Japan)

S. Asahi (Japan)

D. Ejima (Japan)

A. Enomoto (Japan)

Y. Fuke (Japan)

Y. Fukui (Japan)

S. Hashizume (Japan)

C. Hirashima (Japan)

H. Honda (Japan)

M. Hosobuchi (Japan)

H. Hoshi (Japan)

K. Ikura (Japan)

T. Kadowaki (Japan)

M. Kamei (Japan)

Y. Katakura (Japan)

M. Maeda-Yamamoto (Japan)

M. Maki (Japan)

Y. Miura (Japan)

T. Muramatsu (Japan)

M. Nagao (Japan)

N. Nakamichi (Japan)

H. Nakano (Japan)

H. Oda (Japan)

T. Shigehisa (Japan)

S. Shirahata (Japan)

M. Shimizu (Japan)

H. Shinmoto (Japan)

M. Takagi (Japan)

M. Tanokura (Japan)

M. Totsuka (Japan)

H. Tsumura (Japan)

K. Yagasaki (Japan)

M. Yokota (Japan)

Advisory Boards

M. Al-Rubeai (UK)

M. Aizawa (Japan)

S. Arai (Japan)

D. W. Barnes (USA)

M. Carrondo (Portugal)

T. Fujimori (Japan)

K. Funatsu (Japan)

D. W. Jayme (USA)

S. Kaminogawa (Japan)

K. Konstantinov (USA)

Y. Kitagawa (Japan)

K. Nagai (Japan)

T. Nishiyama (Japan)

O. W. Merten (France)

H. Ohgashi (Japan)

H. Ohmura (Japan)

T. Ohno (Japan)

T. Osawa (Japan)

R. Sasaki (Japan)

G. H. Sato (USA)

G. Schmid (Switzerland)

T. Suzuki (Japan)

E. Tsao (USA)

J. Wérenne (Belgium)

F. Wurm (Switzerland)

M. Yap (Singapore)

Animal Cell Technology: Basic & Applied Aspects

Volume 14

Proceedings of the Seventeenth Annual Meeting of the Japanese
Association for Animal Cell Technology (JAACT),
Nagoya, Japan, November 15-18, 2004

Edited by

SHINJI IJIMA

*Department of Biotechnology,
Nagoya University,
Nagoya, Japan*

and

KEN-ICHI NISHIJIMA

*Department of Biotechnology,
Nagoya University,
Nagoya, Japan*

 Springer

A C.I.P. Catalogue record for this book is available from the Library of Congress.

ISBN-10 1-4020-4312-0 (HB)
ISBN-13 978-1-4020-4312-3 (HB)
ISBN-10 1-4020-4457-7 (e-book)
ISBN-13 978-1-4020-4457-1 (e-book)

Published by Springer,
P.O. Box 17, 3300 AA Dordrecht, The Netherlands.

www.springer.com

Printed on acid-free paper

All Rights Reserved

© 2006 Springer

No part of this work may be reproduced, stored in a retrieval system, or transmitted in any form or by any means, electronic, mechanical, photocopying, microfilming, recording or otherwise, without written permission from the Publisher, with the exception of any material supplied specifically for the purpose of being entered and executed on a computer system, for exclusive use by the purchaser of the work.

Printed in the Netherlands.

Contents

Preface	xi
Symposium	
MESENCHYMAL CELLS: METALLOPROTEINASES AND ADHESION ON MICROCARRIERS <i>C. Mosbeux, A. R. dos Santos Pedregal, D. Ribeiro de Sousa, Vincianne Hendric, N. Joseph, M. Bensellam, D. Blankaert, T. Marique, C. Alloin, D. Parent, C. Liesnard, J. P. Van Vooren, S. Lowagie, and J. Werenne</i>	1
CHARACTERIZATION OF PEANUT SPECIFIC T CELLS <i>S. J. Maleki</i>	9
USING METABOLOMICS TO BETTER UNDERSTAND FUNCTIONAL FOODS <i>Dayan B. Goodnowe, Yasuyo Yamazaki, and Bernhard H. J. Juurlink</i>	21
FOOD FACTORS THAT REGULATE INTESTINAL INFLAMMATION: EVALUATION OF THE FACTORS BY USING A COCULTURE SYSTEM <i>Hideo Satsu, and Makoto Shimizu</i>	29
GENERATION OF AN INDUSTRIALLY IDEAL HOST CELL LINE FOR PRODUCING COMPLETELY-DEFUCOSYLATED ANTIBODY WITH ENHANCED ANTIBODY-DEPENDENT CELLULAR CYTOTOXICITY (ADCC) <i>Mitsuo Satoh, Naoko Yamane-Ohnuki, Katsuhiko Mori, Ripei Niwa, Toyohide Shinkawa, Harue Imai, Reiko Kuni-Kamochi, Ryosuke Nakano, Kazuya Yamano, Yutaka Kanda, Shigeru Iida, Kazuhisa Uchida, and Kenya Shitara</i>	39
THERMODYNAMIC AND KINETIC EFFECTS OF HUMAN IgG ₁ DEFUCOSYLATION ON IgG1-Fc γ RIIIa INTERACTION <i>Akira Okazaki, Emi Shoji, Kazuyasu Nakamura, Masako Wakitani, Kazuhisa Uchida, Shingo Kakita, Kouhei Tsumoto, Izumi Kumagai, and Kenya Shitara</i>	47
Oral Session	
EXPRESSION OF RECOMBINANT PROTEIN IN CHO AND HELA CELLS AND ITS FOLLOW-UP USING EGF REPORTER GENE <i>V. Hendrick, D. Ribeiro de Sousa, A. R. dos Santos Pedregal, C. Bassens, P. Rigaux, K. Sato, K. Kotarsky, and J. Werenne</i>	55
ELUCIDATING APOPTOTIC CELL DEATH IN CHO CELL BATCH & FED-BATCH CULTURES <i>Danny C. F. Wong, C. K. Danny C. F. Wong, C. K. Heng, Kathy T. K. Wong, Peter M. Nissom, and Miranda G. S. Yap</i>	61

THE X-LINK INHIBITOR OF APOPTOSIS PROTEIN (XIAP) ENHANCES THE SURVIVABILITY OF C2E7 HYBRIDOMA CELLS UNDER A SERUM DEPRIVED CONDITION <i>B. T. Tey, K. C. Yap, A. M. Ali, and W. S. Tan</i>	67
TRANSCRIPTIONAL PROFILING OF BATCH AND FED-BATCH PROTEIN-FREE 293-HEK CULTURES USING DNA MICROARRAY <i>Yih Yean Lee, Kathy Wong, Peter Morin Nissom, and Miranda G. S. Yap</i>	73
STUDIES ON THE EFFICACY, SAFETY AND QUALITY OF THE TISSUE ENGINEERED PRODUCTS: ENHANCEMENT OF PROLIFERATION OF HUMAN MESENCHYMAL STEM CELLS BY THE NEW POLYSACCHARIDES <i>Saifuddin Ahmed, Toshie Tsuchiya, and Yutaka Kariya</i>	81
STUDIES ON THE EFFICACY, SAFETY AND QUALITY OF THE TISSUE ENGINEERED PRODUCTS: EFFECTS OF A CATALYST USED IN THE SYNTHESIS OF BIODEGRADABLE POLYMER ON THE CHONDROGENESIS OF HUMAN ARTICULAR CARTILAGE <i>Nasreen Banu, Toshie Tsuchiya, Saifuddin Ahmed, and Rumi Sawada</i>	87
THE ROLE OF <i>BIFIDOBACTERIUM</i> IN THE DEVELOPMENT OF GUT IMMUNE SYSTEMS: ANALYSIS USING GNOTOBIOTIC TCR-TRANSGENIC MICE <i>Masato Tsuda, Akira Hosono, Miran Fujioka, Satoshi Hachimura, Ryo Nakamura, Kazuhiro Hirayama, Kikuji Itoh, and Shuichi Kaminogawa</i>	93
THE ROLE OF CD4 ⁺ T CELLS IN IgA PRODUCTION IN MURINE PEYER'S PATCHES FOLLOWING ORAL FEEDING OF <i>BIFIDOBACTERIUM</i> COMPONENTS <i>Yusuke Nakanishi, Akira Hosono, Teiji Kimura, and Shuichi Kaminogawa</i>	101
SUPPLEMENTATION OF SERICIN IS EFFECTIVE IN MAINTENANCE OF ISLET SURVIVAL AND FUNCTION UNDER SERUM-FREE CULTURE <i>Akiko Ogawa, Satoshi Terada, Masao Miki, Toshihisa Kimura, Akio Yamaguchi, Masahiro Sasaki, and Hideyuki Yamada</i>	107
SUPPRESSION OF TWO-STAGE CELL TRANSFORMATION BY ELECTROLYZED REDUCED WATER CONTAINING PLATINUM NANOPARTICLES <i>Ryuhei Nishikawa, Kiichiro Teruya, Yoshinori Katakura, Kazumichi Otsubo, Shinkatsu Morisawa, Qianghua Xu, and Sanetaka Shirahata</i>	113

Poster Session

INFLUENCE OF BOTH GLUCOSE AND GLUTAMINE CONCENTRATION ON MAB PRODUCTION RATE IN CHEMOSTAT CULTURE OF CHO CELLS <i>Hiroshi Matsuoka, Jun-ya Watanabe, and Toshiya Takeda</i>	121
INTRODUCTION OF GENES RELATING TO MUSCULAR DYSTROPHY INTO CHIMERIC CHICKENS BY EMBRYO ENGINEERING <i>Akira Fujiwara, Makoto Mizutani, Tamao Ono, and Hiroshi Kagami</i>	127
PLURIPOTENT CELL CULTURE ENGINEERING AND THE APPLICATION FOR AVIAN BIOTECHNOLOGY <i>Hiroshi Kagami, Tomoki Mushika, Takamasa Noguchi, Yasuhiro Yamamoto, Akira Fujiwara, Naomi Yamakawa, Hisato Okuizumi, and Tamao Ono</i>	135
EFFECT OF OXYGEN TENSION ON THE PROLIFERATION AND THE DIFFERENTIATION OF MOUSE EMBRYONIC STEM CELLS <i>M. Kimura, H. Kurosawa, and Y. Amano</i>	143
ENHANCEMENT OF ANTIBODY PRODUCTION BY ADDITION OF UBIQUINONE-Q ₁₀ <i>Yoshinobu Konno, Motoi Aoki, Masakazu Takagishi, Hiroshi Takasugi, Masamichi Koike, and Shinji Hosoi</i>	149
OBSERVATION OF INDIVIDUAL CELL BEHAVIORS TO ANALYZE MITOGENIC EFFECTS OF SERICIN <i>Tomohiro Toyosawa, Satoshi Terada, Masahiro Sasaki, Hideyuki Yamada, and Masahiro Kino-oka</i>	155
STUDIES OF PASSAGE EFFECT OF HaNPV BACULOVIRUS PRODUCED IN Hz INSECT CELL CULTURE <i>Kanokwan Poomputsa, Kultida Poltawee, Somkiet Techkarnjanarak, and Phenjun Mekvichitsaeng</i>	163
OPTIMIZATION OF RECOMBINANT DENGUE ENVELOPE PROTEIN PRODUCTION IN INSECT CELL CULTURE IN 2.5 L FERMENTER <i>Phenjun Mekvichitsaeng, Somsak Sotasan, and Kanokwan Poomputsa</i> ...	169
TARGETED DISRUPTION OF α -1, 6-FUCOSYLTRANSFERASE (<i>FUT8</i>) GENE BY HOMOLOGOUS RECOMBINATION IN CHINESE HAMSTER OVARY (CHO) CELLS <i>Masayoshi Tsukahara, Ayako Aoki, Keina Kozono, Yoko Maseki, Yukiko Fukuda, Hideaki Yoshida, Kazuo Kobayashi, Makoto Kakitani, Kazuma Tomizuka, and Haruhiko Tsumura</i>	175
IMMUNOSTIMULATION EFFECT OF THE FERMENTED MILK ON HUMAN HYBRIDOMAS AND PERIPHERAL BLOOD LYMPHOCYTES <i>Takuya Sugahara, Katsunori Nakamoto, and Kazushi Hara</i>	185

TRACE ELEMENT OPTIMIZATION ENHANCES PERFORMANCE AND REPRODUCIBILITY OF SERUM-FREE MEDIUM <i>Scott J. Jacobia, Robert W. Kenerson, Lia D. Tescione, Dale F. Gruber, David W. Jayme, Donald G. Munroe, and Stephen F. Gorfien</i>	193
PHENOMENOME PROFILER™ ANALYSIS OF HUMAN COLON CANCER CELL LINES <i>Yasuyo Yamazaki, Shawn Ritchie, and Yanqiu Jiang</i>	201
GENERATION OF NATURAL KILLER CELLS FROM SERUM-FREE EXPANDED CD34 ⁺ CELLS ISOLATED FROM HUMAN UMBILICAL CORD BLOOD <i>I-Ting Kao, Zwe-Ling Kong, Mei-Ling Wu, Li-Wen Hsu, Chao-Ling Yao, and Shiaw-Min Hwang</i>	211
RETINOIC ACID IMPROVES CELL PROLIFERATION AND ANTIBODY PRODUCTION OF HUMAN HYBRIDOMAS NONPROLIFERATIVE IN A FRUCTOSE-BASED MEDIUM <i>Yuichi Inoue, Sanetaka Shirahata, and Yasushi Sugimoto</i>	219
CONSTRUCTION OF RECOMBINANT MONOCLONAL ANTIBODY AGAINST HEPATITIS B SURFACE ANTIGEN BY PHAGE DISPLAY <i>Apichai Prachasuphap, Chaivat Kittigul, Patcharee Sunthoranandh, Panadda Dhepakson, Nongluk Buddhirakkul, and Kruavon Balachandra</i>	227
A HUMAN CATALYTIC ANTIBODY WITH THE LIGHT CHAIN RAISED BY SECONDARY VJ RECOMBINATION IN A HUMAN PLASMA CELL LINE <i>Minoru Iwaki, Hirofumi Tachibana, Ryuichi Sakamoto, and Koji Yamada</i>	233
17BETA-ESTRADIOL REGULATES IMMUNOGLOBULIN M PRODUCTION THROUGH INTERACTION WITH ESTROGEN RECEPTORS <i>Mako Nakaya, Hirofumi Tachibana, and Koji Yamada</i>	239
MDCK CELLS RESISTANT TO METALLOPROTEINASE FROM <i>STREPTOMYCES GRISEUS</i> ACQUIRE ANCHORAGE INDEPENDENT SURVIVAL AND PROLIFERATION ABILITIES ON NON ADHESIVE SUBSTRATE <i>Reiko Tsutsumi, Masanori Shozushima, and Shigehiro Sato</i>	247
THE IMMUNE RESPONSES OF THE PRIME-BOOST REGIMEN WITH rBCG-E12 AND rDIs-E12 CANDIDATE VACCINE <i>P. Leangaramgul, S. Sapsutthipas, K. Balachandra, K. Matsuo, T. Hamano, and M. Honda</i>	255
INCREASE IN THE INSULIN SECRETION OF HIT-T15 CELLS: GAP JUNCTIONAL INTERCELLULAR COMMUNICATIONS ENHANCED BY HYALURONIC ACID <i>Yuping Li, Tsutomu Nagira, and Toshie Tsuchiya</i>	263

CULTURE OF INSULINOMA CELLS ON PANCREAS SECTION <i>Yasuyuki Saito, Satoshi Terada, and Toshiaki Takezawa</i>	271
DOWNREGULATION OF $\alpha_5\beta_1$ INTEGRIN EXPRESSION DURING NEURONAL DIFFERENTIATION IN NEURAL STEM CELLS <i>Dai Muramatsu, Noko Yoshida, Sohei Hishiyama, Yasei Miyamoto, and Tatsuhiro Hisatsune</i>	277
STRATEGIES FOR DEVELOPMENT OF CULTURE MEDIA: APPLICATION TO EMBRYONIC AND ADULT STEM CELLS <i>Shayne Boucher, Paul Price, Ian Lyons, John Daley and David Jayme</i>	285
PREPARATION OF HIGH-TITER RETROVIRAL VECTORS USING TRANSIENT EXPRESSION SYSTEM <i>Akitsu Hotta, Yoshikazu Saito, Ken-ichi Nishijima, Msamichi Kamihira, and Shinji Iijima</i>	293
BIOCHEMICAL ANALYSIS OF CHICKEN OVALBUMIN PROMOTER <i>Mahboob Morshed, Junko Yamamoto, Shusuke Sano, Ken-Ichi Nishijima, Masamichi Kamihira, and Shinji Iijima</i>	301
PRODUCTION OF CHIMERIC ANTIBODIES BY TRANSGENIC CHICKEN BIOREACTORS <i>Yoshinori Kawabe, Akitsu Hotta, Ken-Ichiro Ono, Kazuhisa Esaka, Ken-Ichi Nishijima, Masamichi Kamihira, and Shinji Iijima</i>	309
DETERMINATION OF THE MAJOR FOOD ALLERGEN, OVOMUCOID, WITH AN OLIGOCLONAL ENZYME-LINKED IMMUNOSORBENT ASSAY <i>Junko Hirose, Yukie Murakami-Yamaguchi, Miki Ikeda, and Hiroshi Narita</i>	317
SAFETY EVALUATION OF TISSUE ENGINEERED MEDICAL DEVICES USING NORMAL HUMAN MESENCHYMAL STEM CELLS <i>Rumi Sawada, Tomomi Ito, Yoshie Matsuda, and Toshie Tsuchiya</i>	325
EFFECT OF BIODEGRADABLE POLYMER POLY (L-LACTIC ACID) ON THE CELLULAR FUNCTION OF HUMAN ASTROCYTES <i>Naohito Nakamura and Toshie Tsuchiya</i>	331
IMMUNOLOGICAL ANALYSIS OF EPIDERMAL-TYPE TRANSGLUTAMINASE (TGase 3) IN EPITHELIUM <i>Kiyotaka Hitomi, Kanae Yamamoto, Koji Nishi, Yoshiaki Sugimura, and Masatoshi Maki</i>	339
ANALYSIS OF INTERLEUKIN-6-INDUCED SIGNALING IN MURINE HYBRIDOMA CELL LINES <i>Kazuhiko Takemura, Tatuya Yamashita, and Satoshi Terada</i>	347
IMMUNE REGULATION BY SIALOGLYCOCONJUGATE-BINDING LECTINS <i>Munetoshi Ando, Ken-ichi Nishijima, Shusuke Sano, Aiko Hayashi-Ozawa, Yoshinori Kinoshita, and Shinji Iijima</i>	353

TRANSCRIPTIONAL REGULATION OF THE α -FETOPROTEIN GENE IN HEPATOCYTES <i>Mikio Takahashi, Takeaki Dohda, Hidenori Kaneoka, Yoshitaka Sato, Yujin Inayoshi, Katsuhide Miyake, Masamichi Kamihira, and Shinji Iijima</i>	361
MODULATION OF CYTOKINE AND IMMUNOGLOBULIN A RELEASE BY BETA-(1,3-1,6)-GLUCAN FROM <i>AUREOBASIDIUM PULLULANS</i> STRAIN 1A1 <i>Takahiro Suzuki, Akira Hosono, Satoshi Hachimura, Toshio Suzuki, and Shuichi Kaminogawa</i>	369
INFLUENCE OF NATURAL REDUCED WATER ON RELEVANT TESTS PARAMETERS AND REACTIVE OXYGEN SPECIES CONCENTRATION IN BLOOD OF 320 DIABETES PATIENTS IN THE PROSPECTIVE OBSERVATION PROCEDURE <i>Z. Gadek, Y. Li, and S. Shirahata</i>	377
PROTEOME ANALYSIS OF NEURITE DIFFERENTIATION OF PHYTOESTROGEN-TREATED PC12 CELLS: PRELIMINARY RESULTS <i>Hiroko Isoda, Mariko Seki, Terence P. N. Talorete, and Junkyu Han</i>	387
CAPSAICIN-ENHANCED RIBOSOMAL PROTEIN P2 EXPRESSION AND RECOVERY OF TIGHT JUNCTION PERMEABILITY IN HUMAN INTESTINAL CACO-2 CELLS <i>Junkyu Han, Mitsuaki Akutsu, Terence P. N. Talorete, Toshiyuki Tanaka, and Hiroko Isoda</i>	395
METABOLIC RESPONSES OF EUKARYOTIC DRUG EFFICACY AND TOXICITY <i>D.B. Goodenowe, S. Ritchie, and D. Heath</i>	403
SUPPRESSIVE EFFECT OF FUCOIDAN DERIVED FROM <i>MOZUKU</i> ON <i>IN VITRO</i> INVASION OF HUMAN FIBROSARCOMA HT1080 CELLS <i>Jun Ye, Kiichiro Teruya, Yoshinori Katakura, Hiroshi Eto, and Sanetaka Shirahata</i>	409
INCREASED EXPRESSION, PURIFICATION AND CHARACTERIZATION OF THE WW DOMAIN OF CA150/FBP28 <i>Yusuke Kato, Yoriko Sawano, and Masaru Tanokura</i>	417
IMPROVEMENT OF LIGATION-MEDIATED POLYMERASE CHAIN REACTION (LM-PCR) METHOD FOR GENOME WALKING WITH A SINGLE GENE-SPECIFIC PRIMER <i>Keina Kozono, Ayako Aoki, Masayoshi Tsukahara, and Haruhiko Tsumura</i>	425
Author Index	433
Subject Index	437

Preface

The 17th Annual and International Meeting of the Japanese Association for Animal Cell Technology (JAACT) was held at the Yagoto Mulberry Hotel in Nagoya, Japan from November 15 to 18, 2004. The meeting focused on the industrial applications of animal cell technology. We invited academic and industrial scientists from all over the world to participate and make the JAACT 2004 truly successful and scientifically fruitful. More than 330 participants from 20 countries joined the meeting and gave presentations (plenary lectures, 3; Murakami memorial lecture, 1; ESACT special lecture, 3; presentations by symposists, 37; technical seminars, 3; oral presentations, 33; poster presentations, 91). Fields and titles of 7 symposia were 1. "Process Development & Manufacturing on Biologics", 2. "Food Allergies - Current and Perspectives-", 3. "Evaluation of Anti-Inflammatory and Anti-Cancer Food Factors Using Animal Cell Culture Models", 4. Control and Production Change of Biopharmaceuticals, 5. "Recent Developments in the Small RNA World", 6. "Stem Cell Technology", 7. "Metabolomics as a powerful tool in post-genome era", 8. "Advanced Functional Water for Prevention of Diseases". All presentations (oral and poster) were brought together on the following themes.

1. Cell culture engineering
2. Production of biologicals
3. Functional cell lines
4. Glycoengineering
5. Immunologicals, monoclonal antibodies, and vaccines
6. Transplantation, artificial organs, and organ substitutes
7. Gene therapy
8. Transgenic animals
9. Safety and regulation
10. Cell regulatory factors and signal transduction
11. Functional substances in food and natural sources
12. Animal cells for in vitro assay

The editors hope this volume of Proceedings will greatly contribute to the development of animal cell technology or innovation of life science.

The editors express their sincere gratitude to all the participants, organizers of the symposia, members of the organizing committee for their dedication in assuring the success of the meeting.

We also deeply thank to Nagoya Convention & Visitor Bureau, Daiko Foundation, Kato Memorial BioScience Foundation and Research Foundation for the Electrotechnology of Chubu for their financial supports.

The editors

MESENCHYMAL CELLS: METALLOPROTEINASES AND ADHESION ON MICROCARRIERS

C. Mosbeux¹, A.R. dos Santos Pedregal¹, D. Ribeiro de Sousa¹,
Vincianne Hendrick¹, N. Joseph, M. Bensellam¹, D. Blankaert¹,
T. Marique¹, C. Alloin¹, D. Parent², C. Liesnard², J.P. Van Vooren²,
S. Lowagie¹ and J. Werenne¹

¹Laboratory of Animal Cell Biotechnology, Dept. of Bioengineering,
Faculty of Sciences, Université Libre de Bruxelles, Belgium and ²Erasme Hospital, Brussels,
Belgium.

Abstract: The purpose of this work was to approach the development of a safe and validable process to grow the amounts of adult Mesenchymal Stem Cells (MSC) necessary for future biomedical applications. Using a single use Vue Life bag system integrated in a simple agitations bioreactor we constructed, we have studied the adhesion, migration and growth properties of MSC on different carriers (Cytodex and Bionoc) in comparison to other cells (endothelial/Kaposi sarcoma cells, CHO and HeLa) in relation to the expression of endogenous Metalloproteinases.

Keywords: Mesenchymal Stem Cells; Kaposi sarcoma; endothelial cells; CHO; HeLa; Adhesion; Migration; Mobility; Metalloproteinases; Single use bioreactor.

1. INTRODUCTION

Despite a number of controversial issues including ethical ones, stem cells represent a very important challenge for future therapeutic approaches. Especially adult Mesenchymal Stem Cells (MSC) derived from mesoderm, since it has been documented that they could lead to differentiation of tissues of the other germ layers (-ecto and -endoderm), showing previously unexpected “plasticity”, offer important promises.

As MSC proliferate extensively *in vitro* without obvious senescence or loss of differentiation potential, they may be an ideal source for therapy of inherited, and also for degenerative diseases.

In parallel to the necessary development of conditions securing appropriate differentiation of MSC, one of the numerous challenges in the field of cell based therapy and tissue engineering strategies, is to obtain enough progenitor cells (e.g. 500 millions cells) and to deliver them efficiently to the repair or regeneration site in the body.

This will need the development of culture conditions and devices that

could increase the ability of MSC to proliferate *in vitro* and would permit their migration towards the appropriate location for therapeutic tissue transplantation.

First steps have been taken in this direction using adult rat mesenchymal cells (MSC) as previously characterised and briefly by us (Bensellam *et al.* 2003).

We compared here the adhesion and aggregation properties of Endothelia, Kaposi Sarcoma and Mesenchymal Stem Cells on different solid surfaces.

Their mobility were evaluated in relation to the expression of different metalloproteinases (MMPases after treatment with different factors (PMA, TNF and other Cytokines).

2. MATERIAL AND METHODS

2.1 Cells and culture system

The control of the expansion of Mesenchymal Stem cells in order they can maintain their pluripotentiality and differentiation without the risk of tumoral like invasivity being not a straightforward problem, we started to approach it, by evaluating the interest of using either Cytodex 3 or Bionoc II carriers, and using VueLife bags, given the interest of developing for the future a process that could be easily validated for medical applications.

We first compared in a parallel investigation rat MSC cultivated as adapted (Bensellam *et al.* 2003) from a paper of Wislet-Gendebien *et al.* (2003), to endothelial cells of different origins, including Human Umbilical Endothelial cells (HUVEC) and Human Kaposi Sarcoma cells (Blankaert *et al.* 1998), and to HeLa as well as CHO cells (Hendrick *et al.* 2001).

2.2 Metalloproteinases Zymography

Studying cell adhesion and migration properties in relation to the expression of active MMPases required zymographic analysis as previously described by our group (Blankaert *et al.* 1998).

As MMPases expression was shown to be strongly regulated by MPA under AP1 control in conditions related to properties related to metastasis disseminations (Marique and Wérenne, 2001), we have studied the effect of this tumor promotor as well as the effect of TNF and “conditioned” medium (medium in which cells have been cultivated) or “activated conditioned” medium (same but treated at pH 2 with 10 M HCl and then quickly neutralized with 10 M NaOH) on expression of these enzymes by the different cells, using zymography.

3. RESULTS

3.1. MMPases expression

The following Zymograms (Fig. 1) showed that in HUVEC, after 48h treatment with PMA, the 92 kD MMPases is maximally produced, while in absence of the factor it was nearly undetectable. In Kaposi Sarcoma cells which are, as we have established, of endothelial origin, the 92 kD MMPases is expressed without stimulation, PMA 1nM just increasing it only marginally (Fig. 2). TNF acts synergistically strongly with HUVEC, and much less on Kaposi Sarcoma cells (data not shown), in relation to the basal invasivity properties of this AIDS related tumor.

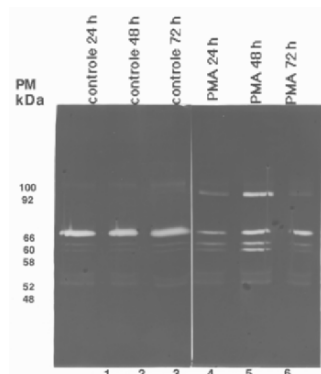


Figure 1. MMPases expression in HUVEC

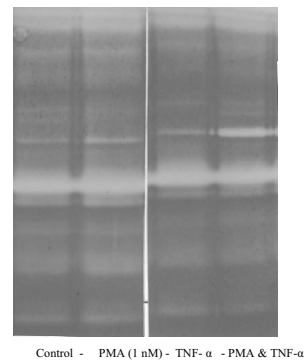


Figure 2. MMPases expression in KAPOSI cells

In MSC conditioned medium, in presence of Foetal Calf Serum, a high molecular weight MMPases (97 kD) was detected, while in absence of Serum its molecular weight is reduced to 91 kD, indicating that a factor of the Serum modulated the enzyme properties (Fig. 3).

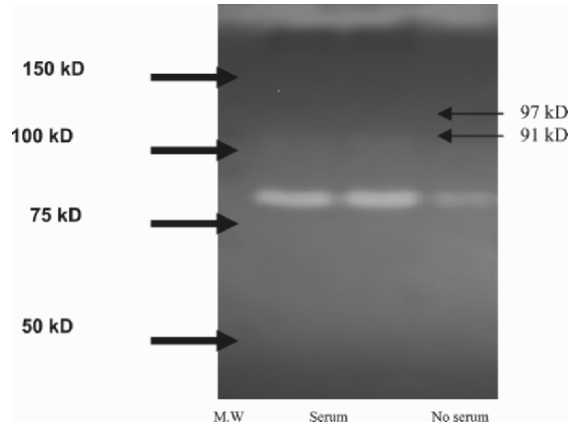


Figure 3. MMPases expression in MSC

3.2. Adhesion and Growth of MSC

We have seeded in VueLife bags either Bionoc II carriers and Cytodex 3 microcarriers, and on both substratum, MSC attached and multiply.

In the Bionoc system (Fig. 4), it is not easy to observe the cells due to the lack of transparency of the material. Moreover, it is not easy to recover the cells by trypsinisation from these microcarriers.

On Cytodex 3, the behavior of MSC depended on the passage of the culture: Higher passage cells (over 45), we have observed that MSC are able to migrate from colonized to empty beads as observed also with HeLa cells. With MSC, cells forms bridges between beads (Fig. 5).

A difference is also observed between Higher and Lower passages MSC, as it was shown that while in both situations, cells migrated from Petri dish to microcarriers added to a monolayer, the Higher passage MSC (over 45) were loosely bound to microcarriers after trypsinisation while Lower passage cells (up to 33) spread happily after trypsinisation to Cytodex 3 (Fig. 6).

Moreover, Higher and Lower passage MSC, grown on Cytodex 3, are able to migrate to TC treated Petri dishes and colonize it, while only Higher passage MSC are able to do so on non TC treated Petri dishes, indicating that different interactions occurred between extracellular matrix and Cells of different passages (Fig. 7).

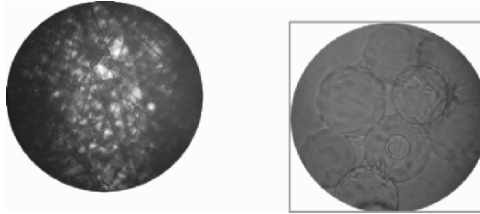


Figure 4. MSC on Bionoc II

Figure 5. MSC on Cytodex 3

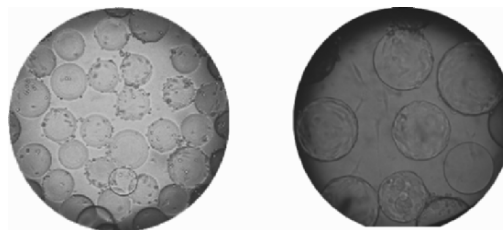


Figure 6. Adhesion of Higher and Lower passage MSC on Cytodex after Trypsinisation

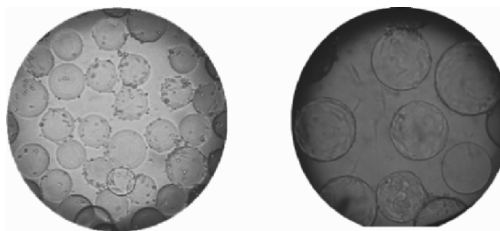


Figure 7. Colonisation of Petri dishes by MSC from confluent Cytodex 3
(left TC treated dish - right untreated dish)

These properties altogether indicate that depending on their number of passage in culture, MSC undergo a striking evolution affecting their interaction with the extracellular matrix and that they are themselves participating in the production of material involved in their adhesion and mobility properties.

Finally (not shown), we observed that compared to a control culture, where migration from a confluent MSC on Petri dish to Cytodex 3 beads, which are trapped in the monolayer is quite limited, it is facilitated under PMA treatment and is inhibited by TGF beta.

4. CONCLUSIONS

It is known that in relation to the potential plasticity of adult MSC, medium composition and passage number, as well as a number of cytokines and related factors, affect their adhesion, aggregation, morphology and differentiation characteristics.

We have in the past shown that in Kaposi Sarcoma, mobility related to the invasivity of the tumor is correlated with a high 92 kD MMPase expression, which may be increased in normal endothelial cells by PMA and TNF. As it was the case in these endothelial cells we showed that these factors modulated the adhesion properties of MSC in a striking way.

Despite it appeared that the control of the expansion of Mesenchymal Stem Cells in order they can maintain their pluripotentiality and differentiation properties without the risk of tumoral like invasivity will not be a straightforward problem, our present results could usefully be taken into account for the development of a culture process in a simple, safe and easily validable bioreactor.

5. REFERENCES

- Bensellam, M., Lowagie, S., Wislet-Gendebien, S., Rogister, B., and Wérenne, J. (2003), unpublished, presented briefly at BELAC Meeting, Brussels, March 21.
- Wislet-Gendebien, S. and Rogister, Bernard, J. *Cell Science* (2003).
- Blankaert, D., Simonart, T., Van Vooren, J.P., Parent, D., Liesnard, C., Farber, C.M., Marique, T. and Wérenne, J. Constitutive Release of Metalloproteinase-9 (92 kD Type IV Collagenase) by Kaposi's Sarcoma Cells (1998), *J. Acquired Immune Deficiency Syndromes and Retrovirology*, 18, 203-209.
- Hendrick, V., Winnepenninckx, P., Abdelkafi, C., Vandeputte, O., Cherlet, M., Marique, T., Renemann, G., Loa, A., Kretzmer, G. and Wérenne, J. (2001), Increased productivity of recombinant tissular plasminogen activator (tPA) by butyrate and shift of temperature: a cell cycle phase analysis, *Cytotechnology*, 36, 71-83.

Marique, T. and Wérenne, J. (2001) Control of 92 kDa Collagenase secretion in mammalian cells by modulation of AP1 activity: an experimentally based theoretical study, *J. Theor. Biol.* 209, 3-8.

CHARACTERIZATION OF PEANUT SPECIFIC T CELLS

S.J. Maleki

U. S. Department of Agriculture, Agricultural Research Service, Southern Regional Research Center, 1100 Robert E. Lee Boulevard, New Orleans, LA 70124

sjmaleki@srrc.ars.usda.gov

1. INTRODUCTION

Approximately 8% of children and 1-2% of adults have some type of food allergy (1). Peanuts, fish, tree nuts, and shellfish account for the majority of food hypersensitivity reactions in adults, while peanuts, milk, and eggs cause over 80% of food hypersensitivity reactions in children (2). Peanut hypersensitivity reactions usually last for a lifetime (3) and are often more severe than to other foods. Several reports (4,5) have detailed fatal and near-fatal anaphylactic reactions occurring in adolescents and adults following the ingestion of peanuts or peanut products.

The development of an IgE response to an allergen involves a series of interactions between antigen-presenting cells (APCs), T cells, and B cells. Initially APCs present small peptide fragments (T-cell epitopes) in conjunction with MHC class II molecules to T cells. T cells bearing the appropriate complementary T-cell receptor (TCR) will bind to the peptide MHC complex leading to further cognate interactions that result in the generation of a "second" signal, T-cell proliferation and cytokine generation (Th2-like lymphocyte activation). Opposing effects of various cytokines, such as IL-4 and IL-13 versus IFN-gamma and TGF-beta, are involved in the regulation of IgE production. Therefore, allergen specific Th2 lymphocytes that are known to secrete high levels of IL-4 and low levels of IL-2 and IFN- γ play an important role in the pathogenesis of allergic disease. The orderly sequence of events necessary to produce allergen-specific IgE, and the critical role T cells play in this process, has been studied in a variety of aero-allergens (6). However, the

role of T lymphocytes and antigen specificity in the induction and regulation of the food allergic response is less well defined.

Currently, the only effective treatment for patients with peanut hypersensitivity is avoidance of any food products that contain the allergen. This is difficult due to the inclusion of peanuts and peanut product as protein extenders in many different foods. Potential immunotherapeutic approaches to food hypersensitivity might include the competitive inhibition of allergen presentation with antibodies specific to the TCR V region or with soluble TCRs that would bind epitopes preventing them from binding to cell associated receptors. Another avenue of approach might be the modulation of T-helper (Th) cell development to favor Th1 cytokine responses by alteration of T-cell epitope structure. All of these approaches require in-depth knowledge of the allergenic proteins, B- and T-cell epitopes and T-cell signaling pathways that lead to the secretion of specific cytokines.

Ara h 2 has been previously identified, cloned from a peanut library and expressed as a recombinant protein. The B-cell epitopes of Ara h 2 have also been mapped and characterized (7). In the current work we have carried out rapid, large-scale purification and detailed characterization of a major peanut allergen. Ara h 2, purified in milligram quantities from peanut bound to specific IgE antibodies from human serum, induced histamine release and caused T-cell proliferation. Upon characterization of the immune response to Ara h 2, the T-cell epitopes of Ara h 2 were mapped using synthetic, overlapping peptides and T cells isolated from the blood of peanut allergic individuals and compared to T-cell epitopes recognized by non-atopic individuals. Identification of these immunodominant epitopes will enable the development of the previously mentioned and possibly novel immuno-therapeutic approaches for peanut hypersensitivity.

2. MATERIALS AND METHODS

2.1 T-CELL PROLIFERATION ASSAY

The peripheral blood lymphocytes (PBLs) of 17 peanut sensitive individuals and 5 non-allergic individuals were isolated from whole blood using ficoll hypaque. Cells were washed and suspended in media at the concentration of 4×10^6 cells/ml and stimulated with 50 ug/ml crude peanut extract (CPE) or 20 ug/ml Ara h 2 every 10-14 days in order to establish peanut or Ara h 2 specific T-cell lines. For the T-cell proliferation assays, 9 wells of a 96 well plate at 2×10^5 PBLs/well were stimulated with media (unstimulated control), crude peanut extracts (CPE, 50 ug/ml), purified wild type Ara h 2 (A2, 10 ug/ml), recombinant native Ara h 2 (rA2, 10 ug/ml, data not shown here), recombinant

mutated Ara h 2 (r-Mut A2, 10 ug/ml, data not shown here), synthetic overlapping peptides of Ara h 2 or crude rice extracts (Rice, 50 ug/ml, as negative control) at 37°C. For the T-cell epitope mapping, 29 synthetic overlapping peptides (SOPs, made by the W. M. Keck Biotechnology Resource Center, New Haven, CT) spanning the entire sequence of Ara h 2 were used to stimulate T cells in 96 well plates. The cells in the 96 well plates were allowed to proliferate at 37°C in the absence (media) and presence of the stimulant (CPE, A2, rA2, r-Mut A2, SOPs, or rice extracts) for 6 days. On day 6 the cells were treated with [³H]-thymidine (1 µCi/well) and re-incubated at 37°C for 6-8 hours and harvested onto glass fiber filters (Packard, Meriden, CT). T-cell proliferation was estimated by determining the [³H]-thymidine incorporation into the DNA of proliferating cells. [³H]-thymidine incorporation is reported as a stimulation index (SI), which is defined as stimulation above media treated (control) cells. Experiments were performed in triplicate and reported as an average of stimulation indexes for all individuals tested, over media treated controls.

2.2 FACS ANALYSIS

For detection of the cell surface receptors CD4 and CD8, cells were first washed twice in cold phosphate-buffered saline (PBS) then resuspended in PBS at a concentration of 1×10^6 cells/ml and incubated with anti-CD4 or anti-CD8 specific monoclonal antibodies (COULTER, PN) according to manufacturers instructions for 30 minutes at room temperature, washed with PBS and fixed with 2% paraformaldehyde. Cells were then subjected to fluorescent analytical cell sorting (FACScan) using a flow cytometer (Becton Dickinson) equipped with a 15 mA argon ion laser. The filter settings for FITC (BP 530/30) and PE (BP 585/42) were used. FITC conjugated murine monoclonal antibody against CD4 or PE conjugated murine monoclonal antibody against CD8 were purchased from Coulter (T4-FITC and T8-RD1, Cyto-STAT/Coulter Clones, COULTER, PN).

2.3 IMMUNOPRECIPITATION AND ELECTROPHORESIS ANALYSIS

T-cell lines derived from peanut sensitive individuals were stimulated with crude peanut extracts (CPE), and then at various times after stimulation (0, 5, and 10 minutes) samples were taken and gently disrupted in lysis buffer. CPE or Ara h 2 specific cell lines were stimulated with CPE, (data for stimulation with r Ara h 2 and mutant r Ara h 2 are not shown). Various times after stimulation (0, 5, and 10 minutes) samples were taken and gently disrupted in lysis buffer. The lysate from each reaction was centrifuged at 10,000 x g

to remove nuclei and debris. The antibodies Anti-ZAP-70 (Transduction Laboratories, Lexington, KY), anti-phosphotyrosine (py-20), antiphosphotyrosine (py-99, Santa Cruz Biotechnology Inc., Santa Cruz, CA) or anti-T-cell receptor- ζ (here referred to as p-18 and p-21, Zymed, San Francisco, CA) were added to the cleared supernatant and allowed to incubate with agitation at 4°C over night. Protein A-sepharose beads were then added to precipitate the antibody/antigen complexes. The pellet was re-suspended in SDS-sample buffer and then electrophoresed on 4-12% polyacrylamide gels. SDS-PAGE resolved proteins were transferred to nitrocellulose electrophoretically. The membranes were blocked in Tris-buffered saline containing 0.05% tween-20 (standard TBST) plus 2% bovine serum albumin (BSA) for 2 hours at room temperature. The membrane was then washed in TBST and incubated anti-Mouse conjugated to Horseradish peroxidase (anti-mouse-HRP, Santa Cruz) for 30 minutes at room temperature. Detection of the bound antibody was performed by exposing blot to ECL Plus Western blot detection system (Amersham Pharmacia Biotech, Buckinghamshire, UK) and subsequent exposure to X-ray film.

3. RESULTS

3.1 DEVELOPMENT AND CHARACTERIZATION OF PEANUT-SPECIFIC T-CELL LINES

Peanut specific T-cell lines were developed from 17 peanut-sensitive patients and 5 control patients (data not shown) using CPE as described in Materials and Methods. These cell lines were then characterized to determine the predominant T-cell type (CD4⁺ or CD8⁺) present in these cell lines and to ensure that the T-cell receptor was engaged by the CPE. In order to determine if helper cells or killer cells were the predominant T-cell type present in each of these cells lines they were stained with fluorescent-labeled antibodies against CD4 and CD8 cell surface markers and subjected to Fluorescent Analytical Cell Sorting (FACS) analysis. The percentage of the total T-cell population, which were CD4⁺ ranged from 42-93% in cell lines developed from peanut sensitive individuals (Fig. 1) while CD8⁺ cells represented only 2-38% of the total T-cell population. In those peanut specific T-cell lines developed from control individuals, 65-87% of the T-cells were CD4⁺ while 2-30% were CD8⁺ (data not shown). These results indicate that the predominant T-cell type mediating peanut specific responses is the T-helper cell subset.

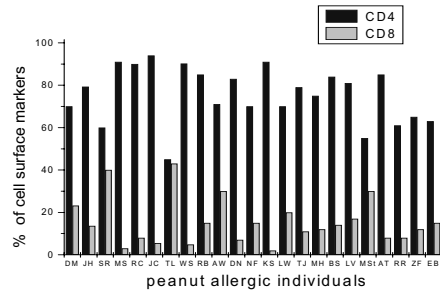


Figure 1. The CD4⁺ and CD8⁺ profiles of the T-cell lines of peanut allergic and non-allergic individuals. T cells were stained with FITC-labeled anti-CD4 and PE-labeled anti-CD8 antibodies. FACS analysis was utilized to determine the percentages of proliferating cells in peanut specific T-cell lines. This figure represents the CD4/CD8 profiles of T-cell lines established from 22 peanut allergic individuals (x-axis).

3.2 IMMUNOPRECIPITATION

Immune-precipitation experiments were performed using an antibody specific to the ZAP-70 protein tyrosine kinase, known to be associated with the TCR- ζ chain (referred to as p18 or p-21 in the figure) when the TCR is engaged, to ensure that CPE was stimulating T cells to proliferate through binding of the T-cell receptor (Fig. 2 A, B). A T-cell line derived from a peanut sensitive individual was stimulated with and then at various times after stimulation (0, 5, and 10 minutes) samples were taken and gently disrupted in lysis buffer. The ZAP-70 antibody was then used to immune-precipitate this protein and any associated proteins. Immune-precipitated proteins were then re-suspended in SDS sample buffer and subjected to Western blot analysis using either the TCR- ζ chain antibody (Panel A) or an antibody that recognizes proteins with phosphorylated tyrosine residues (Panel B). These results show that ZAP-70 associates with the zeta chain of the TCR on stimulation with CPE and that the zeta chain is phosphorylated as a result of peanut allergens binding to the TCR.

Similar experiments were performed to determine the down-stream molecules that are activated as a result of TCR interaction with peanut allergens. As described above, T-cell lines derived from a peanut sensitive individual were stimulated with CPE and then at various times after stimulation (5, 10, and 20 minutes) samples were taken and prepared for immune-precipitation with Anti-ZAP-70 antibodies (Fig. 2 C, D). Western blot analysis of the immune-precipitates was performed using either the ERK antibody, mitogen-activated protein kinases implicated in regulating the activity of a variety of cytokine gene transcription factors, or an antibody that recognizes proteins with phosphorylated tyrosine residues. These results show that ZAP-70 associates with ERKs and that these proteins are phosphorylated for a transient period of time after the T cell is stimulated with peanut allergens.

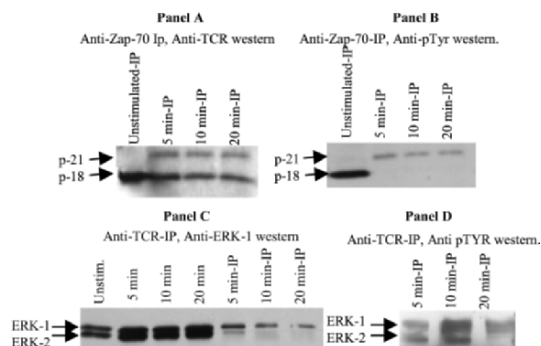


Figure 2. CPE stimulates T-cells to proliferate by activating a T cell signaling pathway.

3.3 PURIFICATION OF ARA H 2 FROM CRUDE PEANUT EXTRACTS

Ara h 2, a major peanut allergen, was purified by ammonium sulfate precipitation followed by conventional column chromatography from CPE. A 25% ammonium sulfate saturation of the crude peanut extract (CPE) resulted in fractionation of the Ara h 2 protein into the pellet with a significant removal of contaminating proteins (Fig. 3A, lane 2). Resolubilized protein was then subjected to anion exchange chromatography (Fig. 3A, lane 3) followed by a final purification step on a hydrophobic column (Fig. 3A, lane 4). This purification process is summarized in Table 1 and resulted in Ara h 2 being purified to near homogeneity from CPE. To confirm that the purification scheme resulted in eliminating all other allergens from the preparation, immunoblot analysis using pooled serum IgE from a population of peanut sensitive patients was performed with samples taken at each stage of purification. Figure 3B shows that the purified proteins were recognized by serum IgE from peanut sensitive patients and that no other IgE-reactive proteins were detected in the purest fractions.

3.4 T-CELL PROLIFERATION IN RESPONSE TO STIMULATION WITH PURIFIED ARA H 2

The ability of the purified Ara h 2 to stimulate the proliferation of T-cell lines isolated from the peripheral blood of peanut-allergic individuals was assessed. The proliferation of twelve CPE-specific T-cell lines from peanut

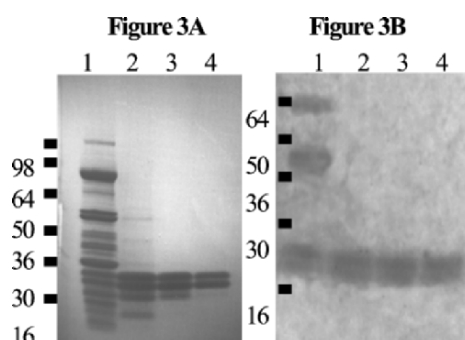


Figure 3. SDS-PAGE and Western blot analysis of Ara h 2 at various stages of purification. SDS-PAGE analysis of Ara h 2 purification process is shown in panel A. Identical samples are transferred to nitrocellulose and probed with anti-human IgE in panel B. Lanes are as follows: lane lanes A1 and B1, crude peanut extract (CPE); lanes A2 and B2, 25% ammonium sulfate pellet; lanes A3 and B3, peak fractions following a DEAE column; lanes A4 and B4, peak fractions containing Ara h 2 following a phenyl sepharose column.

Table 1. The summary of Ara h 2 purification. The milligram (mg) amounts of total protein and Ara h 2, the fold enrichment of the protein and the protein yield with respect to the amount of Ara h 2 in the original crude peanut extract are shown for each purification step exhibited in the first column.

	Total Protein	Ara h 2 (mg)	Fold Enrichment	% Yield
Crude peanut extract	20,000	500	—	—
Ammonium sulfate	500	200	16	40
Anion exchange	150	115	31	23
Hydrophobic column	77	75	39	15

allergic individuals was measured in response to media, CPE, crude rice extracts (negative control), and Ara h 2 (Fig. 4). The stimulation index (SI) for individual T-cell lines stimulated with CPE ranged from 3 to 15 when compared to either media or crude rice extract (negative controls) treated cells. When Ara h 2 was used to stimulate these same T-cell lines the SI range was 2-11 when compared with the same negative controls. For some T-cell lines the SI was nearly the same whether CPE or purified Ara h 2 was used. In other cases, the SI produced when T cells were exposed to Ara h 2 was only a small portion of

that compared to the same T cells stimulated with CPE. CPE-specific T-cell lines could also be developed from normal individuals. However, the number of T-cell lines and the amplitude of the SI were greatly reduced when compared with those from peanut sensitive individuals (data not shown). These results indicate that in some individuals Ara h 2 represents the major allergenic protein found in CPE while in other patients it represents one of a number of different proteins that can stimulate T cells from peanut allergic individuals to proliferate.

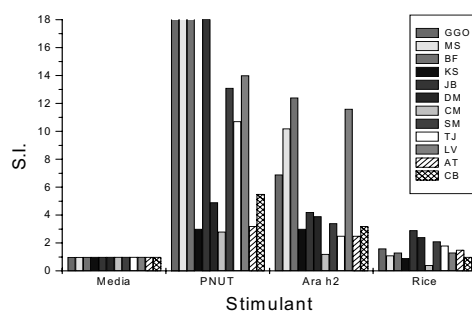


Figure 4. Purified Ara h 2 stimulates the proliferation of T cells of allergic individuals. Isolated T cells are treated with (x-axis) media (untreated), crude peanut extracts (CPE, positive control), Ara h 2 and rice extracts (negative control). T-cell proliferation was estimated by quantitating the amount of 3H-thymidine incorporation into the DNA of proliferating cells and is reported as stimulation index (S.I., y-axis).

3.5 IDENTIFICATION OF THE ARA H 2 T-CELL EPITOPES

Twenty-nine overlapping peptides representing the amino acid sequence of the Ara h 2 protein were synthesized to determine which regions were capable of stimulating CPE-specific T-cell lines to proliferate. Each peptide was 20 amino acids long and was offset from the previous peptide by 5 amino acids. In this manner, the entire length of the Ara h 2 protein could be studied in large overlapping fragments. These peptides were used in a T-cell proliferation assay to identify which Ara h 2 fragments contained T-cell epitopes. CPE-specific T-cell lines that displayed a high SI when stimulated with purified Ara h 2 protein were used to map T-cell epitopes. Experiments were performed with 17 CPE-specific T-cell lines that showed high SIs when stimulated with the intact Ara h 2 protein. Data from all T-cell lines tested were compiled and shown as an average SI for each peptide (Fig. 5). The five T-cell epitopes identified in this manner were centered on amino acid residues 19-33, 39-58, 84-93, 99-109, and 135-148 which correspond to peptides number 908, 913, 924, 926 and 931 in

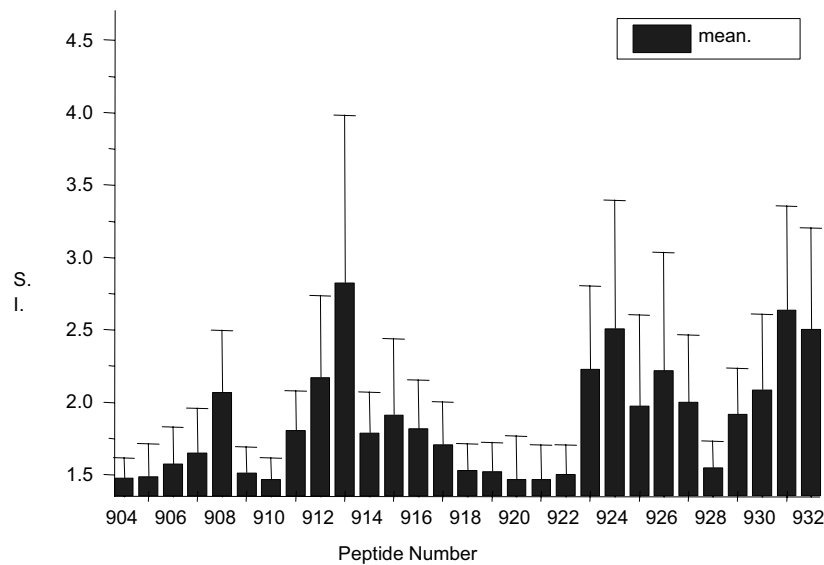


Figure 5. Proliferation of T cells isolated from peanut allergic individuals in response to Ara h 2 derived peptides. T-cell proliferation was measured by 3H-thymidine incorporation in the DNA of proliferating cells and reported here as stimulation index (SI, y-axis). The mean SI of the T cells of all 17 allergic individuals is shown here.

the figure. Most T-cell lines (~70%) were stimulated to proliferate by multiple Ara h 2 regions. In addition, there were no common amino acid sequence motifs shared by all the epitopes.

4. DISCUSSION

To understand food hypersensitivity reactions it is important to identify and characterize the protein allergens that are responsible for the immunologic disorder as well as the immunological responses. What is so different about the protein allergens that causes them to be recognized as pathogenic moieties by the immune system? Why do peanut allergies persist throughout the life of an individual while allergies to similar proteins in other legumes such as soy are outgrown early in life? Various proteins involved in hypersensitivity reactions to peanut have been identified (8, 9, 10, 11, 12), three of which have been cloned and characterized (Ara h 1, Ara h 2 and Ara h 3, 10, 11, and 12 respectively). Identification, isolation of the native Ara h 2 and characterization

of the immune response to the allergen, may prove useful in the development of standardized extracts, in biophysical characterization studies like X-ray crystallography, circular dichroism (CD) and enzyme binding experiments. The biophysical features of *E. coli* produced recombinant Ara h 2 and hypoallergenic mutants of Ara h 2 can be compared with the native Ara h 2 towards development of a possible vaccine or a hypoallergenic peanut.

Identification and isolation of specific food antigens has facilitated identification and molecular characterization of B- and T-cell epitopes of these allergens in peanut, egg and milk. The B-cell epitopes of Ara h 1, Ara h 2, and Ara h 3 have been mapped and identified (11, 12,13) however, the response of T cells to these allergen has not been determined. Ten IgE-binding epitopes were identified for Ara h 2 and epitopes 3, 6, and 7 were recognized by all of the patient sera tested (13). Single amino acid changes in the immunodominant epitopes of Ara h 2 caused loss of IgE binding (7). Here, 5 immunodominant T-cell epitopes have been identified for Ara h 2 only one of which overlaps with a major B-cell epitope. No significant amino acid homology was seen among the epitopes identified. Non-allergic individuals seemed to recognize some of the same epitopes as allergic individuals. Although both T-cell lines from atopic and non-atopic individuals were found to have a Th2-like cytokine secretion profiles, we found that T cells from peanut allergic individuals secrete higher levels of IL-4 in response to treatment with a mutual immunodominant epitope compared to T cells from non-allergic individuals implying a Th2-like response. Previously, a decrease in the level of IFN-gamma was seen in response to treatment of T cells with Ara h 2 with no changes in the level of IL-4 compared to the control suggesting an important role for IFN-gamma in development of peanut specific responses (14). Similar to the findings in this study another group of investigators have confirmed the predominance of CD4+ T cells and demonstrated elevated levels of IL-4 and IL-5 with lower levels of IFN- (production in peanut specific T-cell lines generated from peanut allergic individuals (15). Peanut-specific T-cell lines recognized allergens in association with HLA-DR and -Dp of class II molecules while exhibiting Th2-like cytokine expression profiles whereas, T cells found to cross-react with hazelnut and peanut demonstrated a Th0-like phenotype (16). Although the role of T cells in allergic response is undeniable, very few studies have been done, some with inconsistent findings to understand the mechanisms of T-cell involvement in type I food hypersensitivity. One explanation for some of the apparent discrepancies may be due to the different conditions for antigen preparation, concentrations of antigen, as well as feeding, stimulation and harvesting times of T cells utilized by the various groups. Exploration of T-cell responses to food allergens has only recently begun. Therefore, we may find that minor adjustments while handling cell cultures may result in drastic changes in the proliferative response, cytokine profiles and surface markers of food specific T-cell lines and clones. Regardless, many more experiments are necessary in

order to gain a full understanding of the mechanisms of T-cell action in food allergy.

The ability to identify immunodominant peptides of protein allergens has introduced the possibility of a highly specific immune intervention. Altered forms of known peptides or allergens containing T-cell epitopes can be utilized to control the immune response by induction of anergy or tolerance (17). Hirahara et al. (18) demonstrated immunological tolerance induced by intradermal administration of a peptide, which included the dominant T-cell epitope from a major milk allergen, casein. They also demonstrated a significant immunological tolerance in the antibody response against the whole native protein. Suppression in IgG2a and 2b (Th1-induced subclasses) as well as IgG1 (Th2 induced subclass) of antibody response was observed. This study and others clearly demonstrate that peptides corresponding to dominant T-cell epitopes of allergens can induce immunological tolerance in the T-cell responsiveness to native protein antigens even though the conditions for induction of desired response have not been determined.

5. REFERENCES

1. Ferguson, A. C., Food Allergy. Progress in Food and Nutrition Science 1984; 8: 77-107.
2. Kaminogawa, S., Food Allergy. Oral Tolerance and Immunomodulation-Their molecular and cellular mechanisms. Biosci. Biotech. Biochem. 1996; 60 (11): 1749-1756.
3. Kleinman, R. E., The role of developmental immune mechanisms in intestinal allergy. Annal. Allergy 1983; 51: 222-225.
4. Sampson, H., Immunologically mediated adverse reactions to foods: role of T cells and cutaneous reactions. Annal. Allergy 1984; 53: 472-475.
5. Rumsaeng, V., and Metcalfe, D. D., Food Allergy. Seminars in Gastrointestinal Disease 1996; 7 (3): 134-43.
6. O'Hehir, R. E., Garman, R. D., Greenstein, J. L., and Lamb, J. R., The specificity and regulation of T-cell responsiveness to allergens. Annu. Rev. Immunol. 1991; 9: 67-95.
7. Stanley, S. J., King, N., Burks, A.W., Huang, S. K., Sampson, H., Helm, R. M., West, C. M., and Bannon, G. A. Identification and mutational analysis of the immunodominant IgE binding epitopes of the major peanut allergen Ara h 2. Arch. Biochem. Biophys, 1997; 324 (1): 244-253.
8. Eigenmann, P. A., Burks, A. W., Bannon, G. A., and Sampson H. A., Identification of unique peanut and soy allergens in sera adsorbed with cross-reacting antibodies. J. Allergy Clin. Immunol. 1996; 98 (5) Part 1: 969-978.
9. Burks, A. W., Cockrell, G., Stanley, J. S., Helm, R. M., and Bannon, G. A., Isolation, identification and characterization of clones encoding antigens responsible for peanut hypersensitivity. Int. Arch. Allergy Immunol. 1995; 107: 248-250.
10. Burks, A.W., Williams, L. W., Helm, R. M., Connaughton, C., Cockrell, G., and O'Brien, T. O., Identification of a major peanut allergen, Ara h I, in patients with atopic dermatitis and positive peanut challenges. J. Allergy Clin. Immunol. 1991; 88 (2): 172-179.

11. Burks, A. W., Williams, L. W., Connaughton, C., Cockrell, G., O'Brien, T. O., and Helm, R. M., Identification and characterization of a second major peanut allergen, Ara h 2, with use of the sera of patients with atopic dermatitis and positive peanut challenge. *J. Allergy Clin. Immunol.* 1992; 90 (6) Part 1: 962-969
12. Rabjohn, P. A., Burks, A. W. and Bannon, G. A. Molecular cloning and epitope analysis of the peanut allergen Ara h 3. *J. Clin. Invest.* 1999; 103 (4): 535-542.
13. Burks, A. W., Shin, D., Cockrell, G., Stanley, S. J., Helm, R. M., and Bannon, G. A. Mapping and mutational analysis of the IgE-binding epitopes of Ara h1, a legume vicillin protein and a major allergen in peanut hypersensitivity. *Eur. J. Biochem.* 1997; 254 L: 334-339.
14. Doiron J. B., Burks, A. W., Harbeck, R., Williams, L. W., Trumble, A., Helm, R. M., and Leung, D. Y. M., *J. Allergy Clin. Immunol.* 1994; 93 (1) Part 1: 93-99.
15. de Jong, E. C., Spanhaak, S., Martens, B. P. M., Kapsenberg, M. L., Penninks, A. H., and Weirenga, E. A., Allergen, IgE, mediators, Inflammatory mechanisms: Food allergen (peanut)-specific Th2 clones generated from the peripheral blood of a patient with peanut allergy. *J. Allergy Clin. Immunol.* 1996; 98 (1): 73-81.
16. Higgins J. A., Lamb, J. R., Lake, R. A., and O'Hehir, R. E., Polyclonal and clonal analysis of human CD4⁺ T-lymphocyte response to nut extracts. *Immunol.* 1995; 84: 91-97.
17. Takai, T., Yokota, T., Yasue, M., Nishiyama, C., Yuuki, T., Mori, A., Okudaira, H., and Okumura, Y. Engineering of the major house dust mite allergen Der f 2 for allergen-specific immunotherapy. *Nature Biotech.* 1997; 15: 754-758.
18. Hirahara, K., Hisatsune, T., Choi, C-Y., and Kaminogawa, S., Profound and immunological tolerance in the antibody response against bovine α 1-casein induced by intradermal administration of a dominant T cell determinant. *Clin. Immunol. Immunopath.* 1995; 76:12-18.

USING METABOLOMICS TO BETTER UNDERSTAND FUNCTIONAL FOODS

Dayan B. Goodnowe¹, Yasuyo Yamazaki¹, Bernhard H. J. Juurlink²

¹*Phenomenome Discoveries Inc. 204-407 Downey Road, Saskatoon, SK, S7N 4L8, Canada;*

²*Department of Anatomy and Cell Biology, College of Medicine, University of Saskatchewan, Saskatoon, SK, S7N 5E5, Canada*

Abstract: Decreasing hypertension and inflammation are important human health objectives. Functional foods are being developed to provide an alternative treatment for mild to moderate symptoms as well as for alternatives to pharmaceuticals for long-term health management. Broccoli has been shown to decrease oxidative stress and associated inflammation and hypertension in stroke-prone spontaneously hypertensive rats. This presentation will focus on how comprehensive metabolomics can be used to understand the activity of broccoli in this animal model of hypertension.

Key words: stroke-prone spontaneously hypertensive rat; broccoli sprout.

Metabolomics, the global analysis of small molecules, or metabolites, in biological samples, is the final link in the systems biology chain. To study what genes are expressed under a given set of conditions one measures the change in the concentration and composition of gene transcripts; and, to study what transcripts get translated, one measures the changes in protein content and concentration. It therefore follows that to study how the actual proteins in a system are functioning, one must measure the changes in metabolites content and concentration. The advent of genomics and gene-chip technology gave scientists the ability to monitor and quantitate the changes in the expression of every gene within a genome. Proteomic technologies have made available valuable functional information and have provided the ability to monitor gene products. In the systems biology picture, however, humans truly are more than the sum of our parts; we are more than our genes. To monitor the biology of a system, one must be able to measure

the effects of the environment on gene expression. Because an observed phenotype is the summation of gene expression, resultant protein activity, and environmental influences, metabolomics is required to supply the last piece of the puzzle - the quantifiable measurement of the interaction of genetics and environment. Metabolomics offers measurement of phenotype. The changes observed in the metabolome directly indicate what system changes (e.g. genes or drugs) affect the function of which pathways. As well, the exact point(s) in the pathway affected can be determined. Although proteins involved in these pathways may be useful drug or pesticide targets, it is their activity - not their amount - that is important. This is why the correlation between activity and protein concentration is often poor. Of the 'omics technologies, only metabolomics consistently provides strong correlations between concentration and observed phenotype.

No attention to human health is complete without recognizing the important role that diet and lifestyle play in wellness and disease prevention. It has been estimated that 30 - 40 percent of all cancers can be prevented by lifestyle and dietary measures alone. Since consumption of large quantities of fruit and vegetables is associated with a striking reduction in the risk of developing a variety of inflammations, it is of interest that a number of dietary plants contain substantial quantities of compounds that regulate mammalian enzymes of xenobiotic metabolism. Thus, dietary plants belonging to the family *Cruciferae* and genus *Brassica* (e.g., broccoli and cauliflower) contain substantial quantities of sulforaphane (4-methylsulfinylbutyl isothiocyanate) which is the most potent phase 2 protein inducer found in our food sources (Fahey et al., 1997). A major action of phase 2 proteins, mainly enzymes, is to inactivate electrophiles and strong oxidants (Prester et al., 1993); hence, there has been a research interest in dietary phase 2 protein inducers as a means to prevent cancers (Talalay and Fahey, 2001).

The animal model chosen was the male and female stroke-prone spontaneously hypertensive rats (SHPSp) (Wu et al., 2004). This strain develops severe hypertension (Nagaoka et al., 1976) that is related to increased peroxynitrite formation (Ma et al., 2004) and develops inflammatory changes in blood vessels (Liu et al., 1994, 1996). We chose broccoli sprouts as the source of phase 2 protein inducers. We put stroke-prone spontaneously hypertensive rats ($n = 4-5$ rats per group) on a special diet of AIN-93 (Reeves et al., 1993) plus 200mg/day broccoli sprouts for a period of 4 months and during this period measured their blood pressure and looked at the state of inflammation and oxidative stress in different organs compared to controls which were on AIN-93 diet only. The mentioned diet controls blood pressure and ameliorates inflammatory changes. At the end of study, anesthetized animals were perfused with buffered saline, and

kidneys and plasma were removed and frozen in liquid nitrogen. The frozen tissues were ground in the frozen state, and homogenized tissue powders were used for non-targeted FTMS analysis.

A total of 68 samples (duplicate analysis of control diet SHPsp liver and plasma, male and female $n = 4$; duplicate analysis of broccoli fed SHPsp liver and plasma, $n = 4$ male, $n = 5$ female) were processed via a proprietary extraction method optimized to separate the metabolites into multiple extracts based upon their polarity and acid/base chemistry as shown in Figure 1. Extracts were analyzed by direct injection Fourier Transform Ion Cyclotron Resonance mass spectrometry (FT-ICR-MS). This is currently the highest resolution mass spec technology available, and is the only method that provides the degree of resolution and mass accuracy required to reliably separate metabolites in complex samples. The resulting data set can easily be visualized using DISCOVAmetrics™, a bioinformatics platform that allows multiple samples to be easily compared and mined for both known and novel metabolites.

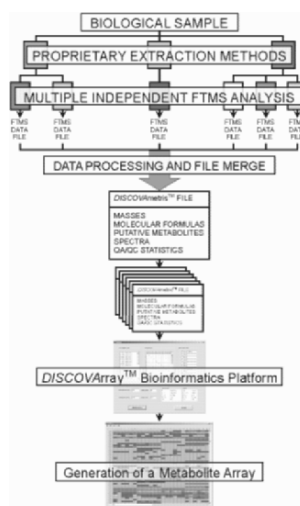


Figure 1. Comprehensive metabolome analysis technology

To evaluate internal reproducibility, each sample was extracted and analyzed in duplicate. The correlations between the two replicates are plotted in Figure 2. The R-squared values for the total average was 0.96.



Figure 2. QAQC reproducibility

Global statistics were performed using all samples, and setting each tissue and gender (n of 16 or 18) equal to one variable, for total of 4 variables. Following log(2) normalization and significance testing (p -values < 0.01). As shown in Figure 3, each tissue was completely separated.

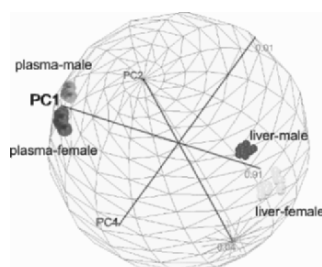


Figure 3. PCA

To evaluate the relative difference between the two treatments (broccoli fed vs. control) in liver and plasma, all male samples were normalized to male control average of each detected metabolite and all female samples were normalized to female control average of each detected metabolite. Hierarchical Clustering Analysis (HCA) plots were generated (see Figure 4).

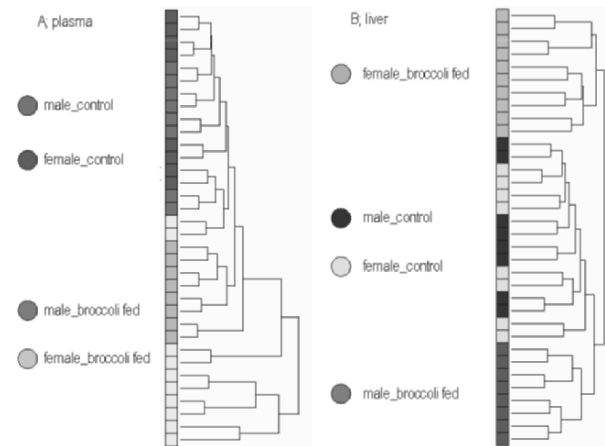


Figure 4. HCA plots

Interestingly, in Figure 4A plasma samples, females exhibit a greater effect of broccoli feeding, while in liver samples at Figure 4B, males and females show different responses to broccoli feeding. Tables 1 and 2 show the number of the significant metabolite changes (p -values < 0.05) between broccoli fed samples vs. control samples in plasma and liver, respectively. According to Table 1, females show a greater effect of broccoli feeding as seen in the HCA result in Figure 4A. In Table 2, a total of 108 metabolites were down-regulated in female liver samples. This phenomenon is totally different from male samples. Focusing on detailed metabolites in plasma, 30 metabolites were up-regulated, including fatty acids, diacylglycerols and triacylglycerols. Additionally this phenomenon was more observed to be greater in female samples. In male liver samples, mainly fatty acids, diacylglycerols and triacylglycerols were up-regulated. On the other hand in female liver samples, glucuronidated metabolites were down-regulated.

Table 1. Number of metabolites which expressed significantly in plasma samples (p -values < 0.05)

	plasma		plasma	
	male + female	male	female	
$> 2.0x$	3	4	9	
$1.2x < 2.0x$	52	33	99	
total up	74	45	127	
$0.5x < 0.8x$	6	7	5	
$< 0.5x$	2	6	2	
total down	15	51	8	
total changed	89	96	135	

Table 2. Number of metabolites which expressed significantly in liver samples (p -values < 0.05)

	liver		liver	
	male + female	male	male	female
$> 2.0x$	0	4		1
$1.2x < 2.0x$	16	44		28
total up	20	85		38
$0.5x < 0.8x$	8	13		83
$\leq 0.5x$	0	0		1
total down	36	58		108
total changed	56	143		146

Summary

The data provided in the current study demonstrates the utility of the comprehensive metabolomics analysis provided in DISCOVAmetrics™ technology. Metabolic analysis is a potentially powerful tool that can be used to address both applied and basic research questions. Broccoli feeding clearly elicited different responses in male and female animals. Such analyses will increase our understanding of the complex pharmacological antioxidants and provide new perspectives for understanding human responses.

REFERENCES

- Fahey, J. W., Zhang, Y. and Talalay, P., 1997, Broccoli sprouts: An exceptionally rich source of inducers of enzymes that protect against chemical carcinogens, *Proc. Natl. Acad. Sci. USA* 94:10367-10372.
- Liu, Y., Jacobowitz, D. M., Barone, F., McCarron, R., Spatz, M., Feuerstein, G., Hallenbeck, J. M., and Siren, A. L., 1994, Quantitation of perivascular monocytes and macrophages around cerebral blood vessels of hypertensive and aged rats, *J. Cereb. Blood Flow Metab.* 14:348-352.
- Liu, Y., Liu, T., McCarron, R. M., Spatz, M., Feuerstein, G., Hallenbeck, J. M. and Siren, A. L., 1996, Evidence for activation of endothelium and monocytes in hypertensive rats, *Am. J. Physiol.* 270:2125-2131.
- Ma, X.-L., Gao, F., Nelson, A. H., Lopez, B. L., Christopher, T. A., Yue, T.-L. and Barone, F. C., 2001, Oxidative inactivation of nitric oxide and endothelial dysfunction in stroke-prone spontaneous hypertensive rats, *J. Pharmacol. Exp. Ther.* 298:879-885.

- Nagaoka, A., Iwatsuka, H., Suzuoki, Z. and Okamoto, K., 1976, Genetic predisposition to stroke in spontaneously hypertensive rats, *Am. J. Physiol.* 230:1354-1359.
- Prester, T., Holtzclaw, W. D., Zhang, Y. and Talalay, P., 1993, Chemical and molecular regulation of enzymes that detoxify carcinogens, *Proc. Natl. Acad. Sci. USA* 90:2965-2969.
- Reeves, P. G., Nielsen, F. H., Fahey, G. C. Jr., 1993, AIN-93 purified diets for laboratory rodents: final report of the American Institute of Nutrition ad hoc writing committee on the reformulation of the AIN-76A rodent diet. *J. Nutr.* 123:1939-1951.
- Talay, P. and Fahey, J. W., 2001, Phytochemicals from cruciferous plants protect against cancer by modulating carcinogen metabolism, *J. Nutr.* 131:3027S-3033S.
- Wu, L., Ashraf, M. H. N., Facci, M., Wang, R., Paterson, P. G., Ferrie, A. and Juurlink, B. H., 2004, Dietary approach to attenuate oxidative stress, hypertension, and inflammation in the cardiovascular system, *Proc. Natl. Acad. Sci. USA* 101:7094-7099.

FOOD FACTORS THAT REGULATE INTESTINAL INFLAMMATION: EVALUATION OF THE FACTORS BY USING A COCULTURE SYSTEM

Hideo Satsu and Makoto Shimizu

Department of Applied Biological Chemistry, Graduate School of Agricultural and Life Sciences, The University of Tokyo, 1-1-1 Yayoi, Bunkyo-ku, Tokyo 113-8657, Japan

Abstract: Immune cells located in the intestinal epithelium interact with intestinal epithelial cells *via* soluble factors. A new *in vitro* model using a coculture system was constructed in this study to analyze the interaction between intestinal epithelial cells and macrophage-like cells. Human intestinal epithelial Caco-2 cells were differentiated on semipermeable membranes. Human monocytic THP-1 cells were differentiated to macrophage-like cells and then cocultured on the basal side of the Caco-2 monolayers. Coculturing for 48 hours resulted in a decrease in the transepithelial electrical resistance of the Caco-2 monolayers and an increased release of lactate dehydrogenase from the Caco-2 cells. This suggests that the coculture with THP-1 induced some disruption in the Caco-2 monolayers. A conditioned medium of the THP-1 cells gave similar results. This disruption was significantly suppressed by adding the anti-TNF- α antibody to the medium, suggesting that TNF- α secreted from THP-1 caused damage to the Caco-2 cells. It is also seems that this phenomenon is similar to that observed with inflammatory bowel disease (IBD). The effects of food factors on the cells in this coculture system were examined. The disruption of the Caco-2 cell monolayers was significantly reduced by adding caffeine to the medium which suppressed the secretion of TNF- α from the THP-1 cells. This model will be useful to study the inflammatory damage to cells in the intestinal epithelium such as IBD, and also the protective functions of food factors involved in this process

1. INTRODUCTION

Numerous studies on the function of food factors have been performed according to various systems for evaluation. Among these, two evaluation systems have mainly been used one involving a

monoculture cell line. Many food samples can be conveniently evaluated by using a culture cell line derived from various tissues, and the intracellular regulatory mechanism of food factors can also be investigated. However, real organisms are more complicated; for example, the food function against cell-to-cell interaction via soluble factors cannot be evaluated. On the other hand, studies using animal models have also been conducted and enable the *in vivo* effect of food factors to be examined. However, it is ethically difficult to examine many food samples in screening experiments on animals, while it is also difficult to reveal the regulatory mechanism of food factors at the cellular level.

On the basis of these phenomena, we focused on an *in vitro* coculture system as a new method for evaluating food factors. This coculture system enabled us to examine the food function for the interaction between different types of cells via soluble factors. Previous studies using a coculture system have reported the interaction between endothelial cells and astrocytes (Dehouck et al., 1994; Fillebeen et al., 1999), as a blood-brain barrier model, and between intestinal epithelial cells and immune cells (Kerneis et al., 1997; Cario et al., 1999). We have previously reported the interaction between Caco-2 cells as a model of human intestinal epithelial cells, and PC12 cells as a model of neuronal cells (Satsu et al., 2001; 2003).

We focused this study on the intestinal immune system, involving the interaction between intestinal epithelial cells and immune cells, and established a new coculture system to examine the cell-to-cell interaction between intestinal epithelial cells and macrophages. The Caco-2 cell line was used as a model for intestinal epithelial cells, and human macrophage/monocyte-like THP-1 cells as a model for macrophages.

2. METHODS AND MATERIALS

2.1 Materials

The Caco-2 cell line was obtained from American Type Culture Collection (Rockville, MD, U.S.A.), and THP-1 cells were purchased from Health Science Research Resources Bank (Osaka, Japan). Dulbecco's modified Eagle's medium (DMEM) was purchased from Nissui Pharmaceuticals (Tokyo, Japan), and fetal calf serum (FCS) was from Sigma (St. Louis, MO, U.S.A.). Non-essential amino acids (NEAA) were purchased from Cosmobio (Tokyo, Japan). Recombinant human TNF- α , recombinant human IFN- γ , recombinant human IL-1 β and recombinant human IL-6 were all purchased from Peprotech

(London, U.K.). Recombinant human IL-8, and biotinylated polyclonal antibodies against human TNF- α , IFN- γ , IL-1 β , IL-6, and IL-8 were from Genzyme Techne (Cambridge, MA, U.S.A.).

2.2 Cell culture

Caco-2 cells were cultured with a medium consisting of DMEM supplemented with 10% FCS, 1% non-essential amino acids, 2% glutamine, 100 U/ml of penicillin, 100 μ g/ml of streptomycin and an appropriate amount of sodium bicarbonate as described previously (Satsu et al., 1997). The cells were incubated at 37°C under a humidified atmosphere of 5% CO₂ in air. The coculture experiments used Caco-2 cells cultured in 12-well cell culture inserts on a semipermeable support membrane (Corning Costar, NY, U.S.A.) that had been precoated with collagen at a density of 1 x 10⁵ cells/ insert. The cell monolayers for the coculture experiments were used after 14 days of culture. THP-1 cells were cultured with a medium consisting of DMEM, 10% FCS, 2% glutamine, 100 U/ml of penicillin, 100 μ g/ml of streptomycin and an appropriate amount of sodium bicarbonate. The THP-1 cells were seeded in a 12-well plate at a density of 3 x 10⁵ cells/well and treated with 200 nM PMA for 4 days to differentiation for subsequent use in the coculture experiment.

2.3 Determination of cell damage to the Caco-2 cell monolayers

The tight junction permeability of the Caco-2 cell monolayer was evaluated by measuring the transepithelial electrical resistance (TER) value. The TER value was measured with a Millicell ERS instrument (Millipore, Bedford, MA, U.S.A.). The viability of the cells was assessed by their ability to maintain lactate dehydrogenase (LDH) inside the cells as measured by an LDH-cytotoxic test kit (Wako, Osaka, Japan).

2.4 Measurement of the cytokine secretion from THP-1 cells

THP-1 cells were cultured with or without 200 nM PMA for 2 days. Each culture medium was collected, and the IL-8, TNF- α , IL-1 β and IFN- γ levels were determined by an enzyme-linked immuno-sorbent assay (ELISA) as previously described (Son et al., 2004).

3. RESULTS AND DISCUSSION

A schematic diagram and the representation of the *in vitro* coculture system used in this study are shown in Fig. 1. The two different types of cell used with this method were not in contact with each other, enabling the cross talk to be observed between the two types of cell via the soluble factors secreted from each cell line.

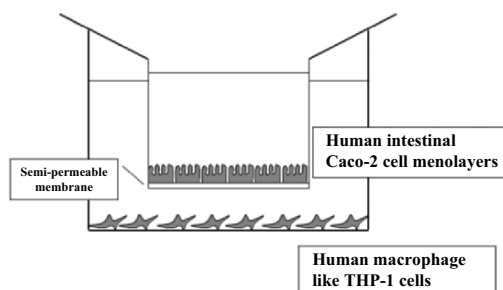


Figure 1. Caco-2 cells were cultured in 12-well cell culture inserts on a semi-permeable support membrane precoated with type-I collagen and formed a monolayer of non-overlapping and contact-inhibited cells. THP-1 cells were cultured on 12-well culture plates in the presence of PMA for 4 days, before the cell culture inserts in which the Caco-2 cells had been cultured were placed in these wells.

Coculturing the Caco-2 monolayers with THP-1 cells induced cell damage to the Caco-2 cell monolayers (Fig. 2). A time-dependent effect was observed: after coculturing for 24 hours, the TER value was 69.1% of the control value, and LDH released from the Caco-2 cell monolayers was 81.9% of the control value, while after coculturing for 48 hours, the TER value had decreased further to 18.8% of the control value, but LDH release had increased to 251% of the control value. These results suggest that the Caco-2 cell monolayers had been damaged by coculturing the macrophage-like THP-1 cells. We next investigated whether the conditioned medium of THP-1 cells could reproduce the phenomena from the coculture with THP-1 cells. Caco-2 cell monolayers cultured in semipermeable membrane inserts were incubated with the conditioned medium prepared from THP-1 for 48 hours. As a result, the conditioned medium of THP-1 cells reproduced the damage to the Caco-2 cell monolayers (data not shown). We studied the effect of the heat-treated conditioned medium on the damage to the Caco-2 cell monolayers. The heat-treated conditioned medium, which had been boiled at 100°C for 10 min, did not increase the LDH release from the Caco-2 cell monolayers. This result suggests that the active factor in the conditioned medium that induced cell damage to the Caco-2 monolayers was unstable under heating, such as a protein would be.

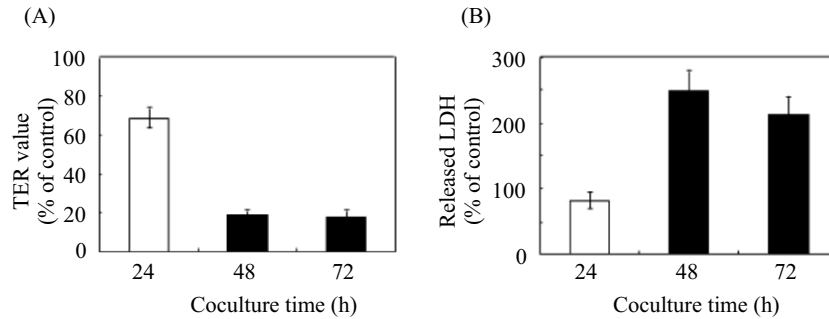


Figure 2. Effect of coculturing with THP-1 cells on the TER value (A) and the LDH release (B) of the Caco-2 cell monolayers. Caco-2 cells were cocultured with or without THP-1 cells for 24, 48, and 72 hours. After being cocultured, the LDH release and TER value of the Caco-2 cell monolayers were measured as described in the Materials and Methods section. Each value is presented as the mean \pm S.E. (n=6).

We focused on the secreted proteins, especially cytokines, to identify the soluble active factor. The secretion of several cytokines was measured by using the sandwich-ELISA method, the secretion of IL-1 β , IL-6, IL-8, and TNF- α from the THP-1 cells being observed. We then studied the effect on THP-1-induced damage to the Caco-2 cell monolayers of neutralizing the antibody against these cytokines. Neutralizing the antibody against IL-1 β had no significant effect on the THP-1-induced damage to the Caco-2 cell monolayers. Neutralizing the antibody against IL-6 and IL-8 also had no significant effect on this THP-1-induced cell damage. However, neutralizing the antibody against TNF- α almost completely suppressed the LDH release from the Caco-2 monolayers (Fig. 3), suggesting that TNF- α was the active factor secreted from the THP-1 cells that induced damage to the Caco-2 cell monolayers. It was also revealed that exposure of the Caco-2 cell monolayers to TNF- α significantly increased the LDH release (data not shown). This result strengthens the supposition that damage to the Caco-2 cell monolayers had been caused by TNF- α secreted from THP-1 cells.

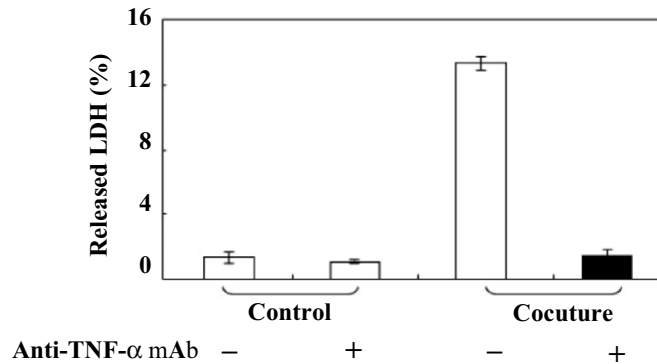


Figure 3. Neutralization of the THP-1-induced increase in LDH release from Caco-2 cell monolayers by the anti-TNF- α antibody. Caco-2 cells were cocultured with THP-1 cells in the presence or absence of the anti-TNF- α antibody (3.2 μ g/ml). After coculturing for 48 hours, the LDH release by the Caco-2 cell monolayers was measured as described in the Materials and Methods section. Each value is presented as the mean \pm S.E. (n=6).

We next examined the effect of one drug used to treat IBD on the damage to Caco-2 cell monolayers by THP-1 cells. The effect of 5-amino salicylic acid (5-ASA), one of the major orally taken drugs for treating IBD, was studied on this occasion. 5-ASA added to both sides of the membrane significantly suppressed the increased LDH release by THP-1 cells (data not shown), indicating that 5-ASA suppressed THP-1-induced damage to the Caco-2 cell monolayers. This result suggests that this coculture system may be a convenient *in vitro* model to screen the factors for suppressing IBD.

We further examined the suppressive effect of food factors on the THP-1-induced damage to Caco-2 cell monolayers. Various food substances were tested, although we focused on caffeine. Adding caffeine to the medium on either the apical or basal side significantly suppressed the increased LDH release from the Caco-2 cell monolayers by coculturing with THP-1 cells (Fig. 4). The effect of caffeine on the secretion of TNF- α from THP-1 cells was further examined to reveal the regulatory mechanism. The secretion of TNF- α from THP-1 cells was significantly decreased by caffeine (data not shown), suggesting that caffeine suppressed the damage to Caco-2 cell monolayers by inhibiting the secretion of TNF- α from the THP-1 cells.

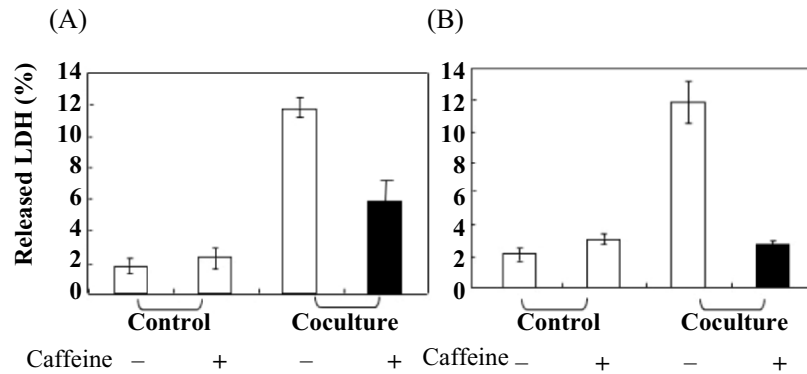


Figure 4. Suppressive effect of caffeine on THP-1-induced increase in LDH release from the Caco-2 cell monolayers. Caco-2 cells were cocultured with THP-1 cells in the presence or absence of 10 mM caffeine on the apical (A) or basolateral (B) side. After coculturing for 48 hours, the LDH release by the Caco-2 cell monolayers was measured as described in the Materials and Methods section. Each value is presented as the mean \pm S.E. (n=6).

We constructed in the present study an *in vitro* coculture system between human intestinal Caco-2 cell monolayers and human macrophage-like THP-1 cells. Coculture with THP-1 cells induced damage to the Caco-2 cell monolayers by TNF- α . Adding the anti-TNF- α antibody completely blocked this cell damage. The addition of 5-ASA, an orally taken drug used to treat IBD, also reduced damage to the Caco-2 cell monolayers, while caffeine, among the food substances tested, suppressed the THP-1-induced cell damage by inhibiting the secretion of TNF- α from THP-1 cells.

One of the most important functions of the human intestines is as a barrier against foreign substances like bacteria and chemicals. In this intestinal immune system, immune cells such as macrophages located in the intestinal epithelium interact with epithelial cells via soluble factors. Any disorder of this interaction causes defective overproduction of some inflammatory cytokines and subsequent mucosal inflammation; for example, IBDs such as Crohn's disease (CD) and ulcerative colitis (UC).

Several function of human intestinal epithelial cells have been reported, including the absorption of nutrients and the barrier function against xenobiotics like pathogenic bacteria or chemical substances. The intestinal immune system involves immune cells such as macrophages located beneath the intestinal epithelial monolayer interacting with epithelial cells via soluble factors. However, under inflammatory

conditions, several inflammatory cytokines are overproduced by immune cells after the intestinal epithelial monolayers have been disrupted.

Although this coculture system is likely to be artificial, it is thought that it may represent an intestinal inflammatory condition such as inflammatory bowel disease (IBD). High-level expression of inflammatory cytokines has commonly been observed in the intestinal epithelium of IBD patients (Stallmach et al., 2004). Furthermore, the administration of the anti-TNF- α antibody, Infliximab, is now being used as a new treatment for IBD (Baert et al., 1999). We therefore examined whether this coculture system could be used as an *in vitro* model of IBD or not. The addition of the anti-TNF- α antibody and 5-ASA significantly reduced the damage to Caco-2 cell monolayers in this study (Fig. 3). These results suggest that this *in vitro* coculture system may at least partly represent intestinal inflammation.

Among the various food factors tested, caffeine significantly suppressed the THP-1-induced damage to Caco-2 cell monolayers as shown in Fig. 4. It is well known that caffeine is contained in such beverages as tea and coffee. Many studies have reported the function of caffeine, and it is also known to inhibit the secretion of TNF- α (van Furth et al., 1995). Our present study shows that caffeine reduced the secretion of TNF- α from THP-1 cells, after suppressing damage to the Caco-2 cell monolayers (Fig. 4). This result suggests caffeine as a candidate for preventing or improving intestinal inflammation. We are now planning a study on the *in vivo* effect of caffeine that uses animal models for intestinal inflammation by a DSS or TNBS treatment.

It is our hope that this coculture system of Caco-2 cells and THP-1 cells may provide a good model of such intestinal inflammation as IBD, and that it will be used to search for effective food factors to treat or prevent intestinal inflammation.

4. ACKNOWLEDGEMENTS

This study was partially supported by grant-aid for Creative Scientific Research by the Japan Society for the Promotion of Science (No.13GS0015). This work was also partially supported by the research grants from the Skylark Food Science Institute and from Kampou Science Foundation.

5. REFERENCES

- Baert FJ, D'Haens GR, Peeters M, Hiele MI, Schaible TF, Shealy D, Geboes K, and Rutgeerts PJ (1999) Tumor necrosis factor alpha antibody (infliximab) therapy profoundly down-regulates the inflammation in Crohn's ileocolitis. *Gastroenterology*. 116(1): 22-28.
- Cario E, Becker A, Sturm A, Goebell H, and Dignass AU (1999) Peripheral blood mononuclear cells promote intestinal epithelial restitution in vitro through an interleukin-2/interferon-gamma-dependent pathway. *Scand. J. Gastroenterol.* 34: 1132-1138.
- Dehouck B, Dehouck MP, Fruchart JC and Cecchelli, R (1994) Upregulation of the low density lipoprotein receptor at the blood-brain barrier: intercommunications between brain capillary endothelial cells and astrocytes. *J. Cell Biol.* 126: 465-473.
- Fillebeen C, Dehouck B, Benaissa M, Dhennin-Duthille I, Cecchelle I, Cecchelli R and Pierce A (1999) Tumor necrosis factor-alpha increases lactoferrin transcytosis through the blood-brain barrier. *J Neurochem* 73: 2491-2500.
- van Furth AM, Seijmonsbergen EM, Langermans JA, van der Meide PH, van Furth R (1995) Effect of xanthine derivatives and dexamethasone on *Streptococcus pneumoniae*-stimulated production of tumor necrosis factor alpha, interleukin-1 beta (IL-1 beta), and IL-10 by human leukocytes. *Clin Diagn Lab Immunol.* 2(6): 689-692.
- Kerneis S, Bogdanova A, Kraehenbuhl JP, and Pringault E (1997) Conversion by Peyer's patch lymphocytes of human enterocytes into M cells that transport bacteria. *Science* 277: 949-952.
- Satsu H, Watanabe H, Arai S, and Shimizu M (1997) Characterization and regulation of taurine transport in human intestinal cell. Caco-2. *J. Biochem.* 121(6):1082-1087.
- Satsu H, Yokoyama T, Ogawa N, Fujiwara-Hatano Y, and Shimizu M (2001) The changes in the neuronal PC12 and the intestinal epithelial Caco-2 cells during the coculture -The functional analysis using in vitro coculture system-. *Cytotechnology* 35: 73-79.
- Satsu H, Yokoyama T, Ogawa N, Fujiwara-Hatano Y, and Shimizu M (2003) The effect of neuronal PC12 cells on the functional properties of intestinal epithelial Caco-2 cells. *Biosci. Biotech. Biochem.* 67(6): 1312-1318.
- Son D-O, Satsu H, Kiso Y, and Shimizu M (2004) Characterization of the carnosine uptake and its physiological function in human intestinal epithelial Caco-2 cells. *Biofactors*, 21(1-4): 395-398.
- Stallmach A, Giese T, Schmidt C, Ludwig B, Mueller-Molaian I, Meuer SC (2004) Cytokine/chemokine transcript profiles reflect mucosal inflammation in Crohn's disease. *Int J Colorectal Dis.* 19(4): 308-315.

GENERATION OF AN INDUSTRIALLY IDEAL HOST CELL LINE FOR PRODUCING COMPLETELY-DEFUCOSYLATED ANTIBODY WITH ENHANCED ANTIBODY-DEPENDENT CELLULAR CYTOTOXICITY (ADCC)

Mitsuo Satoh, Naoko Yamane-Ohnuki, Katsuhiko Mori, Ripei Niwa, Toyohide Shinkawa, Harue Imai, Reiko Kuni-Kamochi, Ryosuke Nakano, Kazuya Yamano, Yutaka Kanda, Shigeru Iida, Kazuhisa Uchida, Kenya Shitara

Tokyo Research Laboratories, Kyowa Hakko Kogyo Co., Ltd., 3-6-6 Asahi-machi, Machida-shi, Tokyo 194-8533, Japan

Abstract: To generate industrially applicable new host cell lines for antibody production with optimizing antibody-dependent cellular cytotoxicity (ADCC) we focused on the most important carbohydrate structure “fucose residues attached to the innermost GlcNAc residue of N-linked oligosaccharides via α -1,6 linkage” (Shields, 2002; Shinkawa, 2003), and succeeded in disrupting both *FUT8* (α -1,6-fucosyltransferase gene) alleles in Chinese hamster ovary (CHO) cell line by sequential homologous recombination. *FUT8*^{-/-} cell lines have morphology and growth kinetics similar to those of the parent. Antibodies produced by the engineered CHO cell lines strongly bound to human Fc γ receptor IIIa (Fc γ RIIIa) and showed approximately two orders of magnitude higher ADCC than anti-CD20 antibodies (RituxanTM) produced by parental cell lines without changing antigen-binding and complement-dependent cytotoxicity (CDC). Moreover, the engineered cell line remains stable, producing completely-defucosylated antibody with fixed quality and efficacy even in serum-free fed-batch culture. Thus, our approaches provide a new strategy for controlling the glycosylation profile of therapeutic recombinant proteins and could be a considerable advantage for the manufacture of glycoprotein therapeutics, especially antibodies.

Key words: recombinant antibody production; antibody-dependent cellular cytotoxicity (ADCC); α -1,6-fucosylation; *FUT8*; siRNA; knockout; fed-batch culture; Chinese hamster ovary (CHO) cells

Introduction

Monoclonal recombinant antibodies IgG, having two N-linked oligosaccharides in the Fc, are commonly used therapeutically. The general structure of IgG N-linked oligosaccharide is complex-type, characterized by a mannosyl-chitobiose core with or without bisecting N-acetylglucosamine (GlcNAc)/L-fucose and other chain variants including the presence or absence of galactose and sialic acid. Although the nature and importance of the oligosaccharides in influencing antibody effector functions was long unrecognized (Ripka, 1986; Kumpel, 1995; Jefferis, 1998; Umana, 1999a; Davies, 2001), the most important carbohydrate structure on antibody-dependent cellular cytotoxicity (ADCC) has just recently been found to be fucose residues attached to the innermost GlcNAc residue of N-linked oligosaccharides via α -1,6 linkage (Nanai, 2000; Shields, 2002; Shinkawa, 2003).

ADCC, a lytic attack on antibody-targeted cells, is triggered after binding of lymphocyte receptors (Fc γ Rs) to the antibody constant region (Fc), and is largely dependent on the Fc oligosaccharide structure. Clinical studies have shown that antibody effector functions, especially ADCC, are very important for clinical efficacy (Lewis, 1993; Clynes, 2000). Patients, suffering Non-Hodgkin's lymphoma, having the Fc γ RIIIa allotype with higher affinity to anti-CD20 IgG1 (RituxanTM) showed the better clinical response than patients with another allotype (Carlton, 2002). Breast cancer patients with complete or partial remission treating with anti-Her2 IgG1 (HerceptinTM) were found to have a higher capability to mediate *in vitro* ADCC of HerceptinTM (Gennari, 2004). Recently, we demonstrated that ADCC is almost solely controlled by the absence of fucose on IgG1, and that galactose and bisecting GlcNAc contribute little or nothing to ADCC (Hanai, 2000; Shinkawa, 2003). Shields *et al.* confirmed this observation (Shields, 2002). Defucosylated RituxanTM shows over 50-fold greater ADCC compared to fucosylated RituxanTM and defucosylated HerceptinTM shows enhanced ADCC with improved Fc γ RIIIa binding. There is no need to concern the immunogenicity of defucosylated form IgG since it is a normal component of natural human serum IgG (Mizuochi, 1982; Harada, 1987). Thus, IgG1 defucosylation is a powerful and elegant mechanism to improve antibody effector function.

In this review, we describe technologies for recombinant antibody production of biologically-active defucosylated form with enhanced ADCC from several aspects, *i.e.*, useful host cell lines, robustness of production processes, and conversion of established antibody-producing cells. Finally, an industrially-ideal production system for completely-defucosylated therapeutic antibody and its impacts on therapeutic fields are discussed.

Antibody has an unusual structure as glycoprotein

In a general concept, carbohydrates on glycoproteins appear to cover their protein portion just like a cachet. However, the carbohydrates play multiple roles, including not only presentation of binding motifs for lectins and/or protection from proteolytic degradation but also stability of the glycoprotein by directly interacting with polypeptide (Wormald and Dwek, 1999; van Zuylen, 1997). The oligosaccharide of IgG is linked to Asn297 in the Fc region where Fc γ RIIIa expressed on effector cells such as natural killer cells binds to. The Asn297-linked oligosaccharide contains a mannosyl-chitobiose core (Man₃-GlcNAc₂), to which fucose, GlcNAc, galactose, mannose, and/or sialic acid are attached (Fig. 1). The crystal structure of IgG Fc region shows that the two oligosaccharides occupy the space between the CH2 domains and extensively contact with the polypeptides (Huber, 1976). Although there is no direct interaction of the carbohydrate with Fc γ R, complete removal of the Asn297-linked oligosaccharides

extinguishes IgG binding to Fc γ Rs, resulting in loss of ADCC (Tao and Morrison, 1989; Radaev, 2001). The unique IgG structure, the location of carbohydrates within protein portion, affects the structure of Fc region and causes the change of antibody effector function ADCC. The antibody defucosylation could contribute to conformational change of the CH2 region to enhance Fc γ RIIIa binding (Okazaki, 2004).

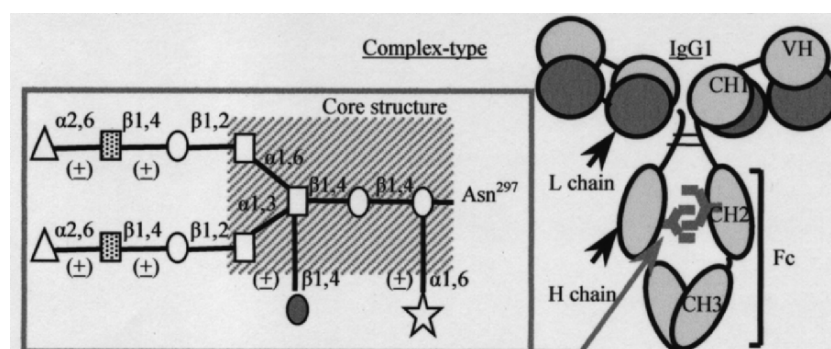


Fig. 1. Oligosaccharide structure of IgG1. Complex-type N-linked oligosaccharide (consists of GlcNAc (○), mannose (□), bisecting GlcNAc (●), fucose (★), galactose (■), sialic acid (Δ)) is attached to the CH2 domains of Fc region IgG1.

Defucosylated antibody production

Recombinant protein expression technology in mammalian cell culture is the principal means of commercial production of therapeutic antibodies; indeed, all approved therapeutic recombinant antibodies are produced using mammalian cells such as Chinese hamster ovary (CHO) and mouse myeloma host cell lines (Table 1). Robust antibody production processes using these host cell lines have been developed. These processes are proven to produce safe and effective antibody molecules with serum half-lives equivalent to those observed for naturally-occurring antibodies. However, it is still remained to be solved to control the oligosaccharide structure of the products to maintain product consistency with desired efficacy because the majority of the recombinant antibody generated by mammalian cells is known to be fucosylated (Kamoda, 2004). A strategy for consistently-regulating recombinant product oligosaccharide structure in mammalian cell culture could be a considerable advantage for the manufacture of therapeutic antibodies. Currently, the methods for generating defucosylated antibody are classified into three categories according to the targeting level of defucosylation (Table 2).

In mammals, almost all antibody fucose residues are attached to the innermost GlcNAc residue of N-linked oligosaccharides via an α-1,6 linkage (Miyoshi, 1999). α-1,6-fucosyltransferase catalyzes the transfer of fucose from GDP-fucose to the GlcNAc residue in an α-1,6 linkage in the medial Golgi cisternae. *FUT8* encodes an α-1,6-fucosyltransferase gene, and no isoforms have yet been cloned (Uozumi N, 1996). To control the fucosylation of recombinant antibody produced by mammalian cells, *FUT8* activity has to be modified somehow. Historically, we had to focus on unique cell line, such as rat hybridoma YB2/0, with reduced intrinsic fucosylation activity (Hanai, 2000). YB2/0 cells, which produce relatively-highly defucosylated (30-50%)

recombinant antibodies, express a more than 10-fold lower level of *FUT8* transcripts than CHO cells, and overexpression of *FUT8* in YB2/0 cells rescues its α -1,6 fucosylation activity rendering it equivalent to that of CHO cells (~10% defucosylated) (Shinkawa, 2003). In the 1st generation there were limitations of defucosylated level of the products and host cells available. Next, the methods for converting host cell lines or normal antibody-producing cells to more desirable cell lines that have ability to produce 60-90% defucosylated antibody were developed using *Lens culinaris agglutinin* (LCA)-resistant clones or small interfering RNA (siRNA) against *FUT8* (Kanda, 2002; Shields, 2002; Mori, 2004). The *FUT8* siRNA-introduced cells that show resistancy to LCA, which recognizes the α -1,6 fucosylated trimannose-core structure of N-linked oligosaccharides, can produce the high-ADCC antibody with the oligosaccharide structure equivalent to the parental one except for the fucose content. Defucosylation level of the product by the siRNA-introduced cells reaches to approximately 60% and stably lasts at the end of serum-free fed-batch culture, which is very important from an industrial application standpoint because manufacture processes must guarantee fixed product properties. Manufacture of a recombinant antibody with structure-desired and consistent carbohydrates is necessary for keeping and controlling therapeutical activity i.e. ADCC of the ingredients.

As an alternative method, overexpression of β -1,4-acetylglucosaminyltransferase III (GnTIII) is reported to indirectly lead to defucosylation of produced antibody with increased bisecting GlcNAc of the oligosaccharide by Dr. Umana (GlycArt Biotechnology AG) in this symposium. The mechanism for the defucosylation induced by GnTIII-overexpression, however, is still remained to be solved because there are some exceptions in which GnTIII hyper-expressing transformed cells mainly produce fucosylated products (Ohno, 1992; Umana, 1999a,b; Davies, 2001; Shinkawa, 2003) and the increase in the content of bisecting GlcNAc is not accompanied by the increase in defucosylation (Hard, 1992; Chen, 1998; Morelle, 2000).

Table 1. Recombinant therapeutic antibodies on the market USA

Product	Company	Type	Antigen	Indication	Host	Approval
ReoPro	Centocor/Lilly	Chimera	gpIIb/IIIa	Thrombosis	SP2/0	1994
Rituxan	IDEC/Genentech/Roche	Chimera	CD20	NHL	CHO	1997
Zenepax	Roche	Humanized	IL-2R	Transplantation	NS0	1997
Remicade	Centocor/J&J	Chimera	TNF α	RA, Cron's	SP2/0	1998
Synagis	MedImmune/Abott	Humanized	RSV	RSV Infection	NS0	1998
Simulect	Novartis	Humanized	IL-2R	Transplantation	SP2/0	1998
Herceptin	Genentech/Roche	Humanized	Her2	Breast Cancer	CHO	1998
Mylotarg	Celltech/AHP	Drug-conjugate	CD33	AML	NS0	2000
Campath	ILEX/Schering	Humanized	CD52	B-CLL	CHO	2001
Zevalin	IDEC/Schering	⁹⁰ Y-conjugate	CD20	NHL	CHO	2002
Humira	Abbott/CAT	Fully human	TNF α	RA	CHO	2002
Bexxar	Corixa/SKB	¹³¹ I-conjugate	CD20	NHL	CHO	2003
Xolair	Genentech/Novartis/Tanox	Humanized	IgE	Allergic asthma	CHO	2003

Table 2. Defucosylated antibody production methods

<p>1st Generation - Production of 30-50% fucose negative antibody</p> <ul style="list-style-type: none"> • Use cell lines with reduced intrinsic fucosylation activity
<p>2nd Generation – Production of 60-90% fucose negative antibody</p> <ul style="list-style-type: none"> • Generation of lectin-resistant cell lines, <i>FUT8</i> RNAi-introduced cell lines from host cells or antibody producing cells
<p>3rd Generation – Production of 100% fucose negative antibody</p> <ul style="list-style-type: none"> • Host cells that are incapable adding fucose, because of <i>FUT8</i> knock out.

An ideal host cell line for completely-defucosylated antibody

Ideally completely-defucosylated antibody should be supplied to patients as therapeutics simply because biological activity of antibody is largely dependent on the fucosylation level and completely-defucosylated antibody shows more potent efficacy both in vitro and in vivo (Niwa, 2004a,b). Industry cannot keep from taking into consideration that a stable supply of therapeutic antibody with uniformed and specified biological activity according to regulation. Production system in which the fucosylation ratios of the products vary in processes depending on the producing clones and/or the culture condition probably causes the fatal problem in terms of industrial application. For the purpose of stable supply of therapeutic antibody with defucosylation, complete and irreversible inactivation of *FUT8* function in producing cells is essential. Thus gene targeting, an extremely rare event in somatic cells (Hanson and Sedivy, 1995), is necessary in the cells employed for antibody production. We succeed in the targeted disruption of both *FUT8* alleles in host cells CHO/DG44 by homologous recombination to generate new cell lines for production of completely-defucosylated antibody (Yamane-Ohnuki, 2004). *FUT8*^{-/-} cell lines have morphology and growth kinetics similar to those of the parent. Antibodies produced by the engineered CHO cell lines strongly bound to human FcγRIIIa and showed approximately two orders of magnitude higher ADCC compared to parental antibody RituxanTM without change in antigen-binding and complement-dependent cytotoxicity (CDC) activities. Moreover, the engineered cell line remains stable, producing completely-defucosylated antibody with fixed quality and efficacy even in serum-free fed-batch culture. *FUT8*^{-/-} cell lines have the great advantage of providing uniformity to biopharmaceutical N-linked glycosylation. *FUT8*^{-/-} cell lines are expected to achieve both improved efficacy and reduction of dose and cost of therapeutic antibody. *FUT8*^{-/-} CHO/DG44 cell lines, the ideal host cells to stably produce high-ADCC therapeutic antibodies, are now available.

References

1. Cartron G, Dacheux L, Salles G, Solal-Celigny P, Bardos P, Colombat P and Watier H (2002) Therapeutic activity of humanized anti-CD20 monoclonal antibody and polymorphism in IgG Fc receptor Fc gamma RIIIa gene. *Blood*. 99: 754-758.
2. Chen YJ, Wing DR, Guile GR, Dwek RA, Harvey DJ and Zamze S (1998) Neutral N-glycans in adult rat brain tissue-complete characterisation reveals fucosylated hybrid and complex structures. *Eur. J. Biochem*. 251: 691-703.
3. Clynes RA, Towers TL, Presta LG and Ravetch JV (2000) Inhibitory Fc receptors modulate in vivo cytotoxicity against tumor targets. *Nat. Med*. 6: 443-446.
4. Davies J, Jiang L, Pan LZ, LaBarre MJ, Anderson D and Reff M (2001) Expression of GnTIII in a recombinant anti-CD20 CHO production cell line: Expression of

- antibodies with altered glycoforms leads to an increase in ADCC through higher affinity for FC gamma RIII. *Biotechnol. Bioeng.* 74: 288-294.
5. Gennari R, Menard S, Fagnoni F, Ponchio L, Scelsi M, Tagliabue E, Castiglioni F, Villani L, Magalotti C, Gibelli N, Oliviero B, Ballardini B, Prada GD, Zambelli A and Costa A (2004) Pilot study of the mechanism of action of preoperative Trastuzumab in patients with primary operable breast tumors overexpressing HER2. *Clin. Cancer Res.* 10: 5650-5655.
 6. Hanai N, Nakamura K, Shoji E, Yamasaki M, Uchida K, Shinkawa T, Imabeppu S, Kanda Y, Yamane N, and Anazawa H (2000) Method for controlling the activity of immunologically functional molecule. WO 00/61739.
 7. Hanson KD and Sedivy JM (1995) Analysis of biological selections for high-efficiency gene targeting. *Mol. Cell Biol.* 15: 45-51.
 8. Harada H, Kamei M, Tokumoto Y, Yui S, Koyama F, Kochibe N, Endo T and Kobata A (1987) Systematic fractionation of oligosaccharides of human immunoglobulin G by serial affinity chromatography on immobilized lectin columns. *Anal. Biochem.* 164: 374-381.
 9. Hard K, Damm JB, Spruijt MP, Bergwerff AA, Kamerling JP, van Dedem GW and Vliegthart JF (1992) The carbohydrate chains of the β subunit of human chorionic gonadotropin produced by the choriocarcinoma cell line BeWo. Novel O-linked and novel bisecting-GlcNAc-containing N-linked carbohydrates. *Eur. J. Biochem.* 205: 785-798.
 10. Huber R, Deisenhofer J and Colman PM (1976) Crystallographic structure studies of an IgG molecule and an Fc fragment. *Nature* 264: 415-420.
 11. Jefferis R, Lund J and Pound JD (1998) IgG-Fc-mediated effector functions: molecular definition of interaction sites for effector ligands and the role of glycosylation. *Immunol. Rev.* 163: 59-76.
 12. Kamoda S, Nomura C, Kinoshita M, Nishiura S, Ishikawa R, Kakehi K, Kawasaki N and Hayakawa T (2004) Profiling analysis of oligosaccharides in antibody pharmaceuticals by capillary electrophoresis. *J. Chromatogr. A.* 1050: 211-216.
 13. Kanda Y, Satoh M, Nakamura K, Uchida K, Shinkawa T, Yamane N, Hosaka E, Yamano K, Yamasaki M and Hanai N (2002) Cells producing antibody compositions. WO 02/31140.
 14. Kumpel BM, Wang Y, Griffiths HL, Hadley AG and Rook GA (1995) The biological activity of human monoclonal IgG anti-D is reduced by beta-galactosidase treatment. *Hum. Antib. Hybrid.* 6: 82-88.
 15. Lewis GD, Figari I, Fendly B, Wong WL, Carter P, Gorman C and Shepard HM (1993) Differential responses of human tumor cell lines to anti-p185HER2 monoclonal antibodies. *Cancer Immunol. Immunother.* 37: 255-263.
 16. Miyoshi E, Noda K, Yamaguchi Y, Inoue S, Ikeda Y, Wang W, Ko JH, Uozumi N, Li W and Taniguchi N (1999) The α 1,6fucosyltransferase and its biological significance. *Biochim. Biophys. Acta.* 1473: 9-20.
 17. Mizuochi T, Taniguchi T, Shimizu A and Kobata A (1982) Structural and numerical variations of the carbohydrate moiety of immunoglobulin G. *J. Immunol.* 129: 2016-2020.
 18. Morelle W, Haslam SM, Ziak M, Roth J, Morris HR and Dell A (2000) Characterization of the N-linked oligosaccharides of megalin (gp330) from rat kidney. *Glycobiology* 10, 295-304.
 19. Mori K, Kuni-Kamochi R, Yamane-Ohnuki N, Wakitani M, Yamano K, Imai H, Kanda Y, Niwa R, Iida S, Uchida K and Shitara K (2004) Engineering Chinese hamster ovary cells to maximize effector function of produced antibodies using *FUT8* siRNA. *Biotechnol. Bioeng.* 88: 901-908.

20. Niwa R, Shoji-Hosaka E, Sakurada M, Shinkawa T, Uchida K, Nakamura K, Matsushima K, Ueda R, Hanai N and Shitara K (2004a) Defucosylated chimeric anti-CC chemokine receptor 4 IgG1 with enhanced antibody-dependent cellular cytotoxicity shows potent therapeutic activity to T-cell leukemia and Lymphoma. *64*: 2127-2133.
21. Niwa R, Hatanaka S, Shoji-Hosaka E, Sakurada M, Kobayashi Y, Uehara A, Yokoi H, Nakamura K and Shitara K (2004b) Enhancement of the antibody-dependent cellular cytotoxicity of low-fucose IgG1 is independent of FcγRIIIa functional polymorphism. *Clin. Cancer Res.* 10: 6248-6255.
22. Ohno M, Nishikawa A, Koketsu M, Taga H, Endo Y, Hada T, Higashino K and Taniguchi N (1992) Enzymatic basis of sugar structures of α-fetoprotein in hepatoma and hepatoblastoma cell lines: correlation with activities of α-1,6-fucosyltransferase and N-acetylglucosaminyltransferase III and V. *51*: 315-317.
23. Okazaki A, Shoji-Hosaka E, Nakamura K, Wakitani M, Uchida K, Kakita S, Tsumoto K, Kumagai I and Shitara K (2004) Fucose depletion from human IgG1 oligosaccharide enhances binding enthalpy and association rate between IgG1 and FcγRIIIa. *J. Mol. Biol.* 336: 1239-1249.
24. Radaev S, Motyka S, Fridman W, Sautes-Fridman C and Sun PD (2001) The structure of a human type III Fcγ receptor in complex with Fc. *J. Biol. Chem.* 276: 16469-16477.
25. Ripka J, Adamany A and Stanley P (1986) Two Chinese hamster ovary glycosylation mutants affected in the conversion of GDP-mannose to GDP-fucose. *Biochem. Biophys. Arch.* 249: 533-545.
26. Shields RL, Lai J, Keck R, O'Connell LY, Hong K, Meng YG, Weikert SH and Presta LG (2002) Lack of fucose on human IgG1 N-linked oligosaccharide improves binding to human FcγRIII and antibody-dependent cellular toxicity. *J. Biol. Chem.* 277: 26733-26740.
27. Shinkawa T, Nakamura K, Yamane N, Shoji-Hosaka E, Kanda Y, Sakurada M, Uchida K, Anazawa H, Satoh M, Yamasaki M, Hanai N and Shitara K (2003) The absence of fucose but not the presence of galactose or bisecting N-acetylglucosamine of human IgG1 complex-type oligosaccharides shows the critical role of enhancing antibody-dependent cellular cytotoxicity. *J. Biol. Chem.* 278: 3466-3473.
28. Tao MH and Morrison SL (1989) Studies of aglycosylated chimeric mouse-human IgG. Role of carbohydrate in the structure and effector functions mediated by the human IgG constant region. *J. Immunol.* 143: 2595-2601.
29. Umana P, Jean-Mairet J, Moudry R, Amstutz H and Bailey JE (1999a) Engineered glycoforms of an antineuroblastoma IgG1 with optimized antibody-dependent cellular cytotoxic activity. *Nat. Biotechnol.* 17: 76-180.
30. Umana P, Jean-Mairet J, Moudry and Bailey JE (1999b) Tetracycline-regulated overexpression of glycosyltransferases in Chinese hamster ovary cells. *Biotechnol. Bioeng.* 65: 542-549.
31. Uozumi N, Yanagidani S, Miyoshi E, Ihara Y, Sakuma T, Gao CX, Teshima T, Fujii S, Shiba T and Taniguchi N (1996) Purification and cDNA cloning of porcine brain GDP-L-Fuc:N-acetyl-beta-D-glucosaminide α1,6fucosyltransferase. *J. Biol. Chem.* 271: 27810-27817.
32. van Zuylen CW, Kamerling JP, and Vliegthart JF (1997) Glycosylation beyond the Asn78-linked GlcNAc residues has a significant enhancing effect on the stability of the alpha subunit of human chorionic gonadotropin. *Biochem. Biophys. Res. Commun.* 232: 117-120.
33. Wormald MR and Dwek RA (1999) glycoproteins: glycan presentation and protein-fold stability. *Struc. Fold. Des.* 15: R115-R160.

34. Yamane-Ohnuki N, Kinoshita S, Inoue-Urakubo M, Kusunoki M, Iida S, Nakano R, Wakitani M, Niwa R, Sakurada M, Uchida K, Shitara K and Satoh M (2004) Establishment of FUT8 knockout chinese hamster ovary cells: an ideal host cell line for producing completely defucosylated antibody with enhanced antibody-dependent cellular cytotoxicity. *Biotechnol. Bioeng.* 87: 614-622.

THERMODYNAMIC AND KINETIC EFFECTS OF HUMAN IgG1 DEFUCOSYLATION ON IgG1-FC γ RIIIA INTERACTION

Akira Okazaki¹, Emi Shoji-Hosaka¹, Kazuyasu Nakamura¹, Masako Wakitani¹, Kazuhisa Uchida¹, Shingo Kakita¹, Kouhei Tsumoto², Izumi Kumagai² and Kenya Shitara¹

¹Tokyo Research Laboratories, Kyowa Hakko Kogyo Co., Ltd., 3-6-6 Asahi-machi, Machida-shi, Tokyo 194-8533, Japan; ²Department of Biomolecular Engineering, Graduate School of Engineering, Tohoku University, Aoba-yama 07, Aoba-ku, Sendai 980-8579, Japan

Abstract: Lack of fucose on human IgG1 oligosaccharide improves its affinity for Fc γ receptor IIIa (Fc γ RIIIa). To address the mechanisms of affinity improvement by the defucosylation, we used isothermal titration calorimetry (ITC) and biosensor analysis with surface plasmon resonance. ITC demonstrated that IgG1-Fc γ RIIIa binding was driven by favorable binding enthalpy (ΔH) but opposed by unfavorable binding entropy change (ΔS). Lack of fucose on IgG1 enhanced the favorable ΔH , leading to the increase in the binding constant of IgG1 for the receptor by a factor of 20 to 30. The increase in the affinity was mainly attributed to an enhanced association rate. A triple amino acid substitution in IgG1, S298A/E333A/K334A, is also known to improve IgG1 affinity for Fc γ RIIIa. ITC demonstrated that the amino acid substitution attenuated the unfavorable ΔS , resulting in a 3 to 4-fold increase in the binding constant. The affinity enhancement by the amino acid substitution was due to a reduced dissociation rate. These results indicate that the mechanism of affinity improvement by the defucosylation is quite distinct from that by the amino acid substitution. Defucosylated IgG1 exhibited higher antibody-dependent cellular cytotoxicity (ADCC) than S298A/E333A/K334A-IgG1, showing a correlation between IgG1 affinity for Fc γ RIIIa and ADCC.

Key words: Isothermal titration calorimetry, surface plasmon resonance, antibody-dependent cellular cytotoxicity

1. INTRODUCTION

The IgG oligosaccharide is linked to Asn297 in Fc region of IgG. IgG Fc region also binds to Fc γ receptors (Fc γ Rs) on the surface of immune cells. The crystal structure of IgG-Fc shows that the two oligosaccharides occupy the space between the CH2 domains and extensively contact with the polypeptides. Complete removal of the Asn297-linked oligosaccharides compromises IgG binding to Fc γ Rs, indicating that the oligosaccharides are involved in IgG binding to Fc γ Rs. Recently, a key role of fucose in IgG1 binding to Fc γ RIIIa and ADCC was demonstrated; lack of fucose from IgG1 improved the affinity for Fc γ RIIIa and ADCC [1,2]. Here, we investigated IgG1-Fc γ RIIIa interaction using isothermal titration calorimetry and surface plasmon resonance to explore the physicochemical basis for affinity improvement by the defucosylation [3]. The S298A/E333A/K334A-IgG1 that also exhibits improved affinity for Fc γ RIIIa [4] was analyzed in parallel to contrast the defucosylation with the amino acid substitution. Furthermore, we compared the enhancements of ADCC brought about by the defucosylation and the amino acid substitution to place these modifications in functional context.

2. MATERIALS AND METHODS

2.1 Recombinant proteins

The cDNAs that encode human Fc γ RIIIa(V¹⁵⁸) and Fc γ RIIIa(F¹⁵⁸) were subcloned into the *Eco*R I-*Bam*H I fragment of pKANTEX93 mammalian cell expression vector. The cDNA portion encoding transmembrane and intracellular domain was replaced by the DNA encoding His₆ tag, so that the resultant receptor protein ended at Gly175 followed by His₆ tag. The recombinant receptors were expressed in YB2/0 cells and purified from culture supernatant by Ni-NTA chromatography (QIAGEN, Valencia, CA). These recombinant proteins were termed sFc γ RIIIa(V¹⁵⁸) and sFc γ RIIIa(F¹⁵⁸).

Rituxan (chimeric mouse/human anti-CD20 IgG1 derived from a CHO cell line) was purchased from Genentech (South San Francisco, CA)/IDEC Pharmaceutical (San Diego, CA) and used as STD-IgG1 in this study. Defucosylated chimeric anti-CD20 IgG1 as dFu-IgG1 was prepared as described previously [2].

2.2 Isothermal Titration Calorimetry

Isothermal titration calorimetry measurements were carried out using a Microcal (Northampton, MA) VP-ITC instrument. IgG1 variants and sFc γ RIIIa were dialyzed against phosphate-buffered saline (PBS, 50 mM Na₂HPO₄, 150 mM NaCl, pH 7.4). sFc γ RIIIa solutions in an injection syringe (43 to 240 μ M) were injected into IgG1 solutions in a cell (2.7 to 16 μ M). The volume of each injection was 10 μ l. IgG1 and sFc γ RIIIa concentrations were determined by absorbance at 280 nm from molar extinction coefficients of 231000 and 38900 M⁻¹ cm⁻¹, respectively. Each titration was accompanied by a dilution-heat measurement in which sFc γ RIIIa was injected into PBS. All titration data were corrected for heat of dilution and analyzed with the software Origin (Microcal) using a single-site binding model. The *c* values were between 5 and 500 for all the measurements in this study.

2.3 Surface Plasmon Resonance

Kinetics of IgG1-sFc γ RIIIa interaction were measured using a BIAcore 2000 instrument and CM5 sensor chips (BIAcore, Uppsala, Sweden). Anti-Tetra His antibodies (QIAGEN) were immobilized onto the chip using amine coupling kit (BIAcore) following the manufacturer's instructions. sFc γ RIIIa was captured by the immobilized anti-His antibodies by injecting sFc γ RIIIa at a flow rate of 5 μ l/min. IgG1 was diluted in HBS-EP buffer (0.01 M HEPES, 0.15 M NaCl, 3 mM EDTA, 0.005% Surfactant P20, pH 7.4) at six different concentrations (from 4.17 nM to 133.3 nM) and each diluted IgG1 was injected over the receptor-captured sensor surface at a flow rate of 5 μ l/min. sFc γ RIIIa and IgG1 bound to the sensor surface were removed by injecting 7.5 mM HCl at a flow rate 10 μ l/min for 30 sec. The experiments were performed at 25°C with HBS-EP as running buffer. Buffer solution without IgG1 was injected over the receptor-captured sensor surface as a blank control. The data obtained by the injection of IgG1 were corrected for the blank control prior to data analysis.

3. RESULTS AND DISCUSSION

3.1 Three IgG1 variants

Three anti-CD20 antibodies were compared in this study: standard IgG1 with fucose and native amino acids (STD-IgG1), defucosylated IgG1 with native amino acids (dFu-IgG1), and S298A/E333A/K334A-

IgG1 with fucose (AAA-IgG1) (Figure 1). STD-IgG1 is equivalent to commercially available Rituxan, which is used in the treatment of non-Hodgkin lymphomas. Rituxan is produced by Chinese hamster ovary (CHO) cells. AAA-IgG1 was also produced by CHO cells whereas dFu-IgG1 was produced by rat hybridoma YB2/0 cells. The monosaccharide composition of STD-IgG1 was similar to that of AAA-IgG1; they had almost fully fucosylated oligosaccharides (Figure 1). By contrast, the fucose content of dFu-IgG1 was 4 % (Figure 1). Thus, STD-IgG1 and AAA-IgG1 are different in amino acid sequence (wild type versus S298A/E333A/K334A), while STD-IgG1 and dFu-IgG1 differ in oligosaccharide composition (mainly fucosylated versus defucosylated). ELISA format assay demonstrated that binding activities to CD20 were identical among these IgG1 variants (data not shown).

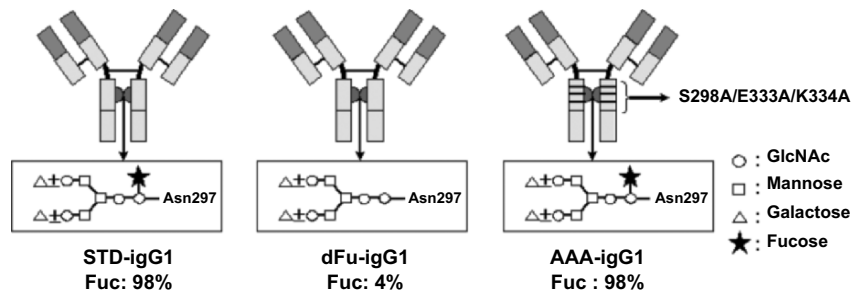


Figure 1. The three chimeric anti-CD20 IgG1s used in this study

3.2 Thermodynamics

The thermodynamic parameters at 15°C are summarized in Table 1. The number of sFcγRIIIa bound to an IgG1 molecule (N) was shown to be one. dFu-IgG1 had a 20 to 30 times higher binding constant for sFcγRIIIa than STD-IgG1, while AAA-IgG1 had a 3 to 4 times higher binding constant for sFcγRIIIa than STD-IgG1. IgG1-sFcγRIIIa binding was driven by favorable binding enthalpy (ΔH) but opposed by unfavorable binding entropy change (ΔS). IgG1-defucosylation improves its affinity for FcγRIIIa by enhancing the favorable ΔH , which contrasts markedly with the entropy-driven improvement of affinity by the amino acid substitution.

Table 1. Thermodynamic parameters for IgG1-sFcγRIIIa(V) interaction

IgG1	N	K_a ($\times 10^6$)	ΔG (kcal/mol)	ΔH (kcal/mol)	$-T\Delta S$ (kcal/mol/K)	ΔC_p (kcal/mol/K)
STD	1.1	1.87±0.07	-8.27±0.03	-20.1±0.5	11.8±0.4	-0.30±0.04
AAA	1.0	6.74±0.73	-9.00±0.06	-17.4±0.3	8.4±0.3	-0.33±0.04
dFu	1.0	58.3±11.3	-10.22±0.12	-26.1±0.7	15.8±0.8	-0.28±0.07

Favorable change in binding enthalpy generally indicates the increase in the non-covalent interactions, such as hydrogen bonds, van der Waals contacts, and salt bridges. Hence, the favorable change in ΔH brought about by the defucosylation suggests the increase in those non-covalent interactions in the complex.

3.3 Kinetics

The kinetic parameters for IgG1 variants-sFcγRIIIa interaction are shown in Table 2. The kinetic analysis demonstrates that the improvement of affinity by the defucosylation is mainly attributed to the enhanced association rate. On the other hand, the improvement by the amino acid substitution is attributed to the reduced dissociation rate.

Table 2. Kinetic parameters for IgG1-sFcγRIIIa(V) interaction

IgG1	k_{ass} ($\times 10^5 \text{ M}^{-1} \text{ s}^{-1}$)	k_{diss} ($\times 10^{-3} \text{ s}^{-1}$)
STD	0.34 ±0.24	7.10 ±0.08
AAA	0.51 ±0.08	4.66 ±0.51
dFu	3.26 ±0.01	6.64 ±0.03

A conformational change on binding is proposed to be a determinant of the association rate. This idea postulates conformational adaptation following the collision of proteins. For the conformational adaptation to proceed, the binding activation energy needs to be overcome. This process, instead of the frequency of collisions between the proteins, constitutes the rate-limiting step in association. The IgG1-FcγRIIIa binding may involve such conformational adaptation and the depletion of fucose could lower the binding activation energy, resulting in faster association.

3.4 ADCC

The ADCC assays of defucosylated IgG1 and S298A/E333A/K334A-IgG1 have been reported [1,2,4]. It was, however, unclear which modification led to greater enhancement of ADCC from the previous reports. In this study, we compared the ADCC activities of STD-IgG1, dFu-IgG1, and AAA-IgG1 to address the question. Two human B cell lymphoma cell lines expressing CD20 molecules, Raji and WIL-2S, were used as target cells. All IgG1 variants exhibited the same binding

activity to these B cell lines in flow cytometric analysis (data not shown). Human peripheral blood mononuclear cells (PBMCs) were used as effector cells. For both target cells, dFu-IgG1 had a greater ADCC activity than STD-IgG1 (Figure 2), indicating that lack of fucose on IgG1 leads to enhanced ADCC as demonstrated in the previous studies [1,2] The ADCC of AAA-IgG1 was in the middle between dFu-IgG1 and STD-IgG1 for both target cells (Figure 2). Thus, the ADCC of these IgG1 variants shows a good correlation with their affinity for Fc γ RIIIa.

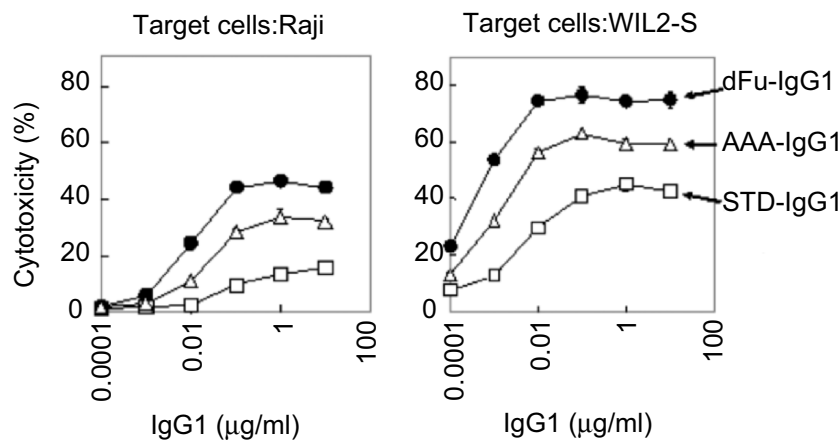


Figure 2. ADCC of the three IgG1s

3.5 Conclusions

Lack of fucose on human IgG1 oligosaccharide enhances binding enthalpy and association rate between IgG1 and Fc γ RIIIa. The structural basis for the affinity improvement by IgG-defucosylation is still an open question.

4. REFERENCES

1. Shields, R. L., Lai, J., Keck, R., O'Connell, L. Y., Hong, K., Meng, Y. G. *et al.* (2002). Lack of fucose on human IgG1 N-linked oligosaccharide improves binding to human Fc γ RIII and antibody-dependent cellular toxicity. *J. Biol. Chem.* 277, 26733-26740.
2. Shinkawa, T., Nakamura, K., Yamane, N., Shoji-Hosaka, E., Kanda, Y., Sakurada, M. *et al.* (2003). The absence of fucose but not the presence of galactose or bisecting N-acetylglucosamine of human IgG1 complex-type

- oligosaccharides shows the critical role of enhancing antibody-dependent cellular cytotoxicity. *J. Biol. Chem.* 278, 3466-3473.
3. Okazaki, A., Shoji-Hosaka, E., Nakamura, K., Wakitani, M., Uchida, K., Kakita, S. *et al.* (2004) Fucose Depletion from Human IgG1 Oligosaccharide Enhances Binding Enthalpy and Association Rate between IgG1 and Fc γ RIIIa. *J. Mol. Biol.* 336, 1239-1249.
 4. Shields, R. L., Namenuk, A. K., Hong, K., Meng, Y. G., Rae, J., Briggs, J. *et al.* (2001). High resolution mapping of the binding site on human IgG1 for Fc gamma RI, Fc gamma RII, Fc gamma RIII, and FcRn and design of IgG1 variants with improved binding to the Fc gamma R. *J. Biol. Chem.* 276, 6591-6604.

EXPRESSION OF RECOMBINANT PROTEIN IN CHO AND HeLa CELLS AND ITS FOLLOW-UP USING EGF REPORTER GENE

V. Hendrick¹, D. Ribeiro de Sousa¹, A.R. dos Santos Pedregal¹, C. Bassens¹, P. Rigaux¹, K. Sato², K. Kotarsky³ and J. Werenne¹

¹Laboratory of Animal Cell Biotechnology, Dept. of Bioengineering, Faculty of Sciences, Université Libre de Bruxelles, Belgium; ²Lund University, Lund, Sweden; ³Tokyo Institute of Technology, Tokyo, Japan.

Abstract: The goal of this paper was to evaluate the potentialities of using chimeric EGFP-Photinus Luciferase reporter gene to follow the expression of the fusion protein by following the fluorescence for the development of recombinant protein production process and to evaluate the conditions in which the use of butyrate stimulation of protein production is effective.

Key words: EGFP; Photinus Luciferase; reporter gene; fusion protein; fluorescence microscopy and photometry; Cytofluorimetry; Butyrate stimulation; CHO; HeLa.

1. INTRODUCTION

Chimeric EGFP-Photinus Luciferase reporter gene has been proposed to improve clone selection and high throughput screening both for CHO and HeLa cells. (K. Kotarsky *et al.* 2001 and 2003).

The construction used as described in the above cited paper is based on a fused gene using an AP-1 sensitive element which is an inducible system.

Both HeLa and CHO cells transfected in this way are known to be induced by ATP and Phorbol esters.

As butyrate has general but unpredictable enhancing properties on protein production, we used this fluorescent/luminescent system to establish the culture conditions required for its efficacy.

2. MATERIAL AND METHODS

HeLa cells and CHO cells, transfected and expressing EGFP and Luciferase (respectively HeLa/HF1 clone and CHO/pCFUSIII clone) were basically grown as described earlier (Kotarsky *et al.* 2001) in DMEM (Biowhitakker-Cambrex); they were also adapted to grow in spinner flasks (Techne 250 ml), in suspension using Bioprol medium (Biowhitakker-Cambrex), and on microcarriers (Cytodex3).

Cell fluorescence was studied by fluorescence microscopy, spectrofluorimetry and cytofluorimetry (FACSalibur, BD), and Luminescence was followed by standard luminometry (Turner Designs TD-20/20) using a Promega Kit system.

3. RESULTS

3.1 Emission spectrofluorimetry and fluorescence microscopy

It was shown (Fig. 1 and Fig. 2) that Butyrate induced fluorescence in both HeLa and CHO transfected cells; the enhancing effect is function of the concentration of the agent, 5 mM being the most active concentration used even if this concentration showed already some cytotoxic action in cells as we described previously for other recombinant protein production systems (V. Hendrick *et al.* 2001).

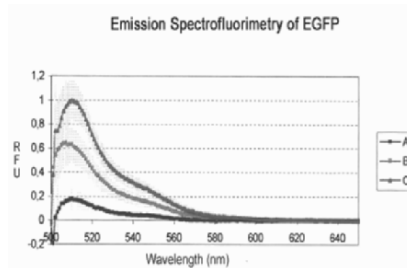


Figure 1. Fluorescence emission in HF1 cells. A – 1 mM butyrate ; B – 2 mM butyrate; C – 5 mM butyrate.

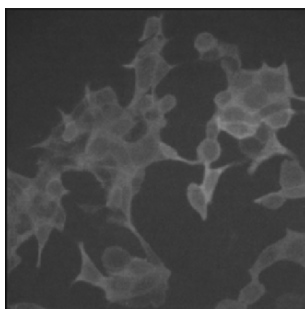


Figure 2. Fluorescence microscopy in HF1 at 5mM Butyrate

Under Butyrate treatment, fluorescence, and also luminescence (not shown) of transfected cells are enhanced in a dose dependant mode, as shown by the different methods used including Cytofluorimetry (data not shown).

3.2 Time course effect of Butyrate

By cytofluorimetry we showed that Butyrate (2mM) has a transitory activation action on fluorescence of the cells (Fig. 3).

The maximal effect is observed between 16 and 24 hours after addition of the inducing agent, indicating that a precise schedule of treatment will be necessary to improve significantly the process.

Both PMA (100nM) and ATP (0.5mM), known to enhance the EGFP fluorescence in transfected cells, exerted a synergistic action with 5mM Butyrate (respectively 4 x for PMA and 1.5 x for ATP).

The ATP presents its enhancing effect up to a saturation level in relation to its mode of action (Kotarsky *et al.* 2001).

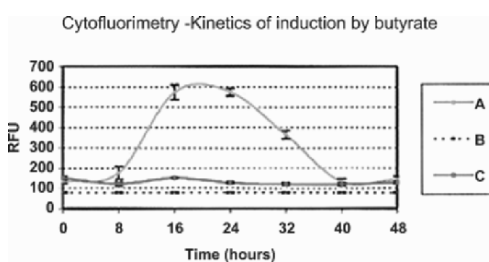


Figure 3. Kinetics of Butyrate induction in HF1 cells. (HF1 clone A : 530 nm; B : Parental HeLa; C : over 650 nm. With Butyrate (2mM)

3.3. Activation by Butyrate of protein expression in HF1 cells

Given the precise time course of the induction of EGFP expression, addition of Butyrate was operated during the culture (either with HF1 adapted to grow in suspension or in culture on microcarriers) was operated at different times of the growth for 16 hours, and the relative Fluorescence compared to a control was measured by Cytofluorimetry (Fig. 4 and 5).

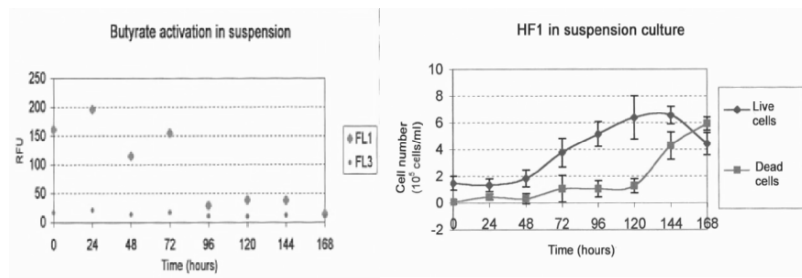


Figure 4. Effect of Butyrate 5 mM on HF1 in suspension

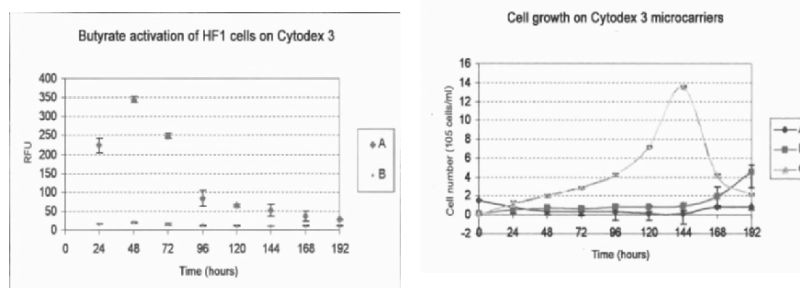


Figure 5. Effect of 5mM Butyrate on HF1 on microcarriers (A– Live cells in suspension; B – Dead cells in suspension; C – Live cells on microcarriers)

It is clear that in both suspension culture and in culture on microcarriers, Butyrate at the concentration of 5mM exerted a highly significant (respectively between 10 and 15 times), but only in the early phase of the growth curve, in both situation, the effect being negligible after 96-100 hours of culture.

4. CONCLUSIONS

Either in suspension or on microcarriers, it was shown that Butyrate enhanced the protein productivity only when added during the early phase of the culture.

We have observed in other systems, as for example the shift-down of temperature with tPA-producing CHO cells, a similar critical time in the cell growth curve above which cell productivity is not enhanced any more.

It appeared that a EGFP fused gene system, could be of interest in order to screen almost on line the productivity of a recombinant protein production.

This was applied with success in the present study for the follow up of the Butyrate action for which we showed that the interest as enhancer of recombinant protein production is limited by the time course of the action of the agent.

It is however of interest for situation in which the productivity is occurring in the early phase of growth

4. REFERENCES

- Hendrick, V., Winnepenninckx, P., Abdelkafi, C., Vandeputte, O., Cherlet, M., Marique, T., Renemann, G., Loa, A., Kretzmer, G. and Wérenne, J. (2001), Increased productivity of recombinant tissular plasminogen activator (tPA) by butyrate and shift of temperature : a cell cycle phase analysis, *Cytotechnology*, 36, 71-83.
- Kotarsky, K., Owman, C and Olde B. (2001), A chimeric reporter gene allowing for clone selection and high-Throughput screening of reporter gene cell lines expressing G-Protein-coupled receptors, *Analytical Biochemistry*, 288, 209-215.
- Kotarsky, K., Antonsson, L., Owman C., and Olde, B. (2003), Optimized reporter gene assays based on a synthetic multifunctional promoter and a secreted Luciferase, *Analytical Biochemistry*, 316, 208-215.

ELUCIDATING APOPTOTIC CELL DEATH IN CHO CELL BATCH & FED-BATCH CULTURES

Danny C.F. Wong,^{1,2} C. K. Danny C.F. Wong,^{1,2} C. K. Heng,² Kathy T.K. Wong,¹ Peter M. Nissom¹ & Miranda G.S. Yap¹

¹*Bioprocessing Technology Institute, Agency for Science and Technology Research (A*STAR), 20 Biopolis Way, #06-01, Centros, Singapore 138668;* ²*Department of Pediatrics, National University of Singapore, 10 Kent Ridge Crescent, Singapore 119260*

Abstract: Chinese Hamster Ovary (CHO) cells are regarded as one of the industrial ‘work-horses’ for complex biotherapeutics production. In these processes, loss in culture viability occurs primarily via apoptosis, a genetically controlled form of cellular suicide. By applying microarray technology using our ‘in-house’ developed CHO cDNA array and a mouse oligonucleotide array for time profile expression analysis, the genetic circuitry that regulates and executes apoptosis induction can be carried out rapidly. We found that in both batch and fed-batch cultures, receptor- and mitochondrial-mediated apoptosis pathways play important roles in apoptosis induction. There are also several other minor pro-apoptotic genes that appear to be upregulated during apoptosis induction in CHO cells. However, although these other genes had been implicated in apoptosis induction, their exact role in apoptosis induction has yet to be elucidated. By having a greater understanding of the regulatory circuitry of apoptosis relevant to cell culture processes, future effective strategies could be developed towards cell death prevention.

1. INTRODUCTION

In industrial batch culture processes, the major cause of viability loss is often nutrient depletion. Fed-batch culture offers a solution towards higher cell density and extended culture viability by addressing this issue through interval feeding of chemically defined culture medium concentrate. Despite nutrient feeding, fed-batch processes are still susceptible to viability loss but at a later time point compared to batch cultures. Therefore, either a critical unidentified nutrient is still missing and/or another insult is triggering cell death. Apoptosis, a genetically

controlled form of cellular suicide has been identified as the major mode of cell death in cell culture. Microarray technology could potentially allow for a better understanding of apoptosis induction in cell culture processes.

2. MATERIALS & METHODS

2.1 CHO Batch and Fed-Batch Cultures

Bioreactor set-up for CHO cell cultures were carried as previously described by Wong *et al.* [1].

2.2 Microarray

Even though CHO cells are the most widely used host for industrial production of recombinant proteins, little genetic information is available for these cells. Furthermore, there are no commercially available Chinese hamster microarray and its genome database is unavailable. Therefore, through a collaborative effort between the Bioprocessing Technology Institute, A*STAR (Singapore) and the Department of Chemical Engineering & Material Science from the University of Minnesota (USA), a CHO cDNA microarray had been constructed with over 5000 sequenced and annotated random transcripts (Version 1.0). Through this effort, we found that there is significant homology between chinese hamster and mouse sequences (65-95%). Therefore, a commercial mouse 65-mer oligonucleotide microarray consisting of approximately 8000 unique genes (Compugen) was used to further complement the CHO cDNA microarray for transcriptional profiling of batch and fed-batch CHO cell cultures.

2.3 RNA extraction, cDNA synthesis

Total RNA was extracted using Trizol reagent (Invitrogen). First strand cDNA probes using oligo-dT priming were then prepared using Superscript II reverse-transcriptase (Invitrogen). Labelling was then carried out using either Cy3 or Cy5 dyes (Amersham) whereby each sample was processed in triplicates consisting of 2 normal-dye labeling and 1 with reversed-dye labelling.

2.4 Hybridization

Hybridization of the probes on the slides was conducted in a manual hybridization chamber (Telechem) for 16 hrs at 42°C. Hybridized arrays were then washed and scanned using an ArrayWorx scanner (Applied Precision).

2.5 Data Normalization & Statistical Analysis

Intensity values data obtained from the scanner were uploaded to an in-house microarray data processing system (Microarray Discovery System). Data normalization, including scale normalization between the slides, was conducted using methods adapted from Yang *et al.*, 2002 [2].

3. RESULTS & DISCUSSIONS

Although fed-batch cultures allowed for higher viable cell densities and longer culture life compared to batch cultures, they are still susceptible to viability loss despite concentrated medium feeding (Figure 1). Consistent with findings by other researchers, viability loss in CHO cells during both batch and fed-batch occurred predominantly via apoptosis.

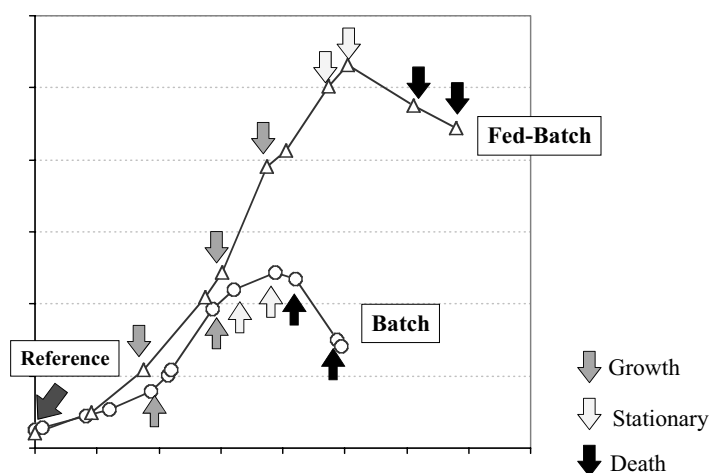


Figure 1. Representative sampling time points from CHO cell batch and fed-batch cultures during exponential growth, stationary and death phases. Time point 0 hr was used as the reference for all sample points.

Interestingly, despite the common notion that apoptosis induction especially via caspases were post-translationally regulated either through protein modification or protein-protein interactions, it was found that some of these changes could be observed transcriptionally. During periods of high viability, most pro-apoptotic genes were observed to be down-regulated but several early pro-apoptotic signaling genes were transcriptionally upregulated during early viability loss. At later stages of viability loss, we detected late pro-apoptotic effector genes such as caspases 3 and 10, DNases and scramblase being upregulated. This sequential upregulation of apoptotic genes showed that microarray could be used as a tool to study apoptotic mechanisms (Figure 2).

	Batch CHO Culture						Fed-Batch CHO Culture					
	Anti-Apoptosis	General	Receptor Signalling	Bcl-2 Family	Caspases	Hallmark Effectors	Anti-Apoptosis	General	Receptor Signalling	Bcl-2 Family	Caspases	Hallmark Effectors
Early Exponential to							Pde1c					Dffa Dnase1
Mid Exponential to	Birc4	Pde1a			Caspase 9		Pde1a	Fas			Caspase 11	Dffa Dnase1
Early Stationary to			Ripk1	Bcl2-like								
Late Stationary to												
Early Death to												
Late Death												

Figure 2. Differential apoptotic gene expression in batch and fed-batch cultures. Many pro-apoptotic genes appear to be up-regulated during the transition into stationary phase when culture viability starts to decrease. (Filtered genes shown here have differential expression of at least 2-fold and p-values <0.05)

It is commonly accepted that there are at least two major signaling pathways for the initiation of apoptosis: receptor mediated and mitochondrial mediated [3]. Based on transcriptional time profiling cDNA microarray experiments, we found that both of these pathways played a major role in apoptosis induction in CHO cells batch and fed-batch cultures (Figure 3).

In CHO cells, we found that apoptosis induction via the receptor-mediated pathway occurred via FADD, RipK1 and Daxx. It has been

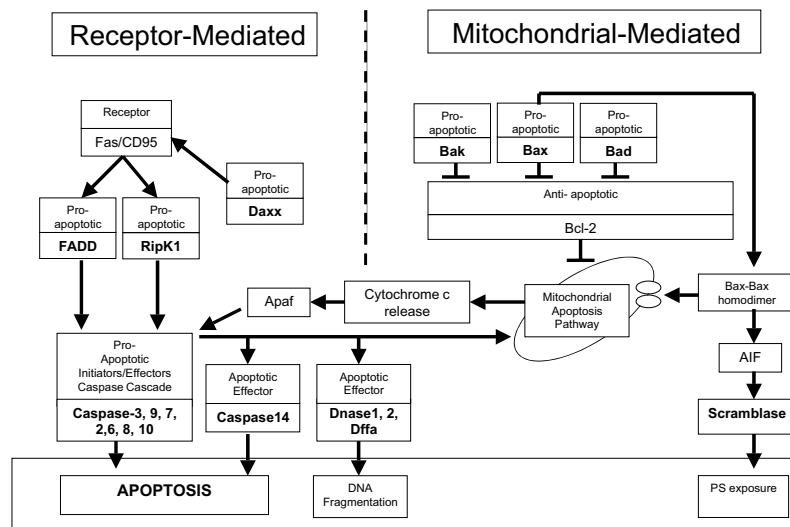


Figure 3. Summary of Receptor- and Mitochondrial-mediated apoptosis induction pathways observed in CHO cell culture.

shown that when a death receptor ligand binds to death receptors, it leads to ligation of preassociated CD95 death receptors [4]. This causes the formation of a death-inducing signaling complex in which Fas-associated death domain (FADD) and/or RipK1 adaptor proteins promote oligomerization and autocatalytic activation of caspase 8. Daxx then augments this signaling pathway further [5].

In the mitochondrial-mediated signaling pathway, it is the mitochondrial intermembrane proteins that play an important role. This signaling pathway is regulated by the interplay of pro-apoptotic and anti-apoptotic members of the Bcl-2 family, which are major regulators of apoptosis [6]. Although the exact mechanism(s) by which Bad, Bax and Bid induces apoptosis is still unclear, all four contained one or more BH3 domain. Bad only possess a short 9-16 amino acid BH3 domain but are otherwise unique while Bid and Bax contain two or three BH3 domains. The BH3 domain is required for binding to and neutralizing the activity of anti-apoptotic Bcl-2 family members.

There are also several other minor pro-apoptotic genes that appear to be upregulated during apoptosis induction in CHO cells. However, although these other genes had been implicated in apoptosis induction, their exact role in apoptosis induction has yet to be elucidated. Therefore, further characterization of these novel genes would provide further insights into the regulatory circuitry of apoptosis.

4. CONCLUSIONS & FUTURE WORK

In batch and fed-batch cultures, receptor- and mitochondrial-mediated apoptosis pathways both play important roles in apoptosis induction. Most interestingly, we found that although the apoptosis inducer(s) in batch and fed-batch cultures are likely to be different, the apoptotic pathways induced are very similar. The elucidation of these two pathways presented some interesting gene targets for apoptosis suppression in CHO cell culture processes. By considering both pathways for the design of future metabolic engineering efforts, we can potentially generate apoptosis resistant cell lines that can lead to significantly higher production yields.

5. REFERENCES

1. Wong D. C. F., Wong, Kathy T. K. Wong, K. M. Goh, L-T. Goh, C. K. Heng and Miranda G. S. Yap (2004) Impact of Dynamic Online Fed-batch Strategies on Metabolism, Productivity and N-Glycosylation Quality in CHO cell cultures. *Biotechnol Bioeng.* Accepted July 2004
2. Yang Y. H., Dubois S., Luu P., Lin D. M., Peng V., Ngai J. and Speed T. (2002). Normalization for cDNA microarray data: a robust composite method addressing single and multiple slide systematic variation. *Nucleic Acids Research*, 30(4), 1-10
3. Laken HA and Leonard MW. (2001) Understanding and modulation apoptosis in industrial cell culture. *Cur. Opinion. in Biotechnol.* 12:1/5-1/9
4. Peter ME and Krammer PH (2003) The CD95(APO-1/Fas) DISC and beyond. *Cell Death and Differentiation*, 10:26-35
5. Baker SJ and Reddy EP. (1998) Modulation of life and death by the TNF receptor superfamily. *Oncogene* 17:3261-3270
6. Strasser A. et al. (2000) Apoptosis signaling *Ann Rev Biochem.* 69:217-245

THE X-LINK INHIBITOR OF APOPTOSIS PROTEIN (XIAP) ENHANCES THE SURVIVABILITY OF C2E7 HYBRIDOMA CELLS UNDER A SERUM DEPRIVED CONDITION

B.T.Tey,^{1,3} K.C.Yap,¹ A. M. Ali,^{3,4} W.S. Tan^{2,3}

¹Department of Chemical Engineering, Faculty of Engineering; ²Department of Microbiology,

⁴Department of Molecular Biology, Faculty of Biotechnology and Molecular Science;

³Institute of Bioscience, Universiti Putra Malaysia, 43400 UPM Serdang, Selangor, Malaysia

Abstract: Hybridoma C₂E₇ cell cultured in a serum deprived condition was only survived not longer than 5 days in a batch culture, whereas for the culture supplemented with 10% of serum showed a far superior proliferation and survivability. The serum supplemented culture was able to survive for more than 9 days in a batch culture and recorded a 6.6 fold increase in maximum cell density. After 5 days of batch culture, the viability of the control culture still more than 50% viable, while for the serum deprived culture the viability of the cells dropped to 17%. The mechanism of the cell death is predominantly via apoptosis which is shown in a classical ladder type pattern on a DNA gel and florescence microscopic analysis. The caspases are the most important apoptotic executors which are responsible for the activation and deactivation of other cellular proteins involved in the apoptotic process or directly involved in cell dismantling. In the cytosol, the activation of caspases can be regulated by another protein called inhibitor of apoptosis protein (IAP). In order to investigate the influence of the XIAP on the apoptosis induced by serum deprivation, we have transfected the hybridoma C₂E₇ cells with XIAP gene. In a culture without any serum supplementation, the XIAP cell was able to maintain greater than 75% viability for over 4 days, while the viability of control cells decreased to below 6%. No further increment was observed in the total cell number for the control cell under serum free conditions, while the XIAP cell recorded a 13% increase in total cell number. This result shows that the XIAP cell is still able to proliferate without the presence of any serum components.

1. INTRODUCTION

Mammalian cells are preferred as the expression system for the complex biomolecules that required the correct post-translational modifications. These post-translational modifications such as glycosylation and acylation are absent in prokaryotic microbial cells. However, the nutritional requirements of mammalian cells are more complex than those of prokaryotic cells. Mammalian cells usually require specific growth factors, which are often added in the form of serum, or other animal originated proteins and lipid components. There are several disadvantages of the uses of serum in mammalian cell cultures. Serum or animal originated components may contain infectious agents like viruses and prions. Therefore, its uses in the manufacturing of therapeutic products are prohibited by the regulatory agency. Furthermore, the high protein content of serum may complicate the down-stream processes.

Approaches such as selection of cell variants or genetically modification the cells have been performed in order to eliminate the requirement for serum from mammalian cell cultures. Other approaches are identification and purification of non-animal originated biologically active proteins to be used as supplements to replace serum during medium formulation. Serum and protein free mediums are now widely used in the commercial cultivation of animal cells. However, mammalian cells cultivated in serum or protein-free medium (Moore et al., 1994) are more susceptible to apoptosis compared to those cultivated in medium containing serum (Singh et al., 1994). In a study, Zanghi et al. (1999) reported that adding serum to protein-free CHO cultures could significantly reduce apoptosis induced by nutrient deprivation. Serum deprivation has also been reported to induce apoptosis in wide range of cell lines such as hybridoma (Singh et al., 1994), myeloma (Tey et al., 2000a), CHO (Tey et al., 2000b), BHK (Mastrangelo et al., 2000b) and COS-1 cells (Fujita et al, 1996).

Apoptosis is a highly regulated process. In order to avoid any unnecessary cell death, inside a healthy cell, the apoptotic machineries are segregated in different cellular compartments. These apoptotic execution tools are only brought together when the death switch is triggered. In mammalian cells, there are three main compartments known to be involved in this segregation. The first compartment is the plasma membrane where the death receptor resides. The second compartment is the mitochondrion, which housed several proteins involved in the apoptotic pathway. The third compartment is the cytosol, which is home to the apoptotic proteases (caspases) (Reviewed in Tey et al., 2001).

The caspases are the most important apoptotic executors which are responsible for the activation and deactivation of other cellular proteins involved in the apoptotic process or directly involved in cell dismantling. In the cytosol, the activation of caspases can be regulated by another protein called inhibitor of apoptosis protein (IAP). At least 8 homologues of this protein have been identified in mammalian cells, 2 in baculoviruses and 4 in *Drosophila*.

These proteins share a common ~70 amino acid motif termed BIR (baculovirus IAP repeat). Among the human IAPs, XIAP is the most characterized and potent caspase inhibitors. It has been reported to inhibit the activity of caspases 3, 7 and 9 (Bergmann et al., 2003). Over-expression of XIAP has been reported to be able to suppress apoptosis in CHO and 293 cell lines (Sauerwald et al., 2002). Hence, the objective of the present study was to investigate the ability of XIAP protein on the reduction of serum dependency and the prevention of apoptosis induced by serum deprivation in hybridoma cell culture.

2. MATERIALS AND METHODS

2.1 Cell Line

The C₂E₇ cell line secreting the Ig M antibody against the MCF-7 breast cancer cells are being used in the present study.

ANALYSIS OF CELL NUMBER, VIABILITY AND APOPTOSIS LEVELS

Cell number and viability were assessed using a haemocytometer with trypan blue exclusion method. Apoptosis and necrosis levels were determined by fluorescence microscopic analysis of nuclear morphology and plasma membrane integrity by double staining with acridine orange (AO) and propidium iodide (PI).

2.2 Batch Culture

Stock culture of the C₂E₇ cell line was established. At mid-exponential phase of the culture, cells were harvested by centrifugation and resuspended at 2×10^5 cells/ml in fresh medium with 10% FBS or without any FBS (0%) and transferred into 75 cm² T-flask with a total working volume of 25 ml. The culture was incubated at 37°C. Samples were taken daily in order to assess viable cell number and viability as mentioned above. Samples were also taken for agarose gel electrophoresis analysis.

2.3 Transfection of Hybridoma Cells

Transfection was conducted using Lipofectamine (Invitrogen Life Technologies, California) as recommended by the manufacturer. Briefly, hybridoma cells were plated in a 35 mm dish at a density of 7×10^5 cells 24 h before being transfected in medium supplemented with FBS. Cells were transfected using a total of 6 µg of plasmid DNA (pcDNA3-myc-XIAP or

pcDNA-myc) (Nomura et al., 2003) and 60 μ l of Lipofectamine reagent per dish. After 6 h culture in serum free medium, the medium was changed to fresh standard medium. Transfected cells were cultured for an additional 72 h. To obtain the stable transfectants, the transfected cells were cultured in the presence of 400 μ g/ml geneticin sulfate.

3. RESULTS AND DISCUSSION

The death mechanism of the C₂E₇ cells under serum deprivation was assessed by exposure of cells to medium without any serum supplementation. Cells were exposed to these conditions for a period of 5 days with the inoculation of about 1.0×10^6 cells/ml, which is comparably higher than the initial inoculation of the control culture (serum enriched) of 2.0×10^5 cells/ml. The maximum cell density of the serum deprived culture was about 1.62×10^6 cells/ml, which is only a mere 60% increase from the inoculation. The growth rate of hybridoma in serum enriched culture was very much higher compared to the serum deprived culture, which can be seen from its 6.6 folds increment in maximum cell density. The viability after 5 days of batch culture under serum-free condition dropped to only 17% while the control culture was still 52% viable (Table 1). The ladder like pattern shown in DNA gel electrophoresis (Data not shown) and fluorescence microscopic data (Table 2) confirmed that cell death occur predominantly via apoptosis. The majority of the cells are categorized in either early or late apoptotic under serum deprived condition.

In order to investigate the influence of the XIAP on the apoptosis induced by serum deprivation, we have transfected the hybridoma C₂E₇ cells with XIAP gene. In a culture without any serum supplementation, the XIAP cell was able to maintain greater than 75% viability for over 4 days, while the viability of control cells decreased to about 6% (Table 3). No further increment was observed in the total cell number for the control cell under serum free conditions, while the XIAP cell recorded a 13% increase in total cell number. This result shows that the XIAP cell is still able to proliferate without the presence of any serum components.

TABLE 1: Influence of Serum on the Growth and Survivability of the Hybridoma C₂E₇ Cells

	Serum Enriched (10% FBS)	Serum Deprived (0%FBS)
Initial Cell Density (cells/ml)	2.0×10^5	1.0×10^6
Maximum Cell Density (cells/ml)	1.32×10^6	1.62×10^6
Increment in Cell Density	6.6 fold	1.6 fold
Viability (%) after 5 days of Cultivation	52%	17%

TABLE 2: Cell Fraction of Hybridoma C₂E₇ Cells after 5 days of cultivation

Cell Type	Serum Enriched (10% FBS)	Serum Deprived (0% FBS)
Viable (%)	59.6	17.0
Early Apoptotic (%)	1.0	45.0
Late Apoptotic (%)	34.6	30.0
Ghost (%)	3.8	5.0
Necrosis (%)	1.0	3.0

TABLE 3: Influence of XIAP on the Growth and Survivability of the Hybridoma C₂E₇ Cells under Serum Deprived Conditions

	XIAP cells	Control cells
Initial Cell Density (cells/ml)	1.60 x 10 ⁵	2.05 x 10 ⁵
Maximum Cell Density (cells/ml)	1.80 x 10 ⁵	4.00 x 10 ⁴
Increment in Cell Density	1.13 fold	0.2 fold (Decrease)
Viability (%) after 5 days of Cultivation	75.8%	6.3%

4. CONCLUSION

The results of the present study show that serum played an important role in preventing apoptosis cell death in in-vitro hybridoma cell culture. The over-expression of XIAP has significantly reduced the cell death rate and allows the hybridoma cells to proliferate without the presence of any serum components.

5. ACKNOWLEDGEMENTS

This work was funded by the IRPA Grant (09-02-04-0454-EA001) from the Ministry of Science, Technology and Innovation, Malaysia. We would like to thank JAACT for the award of a bursary to B. T. Tey and Dr Takeo Nomura (Oita Medical University, Japan) for the pcDNA3-myc-XIAP and pcDNA-myc plasmids used in this study.

6. REFERENCES

- Bergmann, A., Yang, A. Y-P, Srivastava, M. (2003). Regulation of IAP function: coming to grips with the grim reaper. *Current Opinion in Cell Biology* 15: 717-724.
- Fujita, T., Terada, S., Ueda, H. & Suzuki, E. (1996). Over-expression of Bcl-2 improved survival of COS-1 cells and enhanced transient protein production. *Journal of Fermentation and Bioengineering* 82, 589-591.
- Mastrangelo, A.J., Hardwick, J.M., Zou, S.F. & Betenbaugh, M.J. (2000). Part II. Over-expression of *bcl-2* family members enhances survival of mammalian cells in response to various culture insults. *Biotechnology and Bioengineering* 67, 555-564.
- Moore, A., Donahue, C.J., Hooley, J., Stocks, D.L., Bauer, K.D. & Mather, J.P. (1995). Apoptosis in CHO cell batch cultures - examination by flow cytometry. *Cytotechnology* 17, 1-11.
- Nomura, T., Mimata, H., Takeuchi, Y., Yamamoto, H., Miyamoto, E., Nomura, Y. (2003). The X-linked inhibitor of apoptosis protein inhibits taxol-induced apoptosis in LNCaP cells. *Urology Research* 31: 37-44.
- Sauerwald T.M., Betenbaugh M.J., Oyler G.A. (2002). Inhibiting apoptosis in mammalian cell culture using the caspase inhibitor XIAP and deletion mutants. *Biotechnology and Bioengineering*, 77:704-716.
- Singh, R.P., Al-Rubeai, M., Gregory, C.D. & Emery, A.N. (1994). Cell-death in bioreactors - a role for apoptosis. *Biotechnology and Bioengineering* 44, 720-726.
- Tey B.T., Singh R.P., Piredda, L. Piacentini, M., Al-Rubeai, M. (2000a). Bcl-2 mediated suppression of apoptosis in myeloma NS0 cultures. *Journal of Biotechnology*, 79: 147-159.
- Tey B.T., Singh R.P., Piredda, L. Piacentini, M., Al-Rubeai, M. (2000b). Influence of Bcl-2 on cell death during cultivation of a Chinese Hamster Ovary cell line expressing a chimeric antibody. *Biotechnology and Bioengineering*, 68: 31-43.
- Tey B.T., Singh R.P., Al-Rubeai, M. (2001). Programmed cell death-An overview of apoptosis in cell culture. *Asia Pacific Journal of Molecular Biology and Biotechnology* 9: 1-28.
- Zanghi, J.A., Fussenegger, M. & Bailey, J.E. (1999). Serum protects protein-free competent Chinese hamster ovary cells against apoptosis induced by nutrient deprivation in batch culture. *Biotechnology and Bioengineering* 64, 108-119.

TRANSCRIPTIONAL PROFILING OF BATCH AND FED-BATCH PROTEIN-FREE 293-HEK CULTURES USING DNA MICROARRAY

Yih Yean Lee^{1,2}, Kathy Wong^{1,2}, Peter Morin Nissom¹ and Miranda G. S. Yap^{1,2}

¹*Bioprocessing Technology Institute, 20 Biopolis Way, #06-01 Centros, Singapore 138668;*

²*Chemical & Biomolecular Engineering, National University of Singapore*

Abstract: 293-HEK (Human Embryonic Kidney) cells were observed to reach 4 times the cell density in low-glutamine protein-free fed-batch cultures when compared to batch cultures. This was accompanied with a reduction in lactate and ammonia production in fed-batch cultures. Studies with virus infection of both batch and fed-batch cultures have also shown an improvement in virus production of about 10,000-fold in fed-batch.

An endeavor was undertaken to decipher the cellular transcriptional regulation underlying the fed-batch process using microarray. This study presents results focusing on the genes related to amino acid metabolism, tRNA processing and energy metabolism. These processes are intimately related to cell growth and protein production, two issues of importance to bioprocessing. Our results showed that amino acid metabolism enzymes (eg. ASNS, GLUD1, GOT1) and a number of tRNA synthetases (eg. EPRS, YARS, WARS, GARS) were found to have consistent differences in expression patterns between batch and fed-batch, possibly due to differences in nutrient environment of the two cultures. The expression patterns of 3 energy metabolism-related genes, SLC25A5, COX6B and SUCLG2, were also found to be dissimilar in batch compared to fed-batch, indicating disparity in energy efficiency of the cells.

Our results suggest that the microarray platform can effectively be utilized as a tool to monitor transcriptional events of cells in culture. These observations, together with other insights gleaned from further analysis of the data, might be valuable in a rational approach to engineering of robust cell-lines with improved cellular metabolism.

1. INTRODUCTION

293-HEK cells have traditionally been used in the production of adenoviral gene therapy vectors. The use of recombinant adenovirus in gene therapy is currently undergoing extensive research and some of these products are presently undergoing early clinical trials.

DNA microarray technology has evolved into a powerful platform for genomic analysis and has seen increasing employment in the biomedical research arena for profiling gene expressions in a wide variety of studies.

In this study, microarray was used to profile the transcriptional regulation in a low-glutamine fed-batch culture compared to a control batch culture to investigate the corresponding alteration in cellular metabolism and accompanying physiological changes.

2. MATERIALS AND METHODS

2.1 293 Cell Culture

The 293H cells (GibcoBRL) were adapted to a custom modified DMEM/F12 (Hyclone). The fed-batch feed was formulated based on a 10X DMEM/F12 (Hyclone) without protein supplements. Cell pellets were collected at different time points during the course of the cultures and stored at -80°C. Control cell samples were collected from the inoculum cells and treated similarly.

2.2 Bioreactor set-up and fed-batch operations

The instrumentation, reactor set-up and fed-batch operation were previously described (Lee *et al.*, 2003).

2.3 Virus Titer

The method of quantification of the virus productivity was conducted as described in previous publication (Lee *et al.*, 2003).

2.4 RNA purification and labeling

RNA were extracted from samples using Trizol reagent (Invitrogen). 1st-strand cDNA probes were then prepared by oligo-dT priming of RNA using Superscript II reverse-transcriptase (Invitrogen) and labelled using Cy3 or Cy5 dyes (Amersham).

2.5 DNA microarray and data analysis

A 19,584 element microarray was used for the experiments. The microarray was printed in-house from a 18,656 element Human oligonucleotide library (Compugen), with additional controls, on poly-l-lysine coated glass slides. cDNA samples prepared from cells collected from mid-exponential, late exponential and stationary phases of both cultures were compared against a common reference taken from the start of the culture. This allows for the construction of temporal gene expression profiles for comparison of significantly regulated genes in the two cultures. Hybridization of the probes on the slides was conducted in a manual hybridization chamber (Telechem) for a minimum of 16 hrs at 42°C. 4 slides per experiment were used, with 2 reversed-dye labelling. Hybridized arrays were then washed and scanned using an ArrayWorx scanner (Applied Precision). Intensity values data obtained from the scanner were uploaded to an in-house microarray data processing system (Microarray Discovery System). Data normalization, including scale normalization between the slides, was conducted using methods adapted from previous publication (Yang *et al.*, 2002). Gene expression values are expressed as the log₂ intensity ratio of each time point with respect to the control (See Figure 1). Resulting log ratios were then analyzed using the Acuity (Axon) and Genemapp softwares (Dahlquist *et al.*, 2002). Data clustering was conducted using Cluster and visualized using TreeView (<http://rana.lbl.gov/EisenSoftware.htm>).

2.6 Quantitative real-time PCR

Selected gene expression results from microarray data were validated using quantitative real-time PCR. Primers were either obtained from PrimerBank (<http://pga.mgh.harvard.edu/primerbank/>) or designed using the Primer Express software (Applied Biosystems). qRT-PCR runs were conducted with cDNA samples from reference and each phase using Biorad iTaq mastermix (Biorad) in an ABI Prism 7000 (Applied Biosystems). Duplicate runs were conducted for each sample.

3. RESULTS AND DISCUSSIONS

3.1 293 Cell Growth Comparison

Low-glutamine fed-batch cultures reached 4 times the cell density of the batch cultures in repeated runs (Figure 1). An infection study conducted in 2 separate repeated batch and fed-batch runs showed at least 10⁴-fold

improvement in volumetric virus production in the fed-batch cultures compared to batch, reaching a titer of approximately 3×10^{11} pfu/ml (Figure 2).

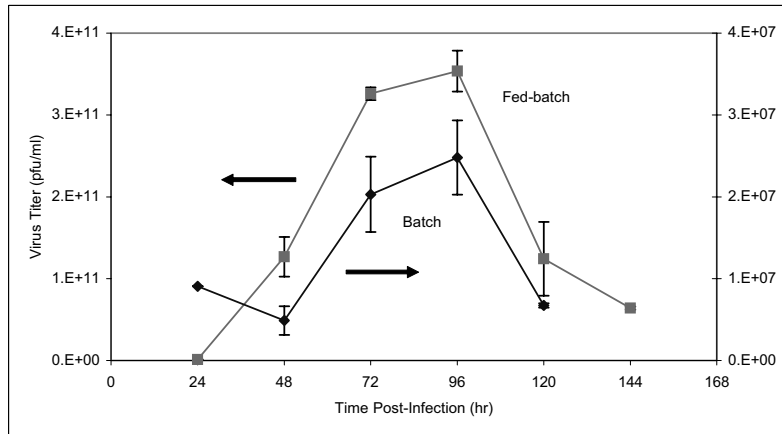


Figure 1. Comparison of batch and fed-batch growth curves with indication of time points where samples were taken for microarray analysis. All samples were collected at viability > 90%.

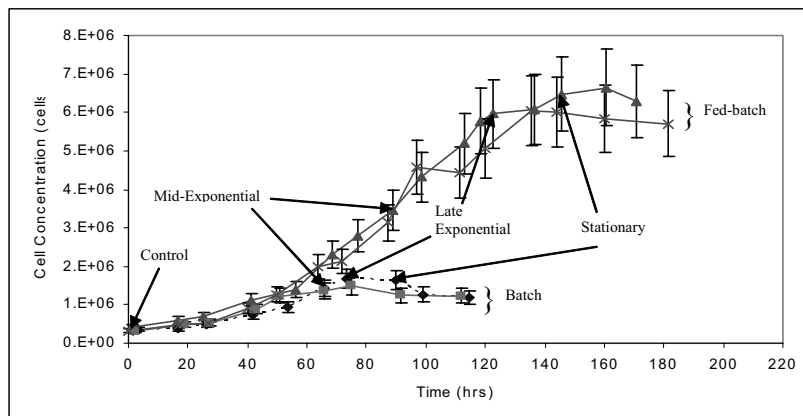


Figure 2. Comparison of batch and fed-batch virus productivity.

3.2 Microarray

3.2.1 Significance Analysis

The significantly regulated genes were filtered out using 2 significance criteria, both with $p\text{-value} \leq 0.05$ (Figure 3). It was observed that a large number of genes were differentially regulated between 1.5 to 2-folds. It could mean that the magnitude of expression regulation reflected in the dataset is

inherently small and hence a less stringent fold change criterion of 1.5-fold might be more appropriate for subsequent analysis.

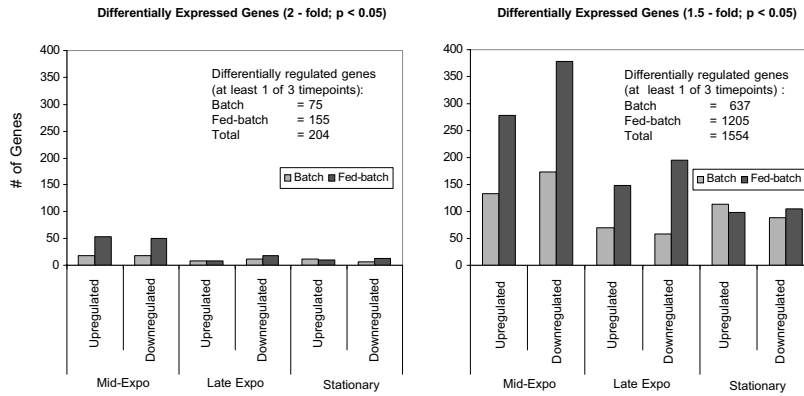


Figure 3. Number of differentially regulated genes of both batch and fed-batch cultures at each of the 3 culture phases using 2 different significance criteria: Fold change ≥ 2 (left) or 1.5 (right) at $p \leq 0.05$.

Based on an absolute fold-change of ≥ 2 (ie. $1 \leq \log \text{ratio intensity} \leq -1$), 204 of the most differentially regulated genes in the dataset was categorized according to their ontology (Figure 4). About half of the differentially expressed genes were unknown or do not have a known functional ontology associated with it despite the relative comprehensiveness of the public human gene database. The 3 highest categories were transcriptional regulation, protein processing and metabolism genes.

Ontologies	# of genes	% of genes
Transcription regulation	19	9
Translation regulation	2	1
Stress response	11	5
Signal transduction	11	5
Protein processing	18	9
Metabolism	17	8
Transport	11	5
Cell cycle	7	3
Apoptosis	5	2
Others	11	5
Unknown	92	45
Total	204	100

Figure 4 . Categorization of 204 most differentially regulated genes based on functional ontologies.

3.2.2 Pathway-Oriented Analysis

A less stringent fold change criteria of 1.5-fold (at $p \leq 0.05$) was used in conjunction with the Genmapp software for the pathway-oriented analysis. A lower fold change criteria was used in order to have enough of a representation of genes in the pathways to make the analysis meaningful. A number of genes related to metabolism, stress response, cell cycle regulation and apoptosis were identified for validation using quantitative real-time PCR.

In order to better appreciate the differences in the transcriptional regulation of these genes, the gene expression profiles were plotted without a cutoff to include the low fold change values and ensure continuity of the plots. The genes presented here focuses on genes related to amino acid metabolism, tRNA processing and energy metabolism, and is only a small number of those found to be significantly regulated.

3.2.2.1. Metabolism-related Genes

Asparagine synthetase (ASNS) catalyses the formation of asparagine from aspartate via the transamination of glutamine to glutamate. It has been shown in literature that its expression, which is under the control of 2 nutrient sensing-response elements (NSRE), is increased in response to either amino acid or glucose deprivation (Zhong *et al.*, 2003). It was observed that the expression of ASNS was similar during the mid and late exponential phases of the culture but was significantly higher in the batch compared to the fed-batch during the stationary phase (Figure 5).

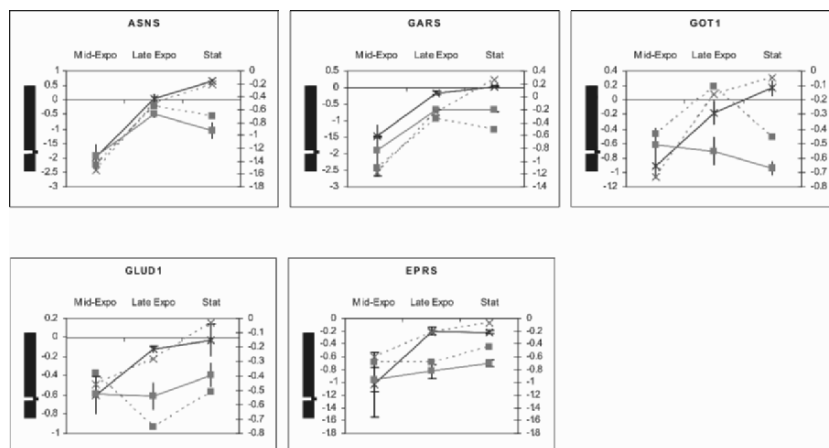


Figure 5. Expression profiles of nutrient-related genes in batch (x) and fed-batch (■). Microarray data represented by broken line (secondary axis) and qRT-PCR results represented by solid lines (primary axis). Positive values denote up-regulation with respect to control and negative values denote down-regulation.

This is a possible indication of higher nutrient deprivation stress experienced by the batch culture.

Glutamate dehydrogenase 1 (GLUD1) catalyzes the oxidative deamination of glutamate to 2-oxoglutarate. Glutamyl-prolyl-tRNA synthetase (EPRS) is the tRNA synthetase that charges the glutamate molecule to its corresponding tRNA during protein biosynthesis. Both these genes are involved in glutamate metabolism and their lower expression in the fed-batch culture (Figure 5) is most likely a direct consequence of the low level of glutamine that was maintained in the fed-batch culture.

tRNA synthetases were first discovered to ligate amino acids to their respective tRNAs signifying their importance in protein biosynthesis. Since then they have also been found to be implicated in a number of other important cellular functions like transcriptional and translational regulation, and apoptosis. A number of tRNA synthetases (eg. EPRS (Figure 5), YARS, GARS (Figure 5), WARS) were found to have similar expression patterns to ASNS. These similarities in expression profiles could be the result of a common environmental trigger but whether this common transcriptional trigger is nutrient-related remains to be determined.

3.2.2.2. Energy Metabolism-related Genes

SLC25A5 is a mitochondrial ATP/ADP carrier and is an important part of the energy metabolism pathway. Cytochrome-C oxidase (COX6B) is the terminal enzyme of the mitochondrial respiratory chain and catalyzes electron transfer from reduced cytochrome C to oxygen.

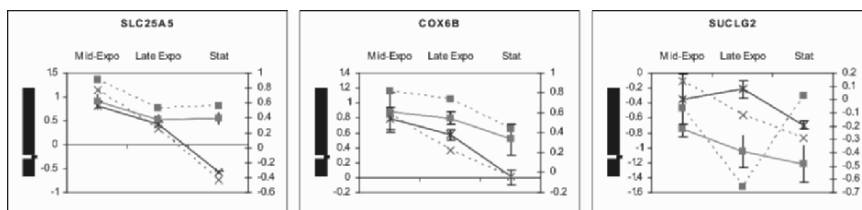


Figure 6 Expression profiles of nutrient-related genes in batch (x) and fed-batch (■). Microarray data represented by broken line (secondary axis) and qRT-PCR results represented by solid lines (primary axis). Positive values denote up-regulation with respect to control and negative values denote down-regulation.

Both these genes showed higher expression in fed-batch compared to batch, indicative of a more active oxidative phosphorylation pathway in the fed-batch.

Succinate CoA-ligase (SUCLG2) is a TCA cycle enzyme catalyzing the conversion of succinyl-CoA to succinate. Downregulation of this gene in fed-batch cultures possibly due to higher oxidative phosphorylation efficiency.

4. CONCLUSIONS

The differential expression of genes related to important pathways between batch and fed-batch cultures have been highlighted in this study. These differences can in general be attributed to the low glutamine level maintained in the fed-batch cultures. These observations, together with other insights gleaned from further analysis of the data, might be valuable in a rational approach to engineering of robust cell-lines with improved cellular metabolism.

5. REFERENCES

- Dahlquist K. D., Salomonis N., Vranizan K., Lawlor S. C., Conklin B. R. (2002). GenMAPP, a new tool for viewing and analyzing microarray data on biological pathways. *Nature Genetics*, 31, 19-20.
- Lee Y. Y., Yap M. G. S., Hu W. S. and Wong T. K. K. (2003). Low-glutamine fed-batch cultures of 293-HEK serum-free suspension cells for adenovirus production. *Biotechnology Progress*, 19(2), 501-509.
- Yang Y. H., Dubois S., Luu P., Lin D. M., Peng V., Ngai J. and Speed T. (2002). Normalization for cDNA microarray data: a robust composite method addressing single and multiple slide systematic variation. *Nucleic Acids Research*, 30(4), 1-10.
- Zhong C, Chen C, Kilberg MS (2003). Characterization of the nutrient-sensing response unit in the human asparagine synthetase promoter. *Biochem J.* Jun 1; 372(Pt 2):603-9.

STUDIES ON THE EFFICACY, SAFETY AND QUALITY OF THE TISSUE ENGINEERED PRODUCTS: ENHANCEMENT OF PROLIFERATION OF HUMAN MESENCHYMAL STEM CELLS BY THE NEW POLYSACCHARIDES

Saifuddin Ahmed,¹ Toshie Tsuchiya¹ and Yutaka Kariya²

¹*Division of Medical Devices, National Institute of Health Sciences, 1-18-1, Kamiyoga, Setagaya ku, Tokyo 158-8501, Japan.*

²*Central Research Laboratories, Seikagaku Corporation, 3-1253 Tateno Higashiyama, Tokyo 207-0021, Japan.*

Abstract: Human mesenchymal stem cells (hMSCs) have the capacity to proliferate and differentiate into multiple cells etc. Polysaccharides can modulate the cell proliferation of human endothelial cell. Here, we investigated the role of different kinds of new polysaccharides to regulate the gap junctional intercellular communication (GJIC) and cell proliferation of cultured normal human dermal fibroblasts (NHDF) cells and hMSCs. The NHDF cells and hMSCs were cultured for 4 days with new polysaccharides. The cultures were then analyzed to verify the extent of GJIC by the scrape-loading dye transfer (SLDT) method, using Lucifer yellow. Alamar blue staining was performed to determine the proliferation of the cultured cells. In NHDF cells, the GJIC was significantly inhibited in cells treated with different kinds of new polysaccharides. On the contrary, in hMSCs, the GJIC was slightly inhibited in all cultured treated cells. But proliferation was enhanced in both cells with different polysaccharides, the extents of cell proliferation was stronger in hMSCs than in NHDF cells. These findings reveal that new polysaccharides seem to play an important role in hMSCs, thus provide a novel tool on tissue engineering.

Key words: GJIC, Proliferation, NHDF, hMSCs.

1. INTRODUCTION

Human mesenchymal stem cells (hMSCs) are multipotent cells have the capacity to proliferate and differentiate into bone, cartilage and adipocytes, and are useful for human cell and gene therapies [1]. Polysaccharides are macromolecules formed from many sugar units connected by glycosidic

linkages. It has two basic functions: serve for monosaccharide storage to make cellular energy and serve as structural components. Sulfated polysaccharide was reported to cause modulation of human endothelial cell proliferation [2]. Sweeney *et al.* also reported that sulfated polysaccharide increases and mobilizes hematopoietic stem cells in mice and nonhuman primates [3]. Furthermore, the inhibition of GJIC can disrupt the balance of cell homeostasis, leading to increase cell proliferation [4]. The aim of this study is to investigate the ability of different kinds of new polysaccharides to regulate the GJIC and cell growth of cultured NHDF cells and hMSCs.

2. MATERIALS AND METHODS

2.1. Materials: 4 different kinds of polysaccharides were used in this experiment.

2.2. Cell Culture: The NHDF cells were obtained from Asahi Techno Glass (Tokyo, Japan), and maintained in Dulbecco's modified Eagle medium (DMEM) supplemented with 10% fetal bovine serum (FBS) in a 5 % CO₂ atmosphere at 37°C. The hMSCs were obtained from Cambrex Bio Science Walkersville, Inc. (Walkersville, USA), and maintained in mesenchymal cell growth medium (MSCGM) supplemented with 10% fetal bovine serum (FBS) in a 5% CO₂ atmosphere at 37°C.

2.3. Scrape-loading and dye transfer (SLDT) assay for detection of GJIC: Cells 1×10^5 /ml (2ml medium/dish) were seeded on to the 35 mm dishes. After 4 hr seeding in a 5% CO₂ atmosphere at 37°C, different kinds of new polysaccharides at the concentration of 2mg/ml, 1ml per dish (35mm dish) was added and incubated at 37°C for 4 days. Then, confluent monolayer cells, after rinsing with Ca²⁺ Mg²⁺ phosphate-buffered saline [PBS (+)] were loaded with 0.1% Lucifer Yellow (Molecular Probes, Eugene, OR, USA)/PBS (+) solution and scraped immediately with a sharp blade. After incubation for 5 min at 37°C, cells were washed three times with PBS (+) and the extent of dye migration length was measured using fluorescence microscope.

2.4. Proliferation assay: 4×10^4 (0.5 ml medium/well) cells per well of 24 well culture plate were seeded. After 4 hr seeding in a 5% CO₂ atmosphere at 37°C, different kinds of new polysaccharides at the concentration of 2mg/ml was added and incubated at 37°C for 4 days. Then, cell proliferation was quantitatively measured by alamar blue (Biosource International, Inc., Camarillo, CA) assay. The assay showed the metabolic activity of the cells by detection of mitochondrial activity. Here, alamar blue used as the indicator dye, was incorporated into the cells, reduced and excreted as a fluorescent product. At the end of 4 days culture, the media from all wells were discarded, and filled with 1 ml/well of 1:20 of alamar blue/fresh medium. The culture plates were incubated at 37°C for 4 h. After the incubation period, two aliquots of 100 µl of solution from each well were transferred into new wells of a Costar 96-well

microplate of tissue culture (Costar type 3595, Corning Co. Ltd.). Equal volume of fresh medium per well (total four wells) served as blanks. The extent of cell proliferation was quantitated by Cytofluor II fluorescence multiwell cell reader (PerSeptive Biosystems, Framingham, MA, USA) at 535-nm excitation and 590-nm emission. The intensity of the blue color obtained was directly proportional to the metabolic activity of the cell populations. Blank values were subtracted from the experimental values to eliminate background readings.

2.5. Statistical analysis: Student's *t* test was used to compare the implanted samples with the controls. Statistical significance was accepted at $p < 0.05$. Values were presented as the mean \pm SD.

3. RESULTS

NHDF cells: In NHDF cells, GJIC was significantly inhibited in cells treated with different kinds of new polysaccharides (** $p < 0.01$) (Figure 1A). But the cell proliferation was significantly increased in cells treated with different kinds of polysaccharides (** $p < 0.01$) (Figure 1B).

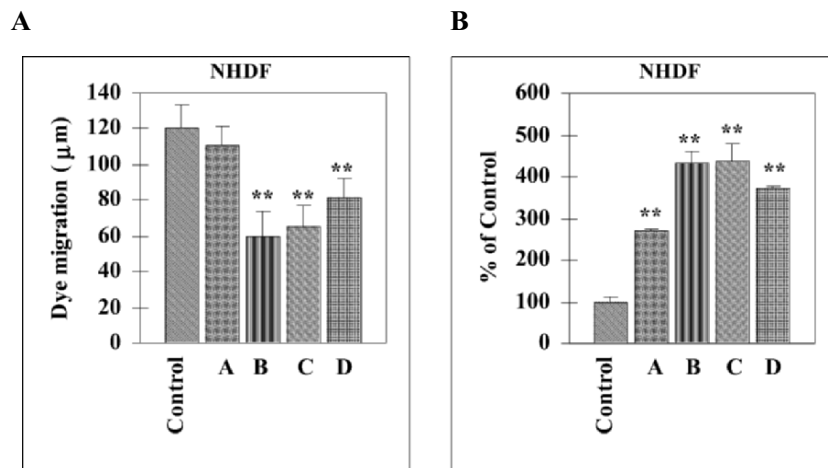


Figure 1. In A, Statistical analysis of SLDT assay and in B, cell proliferation of NHDF cells. ** $p < 0.01$.

hMSCs: In hMSCs, GJIC was also inhibited in all treated cells but significantly in only treated with “D” ($*p < 0.05$, ** $p < 0.01$) (Figure 2A). Here proliferation also was significantly enhanced in cells treated with different kinds of polysaccharides (** $p < 0.01$) (Figure 2B). But stimulatory reaction was much more in hMSC cell than NHDF cell.

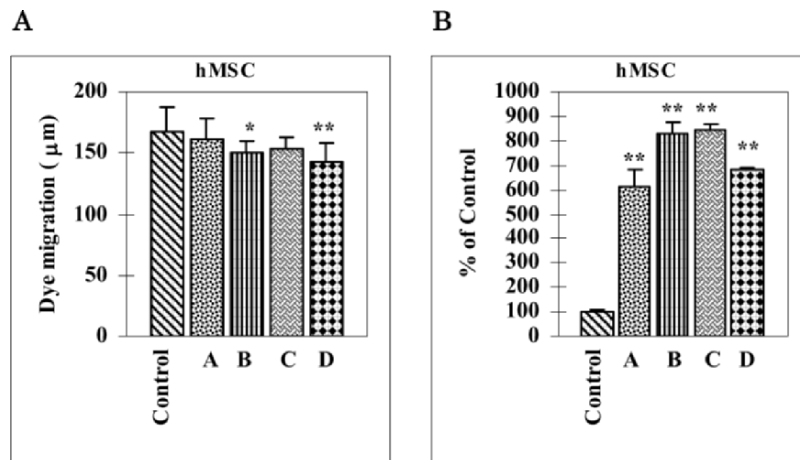


Figure 2. In A, Statistical analysis of SLDT assay and in B, cell proliferation of hMSCs. * $p < 0.05$, ** $p < 0.01$.

4. DISCUSSION

hMSCs are used for tissue engineering of bone and cartilage and provide a versatile model system to study mesenchymal proliferation. In this study we identify several distinct roles of new polysaccharides in hMSC biology, which disclose a role of polysaccharides in hMSC proliferation. GJIC was significantly inhibited in cells treated with different kinds of new polysaccharides in NHDF cells. But in hMSCs, GJIC was slightly inhibited in all cultured treated cells. In contrast, cell proliferation was enhanced by different polysaccharides in hMSCs (6 to 8 folds) more than in NHDF cells (2 to 5 folds) in comparison with controls. As stated earlier, in mice and monkeys, sulfated polysaccharide such as fucoidan caused increase in hematopoietic stem cells [3] and Matsubara *et al.* reported that basement membrane-like extracellular matrix (bmECM) had greater effects on the proliferation of hMSC [5]. Our result also coincided with these reports. Usually, inhibition of the function of connexin is considered to cause the cellular proliferation [4]. Therefore, these findings, that there is a relationship between the inhibitory effects on the connexin function and cellular proliferation, coincided with the result previously reported. Our studies postulated that these new polysaccharides seem to play a significant role in cell proliferation of both NHDF cells and hMSCs. Especially, these new polysaccharides are novel materials to increase the cell number of hMSCs and therefore hMSCs provide a good and clinically relevant model system. In addition, the positive effect of new polysaccharides on hMSC proliferation warrants further studies toward its exploitation in tissue engineering.

5. REFERENCES

- [1] Pittenger, M.F. *et al.* (1999) Multilineage potential of adult human mesenchymal stem cells, *Science*. 284, 143-147.
- [2] Giraux, J.L., Matou, S., Bros, A., Tapon-Brethaudiere, J., Letourneur, D. and Fischer, A.M. (1998) Modulation of human endothelial cell proliferation and migration by fucoidan and heparin, *Eur J Cell Biol.* 77, 352-359.
- [3] Sweeney, E.A., Lortat-Jacob, H., Priestley, G.V., Nakamoto, B. and Papayannopoulou, T. (2002) Sulfated polysaccharides increase plasma levels of SDF-1 in monkeys and mice: involvement in mobilization of stem/progenitor cells, *Blood*. 99, 44-51.
- [4] Klaunig, J.E. and Ruch, R.J. (1990) Role of inhibition of intercellular communication in carcinogenesis, *Lab Invest.* 62, 135-146.
- [5] Matsubara, T. *et al.* (2004) A new technique to expand human mesenchymal stem cells using basement membrane extracellular matrix, *Biochem Biophys Res Commun.* 313, 503-508.

STUDIES ON THE EFFICACY, SAFETY AND QUALITY OF THE TISSUE ENGINEERED PRODUCTS: EFFECTS OF A CATALYST USED IN THE SYNTHESIS OF BIODEGRADABLE POLYMER ON THE CHONDROGENESIS OF HUMAN ARTICULAR CARTILAGE

Nasreen Banu, Toshie Tsuchiya, Saifuddin Ahmed and Rumi Sawada
Division of Medical Devices, National Institute of Health Sciences, 1-18-1, Kamiyoga, Setagaya ku, Tokyo 158-8501, Japan.

Abstract: Among different synthetic biodegradable polymers, polyesters such as poly (glycolic acid) (PGA) is an attractive candidate in orthopedic applications, because of its degradation product glycolic acid is a natural metabolite. The biocompatibility of PGA that was synthesized with and without inorganic tin catalyst, in chondrogenesis of human articular cartilage (HAC) was investigated using a 4 weeks micromass culture system. PGA with tin catalyst caused significant enhancement in chondrocyte proliferation and expression of collagen type II gene. Amounts of total collagen and collagen type II protein were also increased. However, aggrecan gene expression was almost similar to control cultures. On the contrary, PGA without catalyst caused an inhibitory action on the chondrogenesis. From the viewpoint of safety, PGA was not suitable to use as the biodegradable scaffold for cartilage.

Key words: Human articular cartilage, Chondrogenesis, PGA, Tin catalyst.

1. INTRODUCTION

The fields of biotechnology and tissue engineering by using different synthetic biodegradable polymers are general concepts because of its disappearance in the body. In general, synthetic biodegradable polymers offer greater advantage over natural or other materials. The prime advantages include the capacity to change the mechanical properties and degradation kinetics to suit various applications. Synthetic biodegradable polymers, especially polyester

such as poly (glycolic acid) (PGA) plays an important role in orthopedics. PGA, a polymer of glycolic acid can be synthesized under the influence of different catalysts. The common catalysts used include organotin, antimony, lead, and zinc. Organotin compounds are known agents to cause neurotoxicity [1], cytotoxicity [2], immunotoxicity and genotoxicity [3] in human and other experimental animals. Disproportionate dwarfing syndrome, affecting the limbs severely than the trunk, was observed in the rats that had been injected with certain tin compounds [4]. No study yet has reported the chondrogenic effects of PGA, synthesized with and without inorganic tin catalyst. In this study, the biocompatibility of PGA synthesized with and without tin catalyst was investigated using human articular cartilage (HAC) in a micromass culture system.

2. MATERIALS AND METHODS

2.1. Medium and Polymers Used for Cell Culture: Chondrocyte growth medium were commercially obtained from BioWhittaker, Inc., (Walkersville, MD, USA). PGA synthesized with inorganic tin [PGA(Sn)] (Mw = 1,500) and PGA without catalyst (PGA) (Mw = 1,100) were tailor-made and dissolved in dimethyl sulphoxide (DMSO) (Sigma Chemical Co. Irvine, UK).

2.2. Cells and Culture Methods: HAC of the knee joint was commercially obtained from BioWhittaker, Inc., (Walkersville, MD, USA). High-density micromass cultures were started by spotting 4×10^5 cells in 20 μ l of medium onto Costar 24-well microplates for tissue culture (Costar type 3526, Corning Co. Ltd.). After 2 h of attachment period at 37°C in a CO₂ incubator, culture medium (1ml/well) was added into each well. Media were supplemented with DMSO (0.8 μ l/ml), PGA and PGA (Sn) (50 μ g/ml). HAC cultured with DMSO was used as control. The cultures were continued for 4 weeks with medium change twice in a week. At least four cultures were run for each sample.

2.3. Cell Proliferation Study: Cell proliferation was quantitatively estimated by crystal violet (Wako Pure Chemical Industries, Ltd., Osaka, Japan) staining method. After 4 weeks culture, cells were fixed with 100% Methanol, stained by applying 0.1% crystal violet in Methanol, and washed. Again methanol was applied and the absorbance was measured at a wavelength of 590 nm using an ELISA reader (Bio-Tek Instruments, Inc., Winooski, Vt., USA).

2.4. Differentiation Assay: After proper washing with methanol and acetic acid, proliferation assay was followed by the differentiation assay by

staining the cells with 1% (v/v) alcian blue (Wako Pure Chemical Industries, Ltd., Osaka, Japan) in 3% acetic acid, pH 1.0. The cartilage proteoglycans were extracted with 4-M guanidine hydrochloride (GH) and the bound dye was measured at wavelength of 600 nm using an ELISA reader (Bio-Tek Instruments, Inc., Winooski, Vt., USA).

2.5. Analytical Assays: Commercially available assay kit [collagen assay kit, Biocolor Ltd, Newtownabbey, Northern Ireland] was used for the measurement of collagen within the cultured cells as previously described [5]. The amounts of total collagen content (acid and pepsin soluble fractions) and collagen type II protein of the cultured chondrocytes was detected as per manufacturer's instruction. The absorbance of the samples was measured at a wavelength of 540 nm using a spectrophotometer.

2.6. Real-time polymerase chain reaction (PCR): For detection of the presence of proteoglycans, namely collagen type II and aggrecan, single stranded cDNA was prepared from 1 µg of total RNA by reverse transcription (RT) using a commercially available First-Strand cDNA kit (Amersham Pharmacia Biotech, Uppsala, Sweden). Subsequently real-time PCR was done using LightCycler system with LightCycler FastStart DNA Master SYBR Green I (Roche Diagnostics, Penzberg, Germany). LightCycler™- Primer set (Roche Diagnostics) was used for quantitative detection of Collagen type II gene, aggrecan gene, and also a housekeeping gene, glyceraldehyde-3-phosphate dehydrogenase (GAPDH). The quantification data were analyzed with the LightCycler analysis software (Roche Diagnostics).

2.7 Statistical Study: Student's t test was used to compare the sample results. Statistical significance was accepted at $p < 0.05$. All values in this study are reported as means \pm S.D (standard deviation).

3. RESULTS

3.1. Cell Proliferation and Differentiation: Cell proliferation was 1.8 (* $p < 0.05$)-fold increased in PGA (Sn) treated culture compared with DMSO group as the control. Whereas cell proliferation in PGA treated culture was almost similar to DMSO group (Figure 1A). In the case of cell differentiation, PGA (Sn) group showed a slight decrease in cell differentiation compared to DMSO control (Figure 1B).

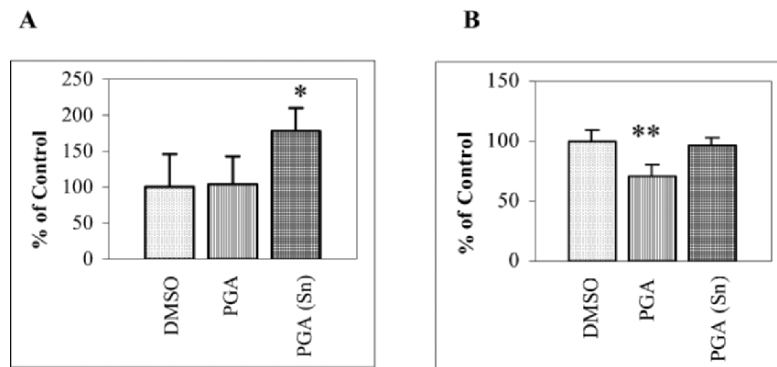


Figure 1. Cell proliferation (A) and cell differentiation (B) of human articular chondrocytes after 4 weeks culture period. * $p < 0.05$, ** $p < 0.01$.

3.2. Extracellular matrix gene expression: Collagen type II gene was strongly expressed in PGA (Sn) than in PGA and control group (Figure 2A). However, aggrecan gene expression was inhibited in the PGA and no difference was observed between PGA (Sn) and the control group (Figure 2B).

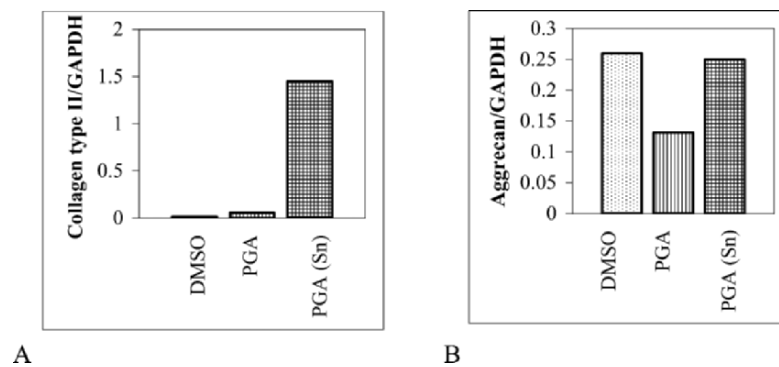


Figure 2. Expression of collagen type II gene (A) and aggrecan gene (B) in cultured chondrocytes, estimated by real time PCR method.

3.3. Measurement of Collagen type II protein and Total collagen amount: The amount of pepsin soluble and cartilage specific protein, collagen type II was significantly increased (** $p < 0.01$) in PGA (Sn) group, but almost no difference in the amount was observed between the PGA and control group (Figure 3A). The amount of total collagen (both acid and pepsin soluble protein) was significantly increased (** $p < 0.01$) in PGA (Sn) group compared with the controls. (Figure 3B).

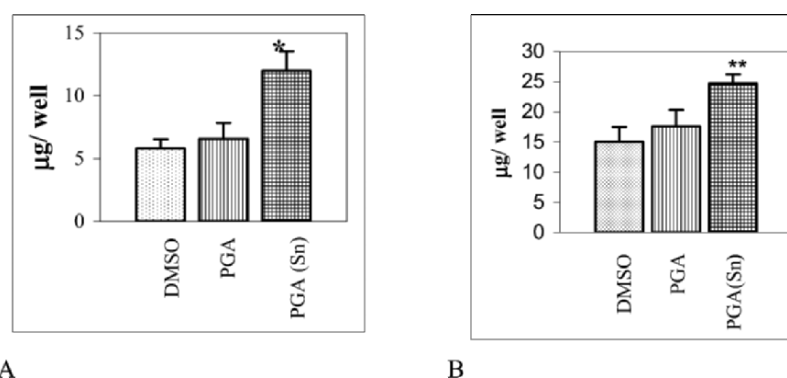


Figure 3. Estimation of the amount of collagen type II protein (A) and total collagen (B) of human articular chondrocytes after 4 weeks of culture. ** $p < 0.01$.

4. DISCUSSION

Different tin compounds had already exhibited general cytotoxic effects on rabbit articular cartilage in monolayer culture [6], and Yamaguchi et al. suggested bone as the critical organ in inorganic tin toxicity in rats [7]. We evaluated the chondrogenic effect of HAC with PGA, synthesized with and without inorganic tin catalyst, in micromass culture system. Oral administration of certain tin compounds was reported to exert stimulatory effect on chondrocyte proliferation of rat [6]. Parallel with this event, proliferation assay of HAC with PGA (Sn) performed in our study also showed stimulatory effect on chondrocyte proliferation in micromass culture (Fig 1). But, PGA showed neither inhibition nor stimulation on the chondrocyte proliferation and thus inorganic tin as catalyst seemed to play a stimulatory role in HAC proliferation. In rat, oral administration of inorganic tin was reported to cause decrease in the proliferation of the chondrocytes accompanied by suppression of DNA synthesis with subsequent inhibition in collagen synthesis [8]. These references suggested a direct relation of inorganic tin in chondrocyte proliferation with the synthesis of collagen protein. In support of these suggestions, our results also showed enhancement of HAC proliferation, expression of collagen type II gene, and amounts of total collagen and collagen type II protein. There was a strong decrease in aggrecan gene expression in PGA compared with control. This study firstly to show the biological action of inorganic tin as catalyst in PGA on human articular chondrogenesis in a micromass culture system. We speculate that nature of tin compound, and also the route of application may play a key role in exhibiting various chondrogenic effects of this metallic compound. In

spite of different positive findings regarding human articular chondrogenesis, from the view points of safety we are considering inorganic tin catalyst is not appropriate to use for synthesis of biodegradable polymers in future clinical applications.

5. REFERENCES

- [1] Chang, L.W. (1990) The neurotoxicology and pathology of organomercury, organolead, and organotin, *J. Toxicol. Sci.* 15, 125-151.
- [2] De Mattos, J.C. et al. (2000) Damage induced by stannous chloride in plasmid DNA, *Toxicol. Lett.* 27, 159-163.
- [3] Chao, J.S., Wei, L.Y., Huang, M.C., Liang, S.C. and Chen, H.H. (1999) Genotoxic effects of triphenyltin acetate and triphenyltin hydroxide on mammalian cells in vitro and in vivo, *Mutat. Res.* 21, 167-174.
- [4] Chang, L.W. (1984) Hippocampal lesions induced by trimethyltin in the neonatal rat brain, *Neurotoxicology.* 5, 205-215.
- [5] Brown, A.N., Kim, B.S., Alsberg, E. and Mooney, D.J. (2000) Combining Chondrocytes and smooth muscle cells to engineer hybrid soft tissue constructs, *Tissue Eng.* 6, 297-305.
- [6] Webber, R.J., Dollins, S.C., Harris, M. and Hough, A.J. Jr. (1985) Effect of alkyltins on rabbit articular and growth-plate chondrocytes in monolayer culture, *J. Toxicol. Environ. Health.* 16, 229-242.
- [7] Yamaguchi, M., Kitade, M. and Osaka, S. (1980) The oral administration of Stannous chloride to rats, *Toxicol. Lett.* 5, 275-278.
- [8] Yamaguchi, M., Sugii, K. and Okada, S. (1982) Inhibition of collagen synthesis in the femur of rats orally administered stannous chloride, *J. Pharm. Dyn.* 5, 388-393.

THE ROLE OF *BIFIDOBACTERIUM* IN THE DEVELOPMENT OF GUT IMMUNE SYSTEMS: ANALYSIS USING GNOTOBIOTIC TCR-TRANSGENIC MICE

Masato Tsuda¹, Akira Hosono¹, Miran Fujioka¹, Satoshi Hachimura²,
Ryo Nakamura¹, Kazuhiro Hirayama³, Kikuji Itoh³, and Shuichi
Kaminogawa¹

¹Department of Food Science and Technology, Nihon University, Fujisawa-shi, Kanagawa, 252-8510, Japan, and ²Department of Applied Biological Chemistry, and ³Department of Veterinary Public Health, The University of Tokyo

Abstract: We have previously established germfree ovalbumin (OVA)-specific T cell receptor transgenic (TCR-Tg) mice. Recent studies have shown that intestinal bacteria affect intestinal immunoresponses and that probiotic bacteria regulate allergic reactions in the host. However, the mechanisms of the development of the gut immune system by intestinal bacteria, especially antigen-specific immune responses, are not well understood. In this study we examined the antigen-specific immunoresponses, in particular of the intestinal immune systems derived from gnotobiotic TCR-Tg mice, associated with *Bifidobacterium* (BIF). The control group was associated with segmented filamentous bacteria (SFB) and 46 strains of clostridia, known to induce the development of the intestinal tissues. The BIF group was associated with *Bifidobacterium pseudocatenulatum* 7041, SFB and clostridia. Lymphocytes were isolated from spleen, Peyer's patch (PP) and lamina propria (LP) of the gnotobiotic TCR-Tg mice, and were co-cultured with OVA. We found that PP and LP cells from BIF mice secreted lower levels of interferon- γ (IFN- γ) and interleukin-6 (IL-6) than those from control mice in response to OVA stimulation. The pattern of regulated cytokine secretion of PP and LP cells from BIF mice was similar to that of CV mice. These results indicate that the colonization by *Bifidobacterium* regulates OVA-specific responses in the intestinal immune system. Our findings suggest that *Bifidobacterium* may contribute to the functional development of the intestinal immune system by down-regulating hyperresponsiveness to specific antigens.

Key words: *Bifidobacterium*, T cell receptor transgenic (TCR-Tg) mice, intestinal immune systems.

1. INTRODUCTION

The gut is consistently exposed to various dietary antigens, pathogenic bacteria, and intestinal commensal bacteria. There are intestinal immune systems specific to the intestinal mucosa whose role is to recognize and remove foreign antigens. It has recently been shown that intestinal bacteria play a role both in the development of intestinal tissues and of these intestinal immune systems.

In particular, members of the genus *Bifidobacterium* are one of the most prominent commensal bacteria in the human intestinal microflora and some species of *Bifidobacterium* have been expected to be probiotic bacteria with their –immunomodulatory activity moderating the response to infection(1-3). It is also possible that the presence of intestinal *Bifidobacterium* may moderate the allergic response. For example, one study examined the fecal flora of 2-year-old children with or without allergy. The allergic children had fewer *Bifidobacterium* in their fecal flora than the nonallergic (4). In addition, in a study using germ-free mice, it was shown that the presence of intestinal bacteria, especially members of the *Bifidobacterium*, was very important for the induction of oral tolerance (5). Thus, it is suggested that *Bifidobacterium* have immunomodulatory effects on intestinal immune systems, although the details of the mechanisms are unclear.

To examine the responsiveness to a specific antigen under conditions of regulated intestinal flora, we previously established the gnotobiotic model of ovalbumin (OVA) specific T cell receptor transgenic (TCR-Tg) mice in which mice were transfected with the sequence encoding the TCR recognizing OVA specifically. Using this experimental system, we have found some differing immunological characteristics when comparing conventional (CV) and germ-free (GF) breeding conditions. GF mice had less-developed intestinal immune tissues as evidenced by the size of Peyer's Patches (PP) from GF mice which were smaller than those from CV mice. Moreover, while immunocellular responsiveness to OVA was different between GF mice and CV mice, it was observed that PP cells from GF mice responded with higher cytokine production than those from CV mice(6). On this basis, we examined the effects of *Bifidobacterium* on the development of intestinal immune systems, focusing on the immune responses to the specific antigen OVA.

2. MATERIALS AND METHODS

2.1 Mice

Germ-free TCR-Tg mice were separated into 2 groups for microflora conditioning - control and BIF. The control group was associated with segmented filamentous bacteria (SFB) and 46 strains of clostridia capable of inducing the development of the intestinal tissues. The BIF group was associated with *Bifidobacterium paseudocatenulatum* 7041 and SFB and clostridia.

2.2 Preparation of the cells from spleen (SP), PP and lamina propria (LP)

Murine small intestines and spleens were excised, and PPs were removed carefully from the intestines. Each single cell suspension from SP or PP was obtained by crushing the respective organ. LP lymphocytes were isolated from the small intestines by means of the following method. We excised PPs from the small intestines, after the intestines were turned inside-out using polyethylene tubing, and wiped carefully a few times with paper toweling. The intestines were cut into approximately 4 cm pieces and washed with HBSS (-) (Hanks' balanced salt solution, Ca, Mg free, containing 5% FCS) with shaking at 37° C for 30 min three times. The supernatant was discarded following filtration with gauze and the intestines were then minced into 5 mm pieces and treated with collagenase (1 mg/ml in HBSS (+) (containing Ca, Mg and 5% FCS)) in a 100 ml-flask with gentle stirring at 37° C for 30 min. After collagenase treatment, the preparation was filtered with gauze and the cells were washed with HBSS (+) followed by centrifugation at 4° C 1,300 rpm for 5 min. The supernatant was then removed. Furthermore, we added 3 ml of 100% Percoll (Amersham Biosciences AB, Uppsala, Sweden) to the cell pellets and added HBSS to 10ml (30% Percoll conc.). The cell suspension was then mixed gently and centrifuged at 20°C, 1,800 rpm for 20 min, after which the supernatant was removed, leaving 1ml of cells in suspension. Subsequently, we added 4.1 ml of 100% Percoll, and topped this up to 10 ml with 10% FCS-RPMI (44% Percoll conc.) and mixed. We then injected 2 ml of 70% Percoll into the bottom of the tube and centrifuged at 20°C, 1,800 rpm for 20 min. Finally, the cells located at the interface between the 44% and 70% Percoll fractions were collected as LP cells and washed with RPMI.

2.3 Cell culture for cytokine production

SP or PP cells (5×10^5 cells) and LP cells (1×10^5 cells) were cultured in 200 μ l of RPMI medium in 96-well culture plates

containing 5%FCS and 0-500 µg/ml of OVA. Supernatants were collected after 48 hours. Spleen cells isolated from Balb/c mice were treated with mitomycin C, and then added (4×10^5 cells) as antigen presenting cells in LP cell cultures.

2.4 ELISA for cytokines

The culture supernatants were assayed for interferon (IFN)- γ , interleukin (IL)-4, IL-5 and IL-6. The amounts of cytokines in the supernatants were measured by a sandwich ELISA method. Rat anti-mouse IFN- γ , IL-4, IL-5 and IL-6 monoclonal antibodies were used as the capture antibody, with biotinylated rat anti-mouse IFN- γ , IL-4, IL-5 and IL-6 monoclonal antibodies, respectively, as the detection antibodies.

3. RESULTS AND DISCUSSION

We examined the effects of *Bifidobacterium* on the responsiveness of gut immune systems to a specific antigen, using gnotobiotic TCR-Tg mice. We did not think that it would be better to compare *Bifidobacterium*-monoassociated mice with germ-free mice in this investigation of intestinal immune responses, because the intestinal tissues of germ-free mice are undeveloped. Consequently, mice associated with SFB and clostridia were set up to be the control group. It has previously been reported that SFB and clostridia promote the development of both intestinal intraepithelial lymphocytes (IEL) and IgA producing cells in the small intestine and of IEL only in the large intestine (7, 8). We confirmed that the shape of PP and the number of PP cells in the mice associated with SFB and clostridia were very similar to that of conventional mice(6). We selected and used *Bifidobacterium pseudocatenulatum* 7041 in this study and the mice associated with *B. pseudocatenulatum* 7041 and SFB and clostridia were defined as the BIF group. It has been reported that *B. pseudocatenulatum* 7041 have a bacterial component which exhibits very strong mitogenic activity for murine splenocytes and PP cells (9). Thus, this *Bifidobacterium* strain enables us to easily evaluate the effects of *Bifidobacterium* on intestinal immune systems.

To examine the effects of *Bifidobacterium* on the antigen-specific cytokine responses in intestinal immune systems, SP, PP and LP cells from control and BIF mice were cultured with OVA and cytokine secretion was measured by ELISA.

Table 1. Production of IFN- γ and IL-6 by PP cells co-cultured with OVA

OVA stimulation ($\mu\text{g/ml}$)	IFN- γ secretion		IL-6 secretion	
	cont	BIF	cont	BIF
0	N.D	N.D	N.D	N.D
50	+	N.D	+	N.D
500	+++	+	+++	+

PP cells from control or BIF mice were co-cultured with 0, 50, or 500 $\mu\text{g/ml}$ OVA. IFN- γ and IL-6 secreted in the culture supernatants were measured by ELISA. Secretion of cytokines was judged based on the results of two or more individual experiments.

In SP cells as the tissue of the systemic immune system, BIF mice produced IFN- γ and IL-6 levels as high as those seen in control mice. PPs are supposed to be the inductive site of the intestinal immune system, and the LP is the effector site. PP cells in BIF mice produced lower levels of IFN- γ and IL-6 than those of control mice. However, IL-4 and IL-5 production by PP cells in both control and BIF mice was not detected. LP cells in BIF mice also produced lower levels of IFN- γ and IL-6 compared with those of control mice. We previously confirmed that PP and LP cells of GF mice responded to OVA with higher IFN- γ and IL-6 production than those of CV mice(6). Thus, we found that the patterns of IFN- γ and IL-6 production in BIF mice were very similar to those of CV mice when compared with GF mice.

The difference in responsiveness to OVA between CV mice and GF mice implies that CV mice have a higher ability to regulate their responses to specific antigens compared with GF mice. In our results, PP and LP cells in BIF mice responded to OVA with lower cytokine production compared with control mice, and cytokine responses to OVA in BIF mice were very similar to CV mice. These results thus suggest that colonization by *Bifidobacterium* may contribute to the functional development of intestinal immune systems, and may have a role in the downregulation of hyperresponsiveness to specific antigens in intestinal immunity, although SFB and clostridia may affect the development of intestinal immune tissues.

Table 2. Production of IFN- γ and IL-6 by LP cells co-cultured with OVA

OVA stimulation ($\mu\text{g/ml}$)	IFN- γ secretion		IL-6 secretion	
	cont	BIF	cont	BIF
0	N.D	N.D	++	+
50	+	+	++	+
500	+++	++	+++	+

LP cells from control and BIF mice were co-cultured with 0, 50, or 500 $\mu\text{g/ml}$ OVA. IFN- γ and IL-6 secreted in the culture supernatants were measured by ELISA. The level of secretion of cytokines was judged based on the results of two or more separate experiments.

4. ACKNOWLEDGEMENT

We thank Dr. Sonoko Habu and Dr. Takehito Sato (Tokai University, School of Medicine) for generously providing the TCR-transgenic mice.

5. REFERENCES

1. Qiao, H., L. C. Duffy, E. Griffiths, D. Dryja, A. Leavens, J. Rossman, G. Rich, M. Riepenhoff-Talty, and M. Locniskar. 2002. Immune responses in rhesus rotavirus-challenged BALB/c mice treated with bifidobacteria and prebiotic supplements. *Pediatr Res* 51:750.
2. Shu, Q., and H. S. Gill. 2001. A dietary probiotic (Bifidobacterium lactis HN019) reduces the severity of Escherichia coli O157:H7 infection in mice. *Med Microbiol Immunol (Berl)* 189:147.
3. Yasui, H., J. Kiyoshima, and H. Ushijima. 1995. Passive protection against rotavirus-induced diarrhea of mouse pups born to and nursed by dams fed Bifidobacterium breve YIT4064. *J Infect Dis* 172:403.
4. Bjorksten, B., P. Naaber, E. Sepp, and M. Mikelsaar. 1999. The intestinal microflora in allergic Estonian and Swedish 2-year-old children. *Clin Exp Allergy* 29:342.
5. Sudo, N., S. Sawamura, K. Tanaka, Y. Aiba, C. Kubo, and Y. Koga. 1997. The requirement of intestinal bacterial flora for the development of an IgE production system fully susceptible to oral tolerance induction. *J Immunol* 159:1739.
6. M. Fujioka, S. Hachimura, A. Hosono, R. Nakamura, K. Hirayama, K. Itoh, and S. Kaminogawa. 2002. Establishment and analysis of germfree T cell receptor transgenic mice. *Animal Cell Technology: Basic & Applied Aspects* 13:243.

7. Umesaki, Y., H. Setoyama, S. Matsumoto, A. Imaoka, and K. Itoh. 1999. Differential roles of segmented filamentous bacteria and clostridia in development of the intestinal immune system. *Infect Immun* 67:3504.
8. Umesaki, Y., Y. Okada, S. Matsumoto, A. Imaoka, and H. Setoyama. 1995. Segmented filamentous bacteria are indigenous intestinal bacteria that activate intraepithelial lymphocytes and induce MHC class II molecules and fucosyl asialo GM1 glycolipids on the small intestinal epithelial cells in the ex-germ-free mouse. *Microbiol Immunol* 39:555.
9. Hosono, A., J. Lee, A. Ametani, M. Natsume, M. Hirayama, T. Adachi, and S. Kaminogawa. 1997. Characterization of a water-soluble polysaccharide fraction with immunopotentiating activity from *Bifidobacterium adolescentis* M101-4. *Biosci Biotechnol Biochem* 61:312.

THE ROLE OF CD4⁺ T CELLS IN IGA PRODUCTION IN MURINE PEYER'S PATCHES FOLLOWING ORAL FEEDING OF *BIFIDOBACTERIUM* COMPONENTS

Yusuke Nakanishi, Akira Hosono, Teiji Kimura, and Shuichi Kaminogawa
Department of Food science and Technology, Nihon University, Fujisawa-shi, Kanagawa 252-8510, Japan

Abstract: Immunomodulatory effects, especially in murine Peyer's patch (PP) cells, were demonstrated following oral administration of *Bifidobacterium* immunomodulators (BIM) to BALB/c mice for 7 consecutive days. The BIM was derived from sonicated *B. pseudocatenulatum* 7041. We previously demonstrated that BIM administration augmented total IgA production including BIM-specific IgA by PP cells and enhanced the secretion of interferon- γ (IFN- γ), interleukin-5 (IL-5), IL-6 and IL-12 by the PP cells. In the present study, the immunoresponses of CD4⁺ PP T-cells have been characterized to elucidate the influences of oral feeding of BIM. Also, we examined how CD4⁺ PP T cells induced IgA production following oral BIM administration. After 7 days of oral administration of BIM, PP cells were obtained from each experimental mouse and CD4⁺ T-cells were isolated using a magnetically activated cell sorting system. The expression of cell-surface antigens on CD4⁺ PP cells was analyzed by flow cytometry. CD4⁺ T cells were co-cultured with BIM in the presence of antigen-presenting cells and the cytokine secretion and IgA production were then measured by ELISA. On CD4⁺ PP T-cells from BIM-fed mice, the expression of CD45RB^{high}, a naïve marker, showed significant enhancement compared with controls. On the other hands, the secretion of cytokines (IFN- γ , IL-6) by CD4⁺ PP T-cells was increased by BIM administration. In addition, these cells increased BIM-specific IgA production but did not induce an increase in the total IgA production.

Key words: *Bifidobacterium*; Peyer's patch; IgA; CD4⁺ T cells.

1. INTRODUCTION

The intestinal microflora is composed of a large number of anaerobic and aerobic bacteria, the makeup of which is changed by aging, diet, stress, and other factors. The intestinal bacteria are supposed to play a crucial role in homeostasis and host defenses through their action as immunomodulators of innate and acquired immune responses. These are harmful bacteria for human health. Recently, “probiotic” bacteria have attracted considerable attention. They are defined as live microbes ingested as food ingredients with the expectation of beneficial effects on our health. Some probiotic bacteria have been reported to have immunopotentiating activity, anti-tumor effects, or anti-allergic effects. In addition, live Gram-positive bacteria such as members of the *Bifidobacterium* or *Lactobacillus* families, as well as some components derived from these bacteria, have been shown to be effective in the prevention of allergy and cancer. However, the immunological mechanisms responsible for the actions of probiotic bacteria have not been clarified in detail. In this study, we have investigated the influence of oral administration of *Bifidobacterium* immunomodulator (BIM) on mucosal immune responses in the intestine. BIM was prepared by sonication of *Bifidobacterium pseudocatenulatum* 7041 derived from human intestinal microflora. We have previously confirmed its strong mitogenic activity on murine lymphocytes [1]. This activity was increased by disruption of the cells, which is perhaps due to the fact that this strain contains water-soluble immunoactive polysaccharides [2, 3]. Therefore, BIM was used to investigate the immunomodulatory effect on mucosal immune responses following oral administration of *Bifidobacterium* components.

2. MATERIALS AND METHODS

Animals. Female 6-week-old BALB/c mice were obtained from Clea Japan (Tokyo, Japan) and were housed in a room, with a 12h light-dark cycle. The mice were naturalized and given MF diet (Oriental Yeast, Tokyo, Japan) before experiments for 3 days. All mice were kept in accordance with the Nihon University guidelines for care of laboratory animals.

Preparation of Bifidobacterium immunomodulator (BIM) derived from sonicated B. pseudocatenulatum 7041, and oral administration of BIM. Sonicated *B. pseudo catenulatum* 7041 was prepared by the method described in the previous report [4]. Mice were orally administered a dose of 10 mg/day of BIM in saline by using a feeding-tube for 7 days. The mice of control group were given saline by the same feeding of tubing. Mice were allowed free access to a pelleted MF diet and sterile deionized water throughout the experimental period.

Preparation of CD4⁺ T cells from PP, and APC from splenocytes. After 7 days oral administration of BIM, PP cells were obtained from each experimental group, and CD4⁺

T cells were isolated by magnetic cell sorting (MACS; Miltenyi Biotec, Bergisch Gladbach, Germany) with anti-mouse CD4-conjugated magnetic microbeads and an LS column following the manufacturer's instructions. APC derived from splenocytes of BALB/c mice, which had no experimental feeding. The cell suspensions of splenocytes were treated with 50 µg/ml mitomycin C (Sigma, St. Louis, MO).

Flow cytometric Analysis. Flow cytometric analysis of CD4⁺ cells was performed using FACScalibur flow cytometer (Becton Dickinson, San Jose, CA) and staining with anti-TCRαβ-biotin, anti-CD4-FITC, and either PE-, anti-CD45RB, anti-CD44, or anti-CD69. Fc receptors (FcγRIII/II) were blocked using anti-mouse CD16/CD32. The above Abs purchased from BD PharMingen. Isotype-matched negative controls were included in the analysis of the cells suspensions. Analysis was done on the Cellquest software. Purity CD4⁺ cells from PP were >93% pure (data not shown).

Preparation of insensitive Thy1.2⁻ PP cells. Thy1.2 (CD90) negative PP cells were isolated by MACS with anti-mouse CD90-conjugated magnetic microbeads and LS column. Insensitive Thy1.2⁻ PP cells derived from PP of BALB/c mice, which had not been given the experimental diet. The isolation technique were as identified above. We checked freedom from CD90 expression cells in Thy1.2⁻ PP cells by FACS (data not shown).

Measurement of total IgA. Total IgA in the culture supernatant was measured by sandwich ELISA. PP cells given the experimental groups were plated on a 48-well plate at 2.5×10^6 cells, and co-culture with 0, 10, 50 µg/ml BIM in RPMI 1640 medium containing 5% fetal bovine serum. CD4⁺ T cells from PP from experimental mice (1×10^6 cells/well) in a total volume of 1 ml were cultured with similar dose of BIM in the presence of insensitive Thy1.2⁻ PP (4×10^6 cells/well) cells from not experimental mice in a 48-well plate. The culture supernatants were collected after 5-7 days for measurement of total IgA. The amounts of total IgA in the supernatants were measured by means of a sandwich ELISA method described as a previous report [4].

Measurement of BIM-specific IgA. BIM-specific IgA was measured by ELISA. Plates were coated with 50 µl of 100 µg/ml BIM. Subsequence handling followed as described above. BIM-specific IgA was qualitatively determined by absorbance at 405 nm.

Culture and cytokine determinants. CD4⁺ T cells from PP cells from experimental mice (2×10^6 cells/well) in a total volume of 1 ml were cultured with 0, 10, and 50 µg/ml BIM in the presence of APC derived splenocytes (8×10^6 cells/well) in RPMI 1640 medium containing 5% FCS in a 48-well plate. The culture supernatants were collected after 24 or 72h and assayed for IL-12 p40 and for IL-5, IL-6, and IFN-γ, respectively. The amounts of IL-5, IL-6, and IFN-γ in the supernatants were measured by means of a sandwich ELISA method described as a previous report [4]. IL-12 measured using OptEIA mouse IL-12 (p40) set (BD PharMingen).

Statistical analysis. Data are expressed as means \pm SD. Differences were examined by one-way analysis of variance (ANOVA), and significant differences found between groups were further evaluated by Tukey's test (SPSS Ver. 10.0, Chicago, IL, USA). Differences were considered significant at $P<0.05$.

3. RESULTS

Total IgA production and BIM-specific IgA of PP cells after BIM administration

There was no significant increase body weight gain among the experimental groups (data not shown). We examined total IgA production by PP cells derived from the experimental mice during a 7-days primary cells culture with different dose of BIM. PP cells had been prepared from the experimental mice. The total IgA production by PP cells of BIM-fed groups was higher than that of control groups all of dose of BIM in vitro. In addition, BIM-specific IgA production by PP cells was enhanced by oral administration of BIM.

Table 1. Effects of oral administration of BIM on total IgA production from murine PP.

BIM stimulation (μ g/ml)	Cont.	BIM-fed.
	Total IgA production	
0	\pm	++
10	+	++
50	+	++
	BIM-spe IgA production	
0	\pm	\pm
10	+	++
50	+	++

PP cells were obtained and pooled for each experimental group respectively, and then the cells were cultured with 0-50 μ g/ml of BIM for 7 days. Total IgA in the culture supernatants was measured by ELISA. BIM-specific IgA in the culture supernatants was qualitatively measured by ELISA. ++, +, \pm was judged based on the results on more than 3 experiments.

PP cells were obtained and pooled for each experimental group respectively, and then the cells were cultured with 0-50 μ g/ml of BIM for 7 days. Total IgA in the culture supernatants was measured by ELISA. BIM-specific IgA in the culture supernatants was qualitatively measured by ELISA. ++, +, \pm was judged based on the results on more than 3 experiments.

Characteristic CD4⁺ T cells induced by oral administration of BIM.

We examined the cytokine production patterns of CD4⁺ T cells derived from PP cells, which were obtained from the oral administrated mice with or without BIM. The prepared CD4⁺ T cells were cultured with BIM in the presence of APC from naïve mice splenocytes in vitro, and the amounts of cytokine in the supernatants were measured. Both of IFN- γ and IL-6 secretion enhanced by administered BIM orally (data not shown). But, the secretion of IL-4 and IL-5 were not detected. To examine the effects of BIM feeding on the state of CD4⁺ PP T cells derived from experimental mice, we analyzed

purified CD4⁺ PP cells by flow cytometric analysis. Oral administration of BIM increased naïve-marker CD4⁺CD45RB^{high} expression cells (cont. 49.6±2.4, BIM-fed. 57.9±6.1). In contrast, activated-marker CD44 or CD69 were not significant difference from control (data not shown).

BIM-affected CD4⁺ T cells enhanced BIM-specific IgA but not induced total IgA.

We tried to demonstrate whether PP CD4⁺ T cells, which derived from BIM administered mice, induced IgA production in PP cells or not. Then, we prepared CD4⁺ T cells derived from BIM or control diet group, and the CD4⁺ T cells were cultured with insensitive Thy1.2⁻ PP cells from non-experimental mice in the presence of BIM respectively. Total IgA production of the culture soup showed not difference from control group. While on the other hand, BIM-specific IgA level in culture from BIM-fed group was higher than that from control group.

Table 2. Effects of activated CD4⁺ T cells by BIM administered on IgA production.

BIM stimulation (µg/ml)	Cont.	BIM-fed.
	Total IgA	
0	±	±
10	+	+
50	±	±
	BIM-spe IgA	
0	±	±
10	+	+++
50	±	++

PP CD4⁺ T⁺ cells were obtained and pooled for each experimental group respectively, then the cells were co-cultured with 0-50 µg/ml BIM in the presence of insensitive Thy1.2⁻ PP cells from not experimental mice for 7 days. Total IgA in the culture supernatants was measured by ELISA. BIM-specific IgA in the culture supernatants was qualitatively measured by ELISA. ++, +, ± was judged based on the results on more than 3 experiments.

4. DISCUSSION

We examined whether sonicated Bifidus components that have strong mitogenic activity influenced the ability of PP cells to produce IgA. We elucidate BIM administration up-regulated proliferation activity of PP cells *in vitro* (data not shown). These results indicate that orally administered BIM was taken up by M cells on the PP and then activated PP cells. We demonstrated that BIM-feeding enhanced cytokine

production, such as IFN- γ , IL-5, IL-6, and IL-12, in the PP cells (data not shown). We also observed that both total IgA and BIM-specific IgA production in the PP derived from BIM-fed animals was higher than that of control group. Additionally, our results show that secretion of both IFN- γ and IL-6 by CD4⁺ T cells were increased by BIM administration. Our results suggest that BIM-feeding induce increased cytokine production in PP cells including CD4⁺ T cells, which enhanced both total IgA and BIM-specific IgA production in the PP. Consequently, when BIM-affected CD4⁺ T cells cultured with insensitive Thy1.2⁻ PP cells from not experimental mice, BIM-specific IgA was increased. These results suggest that CD4⁺ T cells play an important role in induction of IgA production by BIM-feeding in the PP.

5. REFERENCES

- [1] J. Lee, A. Ametani, A. Enomoto, Y. Sato, H. Motosima, F. Ike, S. Kaminogawa, Screening for the immunopotentiating activity of the immune response by Bifidobacterium adolescentis M101-4, *Biosci. Biotech. Ciochem.* 57 (1993) 2127-2132.
- [2] A. Hosono, J. Lee, A. Ametani, M. Natsume, M. Hirayama, T. Adachi, S. Kaminogawa, Comparison of the Immunopotentiating Activity with Structural Characteristics among Water-soluble Polysaccharides Isolated from the Genus Bifidobacterium, *Bioscience Microflora.* 17 (1998) 97-104.
- [3] A. Hosono, J. Lee, A. Ametani, M. Natsume, M. Hirayama, T. Adachi, S. Kaminogawa, Characterization of a water-soluble polysaccharide fraction with immunopotentiating activity from Bifidobacterium adolescentis M101-4, *Biosci Biotechnol Biochem.* 61 (1997) 312-316.
- [4] A. Hosono, A. Ozawa, R. Kato, Y. Ohnishi, Y. Nakanishi, T. Kimura, R. Nakamura, Dietary fructooligosaccharides induce immunoregulation of intestinal IgA secretion by murine Peyer's patch cells, *Biosci Biotechnol Biochem.* 67 (2003) 758-764.

SUPPLEMENTATION OF SERICIN IS EFFECTIVE IN MAINTENANCE OF ISLET SURVIVAL AND FUNCTION UNDER SERUM-FREE CULTURE

Akiko Ogawa¹, Satoshi Terada¹, Masao Miki¹, Toshihisa Kimura², Akio Yamaguchi², Masahiro Sasaki³, and Hideyuki Yamada³

¹*Department of Applied Chemistry and Biotechnology, University of Fukui, 3-9-1 Bunkyo, Fukui 910-8507, Japan;* ²*Department of Surgery, Faculty of Medicine, University of Fukui, 23-3 Shimoaizuki, Matsuoka-cho, Yoshida-gun, Fukui 910-1193, Japan;* ³*Technology Department, Seiren Co., Ltd., 1-10-1 Keya, Fukui 918-8560, Japan*

Abstract: Diabetes is a chronic syndrome due to an insufficiency of insulin production or to insulin tolerance of the target tissue. Islet of Langerhans is the only tissue that produces insulin, the hormone reducing blood glucose level. Therefore islet transplantation is an extremely promising treatment for severe diabetes. Practical islet transplantations have been performed worldwide, including in Japan. However, isolated islets must be transplanted within several hours because their functions and viability reduce as time passes and a suitable islet-culture method for clinical treatment has not been established. Islets are usually cultured in FBS-supplemented medium but the use of FBS has several problems such as batch-to-batch variations and infection from several different pathogens. Therefore the development of a serum-free medium for islets culture is eagerly sought. In the present study, we examined the possibility of sericin as a supplement for islet culture. Rat islets were cultured in RPMI mediums containing sericin, FBS, or no supplement, and the concentration of rat insulin in their supernatants were then measured by ELISA. In the absence of a supplement, half the islets fell apart during culture, while 75% of islets cultured with sericin remained morphologically intact in the presence of sericin. Islets cultured with sericin maintained steady insulin production, while those cultured without supplement rapidly ceased insulin production.

Key words: diabetes, insulin, cell therapy, islet, sericin, serum-free culture

1. INTRODUCTION

More than 16 million people in Japan suffer from diabetes or incipient diabetes. There are some relevant treatments, such as diet therapy and exercise training, but the most effective treatment is insulin injection. However its effect is transient and so patients need to inject insulin daily; thus this treatment has the risk that patients will suffer hypoglycemia, a cause of coma bringing on a critical state if infected with a surfeit of insulin. Thus treatments for diabetes that are both permanent and safe are desired.

Pancreas transplantation or islet transplantation is the only effective treatment for complete recovery. While there is a strong risk of infection during pancreas transplantation surgery, islets can be easily transplanted by infusions [1, 2]. Therefore it is anticipated that islet transplantation will become an effective treatment for diabetes. Already, seven islet transplantations have been performed in Japan, and medical insurance is now applied to islet transplantation in Canada. In the US, Medicare, the tax supported system that provides medical care for old people, is about to be made applicable. Even so, some problems remain before islet transplantation will be established as a general treatment. The major problem is to how build an islet supply system [3, 4].

Pancreas islets are widely cultured in mediums containing fetal bovine serum (FBS). FBS, however, is unfavorable for islet culture because of the risk of virus infection and its batch-to-batch variations. To achieve a safe, high-quality islet culture system, alternative medium supplements have been urgently sought.

This study aimed to establish an effective FBS-independent islet culture for cell therapy. Previously, we reported that sericin improved the proliferation of various cells including mouse hybridoma [5]. In this work, we assess the usefulness of sericin as a novel supplement for serum-free islet culture.

2. MATERIALS AND METHODS

2.1 Rat islets isolation and culture

Rat islets were prepared by collagenase (Nitta Gelatin, Osaka, Japan) digestion, as described previously [6], from male Lewis rats (8-10 weeks old; Charles River Japan, Kanagawa). The obtained islets were cultured

in RPMI medium supplemented with 10% FBS for 2 - 10 days before the experiment proceeded.

2.2 Conditioned medium culture

Morphologically intact rat islets were selected under a stereoscopic microscope and transferred by a micropipette with a 20- μ l culture supernatant into each well of a 96-well round-bottom plate (Sumitomo Bakelite, Tokyo) containing 100 μ l of a fresh 10% FBS-supplemented RPMI medium. To study the effect of sericin on islet survival and insulin production, rat islets were cultured in this conditioned media, no-supplemented, sericin-supplemented, or FBS-supplemented RPMI medium. The medium was exchanged on day 3 according to the following procedure; single rat islets with 20- μ l culture supernatant were collected using a micropipette under a stereoscopic microscope. They were then rinsed with 1 ml of fresh medium with each supplement to take off the culture supernatant before they were transferred to each of the wells that contained 100- μ l fresh medium in a new 96-well round-bottom plate (Figure 1). The culture was ended when disintegration of islets was observed under a stereoscopic microscope.

2.3 INSULIN ANALYSIS

Insulin abundance in the culture supernatants was then determined by ELISA (Sibayagi, Gunma).

3. RESULTS AND DISCUSSION

All rat islets remained assembled until the first medium exchange (Figure 2). After that, four (33%) of the islets in the absence of supplement collapsed, while only two (17%) of them in the presence of sericin and one (8%) of those in the presence of FBS did. On day 6, 11 islets in the presence of FBS remained morphologically intact, while only half of them in the basal medium did. In the presence of sericin, 9/12 (75%) of the islets remained in a morphologically intact state.

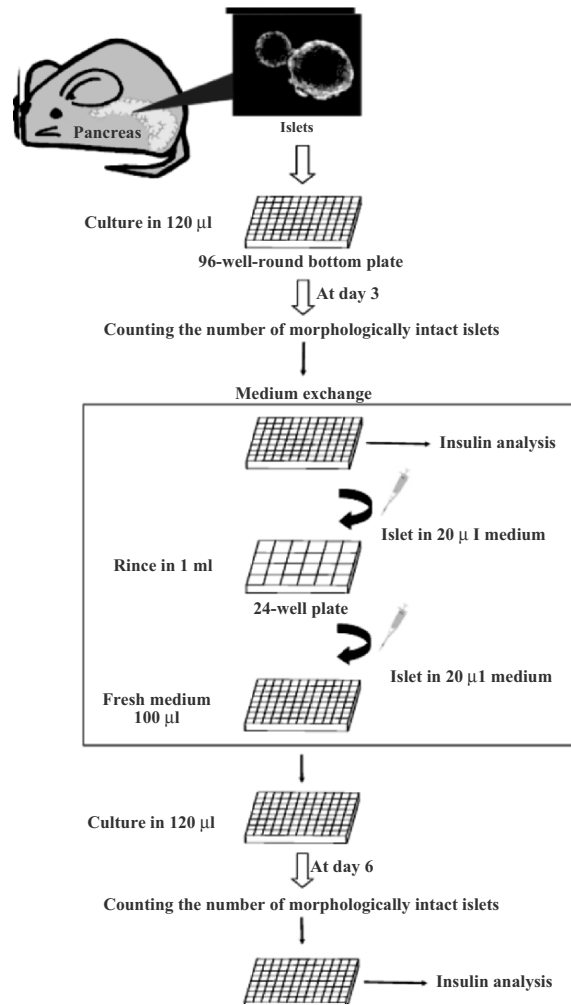


Figure 1. Flow chart of islet serum-free culture.

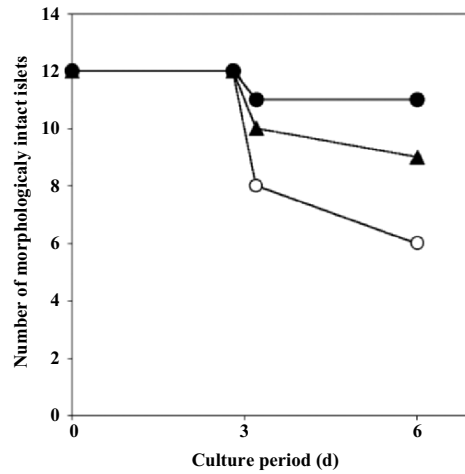


Figure 2. Survival of morphologically intact islets. Each islet was separately harvested into each well of a 96-well round plate. The islets were cultured in the presence of 10% FBS (closed circles), 0.01% sericin (open triangles), or in the absence of any supplement (open circles).

Insulin production of rat islets was measured by ELISA and the results are shown in figure 3. Islets in the presence of FBS produced abundant insulin and this high production was retained over the culture. Islets in the presence of sericin also maintained insulin production, though the amount of insulin was lower than in the presence of FBS. Islets cultured in the absence of any supplement produced only a small amount of insulin during the first 3 days (Figure 3a) and insulin production then ceased.

Most islets cultured in the presence of FBS maintained intact morphology and high insulin production during the culture, whereas only half of the islets cultured in the absence of FBS retained morphology and the insulin production in the culture with the absence of any supplement dramatically decreased. In the presence of sericin, islets successfully maintained morphology and insulin production, but the effects of sericin were inferior to those of FBS. The effects of sericin could be improved by raising the sericin concentration, because the culture of insulinoma produced more insulin in a higher concentration of sericin (data not shown). In conclusion, sericin is an effective medium supplement for islet serum-free culture.

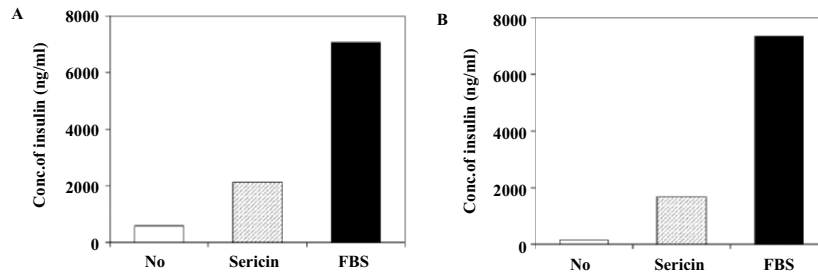


Figure 3. Islet insulin release. Cultured supernatants were collected on days 3 (A) and 6 (B). Insulin concentrations were determined by ELISA. Each column indicates the insulin concentration of each culture's supernatant. Closed, hatched, and open bars indicate islets cultured in the medium supplemented with 10% FBS, 0.01% sericin, and no supplement, respectively.

4. REFERENCES

1. Alejandro, R., Lehmann, R., Ricordi, C., Kenyon, N. S., Angelico, M. C., Burke, G., Esquenazi, V., Nery, J., Betancourt, A. E., Kong, S. S., Miller, J., and Mintz, D. H. (1997) Long-term function (6 years) of islet allografts in type 1 diabetes, *Diabetes*, 46, 1983-1989.
2. Shapiro, A. M., Lakey, J. R., Ryan, E. A., Korbitt, G. S., Toth, E., Warnock, G. L., Kneteman, N. M., and Rajotte, R. V. (2000) Islet transplantation in seven patients with type 1 diabetes mellitus using a glucocorticoid-free immunosuppressive regimen, *N. Engl. J. Med.*, 343, 230-238.
3. Zwiilich, T. (2000) Islet transplants not yet ready for prime time, *Science*, 289, 531-533.
4. Burridge, P. W., Shapiro, A. M. J., Ryan, E. A., and Lakey, J. R. T. (2002) Future trends in clinical islet transplantation, *Transplant. Proc.*, 34, 3347-3348.
5. Terada, S., Nishimura, T., Sasaki, M., Yamada, H., and Miki, M. (2002) Sericin, a protein derived from silkworms, accelerates the proliferation of several mammalian cell lines including a hybridoma, *Cytotechnology*, 40, 3-12.
6. Gotoh, M., Maki, T., Kiyozumi, T., Satomi, S., and Monaco, A. P. (1985) An improved method for isolation of mouse pancreatic islets, *Transplantation*, 40, 437-438.

SUPPRESSION OF TWO-STAGE CELL TRANSFORMATION BY ELECTROLYZED REDUCED WATER CONTAINING PLATINUM NANOPARTICLES

Ryuhei Nishikawa¹, Kiichiro Teruya^{1,2}, Yoshinori Katakura^{1,2}, Kazumichi Otsubo³, Shinkatsu Morisawa³, Qianghua Xu^{1,4} and Sanetaka Shirahata^{1,2}

¹Graduate School of Systems Life sciences, Kyushu University; ²Department of Genetic Resources Technology, Faculty of Agriculture, Kyushu University, 6-10-1 Hakozaki, Higashi-ku, Fukuoka 812-8581, Japan; ³Nihon Trim Co.Ltd., 1-8-34 Oyodonaka, Kita-ku, Osaka 531-0076, Japan; ⁴College of Life Sciences, Zhejiang University, No. 268 Kaixuan Road, Hangzhou 310029, Zhejiang, P.R. China

Abstract: According to the two-stage cell transformation theory, cancer cells first receive initiation, which is mainly caused by DNA damage and then promotion, which enhance transformation. Since murine Balb/c 3T3 cells lose contact inhibition by cell transformation, the cells have been widely used for transformation experiments. Electrolyzed reduced water (ERW) is a health beneficial alkaline drinking water containing high concentration of dissolved hydrogen, and can scavenge intracellular reactive oxygen species (ROS). ERW contains a small amount of platinum (Pt) nanoparticles as atomic hydrogen donor and ROS-scavenger. Therefore, ERW supplemented with Pt nanoparticles (ERW/Pt) can be considered as a model of strong ERW. Here, we report that ERW/Pt can prevent transformation of Balb/c 3T3 cells. ERW was prepared by electrolysis of 0.002 M NaOH. Balb/c 3T3 cells were treated with 3-methyl cholantrene (MCA) as an initiation compound, followed by the treatment with phorbol-12-myristate-13-acetate (PMA) as a promotion compound. The cell transformation induced by MCA/PMA was strongly suppressed by ERW/Pt treatment, especially at the stage of promotion. Analysis of intracellular ROS level showed that ERW/Pt could decrease excess intracellular ROS induced by PMA. These results suggested that ERW/Pt suppressed cell transformation at promotion stage by its ROS scavenging effect.

Key words: active hydrogen; Balb/c 3T3 cells; electrolyzed reduced water; platinum nanoparticles; reactive oxygen species; two-stage cell transformation

1. INTRODUCTION

Intracellular ROS cause irreversible damage to biological macromolecules, resulting in many diseases and cell transformation¹. Electrolyzed reduced water (ERW) is a health beneficial alkaline drinking water which contains high concentration of dissolved hydrogen, and can scavenge intracellular ROS²⁻⁵. ERW was known to improve various diseases such as diabetes^{5,6}, angiogenesis and cancer, and reduce hemodialysis-induced oxidative stress in end-stage renal disease patients⁷. We have revealed that ERW contains a small amount of platinum (Pt) nanoparticles as atomic hydrogen (active hydrogen) donors and ROS-scavengers. Therefore, ERW containing synthesized Pt nanoparticles (ERW/Pt) can be considered as a model of strong ERW. *In vitro* cell transformation assay with Balb/3T3 or C3H10T1/2 cells, has been recognized as being directly relevant to carcinogenesis⁸⁻¹⁰ and regarded as a useful method for the screening of potential carcinogens¹¹⁻¹³. According to the two-stage cell transformation theory, normal cells first receive initiation, which is mainly caused by DNA damage, and then promotion, which enhances cell transformation¹⁴. Here, we report that ERW/Pt can prevent cell transformation of Balb/c 3T3 cells.

2. MATERIAL AND METHODS

2.1 Cell culture

A murine cell line, Balb/c 3T3 A31-1-1 cells was obtained by Japanese Collection of Research Bioresources, and were cultured in a MEM medium (Nissui Pharmaceutical Co. Ltd., Tokyo Japan) supplemented with 10% fetal bovine serum (FBS) at 37°C in a humidified atmosphere of 5 % CO₂.

2.2 ERW, platinum nanoparticles and preparation of medium

ERW preparation was previously described⁵. Briefly, ERW was prepared by electrolysis of 0.002 M NaOH for 1 hr. using a batch-type electrolysis device (Type TI-200S, Nihon Trim Co., Osaka, Japan). Platinum nanoparticles of average size 2 nm were obtained from SENEKA Co., Tokyo, Japan. In order to investigate the two-stage cell transformation assay, culture medium was prepared using ERW instead

of Milli-Q water, and then filtrated by 0.22- μm membrane for sterilization.

2.3 Two-stage cell transformation assay

Balb/c 3T3 cells (1.0×10^4 cells ml^{-1}) were inoculated into 60-mm culture dish. Next, the cells were cultured in the presence of $1.0 \mu\text{g ml}^{-1}$ 3-methyl cholantrene (MCA) from day 1 to day 3 as the initiation stage. After initiation, the cells were cultured with 300 ng ml^{-1} phorbol-12-myristate-13-acetate (PMA) from day 6 to day 21 as the promotion stage. Culture medium was changed every 3 or 4 days intervals. When the culture period reached to 25 ~ 35 days, cells were fixed using methanol and Giemsa stain was performed. Transformed foci were observed by naked eyes, and focus numbers and their sizes were measured. ERW supplemented with various concentrations of Pt nanoparticles were added in the culture medium from day 1 to day 21 and the effect against two-stage transformation was compared.

2.4 Measurement of intracellular ROS

Amount of intracellular ROS, especially the intracellular H_2O_2 produced by PMA was determined by using a fluorescent dye, 2',7'-dichlorofluorescein-diacetate (DCFH-DA)⁵. Balb/c 3T3 cells were incubated for 15 min in the MEM medium with 300 ng ml^{-1} PMA with or without ERW/Pt. After removal of the supernatant, the cells were incubated in $5 \mu\text{M}$ DCFH-DA in Ca^{2+} , Mg^{2+} -free Hank's balanced salt solution for 10 min. The cells were then harvested by trypsinization, washed with PBS, resuspended in PBS and analyzed immediately using a flow cytometer with excitation and emission wavelength of 495 and 525 nm, respectively. Gating was performed to remove cellular debris and apoptotic cells before data were collected.

2.5 Statistical analysis

Statistical analysis was done using the Student's *t*-test. Probabilities of 0.05 or less were considered statistically significant. Statistically significant was represented as *; $P < 0.05$ and ***; $P < 0.005$, compared with treatment of MCA/PMA only.

3. RESULT AND DISCUSSION

3.1 Co-treatment of ERW/Pt suppresses two-stage cell transformation foci

Few foci appeared in the control without MCA/PMA treatment. In the presence of MCA/PMA treatment, many large foci significantly appeared in the culture dishes. Appearance of transformation foci was strongly suppressed by treatment of ERW/Pt (Table 1). Transformation foci were suppressed by addition of Pt nanoparticles to ERW in concentration-dependent manner. ERW supplemented with 1 ppm, 3 ppm and 10 ppm of Pt nanoparticles showed 57.1%*, 65.4%* and 100%*** of transformation foci suppression compared with MCA/PMA only, respectively. However, Pt nanoparticles without ERW could not effectively suppress cell transformation induced by MCA/PMA. It suggested that both ERW and Pt nanoparticles were needed to suppress two-stage cell transformation.

Table 1. Co-treatment of ERW/Pt suppresses two-stage cell transformation foci

MCA/PMA	Treatment	Foci/Dish (Mean \pm SD)	% of Transformation
-	-	1.3 \pm 0.57	2.5*
+	-	52 \pm 10.8	100
+	Pt 1 ppm	57 \pm 7.1	109.6
+	Pt 3 ppm	42 \pm 2.0	80.8
+	Pt 10 ppm	51.7 \pm 5.1	99.4
+	ERW/Pt 1 ppm	22.3 \pm 3.5	42.9*
+	ERW/Pt 3 ppm	18 \pm 1.6	34.6*
+	ERW/Pt 10 ppm	0 \pm 0	0***

*: $P < 0.05$, ***: $P < 0.005$

3.2 ERW/Pt suppress transformation at promotion stage

Treatment of ERW containing 10 ppm of Pt nanoparticles suppressed the cell transformation at the stage of promotion but not at the stage of initiation. ERW containing no synthesized Pt nanoparticles could not suppress the cell transformation. On the treatment of both ERW and Pt nanoparticles, the amounts of transformation foci were suppressed to 1.4%*** at promotion stage, compared to the MCA/PMA treatment only. During all stage treatment of ERW/Pt, transformation was suppressed to 4.3%***. However, the transformation foci were not sufficiently suppressed to 91.3% by the ERW/Pt treatment at initiation stage only. It was almost similar value (91.3%) compared to the MCA/PMA treatment only (Figure 1). Since PMA was well known as a strong inducer of intracellular ROS, it was suggested that both ERW and Pt nanoparticles suppressed the augmentation of intracellular ROS induced by PMA.

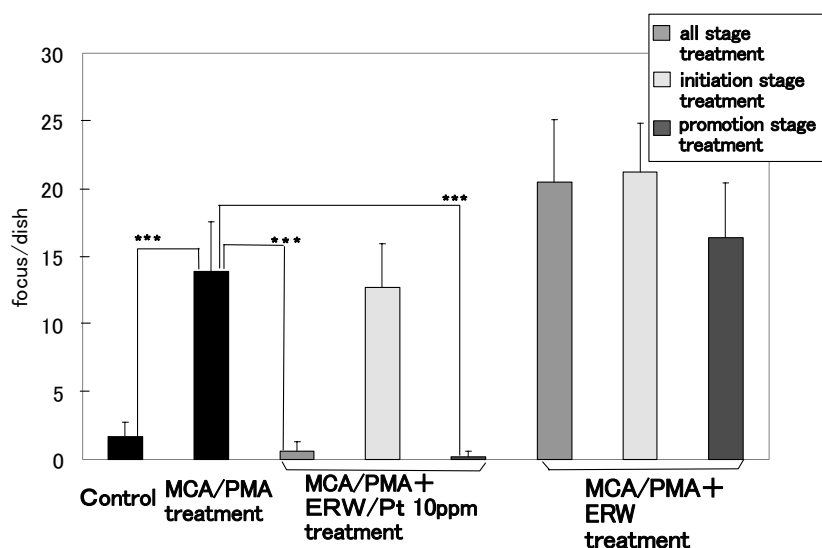


Figure 1. ERW/Pt suppressed cell transformation at promotion stage
 *** $P < 0.005$ compared with MCA and PMA only.

3.3 ERW/Pt did not suppress growth of Balb/c 3T3 cells

To clarify the effect of ERW/Pt on cell proliferation of Balb/c 3T3 cells, the cell growth was examined in the presence of ERW, Pt nanoparticles and both. The growth curve of Balb/c 3T3 cells under the all conditions showed no difference (data not shown). Therefore, ERW, Pt nanoparticles and both did not affect proliferation of Balb/c 3T3 cells, the treatment of ERW/Pt suppressed cell transformation without growth arrest or cell death. The cells treated with only ERW slightly grew faster than control (data not shown).

3.4 ERW/Pt suppress the augmentation of intracellular ROS induced by PMA as well as ascorbic acid-2-phosphate (ASA-2P)

ASA-2P suppress the transformation foci under the condition of $0.2 \mu\text{g ml}^{-1}$ of MCA initiation from day 1 to day 3 and 100 ng ml^{-1} of PMA promotion from day 6 to day 21 (data not shown). ASA-2P is a stable antioxidant, and suppressed Balb/c 3T3 two-stage cell transformation in promotion stage¹⁵. The treatment of ERW with 1 ppm of Pt nanoparticles

suppressed cell transformation stronger than 100 μ M ASA-2P (data not shown). To evaluate the intracellular ROS scavenging effect of ERW/Pt, intracellular ROS was induced by the PMA treatment for 15 min and determined by using DCFH-DA and flow cytometer (Figure 2). ASA-2P, ERW, Pt nanoparticles and ERW/Pt significantly reduced excess intracellular ROS induced by PMA treatment. We have revealed that ERW contains a small amount of Pt nanoparticles as active hydrogen donors and ROS-scavengers^{2,5}. These results suggested that ERW/Pt acted as antioxidant in the cells and suppressed tumorigenesis.

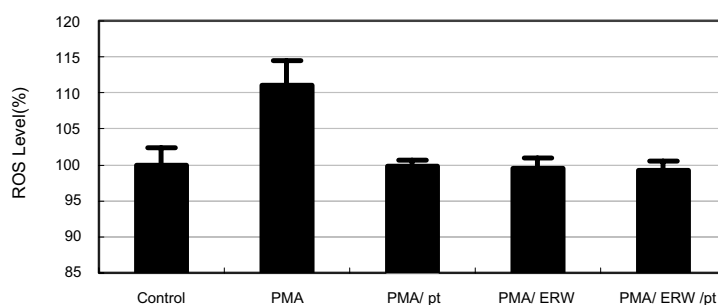


Figure 2. ERW/Pt suppressed intracellular ROS 15 min after PMA treatment. Values were statistically significant at $P < 0.005$ compared with samples additionally treated with PMA.

It was suggested that active hydrogen produced from hydrogen molecules by catalysis on the surface of Pt nanoparticles would scavenge intracellular ROS. ERW/Pt also suppressed ERK^{MAPK} phosphorylation and excess intracellular ROS induced by PMA in murine epidermal JB6 cells (data not shown). In the recent study, intracellular ROS was known to activate MAP kinase, such as ERK^{MAPK} phosphorylation, and then AP-1, NF κ B, iNOS and NOS were activated by MAP kinase. This cascade was related to the cell transformation in promotion stage¹. It was suggested that suppression mechanism for cell transformation of ERW/Pt was similar to effective antioxidant for tumorigenesis such as ASA-2P via reducing excess intracellular ROS.

In conclusion, this is the first report about the suppression of two-stage cell transformation by ERW/Pt nanoparticles. We confirmed that ERW/Pt could scavenge excess intracellular ROS and strongly suppressed cell transformation at promotion stage. The detailed action mechanism of the reducing agents in ERW responsible for the ROS scavenging activity will be reported elsewhere.

4. REFERENCES

1. Dhar, A., Young, M.R., and Colburn, N.H., *Mol. Cell. Biochem.* 234-235: 185-193 (2002).
2. Shirahata, S., Kabayama, S., Nakano, M., Miura, T., Kusumoto, K., Gotoh, M., Hayashi H., Otsubo, K., Morisawa, S., and Katakura, Y., *Biochem. Biophys. Res. Commun.* 234: 269-274 (1997).
3. Shirahata, S., Nishimura, T., Kabayama, S., Aki, D., Teruya, K., Otsubo, K., Morisawa, S., Ishii, Y., Gadek, Z., and Katakura, Y., Anti-Oxidative Water Improves Diabetes, in: *Animal Cell Technology: From Target to Market*, Linder-Olsson, E., et al. eds., (Kluwer Academic Publishers, Dordrecht, 2001), pp. 574-577.
4. Hanaoka, K., *J. Appl. Electrochem.* 31: 1307-1313 (2001).
5. Li, Y., Nishimura, T., Teruya, K., Maki, T., Komatsu, T., Hamasaki, T., Kashiwagi, T., Kabayama, S., Shim, S.-Y., Katakura, Y., Osada, K., Kawahara, T., Otsubo, K., Morisawa, S., Ishii, Y., Gadek, Z., and Shirahata, S., *Cytotechnology* 40: 139-149 (2002).
6. Oda, M., Kusumoto, K., Teruya, K., Hara, T., Maki, T., Kabayama, Y., Katakura, Y., Otsubo, K., Morisawa, S., Hayashi, H., Ishii, Y. and Shirahata, S., Electrolyzed and natural reduced water exhibit insulin-like activity on glucose uptake into muscle cells and adipocytes, in: *Animal Cell Technology: Products from Cells, Cells as Products*, Bernard, A., et al. eds., (Kluwer Academic Publishers, Dordrecht, 1999), pp. 425-427.
7. Huang, K. C., Yang, C. C., Lee, K. T., and Chien, C. T., *Kidney Int.* 64: 704-714 (2003).
8. Kakunaga, T., *Int. J. Cancer* 12: 463-473 (1973).
9. Kennedy, A. R., Promotion and other interactions between agents in the induction of transformation *in vitro* in fibroblasts, in: *Mechanisms of Tumor Promotion, Vol. III, Tumor Promotion and Carcinogenesis in Vitro*, Slaga, T. J., ed., (CRC Press, Boca Raton, 1984), pp. 13-55.
10. Heidelberger, C., Freeman, A. E., Pienta, R. J., Sivak, A., Bertram, J. S., Casto, B. C., Dunkel, V. C., Francis, M. W., Kakunaga, T., Little, J. B., and Schechtman, L. M., *Mutat. Res.* 114: 283-385 (1983).
11. Dunkel, V. C., Pienta, R. J., Sivak, A., and Traul, K. A., *J. Natl. Center Inst.* 67: 1303-1312 (1981).
12. Meyer, A. L., 1983, *Mutat. Res.* 115: 323-338 (1983).
13. Atchison, M., Chu, C., Kakunaga, T., and Van Duuren, B. L., *J. Natl. Cancer Inst.* 69: 503-508 (1982).
14. Tsuchiya, T., and Umeda, M., *Carcinogenesis* 16: 1887-1894 (1995).
15. Tsuchiya, T., Kato-Masatsuji, E., Tsuzuki, T., and Umeda, M., *Cancer Lett.* 160: 51-58 (2000).

INFLUENCE OF BOTH GLUCOSE AND GLUTAMINE CONCENTRATION ON MAB PRODUCTION RATE IN CHEMOSTAT CULTURE OF CHO CELLS

Hiroshi Matsuoka, Jun-ya Watanabe, and Toshiya Takeda

*Department of Biosciences, Teikyo University of Science and Technology,
2525 Uenohara, Yamanashi 409-0193, Japan*

Abstract: Chemostat culture for non-adhesive r-CHO at the wide range of glucose and glutamine feed concentration was carried out in the non-serum media. It was shown that the metabolic conditions were changed by the change of residual glucose and residual glutamine concentration. The specific mAb production rate was independent of glucose concentration, but increased in low glutamine concentration. Intracellular fluxes were estimated from extracellular utilization and production rates. It was elucidated that in low glutamine concentration, fluxes of glycolysis and the TCA cycle were accelerated, and the flux of the direct pathway to α -ketoglutarate increased with decrease of glucose concentration, however the flux of glutamine decomposition was not influenced by glucose concentration.

Key words: CHO, chemostat culture, metabolic engineering, glutamine, glucose

1. INTRODUCTION

Glucose concentration influences the cell metabolism that governs cell growth and monoclonal antibody productivity. Glutamine is also an essential amino acid that provides a major energy source in mammalian cells. It plays the role of both carbon and nitrogen sources. The concentration of glutamine strongly influences the cell metabolism that governs cell growth and monoclonal antibody productivity. Many experiments have been carried out in order to understand the relationship between glucose and glutamine concentrations and cell metabolism, however the quantitative relationship remains unclear (Vriezen, N. and J. P. Dijken (1998), Matsuoka et al. (2001)). Recently, the technique for

calculating metabolic fluxes has been developed and we applied it in our experiments. In this study a chemostat culture was examined in the wide range of glutamine and glucose feed concentration and change of the metabolism by using metabolic flux technique was examined.

2. MATERIALS AND METHODS

A non-adhesive recombinant CHO was used in this experiment. It was cultured in a 1.5 L fermentor with a 800 mL working volume at $37 \pm 0.1^\circ\text{C}$. The values of pH and DO were maintained at 7.2 and 40% of air saturation by CO_2 and O_2 influx through teflon sparger, respectively. Agitation speed was 100 rpm. A chemically defined fresh medium, which was based on IMDM medium and 1% PSN antibiotics mixture, was continuously supplied ($D= 0.30 \text{ d}^{-1}$). Concentrations of glucose, glutamine, glutamate, lactate, and ammonia were measured by Nova Bioprofile400 biochemical analyzer. Other amino acids concentrations were determined by HPLC. Intracellular fluxes were estimated by using the modified metabolic engineering method on the basis of Europa et al. (2000). When the stoichiometric matrix of mass balance, A , was constructed, the metabolic flux vector, x , is,

$$x=(A^T\Psi-I_A)^{-1}A^T\Psi-Ir$$

where r and Ψ are the specific rate vector and the correlation matrix, respectively. The simultaneous equations are constructed by 34 components and 30 equations. The composition of amino acids was used reference data (Akimoto et al. (1997)).

3. RESULTS AND DISCUSSION

Experimental data were collected under seven kinds of steady state conditions (Table 1); residual glutamine concentration was constant and residual glucose concentration was changed (a-e), and residual glutamine concentration was constant and residual glucose concentration was changed (a, f, and g).

Table 1. Glucose and glutamine concentration on glucose limited steady state condition

		a	b	c	d	e	f	g
glucose	feed	23.20	11.80	7.65	2.35	1.14	23.55	23.45
	residual	12.10	0.46	0.23	0.03	0.01	9.83	13.75
glutamine	feed	6.92	8.00	6.72	7.09	7.96	3.56	0.11
	residual	3.14	2.08	2.68	1.91	2.00	0.29	0.00

Figure 1(a) shows that specific rates of glucose uptake and lactate production increase with residual glucose up to 0.5 mM. They are constant more than 0.5 mM of residual glucose. Specific rates of glutamine uptake and ammonia production decrease with residual glucose up to 0.05 mM. They are constant more than 0.05 mM of residual glucose. Figure 1(b) shows that specific rates of glucose uptake and lactate production decrease with residual glutamine. However, specific rates of glutamine uptake and ammonia production are constant in high residual glutamine ($C_{gln} > 0.4$ mM). Figure 2(a) and 2(b) show specific mAb production rates. There are no residual glucose dependency changes of specific mAb production rate. However specific mAb production rate is influenced by residual glutamine concentration. It is rather higher in low glutamine concentration.

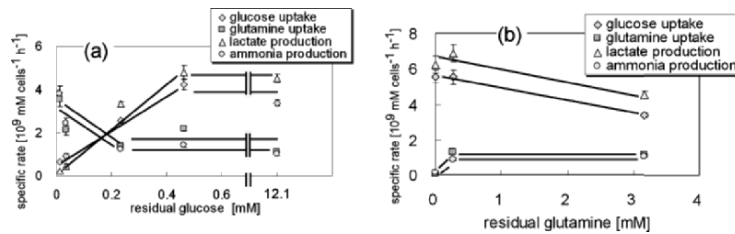


Figure 1. (a) Glucose, and (b) glutamine dependency changes of specific rates

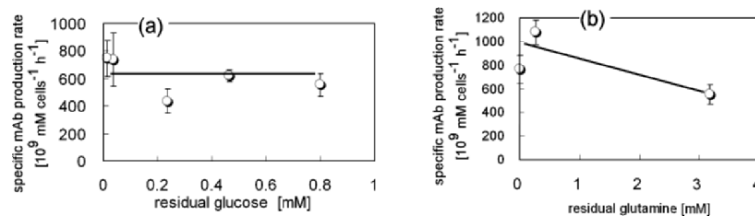


Figure 2. (a) Glucose, and (b) Glutamine dependency mAb production rate

Intracellular fluxes were estimated from extracellular utilization and production rates. Figure 3(a) shows that flux profile of glucose to pyruvate is as same as that of pyruvate to lactate. Up to 0.4 mM of residual glucose, fluxes of glucose to pyruvate and pyruvate to lactate increase with residual glucose. More than 4 mM of glucose these two fluxes are constant. The flux of pyruvate to acetyl-CoA does not influenced on residual glucose. All fluxes as shown in figure 3(b) decrease according to increase of residual glutamine. Figure 4(a) shows that there is no residual glucose concentration dependency changes of

the TCA related fluxes. The TCA related fluxes decrease with increase of residual glutamine as shown in figure 4(b). Figure 5(a) shows that glutamine flux to glutamic acid does not change in the experimental range and glutamic acid flux to α -keto glutalate decreases according to residual glutamine and almost zero more than 0.2 mM glutamine. Figure 5(b) shows that these two fluxes show the same profile. In high glutamine (>0.5 mM) they are not influenced by glutamine concentration, in low glutamine they converge to zero.

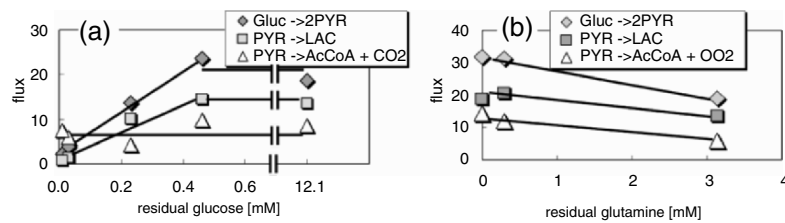


Figure 3. Estimated glycolysis related metabolic fluxes (a) glucose, and (b) glutamine dependency changes

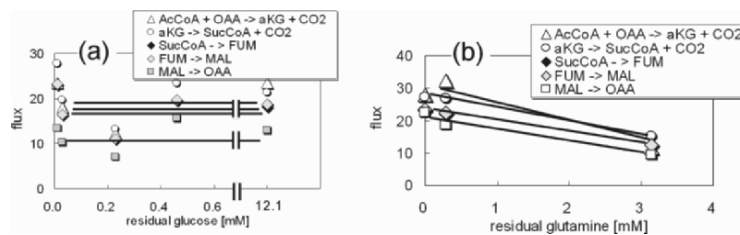


Figure 4. Estimated the TCA cycle related metabolic fluxes (a) glucose, and (b) glutamine dependency changes

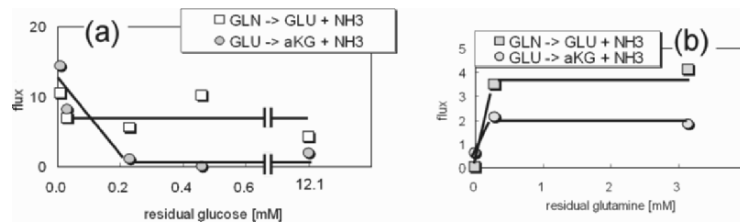


Figure 5. Estimated glutaminolysis related metabolic fluxes (a) glucose, and (b) glutamine dependency changes

4. CONCLUSION

Chemostat culture for non-adhesive r-CHO at the wide range of glucose and glutamine feed concentration was carried out in the non-serum media. It was shown that the metabolic conditions were changed by the change of residual glucose and residual glutamine concentration. The specific mAb production rate was independent of glucose concentration, but increased in low glutamine concentration. Intracellular fluxes were estimated from extracellular utilization and production rates. It was elucidated that in low glutamine concentration, fluxes of glycolysis and the TCA cycle were accelerated, and the flux of the direct pathway to α -ketoglutarate increased with decrease of glucose concentration, however the flux of glutamine decomposition was not influenced by glucose concentration.

5. REFERENCES

- Akimoto, K., Okayasu, T., Ikeda, M., Sorimachi, K., 1997, The amino acid composition of mammalian and bacterial cells. *Amino Acids* 13: 379-391
- Europa, A. F., Gambhir, A., Fu, P-C., Hu, W-S., 2000, Multiple Steady states with distinct cellular metabolism in continuous culture of mammalian cells. *Biotechnol. Bioeng.* 67: 25-34
- Matsuoka, H., Andoh, S., Matsuda, Y., Kaneko, H., Takeda, T., 2001, Influences of glutamine concentration on cellular metabolism in continuous culture of hybridoma. In: *Animal Cell Technology: From Target to Market*, Linder-Olsson, E., Chatzissavidou, N., and Luellau, E. eds., Kluwer Academic Publishers, Dordrecht, pp 175-178
- Vriezen, N., Bastiaan, R., Luyben, K. Ch. A. M., Dijken, J. P. 1997, Effects of glutamine supply on growth and metabolism of mammalian cells in chemostat culture. *Biotechnol. Bioeng.* 54: 272-286

INTRODUCTION OF GENES RELATING TO MUSCULAR DYSTROPHY INTO CHIMERIC CHICKENS BY EMBRYO ENGINEERING

Introduction of Chicken Muscular Dystrophy Gene

Akira Fujiwara^{1),2)}, Makoto Mizutani¹⁾, Tamao Ono²⁾, Hiroshi Kagami²⁾

¹⁾*Nippon Institute for Biological Science, Laboratory Animal Research Station, Kobuchisawa, Yamanashi 408-0041, Japan;* ²⁾*Shinshu University, 8304 Minamiminowa, Nagano 399-4598, Japan*

Abstract: A novel system has been developed to introduce genes relating to muscular dystrophy to chimeric chickens. Fertilized eggs were obtained from New Hampshire chicken; NH-413 strain which have genes relating to Fukuyama type muscular dystrophy. Blastoderms were isolated from these embryos. Cells from the center of area pellucida were specifically isolated from the blastoderms. Excess yolk were removed by PBS and only pluripotent cells were obtained. These cells were used as donor. Recipient embryos were obtained from White Leghorn chicken; Line-M. Approximately 700 cells were removed from the center of the area pellucida of the recipient in stage X blastoderm. The donor cells were microinjected into the subgerminal cavity of the recipients' blastoderms. The manipulated embryos were cultured *ex vivo* until hatching. The generated chimeric chickens had the donor derived brown plumage in the down, suggesting that the cells containing muscular dystrophy were introduced into the chimeras. These chimeric chickens will be raised until sexual maturity. The chimeric chickens will be back-crossed to donor strain; the New Hampshire. In case, these individuals would be germline chimeras, the New Hampshire's offspring would be breed very rapidly. These should be one of the powerful strategies for breeding and regeneration of chickens for an experimental animal model.

Key words: avian; pluripotent cells; cell culture

1. INTRODUCTION

Muscular dystrophy refers to a group of inherited diseases marked by progressive weakness and degeneration of the skeletal, or voluntary, muscles that control movement (Partridge, 1991). The diseases are associated with mutation in the genes encoding several classes of muscle proteins, whose purpose is to maintain the normal function face of the membrane of muscle cells (Imamura et al., 2000). The disease is one of

the most important diseases to be effectively treated. However, there is few clinical treatment for complete recovery. Animal models for the etiological and pathological studies of human muscular dystrophies have been established in mice, dogs and cats (Nonaka, 1998; Partridge, 1991). The diseases symptoms and conditions are not identical among these species because of different pathological manifestations of similar genetic defects. Therefore, establishing additional models will contribute to a better understanding of the mechanisms of muscular dystrophies and provide a basis and applied strategy for clinical therapy trials for such incurable diseases.

Chicken muscular dystrophy with abnormal muscles was first reported in 1956 (Asmundson and Julidan, 1956). The disorder is transmitted codominantly by a single gene, whose phenotype is modified by other “background” genes (Asmundson and Julian, 1956; Kikuchi, T. *et al.* 1981; Wagner, *et al.* 1970). A New Hampshire chicken; Nh-413 strain which have candidate genes relating to Fukuyama type muscular dystrophy was found. The origin (Swift, 1914; Sutasurya *et al.*, 1983; Ginsburg and Eyal-Giladi, 1987; Pardanaud *et al.*, 1987; Urven *et al.*, 1988; Ginsburg and Eyal-Giladi, 1989; Karagenc *et al.*, 1995; Kagami *et al.*, 1997), migratory pathway (Meyer, 1964; Fujimoto, *et al.*, 1976; Ando and Fujimoto, 1983; Muniesa and Dominguez, 1990; Yasuda *et al.*, 1992), collection of pluripotent cell from blastoderm or PGCs has been studied extensively. Based on these knowledge, the technologies of transplanting donor avian pluripotent cells from the stage X blastoderms or PGCs into the recipient embryos was established to generate germline chimeras. These embryo manipulation system has been considered as one of the most powerful for production of avian chimeras (Petitte *et al.*, 1990; Watanabe *et al.*, 1992; Tajima *et al.*, 1993; Naito *et al.*, 1994a,b; Etches *et al.*, 1996; Pain *et al.*, 1996; Etches and Kagami, 1997, Kagami *et al.*, 1997; Tagami *et al.*, 1997) and transgenic birds (Brazolot *et al.*, 1991). Applied these embryo engineering techniques, it was challenged to produced germline chimeras with muscular dystrophy NH-413 strain and a White Leghorn (L-M strain) in Nippon Institute for Biological Science (NIBS). By conducting the strategy, it was aimed to introduce genes relating to muscular dystrophy into chickens.

2. MATERIALS AND METHODS

2.1 Preparation of incubator

The main switch of an incubator (P-008B, Showa, Japan) was put and the water bowl was filled with distilled water. The inside temperature of the incubator was adjusted to 38.5°C.

2.2 Preparation of donor and recipient

The donor embryos were from New Hampshire (NH-413) that have brown feathers. The recipient embryos were from White Leghorn (L-M) that have white feathers. The egg shells of the donor and recipients were washed with distilled water. The shell surfaces were disinfected with 70% ethanol. The eggs were laid for a couple of minutes. The shell was clucked and the contents were moved into a petri dish. The excess egg white was removed from the surface of the embryo. A paper ring was put around the embryo. The yolk membrane was cut off through the ring. The stage X blastoderm itself was obtained (Eyal-Giladi and Kochav, 1976; Eyal-Giladi et al., 1981). Excess yolk and blood around the blastoderm was washed off by PBS. The blastoderms were dissociated and dispersed in DMEM containing 10% chicken serum (Carsience et al., 1993). These cells were used for donor. The White Leghorn's fertilized eggs were used as recipients. The developmental stage of the recipients were also stage X.

2.3 Generation of chicken chimeras

Recipient embryos were irradiated by UV sterilizer for 5 minutes. A disposable needle was attached to a micropipetter. The needle was pushed through the yolk. The top edge of the needle was reached to the subgerminal cavity located beneath at the center of the area pellucida of the recipient's blastoderm. Recipient's cell cluster at the center of the area pellucida of the stage X blastoderm was removed carefully. Initially prepared dispersed donor cells were microinjected into the subgerminal cavity of the center of the area pellucida in the recipient embryo. The manipulated embryos were cultured *ex vivo* by the methods of Perry (1988) and Naito et al. (1990), with minor modifications. The recipient embryo has its own egg yolk. The embryo was placed in a host egg shell that was prepared from a freshly laid egg by cutting off the sharp end. As the initial incubation, the embryos were incubated for 3 days at 38.5°C. Again, the manipulated embryo and egg yolk were transferred to a larger host egg shell. An additional 18 days of incubation was done until they hatch (Hamburger and Hamilton, 1951). In case, brown feather was present, the chicks were judged as the somatic chimeras.

3. RESULTS AND DISCUSSION

In case, donor embryos derived from the freshly laid fertilized eggs of New Hampshire (NH-413) were checked for the developmental stage,

it ranged from stages X to XII. The only the stage X embryos were selected.

When the donor blastoderm of muscular dystrophy NH-413 was incorporated into the recipient embryo of White Leghorn (L-M strain), somatic chimerism was observed by existence of the brown feather pigmentations from the New Hampshire. When a somatic chimera was at 2 weeks of age, the proportion of the donor-derived feather was about 5%. The proportion of the donor derived feather increased from about 15% at 1 month to 30% at 3 months. Generally, the proportion of the donor derived feather has been decreased as the chimera get older. Thus, the increase of donor derived feather in the chimera was very unique phenomena. The reason why it happened is yet to be clarified. However, it could be possible that the cell division and proliferation of cells from muscular dystrophy chicken could be more rapid as compared to that of the normal recipient chicken. The chimera showed frequent abnormalities in behavior. The abnormal behavior was observed since hatching to present. It was considered that the behavior might be attributed by the incorporation of genes relating to the muscular dystrophy. The chimera should be raised sexual maturity and be test mated. If the generated chimera was a germline chimera, the muscular dystrophy gene could be transmitted to the offspring.

The muscular dystrophy symptoms and conditions are different among animal species. This difference seemed mainly due to different pathological manifestations of similar genetic defects. So, establishing chicken model will contribute to elucidate the mechanisms of muscular dystrophies. The accumulation of knowledge and refinement of technologies would provide a basis and applied strategy for clinical therapy trials for s the diseases.

In the present studies, a novel strategy to regenerate a chicken of muscular dystrophy was developed. The strategies should be one of the most effective tools for regeneration of experimental chickens model like the muscular dystrophy.

4. ACKNOWLEDGEMENTS

The authors would like to express their sincere thanks to the technical staff, Nippon Institute for Biological Science, Laboratory Animal Station, for taking care of birds and for preparation of donor and recipient embryos. We are grateful to the students of Laboratory of Animal Developmental Genetics, Faculty of Agriculture, Shinshu

University, for their assistance of experiment. The present studies were supported by the Grants in Aid from the Ministry of Science, Culture, Technologies of the Japanese government, Japan Society for Proportion of Science and Special Funds from the Science and Technology Agency to Hiroshi Kagami.

5. REFERENCES

- Ando Y. and Fujimoto, T. (1983). Ultrastructural evidence that chick primordial germ cells leave the blood-vascular system prior to migrating to the gonadal anlagen. *Dev. Growth Differ.* 25, 345-352.
- Asmundson, V. S. and Julian, L. M. (1956). Inherited muscle abnormality in domestic fowl. *J. Hered.* 47: 248-252.
- Brazolot, C. L., Petite, J. N., Etches, R. J. and Gibbins, A. M. (1991). Efficient transfection of chicken cells by lipofection and introduction of transfected blastodermal cells into the embryo. *Mol. Reprod. Dev.* 30, 303-312.
- Carsience, R. S., Clark, M. E., Gibbins, A. M. and Etches, R. J. (1993). Germline chimeric chickens from dispersed donor blastodermal cells and compromised recipient embryos. *Development* 117, 669-675.
- Etches, R. J., Clark, M. E., Toner, A., Liu, G. and Gibbins, A. M. (1996). Contributions to somatic and germline lineages of chicken blastodermal cells maintained in culture. *Mol. Reprod. Dev.* 45, 291-298.
- Etches, R. J. and Kagami, H. (1997). Genotypic and phenotypic sex reversal. In: *Perspectives in Avian Endocrinology* (ed. R. J. Etches) Bristol UK: Journal of Endocrinology Ltd. (in press)
- Eyal-Giladi, H. and Kochav, S. (1976). From cleavage to primitive streak formation: a complementary normal table and a new look at the first stage of the development of the chicken I. *General Morphology.* *Dev. Biol.* 49, 321-337.
- Eyal-Giladi, H., Ginsburg, M. and Farbarov, A. (1981). Avian primordial germ cells are of epiblastic origin. *J. Embryol. Exp. Morphol.* 65, 139-147.
- Eyal-Giladi, H. (1993). Early determination and morphogenetic processes in birds. In *Manipulation of the avian genome* (ed. R. J. Etches and A. M. Gibbins), pp. 29-37. CRC Press, Boca Raton.
- Fujimoto, T., Ukeshima, A. and Kiyofuji, R. (1976). The origin, migration and morphology of the primordial germ cells in the chicken embryo. *Anat. Rec.* 185, 139-154.
- Ginsburg, M. and Eyal-Giladi, H. (1987). Primordial germ cells of young chick blastoderm originate from the central zone of area pellucida irrespective of the embryo-forming process. *Development* 101, 209- 219.
- Ginsburg, M. and Eyal-Giladi, H. (1989). Primordial germ cell development in cultures of dispersed central disks of stage X chicken blastoderms. *Gamete Res.* 23, 421-428.
- Hamburger, V. and Hamilton, H. L. (1951). A series of normal stages in the development of the chick. *J. Morphol.* 88, 49-92.
- Imamura, am., Araishi, K., Noguchi, S. and Ebashi, S. (2000). A sarcoglycan-dystroglycan complex anchors Dp116 and utrophin in the peripheral nervous system. *Hum. Mol. Genet.* 9, 3091-3100.

- Kagami, H., Clark, M. E., Gibbins, A. M. and Etches, R. J. (1995). Sexual differentiation of chimeric chickens containing ZZ and ZW cells in the germline. *Mol. Reprod. Dev.* 42, 379-387.
- Kagami, H., Tagami, T., Matsubara, Y., Hanada, H., Maruyama, K., Sakurai, M., Kuwana, T. and Naito, M. (1997). The developmental origin of primordial germ cells and the transmission of the donor-derived gametes in mixed-sex germline chimeras to the offspring in the chicken. *Mol. Reprod. Dev.* 48, 501-510.
- Karagenc, L., Ginsburg, M., Eyal-Giladi, H. and Petite, J. N. (1995). Immunohistochemical analysis of germline segregation in preprimitive streak chick embryos using stage-specific embryonic antigen-1 (SSEA-1). *Poult. Sci.* 74, Supplement 1, 26.
- Kikuchi, T., Ishiura, S., Nonaka, I. and Ebashi, S. (1981). Genetic heterozygous carries in hereditary muscular dystrophy of chickens. *Tohoku J. Agr. Res.* 32, 32: 14-26.
- Meyer, D. B. (1964). The migration of primordial germ cells in the chick embryo. *Dev. Biol.* 10, 154-190.
- Muniesa, P. and Dominguez, L. (1990). A morphological study of primordial germ cells at pregastrular stages in the chick embryo. *Cell Differ. Dev.* 31, 105-117.
- Naito, M., Nirasawa, K. and Oishi, T. (1990). Development in culture of the chick embryo from fertilized ovum to hatching. *J. Exp. Zool.* 254, 322-326.
- Naito, M., Tajima, A., Tagami, T., Yasuda, Y. and Kuwana, T. (1994a). Preservation of chick primordial germ cells in liquid nitrogen and subsequent production of viable offspring. *J. Reprod. Fertil.* 102, 321-325.
- Naito, M., Tajima, A., Yasuda, Y. and Kuwana, T. (1994b). Production of germline chimeric chickens, with high transmission rate of donor-derived gametes, produced by transfer of primordial germ cells. *Mol. Reprod. Dev.* 39, 153-161.
- Nonaka, I. (1998). Animal models of muscular dystrophies. *Lab. Anim. Sci.* 48: 8-17.
- Pain, B., Clark, M. E., Shen, M., Nakazawa, H., Sakurai, M., Samarut, J. and Etches, R. J. (1996). Long-term in vitro culture and characterisation of avian embryonic stem cells with multiple morphogenetic potentialities. *Development* 122, 2339-2348.
- Pardanaud, L., Buck, C. and Dieterlen-Liever, F. (1987). Early germ cell segregation and distribution in the quail blastodisc. *Cell Differ.* 22, 47-60.
- Partridge, T. (1991). Animal models of muscular dystrophy – what can they teach us? *Neuropathol. Appl. Neurobiol.* 17: 353-363.
- Perry, M. (1988). A complete culture system for the chick embryo. *Nature* 331, 70-72.
- Petite, J. N., Clark, M. E., Liu, G., Gibbins, A. M. and Etches, R. J. (1990). Production of somatic and germline chimeras in the chicken by transfer of early blastodermal cells. *Development* 108, 185-189.
- Rogulska, T. (1968). Primordial germ cells in normal and transfected duck blastoderms. *J. Embryol. Exp. Morphol.* 20, 247-260.
- Sutasurya, L. A., Yasugi, S. and Mizuno, T. (1983). Appearance of primordial germ cells in young chick blastoderms cultured in vitro. *Develop. Growth Differ.* 25, 517-521.
- Swift, C. H. (1914). Origin and early history of the primordial germ-cells in the chick. *Am. J. Anat.* 15, 483-516.
- Tagami, T., Matsubara, Y., Hanada, H. and Naito, M. (1997). Differentiation of female chicken primordial germ cells into spermatozoa in male gonads. *Dev. Growth Differ.* (in press)
- Tajima, A., Naito, M., Yasuda, Y. and Kuwana, T. (1993). Production of germline chimera by transfer of primordial germ cells in the domestic chicken (*Gallus domesticus*). *Theriogenol.* 40, 509-519.

- Urven, L. E., Erickson, C. A., Abbott, U. K. and McCarrey, J. R. (1988). Analysis of germline development in the chicken embryo using an anti mouse ES cell antibody. *Development* 103, 299-304.
- Yasuda, Y., Tajima, A., Fujimoto, T. and Kuwana, T. (1992). A method to obtain avian germ-line chimeras using isolated primordial germ cells. *J. Reprod. Fertil.* 96, 521-528.
- Wagner, W. D. and Peterson, R. A. (1970). Muscular dystrophy syndrome in the Cornish chicken. *Am. J. Vet. Res.* 31: 331-338.
- Watanabe, M., Kinutani, M., Naito, M., Ochi, O. and Takashima, Y. (1992). Distribution analysis of transferred donor cells in avian blastodermal chimeras. *Development* 114, 331-338.

PLURIPOTENT CELL CULTURE ENGINEERING AND THE APPLICATION FOR AVIAN BIOTECHNOLOGY

Avian Pluripotent Cell Culture Engineering

Hiroshi Kagami¹ Tomoki Mushika¹ Takamasa Noguchi¹ Yasuhiro Yamamoto¹ Akira Fujiwara² Naomi Yamakawa³ Hisato Okuizumi⁴ and Tamao Ono¹

¹*Shinshu University, 8304 Minamiminowa, Nagano 399-4598, Japan;* ²*Nippon Institute for Biological Science, 3331-114 Kamisano, Kobuchisawa, Yamanashi 408-0041, Japan;* ³*Tokyo Metropolitan Institute of Gerontology, 32-2 Sakae-Cho, Itabashi, Tokyo 173-0015, Japan;* ⁴*National Institute of Agrobiological Sciences, 2-1-2 Kannon-Dai, Tsukuba, Ibaraki 305-8602, Japan*

Abstract: Pluripotent cells have been considered as one of the most useful tools for production of transgenic birds, secretion of pharmaceuticals in eggs, regeneration of avian organs and conservation of endangered birds via germline chimeras. To produce the germline chimeras, long term culture of the pluripotent cells is essential. Thus, the avian pluripotent cell culture engineering techniques have been one of the most fundamental subjects in avian biotechnology. Recently, a novel strategy has been established in our lab to culture the pluripotent cells derived from center of the area pellucida in stage X blastoderm in chickens. The cultured cells were positively stained with SSEA-1 and Alkaline Phosphatase. Developmental fate of the cultured cells in chimeras was analyzed. The cultured donor cells were microinjected into the subgerminal cavity of the recipients' blastoderm from which cells in the center of the area pellucida were removed. The manipulated embryos were cultured until hatching. Many of the generated chimeras transmitted donor derived gametes to their offspring. It was considered that the cultured cells derived from blastoderm retained the high potency to differentiate into both germ cells and somatic cells. Prior to microinjection, foreign genes were transfected into the cultured cells. When the chimeric embryos were generated, strong expression of the introduced genes were detected in the embryos. These approaches should open up new frontier for future avian biotechnology.

Key words: avian; pluripotent cells; cell culture

1. INTRODUCTION

The pluripotent cells are derived from early embryos that are undifferentiated cells capable of proliferation and could be self-renewal. Culture engineering of the pluripotent cells; ES cells or EG cells, has opened up new frontier for genetic conservation of rare animals and degenerative medicine. The pluripotent cells were originally obtained from transplantable germ cell tumors or teratocarcinomas derived from the primary germ layers (Martin and Evans, 1975). These technologies were mainly developed in mammals such as mouse or human. In birds, the pluripotent cells have also been considered as one of the most useful tools for production of transgenic birds, secretion of pharmaceuticals in eggs, regeneration of avian organs and conservation of endangered individuals. However, any ES or EG cells are established in birds. To establish these cells in birds, the determination of the origin of avian pluripotent cells and the specific isolation of the cells have been one of the most important subjects (Eyal-Giladi et al., 1981). The presence of pluripotent cells have been detected by the PAS staining or the immunostaining technique. The EMA-1 and SSEA-1 in chickens (Urven et al., 1988; Karagenc et al., 1995) and QH-1 in quail (Pardanaud et al., 1987) have been representative epitopes. Recent progress in embryo engineering techniques (Petitte et al., 1990; Brazolot et al., 1991; Watanabe et al., 1992; Carsience et al., 1993; Tajima et al., 1993; Naito et al., 1994a, b; Kagami et al., 1995; Pain et al., 1996; Etches et al., 1996; Tagami et al., 1997; Etches and Kagami, 1997) would make it possible to detect the cell location more accurately. The replacement of the recipient's cells with a cell cluster from the donor blastoderm which contains the cells would provide a direct evidence to pinpoint the localisation of the pluripotent cells in the early embryos (Kagami et al., 1997; Kagami, 2002; Kagami, 2003).

These isolated cells have been considered very useful vectors to produce germline chimeras that is key step for avian transgenesis or regeneration of birds. To produce the germline chimeras, long term culture of the pluripotent cells is essential. The culture has been tried by use of the blastoderm from a stage X embryo or PGCs (Pain et al., 1996; Petitte et al., 2004). However, no stable techniques have been established to culture the cells in vitro. Thus, to establish the stable avian pluripotent cell culture engineering techniques have been one of the most fundamental subjects in avian biotechnology. In the present studies, development of a novel strategy to establish to culture the pluripotent cells derived from center of the area pellucida in stage X blastoderm (Eyal-Giladi and Kochav, 1976) in chickens was challenged.

2. MATERIALS AND METHODS

2.1 Isolation of blastodermal cells

The fertilized eggs were collected from poultry house everyday and fresh eggs were used for the present studies. The fertilized embryos were from Barred Plymouth Rock chickens (i/i) that have black feathers and are homozygous recessive at the I locus or from White Leghorn chickens (I/I) that have white feathers and are homozygous dominant at the I locus. The embryos used were stage X blastoderm (Eyal-Giladi and Kochav, 1976) in freshly laid and unincubated. The embryo proper was separated from egg yolk and excess yolk and blood were washed off from the embryos with phosphate-buffered saline (PBS). The obtained embryos were observed by stereoscopic microscope to check the developmental conditions. The center of the area pellucida of the blastoderm was carefully isolated from the embryo. The obtained cell cluster was dissociated with trypsin and dispersed in Dulbecco's Modified Eagle's Medium (DMEM) containing 10% chicken serum (Carscience et al., 1993).

2.2 Culture of the blastodermal cells

The fertilized embryos from White Leghorn or Barred Plymouth Rock were incubated for 6 days. The embryo proper was obtained and the excess yolk and blood were washed off by the PBS. The embryo proper were dispersed by repetitive pipeting to single cells. The cells were cultured to make feeder cells. The isolated blastodermal cells were cultured in KAv-1 medium (Kuwana et al., 1996) together with the feeder cells. The morphology was observed during the culture. Pluripotency of the cultured cells was tested by immunological staining with a pluripotency mark AP.

2.3 Production of chimeric embryos

The fresh and cultured donor blastodermal cells from Barred Plymouth Rock chickens were microinjected into the subgerminal cavity of the recipient embryos of White Leghorn at the same stage of the development (stage X). The manipulated embryos were ex vivo cultured by the methods of Perry (1988) with minor modifications. The embryo with its own egg yolk was placed in a host egg shell that was prepared from a freshly laid egg by cutting off the sharp end. The embryos were incubated for 3 days at 38.5°C. Then, the embryo and egg yolk were

transferred to a larger host egg shell that were prepared by cutting off the blunt end of a freshly laid double yolk egg. The embryos were cultured for additional 18 days until the hatching. Somatic chimerism was observed by the presence of black feather pigmentation.

2.4 Production of transgenic embryos

Prior to microinjection, the donor blastodermal cells were transfected with a reporter gene; Lack-Z. The transfected donor cells were microinjected into the recipient embryos at the same stage of the recipients. The manipulated embryos were *ex vivo* cultured in the same condition as described above. The embryo proper was obtained and the excess yolk and blood were removed by washing off the PBS. The gene expression of the foreign reporter gene were detected by immunological staining.

3. RESULTS AND DISCUSSION

When the isolated blastoderms from the freshly laid fertilized eggs were carefully observed under a stereoscopic microscope, some variety in the embryonic developmental stages were identified. The initial stage of the embryos seemed very important for pluripotency *in vitro* culture condition (Petitte et al., 1990; Brazolot et al., 1991; Watanabe et al., 1992; Carsience et al., 1993). Five out of eleven embryos were exactly stage X blastoderm. Thus, only the stage X blastoderms were used for the present experiments.

The cells divided and proliferated very rapidly during first 5 days of incubation. Morphology of the cultured cells differed during the culture from the initial stage of incubation. The mouse ES like colonies were observed around 5 days of incubation. The cell colonies were derived from the blastoderm and they could easily be distinguished from the feeder cells. When the cultured cell were stained with AP, only the colonies shaped cell clusters derived from the blastoderm were stained as red with AP. None of the feeder cells were stained with the AP during incubation. It was suggested that the stained cells retained pluripotency in the *in vitro* culture condition. The AP positive cells were detectable up to 21 days of incubation in case mLIF was added to the culture medium. On the other hand, the AP detectable cells were observed up to 12 days of incubation by use of the medium without mLIF. It was suggested that the mLIF maintained the pluripotency in cultured chicken blastoderma cells, too.

When the donor blastodermal cells from Barred Plymouth Rock chickens were microinjected into the White Leghorn of the same stage of the development, somatic chimerism could be easily identified by the black feather pigmentations derived from the donor after 12 days of the incubation. More than 65% of the generated chimera showed somatic chimerism. These results suggested that the donor cells could be compromised to resulting chimeric embryos and could be differentiated into many somatic tissues or organs. It was suggested that the regeneration of a specific organs could be done in the specific culture conditions.

When chimeras reached to sexual maturity, they were mated with Barred Plymouth Rocks. The distribution of black (*i/i*) and yellow (*I/i*) offspring was recorded to estimate the contribution of the donor (*i*) and the recipient (*I*) to the germline, respectively. Three out of the six chimeras (30%) were confirmed to germline chimeras.

The gene transferred chimeric embryos were cultured in the same condition as described to above. Strong expression of the introduced reporter gene was detected in the chimeric embryos. The expression of the foreign genes were detected by immunological staining. The gene expression was detected in embryos at 4, 5, 7, 18 and 21 days of incubation. All of the detected embryos developed normally. It was suggested that the blastodermal cells are one of the most useful vector cells for avian transgenesis.

In mammalian, manipulation of pluripotent cells such as ES cells or EG cells has opened new possibility for genetic conservation of rare animals and degenerative medicine. In birds, however, there is few strategy to date. This is mainly due to the few knowledge on avian germline development and molecular mechanisms of genetic regulation of avian germ cell differentiation. The developed strategies using by avian pluripotent cells was considered as one of the powerful tools for production of transgenic birds, secretion of pharmaceuticals in eggs, regeneration of avian organs and conservation of endangered birds (Pain et al., 1996; Etches et al., 1996; Tagami et al., 1997; Etches and Kagami, 1997, Kagami, 2002; Kagami, 2003). An advantage to use avian embryos compared to that of the mammalian embryos is the accessibility. As the avian embryo has all the materials inside a egg shell, it led to direct access to the embryo and to manipulate. In the present studies we have established an strategy to culture and manipulate avian pluripotent cells. These approaches should open up new frontier for future avian biotechnology.

4. ACKNOWLEDGEMENTS

The authors would like to express their sincere thanks to Drs. Takahiro Tagami, National Institute of Animal Science and Grassland Science, and Mitsuru Naito, Yuko Matsubara, Takashi Harumi and Michiharu Sakurai, National Institute for Agrobiological Sciences for critical advice on avian cell culture and cytokine. The present studies were supported by the Grants in Aid from the Ministry of Science, Culture, Technologies of the Japanese government, Japan Society for Proportion of Science and Special Funds from the Science and Technology Agency to Hiroshi Kagami. Thanks are also going to all the students of laboratory of Animal Developmental Genetics for helping the present studies and for assistance to take care of the experimental birds.

5. REFERENCES

- Brazolot, C. L., Petite, J. N., Etches, R. J. and Gibbins, A. M. (1991). Efficient transfection of chicken cells by lipofection and introduction of transfected blastodermal cells into the embryo. *Mol. Reprod. Dev.* 30, 303-312.
- Carsience, R. S., Clark, M. E., Gibbins, A. M. and Etches, R. J. (1993). Germline chimeric chickens from dispersed donor blastodermal cells and compromised recipient embryos. *Development* 117, 669-675.
- Etches, R. J., Clark, M. E., Toner, A., Liu, G. and Gibbins, A. M. (1996). Contributions to somatic and germline lineages of chicken blastodermal cells maintained in culture. *Mol. Reprod. Dev.* 45, 291-298.
- Etches, R. J. and Kagami, H. (1997). Genotypic and phenotypic sex reversal. In: *Perspectives in Avian Endocrinology* (ed. R. J. Etches) Bristol UK: Journal of Endocrinology Ltd. 57-67.
- Eyal-Giladi, H. and Kochav, S. (1976). From cleavage to primitive streak formation: a complementary normal table and a new look at the first stage of the development of the chicken I. *General Morphology. Dev. Biol.* 49, 321-337.
- Eyal-Giladi, H., Ginsburg, M. and Farbarov, A. (1981). Avian primordial germ cells are of epiblastic origin. *J. Embryol. Exp. Morphol.* 65, 139-147.
- Kagami, H. (2002). Developmental genetic analysis of the avian primordial germ cells and the application for production of chimeric chickens. *J. Poult. Sci.* 39, 131-139.
- Kagami, H. (2003). Genetic regulation of avian germ cells differentiation and the application for poultry biotechnology. In: *Animal Frontier Sciences* (eds, Sato, E. and Miyamoto, H.) pp. 237-242, Hokuto Shobo, Kyoto, Japan.
- Kagami, H., Clark, M. E., Gibbins, A. M. and Etches, R. J. (1995). Sexual differentiation of chimeric chickens containing ZZ and ZW cells in the germline. *Mol. Reprod. Dev.* 42, 379-387.
- Kagami, H., Tagami, T., Matsubara, Y., Hanada, H., Maruyama, K., Sakurai, M., Kuwana, T. and Naito, M. (1997). The developmental origin of primordial germ cells and the transmission of the donor-derived gametes in mixed-sex germline chimeras to the offspring in the chicken. *Mol. Reprod. Dev.* 48, 501-510.

- Karagenc, L., Ginsburg, M., Eyal-Giladi, H. and Petite, J. N. (1995). Immunohistochemical analysis of germline segregation in preprimitive streak chick embryos using stage-specific embryonic antigen-1 (SSEA-1). *Poult. Sci.* 74, Supplement 1, 26.
- Naito, M., Tajima, A., Tagami, T., Yasuda, Y. and Kuwana, T. (1994a). Preservation of chick primordial germ cells in liquid nitrogen and subsequent production of viable offspring. *J. Reprod. Fertil.* 102, 321-325.
- Naito, M., Tajima, A., Yasuda, Y. and Kuwana, T. (1994b). Production of germline chimeric chickens, with high transmission rate of donor-derived gametes, produced by transfer of primordial germ cells. *Mol. Reprod. Dev.* 39, 153-161.
- Pain, B., Clark, M. E., Shen, M., Nakazawa, H., Sakurai, M., Samarut, J. and Etches, R. J. (1996). Long-term in vitro culture and characterisation of avian embryonic stem cells with multiple morphogenetic potentialities. *Development* 122, 2339-2348.
- Pardanaud, L., Buck, C. and Dieterlen-Liever, F. (1987). Early germ cell segregation and distribution in the quail blastodisc. *Cell Differ.* 22, 47-60.
- Perry, M. (1988). A complete culture system for the chick embryo. *Nature* 331, 70-72.
- Petite, J. N., Clark, M. E., Liu, G., Gibbins, A. M. and Etches, R. J. (1990). Production of somatic and germline chimeras in the chicken by transfer of early blastodermal cells. *Development* 108, 185-189.
- Petite, J. N., Liu, G. and Yang, Z. (2004). Avian pluripotent stem cells. *Mechanism of Development* 121, 1159-1168.
- Tagami, T., Matsubara, Y., Hanada, H. and Naito, M. (1997). Differentiation of female chicken primordial germ cells into spermatozoa in male gonads. *Dev. Growth Differ.* 13, 121-136.
- Tajima, A., Naito, M., Yasuda, Y. and Kuwana, T. (1993). Production of germline chimera by transfer of primordial germ cells in the domestic chicken (*Gallus domesticus*). *Theriogenol.* 40, 509-519.
- Urven, L. E., Erickson, C. A., Abbott, U. K. and McCarrey, J. R. (1988). Analysis of germline development in the chicken embryo using an anti mouse ES cell antibody. *Development* 103, 299-304.
- Watanabe, M., Kinutani, M., Naito, M., Ochi, O. and Takashima, Y. (1992). Distribution analysis of transferred donor cells in avian blastodermal chimeras. *Development* 114, 331-338.

EFFECT OF OXYGEN TENSION ON THE PROLIFERATION AND THE DIFFERENTIATION OF MOUSE EMBRYONIC STEM CELLS

M. Kimura, H. Kurosawa, and Y. Amano

*Division of Medicine and Engineering Science, Interdisciplinary Graduate School of
Medicine and Engineering, University of Yamanashi, 4-3-11 Takeda, Kofu, Yamanashi 400-
8511, Japan*

1. INTRODUCTION

Embryonic stem (ES) cell is a highly expected candidate for the cell source of regenerative medicine, because ES cells retain their totipotency capacity and are able to generate cells of all lineages (Daley *et al.*, 2003; Odorico *et al.*, 2001). However, the technology that controls proliferation and differentiation of ES cells *in vitro* is not established yet. For the self-renewal proliferation, ES cells must be in an undifferentiated state. ES cells can remain in the undifferentiated state in the presence of embryonic fibroblast feeder cells and/or leukemia inhibitory factor (LIF). There is a contrastive relation between proliferation and differentiation of ES cells. Removing the feeder cells and LIF from the ES cell culture, ES cells spontaneously differentiate and chaotically generate various cell types, while the proliferation is suppressed. Strategies to control *in vitro* differentiation of ES cells basically consist of embryoid body (EB) formation, addition of extracellular signals (growth factors), nutrient restriction, engineered expression of master genes, and etc. (Soria, 2001). Generally oxygen is considered to play an important role in the cell culture because oxygen is needed to metabolize nutrients. Therefore, oxygen restriction would result in cessation of proliferation and the initiation of cell differentiation.

The present study was performed to clarify the effect of oxygen on the proliferation and the differentiation of mouse ES cells.

2. MATERIALS AND METHODS

2.1 ES CELL CULTURE

Mouse embryonic stem (ES) cells of the cell line 129SV were cultured on gelatin-coated dishes with feeder cells in the humidified CO₂- incubator (37°C, 20% O₂, 5% CO₂). The immortalized STO fibroblasts were used as feeder layers. The STO cells were cultured in Dulbecco's modified Eagle's medium (DMEM; Gibco, Grand Island, NY) supplemented with 10% inactivated fetal bovine serum (FBS; Gibco), 25 units/ml penicillin, and 25 µg/ml streptomycin. The STO cells were treated with a freshly prepared solution of mitomycin C (Sigma, St. Louis, MO) at 10 µg/ml for 3 h to be incapable of division. Feeder layers for ES cells were prepared by replating the mitomycin C-treated STO cells at approximately 5×10^5 cells per 35 mm dish and incubated overnight. The ES cells (1×10^5 cells per 35 mm dish) were cultured on the feeder layers in DMEM (Gibco) supplemented with 15% KnockOut™ serum replacement (KSR; Gibco), 1 mM sodium pyruvate (Gibco), 0.1 mM nonessential amino acids (Gibco), 0.1 mM 2-mercaptoethanol (Sigma), 25 units/ml penicillin, and 25 µg/ml streptomycin (ES medium). The final volume of ES medium was 1 ml. The undifferentiated state was maintained by 1000 units/ml recombinant murine leukemia inhibitory factor (mLIF; Chemicon, Temecula, CA). For these experiments, ES cells were grown for a maximum of 22 passages in the presence of feeders and mLIF. Oxygen tension of the humidified CO₂-incubator was changed at 5% O₂, 20% O₂, and 40% O₂. The cultures of ES cells for proliferation were carried out under various oxygen tensions. Cell proliferation was estimated by cell counting. Alkaline phosphatase (AP) activity was measured to assess differentiation status.

2.2 EMBRYOID BODY FORMATION

For the EB formation cultures, ES cells, which were cultured for 3 days, were dissociated using 0.1% trypsin-EDTA (Gibco) and suspended in Iscove's modified Dulbecco's medium (IMDM; Gibco) supplemented with 15% inactivated FBS, 1 mM sodium pyruvate, 0.1 mM nonessential amino acids, 0.1 mM 2-mercaptoethanol, 25 units/ml penicillin, and 25 µg/ml streptomycin (EB medium) at a cell density of 5×10^3 cells/ml. The mLIF was not added to the EB-forming cultures. For the EB formation,

the ES cells were seeded at cell density of 1000 cells per well in a 96-well round-bottom plates (Nunc 145399, Low Cell Binding Plates) with 200 μ l EB medium. The plates were incubated statically in the humidified CO₂- incubator (37°C, 5% CO₂) under various oxygen tensions (5% O₂, 20% O₂, and 40% O₂) for 5 days. The formed EBs were microscopically observed. The number of viable ES cells contained in an EB was counted with the hemocytometer after dissociating the EB by incubation in 0.25% trypsin-EDTA (Gibco). Cell viability was determined by the exclusion of Trypan blue dye.

2.3 ATTACHED EB CULTURE TO GENERATE CARDIOMYOCYTES

The EBs, which were formed in the EB formation culture for 5 days, were transferred to the attachment culture for the differentiation of ES cells into cardiomyocytes. The attachment cultures were performed in the EB medium on a 24-well plate (IWAKI No. 3820-024N) coated with 0.1% gelatin under 20% O₂. Twenty-four EBs were seeded on the 24-well plate to be one EB in one well. Periodically, microscopic observation was performed to detect the generation of the beating cells in the populations derived from an EB in each well.

3. RESULTS AND DISCUSSION

3.1 PROLIFERATION AND AP ACTIVITY OF ES CELLS UNDER VARIOUS OXYGEN TENSIONS

As shown in Fig. 1, regardless of the presence of LIF, low oxygen tension (5% O₂) lowered the proliferation of ES cells, while high oxygen tension (40% O₂) hardly affected the proliferation. Inevitably, the AP activity of ES cells also lowered in the 5% O₂ tension regardless of the presence of LIF as shown in Fig. 2. When ES cells were cultivated in the presence of LIF, the effect of the 40% O₂ on the AP activity was not markedly appeared (Fig. 2-A). In the absence of LIF, however, the 40% O₂ retained the higher AP activity from day 3 to day 5 of culture in the comparison with the cultures under other oxygen tensions (Fig. 2-B). During this period, there was no distinguishable difference in the cell number between normal oxygen tension (20% O₂) and the 40% O₂ as

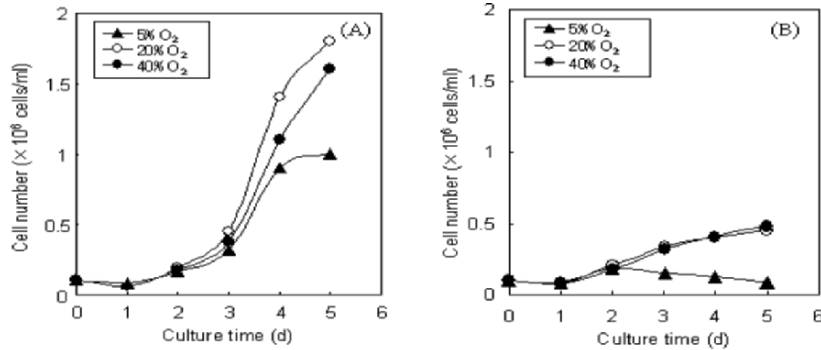


Fig. 1. Effect of oxygen on the proliferation of ES cells under various oxygen tensions in the presence of LIF (A) and in the absence of LIF (B).

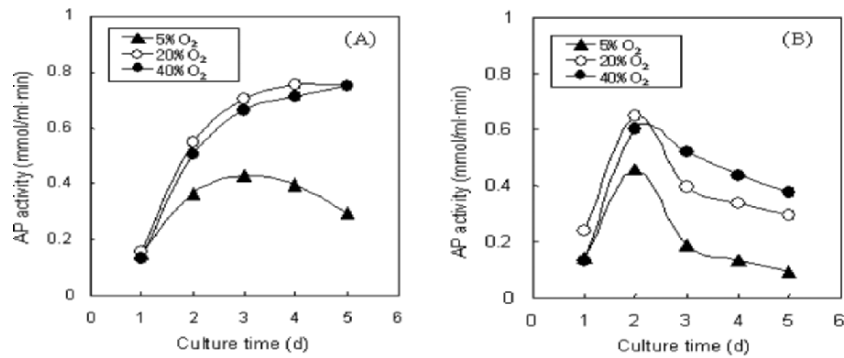


Fig. 2. Effect of oxygen on the AP activity of ES cells under various oxygen tensions in the presence of LIF (A) and in the absence of LIF (B).

shown in Fig. 1-B. Therefore, it is indicated that the AP activity per unit cell number was maintained high under the 40% O_2 . The AP activity is one of indicators for undifferentiated ES cells, and it decreases with the progress of the differentiation of ES cells. It seems that the 40% O_2 suppressed the differentiation of ES cells.

3.2 EFFECT OF OXYGEN TENSION ON THE EB FORMATION

Figure 3 shows the cell number contained in EBs, which are forming under various oxygen tensions. There was no significant difference in the cell number up to day 2 among any oxygen tensions. The effect of oxygen tension on the cell number appeared after the day 2. The cell number increased to about 30,000 cells/EB by day 4 under the oxygen

tensions of 20% O₂ and 40% O₂, but it increased to about 20,000 cells/EB by day 5 under the oxygen tension of 5% O₂. Figure 4 shows the appearance of the EBs at the day 5 of the EB formation culture. As shown in Fig.4, the size of EB formed under the 5% O₂ was the smallest, and the size of EB formed under the 20% O₂ was the largest. The difference between the size of EBs formed under the 20% O₂ and the 40% O₂ was observed, though the cell number in both the EBs was almost same. The EB formed in the 40% O₂ was more compact, and its contour was relatively clear and smooth compared with the EB formed in the 20% O₂.

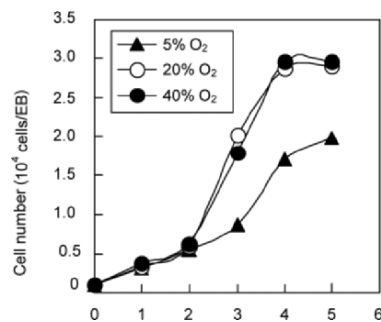


Figure 3. The cell number contained in an EB formed under various oxygen tensions.

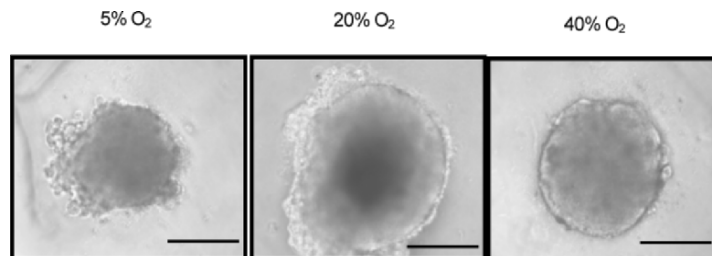


Figure 4. The 5-day-old EBs formed under various oxygen tensions. Scale bar = 200mm.

3.3 Differentiation of EB into cardiomyocytes

All EBs, which were formed under various oxygen tensions, had the capacity for differentiation into cardiomyocytes. Immuno-

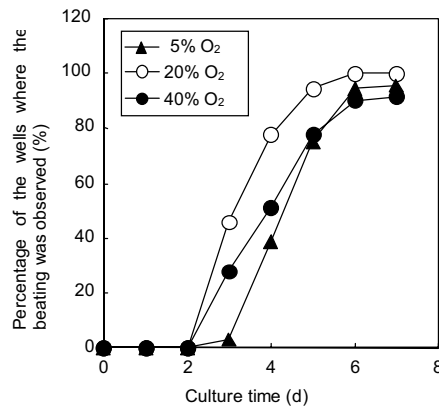


Figure 5. Percentage of the wells where the beating was observed in the outgrowth against the wells attached the EBs.

histochemical stain by cardiac troponin I monoclonal antibody was performed to detect cardiomyocytes. The troponin-positives cells were detected in the outgrowth of the attached EBs (data not shown). Figure 5 shows the percentage of the wells where the beating was observed in the outgrowth against the wells attached the EBs. The generation efficiency of cardiomyocytes was the best in the EB formed under the 20% O₂. The oxygen tensions of 5% O₂ and 40% O₂ became the adverse effect on the formation of EBs.

4. CONCLUSION

Low oxygen tension (5% O₂) lowered the proliferation and the AP activity of ES cells. High oxygen tension (40% O₂) retained the higher AP activity in the comparison with the cultures under normal oxygen tensions (20% O₂). It was supposed that the 40% O₂ suppressed the differentiation of ES cells. The oxygen tensions of 5% O₂ and 40% O₂ became the adverse effect on the formation of EBs.

5. REFERENCES

- Daley, G.Q., Goodell, M.A., and Snyder, E.Y. (2003) Realistic prospects for stem cell therapeutics, *Hematology* 1, 398-418.
- Odorico, J.S., Kaufman, D.S., and Thomson, J.A. (2001) Multilineage differentiation from human embryonic stem cell lines, *Stem Cells* 19, 193-204.
- Soria, B. (2001) In-vitro differentiation of pancreatic β -cells, *Differentiation* 68, 205-219.

ENHANCEMENT OF ANTIBODY PRODUCTION BY ADDITION OF UBIQUINONE-Q₁₀

Yoshinobu Konno¹, Motoi Aoki¹, Masakazu Takagishi¹, Hiroshi Takasugi², Masamichi Koike¹, Shinji Hosoi¹

¹Kyowa Hakko Kogyo Co., LTD., Tokyo research Laboratories, 3-6-6, Asahi-machi, Machida-shi, Tokyo, Japan; ²Kyowa Hakko Kogyo Co., LTD., Tokyo research Laboratories Hofu blanch, 1-1-1, Kyowa-cho, Hofu-shi, Yamaguchi, Japan

Abstract: The productivity has a directly influence to the cost of manufacturing for therapeutic monoclonal antibodies (Mab). We have screened enhancer of specific Mab production rate (SPR) using YB2/0 cell-line. We found that coenzyme Q₁₀ (Q₁₀) as a media ingredient seems to have no significant influence on the cumulative viable cell density, but has the potential to enhance SPR. We added SANOMIT-Q₁₀ (MSE, Hamburg, Germany) to medium, we call SANOMIT-Q₁₀ containing medium as Q-media, at several concentrations and conducted fed-batch culture. Although Q₁₀ is well known strong anti-oxidant, 8-hydroxy-2'-deoxyguanosine (8-OHdG) was no effect by Q-media and Q_{Lactate} / Q_{Glucose} (L/G) was slightly decreased. We evaluate application of Q-media with YB2/0, Chinese Hamster Ovary (CHO), NS0 cell lines. Q-Media enhanced SPR significantly: Case YB2/0: 66.3 %, Case CHO: 28.8%, Case NS0: 31.9 %. On the other hand, the product characteristics have not been affected. For this reason, Q₁₀ seems to be a powerful ingredient to enhance of biotechnology processing.

Key words: Ubiquinone; Coenzyme Q₁₀; Q₁₀; 8-hydroxy-2'-deoxyguanosine; 8-OHdG; Antibody dependent cell mediated cytotoxicity; ADCC; antibody; CHO; NS0; YB2/0.

1. INTRODUCTION

Recently, more than seventeen therapeutic Mabs are lunched in U.S., the minimizing the cost of goods is one of the topics for industrialization of Mabs, since productivity directly has impact on effect for the cost. Therefore, various investigations have been made to improve the productivity, for example: changing temperature, adding n-butyric acids,

iron citrate or ethanolamine and so on. We screened substances and find Q₁₀ has some activity enhance for SPR.

2. MATERIALS AND METHODS

2.1 Materials

First, additions of Q₁₀ (Ubidecarenon, Kyowa, Tokyo, Japan) to the culture medium were used with Tween-80, since Q₁₀ is a lipid soluble compound. Since Q₁₀ is negligibly solved in water, most studies using Q₁₀ have been limited to low concentration. SANOMIT™ Q₁₀ has been developed as a new application includes glycerol and lecithin. We added SANOMIT™ Q₁₀ to culture medium (Q-Media). With production based on a patented nanoparticle technology, Q-Media is a stabilized liquid-in-liquid dispersion with a particle size of less than 50 nm. In case applied endogenously, our results indicated that it seems to be easily and directly absorbed and incorporated into cells

2.2 Cell culture

The anchorage-dependent NS0 cell line was cultivated in 225 cm² T-flask. CHO and YB2/0 were cultivated 250 mL Erlenmeyer flask and/or 1L Bioreactors. CHO, YB2/0 and NS0 cell line expressing proprietary recombinant antibody was cultured in Q-Media. Basal medium were used EX-CELL™ 302 (JRH, Kansas, USA), RPMI-1640, Hybridoma-SFM and CD-Hybridoma (Invitrogen, California, USA). The cultures were inoculated with a density at least of 2×10^5 cells/mL and cultivated until the decline phase at 37°C, pH7.1^{1),2)}.

2.3 Assay

Viable cells and dead cells were counted by Cedex™ using the trypan blue dye exclusion method. Mab concentration was determined by Protein A HPLC. 8-OHdG concentrations were quantified using an ELISA (8-OHdG check, Japan Institute for the control of Aging, Shizuoka, Japan). Glucose and Lactate concentrations were determined by biosensor YSI 2700 (YSI, Ohio, USA). Antibody dependent cell mediated cytotoxicity (ADCC) was detected ⁵¹Cr released assay as reported previously^{3),4)}.

3. RESULTS AND DISCUSSION

3.1 Effect of Q₁₀ in the medium

We screened substances using YB2/0 cell-lines. We found SPR was enhanced in Q₁₀/Tween-80 additive media supplemented with 50 micro-mol/L. On the other hand, Tween-80 additive media was not affected to SPR. Q₁₀, also known as Ubiquinone is applied for healthcare or other uses. Q₁₀ is a lipid soluble compound that inhabits the inside of inner mitochondrial membranes, where it functions as an integral part of the electron transport chain as well as an efficient endogenous lipophilic strong antioxidant. In addition, it has been known that addition of Q₁₀ to cell culture media promotes growth of several cell lines, such as HeLa cell and murine fibroblast cell or bovine embryo cell.

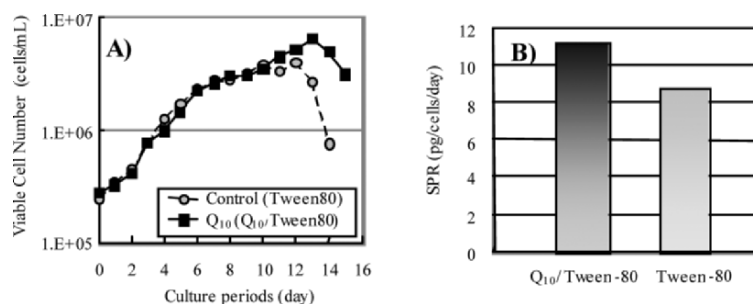


Figure 1. Influence of additive with the Q₁₀/Tween-80 or Tween-80 culture of YB2/0 cell-line in 1 L scale reactor (ABLE, Tokyo, Japan). A) Growth curve, B) Comparison of SPR.

3.2 Oxidative stress response

Q₁₀ is well known strong anti-oxidants. 8-OHdG is well known oxidative DNA damage as a marker. We evaluated 8-OHdG concentrations change in our process. Q-Media supplemented with 500 micro-mol/L is expected antioxidant effect, but no-effect for 8-OHdG concentrations tendency and cumulative cell density. SPR with Q-Media was indicated higher than without Q-media, it was similarly data by Q₁₀/Tween-80.

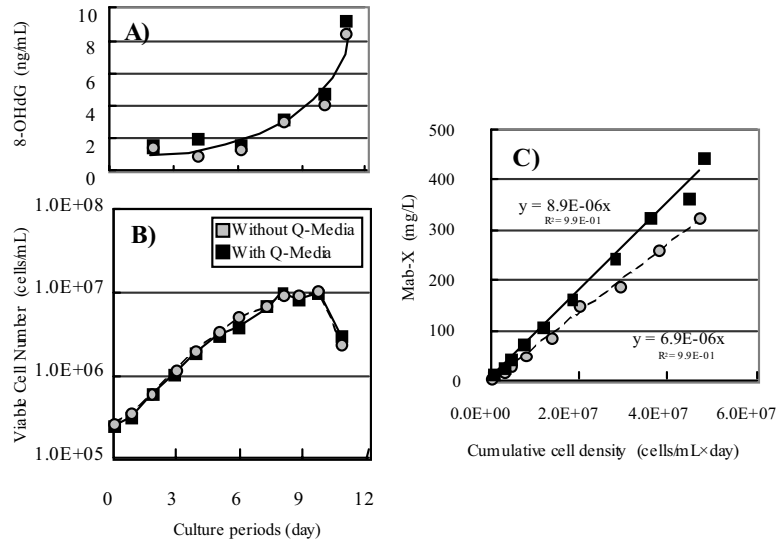


Figure 2. Effect of the Q-Media in 1 L scale reactor fed-batch culture of YB2/0 cell-line for 8-OHdG concentration. A) Time course of 8-OHdG concentrations were not difference with Q-Media (circle) or w/o Q-Media (square), B) Growth curve, C) Mab vs CCD plot.

3.3 Main metabolic

L/G indicates glycolysis and TCA cycle conditions. Higher L/G means glucose turn to lactate through pyruvate, hence energy efficiency is low. High concentration Q-Media supplemented with 160 micro-mol/L indicated slightly decrement of L/G. It is assumed that the possibility of the improvement in electron transport chain by Q-media.

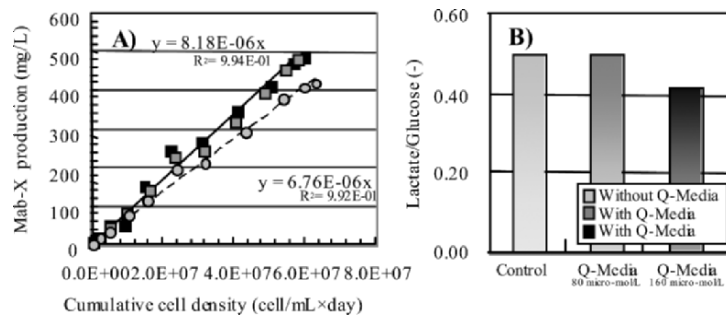


Figure 3. Influence of the Q-Media in 1 L scale reactor. A) Mab-X vs CCD plot indicate SPR, B) Comparison $Q_{\text{Lactate}} / Q_{\text{Glucose}}$

3.4 Application CHO and NS0 cell-lines

YB2/0 indicated SPR enhancement by Q-Media. Similarly, we evaluated CHO and NS0 cell-lines, since CHO and NS0 are common host cell-lines for manufacturing of Mabs. Ratio of enhancement was difference between cell-lines, but SPR enhancement was shown in each cell-line by Q-Media.

Table 1. Experimental information for several cells

Case	Host Cell Line	Product	Cultivation Method (Q ₁₀ concentration)	Media Used	Enhanced the productivity
I	YB2/0	Mab-X	Batch (500 micro-mol/L)	Hybridoma SFM (product from Invitrogen)	66.3%
II	CHO	Mab-Y	Fed-Batch (393 micro-mol/L)	EX-CELL™ 302 (product from JRH Biosciences)	28.8%
III	NS0	Mab-Y	Batch (100 micro-mol/L)	RPMI 1640 + serum fraction (product from Invitrogen)	31.9%

3.5 Biological Activity

Q-Media enhance SPR and easy to handle only adding to basal and/or feed medium. Q-Media did not affect biological activity of Mab, such as antigen binding activity and ADCC. Tease results indicated quality of Mab has no influence by Q-media, which is well known high ADCC Mab production by YB2/0³⁾.

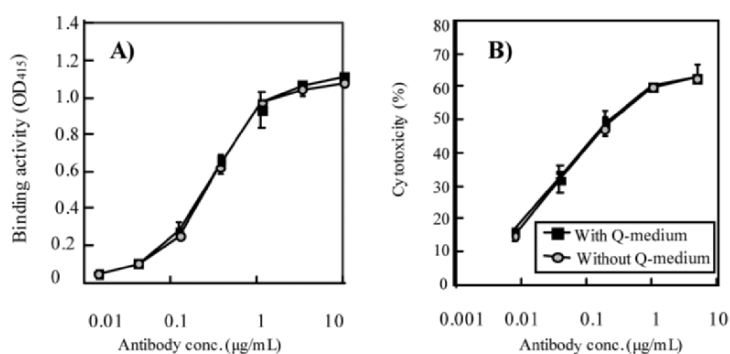


Figure 4. ELISA analysis compare with the Mab from Q-Media or control medium. A) Antigen binding ELISA, B) ADCC

4. CONCLUSION

We found Q₁₀ as the enhancer for Mab production. Q-Media enhanced the productivity of animal cell lines significantly: Case I: 66.3%, Case II: 28.8%, Case III: 31.9 % without influence the antibody biological activity.

ACKNOWLEDGEMENTS

We are grateful to Drs. Kazuyasu Nakamura, Kazuhisa Uchida, Mrs. Eiji Takahashi, Ken Takahashi, Shinji Sakae, Kazutoshi Maki, Noriyuki Takahashi and Ms. Msako Wakitani.

REFERENCES

1. Tatsuya Ogawa, Akashi Narihisa, Yoshinobu Konno, Hiroshi Takasugi, Sugimoto Seiji, Keiichi Yano. Process for producing polypeptide, WO 01/29246 (2001)
2. Yoshinobu Konno, Motoi Aoki, Masakazu Takagishi, Hiroshi Takasugi, Process for producing substance, WO 03/046174 (2003)
3. Toyohide Shinkawa, Kazuyasu Nakamura, Naoko Yamane, Emi Shoji-Hosaka, Nobuo Hanai, Kenya Shitara, et. al., The absence of fucose but not the presence of galactose or bisecting *N*-Acetylglucosamine of Human IgG1 complex-type pligosaccharides shows the critical role of enhancing antibody-dependent cellular cytotoxicity, *J. Biol. Chem.*, 278, 5, 3466-3473, (2003)
4. Junichi Kanazawa, So Ohta, Kenya Shitara, Fumiko Fujita, Masahide Fujita, Masami Okaabeet, et. al., Therapeutic potential of chimeric anti-(ganglioside GD3) antibody KM871: antitumor activity in xenograft model of melanoma and effector function analysis, *Cancer Immunol Immunother*, 49, 253-258 (2000)

OBSERVATION OF INDIVIDUAL CELL BEHAVIORS TO ANALYZE MITOGENIC EFFECTS OF SERICIN

Tomohiro Toyosawa¹, Satoshi Terada¹, Masahiro Sasaki², Hideyuki Yamada², and Masahiro Kino-oka³

¹Department of Applied Chemistry and Biotechnology, University of Fukui 3-9-1 Bunkyo, Fukui 910-8507, Japan; ²Technology Department, Seiren Co., Ltd. 1-10-1 Keya, Fukui 918-8560, Japan; ³Department of Chemical Science and Engineering, Osaka University 1-3 Machikaneyama-cho, Toyonaka 560-8531, Japan

Abstract: Mammalian cell cultures are used in many fields. Various biologically active agents are produced in mammalian cell cultures because of bioactivity derived from glycosylation. *Ex vivo* cultures of various cells including chondrocytes and immunocytes are performed for regenerative medicine and cell therapy. Currently, most of mammalian cell cultures require supplementation of fetal bovine serum (FBS). However, FBS should be avoided due to concerns related to bovine spongiform encephalopathy (BSE) or other infections including viruses that may occur. Therefore, we investigated sericin as an alternative to FBS, and found that sericin could promote proliferation of hybridoma cells. However, mechanisms whereby sericin promotes cell proliferation are still unknown. Microscopic observations indicated that hybridoma cells in the presence of sericin tended to be cohered, implying that sericin might allow cells to aggregate to each other, and interactions between these aggregated cells might induce proliferation, or suggesting that aggregation might be due to proliferation without detachment of cells after cell division. In this study, we attempted to determine whether aggregation of cells in the presence of sericin was due to migration or post-cell divisional detachment. Towards this aim, we used a computer-controlled observation system associated with image analysis. Consequently, results indicated that sericin strengthened attachment between cells after cell division to induce cohesion between cells.

Key words: sericin, silk, serum-free, computer-controlled observation system, aggregation, migration, proliferation, hybridoma

1. INTRODUCTION

Recently, many curative bioproducts for obstinate diseases have been developed in mammalian cell cultures as a novel biotechnological method.

Reasons for producing bioactive reagents in mammalian cell cultures are purely based on physiological activities. Indeed, for example, post-translational modifications such as glycosylation can be performed in such systems. Generally, addition of fetal bovine serum (FBS) or bovine serum albumin (BSA) as an alternative to FBS is required for mammalian cell cultures. However, neither FBS nor BSA is desirable because of concerns for bovine spongiform encephalopathy (BSE). Therefore, alternatives not derived from mammals are eagerly recommended. Ideal alternatives should fulfill the following requirements: 1) they should not derive from mammals, 2) they should be easy to use, 3) they should be effective in proliferation and production. Here, we focused on sericin as a potential alternative. Sericin (1) is derived from silk, and therefore does not incur any concerns for infections from prions and other pathogens. Sericin is a convenient product, partly because it is highly hydrophilic, resulting in good solubility in water, and partly because it is an autoclavable protein. Moreover, we found that sericin promoted proliferation of various cell lines, enhanced antibody productivity of a hybridoma cell line, and protected cells from toxicity by acting as a surfactant. Therefore, it can be expected that sericin could be used as an alternative to FBS in culture media in order to develop serum-free media. However, mechanisms whereby sericin promotes cell proliferation have not been elucidated, except for the observation that hybridoma cells in the presence of sericin tended to aggregate. Whether aggregation is due to attachment after cell division, or acceleration of proliferation is due to aggregation, remains unclear. In order to determine which of these mechanisms is responsible for sericin-induced cell aggregation, a continuous monitoring technique is required.

Several techniques allowing continuous monitoring of cellular behaviors have been developed as it is now accepted that the understanding of cell states would contribute to stable manufacturing processes (2). From cell behaviors, we can obtain important information about cellular activities, and many researchers have developed various observational techniques for improving monitoring of cell cultures (3). However, most of the reported studies used stains for intracellular organelles (4, 5), and therefore it is difficult to apply these techniques to manufacturing processes. Recently, in order to visually capture cellular phenomena as overall outputs through genomic, proteomic and metabolic expressions, non-invasive and time-lapse observations of whole cells have been reported, and applied to evaluation of cellular responses against environmental stimuli (6, 7). In the present study, we tried to elucidate mechanisms of cell proliferation using a computer-controlled observation system combined with image analysis, developed by Kino-oka et al. (8).

2. MATERIALS AND METHODS

Cell Culture

Murine hybridoma cell line 2E3O-3N was maintained in serum-free medium ASF104N (Ajinomoto, Tokyo, Japan) at 37°C under a 5% CO₂ atmosphere. Sericin and BSA were dissolved in ASF104N medium at 0.1% (w/w), and sterilized by filtration.

Assay of proliferation and antibody production

Cell viability and density were determined using the trypan blue exclusion method with a hemacytometer. Monoclonal antibody secretion from hybridoma cells was measured by ELISA.

Image capture

Observation tools were constructed to analyze cellular motion. Three 25 cm² T-flasks containing cells were set on fixed brackets located between an LED lamp (IDM-30/30WT, Imac Co., Shiga, Japan) for illumination, and a high-resolution CCD camera (CS3910, Tokyo Electronic Industry Co., Tokyo, Japan) attached with an objective lens (MPlan60, Nikon Co., Tokyo, Japan) for image capturing (8). Sterile air including 5% CO₂ was introduced into a chamber kept at 37°C. The CCD camera was mounted on stages (ALS-510-H1P, MMU-60X and MMU-60Z; Chuo Precision Industrial, Tokyo, Japan), which could be electrically driven in the *X*-, *Y*- and *Z*-directions to take arbitrary positions on the bottom surface of the flask, and to adjust focus on cells of interest at each position.

Initial images were captured every 20 min at five positions in each flask during cell culture. Captured area and resolution were 0.37 mm² and 1.3 * 10⁶ pixels (1030 lines * 1296 lines), respectively, and each pixel with 10 bits offered 1024 gray scale from black (0) to white (1023). A LabVIEW software (National Instruments, Austin, TX, USA) was used for programming, and all procedures including positional control of the CCD camera on the stages, illumination with the LED lamp and acquisition of the cell images were performed automatically with a personal computer.

3. RESULTS AND DISCUSSIONS

1. Effects of sericin on proliferation of hybridoma cells and antibody production

We initially examined the proliferation of the hybridoma 2E3O-3N cell line in serum-free culture supplemented with sericin in batch cultures. When cells were seeded in medium containing 0.1% sericin, cell proliferation was promoted compared with conditions without supplement (Fig.1a). Mitogenic activity of sericin was similar to that of BSA.

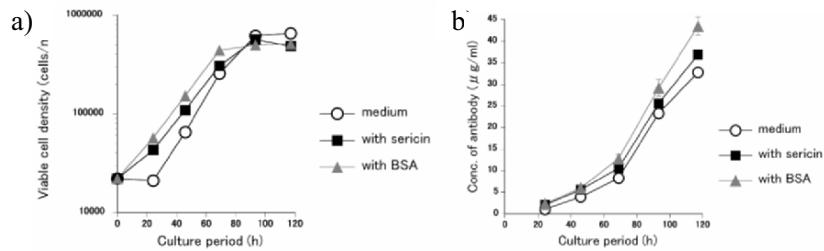
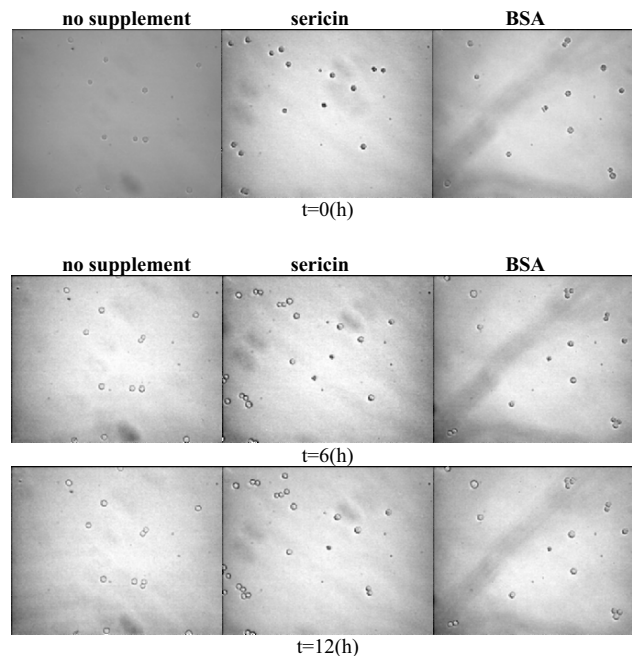


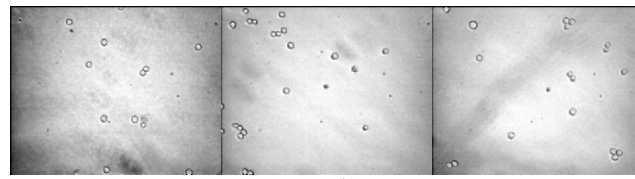
Figure 1a. Effects of sericin on proliferation of hybridoma 2E3O-3N cells. 2E3O-3N cells were cultured in ASF104N medium (Ajinomoto). ASF104N medium was supplemented with either sericin or BSA. Figure 1b. Effects of sericin on monoclonal antibody production. Culture supernatant was collected and antibody concentration was determined by ELISA

Viable cell density of cultures supplemented with sericin or BSA was twice that of cultures without supplement at day 1. Moreover, sericin successfully enhanced monoclonal antibody production (Fig.1b), although BSA was superior to sericin in stimulating antibody production. These results suggested that sericin played an important role in cell culture as an alternative to FBS or other mammalian derived factors.

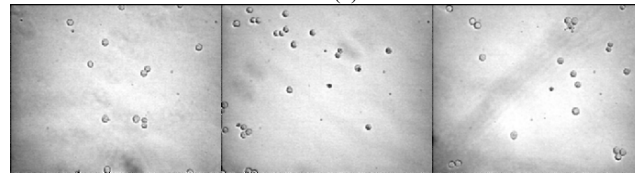
2. Cellular motion of the hybridoma in the presence of sericin

Cellular motion was monitored using the constructed observation tool during culture of the hybridoma in serum-free medium supplemented with sericin, or BSA (Fig. 2). In the presence of sericin, taxis of cells was enhanced while detachment between cells that had just divided decreased. However, individual cells didn't attract to each other, nor adhere together.

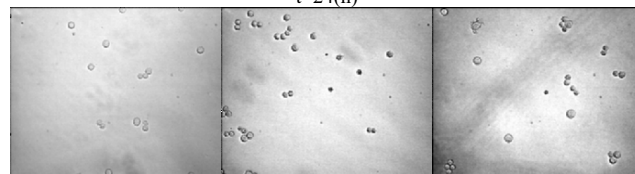




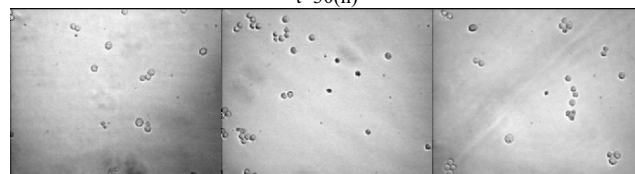
$t=18(h)$



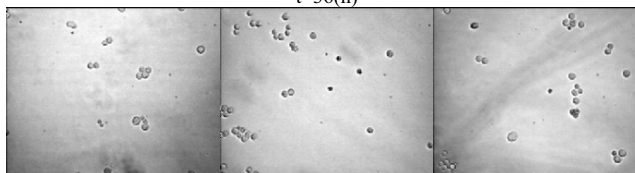
$t=24(h)$



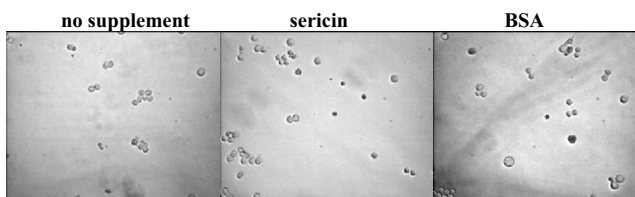
$t=30(h)$



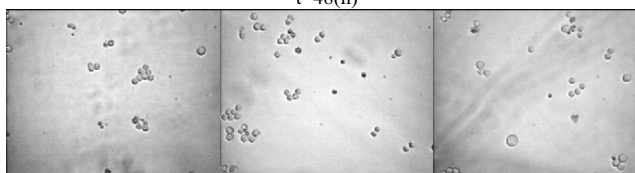
$t=36(h)$



$t=42(h)$



$t=48(h)$



$t=54(h)$

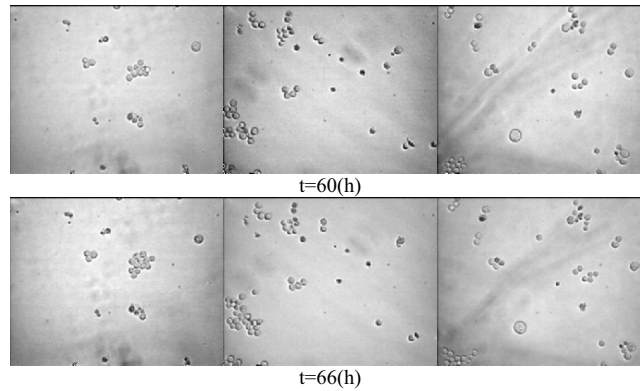


Figure 2. Image of hybridoma cell culture with sericin. 2E3O-3N was cultured in ASF104N medium, supplemented with sericin, supplemented with BSA.

These observations suggested that cohesion of cells that had just divided induced proliferation. Consequently, it was plausible that sericin promoted proliferation of 2E3O-3N cells by inducing cell-cell adhesion between cells at post-cell division (Fig. 3).

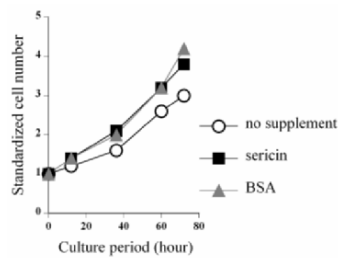


Figure 3. Increase in cell number determined from Fig. 2. Cell number in the same area in the photographs was counted.

Many researchers reported that cell-cell interactions were important for proliferation. For instance, gap junctions composed of two juxtaposed hemichannels present on surfaces of adjacent cells, form a transcellular channel that permits rapid and efficient propagation of ions, metabolites, and second messengers between adjoining cells (9). Moreover, it was also reported that maximal cellular concentrations as well as amounts of monoclonal antibody attainable in batch cultures were dependent on inoculum size (10). All these observations suggest that sericin might stimulate formation of gap junctions or of an autocrine system, to promote proliferation and to enhance antibody production. However, it was also reported that cell-cell interactions often downregulated proliferation (11). Therefore, further studies are desired to elucidate details of mechanisms involved.

4. REFERENCES

- (1) S. Terada, T. Nishimura, M. Sasaki, H. Yamada, and M. Miki, Sericin, a protein derived from silkworms, accelerates the proliferation of several mammalian cell lines including a hybridoma, *Cytotechnology* 40, 3-12 (2002).
- (2) R. Kapur, Fluorescence imaging and engineered biosensors: functional and activity-based sensing using high content screening, *Ann. N.Y. Acad. Sci.* 961, 196-197 (2002).
- (3) J. Folkman, and A. Moscona, Role of cell shape in growth control, *Nature* 273, 345-349 (1978).
- (4) K.A. Giuliano, and D.L. Taylor, Fluorescent-protein biosensors: new tools for drug discovery, *Trends Biotechnol.* 16, 135-140 (1998).
- (5) P.B. Simpson, J.I. Bacha, E.L. Palfresyman, A.J. Woollacott, R.M. McKernan, and J. Kerby, Retinoic acid evoked-differentiation of neuroblastoma cell predominates over growth factor stimulation: an automated image capture and quantitation approach to neuritogenesis, *Anal. Biochem.* 298, 163-169 (2001).
- (6) K. Wu, D. Gauthier, and M.D. Levine, Live cell image segmentation, *IEEE Trans. Biomed. Eng.* 42, 1-12 (1995).
- (7) R. Hartmann-Petersen, P.S. Walmod, A. Berezin, V. Berezin, and E. Beck, Individual cell motility studied by time-lapse video recording: influence of experimental conditions, *Cytometry* 40, 260-270 (2000).
- (8) M. Kino-oka, Y. Agatahama, N. Hata, and M. Taya, Evaluation of growth potential of human epithelial cells by motion analysis of pairwise rotation under glucose-limited condition, *Biochem. Eng. J.* 19, 109-117 (2004).
- (9) J.P. Stains, and R. Civitelli, Cell-to-cell interaction in bone, *Biochem. and Biophys. Res. Commun.* 328, 721-727 (2005).
- (10) S. S. Ozturk, and B. Q. Palsson, Effect of initial cell density on hybridoma growth, metabolism, and monoclonal antibody production, *J. Biotech.* 16, 259-278 (1990).
- (11) K. Asosingh, V. Vankerkhove, I. Van Riet, B. Van Camp, and K. Vandekeken, Selective in vivo growth of lymphocyte function-associated antigen-1-positive murine myeloma cells: Involvement of function-associated antigen-1-mediated homotypic cell-cell adhesion, *Exp. Hematol.* 31, 48-55 (2003).

STUDIES OF PASSAGE EFFECT OF HaNPV BACULOVIRUS PRODUCED IN Hz INSECT CELL CULTURE

Kanokwan Poomputsa¹, Kultida Poltawee¹, Somkiet Techkarnjanarak³, and Phenjun Mekvichitsaeng²

¹*School of Bioresources and Technology, King Mongkut's University of Technology Thonburi, Bangkok, Thailand, 10150;* ²*Pilot Plant Development and Training Institute, King Mongkut's University of Technology Thonburi, Bangkok, Thailand, 10150;*

³*Biochemical Engineering and Pilot Plant Research and Development Unit, National Center for Genetic Engineering and Biotechnology, Bangkok, Thailand, 10150*

Abstract: Serial passage of baculoviruses in insect cell culture leads to rapidly accumulating mutant; also know as “passage effect” which results in changing of virus efficacy. The effect of viral passaging varies between different types of baculovirus. This study aimed to investigate the effect of serial passages on baculovirus (Th-HaNPV) productivity in insect cell culture (Hz cell line) and to determine the overall protein expression (proteomic) changes induced by the serial passage. The viral efficacy in Hz cell culture was determined throughout ten serial passages. The results showed that percentages of infected cells producing polyhedra decreased to 23% at passage 10 (compared to passage 3). The extracellular virus (ECV) titers increased gradually from passage 2 to 5. However, from passage 6 onwards, there was a gradual reduction in ECV production. A 90% decreased of polyhedra produced per cell (PIBs/cell) was also revealed. These results indicated that the viral productivity decrease rapidly during serial passages of Th-HaNPV in Hz cell culture.

Overall protein expression of Th-HaNPV extracellular virus (ECV) during serial passage was also determined by Two-dimensional polyacrylamide gel electrophoresis (2D-PAGE). Serial passage resulted in protein profile changes of ECV. Some proteins of baculovirus (HaNPV) which has not been previously reported were also detected by this technique and may be used as marker proteins to predict the Th-HaNPV viral efficacy.

Key words: Th-HaNPV, passage effect, Hz cell, 2D-PAGE

1. INTRODUCTION

Insect baculoviruses are group of insect biological control agents that received considerable attention. The *Helicoverpa armigera* nucleopolyhedrovirus (HaNPV) is a baculovirus that has the potential to be an effective biocontrol agent for the *Helicoverpa* pest species worldwide. *In vitro* production of baculoviruses on a commercial scale would be an advantage in the production of viral biological control agent. However, serial passaging of some baculoviruses in insect cell culture has been shown to lead to rapidly accumulating mutant, also know as “the passage effect” which a change from the wild-type (referred to as MP for ‘many polyhedra’) to the few polyhedra (FP) mutants can be detected. This resulted in poor production yield and virus efficacy that hinder the use of *in vitro* production of baculoviruses for use as biopesticide. To develop a large-scale *in vitro* production of the Th-HaNPV, it was essential to determine whether or not the passage effect was evident when this virus is serially passaged in cell cultures and what are the characteristics of the Th-HaNPV passage effect.

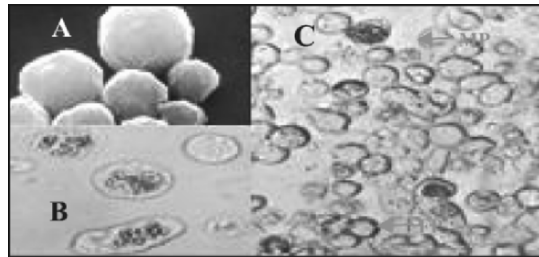


Figure 1. A) Electron micrograph of polyhedral inclusion bodies (PIBs) formed by NPV, which are stable in the environment. B) PIBs in the nucleus of the HaNPV-infected Hz insect cell. C) MP and FP phenotypes found in Th-HaNPV at passage 10.

2. MATERIALS AND METHODS

2.1 Cell and Viruses

Helicoverpa zea (Hz) cell line, isolated from pupal ovarian tissue, was grown in SF900II medium supplemented with 10% foetal bovine serum (FBS) at 27°C. Virus inoculum, HaNPV (Thai isolated, Th-HaNPV), was first established in Hz cells using haemolymph collected from infected larvae from the Central Laboratory and Greenhouse Complex, Kasetsart University, Nakhon Pathom, Thailand.

2.2 Serial passage of Th-HaNPV

Virus stock (P1) was obtained by adding 1 ml of the diluted infected haemolymph to 1.5×10^6 cells in a 25-cm² TC-flask and the medium was harvested 5 days postinfection and used as viral stock. The virus titer was determined by end point dilution assay. Passage 2 (P2) virus stock was made in suspension culture by infecting cells at a density of 5×10^5 cells/ml with P1 stock at MOI of 1 PFU/cell. The infectious medium containing extracellular virus (ECV) was harvested 5 days postinfection and titer determined before used as passage 3(P3) inoculum. The number of polyhedra was determined by lysis of infected cells with 1% SDS for 1 h before counting in a haemocytometer. Serial passages from passages 4 (P4) to 9 (P9) were performed as previously described.

2.3 Two-dimensional gel electrophoresis and protein identification

Protein sample (500 µg) was mixed with IPG rehydration buffer (Amersham-Pharmacia Biotech). The IEF strips (Amersham-Pharmacia Biotech) were allowed to rehydrate overnight, focused, equilibrated and apposed to the second dimension (12%SDS/PAGE) gels. Gels were silver stained and dried between two sheets of cellophane. Protein spots on 2D gels were analyzed with Melanie II 2D-PAGE analysis software.

3. RESULTS AND DISCUSSION

3.1 Viral Efficacy

The viral efficacy can be monitored from the changes of extracellular virus (ECV) and occlusion body (polyhedra) production which had been determined over 10 serial passages in this study. The results (Figure 2) showed that the percentage of infected cells producing polyhedra decreased to 23% at passage 10 (compared to passage 3). The ECV titers increased gradually from passage 2 to 5. The highest ECV titer was obtained at passage 5 (1.6×10^9 pfu/ml). From passage 6 onwards, there was a gradual reduction in ECV production. The number of polyhedra produced per cell decreased from 51 polyhedra per cell at passage 3 to 5 polyhedra per cell at passage 10, representing a 90% reduction in yield. These results indicate that the viral productivity decrease rapidly during serial passages of Th-HaNPV in Hz cell culture and this was similar to HaSNPV and LdMNPV^(1, 2). The information obtained from this study

can be applied for baculovirus (Th-HaNPV) production such as serial passage of HaNPV should not be performed more than 6 passages since very low viral productivity will be obtained.

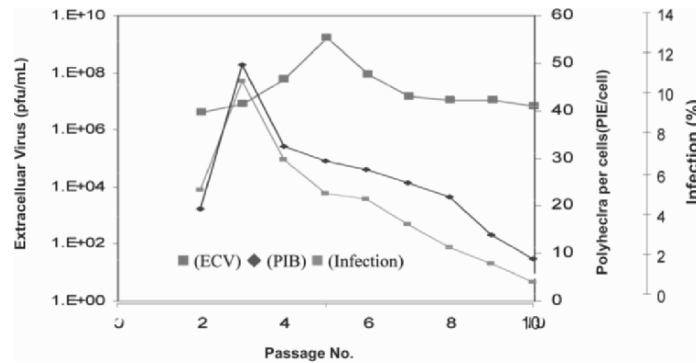


Figure 2. Th-HaNPV virus efficacy over 10 serial passages.

3.2 Viral Protein Profiles

Deletion, rearrangement, and reiteration of viral genome including the insertion of insect host DNA have been reported in mutant baculoviruses when the genome analyses were performed⁽³⁻⁶⁾. The genome information, however, may not clearly explain the changing characteristic of the mutant virus. Studies of protein profiles of the virus during serial passage were therefore performed in this study.

2D-PAGE was used to determine the change of overall proteins expression of extracellular virus (ECV). ECV was obtained from virus stock at passage 2 (reference passage), passage 5 (high ECV titers) and passage 10 (low ECV titers). The results showed that the serial passage resulted in protein profiles changes which could be detected by 2D-PAGE. For example, some proteins believed to be involved in transcriptionally transactivating viral gene and augmenting viral DNA replication such as PE38 and 25KFP which was essential for polyhedron formation and viral occlusion were found to be changed according to their efficacy this study (data not shown). Moreover, other proteins of baculovirus (HaNPV) which has not been previously reported were detected by this technique and may be use as marker protein to predict the viral efficacy (Figure 3, C1).

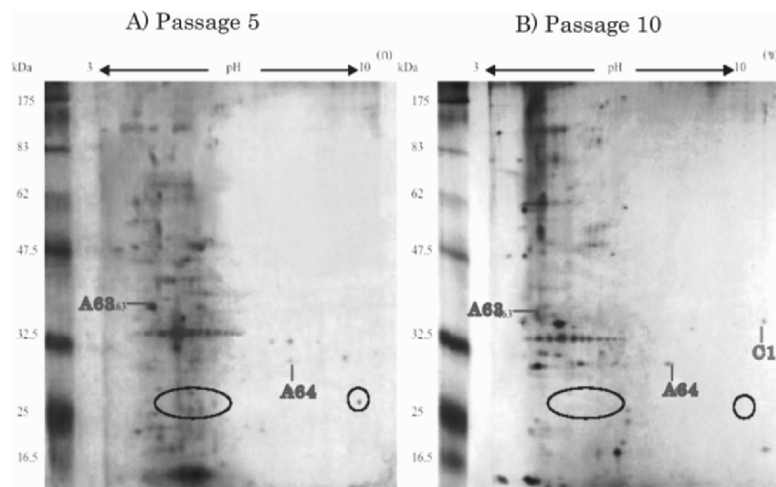


Figure 3. 2D-PAGE of Th-HaNPV extracellular protein from a) Passage 5 and b) Passage 10. Black circles represent proteins that are absent after 10 serial passages which may play some roles in viral efficacy. C1 is an example of protein that is only present when the viral efficacy is decline which may be used as marker protein. A63 and A64 are proteins that did not change during serial passage.

4. REFERENCES

- 1) Kool, M., Voncken, J.W., van Lier, F.L.J., Tramper, J. and Vlak, J.M., 1991, "Detection and analysis of *Autographa californica* nuclear polyhedrosis virus mutants with defective interfering properties", *Virology*, Vol. 183, pp. 739-746.
- 2) Cusack, T. and Mccarthy, W.J., 1989, "Effect of serial passage on genetic homogeneity of plaque variant of *Lymantria dispar* nuclear polyhedrosis virus (Hamden LDP-67)", *Journal of General Virology*, Vol. 70, pp. 2963-2972.
- 3) Lee, H.Y. and Krell, P.J., 1994, "Reiterated DNA fragment in defective genomes of *Autographa californica* nuclear polyhedrosis virus are competent for AcMNPV-dependent DNA replication", *Journal of Virology*, Vol. 202, pp. 418-429.
- 4) Beames, B. and Summers, M.D., 1988, "Comparisons of host cell DNA insertions and altered transcription at the site of insertions in few polyhedra baculovirus mutants", *Virology*, Vol. 162, pp. 206-220.

OPTIMIZATION OF RECOMBINANT DENGUE ENVELOPE PROTEIN PRODUCTION IN INSECT CELL CULTURE IN 2.5 L FERMENTER

Phenjun Mekvichitsaeng, Somsak Sotasan and Kanokwan Poomputsa
*Pilot Plant Development and Training Institute, King Mongkut's University of Technology
Thonburi 83 Mu 8 Takham Bangkhuntien, Bangkok 10150 Thailand*

Abstract: The baculovirus expression vector system (BEVS) has been used to express many functionally authentic recombinant proteins in insect cells. Insect cells are used as hosts for recombinant baculovirus infection which results in recombinant protein production. In this study, recombinant dengue envelope protein production. In this study, recombinant dengue envelope protein was produced from insect cell (SF-9) infected with recombinant dengue baculovirus. Conditions involve the recombinant dengue envelope protein production i.e insect cell medium, insect cell growth phase, cell density, amount of recombinant baculovirus used to infect cells and optimal harvesting time were investigated. The results obtained when study in shake flask (250ml) showed that optimal medium for Sf-9 growth was the mixture of SF-900II and TC100 at ratio 1:1 supplemented with 10% FCS. The optimal growth phase and cell density were at early log phase and 1×10^6 cells/ml, respectively. Optimal multiplicity of infection was 5 (MOI =5) and harvest time was 3 days post infection. The information obtained in this study was then used for large scale production in a 2.5 L stirred tank reactor performed in 1 L working volume. It was found that the optimal agitation rate and dissolved oxygen for insect cell growth was at 90 rpm and 60-80% air saturation, respectively. Maximum recombinant dengue envelope protein production was 13 mg/L which was higher than the production from shake flask.

Key words: Recombinant Protein, Dengue Virus, Insect Cell Culture, Fermenter

INTRODUCTION

Dengue virus is a primary cause of Dengue Hemorrhagic Fever (DHF) that is a major cause of pediatric morbidity and mortality in most tropical countries. Envelope protein of dengue virus is known to stimulate immune of dengue virus' patient. Recombinant dengue viral envelope protein was produced from Baculovirus Expression Vector

System which is known as one of the most powerful and versatile eukaryote expression vector system available. It has been used to express many proteins from different sources. High level of protein production and post translational modification of recombinant protein can be obtained using insect cell as host for baculovirus replication⁽¹⁾. Insect cells were used as hosts for production of recombinant envelope protein when infected with recombinant envelope baculovirus that was engineered by insertion of envelope gene under control of the strong polyhedrin promoter. The recombinant E protein can be used in the diagnostic system as an antigen to detect dengue viral infection.

Recombinant protein production is affected by several factors such as cell density, time of infection (TOI) and availability of nutrients including multiplicity of infection (MOI) and dissolved oxygen. In this study, medium, MOI, TOI, cell density and dissolved oxygen were investigated.

Materials and Methods

1. Cell line and Maintenance

Spodoptera frugiperda (Sf9) insect cells (ATCC-CRL-1711) were maintained in 100 ml of TC 100 medium (Gibco BRL) and Sf-900II medium (Gibco BRL) (1:1) with 10% FCS at 27°C in 250 ml erlenmeyer flask shaking at 120 rpm in an orbital shaker. The cells were sub-cultured to density of 3×10^5 cells/ml when the cell density reached $3-4 \times 10^6$ cells/ml.

2. Cell culture in shake flask

Sf9 cells at 3×10^5 cells/ml were inoculated into 250 ml shake flasks each containing 100 ml of medium shaking at 120 rpm, 27°C. Culture were collected daily for cell count by hemacytometer.

3. Cell culture in 2.5 l fermenter

Sf9 cells at concentration of $3-4 \times 10^6$ cells/ml from 250 ml shake flask was used as inoculum for 2.5 l fermenter with 1 l working volume. The initial cell concentration in fermenter was 3×10^5 cells/ml in every experiments.

4. Baculovirus infection

Sf9 cells were infected at early exponential phase (1 and 2×10^6 cells/ml) with recombinant E baculovirus at various multiplicity of infection (MOI) of 0.1, 1, 5, 10. 1 ml of infected cell was collected daily for cell count and 1 ml was centrifuged at 10,000 rpm for 10 min, cell pellet was collected and resuspended in cell lysis buffer (62.5mM, Tris-HCl pH 6.8, 2%SDS) while supernatant was discarded. Recombinant dengue viral envelope protein from cell lysate was detected by Western blot analysis.

5. Cell density estimation

Cell number was determined by hemacytometer. The cell viability was measured by trypan blue staining.

6. Estimation of recombinant Dengue viral envelope protein concentrations

The recombinant dengue viral envelope protein production was detected by Western blot analysis. The intensity of specific protein bands recognized by monoclonal antibody (3H5) was quantified by image analyzer. On the same membrane, purified recombinant dengue viral envelope protein from *E.coli* at various concentrations were used as standard. The intensities of each specific band were plotted against concentrations. The amount of recombinant dengue viral envelope protein from insect cells was estimated from this standard curve.

RESULTS

1. Medium tested

Ten different mediums were tested by culturing sf9 cell in 250 ml shake flask. The maximum viable cell density and the price of medium were compared in Table 1.

Table 1. Maximum viable cell density and the price of medium in various medium.

Media	Price (bath/ml)	Maximum viable cell density ($\times 10^6$ cells/ml)
1. SF900II+10% FCS	4.494	11.8
2. SF900II+5% FCS	3.977	10.2
3. SF900II	3.460	7.5
4. 45% SF900II+45% TC100+10% FCS	3.114	12.0
5. 47.5% SF900II+47.5 TC100+10% FCS	2.552	9.5
6. 22.5% SF900II+67.5% TC100+2.5% FCS	2.469	5.9
7. 48.75% SF900II+48.75% TC100+2.5% FCS	2.256	8.1
8. 75% MM8+20% SF900II+5% FCS	1.787	0.95
9. 75% MM8+ 20% TC100+5% FCS	1.187	0.53
10. 20% MM8+75% TC100+5% FCS	1.143	1.1

From Table 1 we found that the medium of 45% SF900II+45% TC100+10% FCS was the best medium to cultivate Sf9 cells. The results showed that maximum viable cell density with medium of reasonable price. From this data we used this medium entire experiments.

2. Optimum condition to produce recombinant envelope dengue protein

2.1 MOI and TOI tested in shake flask

Sf9 cells were infected at early exponential phase (1 and 2×10^6 cells/ml) with recombinant E baculovirus at various multiplicity of infection (MOI 0.1, 1, 5, 10). The maximum recombinant envelope protein produced at various MOI were compared and given in Fig. 1 and 2 for cell concentration 1×10^6 cells/ml and 2×10^6 cells/ml, respectively.

Figure 1 and 2 Showed that optimum condition for protein production when infected at cell density of 1×10^6 cells/ml was MOI 5 and TOI 3 days. The optimum condition for protein production when infected at cell density of 2×10^6 cells/ml was MOI 10 and TOI 2 days. Protein production when infected at cell density of 1×10^6 cells/ml was MOI 5 and TOI 3 days was higher than infected at cell density of 2×10^6 cells/ml was MOI 10 and TOI 2 days. Therefore, we used these conditions of infection at cell density of 1×10^6 cells/ml MOI 5 for experiment in fermenter.

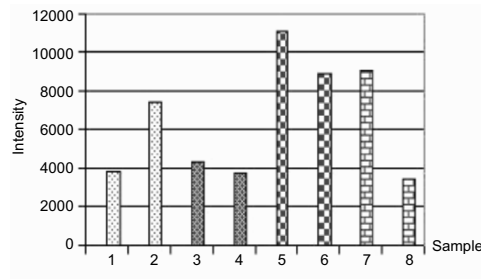


Figure 1. Recombinant envelope protein production from various MOI at the initial cell concentration of 1×10^6 cells/ml (1 ml of cell culture was collected, centrifuged and cell pallet collected was dissolved in 100 μ l lysis buffer)

No.1	MOI 0.1	TOI 7 days:	No.2	MOI 0.1	TOI 8 days
No.3	MOI 1	TOI 7 days:	No.4	MOI 1	TOI 8 days
No.5	MOI 5	TOI 3 days:	No.6	MOI 5	TOI 4 days
No.7	MOI 10	TOI 3 days:	No.8	MOI 10	TOI 4 days

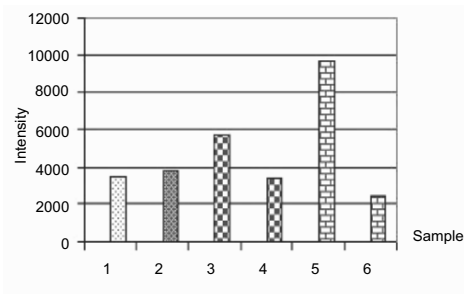


Figure 2. Recombinant envelope protein production from various MOI at the initial cell concentration of 2×10^6 cells/ml. (1 ml of cell culture was collected, centrifuged and cell pallet collected was dissolved in 100 μ l lysis buffer)

No.1	MOI 0.1	TOI 7 days:	Sample No.2	MOI 1	TOI 5 days
No.3	MOI 5	TOI 3 days:	Sample No.4	MOI 5	TOI 4 days
No.5	MOI 10	TOI 2 days:	Sample No.6	MOI 10	TOI 3 days

2.2 Production of recombinant envelope dengue protein in 2.5 l fermenter

2.5 L stirred tank reactor was used with working volume 1 L. From preliminary studied we found that stirring speed of 90 rpm was suitable so we used this rate and varied the dissolved oxygen at 30-50% air

saturated and 60-80% air saturated. Sf9 cell was cultured and infection at cell density of 1×10^6 cells/ml MOI 5.

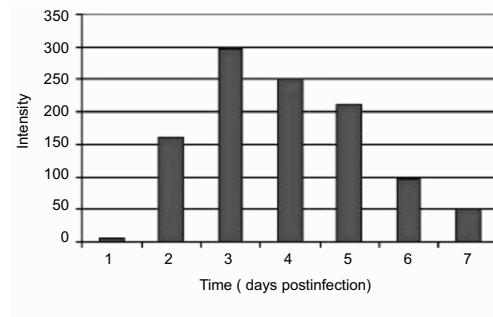


Figure 3. Level of recombinant envelope protein production in stirred tank reactor (2.5 L) with stirring speed of 90 rpm, dissolved oxygen of 30-50% and MOI of 5

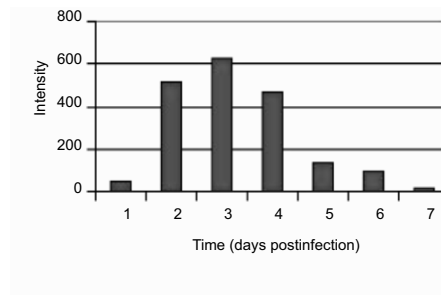


Figure 4. Level of recombinant envelope protein production in stirred tank reactor (2.5 L) with stirring speed of 90 rpm, dissolved oxygen of 60-80% and MOI of 5

From Figure 3 – 4, it was found that the level of dissolved oxygen can affect the level of protein production. The level of protein production at 30-50% dissolved oxygen is much lower than that obtained at 60-80% of dissolved oxygen. This result is found to be in good agreement with that of Kloppinger et al. (1990, 1991) who found that growth and level of protein production of Sf9 cells was affected by both agitation speed and level of dissolved oxygen. At MOI of 5, 1×10^6 cells/ml initial cell

concentration, 90 rpm stirring speed and 60-80 % dissolved oxygen, the highest concentrations of recombinant envelope protein produced are 11.3 and 13.0 mg/l in shake flask and 2.5 L fermentor, respectively, by comparing with standard curve constructed with purified protein extracted from E. coli system.

CONCLUSION

1. It can be deduced that the composition of the medium suitable for growing Sf9 cells to achieved highest cellular density was 45% SF-900 supplemented with 45% TC100 and 10% FCS
2. Optimum conditions for the production of recombinant envelope protein in shake falsk was MOI of 5 and initial cell concentration of 1×10^6 cells/ml while the optimal harvest time was 3 days post infection which led to the concentration of 11.3 mg/L
3. For a 2.5 L stirred tank reactor with 1 L working volume, the optimal conditions which led to the highest recombinant protein production of 13.0 mg/L was MOI of 5, 90 rpm, initial cell concentration of 1×10^6 cells/ml and 60-80 % dissolved oxygen while the optimum harvest time was 3 days post infection

REFERENCES

1. Halstead, S.B., 1989, "Antibody, macrophages, dengue virus infection, shock and haemorrhagic fever: A pathogenic cascade" Review Infection Disease, Vol. 11, pp. 830-839.
2. Kloppinger, M., Fertig, G., Fraune, E. and Miltenburger, H.G., 1990, "Multistage production of *Autographa californica* nuclear polyhydrosis virus in insect cell cultures," Cytotechnology, Vol. 4, pp. 271-278.
3. Kloppinger, M., Fertig, G., Fraune, E. and Miltenburger, H.G., 1990, "High cell density perfusion culture of insect cells of production of baculovirus and recombinant protein." In: Spier, R.E., Griffiths, J.B. and Meignier, B.(eds) Production of biologicals from animal cells culture (10th Meeting of the European Society for Animal cell Culture Technology) pp. 470-476.

TARGETED DISRUPTION OF α -1, 6-FUCOSYLTRANSFERASE (*FUT8*) GENE BY HOMOLOGOUS RECOMBINATION IN CHINESE HAMSTER OVARY (CHO) CELLS

Masayoshi Tsukahara,¹ Ayako Aoki,² Keina Kozono,¹ Yoko Maseki,¹
Yukiko Fukuda,¹ Hideaki Yoshida,² Kazuo Kobayashi,¹ Makoto Kakitani,²
Kazuma Tomizuka,² and Haruhiko Tsumura¹

¹CMC R&D Laboratories, KIRIN Brewery Co., Ltd., 100-1 Hagiwara, Takasaki, Gunma 370-0013, Japan; ²Pharmaceutical Research Laboratories, KIRIN Brewery Co., Ltd., 3 Miyahara, Takasaki, Gunma 370-1295, Japan

Abstract: Targeted disruption of both alleles of the α -1, 6-fucosyltransferase (*FUT8*) gene was successful in CHO cells. The double knockout of *FUT8* was confirmed by Southern and Northern analyses. The frequency of first-round knockout was estimated as 0.53% of G418-resistant clones, more than ten times that of the second round (0.03%). The functional *FUT8* knockout in this cell line was confirmed by its resistance to both LCA and PSA (fucose-recognizing lectins). The HPLC analysis of oligosaccharides in a recombinant monoclonal antibody expressed in this cell line showed a lack of fucose in Asn-linked GlcNAc. The sequential gene-targeting system we used here should be applicable to the modification of properties of recombinant proteins produced by CHO cells.

Key words: gene targeting; α -1, 6-fucosyltransferase (*FUT8*); Chinese hamster ovary (CHO) cell; recombinant monoclonal antibody

1. INTRODUCTION

Targeted disruption of genes of interest has been proven useful not only for the study of gene function but also for permanent modification of cell characteristics. In mammalian cells, efficient gene targeting is limited to a few specific cells, such as mouse embryonic stem (ES) cells¹ and chicken DT40 cells.^{2,3} Chinese hamster ovary (CHO) cells are an attractive mammalian expression host and have been extensively

employed for the production of recombinant protein therapeutics. Genetic modification of CHO cells provides a useful tool for adding extra values to recombinant therapeutic proteins. For example, the lack of fucosylation in recombinant antibodies enhances the activity of antibody-dependent cellular cytotoxicity.^{4,5} So the recombinant monoclonal antibodies produced by the fucosylation enzyme knockout-CHO cells are expected to be clinically effective as a human therapy. On the other hand, several mutants of CHO cells were obtained by a traditional mutagenesis approach. Actually, LEC 13, a CHO cell line deficient in the fucosylation enzyme α -1, 6-fucosyltransferase (*FUT8*), was already obtained by selection according to lectin resistance after mutagen treatment.⁶ However, screenings for mutants are limited to specific characteristics, and unexpected mutations will also occur in selected mutants. Therefore an efficient targeted gene knockout in CHO cells is a prerequisite for industrial application.⁷ Negative selection has been used to decrease nonhomologous random integrations in mouse ES cells.⁸ Recently, Kuroiwa *et al.*⁹ succeeded in sequential gene targeting of a cattle primary fibroblast cell by homologous recombination with positive and negative selection marker genes. In an attempt to produce a knockout cell line in CHO cells, we tried the same strategy using positive and negative selection marker genes. Here, we showed targeted sequential disruption of two alleles of the α -1, 6-fucosyltransferase (*FUT8*) gene, by homologous recombination.

2. MATERIALS AND METHODS

2.1 Construction of *FUT8* KO vector

The genomic DNA corresponding to 9.6 kb of the 5' homologous arm and that corresponding to 2.0 kb of the 3' homologous arm containing part of the first coding exon of the *FUT8* gene were isolated from the Chinese Hamster Lambda Genomic Library (Stratagene, La Jolla, CA). These DNA fragments were subcloned into the 5' and 3' sites of the neomycin-resistant (p*FUT8*-Neo) and puromycin-resistant (p*FUT8*-Puro) genes, respectively (Fig.1).

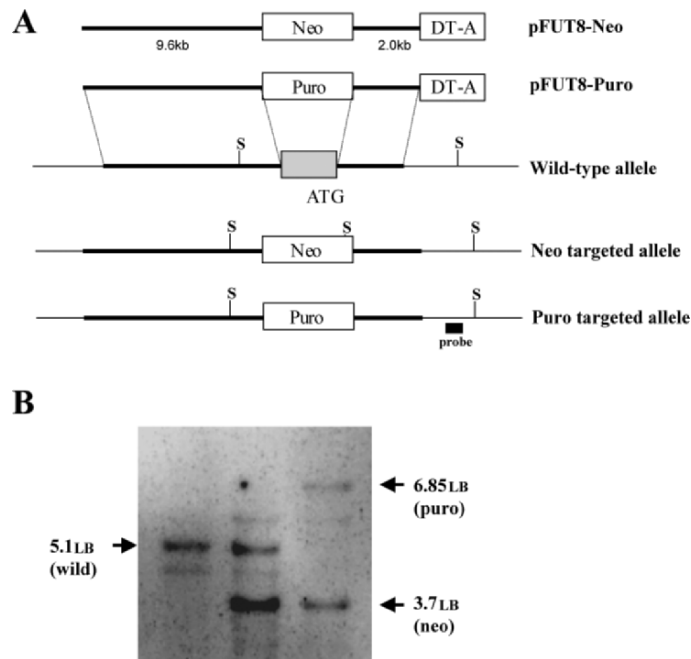


Figure 1. Targeted disruption of α -1, 6-fucosyltransferase (*FUT8*) gene. **(A)** Construct of targeting vectors, wild-type allele, and targeted mutant alleles are shown. The shadow box in the wild-type allele indicates the targeted 134-bp sequence of the *FUT8* gene containing a start codon (ATG). The diphtheria toxin-A (DT-A) fragment gene was attached with the 3' end of the 3' homologous arm for negative selection. Restriction site, S; *SspI*. The strategy to differentiate between the wild-type allele and homologous recombinants using a 3' external probe is shown. **(B)** Southern blot analysis of *SspI*-digested genomic DNA from wild type, *FUT8*^{+/-}, and *FUT8*^{-/-} cells, using the 3'-genomic external probe. Hybridization of *SspI*-digested genomic DNA from wild-type CHO cells to the probe shows a single 5.1-kb DNA band. Targeted integration is revealed by the appearance of an additional diagnostic band: a 3.7-kb band from the targeted allele with the pFUT8-Neo vector and a 6.85-kb band from the targeted allele with the pFUT8-Puro vector.

2.2 Cell culture and transfection

The CHO-K1 cell line was purchased from ATCC (CCL-61). CHO cells were cultured in alpha-minimum essential medium (MEM) supplemented with 10% fetal bovine serum (FBS) at 37°C in a

humidified atmosphere containing 5% CO₂. We transfected 8×10^6 cells in PBS with 37.5 μ g each of pFUT8-Neo and pFUT8-Puro by electroporation set at 950 μ F, 300 V using a Gene Pulser (Bio-Rad, Hercules, CA). After 24 h, we selected the cells under 400 mg/l of G418 and/or 5 mg/l of puromycin for 3 weeks in 96-well plates. For antibody production, the antibody expression vector containing a zeocin-resistant gene was transfected by Lipofectamine (Invitrogen, Carlsbad, CA) according to the manufacturer's instructions. Cells were selected against 300 mg/l zeocin.

2.3 Genomic Southern blot analysis

Genomic DNAs (20 μ g each) isolated from each CHO cell line were digested with *Ssp*I. A DIG-labeled probe was prepared using the PCR DIG Probes Synthesis Kit (Roche Diagnostics, Mannheim, Germany). The labeling by PCR was carried out with primer pairs (5'-AAGGACATCCCC ATCAACACAATG-3' and 5'-AGGGCCAGTCTTAGTCAAACCACC-3') according to the manufacturer's instructions. Each DNA sample was electrophoresed and transferred to Hybond N⁺ (Amersham Biosciences, Piscataway, NJ). The membrane was hybridized with the Dig-labeled probe in DIG Easy Hyb (Roche Diagnostics) overnight at 42°C. Then the blot was washed with a solution of 2 x SSC and 0.1% SDS for 10 minutes at room temperature, and with a solution of 0.1 x SSC and 0.1% SDS for 15 minutes at 65 °C. The signals were visualized by the DIG system (Roche Diagnostics).

2.4 Northern blot analysis

The DIG-labeled DNA fragments used as probes for all experiments were prepared from the CHO cDNA by PCR with the following primer pairs. For *FUT8*: 5'-TCTCTCCGAATACCAGAAGG-3' and 5'-GGTCACCATGGAC TCTTAGG-3'; for glyceraldehyde 3-phosphate-dehydrogenase (*GAPDH*): 5'-CCATCACCATCTTCCAGGAG-3' and 5'-TTCAGTCTGGGATGACC TT-3'. Total RNA was isolated from each CHO clone using Isogen reagent (Nippon Gene Co., Tokyo, Japan). A 20- μ g volume of each RNA sample was electrophoresed and transferred to Hybond N⁺. Visible signals were detected by the same procedure as in genomic Southern blot analysis.

2.5 Lectin resistance assay

Cells were cultured in alpha-MEM with 5% FBS containing 0.5 mg/ml *Lens culinaris* agglutinin (LCA) lectin (Honen, Tokyo, Japan) or *Pisum sativum* agglutinin (PSA) lectin (Honen) for 1 week.

2.6 HPLC analysis of Asn-linked oligosaccharides on antibodies

Antibody was purified with Protein A from culture medium and was dissolved in 100 mM sodium phosphate buffer (pH 7.2) containing 0.5% SDS and 50 mM 2-mercaptoethanol, and was then denatured at 100°C for 5 min. After dilution with 100 mM sodium phosphate buffer and the addition of 0.5% Nonidet P-40, 2.5 units of N-glycanase (Roche Diagnostics) was added to the sample, which was then incubated for 16 h at 37°C. Liberated Asn-linked oligosaccharides were separated from the salts and peptides using an AG 501-X8 mixed-bed resin (Bio-Rad), and from Nonidet P-40 using Bio-Beads S-X8 (Bio-Rad). Reductive pyridylamination and structural analysis of the purified oligosaccharides were carried out essentially according to the method of Kondo *et al.*¹⁰. Pyridylaminated (PA) oligosaccharides were analyzed by HPLC using a reverse-phase column (TSKgel ODS-80TM, TOSOH, Tokyo, Japan). Authentic PA-oligosaccharides and PA-glucose oligomer were purchased from Takara Shuzo Co. (Kyoto, Japan).

3. RESULTS AND DISCUSSION

For the targeting of the first allele of *FUT8*, we screened 934 clones resistant to G418 by genomic PCR. Five independent knockout clones (*FUT8*^{-/-}) were confirmed by Southern blot analysis (data not shown). In this result, the frequency of targeted to random integration was estimated as 0.53% with the pFUT8-Neo vector. Northern blot and RT-Q-PCR analyses of these five knockout clones showed that all clones expressed intact *FUT8* mRNA, and no significant differences in expression levels were observed (data not shown).

For the targeting of the second allele, *FUT8*, one of five heterozygous knockout clones was confirmed to be a single-copy integration and was then transfected with the pFUT8-Puro vector. To avoid integration

of the vector into the first knockout allele, cells were selected in medium containing both G418 and puromycin. After screening of 3,482 clones resistant to both G418 and puromycin, one homozygous knockout clone (*FUT8*^{-/-}) was obtained. A double knockout of the *FUT8* gene was confirmed by Southern blot analysis (Fig. 1B), and the absence of expression was confirmed by Northern blot analysis (Fig. 2). This second-round targeting frequency (0.03%) was less than one-tenth of the first-round knockout frequency. In the DT40 cell line, there was little difference in the targeting frequency between neomycin- and puromycin-resistant genes in the targeting vector.^{11,12} It has been shown that the isogenic sequence is necessary for efficient targeting in mouse ES cells.^{13,14} As a result of the sequence analysis of the intact allele of the targeting region in the heterozygous clone that we used for targeting the second allele, two base deletions were found at 486 bp from the 5' end of the 5' homologous arm of the vector, and no mismatch was found in the 3' homologous arm (data not shown). This heterogeneity between two alleles might explain the lower frequency in the second knockout although we didn't compare the frequency of pFUT8-Neo with that of pFUT8-Puro for the same allele.

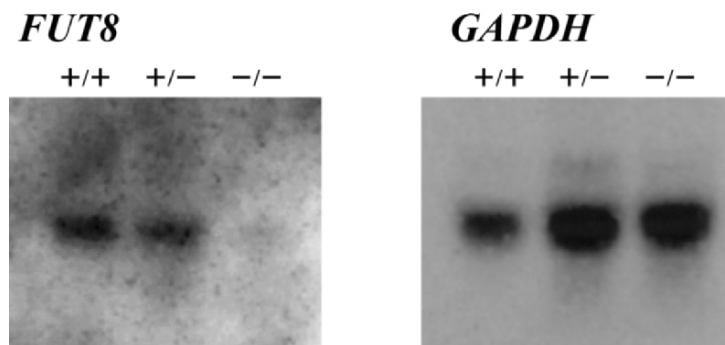


Figure 2. Northern blot analysis for *FUT8* and *GAPDH* mRNA expression. Total RNA was extracted from wild-type, *FUT8*^{+/-}, and *FUT8*^{-/-} cells, electrophoresed, and hybridized with the *FUT8* or glyceraldehyde-3-phosphate dehydrogenase (*GAPDH*) probe.

To confirm the disruption of the *FUT8* gene at the enzyme activity level, the double knockout clone was cultured with two fucose-recognizing lectins. The double knockout clone was grown normally in

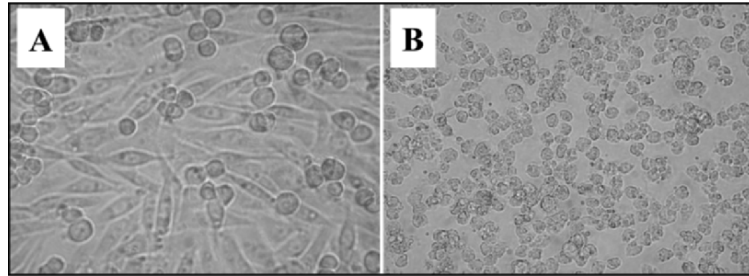


Figure 3. Two days after culture in 0.5 mg/ml LCA of wild-type CHO and *FUT8*^{-/-} clones. (A) *FUT8* double knockout cells were grown normally. (B) wild-type CHO cells were sensitive to LCA.

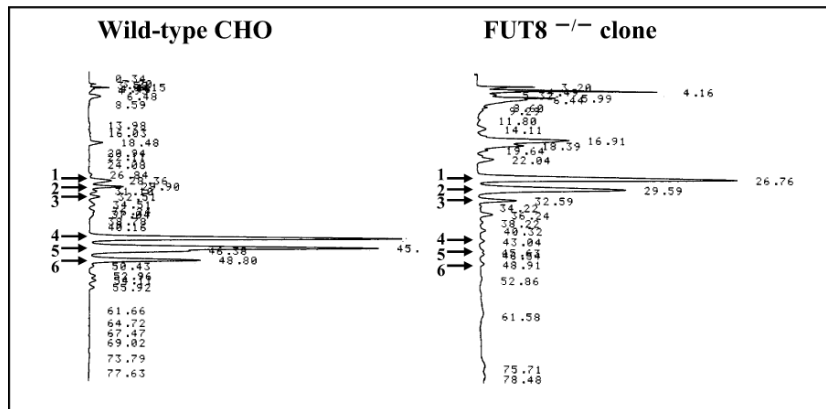


Figure 4. HPLC analysis of Asn-linked oligosaccharides on a recombinant antibody expressed in wild-type CHO cells and *FUT8*^{-/-} double knockout clone. Each signal represented Asn297-N-2-GlcNAc-GlcNAc-mannose-(mannose-GlcNAc)₂, where GlcNAc is N-acetylglucosamine, without fucose (1, 2, 3) and with a fucose attachment of a first GlcNAc arm (4, 5, 6), and/or the attachment of zero (1, 4), one (2, 5), or two (3, 6) terminal galactose units.

medium containing LCA or PSA lectin at the concentration (0.5 mg/ml) for wild-type CHO cells, and all heterozygous clones died (Fig. 3).

Asn-linked oligosaccharides of a recombinant human antibody expressed in the double knockout clone were also analyzed by HPLC to

confirm the disruption of α -1, 6-fucosyltransferase activity. In wild-type CHO cells, three main signals were distinguished by differences in the number of terminal galactose residues. However, in the double knockout clone, only signals at a background level were detected in the retention of fucosylated oligosaccharides (Fig. 4).

Here, we demonstrated the targeted disruption of an endogenous homozygous gene in CHO cells. This approach provides an applicable tool to modify properties of recombinant proteins produced by CHO cells.

4. REFERENCES

1. M. Hooper, K. Hardy, A. Handyside, S. Hunter, M. Monk, HPRT-deficient (Lesch-Nyhan) mouse embryos derived from germline colonization by cultured cells, *Nature* 326 (1987) 292-295.
2. J. M. Buerstedde, S. Takeda, Increased ratio of targeted to random integration after transfection of chicken B cell lines, *Cell* 67 (1991) 179-188.
3. P. Winding, M. W. Berchtold, The chicken B cell line DT40: a novel tool for gene disruption experiments, *J. Immunol. Methods* 249 (2001) 1-16.
4. R. L. Shields, J. Lai, R. Keck, L. Y. O'Connell, K. Hong, Y. G. Meng, S. H. A. Weikert, L. G. Presta, Lack of fucose on human IgG1 N-Linked oligosaccharide improves binding to human FcRIII and antibody-dependent cellular toxicity, *J. Biol. Chem.* 277 (2002) 26733-26740.
5. T. Shinkawa, K. Nakamura, N. Yamane, E. Shoji-Hosaka, Y. Kanda, M. Sakurada, K. Uchida, H. Anazawa, M. Satoh, M. Yamasaki, N. Hanai, K. Shitara, The absence of fucose but not the presence of galactose or bisecting N-acetylglucosamine of human IgG1 complex-type oligosaccharides shows the critical role of enhancing antibody-dependent cellular cytotoxicity. *J. Biol. Chem.* 278 (2003) 3466-3473.
6. J. Ripka, P. Stanley, Lectin-resistant CHO cells: selection of four new pea lectin-resistant phenotypes, *Somat. Cell Mol. Genet.* 12 (1986) 51-62.
7. T. G. Warner, Enhancing therapeutic glycoprotein production in Chinese hamster ovary cells by metabolic engineering endogenous gene control with antisense DNA and gene targeting, *Glycobiology.* 9 (1999) 841-50.
8. T. Yagi, Y. Ikawa, K. Yoshida, Y. Shigetani, N. Takeda, I. Mabuchi, T. Yamamoto, S. Aizawa, Homologous recombination at c-fyn locus of mouse embryonic stem cells with use of diphtheria toxin A-fragment gene in negative selection, *Proc. Nat. Acad. Sci. U S A* 87 (1990) 9918-9922.
9. Y. Kuroiwa, P. Kasinathan, H. Matsushita, J. Sathiyaselan, E. J. Sullivan, M. Kakitani, K. Tomizuka, I. Ishida, J. M. Robl, Sequential targeting of the genes encoding immunoglobulin-mu and prion protein in cattle, *Nat. Genet.* 36 (2004) 775-780.
10. A. Kondo, J. Suzuki, N. Kuraya, S. Hase, I. Kato, T. Ikenaka, Improved method for fluorescence labeling of sugar chains with sialic acid residues, *Agric. Biol. Chem.* 54 (1990) 2169-2170.
11. K. Zimmermann, K. Ahrens, S. Matthes, J. M. Buerstedde, W. H. Str[ä]tling, L. Phivan, Targeted disruption of the GAS41 gene encoding a putative transcription factor indicates that GAS41 is essential for cell viability, *J. Biol. Chem.* 277 (2002) 18626-18631.

12. N. Korfali, S. Ruchaud, D. Loegering, D. Bernard, C. Dingwall, S. H. Kaufmann, W. C. Earnshaw, Caspase-7 gene disruption reveals an involvement of the enzyme during the early stages of apoptosis, *J. Biol. Chem.* 279 (2004) 1030-1039.
13. C. Deng, M. R. Capecchi, Reexamination of gene targeting frequency as a function of the extent of homology between the targeting vector and the target locus, *Mol. Cell. Biol.* 12 (1992) 3365-3371.
14. H. Riele, E. R. Maandag, A. Berns, Highly efficient gene targeting in embryonic stem cells through homologous recombination with isogenic DNA constructs, *Proc. Natl. Acad. Sci. USA*, 89 (1992) 5128-5132.

IMMUNOSTIMULATION EFFECT OF THE FERMENTED MILK ON HUMAN HYBRIDOMAS AND PERIPHERAL BLOOD LYMPHOCYTES

Takuya Sugahara,¹ Katsunori Nakamoto² and Kazushi Hara²

¹Faculty of Agriculture, Ehime University, 3-5-7 Tarumi, Matsuyama, Ehime 790-8566, Japan; ²Shikoku Milk Product Co. Ltd., 1055-1 Minamigata, Touon, Ehime 791-0397, Japan

Abstract: Fat-free bovine milk fermented by more than 10 kinds of various lactic acid bacteria and yeast enhanced monoclonal antibody production of human hybridoma HB4C5 cells 2.8-fold in serum-free medium. Immunoglobulin production of human peripheral blood lymphocytes (PBL) was also stimulated *in vitro*. IgM and IgG production of human PBL was accelerated up to 2.8-fold and 5.4-fold, respectively. Interferon- γ production of human PBL was also accelerated 6.0-fold by 50 $\mu\text{g/ml}$ of the fermented milk. However, interleukin-4 production of PBL was not affected. The activity was enhanced 2.5-fold by the thermal treatment for 30 min at 65°C, and was completely lost by trypsin digestion. The findings suggested that the active substance in the fermented milk was heat stable protein. Gel-filtration and the SDS-PAGE analysis revealed that the molecular weight of the active protein, which was not detected in fat-free bovine milk before fermentation, was 19.0 kDa.

Key words: fermented milk; peripheral blood lymphocytes; immunoglobulin production; interferon-gamma.

1. INTRODUCTION

We have screened immunoglobulin (Ig) production stimulating factors (IPSFs), which enhance Ig production of hybridoma cells and lymphocytes. As a result of investigations, several substances were identified as the IPSF. For instance, lysine-rich histones and poly-lysine accelerated IgM production by human-human hybridoma HB4C5 cells (Sugahara et al., 1994). Some IPSFs were found in foodstuffs. We reported that rice fermented seasoning enhanced Ig production of human

peripheral blood lymphocytes (PBL) (Sugahara et al., 1996). The active substance in the rice fermented seasoning was estimated as a sort of lipid. Hen egg white lysozyme (EC 3.2.1.17) was also identified as the IPSF and the mode of action was investigated (Sugahara et al., 2002).

Bovine milk also contains many biologically functional substances including Ig production stimulators, such as casein, lactoferrin, and β -lactoglobulin. Bovine milk fermented by some sorts of bacteria would have bioactive substances originated by fermentation. Bovine milk cultured with lactic bacteria possesses anti-carcinogenic or anti-mutagenic activities (Hosoda et al., 1992).

In this paper, we focused on fat-free bovine milk fermented by more than 10 kinds of lactic acid bacteria and yeast, and attempted to investigate Ig and cytokine production stimulating activity of the fermented milk.

2. MATERIALS AND METHODS

2.1 Fermented milk

Fat-free bovine milk was fermented for 43 h by more than 10 kinds of lactic acid bacteria and yeast as listed in Table 1. The fermented milk was centrifuged at 100,000 \times g for 30 min, and supernatant was collected. The pH of the supernatant was 4.0. Therefore, the supernatant was dialyzed against 10 mM sodium phosphate buffer (pH 7.4) for neutralization before use.

Table 1. Summary of the bacteria used for fermentation of fat-free milk.

<i>Lactococcus lactis</i> subsp. <i>Lactis</i>
<i>Lactococcus lactis</i> subsp. <i>Cremoris</i>
<i>Streptococcus lactis</i> subsp. <i>diacetylactis</i>
<i>Streptococcus thermophilus</i>
<i>Leuconostoc cremoris</i>
<i>Lactobacillus delbrueckii</i> subsp. <i>bulgaricus</i>
<i>Lactobacillus delbrueckii</i> subsp. <i>lactis</i>
<i>Lactobacillus acidophilus</i>
<i>Lactobacillus casei</i>
<i>Lactobacillus helveticus</i>
<i>Bifidobacterium longum</i>
<i>Saccharomyces cerevisiae</i>

2.2 Cells and cell culture

Human-human hybridoma HB4C5 cells producing lung cancer specific monoclonal IgM were used for the assay of the Ig production

stimulating activity. HB4C5 cell line was a fusion product of a human B lymphocyte from lung cancer patient and a human fusion partner, NAT-30 cells. HB4C5 cells were cultured in ERDF medium (Kyokuto Pharmaceutical, Tokyo, Japan) supplemented with 10 µg/ml of insulin, 20 µg/ml of transferrin, 20 µM ethanolamine, and 25 nM selenite (ITES-ERDF) at 37°C under humidified 5% CO₂-95% air (Murakami et al., 1982).

Human PBL were obtained from peripheral blood of a healthy male donor. Peripheral blood diluted with equal volume of phosphate buffered saline (PBS) was centrifuged at room temperature for 30 min on lymphocyte separation medium (Nycomed Pharma, Oslo, Norway).

2.3 Assay of the immunostimulating activity of the fermented milk

The Ig production stimulating activity was examined by measuring the amount of Ig secreted by HB4C5 cells or human PBL in culture media. HB4C5 cells and human PBL were inoculated in ITES-ERDF medium containing the fermented milk. The assay of the Ig production stimulating activity was performed in a 96-well culture plate. HB4C5 cells and human PBL were inoculated at 1x10⁵ cells/ml and 1x10⁶ cells/ml, respectively. After cultivation in CO₂ incubator at 37°C, the amount of Ig secreted in each culture medium was determined by enzyme-linked immunosorbent assay (ELISA) using anti-human IgM or IgG antibody as mentioned in previous report (Sugahara et al., 1994). Determination of the Ig production stimulating activity of the fermented milk was triplicated.

The assay of cytokine production stimulating activity was performed in a 48-well culture plate. Human PBL were inoculated at 1x10⁶ cells/ml in ITES-ERDF containing the fermented milk and 5.0 µg/ml of LPS. Following cultivation, IL-4 and IFN-γ concentrations in the culture medium were measured by using of each determination kit (Biosource International, CA, USA) on the basis of ELISA. Determination of the amounts of IL-4 and IFN-γ in the culture medium was triplicated.

3. RESULT AND DISCUSSION

3.1 The effect of the fermented milk on IgM production of HB4C5 cells

Human-human hybridoma HB4C5 cells producing monoclonal IgM were used for the assay of the Ig production stimulating activity. HB4C5

cells were inoculated at 1×10^5 cells/ml in ITES-ERDF medium supplemented with various concentrations of the fermented milk. After cultivation for 6 h, the amount of IgM in each culture medium was measured by ELISA. As a result of that, the fermented milk dose-dependently stimulated the Ig production of HB4C5 cells. At the maximum dose (530 $\mu\text{g/ml}$), IgM production of the hybridoma cells was enhanced 2.8-fold.

3.2 Effect of the fermented milk on Ig production of human PBL

The Ig production stimulating effect of the fermented milk on Ig production by human PBL was examined under the serum-free condition. Human PBL were inoculated at 1×10^6 cells/ml in ITES-ERDF medium supplemented with various concentrations of the fermented milk, and cultured for 4 d. The effect on IgM and IgG production was examined. IgM and production by human PBL was facilitated 2.8-fold by the fermented milk at 530 $\mu\text{g/ml}$. IgG production was also enhanced 5.4-fold (Fig. 1). It is suggested from this fact that the effect is due to not increase in cell number, but facilitation of Ig productivity of PBL by the fermented milk.

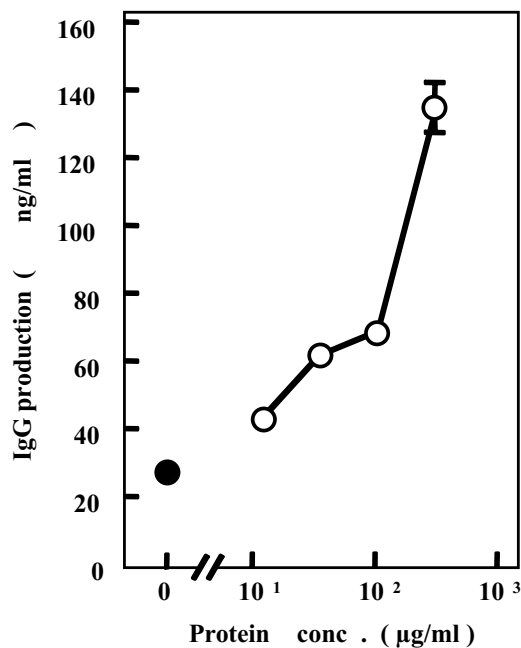


Figure 1. Effect of the fermented milk on IgG production of human PBL.

3.3 Effect of the fermented milk on IL-4 and IFN- γ production of human PBL

The fermented milk stimulated Ig production by human PBL as mentioned above. Then, the effect on cytokine production of human

PBL was examined. Human PBL were cultured in ITES-ERDF medium supplemented with the fermented milk at various concentrations under LPS (5 $\mu\text{g/ml}$) stimulation for 5 d. The production of typical cytokines (IL-4 produced by Th2 cells, and IFN- γ produced by Th1 cells) was assayed. As summarized in Table 2, the fermented milk did not stimulate IL-4 production. On the other hand, IFN- γ production was stimulated 6.0-fold by the addition of 50 $\mu\text{g/ml}$ of the fermented milk.

Table 2. Effect of the fermented milk on cytokine production of human PBL.

Fermented milk ($\mu\text{g/ml}$)	IL-4 (pg/ml)	IFN- γ (pg/ml)
0 (Control)	23.5 \pm 0.2	0.6 \pm 0.2
25.0	26.1 \pm 1.6	3.1 \pm 0.5
50.0	24.7 \pm 1.8	3.6 \pm 0.0

3.4 Heat stability of the fermented milk

The fermented milk was heated at various temperatures for 30 min. Following immediate icing, the Ig production stimulating activity was assayed. HB4 C5 cells were cultured at 1×10^5 cells/ml for 6 h in ITES-ERDF medium supplemented with heat-treated fermented milk. As indicated in Fig. 2, the Ig production stimulating activity of the fermented milk was relatively heat-stable. Distinctively, the activity was facilitated 2.5-fold by thermal treatment at 65°C.

On the other hand, the fermented milk was treated with 50 $\mu\text{g/ml}$ of trypsin for 30 min, and the digestion was terminated by the addition of 250 $\mu\text{g/ml}$ of soybean trypsin inhibitor. Then, the activity was assayed by using of HB4C5 cells. As indicated in Fig. 3, the Ig production stimulating activity against HB4C5 cells was completely lost by trypsin digestion. These results suggest that the active substance in the fermented milk is heat stable protein.

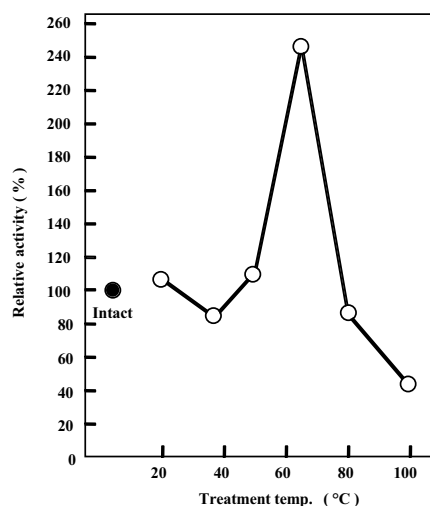


Figure 2. Heat stability of the fermented milk.

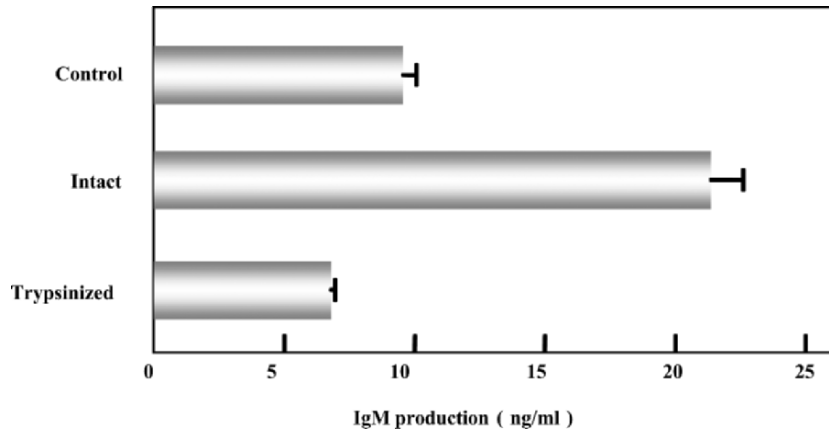


Figure 3. Effect of trypsin digestion of the fermented milk on its activity.

3.5 Identification of the active substance in the fermented milk

The fermented milk was gel-filtrated by use of Superdex 75 HR column (Amersham Biosciences, Piscataway, NJ, USA) equilibrated by PBS. Two peaks were detected by monitoring absorbance at 280 nm and each fraction was collected. The protein components in each peak fraction were analyzed by SDS-PAGE on 15% polyacrylamide gel. The fermented milk before gel-filtration was composed of only two proteins, whose molecular weight was estimated as 19.0 and 14.4 kDa. Fraction 1 and Fraction 2 obtained by gel-filtration contained 19.0 kDa and 14.4 kDa protein, respectively. As a result of assay of Ig production stimulating activity, Fraction 1 had Ig production stimulating activity. This fact suggests that the 19.0 kDa protein is the active substance in the fermented milk. However, the 19.0 kDa protein was not observed in fat-free bovine milk before fermentation. This fact suggests that the 19.0 kDa protein is arisen from fermentation of fat-free milk by bacteria.

4. REFERENCES

- Hosoda, M., Hashimoto, H., Morita, H., Chiba, M., and Hosonome, A., 1992, Studies on antimutagenic effect of milk cultured with lactic acid bacteria on the Trp-P2-induced mutagenicity to TA98 strain of *Salmonella typhimurium*, *J. Dairy Res.* 59:543-549.

- Murakami, H., Masui, H., Sato, G. H., Sueoka, N., Chow, T. P., and Kono-Sueoka, T., 1982, Growth of hybridoma cells in serum-free medium, *Proc. Natl. Acad. Sci. USA* 79:1158-1162.
- Sugahara, T., Sasaki, T., and Murakami, H., 1994, Enhancement of immunoglobulin productivity of human-human hybridoma HB4C5 cells by basic proteins and polybasic amino acids, *Biosci. Biotechnol. Biochem.* 58:2212-2214.
- Sugahara, T., Fukaya, K., and Sasaki, T., 1996, Enhancement of IgM production of human peripheral blood lymphocytes by rice fermented seasoning under serum-free cultivation, *J. Ferment. Bioeng.* 82:77-79.
- Sugahara, T., Yamada, Y., Yano, S., and Sasaki, T., 2002, Heat denaturation enhanced immunoglobulin production stimulating activity of lysozyme from hen egg white, *Biochim. Biophys. Acta* 1572:19-24.

TRACE ELEMENT OPTIMIZATION ENHANCES PERFORMANCE AND REPRODUCIBILITY OF SERUM-FREE MEDIUM

Scott J. Jacobia¹, Robert W. Kenerson¹, Lia D. Tescione¹, Dale F. Gruber¹, David W. Jayme², Donald G. Munroe¹, and Stephen F. Gorfien¹

¹*Invitrogen Corporation, 3175 Staley Road, Grand Island, New York 14072, USA;*

²*Department of Biochemistry, Brigham Young University – Hawaii, 55-220 Kulanui Street, Laie, Hawaii 96762, USA*

Abstract: Optimizing the quantity and composition of trace elements in the AEM (Adenovirus Expression Medium) formulation, resulted in an improved version of AEM, which is a serum-free, low protein, animal-origin free medium designed for adenovirus expression applications for PER.C6[®] and other mammalian cell types. The improved AEM formulation supports higher maximal viable cell growth than other commercially available serum-free media. Optimization of medium trace elements has been shown to support equivalent cell growth in production batches from 100 L to 1500 L. Adding a proprietary trace element mixture to lower performing lots of medium resulted in increased cell growth comparable to better performing lots also containing the mixture. Trace element optimization has been investigated in several additional Gibco[®] serum-free media. The resulting modifications can support maximal viable cell densities 1.5 to 3-fold greater than their predecessors. For example, HEK293 cell growth is supported with peak viable cell densities in excess of 4.0×10^6 viable cells/mL without a lag in cell growth during subsequent passages. Investigation continues to confirm biological productivity and to eliminate recombinant protein constituents and improve biological performance.

Key words: bioproduction; optimization; trace elements; PER.C6[®]; HEK293; CHO-S; HeLa.

PER.C6[®] is a registered trademark of Crucell N.V.

Gibco[®] is a registered trademark of Invitrogen Corporation.

1. INTRODUCTION

A large segment of bioproduction focuses on the expression of recombinant proteins and viruses in mammalian cell culture systems. A goal of industry is to decrease cost while increasing production yields. Therefore increasing cell density and/or specific productivity of these cultures is essential. Properly managing resources is another way of decreasing cost. A robust culture system with predictable and reliable high density cell growth greatly reduces the chance for a sub-standard bioreactor run.

Medium optimization often focuses on amino acid and carbohydrate concentrations and supplemental vitamin and nucleoside levels^{1,2}. Reports have shown a benefit from the addition of cytokines and undefined hydrolysates to cell culture media^{3,4}. Further analysis of existing Gibco[®] serum-free specialty media led to the identification of other important medium components, specifically, the trace elements. The composition and concentration of certain trace elements may have a critical effect on cell growth and productivity⁵. Proper formulation of trace elements in a medium optimized for its other components facilitates scalability, enhances consistency in lot-to-lot performance, elevates maximum viable cell density, and increases culture longevity.

2. MATERIALS AND METHODS

2.1 Small-scale agitated suspension

Parental PER.C6[®], HEK293, CHO-S, and HeLa cells were seeded at $2-3 \times 10^5$ vc/mL in 20 mL cultures. The cultures were incubated at 37°C, 8% CO₂, and agitated at 125 rpm on an orbital shaker. Viable cell densities were determined electronically (Coulter counter) using trypan blue exclusion.

2.2 Antibody quantitation

Spent medium samples were collected from cultures as indicated on the graph. Quantitative HPLC analysis of IgG in cell culture media was performed using a PG ImmunoDetection Sensor Cartridge (Applied Biosystems). The IgG was eluted with sodium chloride at pH 2 – 3 and

detected at 210 nm. Mouse IgG was used as a reference standard, with a range of 15.6 mg/L to 250 mg/L.

2.3 Trace element supplement

The quantitative composition of the trace element supplement cannot be disclosed at this time due to its proprietary nature. Qualitative composition is inclusive of the breadth of trace elements frequently reported for cell culture applications, although we utilized various empirical, analytical and statistical design methods to optimize cell proliferation and biological production, resulting in significant adjustments to standard trace element levels. The trace element supplement was optimized for each respective cell line.

3. RESULTS

3.1 Supplementation of AEM with trace elements

Non-supplemented AEM lots A and B demonstrated parental PER.C6[®] cell growth of approximately 1.0×10^6 and 2.0×10^6 vc/mL respectively (Figure 1). Upon supplementation both lots demonstrated improved PER.C6[®] cell growth in excess of 2.5×10^6 vc/mL. Supplementation not only increased viable cell density of both lots but also increased lot-to-lot consistency. This was demonstrated in greater than 10 lots of AEM medium (data not shown).

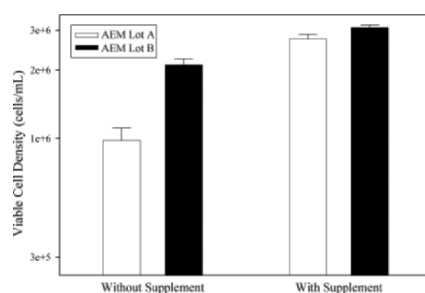


Figure 1. Trace element optimization of two lots of AEM medium; Lot A, a sub-standard lot and Lot B, a standard lot. Bars represent the mean viable cell densities +/- standard deviations of triplicate parental PER.C6[®] cultures as determined during passage 3, day 4.

3.2 Addition of Trace Element Supplement to 293 II SFM

Stock cells were grown in 293 SFM II to a day 4 cell density of approximately 2.5×10^6 vc/mL (99% viable) and passaged into the four test conditions. Due to the relatively high density of the stock cells all passage 1 test cultures lagged. After two subsequent passages all conditions recovered and achieved day 4 cell densities of approximately 2.5×10^6 vc/mL. These cultures were then passaged on day 6 after reaching cell densities in excess of 3.0×10^6 vc/mL. The cells in the unsupplemented medium demonstrated a lag in growth failing to reach 1.0×10^6 vc/mL on day 5 of passage 4 while the cells in the supplemented medium reached a cell density similar to that of the previous passage. Further development of the trace elements in HEK293 media, led to two prototype media, 293 Prototype and 293 CD Prototype. The 293 Prototype is a serum-free, low protein medium, whereas the 293 CD Prototype is chemically defined (CD). These media support increased viable cell densities to approximately 6×10^6 vc/mL compared to 3.5×10^6 vc/mL for 293 SFM II. Increased growth was seen over multiple passages (data not shown).

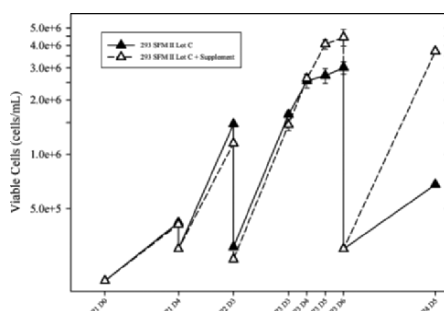


Figure 2. Data represent the mean viable cell densities +/- standard deviations of triplicate HEK293 cultures for passage 3 (P3) and single flasks for passages 1, 2, and 4 (P1, P2, P4).

3.3 Trace element optimized prototypes for other cell lines

A trace element optimized transfected PER.C6[®] medium, PER.C6[®] CD Prototype, supported cell growth to a higher maximum viable cell density as well as increased cell culture longevity in both small-scale (Figure 3) and large-scale (data not shown) agitated suspension than

unsupplemented and supplemented AEM and the commercially available control. The CD Prototype also supported higher antibody production than the control (Figure 3).

Two HeLa formulations with optimized trace elements have been developed, one being a CD formulation which supports growth up to 4×10^6 vc/mL and the other being a low protein, hydrolysate free, serum free formulation which supports growth up to 7×10^6 vc/mL (day 5, passage 5 measurements). In addition to enhancing cell growth, both formulations support an increase in culture longevity. These effects were seen over multiple passages (data not shown).

Trace element optimization of CHO-S prototype media support greater viable cell densities over a longer time span than the catalog control (greater than 6×10^6 vc/mL on days 4, 5, and 6 for the prototypes vs. 6×10^6 vc/mL on day 5 for the catalog control). The maximum viable cell densities were achieved earlier in culture life. The increased cell growth was seen over multiple passages (not shown). This prototype also supported DG44 CHO cell growth similar to that of other Gibco catalog media. Further optimization is necessary in order to support a higher maximum cell density for this cell line.

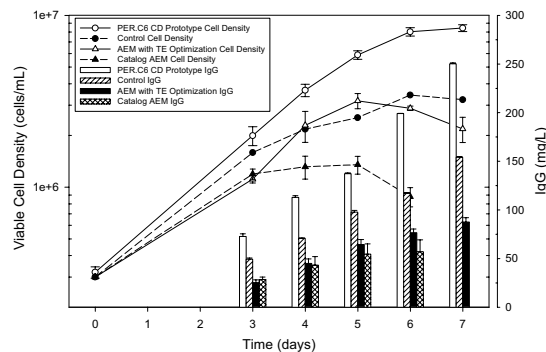


Figure 3. Growth and productivity curve of transfected PER.C6 cultures in unsupplemented and supplemented catalog AEM, PER.C6[®] CD Prototype and commercially available control media.

4. DISCUSSION

The exact mechanism by which trace elements contribute to the robustness of our formulations is not fully understood. Trace metals are associated with greater than 1000 proteins. Some trace elements, such as selenium, zinc, and copper, have been researched extensively. One important trace element, selenium, has long been recognized as an

antioxidant by its participation in glutathione oxidative reactions⁵. Zinc is involved in cellular differentiation, apoptosis, and cellular proliferation⁶. Zinc deficiency in rat glioma cells coincided in a decrease in the growth rate, which was restored with replenishment of zinc^{5,7}. Zinc may promote cell viability by protecting the cell from free radical damage and has been shown to inhibit caspase-3 dependent apoptosis^{8,9}. Copper plays a role in a variety of important enzymes, including cytochrome c oxidase, tyrosinase, p-hydroxyphenyl pyruvate hydrolase, dopamine beta hydroxylase, lysyl oxidase, and Cu/Zn-superoxidase dismutase (SOD)^{10,11}. These enzymes are involved in an array of biological processes required for growth, development, and maintenance. Copper deficiency compromises cellular antioxidant defenses via decreased capability to produce SOD, thereby increasing their susceptibility to oxidative DNA damage^{12,13}. Unfortunately, trace element dynamics is not simply additive but interactions between trace elements display synergistic and antagonistic effects. Zinc and copper are both part of Cu/Zn-SOD; however, they have a strong mutual antagonism, both competing for the same site¹³. The composition and concentrations of the trace elements in a medium determine the effect on cellular toxicity.

Of concern when culturing HEK 293 cells is the necessity to passage them during mid log growth to minimize lags in growth during the subsequent passages. Optimization of trace elements in the medium results in a more robust cell culture system, which eliminates the sensitivity to overgrowth and increases growth consistency over consecutive passages.

We have demonstrated the benefit of trace element optimization in a variety of innovative medium formulations developed for the growth of HEK293, recombinant PER.C6[®], HeLa, and CHO-S cells. These robust formulations are well defined and hydrolysate-free for ease of use, consistency of performance, and raw material sourcing. The optimization of trace elements and elimination of hydrolysates (and other undefined components) are key steps in the development of media which can be consistently produced at large scale.

5. ACKNOWLEDGEMENTS

We would like to thank Crucell NV for access to their parental and transfected PER.C6[®] cells. We would also like to thank Joseph R. Zdanowicz, Richard Hassett, Robert F. Keem, Richard M. Fike, Invitrogen's Media Analytical Services laboratory, Brian M. Burgin, and Steven C. Peppers.

6. REFERENCES

1. S.F. Gorfien, W. Paul, D. Judd, L. Tescione, and D.W. Jayme, Optimized nutrient additives for fed-batch cultures, *BioPharm Int.* 16 (4), 34-40 (2003).
2. D.W. Jayme and D.F. Gruber, in: *Cell Biology: A Laboratory Handbook*, edited by J.E. Celis (Academic Press Limited, London, 1998), pp. 19-26.
3. A. Mizrahi, Primatone RL in mammalian cell culture media, *Biotechnol. Bioeng.* 19 (10), 1557-1561 (1977).
4. C.C. Burteau, F.R. Verhoeye, J.F. Mols, J.-S. Balliez, S.N. Agathos, and Y.-J. Schneider, Fortification of a protein-free cell culture medium with plant peptones improves cultivation and productivity of an interferon- γ -producing CHO cell line, *In Vitro Cell. Dev. Biol. – Animal* 39, 291-296 (2003).
5. E. Ho and B.N. Ames, Low intracellular zinc induces oxidative DNA damage, disrupts p53, NF κ B, and AP1 DNA binding, and affects DNA repair in a rat glioma cell line, *PNAS* 99 (26), 16770-16775 (2002).
6. H. Haase and D. Beyersmann, Uptake and intracellular distribution of labile and total Zn(II) in C6 rat glioma cells investigated with fluorescent probes and atomic absorption, *BioMetals* 12, 247-254 (1999).
7. C.T. Walsh, H.H. Sandstead, A.S. Prasad, P.M. Newberne and P.J. Fraker, Zinc: health effects and research priorities for the 1990s, *Environ. Health Perspec.* 102 (Suppl. 2), 5-46 (1994).
8. F. Chai, A.Q. Truong-Tran, L.H. Ho, and P.D. Zalewski, Regulation of caspase activation and apoptosis by cellular zinc fluxes and zinc deprivation: a review, *Immunol. Cell Biol.* 77, 272-278 (1999).
9. D.K. Perry, M.J. Smyth, H.R. Stennicke, G.S. Salvesen, P. Duriez, G.G. Poirier, and Y.A. Hannun, Zinc is a potent inhibitor of the apoptotic protease, caspase-3, *JBC* 272, 18530-18533 (1997).
10. J.R. Turnlund, in: *Modern Nutrition in Health and Disease*, edited by M.E. Shils, J.A. Olson, M. Shike, and A.C. Ross (Williams and Wilkins, Baltimore, 1999), pp. 241-252.
11. R. Uauy, M. Olivares, and M. Gonzalez, Essentiality of copper in humans, *Am. J. Clin. Nutr.* 67, 952S-959S (1998).
12. Y. Pan and G. Loo, Effect of copper deficiency on oxidative DNA damage in Jurkat T-lymphocytes, *Free Rad. Biol. Medicine* 28, 824-830 (2000).
13. L.M. Gaetke and C.K. Chow, Copper toxicity, oxidative stress, and antioxidant nutrients, *Toxicology* 189, 147-163 (2003).

PHENOMENOME PROFILER™ ANALYSIS OF HUMAN COLON CANCER CELL LINES

Yasuyo Yamazaki¹, Shawn Ritchie¹, Yanqiu Jiang²

¹Phenomenome Discoveries Inc., ²Phenomenome Informatics, 204-407 Downey Road, Saskatoon, SK, S7N 4L8, Canada

Abstract: Phenomenome Profiler is a family of biological data analysis programs designed specifically for the comparison, correlation, and mining of the analytical data generated from the analysis of biological samples. The primary purpose of the Profiler family of products is to rapidly identify the analytically determined components of a complex biological sample that are the most relevant to a particular biological variable. These components are commonly referred to as biomarkers and they can be metabolites, peptides, and/or gene transcripts. To demonstrate the capability of Phenomenome Profiler™ M Series, we analyzed organic extracts of the 12 human cell lines using HPLC-MS atmospheric pressure chemical ionization at positive-ion mode in non-targeted fashion.

Key words: human cell lines; colon cancer; non-targeted LCMS profiling.

The Phenomenome Profiler™ M Series version 1.0 program handles all aspects of a typical metabolomics research project. Since the program can process data files from any mass spectrometer, it is the first truly universal metabolomics solution.

Our Profiler Project Manager Module allows you manage all aspects of your metabolomic projects, seamlessly integrating access to LIMS, raw data tools, and advanced data analysis tools into one user-friendly interface.



Figure 1. Project manager module

- Step 1 - A laboratory information management system (LIMS) built on a relational database structure allows you to save and organize your raw and processed data files in a simple, fast, and intuitive way. A project is logged in using the LIMS module. In this module, you describe the project, the samples that were analyzed and how they were analyzed. An import / export function that allows you to share entire projects with your colleagues.
- Step 2 - A raw data converter that converts mass spectrometric data from any mass spectrometer into profiler's universal file format. The raw data is converted to the Profiler data format. This conversion dramatically reduces the size of your raw data file as well as formatting it to accelerate the rate at which the program can access this data.
- Step 3 - A raw data viewer that allows you open raw data files, display, save, and print extracted ion chromatograms (EIC) and extracted mass spectrums (EMS), as well as advanced data processing functions such as chromatographic smoothing, noise filters, and peak picking to optimize peak processing parameters.
- Step 4 - A raw data calibrator that performs a within-sample retention time calibration and alignment of each LC-MS and GC-MS metabolic profile data to a user-defined list of internal standards or to a reproducible set of endogenous metabolite peaks observed to be present in all samples.
- Step 5 - The calibrated files are then peak picked. A universal peak picker that will smooth and adjust the noise values according to easily defined, user-verified, parameters and then systematically calculate every possible extracted ion chromatogram and create a peak list containing the mass, retention time and intensity for

every metabolite detected. This data is stored in a relational database for future access.

Step 6 - Next, a 2D data array is generated from the peak picked data using Profiler's clustering algorithm. Phenomenome's unique 2D data array creator that combines any number of previously peak picked samples, performs an additional alignment algorithm, and display the entire data set in a 2D table. This is a between-sample alignment. You can easily modified and optimize the algorithm parameters. This between-sample alignment is performed according to the retention time and mass of each metabolite peak. The combined within (step 4) and between (step 6) sample alignment process ensures the most robust data alignment possible and places all of your data into an array that is now amiable for advanced statistical processing.

The array is your portal to view, analyze and interpret your data. The array format is a live table format. This means that although we have dramatically simplified the view of the data by showing only the mass, retention time and peak apex intensities, every cell in the array is "connected" to your raw data for immediate retrieval of the actual raw spectra and chromatography information.

Table 1. Human cell lines

A	112CO	G	HepG2
B	18Co	H	HT29
C	AS15	I	KM12C
D	Colo201	J	SW480
E	Colo205	K	SW620
F	DLD1	L	WiDr

The human cell lines listed above which colon cancer lines (C to F and H to L), and one liver cancer line (G), were grown to approximately 80% confluency, and harvested such that there were equal numbers of cells per sample. Four replicates of each cell line were analyzed randomly.

A total of 48 samples were processed via a proprietary extraction method optimized to separate the metabolites into multiple extracts based upon their polarity and acid / base chemistry.

To demonstrate the capability of Phenomenome Profiler™ M Series, we analyzed organic extracts of the 12 human cell lines using HPLC-MS atmospheric pressure chemical ionization at positive-ion mode in non-targeted fashion.

From the calibrated raw data files, all unique detected mass/retention time pairs representing sample-specific metabolites and metabolite fragments are visualized as a metabolite array, as shown in Figure 2.



Figure 2. Metabolite array

Darker shades of blue represent metabolites with greater intensity. Each column of the array represents one sample, and each row represents a single mass/retention time pairs. The array can then be analyzed and interesting metabolites identified using numerous statistical (unsupervised analysis) and Boolean search tools (supervised analysis) present in the software. In this example, the array has been clustered hierarchically by sample and metabolite, as indicated by the dendrograms at the top and to the left of the array in Figure 2.

Unsupervised analysis

Sophisticated unsupervised data processing capabilities. The M-Series comes with the most advanced principal components (PCA) and hierarchical clustering analysis algorithms in the industry. The visualizations are second to none. More importantly, the visualizations are directly linked to your raw data. You can go directly from the PCA loadings that identify the most important metabolites in the experiment to the actual chromatogram and mass spectrum with the click of a button.

The PCA plot shown in Figure 3 was generated using the entire array dataset for all 12 cell lines. The data was normalized by a log (base10) transformation and p-value cut-off 0.0001. As can be seen, each cell line forms a discrete cluster of four points, suggesting that each cell line contains a highly reproducible unique metabolite profile.

The heat map displays all of the metabolites that were used in the PCA analysis. The screenshot in Figure 4 shows a group of metabolites all having strong positive loadings in the first PC (indicated by green histograms) and another group having strong negative loadings (indicated by red histograms). As you can see, metabolites that are high in sample except A, B and G are the most important metabolites associated with the separation observed along PC1.

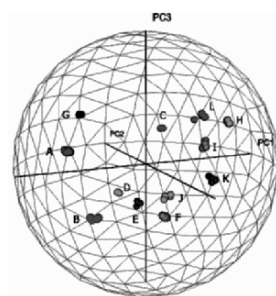


Figure 3. PCA

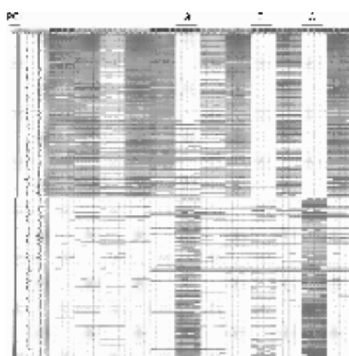


Figure 4. Heat map

Supervised analysis

Advanced Boolean filters allow you to perform an infinite number of pair-wise comparisons between individual samples or between groups of samples with different variable assignments. These data filters rapidly identify metabolites that are differentially expressed between different experimental variables. You can place various statistical and qualitative constraints on the data to further ensure you are only looking at the most important metabolites first.

In the following example in Figure 5, samples within variable assignment set H are compared to samples within variable assignment set A to find all metabolites that are at least five times higher in H than in A with a student's t-test probability score of less than 0.0001. Also, the display of the mean ratio and the actual p-value is requested. Finally, the program found that the below metabolites satisfy these constraints.

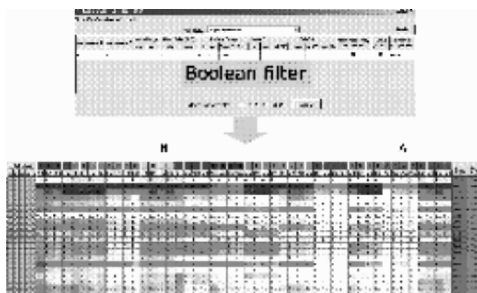


Figure 5. Boolean filter

Array functions

Real-time interaction exists between the array tables (which contain peak apex and intensity data) and the underlying raw chromatography and mass spectrum data. From individual peak display and verification, to spectral averaging, to sophisticated background subtraction and innovative views, you can work with your raw data like never before.

The Row EIC view in Figure 6 displays the extracted ion chromatogram (EIC) of an entire row in the array. In this view, the different variable assignments are grouped together and displayed as an EIC overlay.

Advanced EMS tools in Figure 7 will average the spectra of all the samples within a variable assignment set over the retention time window of the selected peak.

The variable subtraction function is capable of performing complex subtractions between entire sets of samples, as shown in the variable subtraction view in Figure 8.

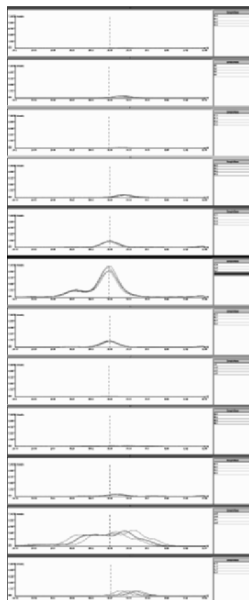


Figure 6. Row EIC

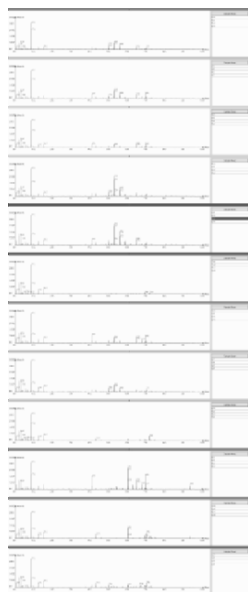


Figure 7. Advanced EMS tools

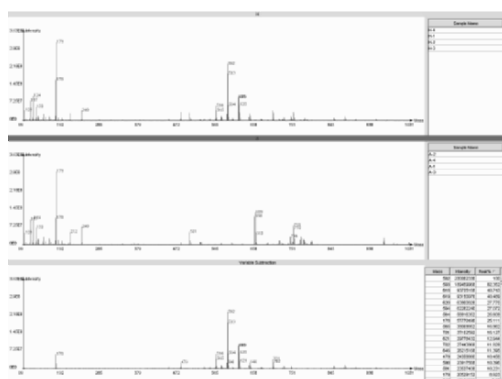


Figure 8. Variable subtraction

Summary

Phenomenome Profiler™ M Series comprises a suite of tools to organize metabolomic mass spectrometry experiments, calibrate raw data, view the data as an interactive array, and perform multivariate statistical analysis.

Using raw LCMS profile data from 12 colon cancer cell lines, the Phenomenome Profiler™ M Series software tools rapidly identified mass/retention time pairs specific to each cell line. The entire mass spectra for each putative biomarker is easily extracted with the advanced MS tools for subsequent *de novo* or database-match identification.

Phenomenome Profiler™ M Series is a universal metabolomics tool, capable of reading and processing data from any mass spectrometer, and sharing raw data and results between multiple users.

GENERATION OF NATURAL KILLER CELLS FROM SERUM-FREE EXPANDED CD34⁺ CELLS ISOLATED FROM HUMAN UMBILICAL CORD BLOOD

I-Ting Kao (1), Zwe-Ling Kong (2), Mei-Ling Wu (1), Li-Wen Hsu (1), Chao-Ling Yao (1), Shiaw-Min Hwang (1)*

*Bioresource Collection and Research Center, Food Industry Research and Development Institute, Hsinchu, Taiwan (1); Alarvita Biolife Corporation, Taipei, Taiwan (2); *Author for correspondence (E-mail address: hsm@firdi.org.tw; telephone: +886-3-522-3191; fax: +886-3-522-4171)*

Abstract: Natural killer cells (CD56⁺CD3⁻) are important effectors of the innate immune system, which contribute to the first line of defense and exhibits antibody-independent, major histocompatibility complex-independent cytolytic activity against infections and tumor cells. Natural killer cell progenitors are derived from the CD34⁺ hematopoietic stem cells (HSCs) population. Human umbilical cord blood has been recognized as a rich source of CD34⁺ HSCs. Although the volume of umbilical cord blood is limited, a serum-free medium for ex vivo expansion of CD34⁺ cells isolated from umbilical cord blood has been developed in authors' laboratory. In this study, expanded CD34⁺ cells were used to differentiate into natural killer cells by a cocktail of cytokines, including IL-2, IL-7, IL-15, Flt-3 ligand and SCF. After induction, natural killer cells were accessed to determine the cellular characteristics weekly by surface antigen analysis and cytotoxic activity against K562 cells. This study demonstrated that the expanded CD34⁺ cells in serum-free medium retained the ability to differentiate into natural killer cells, and provided an extended application of serum-free expanded CD34⁺ cells, besides direct CD34⁺ cell transplantation.

Key words: Ex vivo expanded; Hematopoietic stem cell; Natural killer cell; Umbilical cord blood.

1. INTRODUCTION

Natural killer (NK) cells that express CD56 and CD16, but not CD3 are large granular lymphocytes with innate immunity against viral infections, bacterial infections and tumor cells. NK cells have been recognized as one of the potential candidates for immunotherapy against cancer, because NK cells have the specific and spontaneous ability to eliminate tumor cells without damaging normal cells (Whiteside et al. 1995).

NK cells are differentiated from CD34⁺ hematopoietic stem cells (HSCs) in bone marrow (Carson et al. 1996). Many clinical reports have shown that human umbilical cord blood (UCB) has been recognized as a rich source of HSCs and been used as an alternative to bone marrow transplantation (Gardiner et al. 1998; Grewal et al. 2003). There are various methods to induce, expand and activate NK cells derived from CD34⁺ cells by adding specific cytokines, such as IL-2, IL-7, IL-15, Flt-3 ligand (FL) and stem cell factor (SCF) (Cavazzana-Calvo et al. 1996; Miller et al. 1992; Mrozek et al. 1996; Yu et al. 1998).

We have developed a serum-free medium for expanding HSCs based on isolated CD34⁺ cells from UCB (Yao et al. 2003). The number of CD34⁺ cells increased 27 fold within one-week culture. In this study, the expanded CD34⁺ cells were chosen as the starting cells and the expanded CD34⁺ cells were examined by the potential to differentiate into NK cell lineage. Our results provide that the serum-free expanded CD34⁺ cells isolated from UCB are capable to generate functional NK cells, besides direct CD34⁺ cell transplantation.

2. MATERIALS AND METHODS

2.1 Expansion of CD34⁺ cells

Expansion of CD34⁺ cells isolated from UCB followed the procedure established from our laboratory (Yao et al. 2003).

2.2 Medium preparation

Serum-free medium for CD34⁺ cell expansion was prepared following the procedure established from our laboratory (Yao et al. 2003). NK cell induction medium was composed of IMDM containing a cocktail of cytokines (12.5 ng ml⁻¹ IL-2, 20 ng ml⁻¹ IL-7, 40 ng ml⁻¹ IL-15, 50 ng ml⁻¹ SCF and 50 ng ml⁻¹ FL), 2 mM L-glutamine and 10% fetal bovine serum.

2.3 NK-cell generation from CD34⁺ cells ex vivo

After one-week serum-free expansion of CD34⁺ cells in serum-free condition, we replaced the expansion medium with NK cell induction medium, and seeded the expanded CD34⁺ cells at a cell density of 2×10^5 cells ml⁻¹ in 24-well plate. At weekly intervals, half of the NK cell induction medium was removed and replenished with fresh medium, and maintained the initial cell density as 1×10^6 cells ml⁻¹.

2.4 Flow cytometry analysis of CD34⁺ cells and NK cells

Cells were analyzed by two-color flow cytometry on a FACSCaliber analyzer (Becton-Dickinson). About 1×10^6 cells were stained with FITC-conjugated anti-human CD45 and PE-conjugated anti-human CD34, and gated for CD45⁺CD34⁺ cells with low side scatter. NK cells were labeled with PE-conjugated anti-CD56 and FITC-conjugated anti-CD3 monoclonal antibodies. The NK population was determined as CD56⁺CD3⁻ cells.

2.5 Cytotoxicity assay

After 5 weeks in NK cell induction medium, cells were purified by a positive selection with anti-CD56 magnetic microbeads. Purified CD56⁺ NK cells were used as the effector cells in the cytotoxicity assay. K562 was used as the target cells. The cytotoxicity of NK cells derived from CD34⁺ cells was determined by lactate dehydrogenase (LDH) release assay (CytoTox 96, Promega) according to the manufacturer's instructions. The effector-target ratios (E:T) were 5:1, 2.5:1 and 1.25:1 respectively.

3. RESULTS

3.1 Generation of NK cells from expanded CD34⁺ cells

After the purification with CD133 microbeads, the average purity of CD34⁺ cell was 91.27% as previously described (Yao et al. 2003). The number of CD34⁺ cells increased 27-fold, and the purity of CD34⁺ cell decreased to 36.72% after one-week expansion in serum-free

condition (Figure 1a). In the meantime, the NK cell population that expressed CD56⁺CD3⁻ was only 4.69% (Figure 2a), and the CD56 expression of the expanded CD34⁺ cells was weak (<10² fluorescent magnitude). Subsequently, the expanded CD34⁺ cells were cultured in NK cell induction medium, as described in Material and Methods. The results indicated that the purity of CD34⁺ cells decreased rapidly to 6.92% after one-week induction (Figure 1b), and the population of CD56⁺CD3⁻ cells also decreased to 2.01% (Figure 2b). After 3-week induction, the purity of CD34⁺ cells decreased continuously (Figure 1c), but the population of CD56⁺CD3⁻ cells in the total cells began to increase (Figure 2d). At this time, the fluorescent magnitude of CD56 was dramatically increased to 10³. After 4-week induction, the population of CD56⁺CD3⁻ cells in the total cells increased rapidly to 28.58% (Figure 2e). After 5-week induction, the population of CD56⁺CD3⁻ cells in the total cells reached its maximum, and was 37.88 % (Figure 2f). Almost no CD34⁺ cells were detected at this time (Figure 1d). According to the data of FACS analysis during the induction period, the rapid disappearance of CD34⁺ cells in the first week indicated that these highly enriched HSCs were committed to NK cell lineage in the NK cell induction medium. The NK progenitor cells started to become mature at week 3, and highly expressed CD56 surface marker (>10³ fluorescent magnitude).

In this study, the fresh NK cell induction medium was replenished continuously for 8 weeks. During 8-week induction, the population of CD56⁺CD3⁻ cells was kept increasing to 46.87%, but the total cell density was decreased due to cell death. After one-week induction, the NK cell (CD56⁺CD3⁻) density increased rapidly, and the maximal NK cell density reached to 7.58×10⁵ cells ml⁻¹ at week 5 (Figure 3), and then declined abruptly because the total cell density decreased. After 6-week induction and expansion, the absolute expansion of the NK cells reached a maximum of 6.15×10⁴ folds (Figure 4).

3.2 Cytotoxic activity of generated NK cells

After 5-week induction, the functionality of generated NK cells was determined by K562 cytotoxicity assay. The cytotoxic activity of expanded NK cells against K562 at an E:T ratio of 5:1, 2.5:1 and 1.25:1 was 26.53 ± 3.73%, 18.62 ± 3.95% and 11.34 ± 0.22%, respectively (Figure 5). The results demonstrated that the generated NK cells from the expanded CD34⁺ cells under serum-free condition showed the capability of functional cytotoxicity.

4. DISCUSSION AND CONCLUSION

HSCs (CD34⁺ cells) isolated from UCB can be expanded with a serum-free medium *ex vivo*, and maintain hematopoietic multipotency (Yao et al. 2003). In this study, we show that the expanded CD34⁺ cells could differentiate into NK cell (CD56⁺CD3⁻) lineage by adding IL-2, IL-7, IL-15, SCF and FL.

NK cells derived from serum-free expanded CD34⁺ cells maintained the cytotoxic activity against K562, and surely exhibited immunological function *ex vivo*. NK cells utilize the perforin/granzyme-mediated mechanism to lyse K562 (Vujanovic et al. 1996). Further cytotoxic activity of the generated NK cells against various kinds of tumor cells would be investigated in the future.

The generation of functional from serum-free expanded CD34⁺ cells indicated that the CD34⁺ cell retained its hematopoietic multipotency to differentiate into functional cell lineages after expansion in the serum-free medium. NK cells derived from expanded CD34⁺ cells offered a novel immunotherapy against tumor cells. The generation and activation of NK cells derived from expanded CD34⁺ cells may be a possible solution for insufficient cell number and low cytotoxicity of NK cells in immunotherapy against cancer cells.

5. REFERENCES

- Carson W & Caligiuri M (1996) Natural killer cell subsets and development. *Methods* 9: 327-343.
- Cavazzana-Calvo M, Hacein-Bey S, de Saint Basile G, De Coene C, Selz F, Le Deist F & Fischer A (1996) Role of interleukin-2 (IL-2), IL-7, and IL-15 in natural killer cell differentiation from cord blood hematopoietic progenitor cells and from γ c transduced severe combined immunodeficiency X1 bone marrow cells. *Blood* 88: 3901-3909.
- Gardiner CM, O'Meara A & Reen DJ, (1998) Differential cytotoxicity of cord blood and bone marrow-derived natural killer cells. *Blood* 91: 207-213.
- Giarratana MC, Vergé V, Schmitt C, Bertho JM, Kobari L, Barret C & Douay L (2000) Presence of primitive lymphoid progenitors with NK or B potential in *ex vivo* expanded bone marrow cell cultures. *Exp. Hematol.* 28: 46-54.
- Grewal SS, Barker JN, Davies SM & Wagner JE (2003) Unrelated donor hematopoietic cell transplantation: marrow or umbilical cord blood? *Blood* 101: 4233-4244.
- Miller JS, Verfaillie C & McGlave P (1992) The generation of human natural killer cells from CD34⁺/DR⁻ primitive progenitors in long-term bone marrow culture. *Blood* 80: 2182-2187.
- Mrozek E, Anderson P & Caligiuri MA (1996) Role of interleukin-15 in the development of human CD56⁺ natural killer cells from CD34⁺ hematopoietic progenitor cells. *Blood* 87: 2632-2640.
- Vujanovic NL, Basse P, Herberman RB & Whiteside TL (1996) Antitumor functions of natural killer cells and control of metastases. *Methods* 9: 394-408.

- Whiteside TL & Herberman RB (1995) The role of natural killer cells in immune surveillance. *Curr. Opin. Immunol.* 7: 704-710.
- Yao CL, Liu CH, Chu IM, Hsieh TB & Hwang SM (2003) Factorial designs combined with the steepest ascent method to optimize serum-free media for ex vivo expansion of human hematopoietic progenitor cells. *Enzyme Microb. Technol.* 33: 343-352.
- Yu H, Fehniger TA, Fuchshuber P, Thiel KS, Vivier E, Carson WE & Caligiuri MA (1998) Flt3 ligand promotes the generation of a distinct CD34⁺ human natural killer cell progenitor that responds to interleukin-15. *Blood* 92: 3647-3657.

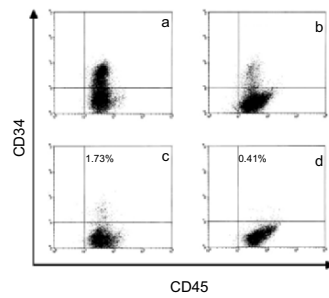


Figure 1. HSC surface marker analysis by flow cytometry of expanded CD34⁺ cells after NK cell induction from week 0 (a), week 1 (b), week 3 (c) and week 5 (d). The HSCs were determined as CD34⁺CD45⁺ cells.

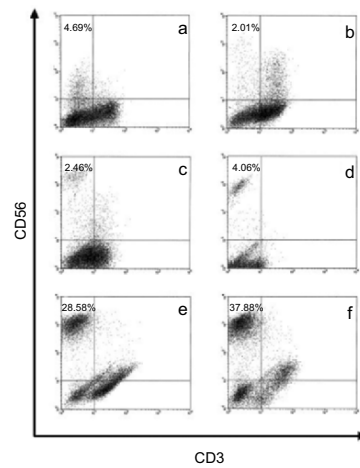


Figure 2. NK cell surface marker analysis by flow cytometry of expanded CD34⁺ cells after NK cell induction from week 0 (a), week 1 (b), week 2 (c), week 3 (d), week 4 (e) and week 5 (f). The NK cells were determined as CD56⁺CD3⁻ cells.

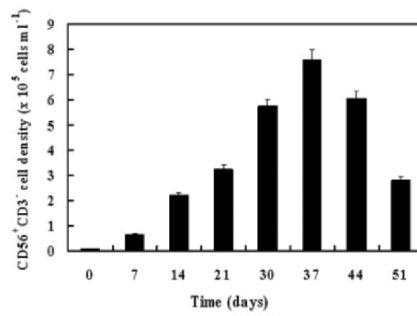


Figure 3. The population of NK cells derived from expanded CD34⁺ cells in the total cell population during the period of induction.

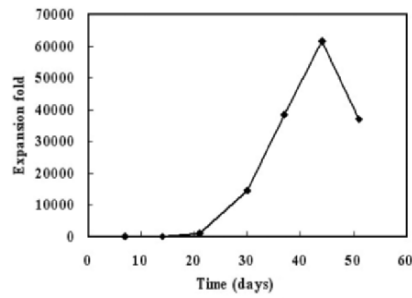


Figure 4. The absolute expansion folds of NK cells derived from expanded CD34⁺ cells during the period of induction.

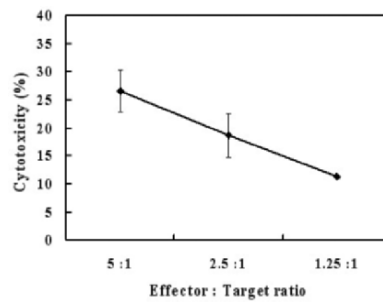


Figure 5. Cytotoxicity against K562 after 5-week induction.

RETINOIC ACID IMPROVES CELL PROLIFERATION AND ANTIBODY PRODUCTION OF HUMAN HYBRIDOMAS NONPROLIFERATIVE IN A FRUCTOSE-BASED MEDIUM

Yuichi Inoue¹, Sanetaka Shirahata² and Yasushi Sugimoto³

¹Faculty of Agriculture, and ³The United Graduate School of Agricultural Sciences, Kagoshima University, 1-21-24 Korimoto, Kagoshima 890-0065, Japan; ²Graduate School of Genetic Resources Technology, Kyushu University, 6-10-1 Hakozaki, Higashi-ku, Fukuoka 812-8581, Japan

Abstract: Fructose-containing cell culture medium is known to cause a decreased lactate production, leading to a decreased change in pH. This is beneficial to the process control of monoclonal antibody (MAb) production by hybridomas. However, not all hybridoma cell lines can be cultured in a fructose-based medium. We found that retinoic acid could improve nonproliferation and boost MAb production in some human hybridoma cell lines by activating fructose metabolism. This study may be useful as a strategy for cell cultures susceptible to lactate production and pH change as well as hybridoma cultures.

Key words: antibody production; cell proliferation; fructose; hybridoma; retinoic acid.

1. INTRODUCTION

Glucose has been used as a sugar source in most cell culture media. However, it is not always suitable for the production of biologicals because it generates a high concentration of lactic acid by glycolysis, leading to a decrease in medium pH below optimal range for cell and product stability. Many investigators have shown that fructose was better than glucose in slow utilization and low lactate production (Imamura et al., 1982; Petch et al., 1996). Despite these facts, fructose has been little used as a sugar source for the production of biologicals

until now. One reason may be the limited availability of fructose for cell lines. In hybridoma cultures, not all cell lines can be cultured in a fructose-based medium. Retinoic acid (RA) has attracted considerable attention as an agent with a broad range of physiological and metabolic effects (Ballow et al., 2003). In addition, it has shown to enhance monoclonal antibody (MAb) production in some human hybridoma cell lines (Aotsuka et al., 1991; Inoue et al., 2000). In the present study, we examined the effect of RA on the fructose-based culture of human hybridoma cell lines.

2. MATERIALS AND METHODS

2.1 Cell line and cell culture

The human hybridoma cell lines AE6 and BD9 were generated by fusing peripheral blood lymphocytes from a healthy adult with a fusion partner A₄H₁₂ derived from human Molt4 cells using an in vitro immunization method (Kawahara et al., 1992). Cells were maintained in the serum-free ITES-ERDF medium (Kyokuto Pharmaceutical Industrial Co., Tokyo, Japan) supplemented with ITS-X Supplements (GIBCO BRL, Tokyo, Japan) which contains 10 µg/ml of insulin, 5.5 µg/ml of transferrin, 2 µg/ml of ethanolamine and 6.7 ng/ml of sodium selenite, at 37°C in humidified 5% CO₂/95% air. Before all experiments, cells were adapted in the ITES-RPMI1640 medium containing 2 g/L of glucose or fructose for one day. All experiments were done in triplicate and the average value was used for analysis.

2.2 Retinoic acid

all-trans-RA (Wako Pure Chemical Industries Ltd., Osaka, Japan) was dissolved in ethanol at a concentration of 1 mM, and stored at -20°C in small aliquots under light protection. For each experiment, stock aliquots were diluted with ethanol, and immediately added to the culture medium at final concentration of 10⁻⁷ M.

2.3 Measurement of glucose, fructose and lactate concentrations

The concentrations of glucose, fructose and lactate were measured by using Glucose CII Test Wako (WAKO), Fructose Assay Kit (SIGMA) and Lactate Reagent (SIGMA), respectively.

2.4 Measurement of antibody concentration and viable cell number

The MAbs concentrations in culture medium were measured by an enzyme-linked immunosorbent assay (ELISA) as described previously (Shoji et al., 1994), using anti-human immunoglobulin (Ig) antibody (IgM #AH1601, IgG # AH1301; Biosource International, Inc., USA) as the first antibody, and anti-human Ig peroxide conjugate antibody (IgM #AH1604, IgG # AH1304; Biosource International, Inc., USA) as the second antibody. Cell number was counted by using a hemacytometer, and viability was determined by the trypan blue dye exclusion method. The fructose concentrations in the medium were measured by using a fructose assay kit (SIGMA, USA).

2.5 RT-PCR analysis

Total RNA was recovered from cells using TRIZOL reagent (GIBCO BRL). Reverse transcription was done using oligo-dT primers as described in the manufacturer's protocol (Amersham Pharmacia Biotech Inc., USA). The following primers were used to amplify the genes of the key enzymes in glycolysis and pentose phosphate cycle, and the β -actin gene as a control (Table 1).

Table 1. Primers for RT-PCR.

Enzymes	Primers	Product size
Hexokinase-1	Forward 5'-TTTACTAGGTCATACGACACGGC-3' Reverse 5'-CCACAAAATCGTGTGTCCG-3'	196 bp
Glucose 6-phosphate dehydrogenase	Forward 5'-GTCAAGGTGTTGAAATG-3' Reverse 5'-CTGGCTCCTGCAGAAGAC-3'	483 bp
Phosphofruktokinase	Forward 5'-CTGAAAGCATGAGACACACTCC-3' Reverse 5'-GTGTCTGACCCAGTCCCG-3'	185 bp
Fructose 1,6-bisphosphatase	Forward 5'-TACGCCAAGGACTTTGACC-3' Reverse 5'-GTGCTTCTCATACACCTTC-3'	362 bp
β -actin	Forward 5'-GACTTCGAGCAAGAGATG-3' Reverse 5'-GCCAGACAGCACTGTGTT-3'	240 bp

PCR amplification reactions were done in 50 μ l reaction volumes containing 5 μ l of 10 x PCR buffer, 4 μ l of 2.5 mM deoxynucleoside triphosphates, 3 μ l of first strand cDNA, 10 pmol of each primer and 1.25 units of *Taq* DNA polymerase (Takara Biomedicals, Osaka, Japan). The mixture was denatured at 94°C for 2 min, followed by 35 cycles at 94°C for 30s, at 55°C for 30s, and at 72°C for 30s. The final elongation step was extended for an additional 5 min. The amplified products were analyzed by electrophoresis on a 1.5% agarose gel and stained by ethidium bromide.

3. RESULTS AND DISCUSSION

3.1 Improvement of cell proliferation and antibody production by RA

The human hybridoma cell line AE6 could not proliferate in a fructose-based ITES-RPMI 1640 medium. However, the addition of RA to the medium improved the proliferation of AE6 cells up to the same level as that in the normal glucose-based medium (see Fig. 1, left). In addition, their IgM production in both glucose-based and fructose-based media supplemented with RA was over four times higher than that in the normal glucose-based medium without RA (see Fig. 1, right), indicating that the enhancement of MAb production by RA was independent of sugar source in culture medium. Similar results were also found in the human hybridoma cell line BD9 that produces IgG.

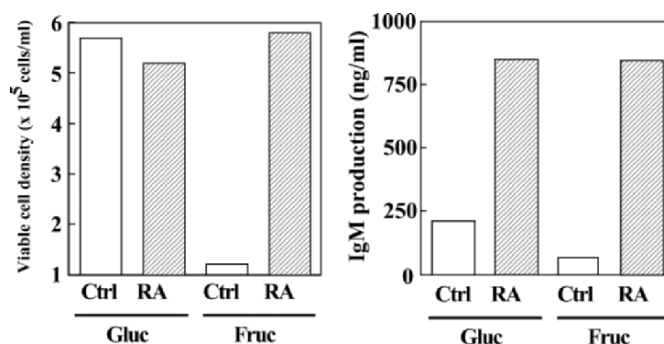


Figure 1. RA improved cell proliferation and IgM production of the human hybridoma cell line AE6 in a fructose-based ITES-RPMI1640 medium. Cells (1×10^5 cells/ml) were cultured in a glucose-based or fructose-based ITES-RPMI1640 medium supplemented with or without 10^{-7} M RA for 4 days. Control (Ctrl) received an equal amount of ethanol without RA. After 4 days, viable cell density and antibody concentration in the medium were measured.

3.2 Sugar consumption and lactate production

The improvement of cell proliferation by RA was not found in the galactose-based or mannose-based medium (data not shown). In the fructose-based medium, fructose consumption was found only in the presence of RA (see Fig. 2), implying that RA activated fructose metabolism of hybridomas. When compared with sugar utilization

between the glucose-based and fructose-based media supplemented with RA, the utilization of fructose was slower than that of glucose. In addition, lactate production in the fructose-based medium supplemented with RA was lower than that in the glucose-based medium supplemented with RA (data not shown). These findings correspond to the results of other investigators (Imamura et al., 1982; Petch et al., 1996).

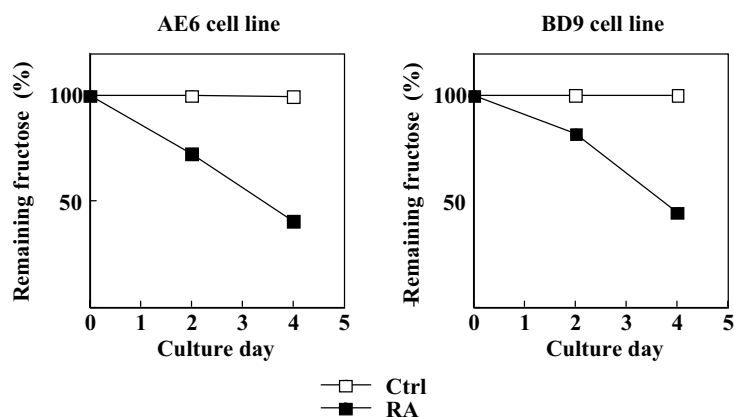


Figure 2. RA activated fructose metabolism of human hybridoma cell lines. Cells (1×10^5 cells/ml) were cultured in a fructose-based ITES-RPMI1640 medium supplemented with or without 10^{-7} M RA for 4 days. Control (Ctrl) received an equal amount of ethanol without RA. After 4 days, fructose concentrations in the medium were measured by using a fructose assay kit.

3.3 RT-PCR analysis of key enzymes for carbohydrate metabolisms

RA has been shown to regulate many gene expressions at the transcription level (Desai et al., 1996). We examined gene expression of key enzymes for glycolysis (hexokinase-1, phosphofruktokinase and fructose 1,6-bisphosphatase) and pentose phosphate pathway (glucose 6-phosphate dehydrogenase) by using RT-PCR analysis. As a result, only fructose 1,6-bisphosphatase expression was found to be significantly increased by RA (see Fig. 3), leading to decrease in lactate production. Fujisawa et al. (2000) reported the identification of a response element for RA in the promoter region of the human fructose 1,6-bisphosphatase gene. These findings support that RA may exert its effect for fructose metabolism of hybridomas. Reitzer et al. (1979) reported that fructose is metabolized essentially through the pentose phosphate cycle in HeLa cells.

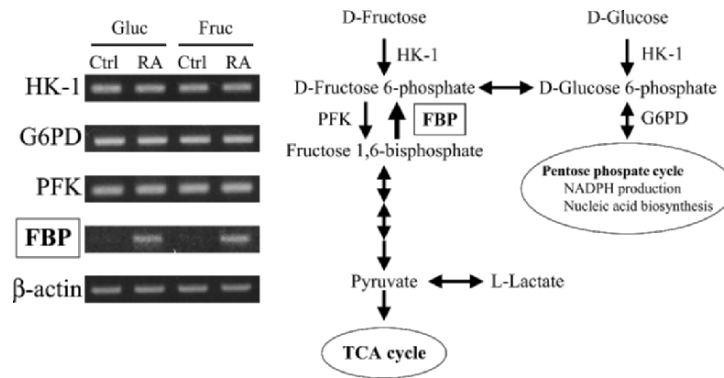


Figure 3. RT-PCR analysis of key enzyme for carbohydrate metabolisms. HK-1: hexokinase-1; G6PD: glucose 6-phosphate dehydrogenase; PFK: phosphofructokinase; FBP: fructose 1,6-bisphosphatase.

4. CONCLUSIONS

We report here that RA can improve nonproliferation and boost MAb production in some human hybridoma cell lines by activating fructose metabolism. However, further study is needed to understand the mechanism underlying the activation of fructose metabolism by RA. This study may be applicable to other cell cultures susceptible to lactate production and pH change.

5. ACKNOWLEDGMENTS

This work is supported in part by a Grant-in-Aid for Young Scientists from Japan Society for the Promotion of Science.

6. REFERENCES

- Aotsuka, Y. and Naito, M., 1991, Enhancing effects of retinoic acid on monoclonal antibody production of human-human hybridomas, *Cell. Immunol.* 133: 498-505.
 Ballou, M., Wang, X., Xiang, S. and Allen, C., 2003, Expression and regulation of nuclear retinoic acid receptors in human lymphoid cells, *J. Clin. Immunol.* 23: 46-54.

- Desai, D., Michalak, M., Singh N. K. and Niles, R. M., 1996, Inhibition of retinoic acid receptor function and retinoic acid-regulated gene expression in mouse melanoma cells by calreticulin, *J. Biol. Chem.* 271: 15153-15159.
- Fujisawa, K., Umesono, K., Kikaw, Y., et al., 2000, Identification of a response element for vitamin D3 and retinoic acid in the promoter region of the human fructose 1,6-bisphosphatase gene, *J. Biochem.* 127: 373-382.
- Imamura, T., Crespi, C. L., Thilly, G. W., and Brunengraber, H., 1982, Fructose as a carbohydrate source yields stable pH and redox parameters in microcarrier cell culture, *Anal. Biochem.* 124: 353-358.
- Inoue, Y., Fujisawa, M., Shoji, M., et al., 2000, Enhanced antibody production of human-human hybridomas by retinoic acid, *Cytotechnology* 33: 83-88.
- Kawahara, H., Shirahata, S., Tachibana, H. and Murakami, H., 1992, In vitro immunization of human lymphocytes with human lung cancer cell line A549, *Hum. Antibod. Hybridomas* 3: 8-13.
- Petch, D. and Butler, M., 1996, The effect of alternative carbohydrates on the growth and antibody production of a murine hybridoma, *Applied Biochem. Biotech.* 59: 93-104.
- Reitzer, L. J., Wice, B. M., and Kennell, D., 1979, Evidence that glutamine, not sugar, is the major energy source for cultured HeLa cells, *J. Biol. Chem.* 254: 2669-2676.
- Shoji, M., Kawamoto, S., Sato, S., et al., 1994, Specific reactivity of human antibody AE6F4 against cancer cells in tissues and sputa from lung cancer patients, *Hum. Antibod. Hybridoma* 5: 116-122.

CONSTRUCTION OF RECOMBINANT MONOCLONAL ANTIBODY AGAINST HEPATITIS B SURFACE ANTIGEN BY PHAGE DISPLAY

Apichai Prachasuphap^{1,2}, Chaivat Kittigul², Patcharee Sunthoranandh², Panadda Dhepakson¹, Nongluk Buddhirakkul¹, Kruavon Balachandra¹

¹Medical Biotechnology Center, Department of Medical Sciences, Thailand,

²Department of Microbiology, Faculty of Sciences, Kasetsart University, Thailand

Abstract: Single chain antibody fragment (scFv) to surface antigen of Hepatitis B virus was generated by phage display technique. The recombinant protein contains variable regions of murine monoclonal antibody HB3 that recognizes a conformational epitope of hepatitis B surface antigen. In this study, immunoglobulin gene was introduced into phagemid vector and rescued by M13 helper phage in *E. coli* TG1. Phage expression and binding activity of recombinant antibody against HBsAg was selected. Infection of *E. coli* HB2151 by selected recombinant phage resulted in stable, efficient expression of scFv that could be secreted into culture medium. The scFv fragment was purified by affinity chromatography and confirmed by immunoblot analysis, which yielded one band of 30 kDa. The activity of recombinant scFv was detected by ELISA, which specifically bound to its cognate antigen at a minimum cutoff sensitivity level of 8 ng/ml. These results indicate that specific binding of a scFv to HBsAg can be used for diagnostic purposes. Further experiments, isolated immunoglobulin gene will be cloned into adenovirus vector for transduction of the encoding cDNA into HBV infected hepatocytes and tested its ability to interfere with the HBV replication cycle that might be a novel gene therapy strategy for intracellular immunization against chronic HBV infection.

Key words: HBV; hepatitis B surface antigen; monoclonal antibody; phage display; recombinant antibody; scFv.

1. INTRODUCTION

Hepatitis B is a serious and common infectious disease of the liver, affecting millions of people throughout the world. The diagnosis of HBV infection is generally made on the basis of serology. Virtually all individuals infected with HBV, either acutely or chronically, will have detectable serum hepatitis B surface antigen (HBsAg). The most sensitive and specific methods used commercially in diagnosis are radioimmunoassays (RIA) and enzyme-linked immunosorbent assays (ELISA) that require a specific antibody against HBsAg. The development of hybridoma technology allowed the generation and production of monoclonal antibody with predefined specificities (Kohler and Milstein, 1975). However, the production of monoclonal antibody may be limited to unstable hybridoma cell lines and time-consuming processes involving animal immunization schedule and/or hybridoma generation. Phage display is an effective way for the isolation and engineering of recombinant antibodies (McCafferty et al., 1990). Furthermore, this can be rescued unstable hybridoma cell lines to recombinant antibodies by used as a source of immunoglobulin gene. Antibodies in the form of recombinant antibody fragments were expressed on the surface of phage. Subsequently, phage bearing antibody with high affinity against the target antigen is enriched after selection and infect to bacterial cells for soluble antibody expression. The expression of antibody will be a way to create inexpensive diagnostic tools or alternatives to rapidly developing monoclonal antibody technology for direct application as therapeutics or biotechnological reagents.

2. METHODS

Total RNA was first isolated from hybridoma cells producing monoclonal antibody specific to Hepatitis B surface antigen. The heavy and light chain mRNA are reverse transcribed into cDNA in two separate reaction using VL forward and VH backward primers and then amplified using two set of primers designed for annealing to opposite ends of the variable region of each chain. The purified heavy and light chain DNA products were assembled into a single gene using DNA linker fragment. The assembled scFv DNA fragment was amplified by PCR using a set of primer containing restriction sites for cloning into pCANTAB-5E phagemid vector. Following restriction digestion and ligation, the ligated vector was introduced into competent *E. coli* TG1 by chemical treated

transformation. Bacterial cells contained phagemid were grown and then infected with M13KO7 helper phage, to yield recombinant phages which display scFv antibody fragment that fused to coat proteins of phage. The phage that displayed scFv antibody fragment were enriched by panning with HBsAg. Then soluble scFv were produced by infect *E. coli* HB2151 with antigen-positive phage. The expressed scFv was purified by affinity chromatography with an epitope-tag antibody column. The antigen binding activity and specificity of purified soluble scFv was confirmed by ELISA and western blot analysis.

3. RESULTS

3.1 Generate scFv fragment and express on bacteriophage

Single chain fragments composed of recombined heavy chain and light chain variable domain with an inserted flexible polypeptide (Gly₄Ser)₄ linker were generated (Figure 1) by randomly joining individual heavy-chain variable domains with light-chain variable domains through gene splicing by jumping-PCR-assembly. Subsequently, scFv fragments were cloned in pCANTAB-5E (Amersham Biosciences) and expressed as fusion proteins with the gene III coat protein of the filamentous bacteriophage M13KO7. The recombinant scFv displayed on the surface of bacteriophage were selected by affinity selection with HBsAg. Only in case of phage EIA response scFv clone were considered specific binders to HBsAg.

3.2 Expression of soluble scFv and Affinity chromatography

For high level expression of soluble scFv in *E. coli*, antigen positive phage clone from phage EIA were used to infect *E. coli* HB2151. After induction with IPTG and incubation overnight at 30°C, soluble antibody was harvested from periplasmic space. Further purification was done using Anti-E Tag column. The purified scFv was analyzed by SDS-PAGE (Figure 2), and one band of recombinant scFv fragment was observed with molecular mass of approximately 30 kDa and could react specifically with anti E-tag antibody by immunoblot analysis.

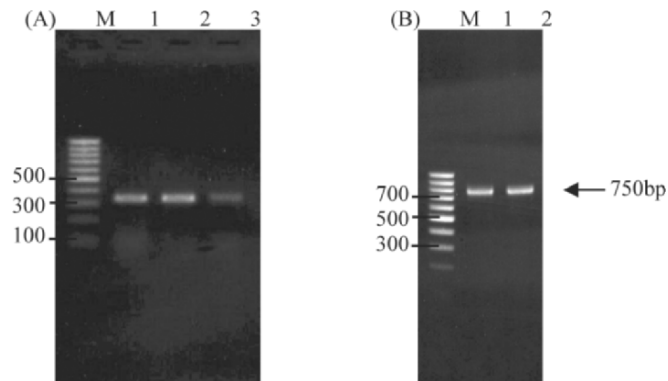


Figure 1. Construction of murine scFv fragments by PCR. (A) Amplification of variable heavy and light chain gene from hybridoma cells producing antibody specific to hepatitis B surface antigen. M = marker, lanes 1-2 present the PCR products of variable light chain gene using different forward primers for amplification of κ light chain and lane 3 present the amplified VH product. (B) scFv fragment was constructed using jumping-PCR-assembly techniques to join heavy-chain and light-chain variable domains with flexible polypeptide (Gly₄Ser)₄ linker. The assembled products of two reactions were 750 bp that indicated by an arrow.

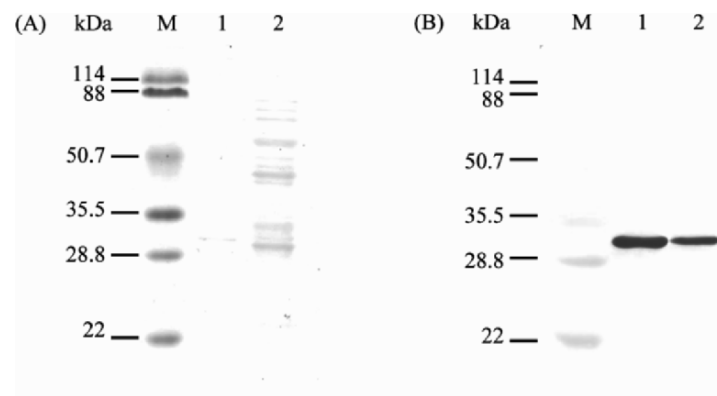


Figure 2. SDS-PAGE and immunoblot analysis of scFv antibody. (A) The protein patterns of purified scFv compared with crude sample. M = marker; lane 1, purified scFv fragment; lane 3, crude sample. (B) Immunoblot analysis of the same patterns with anti E-tag antibody.

3.3 Characterize the activity of recombinant scFv antibody against hepatitis B surface antigen

The sensitivity of scFv for HBsAg detection was determined by coating plates with serial dilution of HbsAg in concentration from 0.5 to

1024 ng/ml. According to ELISA results, the sensitivity of scFv antibody from bacterial culture reacted with HBsAg at a minimum cutoff sensitivity level of 8 ng/ml. Since scFv antibody is specific for HBsAg, this molecule was used in inhibition ELISA studies. Binding to HBsAg by scFv antibody in an ELISA was inhibited by incubation with HBsAg. 25% inhibition of scFv antibody binding was detected at the lowest concentration of HBsAg used (12.5 $\mu\text{g/ml}$). Concentrations of 100 $\mu\text{g/ml}$ HBsAg and above resulted has 98% inhibition. In this result, indicated that decreasing OD with increasing concentrations of soluble antigen.

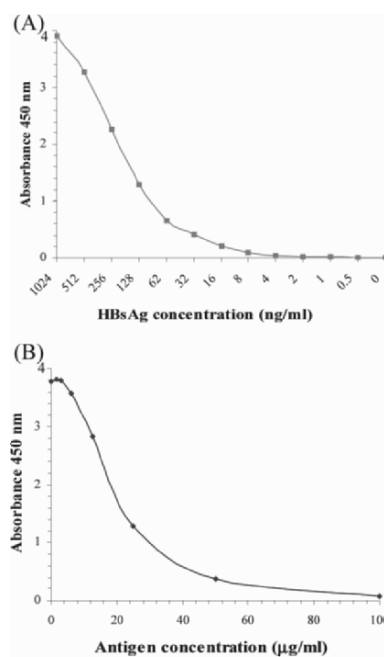


Figure 3. Sensitivity and binding activity of recombinant scFv antibody against HBsAg. (A) Serial dilution of HBsAg were used to coat plates for EIA to determine specific binding of scFv to HBsAg. (B) Competition ELISA to determine affinity of sFv fragments against HBsAg. scFv was incubated with varying concentrations of HBsAg and determined free sFv concentration in solution.

3.4 Screening of Hepatitis B infected serum by ELISA

The double antibody sandwich method was applied to detect HBV infected serum with scFv antibody. Capture antigen on coated plates

were detected with scFv antibody. All HBV infected sera were obtained absorbance greater than 4.0. For non-infected HBV serum, all samples were given absorbance below the negative control. According to this result, not found the fault positive and fault negative including nonspecific background.

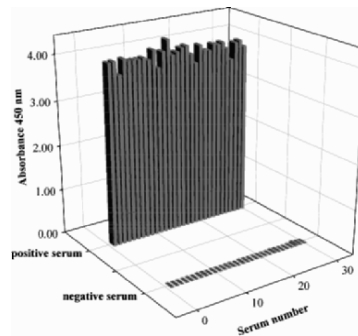


Figure 4. All 60 sera sample from blood donor of Thai Red Cross were analyzed and compared with the result from Thai Red Cross laboratory.

4. CONCLUSION

The results demonstrated that a bacteriophage display is a powerful technique for isolation of a monoclonal antibody when conventional immunological approaches or hybridoma technique is unstable to produce monoclonal antibody. Furthermore, it will be another way to create inexpensive diagnostic tools or alternative method to produce monoclonal antibody rapidly for direct application as therapeutics or biological products.

The affinity of recombinant anti-HBsAg scFv fragment produced in *E. coli* was identical with parent monoclonal anti-HBsAg derived from hybridoma cells. According to the results, anti-HBsAg scFv fragment has sensitivity to detect HBsAg in nanogram level and appears to have high affinity and specificity to HBsAg that is appropriate for using in clinical application.

The severe pathological consequences of persistent HBV infections include the development hepatocellular carcinoma. To achieve antiviral effects in hepatocytes, the encoding cDNA for scFv fragments inhibiting HBV replication will be transduced to hepatocytes using adenovirus vector. If efficient expression of scFv fragment in hepatocytes is encountered, intracellular immunization by viral vector coding for scFv could be a promising approach for treatment of chronic HBV infection.

A HUMAN CATALYTIC ANTIBODY WITH THE LIGHT CHAIN RAISED BY SECONDARY VJ RECOMBINATION IN A HUMAN PLASMA CELL LINE

Minoru Iwaki, Hirofumi Tachibana, Ryuichi Sakamoto, and Koji Yamada
*Department of Bioscience and Biotechnology, Faculty of Agriculture, Kyushu University,
6-10-1 Hakozaki, Higashi-ku, Fukuoka 812-8581, Japan*

Abstract: Immunoglobulin (Ig) gene rearrangements occur in a highly ordered fashion during B-cell development. Continuous rearrangement of the light chain genes has been reported in mature B cells *in vivo*, but not in Ig-secreting plasma cells. In our previous study, we have identified the antibody-secreting human plasma B-cell line HTD8, which actively replaces the production of the original λ light chain with a new λ chain at a high rate. In this study, we examined the peptidolytic activities of the antibodies produced by the plasma cell clones which have occurred secondary recombination to show a possible biological role of the newly-expressed antibodies. An antibody produced by one of the HTD8-derived cells had peptidolytic activities. As a result of sequence analysis, the variable region gene of the antibody light chain belonged to $V_{\lambda}6$ family. The other antibodies with the light chains belonging to $V_{\lambda}6$ family did not have such an activity. The difference among $V_{\lambda}6$ -relating antibodies is a sequence diversification occurring in the combining site between variable and joint regions in the light chain. These results suggest that the peptidolytic activity of the antibody is gained by a sequence diversification occurring in the combining site between variable and joining regions in the light chain.

Key words: catalytic antibody, secondary VJ recombination.

1. INTRODUCTION

B lineage cells recombine Ig gene segments in a highly ordered manner during their differentiation process (1). This mechanism is termed V(D)J recombination and is completed before the immature B cell stage. It was thought that further V(D)J recombination did not occur

after this developmental stage. However continuous rearrangement of the light chain genes has been reported in some cell surface Ig positive (sIg⁺) B-cell lines (2-5) and in mature B cells in vivo (6, 7), but not in Ig-secreting plasma cells. We have shown that long-term culture of a human B-cell hybridoma line with concanavalin A (Con A) induce at a high frequency production of various novel λ light chains, which replaced the original light chain (8, 9). This differential light chain expression led to an alteration of the original antigen binding ability. We call this process light chain shifting (9). We established a plasma cell clone (termed HTD8), which had undergone secondary rearrangement after losing its ability to express the originally rearrangement λ chain at a high frequency. However we have not shown a possible biological role of the newly-expressed antibodies. In this study, we examined the peptidolytic activities of the antibodies produced by the plasma cell clones which have occurred secondary recombination.

2. MATERIALS AND METHODS

2.1 Cells and cell culture

ConA-resistant clones derived from the human Ig-secreting HB4C5 cells (10) were isolated as previously described (11). We have been identified Con A-resistant variants HTD8 cells (12). These cells were cultured in ERDF medium (Kyokuto Pharmacy, Tokyo, Japan) containing 5% fetal calf serum (Whittaker Bioproducts, Walkersville, MD). The cells were cultured for 96 hours in ERDF medium supplemented with 10 μ g/ml of insulin, 20 μ g/ml of transferrin, 20 μ M of ethanolamine, and 25 nM of selenite (ITES-ERDF) at 37°C under humidified 5% CO₂-95% air (13).

2.2 Purification

After cultivation, culture medium was dialyzed. Phenol red was removed from culture medium using activated charcoal. The activated charcoal was removed by centrifugation at 450 x g and 4°C for 20 min. The supernatant of the sample was filtered (0.45 μ m) and freeze-dried. The lyophilizate was dissolved in 50 mM Tris-HCl.

2.3 Fluorescent peptide substrates

Boc-Phe-Ser-Arg-MCA (Substrate for trypsin, tryptase), Pyr-Gly-Arg-MCA (Substrate for urokinase), Z-Phe-Arg-MCA (Substrate for plasma kallikrein), Suc-Leu-Leu-Val-Tyr-MCA (Substrate for chymotrypsin), Leu-MCA (Substrate for aminopeptidase) and Suc-Gly-Pro-Leu-Gly-Pro-MCA (Substrate for collagenase) were purchased from Peptide Institute (Osaka, Japan). These substrates were dissolved in dimethyl sulfoxide and preserved at a concentration of 10 mM. The substrates were diluted 50 μ M with 50mM Tris-HCl (pH 7.6) before use.

2.4 Measurements of peptidolytic activities

Goat anti-human lambda light chain antibody (Biosource International, Camarillo, CA) was used to fix the newly-expressed antibodies. The antibody diluted with phosphate-buffered saline (PBS) was added to a 96-well plate, and incubated for 2 h at 37°C. After washing with 0.05% Tween20-PBS (T-PBS), each well was blocked with 25% Block Ace (Dainihon) for 2 h at 37°C. After blocking reaction, the plate was washed with 0.05% T-PBS. One hundred μ l of samples were added to a 96-well plate for 1 h at 37°C, the plate was washed with 0.05% T-PBS. The fluorescent peptide substrates were added and measured fluorescent intensities for 6 hours at 37°C.

2.5 Inhibition of peptidolytic activity

The method is the same as measurements of peptidolytic activities. Before 100 μ l of fluorescent peptide substrates were added, the antibody (goat anti-human IgM) was reacted with the fixed antibodies in the 96-well plate, and incubated for 90 minutes at 37°C.

2.6 Nucleotide sequence analysis

The nucleotide sequences of the antibody variable regions were determined by the previously reported method (14) using the DyeDeoxy terminator kit (Perkin-Elmer) with the DNA sequencer ABI 310 (Perkin-Elmer) according to the manufacturer's instruction.

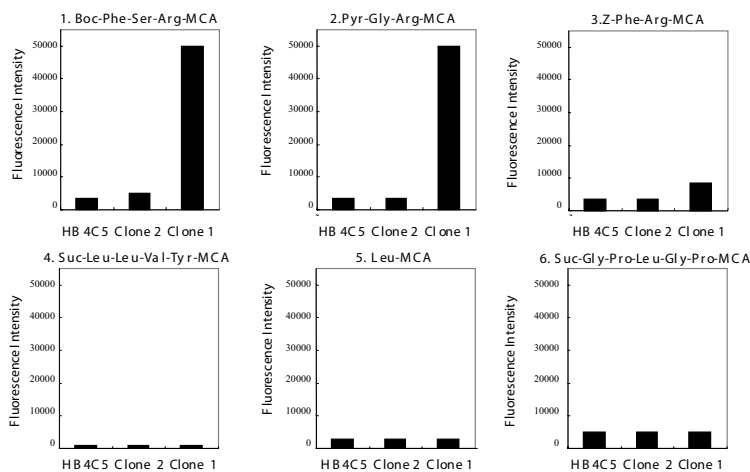


Figure 1. Measurements of peptidolytic activities. Peptidolytic activities of newly-expressed antibodies were measured with fluorescent peptide substrates for 6 hours at 37°C. Goat anti-human lambda light chain antibody was used to fix the newly-expressed antibodies. Final concentration of the antibodies was 500 ng/well. Final concentration of fluorescent peptide substrates was 50 μM.

3. RESULTS AND DISCUSSION

3.1 Peptidolytic activities of the newly-expressed antibody

We measured peptidolytic activities of the antibodies using fluorescent peptide substrates (Fig. 1).

The antibodies produced by HB4C5 did not have the peptidolytic activity. The antibody with the light chains belonging to $V_{\lambda 6}$ family produced by the clone 2 cells also did not have the peptidolytic activity. However, the antibody with a $V_{\lambda 6}$ family light chain from the clone 1 cells had the trypsin-like, urokinase-like, and plasma kallikrein-like activities.

3.2 Inhibition of peptidolytic activity

Peptidolytic activity was inhibited by goat anti-human IgM. (Fig. 2)

When conventional IgG was used as an antibody of a negative control, peptidolytic activity was not inhibited. These results suggest that the antibody produced by the clone 1 cells have peptidolytic activities.

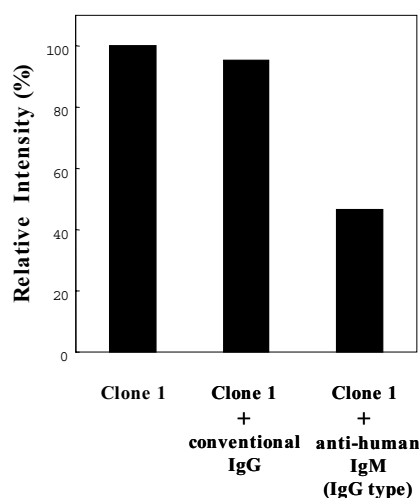


Figure 2. Inhibition of peptidolytic activity. The antibody produced from clone 1 cells was reacted with either anti-human IgM or conventional IgG for 90 minutes at 37°C, then we measured trypsin-like activity for 18 hours using the fluorescent peptide substrate, Boc-Phe-Ser-Arg-MCA. Conventional IgG was used as a negative control.

3.3 Nucleotide sequence analysis

The nucleotide sequences of the variable region of the light chains belonging to $V_{\lambda 6}$ family were determined.

There were 7 clones with the light chains belonging to $V_{\lambda 6}$ family. The difference among antibodies is only a sequence diversification occurring in the combining site between variable and joint regions (N region) in the light chain. Among the $V_{\lambda 6}$ -relating antibodies, only the clone 1 cells had peptidolytic activities. These results suggest that the peptidolytic activity of the antibody is gained by a sequence diversification occurring in N region in the light chain.

4. REFERENCES

1. Rolink, A., Melchers, F., 1991, Molecular and cellular origins of B lymphocyte diversity, *Cell* 66: 1081-94
2. Hardy, R. R., Jeffery, L. D., Kyoko, H., Gina, J., Leonore, A. H., and Leonard, A. H., 1986, Frequent Λ light chain gene rearrangement and expression in a Ly-1 B lymphoma with a productive Kappa chain allele, *Proc. Natl. Acad. Sci. USA* 83: 1438-1442

3. Levy, S., Campbell, M.J., Levy, R., 1989, Functional immunoglobulin light chain genes are replaced by ongoing rearrangements of germline V kappa genes to downstream J kappa segment in a murine B cell line, *J. Exp. Med.* 170: 1-13
4. Harada, K., Hideo, Y., 1991, Lack of feedback inhibition of V κ gene rearrangement by productively rearranged alleles, *J. Exp. Med.* 173: 409-415
5. Berimstein, N., Levy, S., Levy, R., 1989, Activation of an excluded immunoglobulin allele in a human B lymphoma cell line, *Science* 244: 337-339
6. Papavasiliou, F., Casellas, R., Suh, H., Qin, X., Besmer, E., Pelanda, R., Nemazee, D., Rajewsky, K., Nussenzweig, M., 1997, V(D)J recombination in mature B cells a mechanism for altering antibody responses, *Science* 278: 298-301
7. Hertz, M., Kouskoff, V., Nakamura, T., Nemazee, D., 1998, V(D)J recombinase induction in splenic B lymphocytes is inhibited by antigen-receptor signaling, *Nature* 394: 292-295
8. Tachibana, H., Kido, I., Murakami, H., 1994, Heterogeneous expression of human antibody lambda chains by concanavalin A-resistant hybridomas lead to changed antigen binding, *J. Biol. Chem.* 269: 29061-29066
9. Tachibana, H., Ushio, Y., Krungkasem, C., Shirahata, S., 1996, Inducing the loss of immunoglobulin lambda light chain production and the rearrangement of a previously excluded allele in human plasma B cell lines with concanavalin A, *J. Biol. Chem.* 271: 17404-17410
10. Murakami, H., Hashizume, S., Ohashi, H., Shinohara, K., Yasumoto, K., Nomoto, K., Omura, H., 1985, Human-human hybridomas secreting antibodies specific to human lung carcinoma, *In Vitro Cell Dev Biol.* 21: 593-596
11. Tachibana, H., Shirahata, S., Murakami, H., 1992, Generation of specificity-variant antibodies by alteration of carbohydrate in light chain of human monoclonal antibodies, *Biochem. Biophys. Res. Commun.* 189: 625-632
12. Tachibana, H., Haruta, H., Yamada, K., 1999, Light chain shifting: identification of a human plasma cell line actively undergoing light chain replacement, *Blood* 93: 198-207
13. Murakami, H., Masui, H., Sato, H., Sueoka, N., Chow, P., Kano, T., 1982, Growth of hybridoma cells in serum-free medium: ethanolamine is an essential component, *Proc. Natl. Acad. Sci. USA* 79: 1158-1162
14. Tachibana, H., Haruta, H., Ueda, K., Chiwata, T., Yamada, K., 2000, Induction of light chain replacement in human plasma cells by caffeine is independent from both the upregulation of RAG protein expression and germ line transcription, *J. Biol. Chem.* 275: 5927-5933

17BETA-ESTRADIOL REGULATES IMMUNOGLOBULIN M PRODUCTION THROUGH INTERACTION WITH ESTROGEN RECEPTORS

Mako Nakaya, Hirofumi Tachibana and Koji Yamada

Department of Bioscience and Biotechnology, Faculty of Agriculture, Kyushu University, 6-10-1 Hakozaki, Higashi-ku, Fukuoka 812-8581, Japan

Abstract: Estrogens have diverse effects on cell growth, differentiation and homeostatic functions, and have been shown to play an important role in regulating immune system. Most of these E2 functions are mediated by estrogen receptors (ERs). Recently, it was reported that ERs were expressed immunocompetent cells, such as B cell, T cell, Natural killer cell and macrophage. In this study, it was examined that effect of 17 β -Estradiol (E2) on antibody production by splenocytes isolated from C57BL/6N mice. E2 regulates immunoglobulin M (IgM) production by mouse splenocytes. IgM production was enhanced 2.0-fold at 10^{-10} M E2. This enhancing effect of E2 was canceled by ER antagonist ICI 182780. Previously, it was reported that two subtypes of ERs, such as ER α and ER β . Both ER α selective agonist, 4,4',4''-(4-propyl- [1H]-prazole-1, 3, 5-triyl)trisphenol and ER β selective agonist, 2,3-bis-(4-hydroxyphenyl)-propionitrile enhanced the production of IgM as well as E2. Recently, ERs are expressed in plasma membrane as well as in nucleus. E2 conjugated to bovine serum albumin (E2-BSA) is a plasma membrane-associated ER specific ligand. E2-BSA has no effects on IgM production by mouse splenocytes. In conclusion, our results indicate that E2 up-regulates the production of IgM through interaction with ER α and ER β by mouse splenocytes. The enhancing effect of E2 was not induced by plasma membrane-associated ER.

Key words: 17 β -estradiol; splenocytes; immunoglobulin M; estrogen receptor.

1. INTRODUCTION

Sex hormones such as 17 β -estradiol (E2) have an important role in the immune system (Paavonen, 1994) as well as in the reproductive organs. Previous reports have been shown that E2 regulates interleukin (IL)-2, IL-4 and interferon (IFN) - γ mRNA transcription (Karpuzoglu-Sahin et al., 2001), and activates IL-1 β promoter in a macrophage cell line (Ruh et al., 1998). We have also reported that estrogenic compounds suppress lipopolysaccharide (LPS) induced IFN- γ production by mouse splenocytes (Nakaya et al., 2003).

The activations of E2 are mediated through the estrogen receptors (ERs). There are two ER subtypes termed ER α and ER β . Which act as ligand-dependent transcription factors. While it is well known that E2 can bind to and activate ERs, and that ligand-bound ERs then stimulate the transcription of estrogen responsive genes (Barkhem et al., 1998). Recent reports have shown that ER α is important for full development of thymus and spleen in male ER knocked-out mice (Staples et al., 1999), and estrogen treatment of oophorectomized ER β knocked-out mice induces thymic atrophy (Erlandsson et al., 2001), and ERs are expressed immunocompetent cells, such as B cell, T cell, NK cell and macrophage (Sakazaki et al., 2002; Curran et al., 2001). These findings suggest that E2 and ERs have very important roles in immune system. In addition, it has been reported that E2 may bypass the nucleus through a newly recognized ERs that are located on the plasma membrane (Chen et al., 1999). The plasma membrane-associated ERs have nongenomic activations. However, physiological meanings and functions of plasma membrane-associated ERs are poorly understood.

In this study, we revealed the effect of E2 on immunoglobulin (Ig) M productions by mouse splenocytes. We focused on which the effect of E2 on IgM production by splenocytes is mediated through ER α or ER β , or both. In addition, we examined whether the effect of E2 on IgM production is mediated through plasma membrane-associated ERs or not.

2. MATERIALS AND METHODS

2.1 Reagents

Male 8-10 week-old C57BL/6N mice were obtained from Seac Yoshitomi Ltd (Fukuoka, Japan). Phenol red-free RPMI 1640 medium was derived from Irvine Scientific (Santa Ana, CA). Fetal bovine serum

(FBS) was obtained from Biofluids (Rockville, MD). LPS, E2, E2 conjugated to bovine serum albumin (E2-BSA) and E2-BSA-FITC were purchased from Sigma (St. Louis, MO). 4,4',4''-(4-propyl-[1H]-prazole-1,3,5-triyl) trisphenol (PPT), 2,3-bis-(4-hydroxyphenyl)-propionitrile (DPN) and ICI 182780 were purchased from TOCRIS (Bistol, UK). Block Ace was purchased from Dainihon Pharmaceutical (Osaka, Japan).

2.2 Cells and cell culture

The spleen was excised from C57BL/6N mouse sedated under diethyl ether anesthesia, and the splenocytes were isolated. Splenocytes were inoculated at 2×10^6 cells/ml in phenol red-free RPMI1640 medium containing 5% charcoal-treated FBS and estrogen along with 7.8 $\mu\text{g/ml}$ of LPS, and cultured at 37°C in a humidified atmosphere containing 5% CO₂. This experiment was carried out according to the guidelines for animal experimentation set by the Faculty of Agriculture and Graduate Course of Kyushu University No. 6 of the Japanese government.

2.3 Enzyme-linked immunosorbent assay for mouse antibodies

The amounts of IgM in culture medium were measured by sandwich enzyme-linked immunosorbent assay (ELISA) as previously reported (Takasugi et al., 2001). Goat anti-mouse IgM (Zymed, Sun Francisco, CA) were used to fix IgM. The antibody solution was diluted 1000 times with 50 mM sodium carbonate-bicarbonate buffer (pH 9.6). Each well of ELISA plate was treated with 100 μl of the antibody solutions for 1 h at 37°C. Then, each well was blocked with 25% of Block Ace for 2 h at 37°C. Following blocking reaction, each well treated with 50 μl of culture supernatant for 1 h at 37°C. The well was then treated with 100 μl of HRP-conjugated goat anti-mouse IgM (Zymed) diluted 1000 times with 10% Block Ace for 1 h 37°C. Then, 0.6 mg/ml of 2,2'-azino-bis(ethylbenzothazoline-6-sulfonic acid diammonium salt) (ABTS) dissolved in 0.03% H₂O₂-0.05 M citrate buffer (pH 4.0) was added to wells at 100 μl , and the absorbance at 405 nm was measured after the addition of 100 μl 1.5% oxalic acid for termination of the coloring reaction. The wells were rinsed 3 times with 0.05% Tween20-PBS between each step.

2.4 Antagonist of ER

The splenocytes were treated with 10^{-10} M E2 under the coexistence of estrogen receptor antagonist ICI 182780 for 24 h. The cells were pre-incubated with 10^{-5} M ICI 182780 for 30 min before E2 application, and cultured with E2 for 24 h to investigate the participation of ER in regulation of IgM production by E2.

2.5 ER α , ER β and plasma membrane-associated ER

The splenocytes were treated with nuclear ER α agonist PPT or ER β agonist DPN for 24 h. E2-BSA binds only to plasma membrane-associated ER. The splenocytes were treated with E2-BSA for 24 h. All of these studies were performed in the presence of 7.8 μ g/ml LPS. Splenocytes suspension was adjusted at 1×10^6 cells/ml with PBS. E2-BSA-FITC (10^{-6} M) was added to the cell suspensions and the mixtures were stood for 1 h at room temperature. After washing twice, the cells were fixed with 3.7% formaldehyde for 5 min at room temperature. Samples were mounted on microscope slides by using of a 1:1 (v/v) mixture of glycerol and Vectashield (Vector) containing 2% (w/v) of 1,4-diazabicyclo[2,2,2]octane (DABCO, Merck, Darmstadt, Germany). The specimen was analyzed with Leica confocal laser scanning microscope unit. FITC was detected by 488 nm argon laser.

2.6 Statistical analysis

All data are expressed as the means \pm SD. Statistical significance was analyzed by Student's t test (Table 1, Fig. 1 and 3) or Scheffe's F-test (Fig. 2). Each value of $p < 0.05^*$, $p < 0.01^{**}$ or $p < 0.001^{***}$ is considered to be statistically significant.

3. RESULT AND DISCUSSION

Estrogens have diverse effects on cell growth, differentiation and homeostatic functions. Estrogens decrease low-density lipoprotein and lipoprotein A, increase high-density lipoprotein levels, and promote vasodilatation and blood flow.

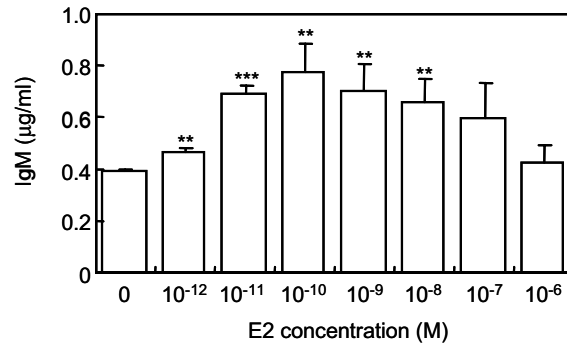


Figure 1. Effect of 17 β -estradiol on immunoglobulin M production by splenocytes of C57BL/6N mice. Splenocytes were treated with 10⁻¹² - 10⁻⁶ M E2 in the presence of 7.8 μ g/ml LPS for 24 h. Level of IgM was measured by ELISA. Data are means \pm SD (n=3). Data with asterisk marks are significantly different from the values of the control group at $p < 0.05$ *, 0.01** or 0.001***.

We first evaluated the effect of E2 on the production of IgM by splenocytes isolated from male C57BL/6N mice. As shown in Fig. 1, the production of IgM was obviously accelerated by E2, and enhanced by 2.0-fold at 10⁻¹⁰ M. This E2 concentration is equivalent to the circulating concentration of postmenopausal women treated hormone replacement therapy (Roger and Eastell, 1998).

Then, it was investigated whether ERs participate in the regulation of IgM production or not. Splenocytes were treated with E2 in the presence of ICI 182780, an ER antagonist, blocks forming ER dimer and decomposes ERs (Wakeling and Bowler, 1992; Parisot et al., 1995). As shown in Fig.2, the enhancing effect of E2 on IgM production was

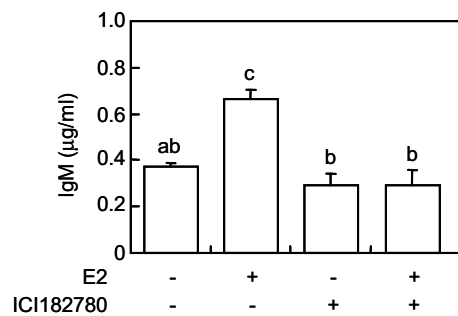


Figure 2. Effect of an ER antagonist ICI 182780 on 17 β -estradiol stimulated IgM production. Splenocytes were stimulated with 10⁻¹⁰ M E2 in the presence or absence of 10⁻⁵ M ICI 182780 for 24 h with 7.8 μ g/ml LPS. The cells were pre-incubated with ICI 182780 for 30 min before E2 application. Data are means \pm SD (n=3). Letters that are different from each other denote significant difference at $p < 0.05$ (Scheffe's F test).

completely canceled by 10^{-5} M ICI 182780. This suggests that up-regulation of IgM production by E2 is mediated through ERs. ERs were classified into two kinds of subtype ER α and ER β . Thus, it was evaluated which kind of ERs is concerned with the regulation of IgM production by using agonists specific to ER α (PPT) and ER β (DPN). PPT is an ER α agonist, and possesses 410-fold selectivity for ER α over ER β (Harris et al., 2002).

As shown in Table 1, both PPT and DNP significantly enhanced IgM production, as well as E2. These results suggest that the up-regulation of IgM production by E2 is mediated by both ER α and ER β .

Table 1. Effect of ER α and ER β agonists on IgM production by mouse splenocytes.

(M)	IgM (ng/ml)	
	PPT	DPN
0	576.8 \pm 41.5	406.7 \pm 39.6
10^{-9}	870.8 \pm 105.9*	855.9 \pm 48.8***
10^{-8}	1004.1 \pm 91.8**	826.4 \pm 77.8***
10^{-7}	1048.5 \pm 117.6*	706.5 \pm 84.8***

Splenocytes were stimulated with 10^{-9} - 10^{-7} M PPT (ER α agonist), or 10^{-9} - 10^{-7} M DPN (ER β agonist) for 24 h in the presence with 7.8 μ g/ml LPS. Data are means \pm SD (n = 3). Data containing asterisk marks are significantly different from the values in the control group at $p < 0.05^*$, 0.01^{**} or 0.001^{***} .

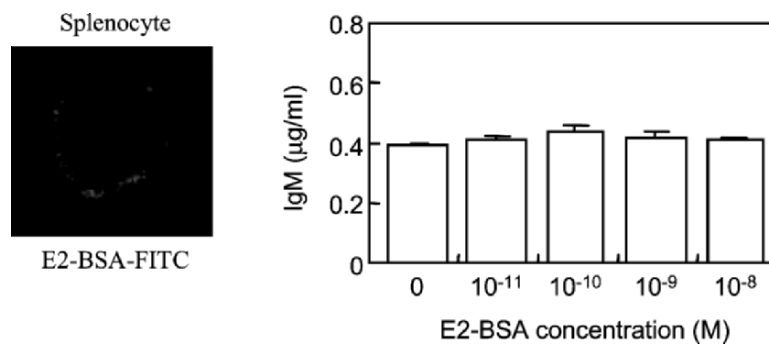


Figure 3. Effect of E2-conjugated BSA IgM on production by mouse splenocytes. Splenocytes were treated with 10^{-6} M E2-BSA-FITC for 1 h at room temperature. The cells were fixed with 3.7% formaldehyde for 5 min at room temperature. The specimens were analyzed with a Leica confocal laser scanning microscope unit. Splenocytes were treated with 10^{-11} - 10^{-8} M E2-BSA in presence of 7.8 μ g/ml LPS for 24 h. Data are presented as means \pm SD (n=3).

It is well-known that ERs are located on plasma membranes as well as in nucleus (Chen et al., 1999). Then, we examined whether plasma

membrane-associated ER participates in the regulation of IgM production or not. Though E2 can bind to ERs in both locations, E2-BSA can bind only to plasma membrane-associated ER. Splenocytes were treated with E2-BSA labeled with FITC. As shown in Fig. 3, plasma membrane-associated ER on splenocytes were stained by E2-BSA-FITC, however, IgM production of splenocytes was not stimulated by E2-BSA.

In this study, we demonstrated that E2 enhances the IgM production of splenocytes isolated from C57BL/6N mice. E2 up-regulates the IgM production through both of ER α and ER β .

4. REFERENCES

- Barkhem, T., Carlsson, B., Nilsson, Y. et al. (1998) Differential response of estrogen receptor α and estrogen receptor β to partial estrogen agonist/antagonist. *Mol. Pharmacol.* 54, 105-112.
- Chen, Z., Yuhanna, I.S., Galcheva-Garegova, Z. et al. (1999) Estrogen receptor α mediates the nongenomic activation of endothelial nitric oxide synthase by estrogen. *J Clin Invest.* 103, 401-406.
- Curran, M.E., Berghaus, L., Verneti, J.N. et al. (2001) Natural killer cells express estrogen receptor- α and estrogen receptor- β and can respond to estrogen via a non-estrogen receptor- α -mediated pathway. *Cellular Immunology* 214, 12-20.
- Erlandsson, M.C., Ohlsson, C., Gustafsson, J.A. et al. (2001) Role of oestrogen receptors alpha and beta in immune organ development and in oestrogen-mediated effect on thymus. *Immunology* 103(1), 17-25.
- Harris, H.A., Katzenellenbogen, J.A., Katzenellenbogen, B.S. (2002) Characterization of the biological roles of the estrogen receptors, ER α and ER β , in estrogen target tissues *in vivo* through the use of an ER α -selective ligand. *Endocrinology* 143(11), 4172-4177.
- Karpuzoglu-Sahin, E., Zhi-Jun, Y., Lengi, A. et al. (2001) Effect of long-term estrogen treatment on IFN-gamma, IL-2 and IL-4 gene expression and protein synthesis in spleen and thymus of normal C57BL/6 mice. *Cytokine* 14, 208-217.
- Meyers, M.J., Sun, J., Carlson, K.E. et al. (2001) Estrogen receptor-beta potency-selective ligands: structure-activity relationship studies of diarylpropionitriles and their acetylene and polar analogues. *J. Med. Chem.* 44, 4230-4251.
- Nakaya, M., Yamasaki, M., Miyazaki, Y., Tachibana, H. et al. (2003) Estrogenic compounds suppressed interferon-gamma production in mouse splenocytes through cell-cell interaction. *In Vitro Cell Dev. Biol. Anim.* 39, 383-387.
- Paavonen, T., (1994) Hormonal regulation of immune responses. *Ann. Med.* 26, 255-258.
- Parisot, J.P., Hu, X.F., Sutherland, R.L. et al. (1995) The pure antiestrogen ICI 162,780 binds to a high-affinity site distinct from estrogen receptor. *Int. J. Cancer* 62:480-484.
- Roger, A. and Eastell, R. (1998) Effect of estrogen therapy of postmenopausal women on cytokines measured in peripheral blood. *J. Bone Miner Res.* 13, 1577-1586.
- Ruh, M.F., Bi, Y., D'Alonzo, R. et al. (1998). Effect of estrogens on IL-1 β promoter activity. *J. Steroid Biochem. Mol. Biol.* 66, 203-210.
- Sakazaki, H., Ueno, H., and Kakamuro, K. (2002) Estrogen receptor α in mouse splenic lymphocytes: possible involvement in immunity. *Toxicology Letters* 133, 221-229.

- Staples, J.E., Gasiewicz, T.A., Fiore, N.C. et al. (1999) Estrogen receptor alpha is necessary in thymic development and estradiol-induced thymic alterations. *J. Immunol.* 163, 4168-4174.
- Takasugi, M., Tamura, Y., Tachibana, H. et al. (2001) Development of assay system for immunoglobulin production regulatory factors using whole cell cultures of mouse splenocytes. *Biosci. Biotechnol. Biochem.* 65(1), 143-149.
- Wakeling, A.E. and Bowler, J. (1992) ICI 182,780, a new antiestrogen with clinical potential. *J Steroid Biochem. Mol. Biol.* 43, 173-177.

MDCK CELLS RESISTANT TO METALLOPROTEINASE FROM *STREPTOMYCES GRISEUS* ACQUIRE ANCHORAGE INDEPENDENT SURVIVAL AND PROLIFERATION ABILITIES ON NON ADHESIVE SUBSTRATE

Reiko Tsutsumi¹, Masanori Shozushima² and Shigehiro Sato¹

¹Department of Microbiology, School of Medicine, Department of Radiology, ²School of Dentistry, Iwate Medical University, 19-1 Uchimaru, Morioka, Iwate 020-8505, Japan

Abstract: Using the bacterial metalloproteinase (MEP), derived from *Streptomyces griseus*, a suspension culture of MDCK (Madin-Darby canine kidney) cells was maintained for several months. The established cell line, designated as 6M-4, has unique characteristics, which allowed it to be cultured adherently on a polystyrene matrix, and anchorage-independently on a polystyrene matrix with MEP or on a non-adhesive substrate coated with poly 2-methacryl-oxethyl phosphorylcholine (MPC). The higher yield of influenza virus produced in a suspension culture of 6M-4 cells is practically beneficial in large-scale culture. Some phenotypic characteristics of the 6M-4 cells were compared with the parental MDCK cells. 6M-4 cells consist of at least two types of cells, which have different growth characteristics in soft agar. One type of cells that are incapable of growing in soft agar was favorable for the suspension culture because they do not grow in large aggregates.

Key words: MDCK; Suspension culture; Anoikis-resistance; Non adhesive matrix; MPC coating; Influenza virus.

1. INTRODUCTION

Normal epithelial, endothelial and muscle cells require attachment to the extra cellular matrix (ECM) to grow or survive, and removal of anchorage-dependent cells from their association with the ECM results in apoptotic cell death, known as a anoikis. MDCK is an anchorage-

dependent Madin-Darby canine kidney-derived epithelial cell line and is normally anoikis sensitive. For the large-scale culture of the influenza virus, a suspension culture of MDCK has been devised by introducing solid carriers to the media or using a roller bottle (Tree *et al.* 2001). The latter technique is a typical protocol recommended for the adaptation of the cells to suspension culture. The mechanism of the transition from adherent to suspension growth is being reexamined in terms of connections between integrin signaling and the apoptotic machinery. Many factors are involved in anoikis resistance and vice versa. Recent studies have revealed the participation of metalloproteinases (MMPs) and tissue inhibitors of MMP (TIMPs) on cell survival signaling pathways. We have therefore examined a foreign metalloproteinase to select anoikis resistant MDCK cells, named 6M-4: practical benefit that any of the suspension cultures with MEP on normal tissue culture matrix could produce influenza virus comparable with the adherent parental MDCK was also described.

2. MATERIALS AND METHODS

2.1 Cells and Culture-wares

MDCK cells were purchased from ATCC (NBL-2, CCL 34) and cultured in Minimum Essential Medium containing 10% FBS (MEM-10) at 37°C under 5% CO₂. The culture bottle and the 96-well micro-plate coated with poly (2-methacryloyloxyethyl phosphorylcholine), MPC, were purchased from NUNC (Nalge Nunc International, Rochester, NY, USA).

2.2 Development 6M-4 cells

MDCK was cultured in a polystyrene culture flask (Nalge Nunc International, No136196) in the presence of 50 µg/ml metalloproteinase (MEP) prepared from *Streptomyces griseus*, which received as a gift from Dr. S. Fujisaki (Institute of Enzyme Research, Osaka, Japan). The cells that were capable of growing in a suspension medium containing MEP were recovered and maintained as adherent cells (6M-4) in MEM-10 without MEP.

Colony selection was carried out by the dilution method on a 96 well polystyrene-plate and by the selection of cells in soft agar. For the

latter selection, cells were suspended in 15 ml of 0.3% agar, supplemented with complete growth medium. This cell suspension was allowed to solidify at room temperature on 10 ml of a 0.5% agar base layer containing growth medium in 10 cm dishes.

2.3 Variability and apoptosis assay

The variability of cells was checked with a LIVE/DEAD Variability/Cytotoxicity Kit (Molecular Probes, Inc. Eugene, OR, USA) according to the manufacturer's protocol. Apoptotic cells were stained with FITC-labeled annexin using a Apoptosis Detection Kit (Trevigen, Inc. Gathersburg, MD, USA) and the cells were analyzed with FACSCalibur™ (BD Bioscience, San Diego, CA, USA).

2.4 Proliferation assays

The proliferation of cells was tested using four methods. Namely, the respiratory activity was measured using an alamarBlue™ Assay (Trek diagnostic System Inc. Westlake, OH, USA). After a constant culture duration, the fluorescence of the reduced alamarBlue™ was monitored at an emission wavelength of 590 nm using a Luminescence spectrometer LS 50B (Perkin-Elmer Ltd., Buckinghamshire, UK). The incorporation of ³H-thymidine (Amersham Biosciences Corp. Piscataway, NJ, USA) into high molecular weight DNA in the 96 well microplate was assayed, essentially, according to the procedure as described (Shevach 1996). A 24 hour labeling period each day allowed termination by the addition of Triton X (0.1% final) solution and the cultures were harvested with a semi-automated cell harvesting apparatus and counted in a β counter LSC-1000 (ALOKA Co., LTD. Tokyo, Japan). For the detection of the cells that were synthesizing DNA, they were labeled with BrdU and followed by FITC-labeled antibody binding using a BrdU Flow Kit (BD Pharmingen, San Diego, CA, USA).

2.5 Influenza virus inoculation

A clinical isolate of influenza virus A was inoculated to adherent MDCK cells and to the suspension culture of 6M-4 cells and the virus suspension was recovered on day 7. The virus titer was determined by observation of the cytopathic effect (CPE) development according to the standard procedure (Hierholzer *et al.* 1995).

3. RESULTS

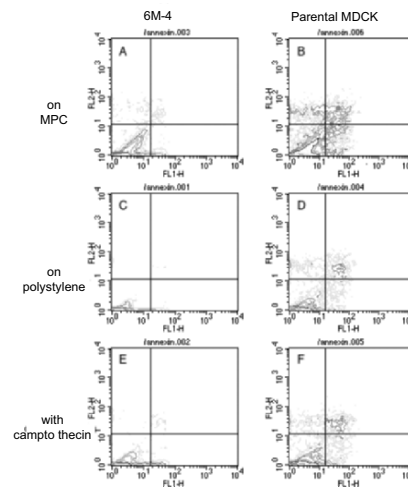
3.1 Morphological appearance and variability of 6M-4 cells

A floating sub line (6M-4) of adherent MDCK cells were selected from the MEP resistant floating cells. The fundamental differences in growth pattern are the growth as floating aggregates for 6M-4 cells versus the suspension cell death for the parental MDCK cells on a non-adhesive MPC matrix. The 6M-4 cell lines grew adherently without MEP. The validity of the cells, using calcein-AM and ethidium homodimer, confirmed that the 6M-4 cells, floating in the presence of MEP, were ethidium homodimer negative. As expected, a large fraction of the parental MDCK population cultured with MEP became ethidium homodimer positive.

3.2 Assessment of cell survival and proliferation avoiding anoikis

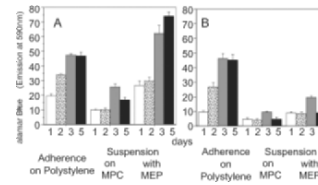
3.2.1 Annexin V binding

The externalization of phosphatidylserine after the detachment of cells was examined by Annexin V binding. As shown in Fig. 1, 6M-4 cells were apparently anoikis resistant during the first 6h on both the MPC and polystyrene matrix. A larger fraction of the parental MDCK cells on the MPC matrix presented double positive signals than those on the polystyrene matrix. After a 6 hour-exposure to camptothecin, which is an inhibitor of the gyrase responsible for DNA replication, the 6M-4 cells were still resistant to Annexin V binding compared to the MDCK cells, although overnight contact with the drug was completely lethal.



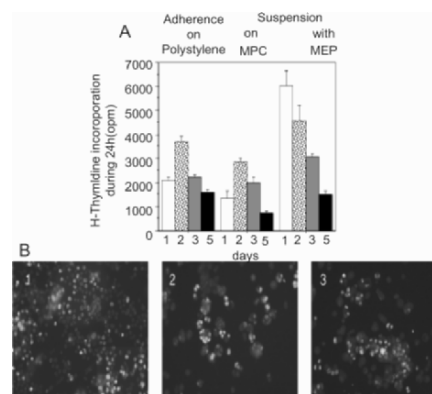
3.2.2 Respiratory activity

The quantitative respiratory activity of cells was measured using a REDOX indicator, alamarBlue™ during the 6 days. As shown Fig. 2, the 6M-4 cells were resistant to MEP in contrast to the sensitivity of the parental MDCK cells. An unexpected stimulation of oxidative activity was observed by the addition of MEP to the 6M-4.



3.2.3 ³H-thymidine and BrdU incorporation into 6M-4 cells

Cell proliferation was directly examined using precursors of DNA synthesis. Quantitative ³H-thymidine incorporation into the cells during the 6 days was measured. The adherent and suspension 6M-4 cells showed a similar incorporation pattern during the culture period. Stimulation by MEP was observed, as well as the result of the respiratory assay, as shown in Fig. 3. As shown in Fig. 4-B, BrdU was incorporated into the suspension 6M-4 cells as well as the adherent cells. Interestingly, synchronous BrdU incorporation was observed in adjacent cells in floating aggregates.



3.3 Influenza virus production in 6M4 cells

To confirm the capacity to produce influenza virus in the suspension 6M-4 culture, a clinical isolate of influenza virus, A/H3, was inoculated

to the adherent and suspension 6M-4 cells. As shown in Table 1, influenza A was amplified efficiently in both the adherent and suspension 6M-4 cells as well as in the parental MDCK cells. No negative influence due to MEP was observed.

	Adherent cell with 0.1% trypsin		Suspension cell with
	Parental MDCK	6M-4	50 μ g/ml MEP
TCID ₅₀ /0.1ml	2 ^{12.3}	2 ¹³	6M-4 2 ¹⁴

3.4 Grouping of 6M-4 cells depending on growth in soft agar

As described above, 6M-4 cells consist of a morphologically heterogeneous population, so, we attempted clonal selection using the dilution and soft agar culture methods. We found at least two populations in the 6M-4 cells, namely, one group capable of growing in soft agar and the other incapable of proliferating in soft agar but able to survive. Both populations maintained the characteristics of adherence to polystyrene and resistance to anoikis and MEP. The former populations formed larger aggregates in the suspension and the latter formed smaller aggregates, which seem favorable for practical use.

4. DISCUSSION

We attempted a new technique to obtain a suspension subline from the routine adherent MDCK cultures. At first, the adherent MDCK cells were trypsinized normally, and passaged under various concentrations of MEP (Fujisaki *et al.* 2000). We focused on the floating cells resistant to the long-term exposure of MEP. During the selection we found that the floating cells consisted of various subpopulations with different facilities for adherence on a polystyrene matrix in the absence of MEP. Then, we directed our target cells to those floating in the presence of MEP but adherent in the absence of MEP. Using the adherent conditions, dead cells could be easily removed during the passage. After several passages, we selected the subline 6M-4, which was used in this report.

In contrast to the parental MDCK, we found that 6M-4 cells remained anoikis-resistant and grew under anoikis-inducing conditions (poly 2-methacryloyloxyethyl phosphorylcholine (MPC)-treated flask). Furthermore, we observed that this resistant cell line remained anoikis-resistant after at least 10 passages by one-fourth dilution once per week

under adherent conditions. Therefore, we were able to maintain 6M-4 cells under both adherent and suspension conditions. This indicates that once the resistant phenotype was acquired, it remained stable.

To develop techniques for suspension culture of many mammalian cell lines, we obtained an idea that was made previously that involved the use of the bacterial neutral protease from *Bacillus polymyxa*, dispase (Nagata *et al.* 1986). They described the wide variation among cell lines in the mode of action of the enzyme on the detachment of cells from the matrix, the dispersion of cells into single cells or into clusters, the cytotoxicity, and the successful dispase suspension culture. They reported that epithelial cell lines of kidney origin, MDCK and RK13, were relatively resistant to dispase treatment, and Vero cells were even more difficult to detach. Different from dispase, the MEP used in this report was able to detach MDCK to single cells in the absence of serum. In the culture medium containing serum, MEP detached the adherent MDCK cells as a sheet, similar to the effect of dispase. Adherent 6M-4 detached more easily from the polystyrene matrix as a cell sheet than the parental MDCK cells by both proteases, suggesting that some changes had occurred between the two populations in their adhesion molecules, such as integrins.

The production system of the influenza virus for vaccines or diagnostic antigens is restricted to the use of MDCK cell cultures and embryonated hens' eggs. The stable suspension culture conditions as described here, without any solid or porous carriers, have many advantages for the large-scale culture of the influenza virus.

5. REFERENCES

- Fujisaki S, Fujisaki T, Yoshida J, Fujisaki Y, Mitani M, Nakamura M, Otake N. (2000) [Proposed mechanism of action of metallo- endopeptidase-F in the treatment of patients with chronic hepatitis B or C infection] [Article in Japanese] *Jpn. J. Antibiot.* 53, 135.
- Hierholzer JC and Killington RA (1995) Virus isolation and quantitation, In: Mahy BWJ and Kangro HO, eds. *Virology Methods Manual*. Academic Press Ltd, London, UK, 25.
- Nagata M, Matsumura T. (1986) Action of the bacterial neutral protease, dispase, on cultured cells and its application to fluid suspension culture with a review on biomedical application of this protease. *Jpn. J. Exp. Med.* 56, 297.
- Shevach EM. (1996) Labeling cells in microtiter plates for determination of 3H-thymidine uptake. In: Coligan JE, Kruisveek AM, Margulies DH, Shevach EM, Sterober W and Coico R, eds. *Current protocols in immunology*. John Wiley & Sons, Inc. Hoboken, NJ, USA. A.3D1.
- Tree JA, Richardson C, Fooks AR, Clegg JC, Looby D. (2001) Comparison of large-scale mammalian cell culture systems with egg culture for the production of influenza virus A vaccine strains. *Vaccine.* 19, 3444.

THE IMMUNE RESPONSES OF THE PRIME-BOOST REGIMEN WITH rBCG-E12 AND rDIs-E12 CANDIDATE VACCINE

P. Leangaramgul(1), S. Sapsutthipas(1), K. Balachandra(1), K. Matsuo(2), T. Hamano(2), M. Honda(2)

(1)Medical Biotechnology Center, Department of Medical Sciences, Ministry of Public Health, Tivanon Rd., Muang, Nonthaburi, 11000, Thailand. (2)AIDS Research Center, National Institute of Infectious Diseases, Shinjuku-ku, Tokyo 162-8640, Japan

Abstract: In the previous study, a research group in NIID, Japan demonstrated that the V3 sequence of 12 amino acids of HIV-1 CRF01_AE (E12 epitope) fused with mycobacterial α -antigen was secreted from BCG cells (rBCG-E12) and could induce NT-Ab against CRF01_AE primary isolates. However, the NT-Ab titer in guinea pig was not enough to obtain protective efficacy. So, we attempted to boost the NT-Ab by rDIs expressing E12 epitope- α -antigen fusion protein (rDIs-E12).

We have started the second generation AIDS vaccine research project and successfully constructed rDIs-E12 which expressed E12 epitope under control of vaccinia p7.5 promoter in infected chicken embryo fibroblast cell. The rBCG-E12 clone that could secrete E12 epitope under control of α -antigen promoter was provided us by NIID, Japan group. The expression of α -antigen-E12 fusion protein in the both rDIs-E12 and rBCG-E12 were checked by Western blot analysis using HIV⁺ human serum and the size of the fusion protein was approximately 32 kDa. To test immunogenicity, we primed Balb/c mice with rBCG-E12 and boosted with rDIs-E12 to analyze effect of prime-boost regimen for NT-Ab production. The ELISPOT was performed for the quantitation of antigen-specific CD8 T cells responses. We found that the E12 itself could not stimulate CTL response, it might not be CTL epitope in Balb/c mice. The rBCG and rDIs vectors could stimulate CTL activity, this means CTL activity was induced with alpha antigen and PPD. The CTL responses increase after second boosting with rDIs. The ELISA was also performed for check the antibody titer against E12 and alpha antigen. There are antibody titer against alpha antigen but no antibody titer against E12 peptide. From the experiment, we conclude that priming with rBCG-E12 and boosting with rDIs-E12 could stimulate CTL responses and have boosting effect but could not stimulate antibody titer. Further study will develop the regimen of immunization and using new epitope for candidate vaccine.

Key words: HIV, Vaccine, Immune response, CTL, BCG, Vaccinia.

1. INTRODUCTION

The development of an effective prophylactic vaccine for human immunodeficiency virus type 1 (HIV-1) is hindered by the lack of a known immunologic correlate of protection. However, until an efficacy trial is undertaken, those evaluating candidate vaccines must rely on criteria chosen from other clinical settings, such as the immune responses found in HIV-1 infected long-term nonprogressors and in HIV-1 exposed but uninfected, and primate vaccine studies. It is widely believed that two of more important responses for preventing or controlling HIV infection are a vigorous CD8⁺ cytotoxic T lymphocyte (CTL) response (CD8⁺ CTL) and the development of antibody that would neutralize primary transmitted viruses (1-4).

Genetic diversity in HIV-1 is well evidenced from the large number of different HIV-1 strain isolated around the world, which have been divided into three groups. The major group has been further divided into 10 nucleotide sequence defined subtypes (5, 6). In Thailand, two major subtypes of HIV-1 are prevalent: clade B^{*} (Thai subtype B) in intravenous drug abusers and clade E (Thai subtype A) in heterosexuals (7, 8).

Most of the candidate vaccines currently in production are based on B clade virus which, although prevalent in the developed countries, is not the clade which is found in most parts of the developing countries. HIV-1 clade B-derived vaccine could hardly prevent infection of clade E virus (9).

Recombinant live attenuated *Mycobacterium bovis* BCG (BCG) vector-based vaccine targeted to HIV-1 and simian immunodeficiency virus were reported to induce both humoral and cellular immune responses in animal models against a variety of antigens such as Gag, Env and Nef (10-14). The BCG immunization is known to generate primary Th1 and delayed-type hypersensitivity responses that are considered to be suitable for a vaccine development for HIV-1.

Recombinant viral vectors are believed to have similarity to live attenuated vaccines. The expression vector results in antigen processing through the major histocompatibility (MHC) class I pathway, which induces CD8⁺ CTL. Earlier studies have evaluated the safety and immunogenicity of recombinant vaccinia vector (15, 16).

The objectives of this study are to construct the new candidate HIV-1 subtype E vaccine, rBCG-E12 and rDIs-E12 and to develop a prime-boost strategy with the goal of eliciting broadly neutralizing antibodies against HIV-1 to provide sterilizing immunity for this virus.

2. MATERIALS AND METHODS

1 Design and construction of recombinant vaccinia virus (rDIs-E12) and recombinant BCG (rBCG-E12)

E12 epitope sequence was synthesized from the 12 amino acids (aa) E12 consensus sequence of HIV subtype E and inserted into the *Xho*I site of alpha-antigen in pUCvvp7.5-tPA in which a signal sequence of tissue plasminogen activator gene drives secretion of alpha antigen-E12 fusion protein. A fragment of p7.5-tPA-alpha K-E12 was inserted into the *Hind*III site of pUC/DIs as transfer vector.

Recombinant vaccinia virus (rDIs) was constructed by using this transfer vector and rDIsLacZ as the parental virus. The recombinant viruses were propagated in Chicken Embryo Fibroblast (CEF) cells.

Infection was performed onto CEF cells grown in 6-wells plate. Transfection was performed with 20 μ g of pUC/DIs/p7.5-tPA-alpha K-E12 using CLONFECTIN (Clontech). Recombinant DIs virus expressing E12 epitope was selected by two consecutive rounds as colorless plaques when stained with X-gal. The recombinant clones were grown in CEF cell cultures and checked the expression by Western blot analysis.

The recombinant BCG-E12 (rBCG-E12) that could secrete E12 epitope under control of α -antigen promoter was provided by NIID, Japan group. A fragment of α -K antigen-E12 was inserted into the shuttle vector, pSO246 which was stable in BCG and then transformed into BCG Tokyo strain by electroporation with kanamycin resistance selection. The rBCG-E12 clone was checked the expression by Western blot analysis (18).

II Evaluation of the vaccine candidate by animal model

An optimal immune induction would be obtained by a prime-boost regimen of vaccination. The mice groups are shown in Table 1. The balb/c mice were administered intradermal with rBCG-E12 or rBCG- α antigen. Eight weeks after inoculation, three mice of each group were sacrificed to assess humoral and cellular immune responses. The other mice were boosted with rDIs-E12 at 2 months after first inoculation. Two weeks after boosting three mice of each group were sacrificed for immune response checking and the remained mice were boosted with rDIs-E12 for further stimulate immune responses. Two weeks after final inoculation, all mice were sacrificed to assess immune responses.

The assessments of CTL responses were detected with gamma interferon by using the ELISPOT technique. The antibody responses were checked by ELISA for anti-V3 peptide (E12 peptide) and anti-alpha antigen.

3. RESULTS

I Design and construction of rDIs-E12 and rBCG-E12 candidate vaccine

A synthetic DNA fragment encoding the 12 amino acids (aa) V3 sequence of clade E consensus HIV (E12 epitope) was inserted into the *Xho*I site of alpha-antigen in pUCvvp7.5-tPA in which a signal sequence of tissue plasminogen activator gene drives secretion of alpha antigen-E12 fusion protein. A fragment of p7.5-tPA-alpha K-E12 about 2.3 kb was cloned into the *Hind*III site of pUC/DIs (4.7 kb) as transfer vector. The positive clone was selected by *Hind*III cut and obtained only one clone (#3) as shown in Figure 1.

These transfer vectors, pUC/DIs-E12 that harbored E-12 epitope gene in the cloning site of pUC/DIs, were used for the construction of recombinant DIs using rDIs-LacZ as the parental virus. We obtained recombinant vaccinia virus (rDIs-E12) that selected from colorless virus plaques stained with X-gal, purified two times by repetitive selection, and propagated in CEF cells.

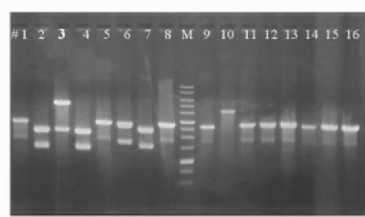


Figure 1. Agarose gel electrophoresis analysis of pUC/DIs-E12 16 clones, which were digested with *Hind*III. Clone #3 contained 2.3 kb α -K antigen E12 gene and 4.7 kb pUC/DIs plasmid. *M* was represented for 1 kb DNA ladder.

II Expression and characterization of rDIs-E12 and rBCG-E12

The expression of alpha antigen E12 epitope fusion protein from rDIs-E12 and rBCG-E12 were checked by Western blot analysis using HIV⁺ human serum as primary antibody. We found that the alpha-K E12 fusion protein could express in culture supernatant of rDIs-E12 and shown molecular weight of approximately 32 kDa as shown in Figure 2.

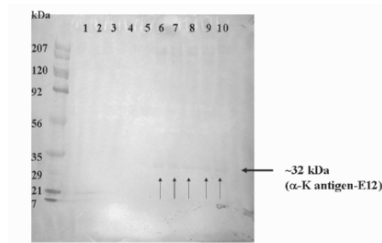


Figure 2. Western blot analysis of α -K antigen-E12 fusion protein from rDIs-E12 using HIV⁺ human serum as primary antibody. Lanes1-5; Cell lysate, Lanes6-10; Culture supernatant. Lanes1,6; rDIs-E12 #1-1, Lanes2,7; rDIs-E12 #1-2, Lanes3,8; rDIs-E12 #2-1, Lanes4,9; rDIs-E12 #4-1, Lanes5,10; rDIs-E12 #4-2. The positive bands of α -K antigen E12 were shown molecular weight approximately 32 kDa in culture supernatant.

III Evaluation of the vaccine candidate by animal model

ELISPOT

Since IFN- γ is a crucial component of antimycobacterial immunity, the induction of this cytokine in both the candidate vaccine and vector control of immunized mice was quantitatively assessed by the ELISPOT technique. The rBCG prime and rDIs-E12-boost group showed significant enhancement of ELISPOT activity against PPD (containing alpha antigen) as shown in Figure3. However, they did not show any significant activity against E12 peptide (Figure 4), indicating that V3 epitope of CRF01_AE did not act as a CTL epitope in Balb/c mice.

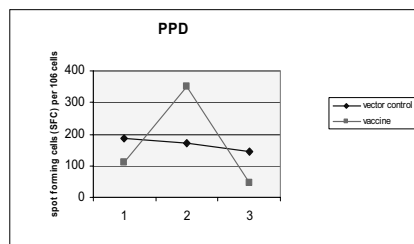


Figure 3. CTL activity against PPD: 1 = priming, 2 = first boosting, 3 = second boosting

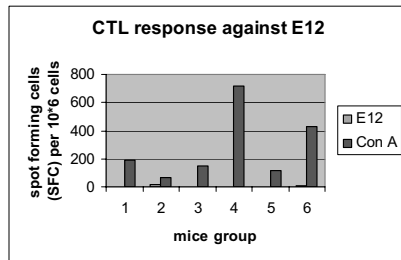


Figure 4. CTL activity against E12 compared with ConA (positive control); mice groups 1-6 are shown in Table 1

ELISA

Using an enzyme-linked immunosorbent assay (ELISA), the antigen specific E12 peptide, alpha-T antigen, and alpha-K antigen antibody titers were determined for sera from vaccinated animals as shown in Table 1. There were antibody titer against alpha-T antigen and alpha-K antigen in all groups of mice but no antibody titer against E12 peptide.

Table 1. Humoral response to E12 peptide, alpha-T antigen, and alpha-K antigen in vaccinated mice.

Categories	Mice Group	Injection	Antibody Titer		
			E12 peptide	alpha-T antigen	alpha-K antigen
Candidate Vaccine	1	rBCG-E12	500	2000	1000
	2	rBCG-E12 + rDIs-E12	500	2000	2000
	3	rBCG-E12 + rDIs-E12 + rDIs-E12	UC	4000	2000
rBCG control	4	rBCG-pSO246	UC	4000	2000
	5	rBCG-pSO246 + rDIs-LacZ	UC	4000	1000
	6	rBCG-pSO246 + rDIs-LacZ + rDIs-LacZ	UC	4000	500
rDIs control	7	rDIs-LacZ	UC	2000	1000
	8	rDIs-E12	UC	250	250
	9	rDIs-E12 + rDIs-E12	UC	2000	250

UC = Under Cut-off

4. DISCUSSION

In the present study, we have successfully constructed rDIs-E12 and rBCG-E12 candidate vaccines. To clarify the enhancement of HIV-1 specific immune response by the consecutive vaccine regimen using these two vaccine constructs, we have examined E12-specific ELISPOT (cellular immunity) and antibody production in mice.

From the ELISPOT experiments, the prime-boost regimen enhanced effector cell response for alpha antigen but could not enhance that for E12 peptide. Although the V3 epitope in HIV subtype B contains CTL epitope restricted by mouse class I H2d (17), to our knowledge, there is no report on such CTL epitope in HIV CRF01_AE,

and the lack of CTL induction should be ascribed to not matching class I-restriction in the HIV-1 subtype. However, the ELISPOT response against alpha antigen was significantly boosted by rDIs-E12, suggesting that the prime-boost regimen could have an effect for enhancing cellular immunity.

Regarding antibody response, rBCG-E12 immunization induced NT antibody production in guinea pigs (18) and in mice (data not shown). However, the rDIs-E12 boosting could not enhance anti-E12 peptide antibody titer. Taking account of enhancing anti-alpha antigen antibody titer by the same regimen, the antigenicity of E12 peptide inserted in rDIs-E12 was not enough for enhancing anti-E12 antibody, implying that the conformation of E12-alpha antigen fusion protein in rDIs-E12 may be different from that in rBCG-E12. To produce NT antibody for better HIV vaccine development, it should be tested to construct and evaluate such prime-boost regimen for the other Env construct of both rBCG and rDIs vector systems.

5. ACKNOWLEDGEMENT

This work was supported by Japan Foundation for AIDS Prevention (JFAP) and Small Grants Program from International Society for Infectious Diseases (ISID), USA.

6. REFERENCES

- 1) Haynes BF, Pantaleo G, Fauci AS. Toward an understanding of the correlates of protective immunity to HIV infection [see comment]. *Science* 1996; 271: 324-328.
- 2) Graham BS, Wright PF. Candidate AIDS vaccine. *N Eng J Med* 1995; 333: 1331-1339.
- 3) Hamano T, Sawanpanyalert P, Yanai H, Piyaworawong S, Sapsutthipas S, Phromjai J, Hara T, Yamazaki S, Warachit P, Honda M, and Matsuo K. Acquired gag gene expression in human immunodeficiency virus type 1 seronegative high-risk drug users. *The Lancet submitted* 2002.
- 4) Hamano T, Chotpitayasonondh T, Siriwasin W, Phromjai J, Sapsutthipas S, Warachit P, Honda M, and Matsuo K. Surface marker analyses of CD8⁺ T lymphocyte in human immunodeficiency virus type 1, subtype E (CRF01_AE) infected infants, mothers and cord bloods. *J Immunology submitted* 2002.
- 5) Simon F, Mauciere P, Roques P, Loussert-Ajaka I, Muller-Trutwin MC, Saragosti S, MC, Georges-Courbot, F. Barre-Sinoussi and F. Brun-Vezinet. Identification of a new human immunodeficiency virus type 1 distinct from group M and group O. *Nat Med* 1998; 4: 1032-1037.
- 6) Sabbarao S, and Schochetman G. Genetic variability of HIV-1 1996; *AIDS 10* (Suppl. A): S13-S23.
- 7) Ou C-Y, Takebe Y, Weniger BG, *et al.* Independent introduction of two major HIV-1 genotypes into distinct high-risk populations in Thailand. *Lancet* 1993; 341: 1171-1174.
- 8) Balachandra K, Matsuo K, Sutthent R, Hoisanka N, Boonthorn N, Sawanpanyalert P, Warachit P, Yamazaki S, and Honda M. Characteristic of HIV-1 V3 loop region based on seroreactivity and amino acid sequences in Thailand. *Asian Pacific Journal of Allergy and Immunology* 2002; 20: 93-98.
- 9) Girard M, Yue L, Barre-Sinoussi F, van der Ryst E, Meignier B, Muchmore E, *et al.* Failure of a human immunodeficiency virus type 1 (HIV-1) subtype B-derived vaccine to prevent infection of chimpanzees by an HIV-1 subtype E strain. *J Virol* 1996; 70: 8229-8233.

- 10) Aldovini A, Young R. Humoral and cell-mediated immune responses to live recombinant BCG-HIV vaccine. *Nature* 1991; 351: 479-482.
- 11) Kameoka M, Nishino Y, Matsuo K, *et al.* Cytotoxic T lymphocyte response in mice induced by a recombinant BCG vaccination which produces an extracellular α -antigen that fused with the human immunodeficiency virus type 1 envelope immunodominant domain in the V3 loop. *Vaccine* 1994; 12: 153-158.
- 12) Lagranderie M, Balazuc A-M, Gicquel B, Gheorghiu M. Oral immunization with recombinant *Mycobacterium bovis* BCG simian immunodeficiency virus nef induces local and systemic cytotoxic T-lymphocyte responses in mice. *J Virol* 1997; 71: 2303-2309.
- 13) Tover CK, de la Cruz VF, Fuerst TR, *et al.* New use of BCG for recombinant vaccine. *Nature* 1991; 351: 456-460.
- 14) Yosutomi, Koenig S, Woods RM, *et al.* A vaccine elicited, single viral epitope-specific cytotoxic T lymphocyte response does not protect against intravenous cell-free simian immunodeficiency virus challenge. *J Virol* 1995; 69: 2279-2284.
- 15) Grabam BS, Beishe RB, Clements ML, *et al.* Vaccination of vaccinia-naïve adults with human immunodeficiency virus type 1 gp160 recombinant vaccinia virus in a blinded, controlled, randomized clinical trial. *J Infect Dis* 1992; 166: 244-252.
- 16) Corey L, McElrath MJ, Meinhold K, *et al.* Cytotoxic T cell and neutralizing antibody responses to HIV-1 envelope with a combination vaccine regimen. *J Infect Dis* 1997; 176: 924-932.
- 17) Takahashi H, Cohen J, Hosmalin A, *et al.* An immunodominant epitope of the human immunodeficiency virus envelope glycoprotein gp160 recognized by class I major histocompatibility complex molecule-restricted murine cytotoxic T lymphocytes. *Proc Natl Acad Sci USA* 1988; 85: 3105-9.
- 18) Chujoh Y, Matsuo K, Yoshizaki H, *et al.* Cross-clade neutralizing antibody production against human immunodeficiency virus type 1 clade E and B' strains by recombinant *Mycobacterium bovis* BCG-based candidate vaccine. *Vaccine* 2001; 20: 797-804.

INCREASE IN THE INSULIN SECRETION OF HIT-T15 CELLS:

Gap Junctional Intercellular Communications Enhanced by Hyaluronic Acid

Yuping Li, Tsutomu Nagira and Toshie Tsuchiya

*Division of Medical Devices, National Institute of Health Science, Kamiyaga 1-18-1,
Setagaya-ku, Tokyo, Japan*

Abstract: Gap junctional intracellular communications (GJIC) were found in almost all types of vertebrate cells. The β -cells of the endocrine pancreas are connected by gap junctions, and the membrane specializations are thought to provide channels for direct cell-to-cell and cell-to-matrix communications. Previous studies suggested that GJIC may participate in the control of insulin secretion. It has been suggested that hyaluronic acid (HA) increases the function of GJIC—*via* the expression of Connexin43, a major protein component of gap junctions. However, the effects of HA on insulin secretion and gap-junctions between β -cells remains unclear. To determine whether insulin secretion is affected by gap-junctions after HA-treatment, we exposed HIT-T15, a clonal pancreatic β -cell line, in various concentrations of HA for 72 h, and detected their base- and glucose-stimulated insulin secretion, using an insulin assay kit by ELISA technique. The cellular functions of GJIC were assayed by dye transfer method using the dye solution of Lucifer Yellow. HA-treatment resulted in the enhancement of GJIC and the increase of insulin release. The results obtained in this study suggest that HA increases the insulin secretion of HIT-T15 cells by the enhancement of GJIC.

Key words: hyaluronic acid; gap junction; HIT-T15 cells; insulin secretion.

1. INTRODUCTION

Gap junctions are channels between cells for the passage of ions, small metabolites, and second messengers. The physical link is responsible for electrical and metabolic communications in several types of cells, including the insulin-producing pancreatic β -cells. The insulin secretion from pancreatic β -cells is a multicellular event arising as an emergent property due to β -cell intercellular communications. Among

the several mechanisms to control cell-to-cell communications between pancreatic β -cells, the one mediated by gap junctions is believed to be essential for the recruitment and synchronization of insulin-secreting cells. Previous studies showed that the proper insulin secretion from pancreatic islets depends on a communication network coordinating the activities of individual insulin-producing cells. The single β -cells unconnected with connexin channels show poor expression of the insulin gene and release low amounts of the hormone after stimulation, whereas both insulin biosynthesis and release are rapidly improved due to the restoration of β -cell contacts [1, 2]. It is known that HA-treatment enhances the function of GJIC in normal human dermal fibroblasts [3] and the expression of Connexin43 in rat calvarial osteoblast [4]. In this study, we used HIT-T15 cells, the clonal pancreatic β -cell line, to observe the relative effect of HA on insulin secretion and gap-junctions between β -cells. The results obtained indicate that HA increases insulin secretion of HIT-T15 cells by the enhancement of GJIC.

2. MATERIALS AND METHODS

2.1 Preparation of media and culture dishes

The high-molecular-weight (HMW) HA polysaccharide was dissolved in distilled water at a concentration of 4 mg/ml. Each 35-mm culture dish was coated at a final concentration of 0.01 to 2.0 mg/ml. The HA-coated dishes were dried further under sterile air flow at room temperature for 12 h before use. In order to investigate the effect of HA-addition on the functions of HIT-T15 cells, many media were prepared with various concentrations of HA.

2.2 Cell culture

The hamster pancreatic β -cell line, HIT-T15, were cultured in RPMI 1640 medium containing 10% fetal bovine serum (FBS), 2 mM L-glutamine, 25 mM HEPES, 100 IU/ml penicillin-G and 100 μ g/ml streptomycin. HIT-T15 cells in RPMI 1640 medium were maintained in a humidified 5% CO₂ incubator at 37°C. The subcultured cells were seeded at a density of 1.0~5.0 $\times 10^5$ cells/ml in multiwell plates or culture dishes. When they reached more than 80% confluence, the cells were used for various studies. Throughout the cell growth period the culture media were exchanged every 2-3 days.

2.3 Measurement of cell viability

HIT-T15 cells (1×10^5) were incubated into the various concentrations of HA-coated 24 wells plate, or after the cells were seeded onto 24 well plates and pre-incubated in a 10%FBS/RPMI 1640 medium overnight, the medium was exchanged for 10%FBS/HA/RPMI 1640 medium prepared. After 72 h of HA-treatment, the cell viability was determined by alamarBlue™ assay, according to the manufacturer instructions. Control cells received fresh medium without HA.

2.4 Measurement of insulin release

HIT-T15 cells were treated as described above. After washing with KRB buffer, the cells were incubated with KRB buffer for 60 min. The amount of insulin release in the spent medium was determined by ELISA insulin kit, according to the manufacturer instructions.

2.5 Scrape-loading and dye transfer (SLDT) assay

HIT-T15 cells (5×10^5) were treated as described above. The cells were washed three times with PBS (+) before the addition of the fluorescent dye. The cells were scraped using a surgical blade and loaded with 0.1% Lucifer Yellow solution for 5 min at 37°C. The dye solution was discarded, washed three times with PBS (+) solution to remove detached cells and background fluorescence. The distance of dye transfer was measured at room temperature under the fluorescence microscope equipped with a type UFX-DXII and Super High Pressure Mercury Lamp Power Supply (NIKON, Japan).

3. RESULTS AND DISCUSSION

In order to evaluate the effect of HA on cell viability, HIT-T15 cells were treated with HA-coated or -added for 72 h. At the same incubated time, the cell viability of HIT-T15 cells grown on high concentration HA-coated dishes (≥ 2.0 mg/dish) was significantly less than low concentration HA-coated and control (Fig. 1). However, there was no difference in cell viability between the HA-added and control (data not shown). Previous studies have shown that HMW (310 kDa and 800 kDa) HA-coating resulted in low adhesiveness to the cells. Because the HMW HA-coated surface provides a stable anionic surface that prevents cells attachment at the early time. In this study, after 12 h, the cells in low

concentration HA (1680 kDa)-coated dishes (0.01, 0.5, 1.0 mg/dish) already had attached and confluent but not in high concentration HA-coated dishes (2.0 mg/dish). These results indicated that the changes of cell viability by HA-treatment may depend on the cell attachment activity.

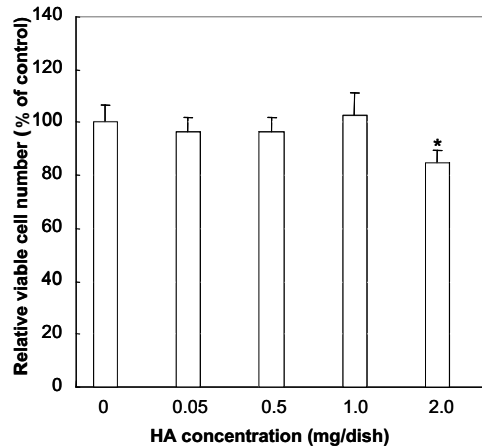


Figure 1. Viability of HIT-T15 cell after 72 h of HA-treatment. The viable cell numbers of HIT-T15 cell were determined by alamarBlue™ assay as described in Section 2. Each value denotes the mean \pm S.D. * $P \leq 0.05$ compared to untreated control.

HIT-T15 cells, retain glucose-stimulated insulin secretion, showed a increase in insulin secretion as a function of stimulation. Thus, their insulin output was 13.25 ± 0.96 and 19.63 ± 0.98 pg/ μ g protein in the base and glucose-stimulation (11.1 mM), respectively (n = 9 dishes from three independent experiments) (data not shown). When these cells were exposed to low concentration of HA-coating (0.25, 0.5, 1.0 mg/dish), their insulin secretion was significantly increased in the absence or presence of glucose-stimulation. By contrast, high concentration of HA-coating (2.0 mg/dish) failed to increase its insulin secretion (Fig. 2).

On the other hand, when HIT-T15 cells were treated with HA-addition for 72 h, the increasing effect was not exhibited. The insulin secretion was without difference between control and HA-addition (data not shown). Previous studies have indicated that HA-treatment enhances the function of GJIC in normal human dermal fibroblasts [3] and the expression of Connexin43 in rat calvarial osteoblast [4]. The increasing evidence suggests that gap junction proteins and/or GJIC participate in the multifactorial control of insulin secretion. Thus, the increase in insulin secretion by HA-coating might have relation to gap junctions.

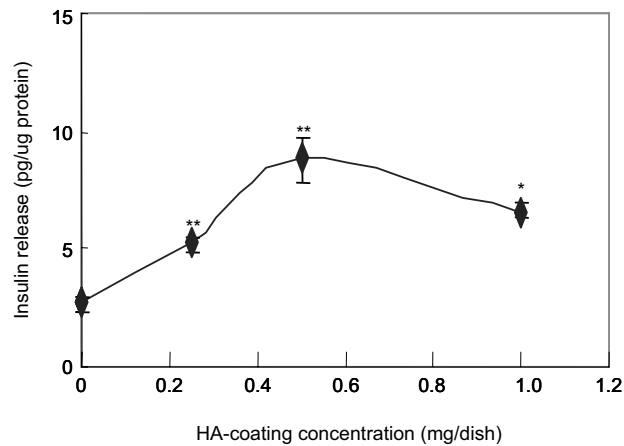


Figure 2. Concentration-dependent effects of HA-coating on insulin secretion from HIT-T15 cells. Treated with HA for 72 h, HIT-T15 cells were incubated with KRB buffer for 60 min. The released insulin in the spent medium was determined by ELISA insulin kit. Each value denotes the mean \pm S.D. of three separate experiments. * $P \leq 0.05$, ** $P \leq 0.01$ compared to control.

To test whether the HA-coating affects the gap junctions in pancreatic β -cells, we assessed the function of GJIC using Lucifer Yellow by SLDT assay. A scrape line was made on the cell grown to confluence, and the fluorescent dye penetrated the adjacent cells. The distance of dye transfer was determined.

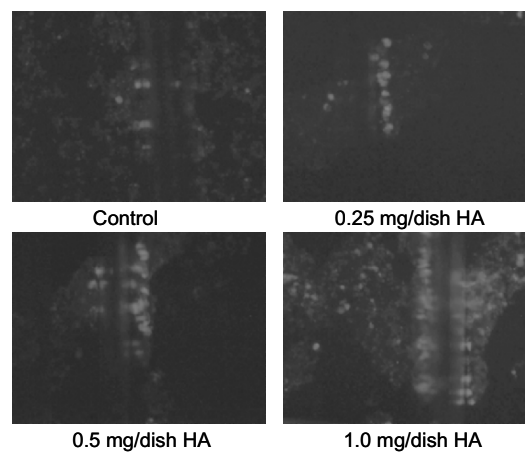


Figure 3. Time-course effects of various concentrations of HA-coating on the dye transfer ratio of HIT-T15 cells.

Fig. 3 shows the patterns of dye transfer in HIT-T15 cells treated with HA. The dye transfer extent of the cells grown on the HA-coated dishes

was more than that of the control, which indicated that GJIC function was activated by the HA-coating. The effect of HA is influenced by the concentration of FBS and the nutrients in medium, because the serum contains many components such as hormone, growth factor (FGF, etc.), cell adhesion molecule (N-CAM and cadherins), and transportation protein [4]. As a result, the HIT-T15 cells can use these nutrients and the nutrient-enriched substrata, e.g., natural extracellular matrixes with HA bound, to change the cell aggregations. Therefore, HA might play an important role in the increase of GJIC.

With the evidence above, it is known that the gap junction channels play a role in the regulation of β -cell secretion [5, 6]. It has been shown that the increase in connexin, e.g., gap junction proteins Cx43, affects the electrical coupling, synchronization of $[Ca^{2+}]_i$ oscillations, and insulin secretion, and the insulin secretion is evoked by a variety of metabolizable and nonmetabolizable secretagogues that activate different intracellular pathways [7-10]. In this study, we have found that the functional gap junction is promoted by low concentration HA-coating in spite of the inhibitory effects on the cell viability in high concentration HA-coating dishes. However, further intensive investigation should be promoted on the detailed action mechanism of HMW-HA responsible for the insulin-secreting activity.

4. CONCLUSIONS

The function of GJIC is considered to be a useful marker for evaluating tissue-engineered products. The data obtained in this study shows that gap junctions contribute to regulating some still-unknown mechanism to couple the stimulus-secretion of HIT-T15 cells under the condition of low concentration HA-coating. These results give useful information on how to design biomaterials of polysaccharides such as HA, when the GJIC is an important function for evaluating biocompatibility of biomaterials.

5. REFERENCES

1. Meda P., Bosco D., Chanson M., Giordano E., Vallar L., Wollheim C. and Orci L. (1990) Rapid and reversible secretion changes during uncoupling of rat insulin-producing cells. *J Clin Invest* 86:759-768

2. Vozzi C., Ullrich S., Charollais A., Philippe J., Qeci L. and Medz P. (1995) Adequate connexin-mediated coupling is required for proper insulin production. *J Cell Biol* 131: 1561-1572
3. Park JU. and Tsuchiya T. (2002) Increase in gap-junctional intercellular communications (GJIC) of normal human dermal fibroblasts (NHDF) on surfaces coated with high-molecular-weight hyaluronic acid (HMW HA). *Inc J Biomed Mater Res* 60: 541-547
4. Nagahata M., Tsuchiya T., Ishiguro T., Matsuda N., Nakatsuchi Y., Teramoto A., Hachimori A. and Abe K. (2004) Anovel function of N-cadherin and Connexin 43: marked enhancement of alkaline phosphatase activity in rat calvarial osteoblast exposed to sulfated hyaluronan. *Biochem Biphys Res Commun* 315: 603-611
5. Meda P. (1996) The role of gap junction membrane channels in secretion and hormonal action. *J Bioenery Biomembr* 28: 369-377
6. Charollais A., Gjinovci A., Huarte J., Bauquis J., Nadal A., Martin F., Andreu E., Sanchez-Andres JV., Calabrese A., Bosco D., Soria B.,m B., Herrera PL. and Meda P. (2000) Junctional communication of pancreatic beta cells contribetes to control of insulin secretion and glucose tolerance. *J Clin Invest* 106: 235-243
7. Cakabrese A., Zhang M., Serre-Beinier V., Caton D., Mas C., Satin SL. and Meda P. (2003) Connexin 36 controls synchronization of Ca^{2+} oscillations and insulin secretion in MIN6 cells. *Diabetes* 52: 417-424
8. Meda P., Chanson M. and Pepper M. (1991) *In vivo* modulation of connexin-43 gene expression an djunctional coupling of pancreaticc β -cells. *Exp Cell Res* 192: 469-480
9. Meda P., Pepper MS. and Traub O. (1993) Differential expression of gap junction connexins in endocrine and exocrine glands. *Endocrinology* 133: 2371-2378
10. Charollais A., Serre V., Mock C., Cogne F., Bosco D. and Meda P. (1999) Loss of α_1 connexin does not alter the prenatal differentiation of pancreatic β -cells and leads to the identification of another islet cell connexin. *Dev Genetics* 24: 13-26

CULTURE OF INSULINOMA CELLS ON PANCREAS SECTIONS

Yasuyuki Saito^{1,2}, Satoshi Terada¹, and Toshiaki Takezawa²

¹Department of Applied Chemistry and Biotechnology, University of Fukui, 3-9-1 Bunkyo, Fukui 910-8507, Japan; ²Laboratory of Animal Cell Biology, National Institute of Agrobiological Sciences, Ikenodai 2, Tsukuba, Ibaraki 305-0901, Japan

Abstract: Cell therapy using pancreatic islets is a promising lifelong treatment for type 1 diabetes mellitus. However, before cell therapy can be extensively used, there are some problems that need overcome. Of these, we focused on the need for improved cell function during *in vitro* culture. The sources of cells for cell therapy for diabetes are classified into two categories; primary cells isolated from a donor pancreas and established cell lines. The function of isolated primary cells decreases rapidly during *in vitro* culture and the function of established cell lines is too low for transplantation. To maintain and/or improve cell function during *in vitro* culture we designed TOSHI-substrata (substrata made of tissue / organ sections for histopathology), and investigated its effect on pancreatic cell lines derived from insulinomas. Before investigation, we estimated the influence of optimum cutting temperature (OCT) compound, which is used in preparation of the TOSHI-substrata, to confirm whether or not it significantly affects cell culture. We then cultured the cells on the TOSHI-substrata and found that they spontaneously aggregated; proliferation of the cells on the TOSHI-substrata was also slightly inferior to that on control glass slides, suggesting that culturing on pancreas sections might allow redifferentiation of the cell line or recovery of islet function.

1. INTRODUCTION

Cell therapy currently has several problems that need solved. For example, the function of cells isolated from a donor pancreas decreases rapidly during *in vitro* culture, while the function of established cell lines is extremely low. In addition, transplanted cells are exposed to several stresses, such as hypoxia, before secondary vascularization. Thus a large

cell mass is needed for cell therapy. We previously reported that over-expression of the anti-apoptosis genes *crmA* and *bcl-2* in an insulinoma cell line suppressed cell death induced by hypoxia and prolonged the culture period (1), and that sericin protein derived from silkworm cocoons improved the serum-free culture of rat islet cells (2).

Under *in vivo* conditions, pancreatic islets are surrounded by extracellular matrices (ECMs), and interactions between cells and the ECMs regulate cell activity. Therefore, to maintain and improve cell function during *in vitro* culture, culture methods using substrata such as collagen and laminin have been developed. TOSHI-substratum, which was prepared from thin tissue/organ sections, conserves not only ECMs, but also components of the original tissue *in vivo* and was previously reported to be useful for differentiation of several cell lines including PC-12 (3). Pancreas-derived TOSHI-substratum might therefore improve the function of β -cell lines including insulin production.

2. MATERIALS AND METHODS

2.1 Cell lines and culture conditions

The rat insulinoma cell line RIN-5F and hamster β -cell line HIT-T15 were cultured in RPMI 1640 medium (Nissui, Tokyo, Japan) supplemented with 10% (v/v) FBS, 10 mM HEPES, 0.2% NaHCO₃, 2 mM glutamine, and 0.06 mg/ml kanamycin. The culture was performed at 37°C in air containing 5% CO₂.

2.2 Preparation of Toshi-substrata made of adult bovine pancreas

A pancreas was excised from a cow, trimmed to an appropriate size, embedded in an optimum cutting temperature (OCT) compound (Miles Inc., Elkhart, IN, USA) then rapidly frozen. The frozen pancreas was cut into 5 or 10 μ m-thick sections using a cryomicrotome. Each section was spread on a glass slide (Matsunami Glass Ind., Osaka, Japan) and air-dried. For preparation of the TOSHI-substratum, each section-mounted glass slide was placed in a petri dish and immersed three times in PBS supplemented with 0.06 mg/ml kanamycin for 10 minutes to remove the OCT compound, and then in RPMI-1640 to optimize the section as a culture substratum.

2.3 Cell proliferation assay

Cell proliferation was assessed by neutral red (NR) assay. The culture medium was replaced with NR assay solution consisting of 40 µg/ml NR dye (Tokyo Kasei Kogyo Co., Ltd. Tokyo, Japan) in fresh medium, and incubated for 3 hours at 37°C. The NR assay solution was then discarded and the cells were immersed twice for 10 minutes in solution of 1% CaCl₂/0.5% formaldehyde. The NR dye was extracted into supernatant with solution consisting of 1% (v/v) acetic acid/50% (v/v) ethanol. After 10 minutes at room temperature, the absorbance of the extracted dye was recorded on a microplate reader at 540 nm.

2.4 Insulin assay

The insulin concentration in the culture supernatant was determined by ELISA using a rat insulin ELISA kit (Sibayagi, Gunma, Japan).

2.5 Histological Observation

The cells cultured on the TOSHI-substrata were fixed in 10% formalin neutral buffer solution and stained with hematoxylin and eosin (HE). These HE-stained specimens were observed by optical microscopy.

3. RESULTS AND DISCUSSION

3.1 Influence of the OCT compound on cell culture

The OCT compound is used in preparation of TOSHI-substrata, and although the TOSHI-substrata were rinsed with PBS several times, some OCT compound might remain. Therefore the influence of the OCT compound on cell culturing was examined. RIN-5F cells were seeded on a glass slide spread with OCT. Fig. 1 shows that the proliferation and insulin secretion of RIN-5F cells on this glass slide were similar to that on control glass slides. This result suggests that the OCT compound is not cytotoxic.

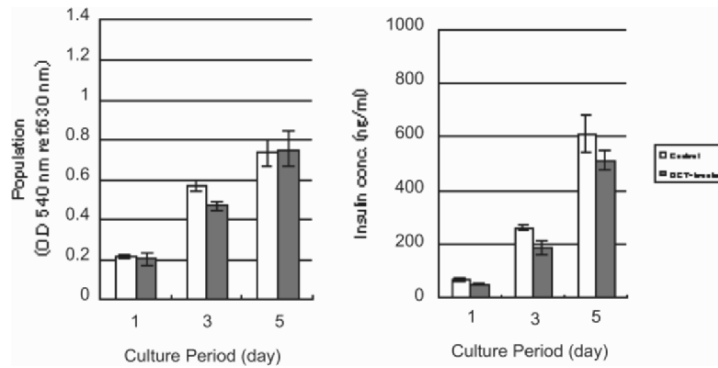


Figure 1. Proliferation (A) and insulin secretion (B) of the pancreatic cell line RIN-5F on a glass slide spread with OCT compound. RIN-5F cells were seeded at a density of 5.8×10^4 cells/cm² and cultured either on a glass slide spread with OCT compound (open) or on a control glass slide (closed). (A) Proliferation was determined by neutral red assay and (B) insulin concentration in the culture supernatant was measured by ELISA.

3.2 Cell culture on Toshi-Substrata made of adult bovine pancreas

3.2.1 Effect of Section Thickness on Cell Morphology

Pancreas-derived TOSHI-substrata cut into 5 or 10 μm -thick sections were prepared and the effect of section thickness on the culture was examined. HIT-T15 cells were seeded on the TOSHI-substrata and microscope observation revealed that they adhered and spontaneously aggregated on both sized sections (Fig. 2); no significant difference was observed. This suggests that the TOSHI-substrata can induce cells to aggregate regardless of section thickness.

3.2.2 Effect of TOSHI-substrata on Cell Proliferation

To define the effect of the TOSHI-substrata on cell proliferation, an NR assay was conducted; a culture on a glass slide was compared as a negative control. The absorbance of dye extracted from RIN-5F cells on the TOSHI-substrata at day 1 was similar to that on the control glass

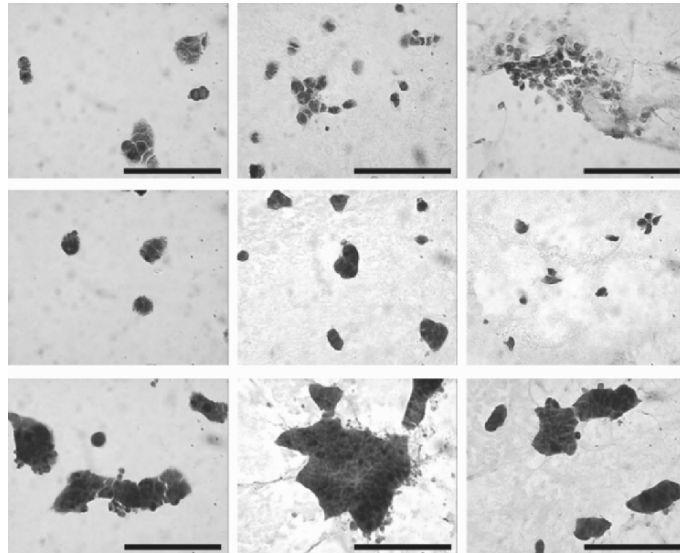


Figure 2. Morphology of HIT-T15 cells on pancreas-derived TOSHI substrata cut into 5 or 10-µm thick sections. HIT-T15 cells were seeded at a density of 7.6×10^4 cells/cm² and cultured either on a control glass slide (A,D,F), or TOSHI-substrata sectioned into 5- (B,E,H) or 10-µm sections (C,G,I). These samples were stained with HE and observed by optical microscopy. Samples show results after 1 day culture (A,B,C), 4 days culture (D,E,F) and 7 days culture (G,H,I). Scale bars indicate 100 µm.

slide, but that at day 3 was slightly lower than that of the control. These results suggest that the adhesion of RIN-5F cells to TOSHI-substrata occurred as well as it did on the control glass slide, but proliferation of the RIN-5F cells was slightly suppressed on the TOSHI-substrata.

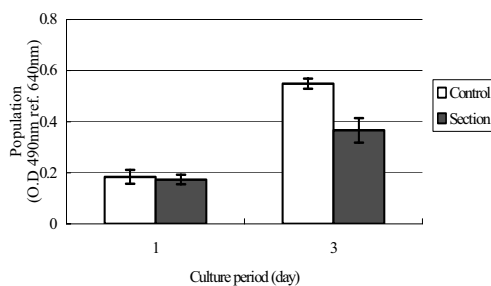


Figure 3. Proliferation of RIN-5F cells on the TOSHI-substratum. RIN-5F cells were seeded at a density of 6.9×10^4 cells/cm² and cultured either on a control glass slide (open) or TOSHI-substrata sectioned into 5-mm thick sections (closed). Proliferation was investigated by neutral red assay.

4. CONCLUSION

In this study, the effect of TOSHI-substrata made of pancreas on pancreatic cell lines in culture was investigated. Cells on the pancreas sections spontaneously aggregated like pancreas islets. Furthermore, the proliferation of cells on the pancreas sections was slightly inferior to that on the control glass slide. These results suggest that cultures on pancreas sections might allow redifferentiation of cells or stimulate pancreatic activity. An assay of pancreatic function should be conducted in the future.

5. ACKNOWLEDGMENTS

This work was partly supported by a Grant-in-Aid for Scientific Research from JSPS to S. Terada and by a MAFF/Pioneer grant to T. Takezawa.

6. REFERENCES

- (1) A. Ogawa, S. Terada, Y. Saito, T. Kimura, A. Yamaguchi and M. Miki (2004) *Crma* and *Bcl-2* protect a cell line derived from islet of Langerhans, RIN-5F from hypoxia-induced apoptosis. *Biochem. Eng. J.*, 20, 209.
- (2) A. Ogawa, S. Terada, T. Knanayama, M. Miki, M. Morioka, T. Kimura, A. Yamaguchi, M. Sasaki and H. Yamada (2004) Improvement of Islet Culture with Sericin. *J. Biosci. Bioeng.*, 98, 217.
- (3) T. Takezawa, T. Takenouchi, K. Imai, T. Takahashi and K. Hashizume (2002) Cell culture on thin tissue sections commonly prepared for histopathology. *FASEB J.*, 16, 1847.

DOWNREGULATION OF $\alpha_5\beta_1$ INTEGRIN EXPRESSION DURING NEURONAL DIFFERENTIATION IN NEURAL STEM CELLS

Dai Muramatsu, Naoko Yoshida, Sohei Hishiyama, Yusei Miyamoto, Tatsuhiro Hisatsune

Department of integrated biosciences, University of Tokyo, Bioscience building 402, 5-1-5 Kashiwanoha, Kashiwa, Chiba 277-8562, Japan

Abstract: During neuronal differentiation, dynamic morphological and physiological changes found in neural stem cells imply the involvement of cell adhesion molecules. Integrins, which are major family of cell adhesion molecule play a central role in migration, proliferation and differentiation in various cells through extrinsic and intrinsic cellular signals. In this study, we indicated that integrin $\alpha_5\beta_1$ are involved in neuronal differentiation in neural stem cells under the neurogenin1 expression.

1. INTRODUCTION

Neural stem cells have ability for self-renewal and give rise to neurons, astrocytes and oligodendrocytes through asymmetric division (Temple 1989; Davis and Temple, 1994). During brain development, neural stem cells generate all the cell types in temporally distinct phases, neurons first, followed by astrocytes and then oligodendrocytes (McKay 1997; Anderson 2001).

Dynamic morphological changes found in neural stem cells during neuronal differentiation imply the involvement of cell adhesion molecules during differentiation (Temple et al., 1989; Cattaneo et al., 1990; Davis and Temple 1994). Cell adhesion molecules integrins play critical roles in regulation to morphological and physiological properties in various cells. In developing central nervous system, our previous study demonstrated that the neural stem cells, which expressed integrin α_5 and β_1 subunit in low level, called $\alpha_5\beta_1^{\text{low}}$ cells, sufficiently differentiated into neurons (Yoshida et al., 2003). But it has not been

understood how the decrease of integrin $\alpha_5\beta_1$ expression was caused and how it influenced on neural stem cells during neuronal differentiation.

In this study, we examined integrin $\alpha_5\beta_1$ expression profile in neural stem cells with the gene transfer of neurogenin1 (Ngn1), which is a member of neural basic helix-loop-helix transcription factors (Ma *et al.*, 1996; Sun *et al.*, 2002). Ngn1 is expressed in neural stem cells during early developmental stage of telencephalon and induces neuronal differentiation (Lee *et al.*, 1997; Fode *et al.*, 2000; Parras *et al.*, 2002).

We show that the increase of integrin $\alpha_5\beta_1^{\text{low}}$ cells was sufficiently induced by Ngn1 expression and $\alpha_5\beta_1^{\text{low}}$ cells differentiated into neurons.

2. MATERIALS AND METHODS

2.1 Cell culture

In this study, we used MSP-1 cells, which are neural stem cell lines established from p53 knockout mice telencephalons (Yamada *et al.*, 1999). MSP-1 cells were plated on poly-ornithine/fibronectin-coated dishes in DMEM/ F12 supplemented with N2 supplement containing basic-FGF (10ng/ml) and maintained in this manner overnight. After retrovirus infection cells were cultured from 1 to 4 days. Mediums were replaced with new same mediums at Day 2.

2.2 Virus production

Retrovirus vector plasmid pMY-IRES-EGFP and pMY-IRES-EGFP, which contains rat Ngn1 coding region, were kindly provided by Dr. Nakashima (Kumamoto University). Retroviruses were produced from GP-293 packaging cell line (CLONTECH). Cells were transiently transfected at about 80% confluence with pVSV-G using the TransFast Transfection Reagent (Promega). Supernatants were collected 48hr after transfection, filtered through 0.45 μm mixed cellulose ester filter (ADVANTEC) and concentrated at 6000 \times g, 4°C for 18hr. Pellets were suspended in DMEM/F12 supplemented with N2 supplement and stored at -80°C.

2.3 FACS Analysis

Flow cytometric analyses were performed using a FACScan flow cytometer (Beckton Dickinson, San Jose, CA). Cells were resuspended

to a density of 5×10^4 cells/50 ml in Ca^{2+} - and Mg^{2+} -free HBSS containing 0.1% BSA and 0.1% sodium azide, and then mixed with a 1/25 dilution of biotin-conjugated monoclonal antibody (mAb) recognizing α_5 or β_1 integrin subunits (PharMingen, San Diego, CA) for 20 min on ice. Cell-mAb complexes were washed twice with Ca^{2+} - and Mg^{2+} -free HBSS containing 0.1% sodium azide and resuspended on ice in a 1/50 dilution of streptavidin-phycoerythrin (st-PE) (PharMingen) for 20 min. After washing once with Ca^{2+} - and Mg^{2+} -free HBSS containing 0.1% sodium azide, cells were resuspended in Ca^{2+} - and Mg^{2+} -free HBSS containing 0.1% BSA, 0.1% sodium azide and 0.5 mg/ml propidium iodide (PI) (Wako). For α_5 and β_1 subunit double-staining, cells were first incubated with α_5 antibody followed by a 1/200 dilution of anti-rat IgG-PE (Southern Biotechnology Associates, Birmingham, AL) before a subsequent incubation with biotin-conjugated β_1 antibody followed by 20 ml/test of streptavidin-allophycocyanin (st-APC; Beckton Dickinson). Dead cells were excluded by gating on the forward and side scatter plots and eliminating PI positive events.

2.4 Immunocytochemistry

Cultured cells were fixed with 4% paraformaldehyde (Wako) in PBS for 15 min at room temperature and incubated in a PBS blocking solution containing 3% normal goat serum (Life Technologies), 0.1% Triton X-100 (Wako) for 2 h at room temperature. Incubation was continued overnight at 4°C in blocking solution containing a 1/750 dilution of the mAb anti-MAP-2a2b (microtubule-associated protein-2) (neuron-specific marker) (Sigma). After washing with PBS 3 times, the cells were incubated in PBS containing a 1/400 dilution of anti-mouse IgG rhodamine (Chemicon, Temecula, CA) for 2 h at room temperature. Thereafter, cells were counterstained for 10 min in PBS containing 1 mg/ml DAPI (Sigma) and the cells were mounted in DABCO/immunoblot. Labeled cells were analyzed by confocal scanning laser microscopy (Leica, Mannheim, Germany).

3. RESULT

To examine the relation between integrin $\alpha_5\beta_1$ subunits and Ngn1, we performed FACS analysis on MSP-1 infected with either Ngn1 or control-EGFP retroviruses respectively. From Day 1 to Day 4, we examined the proportion of $\alpha_5\beta_1^{\text{low}}$ cells in the infected cells ($\alpha_5\beta_1^{\text{low}} < 10^2$

fluorescence intensity). The results were shown in Fig.1. The proportion of $\alpha_5\beta_1^{\text{low}}$ cells infected with Ngn1 significantly increased from Day 2 to Day 3. Interestingly, FACS analysis showed that $\alpha_5\beta_1^{\text{low}}$ cells infected with Ngn1 slightly decreased at Day 4 compared with Day 3. This decrease in integrin $\alpha_5\beta_1^{\text{low}}$ cells is considered to be in agreement with integrin $\alpha_5\beta_1$ subunit expression pattern in neuronal differentiation (Bi et al., 2001). On the other hand in control-EGFP infected cells, there was no increase in number of $\alpha_5\beta_1^{\text{low}}$ cells. Thus, these data suggest that Ngn1 downregulates integrin $\alpha_5\beta_1$ expression in neural stem cells.

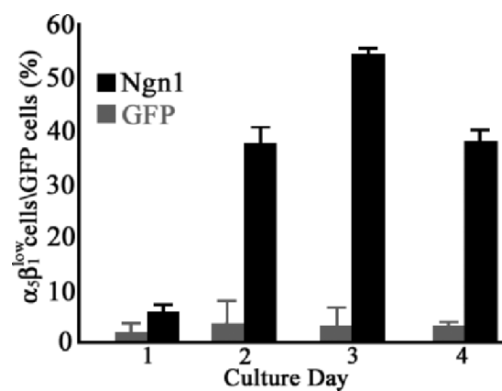


Figure 1. FACS profiles of integrin $\alpha_5\beta_1^{\text{low}}$ cells in MSP-1 cells infected with Ngn1 and Control-EGFP. The increase in the proportion of integrin $\alpha_5\beta_1^{\text{low}}$ cells to the total population of Ngn1-infected neural stem cells during neuronal differentiation. The percentage values were obtained from FACS analysis by gating Ngn1, GFP-infected cells.

We next performed Immunocytochemistry to examine MAP2-2a2b expression in the MSP-1 cells infected with Ngn1- and control-EGFP respectively (Fig. 2). At Day 4, Ngn1 infected cells adopted a neuronal morphology and expression of MAP-2a2b were detected (Fig. 2A). In contrast, control-EGFP infected cells maintained undifferentiated morphologies and MAP-2a2b were not detected (Fig. 2B).

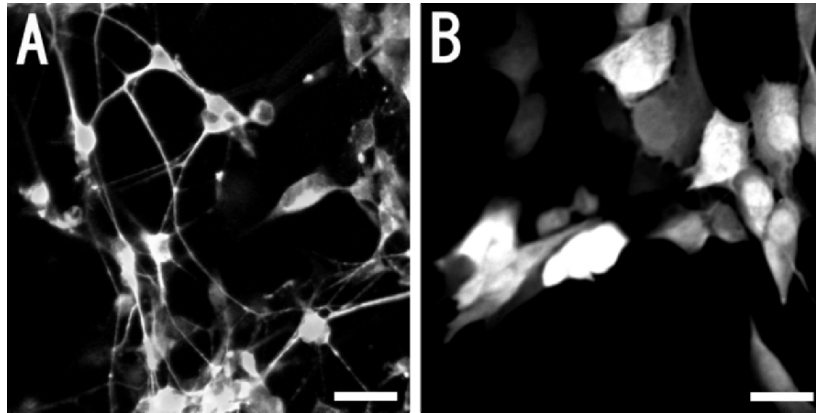


Figure 2. MSP-1 cells infected with Ngn1-IRES-EGFP differentiated into neurons. Cultures infected with the retroviruses encoding Ngn1-IRES-EGFP(A) or control-EGFP(B) were grown for 4 days in 10 ng/ml bFGF, fixed and double-stained with the antibodies to MAP-2a2b and DAPI. Scale bars = 20 μ m.

4. CONCLUSION

In this study, we demonstrated that Ngn1 downregulates integrin $\alpha_5\beta_1$ expression. Low level of integrin $\alpha_5\beta_1$ expression possibly leads neural stem cells to exit cell cycle and then induces neuronal differentiation. In contrast, high level of integrin $\alpha_5\beta_1$ expression activates cell cycle and promotes neural stem cells to proliferate for self-renewal (Fig. 3).

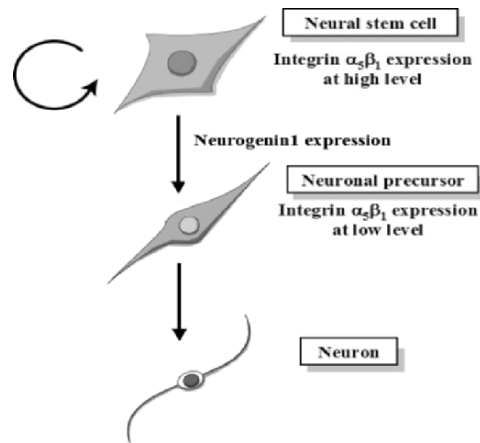


Figure 3. Working model: integrin expression and neuronal differentiation. In neural stem cells, the decrease in expression of integrin $\alpha_5\beta_1$ induces neuronal differentiation. High level of integrin $\alpha_5\beta_1$ expression probably maintains neural stem cells properties.

5. REFERENCES

- Anderson, D. J. (2001). Stem cells and pattern formation in the nervous system: The possible versus the actual. *Neuron* 30, 19-35.
- Bi, X., Lynch, G., Zhou, J., and Gall, C. M. (2001). Polarized distribution of $\alpha 5$ integrin in dendrites of hippocampal and cortical neurons. *J. Comp. Neurol.* 435, 184-193.
- Cattaneo, E., and McKay, R. (1990). Proliferation and differentiation of neuronal stem cells regulated by nerve growth factor. *Nature* 347, 762-765.
- Davis, A. A., and Temple, S. (1994). A self-renewing multipotential stem cell in embryonic rat cerebral cortex. *Nature* 372, 263-266.
- Fode, C., Ma, Q., Casarosa, S., LeMeur, M., Dierich, A., Ang, S. L., Anderson, D. J., Guillemot, F. (2000). A role for neural determination genes in specifying the dorsoventral identity of telencephalic neurons. *Genes Dev* 14, 67-80.
- Lee, J. E., Price, J., Thurlow, L. (1997). Basic helix-loop-helix genes in neural development. *Curr. Opin. Neurobiol* 7, 13-20.
- Ma, Q., Kintner, C. and Anderson, D. J. (1996). Identification of neurogenin, a vertebrate neuronal determination gene. *Cell* 87, 43-52.
- McKay, R. (1997). Stem cells in the central nervous system. *Science* 276, 66-71.
- Parras, C. M., Schuurmans, C., Scardigli, R., Kim, J., Anderson, D. J., Guillemot, F. (2002). Divergent functions of the proneural genes Mash1 and Ngn2 in the specification of neuronal subtype identity *Genes Dev* 16, 324-338.
- Sun, Y., Nadal-Vicens, M., Misono, S., Lin, M. Z., Zubiaga, A., Hua, X., Fan, G., Greenberg, M.E. (2001). Neurogenin promotes neurogenesis and inhibits glial differentiation by independent mechanisms. *Cell* 104, 365-376.

- Temple, S. (1989). Division and differentiation of isolated CNS blast cells in microculture. *Nature* 340, 471-473.
- Yamada, K., Hisatsune, T., Uchino, S., Nakamura, T., Kudo, Y., Kaminogawa, S., 1999. NMDA receptor mediated Ca^{2+} responses in neurons differentiated from p53^{-/-} immortalized murine neural stem cells. *Neurosci. Lett.*, 264, 165-167.
- Yoshida, N., Hishiyama, S., Yamaguchi, M., Hashiguchi, M., Miyamoto, Y., Kaminogawa, S., Hisatsune, T., 2003. Decrease of in expression of alpha 5 beta 1 integrin during neuronal differentiation of cortical progenitor cells. *Exp. Cell. Res.*, 287, 262-271.

STRATEGIES FOR DEVELOPMENT OF CULTURE MEDIA: APPLICATION TO EMBRYONIC AND ADULT STEM CELLS

Shayne Boucher¹, Paul Price¹, Ian Lyons¹, John Daley¹ and David Jayme²

¹*Invitrogen Corporation, 3175 Staley Road, Grand Island, New York 14072, USA;*

²*Department of Biochemistry, Brigham Young University – Hawaii, 55-220 Kulamui Street, Laie, Hawaii 96762, USA*

Abstract: Both exploratory research and proposed clinical applications of human stem cells and derived cell populations demand refinements in the nutrient environment. Significant early research has been performed with serum supplementation, using FBS lots that were carefully selected for performance characteristics based on expansion and maintenance of the undifferentiated phenotype. However, the ill-defined composition and lot-to-lot variability in proliferation and differentiation factors inherent to serum and potential foreign protein immunogenicity and adventitious agent contamination make serum unattractive for these applications.

This laboratory continues to refine its approach to develop serum-free specialty nutrient formulations for targeted expansion and differentiation of adult and embryonic stem cell populations. Modifications of AIM-V Medium, originally developed for lymphokine activated killer (LAK) cell adoptive immunotherapy, may be modified for studies in T cell-mediated therapy and dendritic cell applications. KnockOut[®] formulation modifications and serum replacements have reduced variability in embryonic stem cell expansion and differentiation studies, facilitated isolation of novel stem cell lines and permitted feeder-free cultivation under some limited conditions. Neurobasal[®] media and specialized supplements (e.g., B27 modifications) have enhanced neurosphere formation, increased the number of neurospheres, and supported the ability to generate differentiated CNS cell types. Where total serum replacement has been technically challenging to date, such as the three-dimensional cultivation of neurospheres or mesenchymal stem cell populations, several modifications of Advanced Media have permitted substantial reduction in serum requirement to yield differentiated tissue phenotypes.

Significant hurdles remain for optimization of cultivation options for clinically relevant expansion and targeted differentiation of stem cells, and for effective selection and lineage identity verification. However, reduction or elimination of serum from the culture environment represents a significant interim step toward that objective.

Key words: stem cell, differentiation, serum-free culture, expansion, nutrient optimization.

1. INTRODUCTION

Stem cells and other progenitor populations have been manipulated historically in cell culture using pre-screened serum lots. However, the biochemical variability of this undefined serum additive creates undesirable impacts on cellular maintenance, proliferation and differentiation. Additionally, the ultimate therapeutic endpoint of such regulated culture manipulations would prefer superior biochemical definition and biosafety of a serum-free culture environment, particularly using constituents of non-animal origin.

We have selected four specific culture applications of progenitor populations and provided initial exploratory data targeted to reduce or eliminate the requirement for serum supplementation, with the eventual goal of establishing a chemically-defined, serum-free system that will be technically robust and regulatory friendly. The four test systems include expansion and targeted differentiation of: embryonic stem cells; neural stem cells; mesenchymal stem cells; and hematopoietic stem cells (specifically dendritic cell precursors).

Each test system was expanded in serum-free or reduced serum culture, with undifferentiated state confirmed by appropriate biomarkers. Cytokine cocktails were added to expanded populations to induce differentiation along targeted lineages.

2. MATERIALS AND METHODS

2.1 Embryonic stem cell cultivation

Mitomycin C-treated primary embryonic fibroblast feeder cells were plated at a density of $\sim 5 \times 10^4$ cells/cm² in KnockOut D-MEM or D-MEM containing glutamine, antibiotics, and 10% (heat-inactivated) ES

Cell Qualified FBS [1-2]. Feeder cells were incubated at 37°C, 5% CO₂ for 24-72 hours to enable cell attachment. D3 murine ES cells were dissociated using 0.25% Trypsin/1 mM EDTA and centrifuged for five minutes at 200 x g. Cells were resuspended in KnockOut D-MEM or D-MEM with same supplements plus Non-Essential Amino Acids Solution, 2-mercaptoethanol and 15% KnockOut SR or ES Cell Qualified FBS, and seeded at ~20 cells/ cm². The plates were incubated for seven days and colonies were fixed and stained for alkaline phosphatase activity (a marker of undifferentiated ES cells). Each ES cell colony was assessed visually for differentiation based on colony size, shape, border definition, and intensity of alkaline phosphatase staining.

2.2 Neural stem cell cultivation

Neural stem cells (NSCs) were generated from E18 cortical tissue, processed and grown as neurospheres in non-agitated ultra low attachment (ULA) 6-well culture dish (Corning) in a 5% CO₂, 37°C incubator [3-4]. The control medium was DMEM/F12, 1x N2, 10 ng/ml EGF and 20 ng/ml basic FGF (Invitrogen). The test medium was Neural sySTEM EX, a medium prototype, with 2 mM L-glutamine, 1x B27™ without retinol acetate (RA), 10 ng/ml EGF and 20 ng/ml basic FGF. Viable cells were counted by trypan blue exclusion using a hemacytometer. Cells were seeded at a density of 1-2x10⁵ cells/ml for all proliferation experiments.

2.3 Mesenchymal stem cell cultivation

Human bone marrow (Cambrex) was mixed 1:2 within 24 hours of collection with Hank's balanced salt solution without Ca²⁺ or Mg²⁺ [5-6]. Mononuclear cells were isolated by passage over Histopaque density gradient (1.077) and centrifuging. Washed mononuclear cells were labeled with anti-CD34⁺ antibody (Miltenyi Biotec) and passed over a midi-Max magnetic bead column (Miltenyi Biotec). CD34⁺ cells were collected, washed 1x with DPBS and centrifuged. Pelleted cells were resuspended in Advanced DMEM with 10% FBS, seeded into a T-75 flask, and incubated at 37°C, 5%CO₂ for 24 hours. Non-attached cells were removed and the flask washed 1x with DPBS. Fresh Advanced DMEM (10% FBS) was added and the flask incubated until the cells reached 80-90% confluency with re-feeding every 5-6 days. Passaged MSC were plated into six well plates at a concentration of 4 x 10³ cells per mL. Cells were grown for 6 days at 37°C, 5% CO₂. Cells were harvested by trypsinization and counted electronically (Coulter).

2.4 Hematopoietic stem cell cultivation

Cord blood CD34⁺ enriched cells were cultured for 7 days in AIM-V, StemPRO-34 and three competitive media supplemented with recombinant human cytokines [7-8]. The cytokine combination consisted of stem cell factor (SCF), Flt-3 ligand, interleukin-3 (IL-3), IL-6 and granulocyte colony stimulating factor (G-CSF). On day 7, the cultured cells were harvested, washed and equal number of cells was then cultured in each of the media for 7 days in granulocyte-macrophage colony stimulating factor (GM-CSF) and IL-4. Cells were then cultured for an additional 4 days in GM-CSF, IL-4 and tumor necrosis factor-alpha. Phenotypic analysis by flow cytometry used fluorochrome-conjugated monoclonal antibodies (CD14, HLA-DR, CD11c, and CD80).

3. RESULTS

3.1 Embryonic stem cell applications

Murine ES cells were cultivated for 7 days in either standard DMEM or a modified formulation, KnockOut DMEM. Cultures were supplemented (15%) with either ES Cell-Qualified FBS or a serum replacement, KnockOut SR. Undifferentiated ES cell growth was scored based upon visual criteria and alkaline phosphatase staining. Substitution of KnockOut DMEM for standard DMEM maintained the undifferentiated state more effectively in both FBS and KnockOut SR-supplemented cultures. KnockOut SR produced a 2-fold improvement in % undifferentiated cultures in each test medium, compared with FBS-supplemented control cultures.

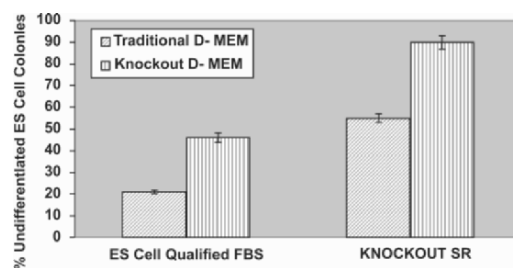


Figure 1. Comparison test of traditional D-MEM and KnockOut D-MEM for culturing ESC colonies under serum and serum replacement conditions. Test shows that combination of KnockOut D-MEM and Knockout SR maintains ESC colonies in an undifferentiated state.

3.2 Neural stem cell applications

Single cell suspensions from E18 rat embryonic cortices were plated at two densities ($1 \times 10^5/\text{ml}$ and $2 \times 10^5/\text{ml}$) in two serum-free formulations, N2-supplemented DMEM/F12 or Neural sySTEM EX, and expanded for one week. Expanded populations were confirmed to be predominantly neural SC as demonstrated by nestin immunostaining of neurospheres, and dual staining for neural marker, β -tubulin III, and nuclear stain, DAPI (data not shown). Figure 2 illustrates that neural SC expansion was significantly accelerated in Neural sySTEM EX medium.

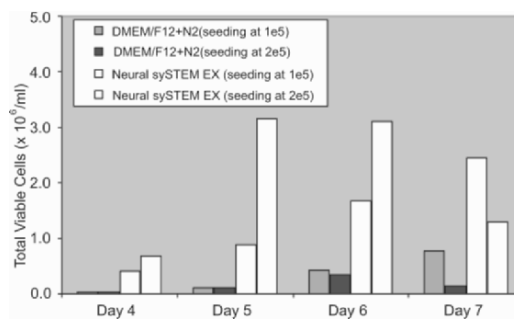


Figure 2. Single cell suspensions from E18 rat embryonic cortices were plated at $1 \times 10^5/\text{ml}$ and $2 \times 10^5/\text{ml}$ in two serum-free media. Growth of undifferentiated neural stem cells was monitored daily (4 to 7 days).

3.3 Mesenchymal stem cell applications

Cultivation of mesenchymal SC under totally serum-free conditions with sustained attachment and undifferentiated phenotype has been problematic. A growth factor enriched version of DMEM (Advanced DMEM) permitted serial cultivation of undifferentiated mesenchymal SC with substantial reduction of supplemental FBS (data to 1% FBS are illustrated in figure 3).

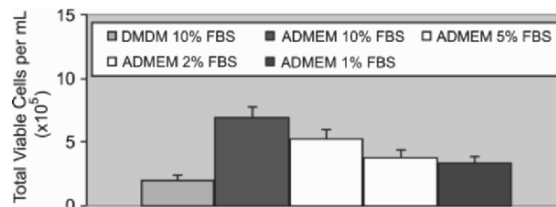


Figure 3. Expansion of MSC in standard DMEM + 10% FBS or Advanced D-MEM supplemented with reduced (1, 2, 5 or 10%) FBS.

3.4 Hematopoietic stem cell applications

Serum-free media have been utilized for nearly two decades for *ex vivo* expansion of lymphokine-activated killer (LAK) cells and other mobilized lymphocytic populations. We evaluated breadth of utility of AIM V Medium for expanding hematopoietic progenitor populations that might ultimately be utilized for expansion of human T cells or dendritic cells in comparison with other commercially-available serum-free formulations.

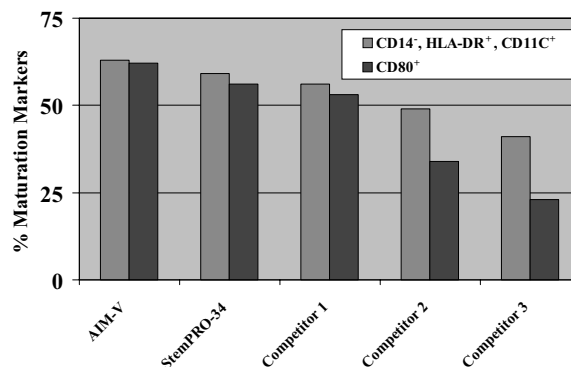


Figure 4. Comparison test of AIM-V and other media types in maturation of CD34⁺ cord blood cells into dendritic cells after eleven days of cultivation with cytokine cocktail rhGM-CSF, IL-4, and TNF α . Tests indicate that AIM-V is a robust formulation for generating dendritic cells from CD34⁺ cord blood cells.

4. DISCUSSION

Stem cell populations may be expanded *ex vivo* in serum-free or serum-reduced nutrient formulations with minimal differentiation. Stem cell culture applications are at various stages of maturity. For embryonic stem (ES) cells, the goal is to define optimal osmolality, feeder requirements, and media formulation for culturing primate ES cells to identify and elucidate signaling pathways for pluripotency and differentiation. For neural stem cells, the goal is to standardize culture strategies to translate research findings into cell therapy applications. Closer to clinical trials, mesenchymal stem cells require serum-free systems to promote expansion and differentiation into desired cell types. For hematopoietic stem cells used in cell-based cancer therapy, the drive is to eliminate animal origin components from the expansion and

maturation medium and to explore more efficient methods of signal pathway induction.

Optimized formulations have been developed that may be preferentially used for specific stem cell culture applications:

- KnockOut formulations reduced variability of murine & human embryonic stem cell expansion and differentiation.
- Iterative improvement of nutrient media enhanced generation of neural stem cell populations.
- Advanced Media reduced serum requirements for plating and maintaining mesenchymal stem cells.
- Modified or supplemented AIM-V increased its utility for T-cell or dendritic cell-based immunotherapy applications.

Additional effort is required to eliminate medium constituents of animal origin and to design a reproducible, biochemically-defined nutrient environment to address technical and regulatory requirements for proposed stem cell-based therapies.

5. ACKNOWLEDGEMENTS

We thank Mary Lynn Tilkins for technical input and assistance in preparing this paper. Invitrogen provided funding for this study.

6. REFERENCES

1. Amit, M. et al. Feeder and serum free culture of human embryonic stem cells. *Biol Reprod.* 70: 837-845 (2004).
2. Robertson, E.J. ed. *Teratocarcinomas and Embryonic Stem Cells: A Practical Approach*, Oxford: IRL Press (1987).
3. Price, P. & Brewer, G. "Serum-Free Media for Neural Cell Cultures: Adult and Embryonic." *Protocols for Neural Cell Culture, 3rd Ed.*, 255-264 (2002).
4. Gritti, A. et al. "Cultures of Stem Cells of the Central Nervous System." *Protocols for Neural Cell Culture, 3rd Ed.*, pp. 173-197 (2002).
5. Friedenstein, A.J. et al. Stromal cell responsible for transferring the microenvironment of the hematopoietic tissues: cloning *in vitro* and retransplantation *in vivo*. *Transplantation* 17: 331-340 (1974).
6. Bruder, S.P. et al. Growth kinetics, self-renewal, and the osteogenic potential of purified human mesenchymal stem cells during extensive subcultivation and following cryopreservation. *J. Cell. Biochem.* 64: 278-294 (1997).
7. Syme, R. & Gluck, S. Effects of cytokines on the culture and differentiation of dendritic cells *in vitro*. *J. Hematotherapy & Stem Cell Res.* 10: 43-51 (2001).
8. Kontani, K et al. Dendritic cell vaccine immunotherapy of cancer targeting MUC1 mucin. *Int. J. Mol. Med.* 12: 493-502 (2003).

PREPARATION OF HIGH-TITER RETROVIRAL VECTORS USING TRANSIENT EXPRESSION SYSTEM

Akitsu Hotta, Yoshikazu Saito, Ken-ichi Nishijima, Masamichi Kamihira, Shinji Iijima

*Department of Biotechnology, Graduate School of Engineering, Nagoya University,
Furo-cho, Chikusa-ku, Nagoya 464-8603, Japan*

Abstract: Retroviral vectors are widely used as a tool for introduction of a foreign gene into host genome. High viral titer preparation is required for generation of transgenic animals. In this regard, we introduced Q vector, a transient production system of retroviral vectors, to achieve high titers. In this system, an LTR promoter was replaced by CMV promoter to increase the transcription level of virus genomic RNA, and SV40 replication origin allows episomal replication of plasmids in cells expressing SV40 large T antigen. We used this Q vector as a backbone and introduced a murine stem cell virus (MSCV) *cis* elements and vesicular stomatitis virus G glycoprotein (VSV-G) as an envelope. After optimization of the transfection conditions and cell culture medium, viral titer was increased up to 10^6 IU (infectious unit)/ml. This titer level was comparable to that produced by packaging cell lines.

Key words: retroviral vector; murine stem cell virus (MSCV); Q vector; CMV promoter; SV40 replication origin; vesicular stomatitis virus G protein (VSV-G); gene therapy.

1. INTRODUCTION

Retroviral vectors are a powerful tool to introduce a foreign gene into host genome (Miller, 2002) and thus are widely used for gene therapy (Weber et al., 2001), gene transduction for cells and establishment of transgenic animals (Kamihira et al., 2004). For these purposes, high titer viral preparation, more than 10^8 IU/ml is required (Chan et al., 2001; Lin et al., 1994). In general, the most common ways to prepare high-titer viral solution is the establishment of packaging cell lines (VandenDriessche et al., 2003). Although packaging cells are a powerful tool to prepare retroviral vectors with high titer, the establishment of

such cell lines from many clones is a time-consuming process. In this study, we used Q vector (Julius et al., 2000) as a backbone, and introduced the mouse stem cell virus (MSCV)-derived *cis* elements to avoid the gene silencing specific to undifferentiated stage (Cherry et al., 2000). The MSCV belongs to murine leukemia viruses. Furthermore, we used vesicular stomatitis virus G glycoprotein (VSV-G) to produce a pseudotyped vectors. The VSV-G pseudotyped virus can infect broad range of species and can be concentrated up to 1000-fold by ultracentrifugation (Burns et al., 1993).

To produce the VSV-G pseudotyped retroviral vector in the MSCV system, GP293 cells that express Gag-pol protein were transfected with the vector plasmid and pVSV-G. Viral genomic RNA was expressed from MSCV LTR promoter and VSV-G was expressed from the CMV promoter. In the Q vector system, 293FT cells were transfected with vector plasmid, pcDNA4/gag-pol and pLP/VSV-G (Table 1). To increase the transcription level of viral RNA, 5' LTR promoter was substituted with CMV promoter. Furthermore, SV40 replication origin was introduced into all three plasmids and allows episomal replication in the 293FT cells which express SV40 large T antigen. This report proposes a quick and high-titer production of VSV-G pseudotyped MSCV based Q-vector.

Table 1. Virus producer methods that used in this paper.

	GP293 cells	293FT cells	Packaging cells
Genome RNA	pMGRN	pQMGRN	(Genomic)
Gag-pol	(Genomic)	pcDNA4/gag-pol	(Genomic)
Envelope	pVSV-G	pLP/VSV-G	pVSV-G

2. MATERIALS & METHODS

Viral producer cells, GP293 (Clontech), 293FT (Invitrogen) and GP293-G4 (Mizuarai et al., 2001) cell lines were maintained in high glucose DMEM media (Sigma) supplemented with 10% FBS (BioWest), 0.1 mM MEM non-essential amino acids (Invitrogen), 2mM L-glutamine (Sigma) and penicillin-streptomycin (Wako) on collagen-coated dishes (Iwaki). Virus producer cells were transfected with GFP or β -galactosidase (*lacZ*) coding virus vector plasmid and appropriate expression plasmids (see Table 1 and Results) to produce the viral particles using Lipofectamine 2000 (Invitrogen). The supernatant was collected 48 h posttransfection, centrifuged at 3,000 rpm for 15 min at 4°C to remove cell debris, and infected to NIH3T3 cells (RIKEN) in the presence of 8 μ g/ml polybrene (Sigma) to determine the viral titer. NIH3T3 cells were grown in high glucose DMEM supplemented with

10% FBS, penicillin and streptomycin. At 48 h postinfection, GFP positive NIH3T3 cells were counted by a flow cytometer (Particle analyzing system; Partec). Non-infected cells were always no greater than 3% of GFP positive cells. β -Galactosidase producing cells were counted after the enzyme reaction with x-gal. No stained cells were observed when non-viral supernatants were treated.

All trans retinoic acid (Sigma) and trichostatin A (Wako) were dissolved in ethanol at the concentrations of 10 mM and 5 mM, respectively. Six hours after transfection, reagents with appropriate concentration were added to the medium.

3. RESULTS

We firstly studied effects of VSV-G on virus titer by changing the amount of the expression vector for the transfection, since the protein has cytotoxic effects on host cells (Ory et al., 1996). We found that 100 to 200 ng of VSV-G expression plasmid DNA per 24 well plate (Iwaki) gave a good result (data not shown). We performed similar experiments on virus vectors and *gag/pol* (for 293FT cells) expression plasmids to determine the amount of DNA which gave the best results (data not shown). In the following experiments, 200 ng of VSV-G expression plasmid, and 600 ng of MSCV or Q-vector were used for the virus production with GP293 cells. For 293FT cells, 330 ng of *gag/pol* expression vector were transfected in addition to virus vector and VSV-G.

Table 2. Viral titers of GFP coding vectors produced by GP293, 293FT cells and packaging cell line GP293-G4.

Producer cells	Vector plasmid	Mean titer \pm S.D. [IU/ml]
GP293	pMGRN	4.5 \pm 1.1 \times 10 ⁵
GP293	pQMGRN	9.3 \pm 0.9 \times 10 ⁵
293FT	pMGRN	5.1 \pm 1.5 \times 10 ⁵
293FT	pQMGRN	1.3 \pm 0.2 \times 10 ⁶
GP293-G4		3.0 \pm 0.3 \times 10 ⁶

Table 3. Viral titers of lacZ coding vectors produced by GP293 and 293FT cells.

Producer cells	Vector plasmid	Mean titer \pm S.D.[IU/ml]
GP293	pMSCV/N Δ A β	5.1 \pm 2.0 \times 10 ⁴
GP293	pQMSCV/N Δ A β	1.8 \pm 0.2 \times 10 ⁵
293FT	pMSCV/N Δ A β	2.9 \pm 0.3 \times 10 ⁵
293FT	pQMSCV/N Δ A β	6.7 \pm 2.6 \times 10 ⁵

When MSCV and Q vector derived viruses were produced in *gag/pol* expressing GP293 cells (large T negative), Q-vector gave higher virus titer compared to MSCV such that 2.1-fold for GFP and 3.5-fold for *lacZ* virus vectors, respectively (Tables 2 and 3). Since Q-vector contains CMV promoter instead of that in virus LTR, this increase may depend on promoter activity. We then compared the virus production of Q-vector system in large T positive 293FT cells and GP293 cells. Former cells gave 1.4 (GFP) and 3.7 (*lacZ*)-fold increasing titer compared to the latter cells, respectively.

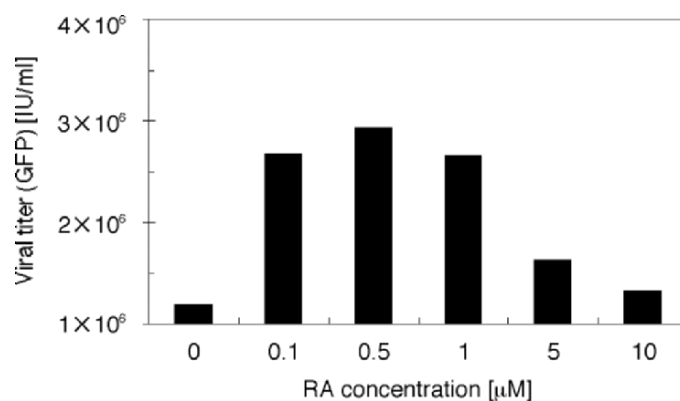


Figure 1. Addition of retinoic acid (RA) increased the viral titer.

Since Q-vector contains SV40 replication origin, the increase in gene copy number up to 1000-fold is expected in large T antigen expressing cells (Chittenden et al., 1991). However, judging from virus titer obtained, the gene amplification seems not to occur as expected. To clear this point, circular DNA was isolated from cells (Hirt, 1967) and quantified by dot blot method. We found that the amount of circular form virus DNA was increased almost 5.6-fold in large T expressing 293FT cells but the amplification was much less than positive control (pcDNA4) under the same condition (25-fold). By now, the reason for relatively lower rate of amplification has not yet been clear, but the complex structure of virus genome such as LTR and packaging signal that easily form secondary structure may hamper the full induction.

Another characteristics of Q-vector system is that CMV promoter is included in LTR instead of virus U3 promoter in order to increase the expression of viral genomic RNA. So as to improve the genomic RNA production by the CMV promoter, retinoic acid which was reported to

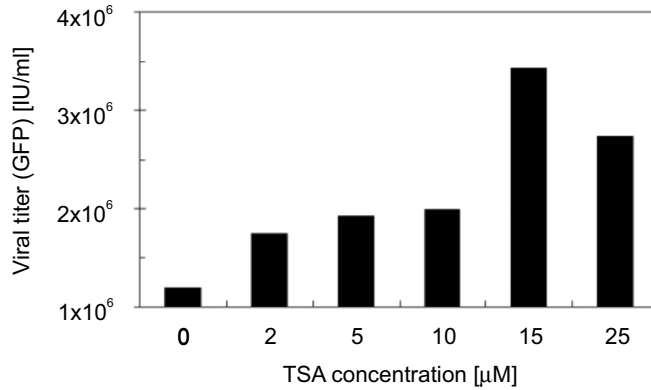


Figure 2. Addition of trichostatin A (TSA) increased viral titer.

activate CMV promoter (Ghazal et al., 1992) was added at various concentrations (Fig. 1). By adding at a concentration of 5 μM , virus titer increased 2.4-fold. Since retinoic acid is known to activate Molony leukemia virus LTR promoter (Collins, 1988), we then checked the activation of the LTR promoter and found that several-fold activation can be obtained by adding the reagent (data not shown). Histone deacetylase inhibitor trichostatin A was reported to amplify virus titer more than 30-fold (Tobias et al., 2000). As shown in Fig. 2, the reagent increased the virus titer at 2.8-fold. This difference between our results and previous reports may be due to the dependence of the effects on the amount of virus particle produced: virus titer increased from 10^3 to 10^5 in previous report but high virus titer of 10^5 order had already been obtained in our system.

4. DISCUSSION

We determined the optimal condition of transient retroviral production using Q vector system. Optimization of plasmids ratio at the transfection allows the high titer production of retroviral vectors. Although we chose GFP and *lacZ* genes as the reporter genes in this study, this system can be used for other genes, such as therapeutic gene like human tumor necrosis factor receptor and human IgG Fc region (TNFR-Fc) fusion protein for autoimmune disease therapy (Hotta et al., unpublished results).

This transient expression system could produce more than 10^6 IU/ml of retroviral vectors constantly without time-consuming cloning

processes, and this titer was comparable to that produced by packaging cell lines (compare Table 2 and Figs. 1,2). Furthermore, since we used VSV-G pseudotyped vectors, produced virus particles can be concentrated to more than 10^9 IU/ml by ultracentrifugation. Thus, this system provides a quick and high-titer preparation of retroviral vectors and this kind of optimization will be applicable to industrial and clinical use.

5. REFERENCES

- Burns J.C., Friedmann T., Driever W., Burrascano M., Yee J.K., 1993, Vesicular stomatitis virus G glycoprotein pseudotyped retroviral vectors: concentration to very high titer and efficient gene transfer into mammalian and nonmammalian cells, *Proc. Natl. Acad. Sci. U. S. A.* 90(17): 8033-8037.
- Chan A.W., Chong K.Y., Martinovich C., Simerly C., Schatten G., 2001, Transgenic monkeys produced by retroviral gene transfer into mature oocytes, *Science*. 291(5502): 309-312.
- Cherry S.R., Biniszkiwicz D., van Parijs L., Baltimore D., Jaenisch R., 2000, Retroviral expression in embryonic stem cells and hematopoietic stem cells, *Mol. Cell. Biol.* 20(20): 7419-7426.
- Chittenden T., Frey A., Levine A.J., 1991, Regulated replication of an episomal simian virus 40 origin plasmid in COS7 cells, *J. Virol.* 65(11): 5944-5951.
- Collins S.J., 1988, Retinoic acid-induced differentiation of retrovirus-infected HL-60 cells is associated with enhanced transcription from the viral long terminal repeat, *J. Virol.* 62(11): 4349-4352.
- Ghazal P., DeMattei C., Giulietti E., Kliewer S.A., Umesono K., Evans R.M., 1992, Retinoic acid receptors initiate induction of the cytomegalovirus enhancer in embryonal cells, *Proc. Natl. Acad. Sci. U. S. A.* 89(16): 7630-7634.
- Hirt B., 1967, Selective extraction of polyoma DNA from infected mouse cell cultures, *J. Mol. Biol.* 26(2): 365-369.
- Julius M.A., Yan Q., Zheng Z., Kitajewski J., 2000, Q vectors, bicistronic retroviral vectors for gene transfer, *Biotechniques*. 28(4): 702-708.
- Kamihira M., Nishijima K., Iijima S., 2004, Transgenic birds for the production of recombinant proteins, *Adv. Biochem. Eng. Biotechnol.* 91: 171-189.
- Lin S., Gaiano N., Culp P., Burns J.C., Friedmann T., Yee J.K., Hopkins N., 1994, Integration and germ-line transmission of a pseudotyped retroviral vector in zebrafish, *Science*. 265(5172): 666-669.
- Miller A.D., 2002, Chapter 9; Development and application of retroviral vectors, in *Retroviruses*, Coffin J.M., Hughes S.H., Varmus H.E., ed., Cold Spring Harbor Laboratory Press.
- Mizuarai S., Ono K., Yamaguchi K., Nishijima K., Kamihira M., Iijima S., 2001, Production of transgenic quails with high frequency of germ-line transmission using VSV-G pseudotyped retroviral vector, *Biochem. Biophys. Res. Commun.* 286(3): 456-463.
- Ory D.S., Neugeboren B.A., Mulligan R.C., 1996, A stable human-derived packaging cell line for production of high titer retrovirus/vesicular stomatitis virus G pseudotypes, *Proc. Natl. Acad. Sci. U. S. A.* 93(21): 11400-11406.

- Tobias C.A., Kim D., Fischer I., 2000, Improved recombinant retroviral titers utilizing trichostatin A, *Biotechniques*. 29(4): 884-890.
- VandenDriessche T., Collen D., Chuah M.K., 2003, Biosafety of onco-retroviral vectors, *Curr. Gene Ther.* 3(6): 501-515.
- Weber E., Anderson W.F., Kasahara N., 2001, Recent advances in retrovirus vector-mediated gene therapy: teaching an old vector new tricks, *Curr. Opin. Mol. Ther.* 3(5): 439-453.

BIOCHEMICAL ANALYSIS OF CHICKEN OVALBUMIN PROMOTER

Mahboob Morshed, Junko Yamamoto, Shusuke Sano, Ken-ichi Nishijima, Masamichi Kamihira and Shinji Iijima

Department of Biotechnology, Nagoya University, Furo-cho, Chikusa-ku, Nagoya 464-8603, Japan

Abstract: In this study, we report the changes of DNA methylation in chicken ovalbumin promoter-enhancer upon the induction of its expression. Genomic DNA of the oviduct, which was obtained from either immature chickens, estradiol-treated chickens or laying hens, was analyzed by the bisulfite method followed by PCR amplification and sequence determination. Primers were used for different regions of the ovalbumin promoter. Most CpG sites were methylated in untreated immature chickens, probably consistent with the lack of expression. In ovalbumin expressing chickens, some CpGs were selectively demethylated. These include transcription start site, DNase I hypersensitive sites II and III but not the DNase I hypersensitive site IV. These results show that some CpGs in the ovalbumin promoter region are specifically demethylated upon ovalbumin expression.

Key words: chicken; ovalbumin; promoter; DNA methylation.

1. INTRODUCTION

DNA methylation is one of the mechanisms of modifying gene expression, especially it establishes a silent state of chromatin.^{1,2} By collaborating with proteins, DNA methylation plays important roles in the silencing of repetitive sequences or in genomic imprinting. It has also been reported that DNA methylation participated in some tissue-specific gene expression.³ Chicken ovalbumin is the major protein in egg white and

accounts for approximately 54% of the total protein of egg white.⁴ Ovalbumin promoter has been used as an excellent model system for the hormonal development and tissue-specific regulation of gene expression. In this study, we analyzed the methylation status of chicken ovalbumin promoter.

2. MATERIALS AND METHODS

2.1 Animals

Four-day-old female chickens and laying hens were purchased from Chubu Kagaku (Nagoya, Japan). To induce ovalbumin expression in immature chickens, the chickens were injected daily with 1 mg of estradiol for 12 days.

2.2 DNA extraction

Oviduct tissue was excised from untreated chickens, estradiol-treated chickens and laying hens. Freshly isolated tissues (0.5 g) were washed twice in PBS, minced and then lysed in 5 ml of a solution containing 10 mM Tris (pH: 8.0), 100 mM EDTA, 0.5% (w/v) SDS and 0.5 mg/ml proteinase K. Following incubation at 55°C overnight, the lysate was extracted twice with phenol-chloroform and then chloroform-isoamyl alcohol. Finally DNA was dialyzed to a buffer A (20mM Tris (pH 8.0), 10mM EDTA and 0.1M NaCl) and buffer B (10mM Tris (pH 8.0), 10mM EDTA and 10mM NaCl) 6 times for 3 days and stored at 4°C until use.

2.3 Bisulfite genomic sequencing for determination of DNA methylation

Sequencing of bisulfite-modified genomic DNA allows us to determine the methylation status of any cytosine in chromosomal DNA. This method is based on the deamination of cytosine but not of 5-methyl cytosine to uracil by a series of reaction using bisulfite. PCR amplification and sequencing of modified DNA results in a sequence pattern showing conversion of all unmethylated cytosine to thymine (since uracil is read by Taq polymerase as a thymine), whereas 5-methyl cytosine remains as cytosine. Bisulfite conversion was performed by the method reported by Clark *et al.*⁵ with some modifications. Twenty micrograms of DNA was denatured by adding freshly prepared NaOH solution to a final concentration of 3.3 M in a 100 µl

reaction volume and incubated for 20 minutes at 37°C. Freshly prepared bisulfite solution containing 2.6 M sodium bisulfite and 10 mM hydroquinone was added directly to the denatured DNA to a final volume of 1200 µl, and then samples were gently mixed, overlaid with mineral oil and incubated at 55°C for 6 hours. After the DNA was desalted using Wizard DNA Clean-Up System (Promega, Madison, MI) and dissolved in 100 µl of 1 mM Tris-HCl (pH 8.0), then NaOH was added to a final concentration 2.2 M and incubated for 20 minutes at 37°C. After adding 10 M of ammonium acetate to the final concentration of 3 M, DNA was recovered by ethanol precipitation and dissolved in 50 µl of 1 mM Tris-HCl (pH 7.6) and stored in -20°C until use.

Amplifications were performed in 50 µl reaction mixtures containing 1-4 µl bisulfite-treated genomic DNA, 400 µM dNTPs, 0.2 µM primers, 2.5 mM MgCl₂, 0.5 µl LA Taq DNA polymerase (TaKaRa, Osaka, Japan).

Table 1. Primers used in this study

Region (kb)		Primer sequence
-6.3 to -5.9	Direct	5'-GGTttTttTAGGGAATGtTGTATGTGT-3'
	Reverse	5'-GGTGGATCCC AaaTCATACTAaaAaTCCTTaaCC-3'
-5.8 to -5.3	Direct	5'-GAGGGAtTGGTtTTGtTtTGGG-3'
	Reverse	5'-AaTCTaCATCCTaAaATCAaCAaaCCC-3'
-5.3 to -4.6	Direct	5'-GGttTGtTGATtTtAGGATGtAG-3'
	Reverse	5'-CACAAaaTaaTACAATCACCCA-3'
-4.4 to -4.1	Direct	5'-CCAGGATAATGGTAGGTTAAGtAATAGATAtAGAGTTTG-3'
	Reverse	5'-aCCTCACCTaCATaCAAAaCCTTTCAC-3'
-4.0 to -3.2	Direct	5'-AGGAATtATTGAtTGTAtAGTGAAGGG-3'
	Reverse	5'-CCTaCCCAaCACAACTaTaCAAAaC-3'
-2.8 to -2.3	Direct	5'-GTAGGtTGGAA TtaGGAtAtTATGTGG-3'
	Reverse	5'-AaCACTCTaACCCTCTaCAaCAaCCCAT-3'
-2.5 to -1.9	Direct	5'-GTAGtAATGGAAGAtTGATATTGGAGAAA-3'
	Reverse	5'-AATAACAACAaaCTaCTTCTCACCTaT-3'
-1.6 to -1.0	Direct	5'-GTAGATTAGGAtAGAATTATTtTGGAG-3'
	Reverse	5'-CCATTaAaCTTCAaTTACAACCAaATA-3'
-0.9 to -0.2	Direct	5'-AAAtAGTgTTTAtAGAGGtAGAATGG-3'
	Reverse	5'-CCATTaAaCTTCAaTTACAACCAaATA-3'
-0.1 to +0.4	Direct	5'-CCAGGATCCAGTtTGATGGATTAGtAGAAAtAGGTAGAA-3'
	Reverse	5'-GGTGGATCCATaATTTaCTCTCTaTCACTCT-3'

Amplification involved a first denaturation at 94°C for 2 min, followed by amplification of target DNA for 35 cycles (denature at 94°C for 15 sec, annealing at 48-55°C for 30 sec and extension at 68°C for 60 sec). Ten sets of primers were used, location and sequences are indicated in Table 1. In primers sequence small letters show the modified nucleotides: conversion

from cytosine to uracil by bisulfite reaction are appeared as 't' in direct primers and as 'a' in reverse primers that anneal the other strand of PCR product. Amplified fragments were cloned into pT7Blue-2 vector (Novagen, Madison, WI). Individual clones were sequenced using BigDye Terminator v3.1 Cycle Sequencing Kit (Applied Biosystems, Warrington, UK).

3. RESULTS AND DISCUSSION

The expression of the ovalbumin gene is induced in accordance with the development of oviduct tissue, which in turn is developmentally regulated but is also possible to be induced artificially by administering steroid hormones to immature female chickens.^{6,7} We confirmed that laying hens and 12-day estradiol-treated chickens expressed ovalbumin either in the level of mRNA or of protein (data not shown). Untreated immature chickens did not express ovalbumin as expected. Oviducts from these chickens were used for the following experiments.

The length between the transcription start site of the ovalbumin and the end of the neighboring gene (*Y*) is about 8 kb. Within this region, there are four DNase I hypersensitive sites (DHSs).⁸ The first DHS includes the transcription start site and extends up to 300 bp upstream and three other DHSs are centered at -0.80, -3.3 and -6.0 kb upstream (Fig. 1). It has been reported that the appearance of these regions was associated with ovalbumin expression: these were present in laying hens and in chickens artificially induced by steroids while being absent from erythrocytes in which the ovalbumin gene was not expressed.⁹ It is generally postulated that DHSs contain important regions for transcriptional regulation. There are several reported regulatory elements which regulate the transcription of the ovalbumin located inside DHSs. DHS I contains a proximal promoter about 90 bp in the length and a negative regulatory region spanning -90 to -300 bp.¹⁰ DHS II is reported to be responsible for the induction of steroid hormones (usually used as a mixture of estradiol and glucocorticoid) using primary culture of oviduct cells obtained from estradiol-induced immature oviducts.⁹⁻¹² An estrogen-responsive enhancer element is present in DHS III.¹³ There is also a tissue-specific silencer element that overlaps with DHS III. This represses the expression of reporter gene in the liver but not in the oviduct.¹⁴ There is no evidence for function or binding proteins on DHS IV.

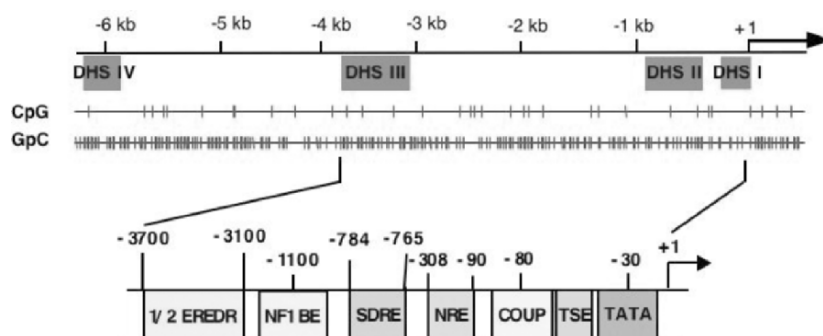


Figure 1. Putative regulatory elements in the 5'-flanking region of the chicken ovalbumin gene. 1/2 EREDR: Half estrogen response element direct repeat; NF1BE: Nuclear factor 1 binding element; SDRE: Steroid-dependent response element; NRE: Negative regulatory element; COUP: Chicken ovalbumin upstream promoter; TSE: Tissue specific element; Modified from Muramatsu and Sanders.¹⁵(Figure is not drawn to scale).

Within the 6.3 kb upstream of the ovalbumin promoter (including transcription start site), there are 36 CpG sites which are distributed almost uniformly in the promoter region and do not form a CpG island (Fig. 1). First, we analyzed the methylation status of immature chickens (Fig. 2). Most CpG sites were methylated throughout the promoter-enhancer region. Some CpG sites near DHS II and the transcription start site were not methylated even in the absence of expression. These were not methylated in erythrocytes either (data not shown), suggesting that demethylation of these sites is not related to tissue specific expression of the ovalbumin.

Several regions of CpGs are selectively unmethylated in both estradiol-treated chickens and laying hens as shown in Fig. 2. First three CpGs in the transcribed region were demethylated. The first is inside the first exon and the other two sites are in the first intron. Such selective demethylation of the 5'-region was reported for other genes.¹⁶ Inside DHS II, a CpG site was specifically demethylated upon ovalbumin expression. This specific demethylation might be related with the gene transcription and also this CpG site is located very near to SDRE which is steroid inducible element. Sanders group proved that the promoter region from -0.9 kb to +1 (DHS II CpG site and SDRE are included in this promoter region) is sufficient for steroid induction when transfected in primary cultures of oviduct cells.¹⁰

In our analysis, partial demethylation for DHS III was observed in the ovalbumin expressing chickens. But the downstream and upstream regions of DHS III were strongly methylated even in laying hens. We analyzed more than ten clones of bisulfite modified DNA of the DHS III region and the results showed that about half were methylated while the others were

unmethylated. But we did not obtain any partial methylation state in the case of DHS II of estradiol-treated chickens and laying hens and there was also a clear change in the methylation pattern between immature chickens, estradiol-treated chickens and laying hens (Fig. 2). Our results suggest that some regulatory mechanisms induce demethylation in some regions of this promoter and further DNA methylation is an epigenetic process, cells existed in a mixed population of different methylation states.

The CpG site in DHS IV was completely methylated in both estradiol-treated chickens and laying hens (Fig. 2). This could be a reflection of the lack of functional importance of this region. In fact, the expression of the reporter CAT gene was sufficient by the ovalbumin promoter -3.2 kb to $+1$ in the oviduct and was not affected by the existence of -4 kb to -8 kb covering DHS IV.¹⁴ These results suggest that our methylation analysis is in good accordance with other experimental methods which indicate the importance of gene regulation. Further analysis would be helpful to fully understand the biochemical and functional features of the ovalbumin promoter.

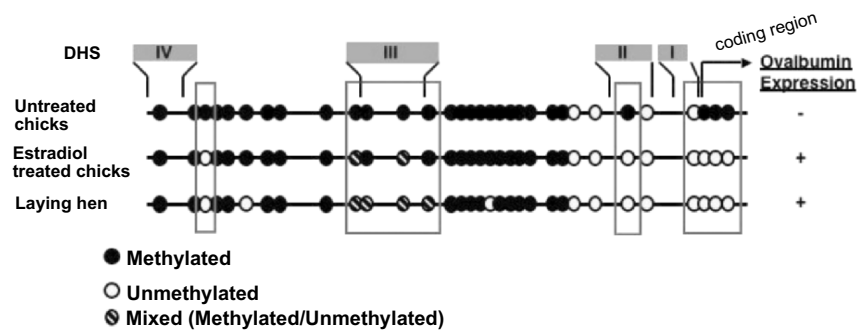


Figure 2. CpG methylation pattern of ovalbumin promoter of immature chickens, estradiol-treated chickens and laying hens. (Figure is not drawn to scale).

4. REFERENCES

1. B. Richardson, Impact of aging on DNA methylation, *Ageing Research Reviews* 2, 245-261 (2003).
2. A. P. Bird, and A. P. Wolffe, Methylation-induced repression-belts, braces and chromatin, *Cell* 99, 451-454 (1999).
3. Y-G. Ko, K. Nishino, N. Hattori, Y. Arai, S. Tanaka, and K. Shiota, Stage by stage change in DNA methylation status of *Dnmt 1* locus during mouse early development, *J. Biol. Chem.* 280, 9627-9634 (2005).

4. A. B. Gilbert, Egg albumen and its formation, in: *Physiology and Biochemistry of the Domestic Fowl* vol 3, edited by D. J. Bell and B. M. Free (Academic Press, 1984), pp. 1291-1329.
5. S. J. Clark, J. Harrison, C. L. Paul, and M. Frommer, High sensitivity mapping of methylated cytosines, *Nucleic Acids Res.* 22, 2990-2997 (1994).
6. R. D. Palmiter, Quantitation of parameters that determine the rate of ovalbumin synthesis, *Cell* 4, 189-197 (1975).
7. R. D. Palmiter, E. R. Mulvihill, J. H. Shepherd, and G. S. McKnight, Steroid hormone regulation of ovalbumin and conalbumin gene transcription, *J. Biol. Chem.* 256, 7910-7916 (1981).
8. J. S. Kaye, M. Bellard, G. Dretzen, F. Bellard, and P. Chambon, A close association between sites of DNase I hypersensitivity and sites of enhanced cleavage by micrococcal nuclease in the 5'-flanking region of the actively transcribed ovalbumin gene, *EMBO J.* 3, 1137-1144 (1984).
9. J. S. Kaye, S. Pratt-Kaye, M. Bellard, G. Dretzen, F. Bellard, and P. Chambon, Steroid hormone dependence of four DNase I-hypersensitive regions located within the 7000-bp 5'-flanking segment of the ovalbumin gene, *EMBO J.* 5, 277-285 (1986).
10. M. M. Sanders, and G. S. McKnight, Positive and negative regulatory elements control the steroid-responsive ovalbumin promoter, *Biochemistry* 27, 6550-6557 (1988).
11. L. A. Schweers, and M. M. Sanders, A protein with a binding specificity similar to NF-kB binds to a steroid-dependent regulatory element in the ovalbumin gene, *J. Biol. Chem.* 266, 10490-10497 (1991).
12. D. M. Dean, P. S. Jones, and M. M. Sanders, Alterations in chromatin structure are implicated in the activation of the steroid hormone response unit of the ovalbumin gene, *DNA and Cell Biology* 20, 27-39 (2001).
13. S. Kato, L. Tora, J. Yamauchi, S. Masushige, M. Bellard, and P. Chambon, A far upstream estrogen response element of the ovalbumin gene contains several half-palindromic 5'-TGACC-3' motifs acting synergistically, *Cell* 68, 731-742 (1992).
14. T. Muramatsu, T. Imai, H. Park, H. Watanabe, A. Nakamura, and J. Okumura, Gene gun-mediated *in vivo* analysis of tissue-specific repression of gene transcription driven by the chicken ovalbumin promoter in the liver and oviduct of laying hens, *Mol. Cell. Biochem.* 185, 27-32 (1998).
15. T. Muramatsu, and M. M. Sanders, Regulation of ovalbumin gene expression, *Poultry Avian Biol. Rev.* 6, 107-123 (1995).
16. C. D. Smet, A. Loriot, and T. Boon, Promoter-dependent mechanism leading to selective hypomethylation with the 5'-region of gene *MAGE-A1* in tumor cells, *Mol. Cell. Biol.* 24, 4781-4790 (2004).

PRODUCTION OF CHIMERIC ANTIBODIES BY TRANSGENIC CHICKEN BIOREACTORS

Yoshinori Kawabe, Akitsu Hotta, Ken-ichiro Ono, Kazuhisa Esaka, Ken-ichi Nishijima, Masamichi Kamihira and Shinji Iijima

Department of Biotechnology, Graduate School of Engineering, Nagoya University, Furo-cho, Chikusa-ku, Nagoya 464-8603, Japan

Abstract: Recombinant antibodies have been successfully used as pharmaceuticals for diseases such as cancer and rheumatoid, and an effective mass production method for therapeutic antibodies is urgently desired. Transgenic chicken proposed as a transgenic bioreactor is expected to be one of the candidates for mass production procedure of recombinant proteins. In the present study, we constructed retroviral vectors in which H- and L-chains of anti-CD2 chimeric antibody were produced from a single transcript mediated by an IRES sequence (MSCV/GΔAL-IRES-H). Transgenic chickens were generated by injecting concentrated retroviral vector solution into the chicken embryos after 55 h incubation and followed by *in vitro* embryo culture. L- and H-chain genes encoded by the retroviral vector were detected in genomic DNA extracted from the tissues of hatched chickens by Southern blotting. The chickens stably produced the chimeric antibody in the serum and eggs for long term. The chimeric antibody purified from egg white laid by a transgenic hen exhibited the antigen recognition activity. These results indicate that transgenic chicken bioreactor is promising for commercial production of recombinant antibodies.

Key words: Transgenic chicken, Chimeric antibodies, Internal ribosome entry site.

1. INTRODUCTION

By hybridoma technology (Köhler and Milstein, 1975) and a development of antibody technology, therapeutic potential of monoclonal antibodies were widely recognized as a magic bullets (Chadd and Chamow, 2001; Gura, 2002; Brekke and Sandlie, 2003;

Sanz et al., 2004). Animal cell culture has become a major system for the production of therapeutic antibodies using chinese hamster ovary, CHO cells. Antibody molecule produced by the animal cells is folded properly and glycosylated (*Roque et al.*, 2004). However, since the production cost in cultured animal cells is usually high due to using the relatively expensive media and low productivity, an alternative mass production procedure for recombinant antibodies is urgently desired.

Recently, the production of pharmaceutical proteins using transgenic livestock has been attempted (*Pollock et al.*, 1999; *Rudolph*, 1999; *Dyck et al.*, 2003), but the generation of transgenic livestock has a disadvantage such as a long-term breeding period (*Bruce and Whitelaw*, 2004). As an alternative transgenic bioreactor, avian species such as chicken and quail have attracted an attention for the production of pharmaceutical proteins in eggs since chickens have short generation times. Furthermore, it is reported that chickens exhibit glycosylation patterns that are very similar to humans, although other livestock animals such as goats, cows and sheep have slightly different patterns (*Raji et al.*, 2000). The absence of the prion problem in chicken is also emphasized.

In the past decade, many researches have attempted to generate transgenic birds (*Salter et al.*, 1985; *Bosselemen et al.*, 1989; *Vick et al.*, 1993; *Love et al.*, 1994; *Sherman et al.*, 1998; *Mizuarai et al.*, 2001; *Havery et al.*, 2002; *Mozdziak et al.*, 2003; *Rapp et al.*, 2003; *Chapman et al.*, 2004; *McGrew et al.*, 2004., *Sang*, 2004; *Kamihira et al.*, 2005), but reasonably high production of recombinant proteins with a complicated structure such as full antibodies has not been reported.

Here, we report the generation of transgenic chickens producing a full antibody using a VSV-G pseudotyped replication-defective retroviral vector for antibody gene transfer.

2. MATERIALS AND METHODS

Plasmid construct. The retroviral vector was constructed in which H- and L-chains of anti-CD2 chimeric antibody were produced from a single transcript mediated by an EMCV-derived IRES sequence (MSCV/G Δ AL-IRES-H) as described in our previous report (*Hotta et al.*, 2004). The schematic drawing of the structure of plasmid is shown in Fig. 1.

Microinjection of viral vector and embryo culture. A concentrated retroviral vector solution was injected into the heart of chicken embryos with a glass micropipette. The injected embryos were cultured to hatch

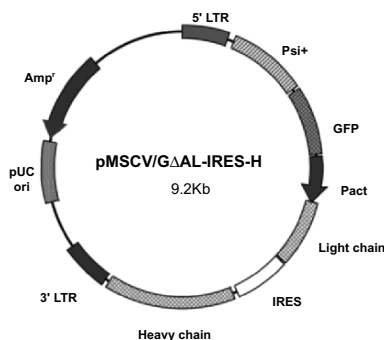


Figure 1. Schematic drawing of the pMSCV/GΔAL-IRES-H.

by an *in vitro* embryo culture method as described in our previous report (Kamihira *et al.*, 2005).

Measurement of antibody concentration. The antibody concentration in the serum and eggs of transgenic chickens was determined by the solid-phase ELISA.

Purification of the antibody. The antibody produced in the egg white of transgenic hen was collected by ammonium sulfate precipitation and purified by a protein A beads.

Western blot analysis. Western blotting was performed to check the chimeric antibody produced in the serum and eggs of transgenic chickens and was also carried out to assay the antigen recognition ability of the antibody purified from the egg white.

3. RESULTS

Transgenic chickens were generated by injecting a concentrated retroviral vector solution into the heart of chicken embryos after 55 h incubation and the injected embryos were cultured to hatch by *in vitro* embryo culture method. The titer of the viral solution used for infection was $2.4\text{--}9.0 \times 10^8$ cfu/ml. In four trials, the viral vector was injected into a total of 36 embryos, 3 of which hatched; the hatchability was 8.3%.

For hatched chickens, the antibody expression in the serum was analyzed once a month with solid-phase ELISA. The antibody expression in the serum remained stable for over a year with the production level ranging from several to thirty $\mu\text{g/ml}$. After sexual maturation of hens, eggs were collected and the expression level of antibody in their eggs was also measured. The antibody was detected in both egg white and yolk (Table 1).

Table 1. The antibody productivity of transgenic chickens

Bird No.	Sex (M: Male, F; Female)	Antibody concentration ($\mu\text{g/ml}$)		
		Serum	White	Yolk
#1	F	14.8 \pm 3.90	18.4 \pm 4.91	1.67 \pm 0.46
#2	M	29.2 \pm 6.25	–	–
#3	F	7.80 \pm 2.59	19.3 \pm 4.91	3.73 \pm 0.99

The structure and function of the chimeric antibody produced by transgenic chickens were analyzed. The chimeric antibody was purified from the egg white laid by transgenic hen using Protein A beads. By the Western blotting, heavy and light chains were detected in the samples from serum, egg white and yolk of transgenic chickens on a gel under reducing conditions (Fig. 2). A human IgG and the chimeric antibody purified from the egg white were used as a positive control. These results suggest that the antibody in both serum and eggs of transgenic chicken was intact without degradation.

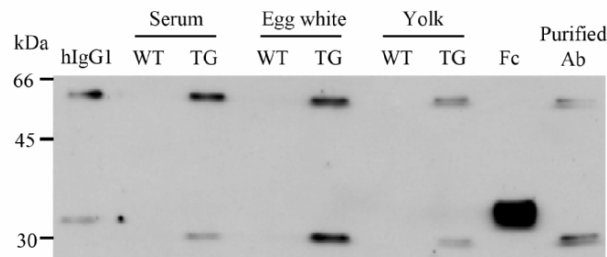


Figure 2. Western blotting of chimeric antibody produced by transgenic chickens.

Then, to detect the antigen recognition ability of chimeric anti-CD2 antibody purified from the egg white, Western blot analysis was carried out using the lysate from CD2-positive Jurkat cells. A human IgG was used as a positive control. The chimeric anti-CD2 antibody purified from the egg white specifically recognized CD2 molecules derived from Jurkat cells (Fig. 3).

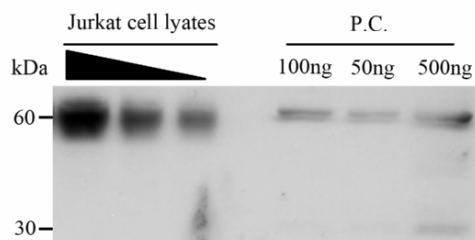


Figure 3. Antigen recognition ability of chimeric antibody produced by transgenic chicken.

4. DISCUSSION

We report in this study the construction a replication-defective retroviral vector with the bicistronic expression and generation of transgenic chicken producing chimeric anti-CD2 antibody by injecting a concentrated retroviral vector into the heart of chicken embryos. A chimeric antibody produced by transgenic chickens remained intact (Fig. 2) and exhibited antigen recognition ability (Fig. 3). In the present case, the bicistronic expression system was used for the expression of light and heavy chain genes; light chain was translated by ribosome scanning mechanism from the cap site and the translation of heavy chain was started from the IRES sequence. As shown in our previous report (Hotta *et al.*, 2004), an optimization of valance in expression level of heavy and light chain is very important for effective assembly of antibody. In this regard, optimization of IRES activity with other IRES sequence possibly increase the productivity (Bonnal *et al.*, 2003) since the translation from EMCV-derived IRES sequence seems to be less efficient comparing to cap-dependent translation (Mizuguchi *et al.*, 2000).

Until now, biopharmaceuticals that could be produced by transgenic avian are limited to a secreted protein with a simple structure (Harvey *et al.*, 2002; Rapp *et al.*, 2003). In this study, we succeeded in the production of protein with a complicated structure such as full antibodies. Thus, we think that transgenic chicken bioreactor for the production of pharmaceutical proteins will be a realistic method in near future.

5. REFERENCES

- Brekke, O. H., and Sandlie, I., 2003, Therapeutic antibodies for human diseases at the dawn of the twenty-first century, *Nat. Rev. Drug. Disc.* 2: 52-62.

- Bonnal, S., Boutonnet, C., Prado-Lourence, L., and Vanger, S., 2003, IRESdb: the internal ribosome entry site database, *Nucleic Acids Res.* 31: 427-428.
- Bosselmen, R. A., Hsu, R. V., Boggs, T., Hu, S., Brusxewski, J., Ou, S., Kozar, L., Martin, F., Green, C., Jacobson, F., Nicolson, M., Schultz, J. A., Seman, K. M., Rishell, W., and Stewart, R. G., 1989, Germline transmission of exogenous genes in the chicken, *Science* 243: 553-555.
- Bruce, C., and Whitelaw, A., 2004, Transgenic livestock made easy, *Trends in Biotechnol.* 22: 157-160.
- Chadd, H. E., and Chamow, S. M., 2001, Therapeutic antibody expression technology, *Current Opinion in Biotechnology* 12: 188-194.
- Chapman, S. C., Lawson, A., MacArthur, W. C., Wiese, R. J., Loechel, R. H., Burgos-Trinidad, M., Wakefield, J. K., Ramabhadran, R., Mauch, T. J., and Schoenwolf, G. C., 2004, Ubiquitous GFP expression in transgenic chickens using a lentiviral vector, *Development* 132: 935-940.
- Dyck, M. K., Lacroix, D., Pothier, F., and Sirard, M-A., 2003, Making recombinant proteins in animals - different systems, different applications, *Trends in Biotechnol.* 21: 394-399.
- Gura, T., 2002, Magic bullets hit the target, *Nature* 417: 584-586.
- Harvey, A. J., Speksnijger, G., Baugh, L. R., Morris, J. A., and Ivarie, R., 2002, Expression of exogenous protein in the egg white of transgenic chickens, *Nat. Biotechnol.* 19: 396-399.
- Hotta, A., Kamihira, M., Itoh, K., Morshed, M., Kawabe, Y., Ono, K., Matsumoto, H., Nishijima, K., and Iijima, S., 2004, Production of anti-CD2 chimeric antibody by recombinant animal cell, *J. Biosci. Bioeng.* 98: 298-303.
- Kamihira, M., Ono, K., Esaka, K., Nishijima, K., Kigaku, R., Komatsu, H., Yamashita, T., Kyogoku, K., and Iijima, S., 2005, High-level expression of scFv-Fc fusion protein in serum and egg white of genetically manipulated chickens using a retroviral vector, *J. Virol.* in press.
- Köhler, G., and Milsten, C., 1975, Continuous cultures of fused cells secreting antibody of predefined specificity, *Nature* 256: 495-497.
- Love, J., Gribbin, C., Mather, C., and Sang, H., 1994, Transgenic birds by DNA microinjection, *Bio/Technology* 12: 60-63.
- McGrew, M. J., Sherman, A., Ellard, F. M., Lillico, S. G., Gilhooley, H. J., Kingsman, A. J., Mitrophanous, K. A., and Sang, H., 2004, Efficient production of germline transgenic chickens using lentiviral vectors, *EMBO reports* 5: 728-733.
- Mizuguchi, H., Xu, Z., Ishii-Watabe, A., Uchida, E., and Hayakawa, T., 2000, IRES-dependent second gene expression is significantly lower than cap-dependent first gene expression in a bicistronic vector, *Mol. Ther.* 1: 376-382.
- Mizuarai, S., Ono, K., Yamaguchi, K., Nishijima, K., Kamihira, M., and Iijima, S., 2001, Production of transgenic quails with high frequency of germ-line transmission using VSV-G pseudotyped retroviral vector, *Biochemi. Biophys. Res. Commun.* 286: 456-463.
- Mozdziak, P. E., Borwornpinyo, S., McCoy, D. W., and Petite, J. N., 2003, Development of transgenic chickens expressing bacterial β -galactosidase, *Dev. Dynamics* 226: 439-445.
- Pollock, D. P., Kutzko, J. P., Birck-Wilson, E., Williams, J. L., Echelard, Y., and Meade, H. M., 1999, Transgenic milk as a method for the production of recombinant antibodies, *J. Immunol. Methods* 231: 147-157.
- Raji, T. S., Briggs, J. B., Borge, S. M., and Jones, A. J. S., 2000, Species-specific variation in glycosylation of IgG: evidence for the species-specific sialylation and branch-specific galactosylation and importance for engineering recombinant glycoprotein therapeutics, *Glycobiology* 10: 477-486.

- Rapp, J. C., Harvey, A. J., Speksnijder, G. L., Hu, W., and Ivarie, R., 2003, Biologically active human interferon α -2b produced in the egg white of transgenic hens, *Trans. Res.* 12: 569-575.
- Roque, A. C. A., Lowe, C. R., and Taipa, M. Â., 2004, Antibodies and genetically engineered related molecules: production and purification, *Biotechnol. Prog.* 20: 639-654.
- Rudolph, N. S., 1999, Biopharmaceutical production in transgenic livestock, *Trends Biotechnol.* 17: 367-374.
- Salter, D. W., Smith, E. J., Hughes, S. H., Wright, S. E., Fadly, A. M., Witter, R. L., and Crittenden, L. B., 1985, Gene insertion into chicken germ line by retroviruses, *Poult. Sci.* 65: 1445-1458.
- Sang, H., 2004, Prospects for transgenesis in the chick, *Mech. Dev.* 121: 1179-1186.
- Sherman, A., Dawson, A., Mather, C., Gilhooley, H., Li, Y., Mitchell, R., Finnegan, D., and Sang, H., 1998, Transposition of the *Drosophila* element *mariner* into the chicken germ line, *Nature Biotechnol.* 16: 1050-1053.
- Sanz, L., Blanco, B., and Vallina, L. A., 2004, Antibodies and gene therapy: teaching old 'magic bullets' new tricks, *Trends Immunol.* 25: 85-91.
- Vick, L., Li, Y., and Simkiss, K., 1993, Transgenic birds from transformed primordial germ cells, *Proc. R. Soc. London B Biol. Sci.* 251: 179-182.

DETERMINATION OF THE MAJOR FOOD ALLERGEN, OVOMUCOID, WITH AN OLIGOCLONAL ENZYME-LINKED IMMUNOSORBENT ASSAY

Oligoclonal sandwich ELISA for ovomucoid

Junko Hirose¹, Yukie Murakami-Yamaguchi², Miki Ikeda², Hiroshi Narita²

¹Department of Life Style Studies, School of Human Cultures, The University of Shiga Prefecture, Shiga 522-8533, Japan; ²Department of Food and Nutrition, Kyoto Women's University, Kyoto 605-8501, Japan

Abstract: Ovomucoid (OM), a glycoprotein of a molecular weight of 28 kDa, is thought to be the major allergen in egg white. We have established three monoclonal antibodies (mAbs) against OM. MAb 5C is specific to native OM, mAb 6H is specific to heated OM, and mAb 7D is specific to carbohydrate moiety of OM, which recognizes native and heated OM equally. Then, an enzyme-linked immunosorbent assay (ELISA) capable to determine the total OM content, irrespective of the degree of heat denaturation of OM, was constructed by using mAb 7D. Furthermore, two novel methods have been developed to improve the ELISA. First, its sensitivity was enhanced 100 times by using an oligoclonal cocktail of mAbs 7D, 5C, and 6H as a second antibody. Second, it was shown that usage of denaturing reagents such as SDS and β -mercaptoethanol for extraction of allergens from foods was acceptable for ELISA within a range of stability of a first antibody on a solid phase. Properties of the oligoclonal sandwich ELISA system thus constructed will provide important information for establishing a common international method for allergen determination.

Key words: allergen labeling, enzyme-linked immunosorbent assay, food allergy, monoclonal antibody, ovomucoid.

1. INTRODUCTION

From the viewpoint of preventing the occurrence of health hazards caused by foods containing allergens, mandatory labeling of five specified ingredients (eggs, milk, wheat, buckwheat, and peanuts) has started from 2002 in Japan for the first challenge in the world (Kanagawa & Imamura, 2002). For the accomplishment and confirmation of this labeling, two types of enzyme-linked immunosorbent assays (ELISAs) using polyclonal antibodies were introduced according to the Notification #1106001 from The Japanese Ministry of Health, Labour and Welfare (Honjoh *et al.*, 2002; Takahata *et al.*, 2002). However, they are requested to be further improved along with scientific progress as soon as possible.

Hen's egg is the material that causes food allergy most frequently (Imai & Iikura, 2003) and approximately two-thirds of children diagnosed as food allergy are reactive to egg white (Sampson & Ho, 1997). Ovomuroid (OM), a glycoprotein of a molecular weight of 28 kDa, is thought to be the major allergen in egg white (Bernhisel *et al.*, 1994). In this study, we report three kinds of monoclonal antibodies (mAbs) and sandwich ELISAs that can recognize native and/or thermally induced denatured forms of OM (Hirose *et al.*, in press). Furthermore, two novel methods have been developed to improve this ELISA.

2. MATERIALS AND METHODS

Preparation of OM

Native OM (N-OM) was chromatographically purified. To freshly prepared hen's egg white was added an equal volume of 0.1M Acetate buffer pH3.8 and the mixture was dialyzed against the same buffer overnight. After centrifugation, resulting supernatant was applied to a column of carboxymethyl-Toyopearl 650M (TOSO, Tokyo, Japan). OM was eluted by a linear gradient of 0-0.2M of NaCl in 20 mM Acetate buffer pH4.6. Heated OM (H-OM) was prepared by heating 1 mg/ml of N-OM in 10 mM phosphate-buffered saline pH7.4 (PBS) at 100°C for 30 min.

Monoclonal antibodies

Hybridomas producing mAbs were established by fusion of splenocytes of BALB/c mice immunized with N- or H-OM and myeloma cells (NSI/1-Ag4-1) essentially as described previously (Narita *et al.*, 1995). Those with interest were cloned twice and mAbs named after

them were prepared from their ascitic fluids and purified on Protein G-Sepharose columns (Amersham Biosciences Corp. NJ, USA). Portions of purified mAbs were biotinylated with EZ-Link sulfo-NHS-LC-Biotin (Pierce, IL, USA).

Sandwich ELISA

Wells in an ELISA plate (Nunc, Roskilde, Denmark) were first coated commonly with 5 µg/ml of mAb 7D. After blocking, standard OM or samples were added to the wells. Then, the amount of OM bound to a well was assayed indirectly by using alkaline phosphatase-conjugated streptavidin (Oncogene, Boston, USA) via biotinylated second mAb(s), after which each sandwich ELISA system was named. Absorbance at 405 nm was measured for the enzyme reaction.

3. RESULTS AND DISCUSSION

Monoclonal antibodies and sandwich ELISAs for OM

We have established 3 hybridoma clones designated 5C, 7D, and 10D. They produce respective mAbs with characteristic reactivity against OM. MAb 5C is specific to N-OM, mAb 6H is specific to H-OM, and mAb 7D is specific to the carbohydrate moiety of OM, therefore capable to recognize N- and H-OMs equally (Hirose *et al.*, in press). These mAbs did not cross-react with proteins from other sources such as cow's milk, wheat flour, buckwheat flour, soy bean, peanut, yeast extract and meats from beef, pork and chicken on ELISA.

Then, we developed the sandwich ELISA systems capable to distinguish N-OM and/or H-OM (Systems 5C, 6H, and 7D in Fig. 1). MAb 7D was selected as the common first antibody because of its binding capacity to both N- and H-OMs and each biotinylated mAb was used as the second antibody. Property of each sandwich ELISA was dependent on that of the biotinylated second antibody. In the case of biotinylated mAb 5C, System 5C was sensitive to N-OM about 30 times higher than to H-OM. In the case of biotinylated mAb 6H contrarily, System 6H was almost specific to H-OM. Several ng/ml of N- or H-OM was able to be selectively detected by each system. Although a sandwich ELISA is usually unable to set up by a single mAb, it was successful in the case of mAb 7D because of 4 or 5 carbohydrate chains per

one molecule of OM. System 7D showed equal reactivity against N- and H-OMs, indicating the possibility to determine total OM content irrespective of the degree of heat denaturation of OM. It is a very important nature required for the allergen detection system because of the allergenicity of H-OM (Hirose *et al.*, in press). The detection limit of System 7D was rather high and about 100 ng/ml for both N- and H-OMs.

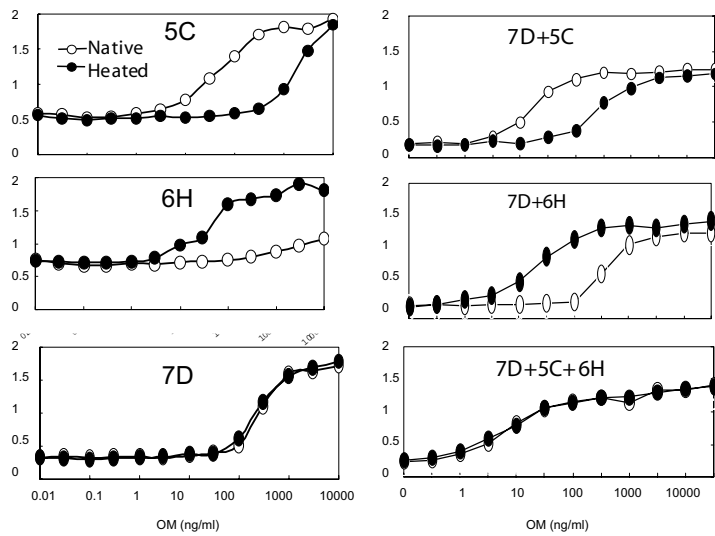


Figure 1. ELISAs for the quantitative analysis of N- and H-OMs.

Sandwich ELISAs were constructed with mAb 7D as a common solid phase antibody and 50 μ l of biotinylated second mAb(s). In Systems 5C, 6H, and 7D was used 0.5 μ g/ml of each biotinylated mAb. For the oligoclonal ELISA, 0.5 μ g/ml each of biotinylated mAbs 5C and 7D were used in System 5C · 7D, 0.2 μ g/ml of biotinylated mAb 6H and 0.5 μ g/ml of biotinylated mAb 7D in System 6H · 7D, and 0.2 μ g/ml of biotinylated mAb 6H and 0.5 μ g/ml each of biotinylated mAbs 5C and 7D in System 5C · 6H · 7D. N-OM (open circle) and H-OM (closed circle) were used as standards.

Oligoclonalization of ELISA

For the improvement of the sensitivity of system 7D, oligoclonalization of second antibody was examined, because ELISA constructed with polyclonal antibody usually exhibits higher sensitivity than that with mAb. When a mixture of biotinylated mAbs 5C and 7D

was used as a second antibody, sensitivity only to N-OM was improved about 30 times (System 5C·7D in Fig. 1). Contrarily by using that of biotinylated mAbs 6H and 7D, similar enhancement of sensitivity was seen only to H-OM in turn (System 6H·7D in Fig. 1). Then by using that of three biotinylated mAbs, the original sensitivity of System 7D was finally improved about 100 times for both N- and H-OMs (System minimum and essential to get that sensitivity. Increase of biotinylated mAb 6H was inhibitory. We used only mAb 7D as a solid antibody here, because we can determine N- and/or H-OM according to the purpose by selecting proper second antibody from biotinylated mAb 7D, 5C, 6H, or a mixture of them. Optimization of an oligoclonal ELISA should be examined in each case.

Extraction with denaturing reagents

To enhance the overall sensitivity of the assay system, it is important to improve not only determination method but also extraction method. We found that mAb 7D immobilized onto a ELISA plate was stable even in the presence of 0.1% SDS and 0.1M β -mercaptoethanol at 37°C for 60 min (data not shown). It has been known that proteinous samples can be usually well solubilized in the condition of sample preparation for SDS-PAGE (Laemmli, 1970). Then, we decided to extract OM from foods in 1% SDS and 1M β -mercaptoethanol at 100°C for 5 min. After cooling and 20 times dilution with PBS, OM was determined with oligoclonal System 5C-6H-7D (Table 1). There was not big difference between the values extracted with or without denaturing reagents in the case of simple or moderately processed foods. However, 6-30 fold difference were seen for foods processed under complex and/or severe conditions. Extraction with the denaturing reagents was effective even for well soluble and non-heat precipitable protein such as OM, much more for many other proteins that are insoluble or difficult to be soluble in water and heat-precipitable. Moreover, if a food is proved to be not containing allergens or non-allergenic by an *in vitro* tests because of some masking effects such as modification, aggregation (Kato *et al.*, 2001), and immune complex formation (Hirose *et al.*, 2001), its allergenicity after eating is uncertain. Extraction with denaturing reagents might enable us to determine antigens in foods closer to an absolute quantity by removing masking factors.

Table 1. Determination of OM in foods extracted with or without denaturing reagents.

Fresh chicken egg was boiled in water for 20 min or retorted for 20 min at 120°C. Kamaboko (a traditional Japanese food, semicylindrically shaped fish paste), steamed bun, hard biscuit, and Chinese noodle with labels of egg usage were purchased at a market. After homogenizing whole eggs and foods individually, two gram each was mixed vigorously in 38 ml of PBS with or without 1% SDS and 1M β -mercaptoethanol (Mer). Samples extracted with denaturing reagents were boiled at 100°C for 5 min and cooled. After centrifugation at 13,000g for 10 min, a portion of the supernatant was diluted 20 times with PBS and OM was determined by System 5C·6H·7D in Fig.1. Values were expressed as mg/g.

Food	Extraction	
	without SDS & Mer	with SDS & Mer
Raw egg	10.3	13.3
Boiled egg	11.2	11.4
Retorted egg	7.5	8.5
Kamaboko	0.080	0.054
Steamed bun	0.025	0.179
Hard biscuit	0.021	0.298
Chinese noodle	0.004	0.105

There is an international movement for allergen labeling, as seen in the agreement of the Joint FAO/WHO Codex Alimentarius Commission Session in 1999. In consideration of worldwide distribution of foods today, development of an international common method is required for the adequate determination of allergens. Oligoclonal system is suitable for the purpose because it is more stable than polyclonal system in specificity and quantity due to the nature of mAbs.

4. REFERENCES

- Bernhisel-Broadbent J, Dintzis HM, Dintzis RZ, and Sampson HA (1994) *J Allergy Clin Immunol* 93: 1047-1059.
- Hirose J, Ito S, Hirata N, Kido S, Kitabatake N and Narita H (2001) *Biosci Biotechnol Biochem* 65: 1438-1440.
- Hirose J, Kitabatake N, Kimura A and Narita H (2004) *Biosci Biotechnol Biochem*, 68(12), in press.
- Honjoh T, Muraoka S, Mamekoshi S and Sakai M (2002) *Food and Food Ingredients J Jpn* 206: 13-22.
- Imai T and Iikura Y (2003) *Jpn J Allergol* 52: 1006-1013.

- Kanagawa Y and Imamura T (2002) *J Food Hyg Soc Jpn* 43: 269-271.
Kato Y, Oozawa E, Matsuda T (2001) *J Agric Food Chem* 49: 3661-3665.
Laemmli UK (1970) *Nature* 227: 680-685.
Narita H, Asaka Y, Ikura K, Matsumoto S and Sasaki R (1995) *Eur J Biochem* 228: 855-862.
Sampson HA and Ho DG (1997) *J Allergy Clin Immunol* 100: 444-451.
Takahata Y and Morimatsu F (2002) *Food and Food Ingredients J Jpn* 206: 23-32.

SAFETY EVALUATION OF TISSUE ENGINEERED MEDICAL DEVICES USING NORMAL HUMAN MESENCHYMAL STEM CELLS

Rumi Sawada, Tomomi Ito, Yoshie Matsuda, and Toshie Tsuchiya
Division of Medical Devices, National Institute of Health Sciences

Abstract: For safety evaluation of tissue engineered medical devices using normal human mesenchymal stem cells (hMSC), in this study, some genes expressions in hMSC were compared with those in two kinds of the tumor cells (HeLa and HepG2). Effects of the passage number of hMSC on the gene expressions were also investigated using quantitative real-time RT-PCR. The proliferation speed of hMSC was lowered with the cell passage number. The mRNA expressions of c-myc oncogene and nucleostemin in the tumor cells (HeLa and HepG2) were significantly higher than in the stem cells (hMSC). And the mRNA expressions of them in hMSC decreased with the passage number. Wnt-8B mRNA was expressed in the tumor cells (HeLa and HepG2), but not in the stem cells (hMSC) in any passage number. Although these results suggest change in these expression levels are not directly related to the tumorigenesis of hMSC, it is discussed that mRNA expression levels of c-myc oncogene, nucleostemin, and Wnt-8B can be used as an index of hMSC tumorigenesis.

Key words: hMSC, tumorigenesis, c-myc, nucleostemin, Wnt-8

1. INTRODUCTION

Several recent studies demonstrate the potential of tissue engineering for regenerative therapy using somatic stem cells. Human mesenchymal stem cells (hMSC) derived from bone marrow aspirates have the potentiality to differentiate into osteocytes, chondrocytes, myocytes, stromal cells, tenocytes, adipocytes, and so on. Therefore, the autologous cell or tissue transplantation using hMSC was noticed as the medical treatment under the various kinds of clinical conditions. On the

other hand, owing to the similarity to the tumor cells, the stem cells also possess the ability of cell proliferation. Consequently, it is required to evaluate the safety of hMSC when that is used for tissue engineered medical devices. In this study, hMSC was compared with two kinds of the the tumor cells, HeLa (human cervix cancer) and HepG2 (human hepatoma), by investigating the differences in some genes expressions of each cells. Effects of the passage number of hMSC on the gene expressions were also investigated using quantitative real-time RT-PCR.

2. MATERIALS AND METHODS

Cell culture. Human mesenchymal stem cells (hMSC) purchased from the Cambrex Bio Science Walkersville, Inc. (MD, USA) was cultured in Mesenchymal Stem Cell Basal Medium (MSCBM; Cambrex Bio Science Walkersville, Inc.) supplemented with Mesenchymal Cell Growth Supplement (MCGS; Cambrex Bio Science Walkersville, Inc.), L-Glutamine and Pen/Strep at 37°C under a 5% CO₂ atmosphere. The cells was seeded at a density of 6,000 cells / cm² and subcultured when they are just sub-confluent (approximately 90% confluent) up to 10th passage.

Quantitative RT-PCR. For quantitative RT-PCR, total RNA was extracted from hMSC of 1st, 3rd, 5th and 10th passage cultures with ISOGEN (NIPPON GENE CO., LTD.). RNA was then reverse-transcribed into cDNA using First Strand cDNA Synthesis Kit for RT-PCR (AMV) (Roche Diagnostics; Tokyo, Japan). Primers and annealing temperatures for the c-myc oncogene, nucleostemin, and Wnt-8B are summarized in Table 1. Amplifications of them were carried out for 10s at 95°C, for 15s at each annealing temperature, and for 12s at 72°C for 40 cycles. PCR was performed in Light Cycler Fast Start DNA Master SYBR Green I (Roche Diagnostics) in Roche Light Cycler (software version 4.0).

Table 1. Primers and annealing temperatures used for Real time RT-PCR

Gene name	GenBank™ accession number	Primer orientation	Nucleotide sequence	Starting sequence position	Size for the PCR amplicon(bp)	Annealing Temp (°c)
c-myc	V00568	Forward	5'- GCG AAC ACA CAA CGT C -3'	1626	315	50
		Reverse	5'- CAA GTT CAT AGG TGA TTG CT -3'	1940		
nucleostemin	X91940	Forward	5'- CCA TTC GGG TTG GAG TAA -3'	782	284	50
		Reverse	5'- CTG TCG AGC ATC AGC C -3'	1065		
Wnt-8B	NM_014366	Forward	5'- AGT GAC AAT GTG GGC T -3'	331	244	60
		Reverse	5'- CGT GGT ACT TCT CCT TCA G -3'	574		

3. RESULTS

In this study, for safety evaluation of tissue engineered medical devices using normal human mesenchymal stem cells (hMSC), some genes expressions in hMSC were compared with those in two kinds of the tumor cells (HeLa and HepG2). At first, effect of the passage number on hMSC proliferation was investigated. The proliferation speed of hMSC was lowered with the cell passage number (Fig. 1).

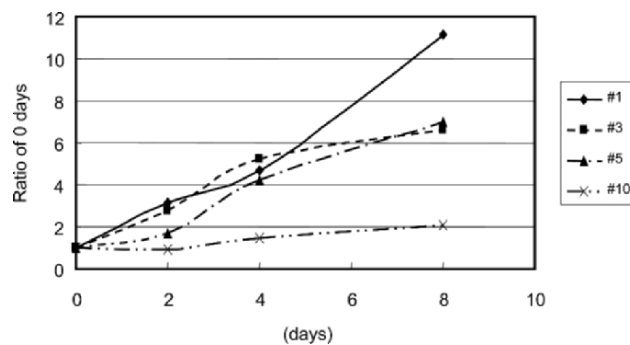


Fig. 1. Effect of the passage number on the cell growth curves of hMSC.

The mRNA expressions of c-myc oncogene in the tumor cells (HeLa and HepG2) were significantly higher than in the stem cells (hMSC) (Fig. 2). The mRNA expressions of c-myc oncogene in hMSC in the 3rd and 5th passages were higher than in the 1st and 10th passages (Fig. 3). Similarly to c-myc, the mRNA expressions of nucleostemin in the tumor cells (HeLa and HepG2) were significantly higher than in the stem cells (hMSC) (Fig. 4). The mRNA expressions of nucleostemin in hMSC decreased with the passage number (Fig. 5). Wnt-8B mRNA was expressed in the tumor cells (HeLa and HepG2), but not in the stem cells (hMSC) in any passage number (Fig. 6).

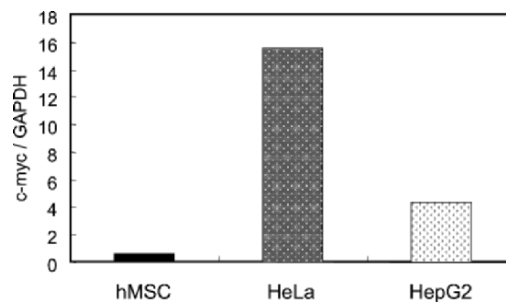


Fig. 2. The mRNA expression c-myc oncogene in hMSC, HeLa, and HepG2.

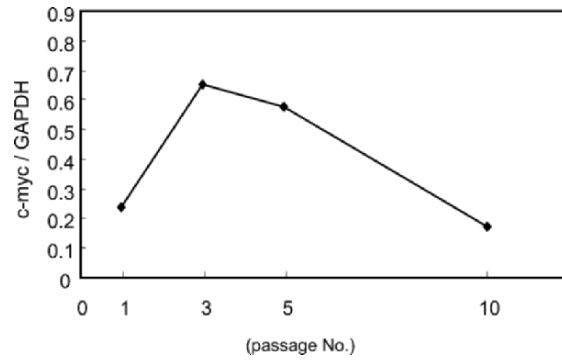


Fig. 3. Effect of the passage number on the mRNA expression c-myc oncogene in hMSC.

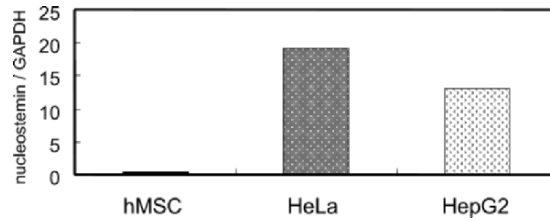


Fig. 4. The mRNA expression nucleostemin in hMSC, HeLa, and HepG2.

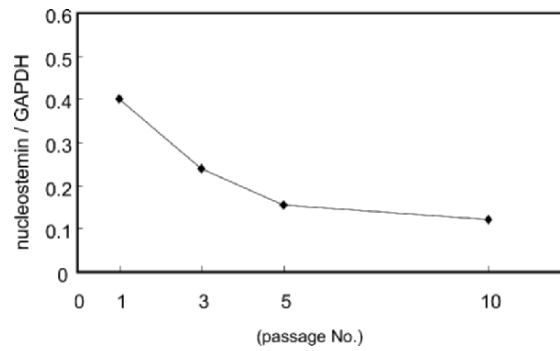


Fig. 5. Effect of the passage number on the mRNA expression of nucleostemin in hMSC.

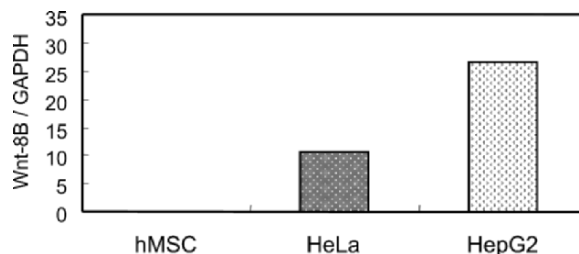


Fig. 6. The mRNA expression Wnt-8B in hMSC, HeLa, and HepG2.

4. DISCUSSION

In this study, effects of the passage number on the gene expression in hMSC were investigated. At first, *c-myc* oncogene and Wnt-8B concerned with cell proliferation and tumorigenesis were noticed by gene chip analysis (data not shown). Therefore, *c-myc* oncogene and Wnt-8B mRNA expressions in four kinds of passage numbers (#1, #3, #5, and #10) of hMSC were measured by quantitative real time RT-PCR. Furthermore, nucleostemin that concerned with proliferation of both stem cells and tumor cells (1) was also investigated. The proliferation speed of hMSC was lowered with the cell passage number (Fig. 1).

The mRNA expressions of *c-myc* oncogene, Wnt-8B, and nucleostemin in 1st, 3rd, 5th, and 10th passage of hMSC were investigated using quantitative real time RT-PCR. The mRNA levels of *c-myc* oncogene were decreased with the passage number from 3rd to 10th (Fig. 3). The mRNA expression of nucleostemin was decreased with the passage number (Fig. 5). In all three genes, their mRNA expressions of the stem cells (hMSC) were significantly lower than two kinds of tumor cells (HeLa and HepG2) (Fig. 2, 4, and 6). In hMSC, Wnt-8B was not expressed in any passage numbers. Although these results suggest that change in these expression levels are not directly related to the tumorigenesis of hMSC, it is discussed that mRNA expression levels of *c-myc* oncogene, nucleostemin, and Wnt-8B can be used as an index of hMSC tumorigenesis.

5. REFERENCES

- 1) Tsai R.Y.L. and McKay R.D.G., A nucleolar mechanism controlling cell proliferation in stem cells and tumor cells, *GENES & DEVELOPMENT* 16, 2991-3003 (2002).

EFFECT OF BIODEGRADABLE POLYMER POLY (L-LACTIC ACID) ON THE CELLULAR FUNCTION OF HUMAN ASTROCYTES

Naohito Nakamura and Toshie Tsuchiya

*Department of Medical Devices, National Institute of Health Science, Kamiyoga
1-18-1 Setagaya-ku, Tokyo, Japan*

Abstract: The objective of this study is to assay the efficiency and safety of poly (L-lactic acid) (PLLA) on human neural tissues. We used normal human astrocytes (NHA) to clarify effects of PLLA on their proliferation and differentiation. We cultured NHA with PLLA for one week, and determined NHA cell number and neural cell specific marker genes to assay their proliferation and development, respectively.

Cell proliferation was determined by tetrazolium salt (MTT) assay. The cell number of astrocytes cultured with 50 µg/ml PLLA was 70% of control. It has been suggested that a part of astrocytes had neural precursor cell activity that give rise to neuron, oligodendrocyte and astrocyte. We compared gene expression of neural cell specific markers. Expression of Nestin, a specific gene for neural precursor cell was decreased in a dose-dependent manner, while expression of specific genes for neuron markers and astrocyte markers were not different from that of control.

PLLA suppressed astrocyte proliferation in dose dependent manner. A neural precursor cell marker decreased when astrocytes were cultured with PLLA. These findings suggest that PLLA reduces proliferation and developmental potential of astrocytes.

Key words: Astrocyte, PLLA, proliferation, development

1. INTRODUCTION

Brain and neural clinical hospitality have been rapidly advancing, including implantation techniques. Otherwise discreditable accidents sometimes happened. It is necessary to study efficiency and safety of techniques and materials for brain and neural cell proliferation and development. Precise mechanisms by which neurogenesis and gliogenesis are regulated in the central nervous system (CNS) remain to be elucidated. Telencephalic neuroepithelial cells contain neural precursors that give rise to the neuronal lineage and the glial lineage, which includes astrocytes and oligodendrocytes (1, 2). The fate of neural precursors in the developing brain is believed to be determined by intrinsic cellular programs and by external cues, including implantation of biomaterials and cytokines (3). Doetsch et al. demonstrated that subventricular zone (SVZ) astrocytes act as neural stem cells in both the normal and regenerating brain (4). Neural stem cells, endogenously present in spinal cord *in vivo*, proliferate in response to injury, yet the vast majority of newly generate cells are glial fibrillary acidic protein (GFAP)-positive astrocytes (5). In addition, adult hippocampus-derived neural stem cells, when implanted into adult brain in such a region as cerebellum or striatum, have been reported to differentiate predominantly into glial cells (2, 6, 7).

Biodegradable polymers have been attractive candidates for scaffolding materials because they degrade and the new tissues are formed, although adverse events such as foreign-body reaction, inflammation and tumor formation were reported in clinical human and animal study. These scaffolds have shown great promise in the research of engineering a variety of tissues. Biodegradable polymer poly (L-lactic acid) (PLLA) is frequently implanted in cranial surgery etc. However, to engineer clinically useful tissues and organs is still a challenge. The understanding of the principles of scaffolding is far from satisfactory, still more its effect and safety on neural tissues are not known. We previously reported PLLA suppressed proliferation and differentiation of fetal rat midbrain neural precursor cells (8). In this report, we investigated the effect of PLLA on normal human astrocytes (NHA).

2. MATERIALS AND METHODS

Astrocyte cell culture

We used normal human astrocyte (Cambrex Bio Science, Walkersville, MD). NHA were seeded into 12-well plates for quantitative RT-PCR at a density of 2×10^4 /well, or 24-well plates for MTT assay at a density of 1×10^4 /well in ABM medium(Cambrex Bio

Science) supplemented with 5% FCS, rhEGF and IGF, and cultured in a humidified atmosphere of 5% CO₂ in 95% air at 37°C.

PLLA preparation

Stock solutions of PLLA were made in dimethyl sulfoxide (DMSO) and final concentration of DMSO was 0.1%; this concentration did not affect proliferation and development of NHA. Control cultures were incubated with 0.1% DMSO. Stock solutions of lactic acid and tin chloride were made directly in ABM medium.

MTT assay

After cell culturing for 1 week with PLLA, the viability of NHA cells was determined by MTT assay. The TetraColor ONE (Seikagaku Kogyo, Tokyo, Japan) was used to measure changes of cell numbers. This assay is a nonradioactive alternative to tritium-thymidine incorporation. The system measures the conversion of tetrazolium salt compound into a soluble formazan product by the mitochondria of living cells. NHA in 24-well plates were cultured as described above. One week after NHA cultured with vehicle or PLLA, the media were replaced with 300 µl of fresh medium containing 6 µl TetraColor ONE reagent. After 2h, samples were measured in a micro plate reader.

Expression of neural cell marker genes

Total RNA was prepared from NHA using a modified acid guanidium thiocyanate-phenol-chloroform method. The total RNA treated with RNase-free DNase (Boehringer Mannheim, Mannheim, Germany) were subjected to reverse transcription using oligo d(T) primer (Toyobo, Tokyo, Japan) and superscript II reverse transcriptase (Gibco BRL, Gaithersburg, MD) at 42°C for 30 min followed by RNase H treatment. Aliquots of the cDNA (1/20) were used as templates for PCR analysis using Lightcycler system (Roche, Mannheim, Germany). PCR amplification was performed in a total volume of 20 µl mixture including 1 µl of RT reaction, 2 µl Light Cycler-Fast Start Reaction Mix SYBR Green 1 (Roche, Mannheim, Germany), 0.5 µM/liter of each primer, and 3 mmol/liter MgCl₂. The PCR program consisted of 40 cycles of 8 sec at 94°C, 5 sec at 65°C, 10 sec at 72°C. Primer sequences for amplification are 5'-CTAAGGAGGAGATTGGACAGG-3' and 5'-AGTGGTGGCAGTGATTT CAGT-3' for Nurr-1 amplification, 5'-TCCGCTGCTCGCCGCTCCTAC-3' and 5'-TCATCTCTGCCCGCTCACTGG -3' for GFAP amplification, 5'-TCGCCCTGCCCACTTGACTTC-3' and 5'-TTCCACACCTCCACGCTC TGA-3' for Id-3 amplification, 5'-GAGATCAGAGCCCAGGATGCT-3' and 5'-CTGAGGGGTGGTGCCAAGGAG -3' for Nestin amplification, 5'-ACCACAGTCCATGCCATCAC-3' and 5'-

TCCACCACCCTGTTGCTGT A-3' for GAPDH. RNA preparation and RT-PCR in the present study were performed in triplicate.

Statistical analysis

The Fisher's PLSD was used to compare the PLLA concentration and relative expression levels of neural specific marker mRNA.

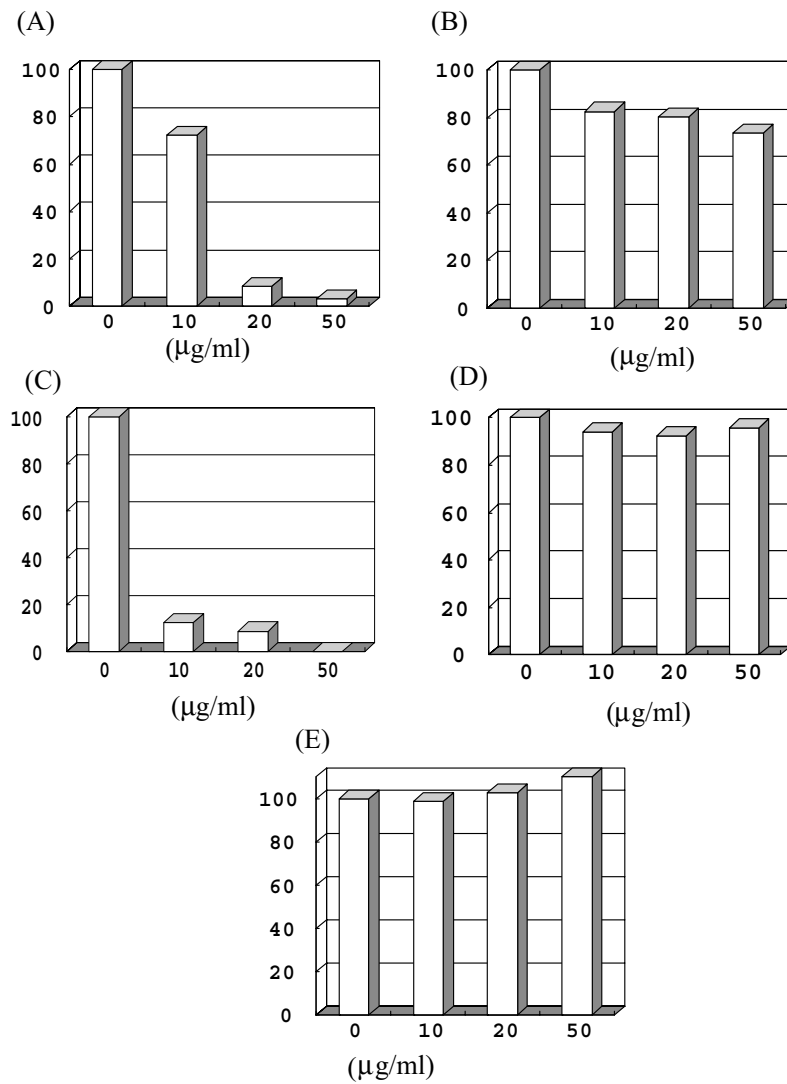


Fig. 1 Effect of PLLA on NHA proliferation (A) PLLA 3.000 (B) PLLA 5.000 (C) PLLA 11.000 (D) Lactic acid (E) Tin chloride

3. RESULTS AND DISCUSSION

NHA proliferation

We used three kinds of PLLA. PLLA 3000 (PLLA, Mw 3000) is made without catalyst. PLLA 6000 (PLLA, Mw 5000) is made with organic tin catalyst. PLLA 11000 (PLLA, Mw 11000) is made with catalyst tin chloride, contains 590 ppm tin. After a week culture with PLLA, we detected cell number of NHA using MTT assay. Cell numbers were decreased in a dose-dependent manner of PLLA (Fig. 1A-C). The cell number of NHA cultured with 50 µg/ml of PLLA 3000, PLLA 5000 and PLLA 11000 were 15%, 70% and 7.8% of that of control respectively.

Whether tin ion included in PLLA affected NHA proliferation or not, we added tin chloride to NHA culture medium (Fig. 1D). The concentration of tin chloride at 50 ng/ml did not affect NHA proliferation. PLLA is hydrolysed in medium, we assayed lactic acid (LA), a monomer of PLLA was also tested by the MTT assay using NHA cells. (Fig. 1E). There was no effect on the cell number of NHA culture with LA monomer. The cause of PLLA effect for NHA was neither included tin ion nor degraded LA monomer. It was probably the effect of PLLA itself and/or degraded LA oligomers.

Lam and his co-workers demonstrated that predegraded PLLA (P-PLLA; 25 kGy gamma-irradiation) caused signs of cell damage, cell death, and cell lysis due to phagocytosis of a large amount of P-PLLA particles (9). Phagocytosis of LA oligomers or degraded PLLA particles may affect the proliferation and development of NHA. It is necessary to know culture medium with PLLA contains how much PLLA particles, PLLA oligomer and organic tin.

Gene expression of neural cell specific markers

It has been suggested that a part of astrocytes contain neural precursor cell activity that give rise to neuron, oligodendrocyte and astrocyte itself. The recent discovery of stem cell populations in the CNS has generated intense interest, since the brain has long been regarded as incapable of regeneration (5, 10, 11). Neural stem cells (NSCs) have capability for expansion and differentiation into astrocytes, oligodendrocytes, and neurons in vitro (12, 13). NSCs have been suggested to have therapeutic potential for central nervous system regeneration (14-16).

They express their original specific genes, neural cell specific markers. Neural precursor cells express Nestin, a class IV intermediate filament protein. Differentiated neuron expresses Nurr-1, a transcription factor and Id-3, a transcription inhibitory factor. Astrocyte expresses

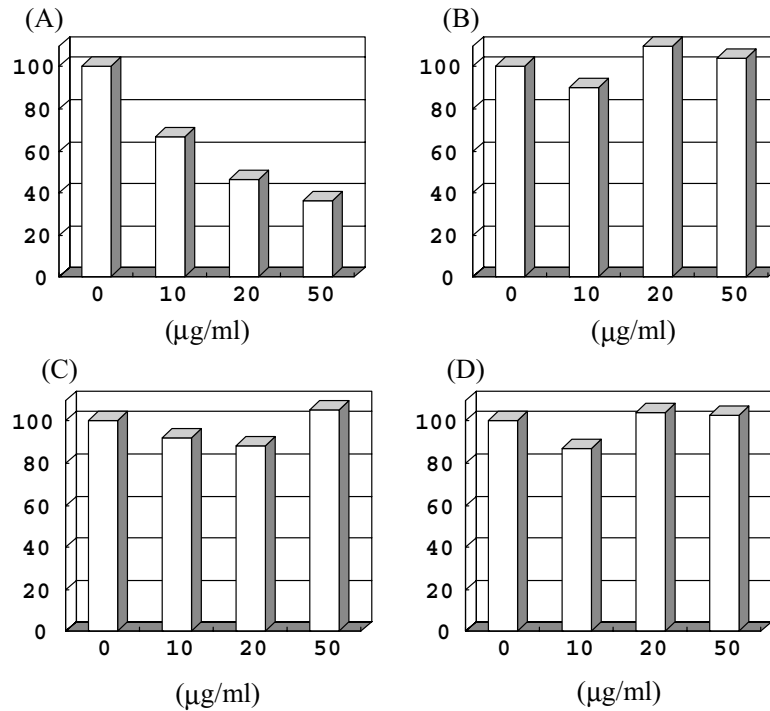


Fig. 2 Effect of PLLA on neural specific gene expression.
(A) Nestin (B) Nurr-1 (C) GFAP (D) Id-3

GFAP, a glial filamentous acidic protein. We compared gene expression of neural cell specific markers. Expression of Nestin, a neural precursor cell marker decreased with the dose of PLLA5000. The expression of Nestin in NHA cultured with 50 µg/ml PLLA was 30% of control (Fig. 2A). Expressions of the other genes that assayed in this study were similar to control (Fig. 2B-D).

Expression of Nestin was decreased when NHA were cultured with PLLA suggested that PLLA decreased population of neural precursor cells. There were two kinds of possibilities. (1) PLLA leads NHA to gliogenesis. Nakashima et al. reported that Gliogenesis significantly reduced the number of cells expressing Nestin and the number of cells expressing microtubule-associated protein 2 (MAP2), a neuronal marker. (2) When neural precursor cells specifically phagocytosed PLLA, they go to programmed cell death, apoptosis or loose their developmental potential as neural precursor cells. Lam et al. demonstrated that PLLA caused signs of cell damage, cell death, and cell lysis due to phagocytosis of a large amount of P-PLLA particles. Phagocytosis of PLLA may affect proliferation and development of NHA.

4. REFERENCES

- [1] McKay, R. (1997) Stem cells in the central nervous system. *Science* 276, 66-71.
- [2] Gage, F. H. (2000) Mammalian neural stem cells. *Science* 287, 1433-1438.
- [3] Nakashima K. et al. (2001) BMP2-mediated alteration in the developmental pathway of fetal mouse brain cells from neurogenesis to astrocytogenesis. *Pro. N. A. S.* 98, 5868-5873.
- [4] Doetsch F. et al. (1999) Subventricular zone astrocytes are neural stem cells in the adult mammalian brain. *Cell* 97, 703-716.
- [5] Johansson C. B. et al. (1999) Identification of a neural stem cell in the adult mammalian central nervous system. *Cell* 96 25-34.
- [6] Gage F. H. et al. (1995) Survival and differentiation of adult neuronal progenitor cells transplantation to the adult brain. *Pro. N. A. S.* 92, 11879-11883.
- [7] Suhonen J. et al. (1996) Differentiation of adult hippocampus-derived progenitors into olfactory neurons in vivo. *Nature (London)* 383, 624-627.
- [8] Tsuchiya T. et al. (2002) Effects of biodegradable polymers on the cellular function of chondrogenesis. (in Japanese) *Bio Industry* 19, 30-37.
- [9] Lam K. H. et al. (1993) The effect of phagocytosis of poly (L-lactic acid) fragments on cellular morphology and viability. *J. Biomed. Mater. Res.* 27, 1569-1577.
- [10] Reynolds B. A. et al. (1992) Generation of neurons and astrocytes from isolated cells of the adult mammalian central nervous system. *Science* 1707-1710.
- [11] Richards L. J. et al. (1992) De novo generation of neuronal cells from the adult mouse brain. *Pro. N. A. S.* 89, 8591-8595.
- [12] Svendsen C. N. et al. (1996) Survival and differentiation of rat and human epidermal growth factor-responsive precursor cells following grafting into the lesioned adult central nervous system. *Exp. Neurol.* 137, 376-388.
- [13] Flax J. D. et al. (1998) Engraftable human neural stem cells respond to development cues, replace neurons, and express foreign genes. *Nat. Biotech.* 16, 1033-1039.
- [14] Woodbury D. et al. (2000) Adult rat and human bone marrow stromal cells differentiate into neurons. *J. Neurosci. Res.* 61, 364-370.
- [15] Sanches-Ramos J. et al. (2000) Adult bone marrow stromal cells differentiate into neural cells in vitro. *Exp. Neurol.* 164, 247-256.
- [16] Deng W. et al. (2001) In vitro differentiation of human marrow stromal cells into early progenitors of neural cells by conditions that increase intracellular cyclic AMP. *Biochem. Biophys. Res. Commun.* 286, 779-785.

IMMUNOLOGICAL ANALYSIS OF EPIDERMAL-TYPE TRANSGLUTAMINASE (TGase 3) IN EPITHELIUM

Kiyotaka Hitomi, Kanae Yamamoto, Koji Nishi, Yoshiaki Sugimura,
and Masatoshi Maki

*Graduate School of Bioagricultural Sciences, Nagoya University, Chikusa, Nagoya,
464-8601, Japan*

Abstract: Transglutaminases (TGase) are enzymes that catalyze the Ca^{2+} dependent cross-linking reaction between a γ -carboxyamide group of glutamine and an ϵ -amino group of lysine or other primary amine. Among these isozymes, TGases 1 and 3 are involved in the formation of the cornified envelope, where they function to cross-link structural proteins during epidermal terminal differentiation.

We developed monoclonal antibodies against human recombinant TGase 3. Using these antibodies, we analyzed TGase 3 expression in epidermis as well as cultured epidermal keratinocytes as a function of differentiation. In skin epidermis, TGase 3 was expressed in the cells of granular and cornified layers consistent with its role in cornified envelop formation. In the primary cultured keratinocytes, TGase 3 was expressed entirely in the cytoplasm of differentiating cells.

TGase 3 activation during keratinocyte differentiation involves cleavage of a 77 kDa zymogen by limited proteolysis to release 47 and 30 kDa fragments. Although the dispase (bacterial protease) was only known enzyme for limited proteolysis *in vitro*, the responsible protease *in vivo* had not been clear. Recently, cathepsins S and L appeared to proteolyze the recombinant TGase 3. We have confirmed the enzymatic activation of TGase 3 zymogen by cathepsins and then determined the cleavage sites by these proteases.

Key words: transglutaminase, epidermis, keratinocyte, cathepsin.

1. INTRODUCTION

Transglutaminases (TGase) are enzymes that catalyze the Ca^{2+} dependent cross-linking reaction between a γ -carboxamide group of glutamine and an ϵ -amino group of lysine or other primary amine¹. To date, eight human TGase isozymes (Factor XIII, TGases 1-7) have been found comprising a large protein family. Among these isozymes, TGases 1 and 3 are involved in the formation of the cornified envelope, where they function to crosslink structural proteins such as involucrin, loricrin and small proline-rich proteins during epidermal terminal differentiation². Since the cornified envelope plays a role as a barrier function, TGases is critical for the skin formation.

Although structural and biochemical characterization of recombinant TGase 3 has been reported, it has been difficult to investigate the distribution of TGase 3 due to the low levels of expression in the skin and cultured keratinocytes^{3,4,5}. Because the primary structures of the TGases (1, 2, 3, and 5) are quite similar, it is important to develop antibodies that were monospecific for TGase 3, particularly for immunohistochemical analysis. Therefore, in order to characterize the expression profile in epidermal keratinocytes more specifically, we developed monoclonal antibodies against human recombinant TGase 3.

TGase 3 activation during keratinocyte differentiation involves cleavage of a 77 kDa zymogen by an unknown protease to release fragments of 47 and 30 kDa fragments which then associate non-covalently to form the active enzyme³. *In vitro*, dispase, a bacterial enzyme, is able to proteolyze the zymogen form resulting in proteolytic activation. The responsible enzyme for TGase 3 activation has remained unknown. While TGase 1 is proteolyzed for activation by calpain, a Ca^{2+} dependent cellular protease, TGase 3 could not be digested⁶. Additionally, responsible enzyme was investigated based on the information of abnormal cornification in the cystatin M/E knockout mice⁷.

2. MATERIALS AND METHODS

2.1 Establishment of monoclonal antibodies

As antigen, recombinant human TGase 3 was expressed and purified from bacteria expression system as described previously. Splenocytes from the immunized mice were prepared and hybridomas were established using mouse myeloma Sp2 by standard methods. Among the various hybridomas, the line

secreting most specific monoclonal antibody (C2D) against human TGase 3 were selected by ELISA.

2.2 Immunochemical analysis of TGase 3

For the preparation of total cellular lysates from human skin, frozen epidermis was homogenized in liquid nitrogen. The powder was solubilized with Urea/Tris extraction buffer. Immunohistochemical analysis was performed on formalin-fixed human skin embedded in paraffin using the avidin-biotin peroxidase method. The immunoreaction was detected using diaminobenzidine.

2.3 Digestion and activation of recombinant TGase 3

Recombinant human cathepsins S and L were used for digestion of recombinant TGase 3. In each case, the molar ratio (cathepsins: TGase) is around 1:100 in an appropriate buffer. In the case of dispase, reaction condition was similar to the method as described previously⁴. The reaction was stopped by the addition of E-64, an inhibitor for cystein protease upon measurement of enzyme activity. The enzymatic activity was determined by the measurement of incorporated biotinylated cadaverine into dimethylcasein.

3. RESULTS AND DISCUSSION

3.1 Preparation of recombinant TGase proteins and monoclonal antibodies

It has been difficult to pursue the TGase 3 localization using polyclonal antibodies because the primary structures of these TGases are quite similar. Therefore, we generated monoclonal antibodies that specifically detect human TGase 3⁸.

In order to confirm the specificity of the antibody, cross-reactivity to isozymes present in the skin (TGases 1, 2, and 5) was investigated. Each recombinant TGase was prepared in *E.coli* and the extracts was analyzed by SDS-PAGE.

In the Western blotting analysis, only human TGase 3 was detected as a single band by C2D, demonstrating the specificity of the monoclonal antibody for TGase 3 (Fig. 1). TGase 3 was detected in the human skin extract (Fig.1), mainly existing as a zymogen form. This result is similar with that obtained in the case of polyclonal antibody⁹.

3.2 Human TGase 3 is expressed in differentiating layers of stratified cornified epithelia

To examine the distribution of TGase 3 in the skin, we performed immunohistochemical staining using the monoclonal antibody, C2D (Fig. 2).

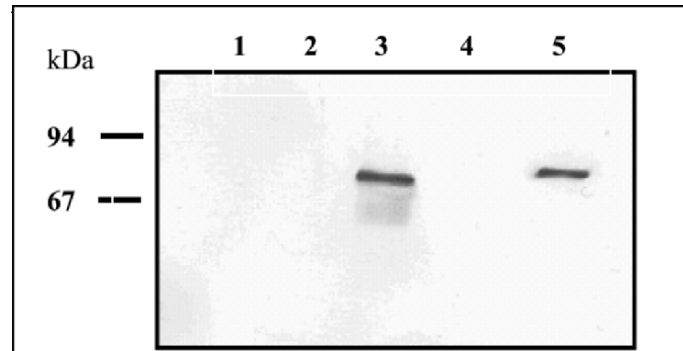


Figure 1. Cross reaction of monoclonal antibody with various TGase isozymes. TGase 1 (lane 1), TGase 2 (lane 2), TGase 3 (lane 3), TGase 5 (lane 4), human skin extract (lane 5).

In the human epidermis, the upper spinous and granular layers were clearly labeled by the antibody, demonstrating that TGase 3 is expressed late in the epidermal differentiation program. This result is consistent with that in Western blotting analysis of cultured keratinocytes (data not shown). In the case of differentiated keratinocytes, TGase 3 is detected in the cytoplasm (data not shown).

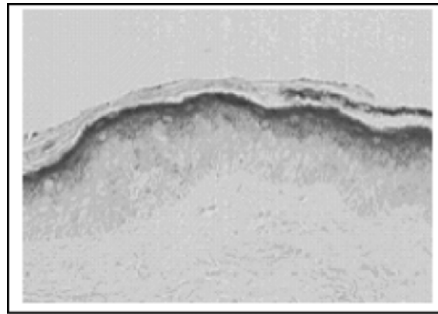


Figure 2. Detection of TGase 3 in the human skin epidermis by monoclonal antibody. The outer layer was stained.

3.3 Limited proteolysis and activation of TGase 3 by cathepsin

With respect to TGase 3, no protease(s) responsible for proteolytic activation has been found so far. However, very recently, using cystatin M/E knockout mice, legumain appeared to be involved in the activation of TGase 3. In the proposed model by Zeeuwen *et al.*, legumain activate cathepsins S and L, which resulted in the elevated crosslinking of loricrin, a substrate protein of TGase 3⁷. Therefore, to directly examine the proteolytic activation of TGase 3 by the proteases, recombinant TGase 3 was reacted with the cathepsins. Cathepsins are lysosomal protease responsible for digestion of various cellular proteins. Although most cathepsins are active in the acidic pH in the lysosome, both cathepsins S and L proteolyze even at the neutral pH.

As shown in the Fig. 3, cathepsin L proteolyzed 77 kDa of TGase 3 into the 47 and 30 kDa fragments as in the case of dispase digestion. The sizes of the cleaved fragments are very close to that obtained by dispase digestion. In the case of cathepsin S, digestion also showed the similar results (data not shown). E-64, a cysteine protease inhibitor, prevented both proteolysis, suggesting the digestion by cathepsins is specific. When using other major cathepsins, cathepsins B and D, could not proteolyze TGase 3 (data not shown).

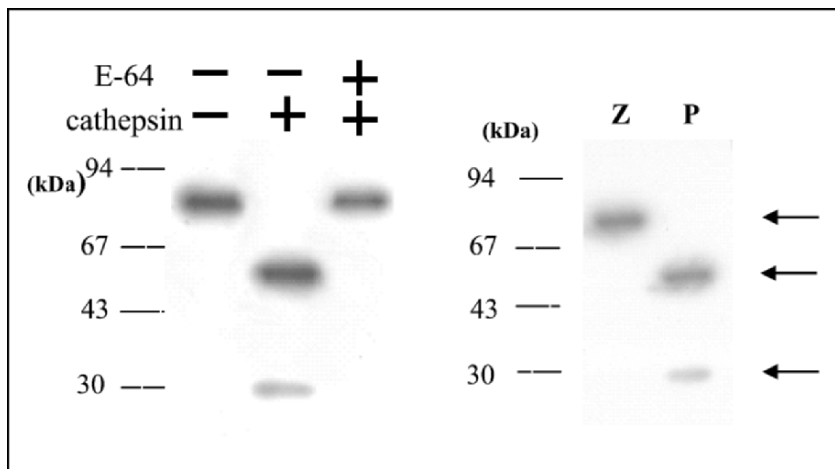


Figure 3. Recombinant TGase 3 was proteolyzed by cathepsin L (left) and dispase (right). The reaction products were subjected to the 10% SDS-PAGE following the Western blotting by polyclonal antibody against TGase 3. In the right figure, Z and P indicate the zymogen and proteolyzed form of TGase 3.

Next, we investigated whether the proteolysis resulted in the enzymatic activation of TGase 3. The TGase enzyme activity was determined by measurement of the incorporation of biotinylated cadaverine (primary amine) into dimethylcasein. As shown in the Fig. 4, compared to the zymogen form, proteolyzed TGase 3 by cathepsin L showed the apparent enzymatic activity. As in the case of cathepsin S digestion, similar result was obtained (data not shown).

Whether this proteolysis is responsible *in vivo* still remained unresolved. We determined the cleavage site of the N-terminal sequence of 30 kDa fragment that was released by the digestion with cathepsins S and L (data not shown). Investigation using the specific antibody recognizing this cleavage site is in progress.

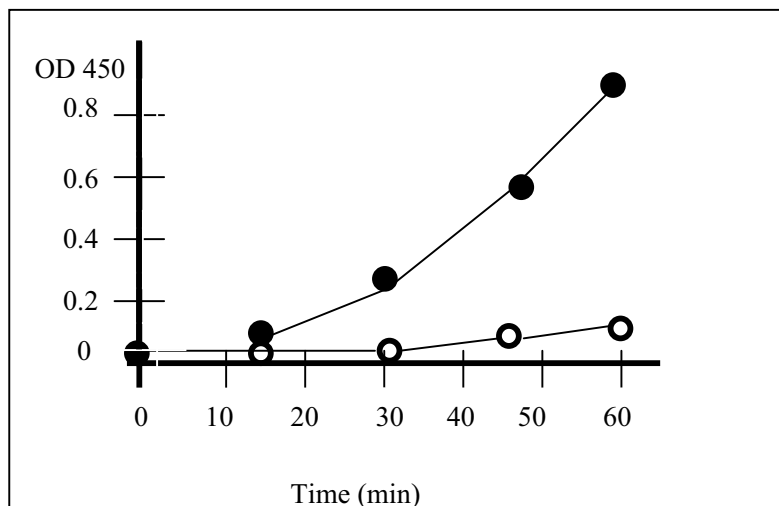


Figure 4. The enzymatic activity of TGase 3 digested by cathepsin L was measured. The open and closed circle indicates the zymogen and proteolyzed TGase 3, respectively. The enzymatic activity is indicated as OD450 of the reaction product.

4. ACKNOWLEDGEMENTS

We thank Prof. Beverly-Crunk Dale and Prof. Richard Presland (University of Washington, U.S.A.) for the collaboration of immunohistochemical analysis. We thank also Prof. Zweeuen (University Medical center, Nijmegen, The Netherlands) for the collaboration of proteolysis by TGase 3.

5. REFERENCES

- [1] Lorand L, Graham RM, Transglutamiases: crosslinking enzymes with pleiotropic functions, *Nat. Rev. Mol. Cell. Biol.* 4, 140-156 (2003)
- [2] Kalinin AE, Kajava AV, Steinert PM. Epithelial barrier function: assembly and structural features of the cornified envelope, *BioEssays* 24, 789-800 (2002)
- [3] Kim IJ, Gorman JJ, Park SC, Chung SI, Steinert PM. The deduced sequence of the novel protransglutaminase E (TGase 3) of human and mouse. *J. Biol. Chem.* 268, 12682-12690 (1993)
- [4] Hitomi K, Horio Y, Ikura K, Maki M. Analysis of epidermal-type transglutaminase expression in mouse tissues and cell lines. *Int J Biochem Cell Biol* 33, 491-498 (2001)

- [5] Ahvazi B, Kim HC, Kee S-H, Nemes Z, Steinert PM, Three-dimensional structure of the human transglutaminase 3 enzyme: binding of calcium ions changes structure for activation, *EMBO J.* 21, 2005 (2002)
- [6] Kim S-Y, Kim I-G, Chung S-I, Steinert PM, The structure of the transglutaminase 1 enzyme: Deletion cloning reveals domains that regulate its specific activity and substrate, *J Biol Chem*, 269, 27979-27986 (1994)
- [7] Zeeuwen PL, van Vlijmen-Willems IM, Olthuis D, Johansen HT, Hitomi K, Hara Nishimura I, Powers JC, James KE, op den Camp HJ, Lemmens R, Schalkwijk J. Evidence that unrestricted legumain activity is involved in disturbed epidermal cornification in cystatin M/E deficient mice. *Hum Mol Genet.* 13, 1069-1079 (2004)
- [8] Hitomi, K. Preslansd RB, Nakayama T., Fleckman P., Dale BA, Maki M. *J. Dermatol. Sci* 32, 95-103 (2003)
- [9] Hitomi K, Horio Y, Ikura K, Maki M. Analysis of epidermal-type transglutaminase expression in mouse tissues and cell lines. *Int J Biochem Cell Biol* 33, 491-498 (2001)

ANALYSIS OF INTERLEUKIN-6-INDUCED SIGNALING IN MURINE HYBRIDOMA CELL LINES

Kazuhiko Takemura, Tatuya Yamashita and Satoshi Terada

Department of Applied Chemistry and Biotechnology, Faculty of Engineering, University of Fukui3-9-1, Bunkyo, Fukui, 910-8507, Japan

Abstract: Interleukin-6 (IL-6) is a multifunctional cytokine that plays important roles in the immune response, inflammation, differentiation, and growth control in various cells. It is also reportedly involved in a variety of diseases. We found that a murine hybridoma cell line, 2E3, derived from P3U1 myeloma cells and its subclone, 2E3-O, adapted to serum-free medium differed in growth responses to IL-6. When treated with IL-6, the growth of 2E3 cells was accelerated, while that of 2E3-O cells was significantly suppressed. Because studying differences between the two cell lines could yield important insights into IL-6-induced signaling, we comprehensively analyzed the protein expression profiles of both cell lines and detected several unique spots in 2E3-O cells.

1. INTRODUCTION

Interleukin-6 (IL-6) is a growth factor for B cell hybridoma / plasmacytoma cells [1], and a potent factor that acts on hybridoma cells to regulate antibody production. We previously investigated the effect of recombinant human IL-6 on the growth of a mouse hybridoma 2E3-O cell line in serum-free medium, and found that IL-6 suppressed growth of this cell line and enhanced antibody production up to five-fold [2].

IL-6 specifically binds to a cell surface receptor consisting of two subunits, ligand-binding IL-6R α and signal-transducing gp130 [3] (Fig. 1).

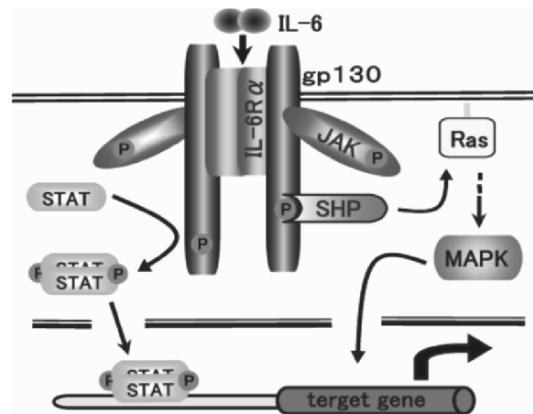


Figure 1. Signal-transduction mechanism of IL-6 through gp130 (modified from ref.14).

Binding of IL-6 to IL-6R α induces homodimerization of gp130 and activation of several members of the Janus kinase (JAK) family, JAK1, JAK2, and Tyk2 [4-6], and in turn the activated JAKs kinase phosphorylate gp130 [7]. Following activation of these kinases, two important downstream pathways are induced [8-10]. First, the phosphorylated gp130 binds to signal transducers and activators of transcription 3 (STAT3), which is phosphorylated by JAK kinases, before homodimers of the phosphorylated STAT3 rapidly migrate to the nucleus then bind to IL-6 response elements on the promoters of IL-6-induced genes [11]. Second, the phosphorylated gp130 activates the Ras-dependent mitogen-activated protein kinase (Ras-MAPK) cascade through its SHP-2 region. This cascade ultimately leads to activation of transcription factors, such as ternary complex and activator protein-1 [12-13]. These signaling pathways might interact with each other and contribute to a variety of biological activities.

In the present work, we used two-dimensional electrophoresis to analyze the signal-transduction mechanisms in cells that differ in their growth responses to IL-6.

2. MATERIALS AND METHODS

2.1 CELL LINE AND CULTURE CONDITIONS

The hybridoma cell line 2E3 was derived from a mouse myeloma P3X63 AG8U.1 by electric fusion with mouse spleen cells [2]. Next,

2E3 cells were cultured in RPMI1640 medium supplemented with 10% FBS. The cell line 2E3-O is a subclone of the 2E3 cell line, and was adapted to serum-free ASF-103 medium (Ajinomoto, Japan). Recombinant human IL-6 was purchased from Wako Junyaku (Japan). Both cell lines were grown at 37°C in humidified air containing 5% CO₂. Viable and dead cells were determined by counting in a hemocytometer under a phase contrast microscope using trypan blue exclusion.

2.2 TWO-DIMENSIONAL ELECTROPHORESIS ANALYSIS

2.2.1 First dimension

Immobilized pH gradient (IPG) strips (Amersham Bioscience, USA) were rehydrated at room temperature overnight. After mounting the strips in the electrofocusing chamber unit (Anatech, Japan), proteins were separated according to their isoelectric points with the steps shown in table 1.

2.2.2 Second dimension

The isoelectrically focused IPG strips were equilibrated with 13 mM DTT and 25 mM iodoacetamide. Each strip was then mounted onto SDS-gel, and the proteins were separated in 20-40 mA/slab according to their molecular weight until the BPB dye approached the bottom of the gel.

2.2.3 Staining and spot analysis

Immediately after electrophoresis, the gels were fixed overnight in 50% methanol and 5% acetic acid. The gels were then stained using a Protein Silver Staining Kit (Amersham Bioscience) and analyzed with ImageMasterTM 2D software (Amersham Bioscience).

Table.1. Steps of electrofocusing

Step	Voltage	Time (hours)	Step	Voltage	Time (hours)
1	500 V	2 h	5	2000 V	1 h
2	700 V	1 h	6	2500 V	1 h
3	1000 V	1 h	7	3000 V	1 h
4	1500 V	1 h	8	3500 V	14 h

3. RESULTS AND DISCUSSION

3.1 EFFECT OF IL-6 ON HYBRIDOMA PROLIFERATION

We investigated the effect of IL-6 on the growth of two hybridoma cell lines. After culturing in 24-well plates with purified IL-6 for two days, cell number was counted. In the presence of IL-6, the growth of 2E3 cells was slightly accelerated, while that of its subclone 2E3-O adapted to serum-free medium was significantly suppressed (Fig.2). This result suggests that the IL-6-induced growth signal mechanism might differ in each cell line.

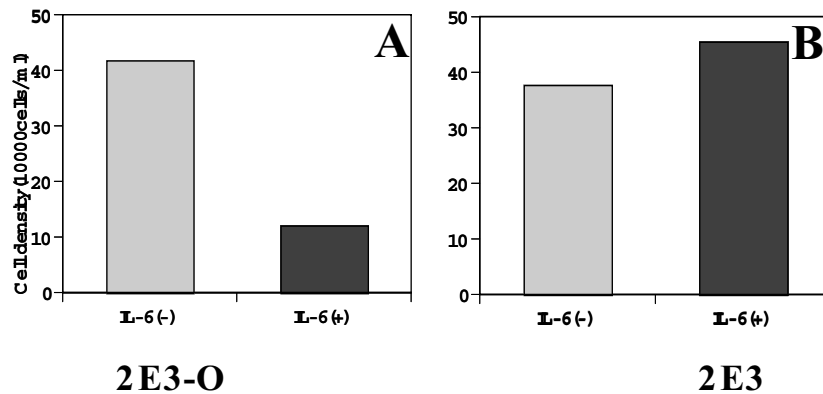


Figure 2. Effects of IL-6 on the proliferation of hybridomas. A) The 2E3 cell line was cultured with 1 ng/ml of IL-6, and B) the 2E3-O line with 100 ng/ml of IL-6. Each cell line was cultured with IL-6 for two days, before cell density was determined.

3.2 PROTEOME ANALYSIS USING TWO-DIMENSIONAL ELECTROPHORESIS

To investigate the protein profiles of 2E3 and 2E3-O, we used two-dimensional gel electrophoresis, which is currently the only analytical and preparative method capable of separating proteins. The results are shown in Fig. 3. Several different spots between 2E3 and 2E3-O were detected in the area marked in Fig. 3 and enlarged in Figs.4A and B. These areas were analyzed using ImageMasterTM 2D software, and two unique protein spots were found in the 2E3-O cells with statistical significance.

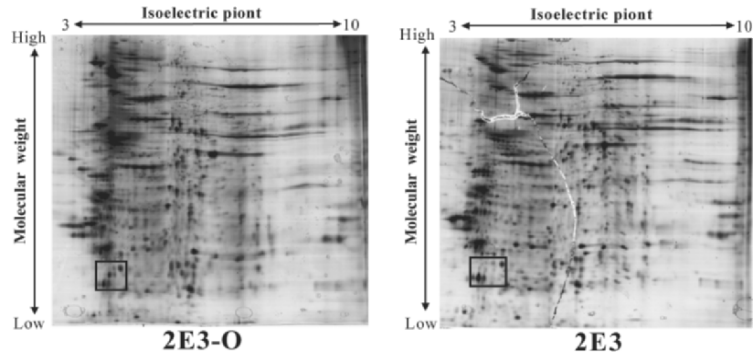


Figure 3. Two-dimensional protein profile of the 2E3 cell line and its subclone 2E3-O cell line. The vertical axis indicates the molecular weight, while the horizontal axis indicates the isoelectric point.

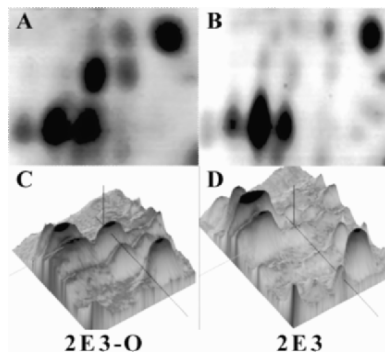


Figure 4. The results of analysis using ImageMaster™ 2D software. A) and B) represent enlargements of the squared areas marked in Figs.3. C) and D), 3D-results.

4. ACKNOWLEDGEMENTS

We thank Ms Y. Tanaka and Ms M. Sassa for their helpful advice.

5. REFERENCES

- (1) Van Damme J, Opendakker G, Simpson RJ, Rubria MR, Cayphas S, Vink A, Billian A, Van Snick J (1987) Identification of the human 26-KD protein, interferon 2, as a B-cell hybridoma / plasmacytoma growth factor induced by interleukin 1 and tumor necrosis factor, *J Exp Med* 165, 914

- (2) Makishima F, Terada S, Mikami T and Suzuki E (1992) Interleukin-6 is antiproliferative to a mouse hybridoma cell line and promotive for its antibody productivity, *Cytotechnology* 10, 15
- (3) Akira T, Taga T, and Kishimoto T (1993) Interleukin-6 in biology and medicine, *Adv. Immunol* 13, 54
- (4) Narazaki M, Witthuhn K, Yosida O, Silvennoinen K, Yasukawa K, Ihle J, Kisimoto T, and Taga T (1994) Activation of JAK2 kinase mediated by the interleukin 6 signal transducer gp130, *Proc. Natl. Acad. Sci. USA* 91, 2285
- (5) Matuda T, Yamasaki Y, and Hirano T (1994) Interleukin-6-induced tyrosine phosphorylation of multiple proteins in murine hematopoietic lineage cells, *Biochem. Biophys. Res. Commun.* 200, 821
- (6) Guschin D, Rogers N, Briscoe J, Witthuhn B, Waltling D, Horn F, Pellegrini S, Yasukawa K, Heinrich P, Stark G.R, Ihle J.N, and Kerr I.M (1995) A major role for the protein tyrosine kinase JAK1 in the JAK/STAT signal transduction pathway in response to interleukin-6, *EMBO J.* 14, 1421
- (7) Kismoto T, Akira S, Narazaki M, and Taga T (1995) Interleukin-6 family of cytokines and gp130, *Blood* 86, 1243
- (8) Kisimoto T, Taga T, and Akira S (1994) cytokine signal transduction, *Cell* 76, 253
- (9) Sadowski H, Shuai K, and Darnell J.E (1993) A common nuclear signal transduction pathway activated by growth factor and cytokine receptors, *Science* 261, 1739
- (10) Zhong Z, Wen Z, and Darnell J.E (1994) STAT3: A stat family member activated by tyrosine phosphorylation in response to epidermal growth factor and interleukin-6, *Science* 264, 49
- (11) Akira S, Nishio Y, Inoue M, Wang X-j, Wei S, Matsusaka T, Yoshida K, Sudo T, Naruto M, and Kishimoto T (1994) Molecular cloning of APRF, a novel IFN-stimulated gene factor 3 p91-related transcription factor involved in the gp130-mediated signaling pathway, *Cell* 77, 64
- (12) Nakajima T, Kinoshita S, Sasagawa T, Sasaki K, Naruto M, Kishimoto T, and Akira S (1993) Phosphorylation at threonine-235 by a ras-dependent mitogen-activated protein kinase cascade is essential for transcription factor NF-IL-6, *Proc. Natl. Acad. Sci. USA* 90, 2207
- (13) Neumann C, Zehentmaier G, Danhauser-Riedel S, Emmerich B, and Hallek M (1996) Interleukin-6 induced tyrosine phosphorylation of the Ras activating protein Shc, and its complex formation with Grb2 in human multiple myeloma cell line LP-1, *J. Immunol* 26, 379
- (14) Taga T and Kisimoto T (1999) Gp130 and the interleukin-6 family of cytokines, *Annu. Rev. Immunol* 15, 797

IMMUNE REGULATION BY SIALOGLYCOCONJUGATE-BINDING LECTINS

T cell costimulation by L-selectin

Munetoshi Ando, Ken-ichi Nishijima, Shusuke Sano, Aiko Hayashi-Ozawa,
Yoshinori Kinoshita, and Shinji Iijima
*Department of Biotechnology, Nagoya University, Furo-cho, Chikusa-ku, Nagoya 464-8603,
Japan*

Abstract: L-selectin that binds 6-sulfo sLe^x mediates the first step in the leukocyte-endothelial cell interaction as a rolling receptor on T cells. Furthermore, it is suggested that L-selectin plays a fundamental role as a signal transduction molecule. Here, we show the costimulatory activity of L-selectin in murine T cells using anti L-selectin monoclonal antibody, MEL14. Purified T cells proliferated in response to immobilized anti-CD3 antibody alone, and immobilized MEL14 enhanced this proliferation. Next, we assessed whether signaling via L-selectin can rescue unresponsiveness of T cells. MEL14 significantly enhanced the proliferation of responding T cells obtained from PBS-injected mice, however, unresponsive T cells from SEB-injected mice was not proliferated by the *in vitro* stimulation of SEB even in the presence of MEL14. This result indicates that signaling via L-selectin does not rescue the unresponsiveness of T cells. Then we analyzed how MEL14 enhanced T cell proliferation. We demonstrated that enhancement of T cell proliferation by MEL14 is not due to increase in IL-2 production, which is a common feature of non-CD28 type costimulatory molecules.

Key words: L-selectin, costimulation, T cells

1. INTRODUCTION

Sialic acids reside in terminals of many glycoproteins and glycolipids especially in higher animals. In this outward exposed position, sialic acids contribute significantly to the structural and functional properties of these molecules on cell surfaces via regulating cellular and molecular interactions. For example, sialic acid is involved in the first step of the leukocyte-endothelial cell interaction called rolling that proceeds the

adhesion of leukocytes and is crucial in the regulation of the immune responses during infection or in recirculation of lymphocytes to lymphatic organs.¹ Rolling is mediated by transient interactions of L-selectins on leukocytes with their sialic acid-containing glycoprotein-ligands on endothelial cells under certain situations.² Mice deficient in L-selectin, which binds 6-sulfo sialyl-Le^X, suffer from a lack of T cell homing and local inflammation,³ indicating essential roles of L-selectin in this type of immune regulation. Although the cytosolic domain of L-selectin is very short, engagement of L-selectin induces the activation of various signaling molecules, such as extracellular signal-regulated protein kinase (ERK),⁴ c-Jun NH₂-terminal kinase (JNK),⁵ p38 mitogen-activated protein kinases (MAPK),⁶ small G proteins Ras⁴ and Rac,^{4,7} calcium influx,⁸ and ceramide.⁹ There is less information available on the involvement of L-selectin in signal transduction in primary T lymphocytes.

The activation of T cells requires two types of signals. One is antigen-dependent and is mediated by the T cell receptor-CD3 complex which recognizes antigen bound to MHC. The other is antigen-independent costimulation that is provided by soluble factors and/or surface ligands on antigen-presenting cells to interacting with their counterreceptors on the T cells. To date, various molecules are suggested to have costimulatory activity. Among them, CD28 is the most important for initiating immune responses, since CD28 induces IL-2 production that leads to T cell proliferation. In CD28-disrupted mice, T cell response is severely impaired, but they are still detectable levels.^{10,11} These indicate that CD28 have essential roles in T cell activation but that other costimulatory pathways are also physiologically relevant. Although anti-L-selectin antibody alone does not induce T cell proliferation, it enhances the proliferation of mouse T cells in mixed lymphocyte reaction¹² or of human peripheral blood lymphocytes under anti-T cell receptor antibody stimulation.¹³ Therefore, L-selectin is a candidate for another costimulatory pathway, although precise mechanism for proliferation remains to be elucidated. Here, we study the costimulatory activity of L-selectin for primary murine T cells using anti L-selectin monoclonal antibody, MEL14.

2. MATERIALS AND METHODS

Reagents. Anti-CD3 antibody 145-2C11 which binds to CD3 ϵ -chain in T cell receptor complex, and anti-L-selectin antibody MEL14 were

purified from ascites with POROS Protein G plastic column. Anti-CD28 antibody 37.51, which stimulates T cells, was purchased from Pharmingen (CA, USA). Control rat IgG2a was purchased from Southern Biotechnology (Birmingham, USA). Staphylococcal enterotoxin B (SEB), one of the bacterial superantigens, was purchased from Toxin Technology (WI, USA). Anti-phospho-p44/42 (ERK) MAPK antibody (#9101) was obtained from Cell Signaling Technology (MA, USA).

T cell proliferation assay. The inguinal and popliteal lymph node cells were isolated from male BALB/c mice. Whole lymph node cells (1×10^5) or T cells purified with Nylon Fiber (Wako; Osaka, Japan) as manufacturer's recommendation were cultured in microtiter plates in 200 μ l of RPMI1640 medium supplemented with 5×10^{-5} M 2-mercaptoethanol, 100 U/ml of penicillin G, 100 μ g/ml of streptomycin and 10% fetal calf serum (Biowittaker; MD, USA) for 3 days, and the incorporation of ^3H -thymidine (18.5 kBq/well) of last 16 h of culture was measured. At the initiation of the culture, 2.5 μ g/ml of SEB or 0.1 μ g of immobilized antibody (s) was added for stimulation. To obtain unresponsive state of T cells, mice were injected with either phosphate-buffered saline (PBS) or 5 μ g of SEB at the footpads, and lymph node cells were collected 5 days postinjection.

RT-PCR analysis. T cells (1×10^6) were cultured in 1 ml of medium in 24 well plates for 24 h. Total RNA was extracted by QuickPrepTM total RNA Extraction Kit (Amersham Pharmacia Biotech; Tokyo, Japan) and reverse-transcribed with ReverTra Ace (Toyobo; Osaka, Japan) with oligo-dT as a primer. The primers used for PCR were mouse IL-2 forward (5'-GCTCTACAGCGGAAGCACA-3') and reverse (5'-TCCTCAGAAAGTCCACCACAGT-3'). The expression level was normalized by the amount of amplified actin cDNA.

3. RESULTS

3.1 Anti-L-selectin antibody enhanced the proliferation of T cells induced by anti-CD3 antibody

To examine whether anti-L-selectin antibody, MEL14, enhances the proliferation induced by bacterial superantigen, mouse whole lymph node cells were stimulated *in vitro* with SEB and MEL14 in soluble form. MEL14 induced the marked enhancement of the proliferation, while control rat IgG2a did not affect the proliferation (data not shown). This

result suggests that L-selectin has a potential as T cell costimulator when lymph node cells were stimulated with superantigen.

To assess the direct action of T cells, the effects of MEL14 on purified T cells were examined. T cells proliferated in response to immobilized anti-CD3 antibody alone, and immobilized anti-CD3 plus MEL14 enhanced the T cell proliferation (Fig. 1). Therefore, MEL14 directly acts on T cells to enhance proliferation. It has been demonstrated that L-selectin engagement leads to cell signaling not only by antibody cross-linking but also via ligation with naturally occurring ligands such as GlyCAM-1 or sulfatide.¹⁴ Therefore, purified T cells were stimulated by sulfatide. Sulfatide also enhanced the proliferation of T cells twice upon stimulation with anti-CD3 antibody (Fig. 1), supporting that MEL14 activates T cells in a similar manner to saccharide ligands.

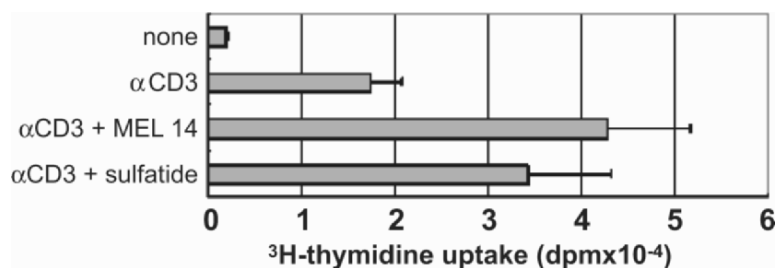


Figure 1. Proliferation assay of purified T cells stimulated by immobilized antibodies.

3.2 Anti-L-selectin antibody did not overcome unresponsive state of T cells induced by superantigen

It is essential for homeostasis of the immune system to maintain the peripheral tolerance. T cell inactivation, in which T cells exhibit only weak responses on antigenic stimulation as to impaired IL-2-production and proliferation, is called anergy and recognized as one of the mechanisms to downregulate immune responses.¹⁵ We used SEB-induced anergy as a model system of unresponsiveness induced *in vivo*. Although MEL14 significantly enhanced the proliferation of responding T cells obtained from PBS-injected mice, the proliferation of unresponsive T cells from SEB-injected mice was not induced by the *in vitro* stimulation of SEB even in the presence of MEL14 (Fig. 2). This result indicates that signaling via L-selectin does not rescue the unresponsiveness of T cells.

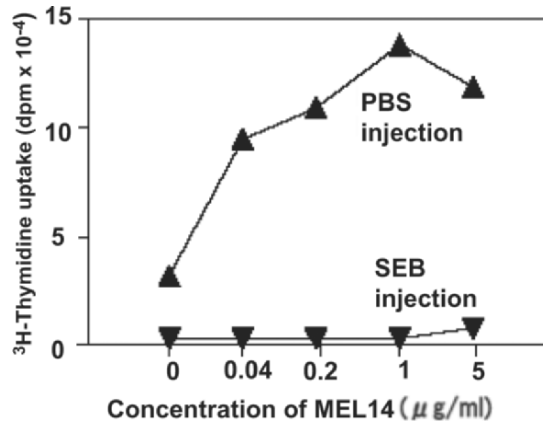


Figure 2. Proliferation assay of the SEB-induced unresponsive T cells.

3.3 Anti-L-selectin antibody did not enhance the expression of IL-2 mRNA in T cells

Next, we assessed how anti-L-selectin antibody enhances the proliferation of T cells induced by anti-CD3 antibody. It is possible that enhanced proliferation of T cells is due to the enhanced production of growth factors. IL-2 is secreted by T lymphocytes after stimulation with mitogen, antigen, or alloantigen and functions as a growth factor for many subsets of T cells via IL-2 receptors. We examined whether costimulation of L-selectin enhances IL-2 production. The result shows that costimulation of L-selectin did not enhance its expression, whereas CD28 induced a high level production of IL-2 mRNA (Fig. 3). Thus, enhancement of T cell proliferation by MEL14 is not due to increase in IL-2 production.

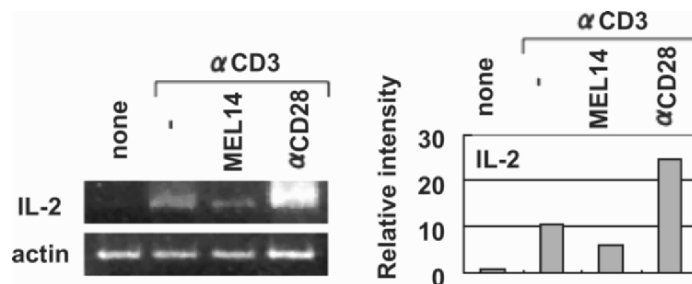


Figure 3. Reverse transcriptional PCR analysis of purified T cells stimulated by antibodies.

4. DISCUSSION

We report in this study the costimulatory activity of L-selectin to control T cell proliferation. As shown in Fig. 3, the production of IL-2 was not enhanced by anti-L-selectin antibody, in clear contrast to major costimulator CD28. The enhancement of T cell proliferation without facilitating IL-2 production is a common feature of other non-CD28 type of costimulatory molecules such as CD2, CD44 and CD11a.¹⁶ We have obtained the result that activation of ERK was enhanced by both L-selectin and CD28 (data not shown) that might lead the enhancement of T cell proliferation. Thus, it is likely that the mechanism of T cell costimulation is partially but not completely different between these molecules.

Given the potential clinical importance of the induction and maintenance of tolerance, many investigators have examined the biochemical events that define the anergic state. These studies have shown that some signaling molecules (lck, ZAP-70, TCR ζ and ϵ chains, Ras, JNK, ERK, AP-1, and NF-AT) were selectively inactive while activation of some molecules (fyn, intracellular free Ca^{2+} , PLC- γ 1, phosphatidylinositol 1,4,5 triphosphate, and Rap1) were even higher in anergic T cells compared with responsive cells.^{17,18,19} The result shown in Fig. 2 indicates that signaling via L-selectin does not rescue the unresponsiveness of T cells. In this regard, it is noteworthy that kinase activity of lck, which is required for ERK activation by L-selectin in Jurkat cells,⁴ is diminished in unresponsive T cells.²⁰ This implies a possibility that common upstream signaling pathway is inactivated in unresponsive T cells, and that candidate of such molecule is lck.

L-selectin interacts with the receptor on the vascular surface, therefore, it is possible that L-selectin may transmit intracellular signals when T cell is interacting with endothelial cells. Since endothelial cells express functional MHC class II molecules but do not express the ligands for CD28 even after various stimuli,²¹ the other costimulatory mechanism including that via L-selectin may work. Further investigation will reveal the underlying mechanism of the T cell costimulation that is important to regulate immune responses.

5. REFERENCES

1. T. A. Springer, Traffic signals for lymphocyte recirculation and leukocyte emigration: The multistep paradigm, *Cell* 76, 301-314 (1994).
2. S. D. Rosen, Ligands for L-selectin: Homing, Inflammation, and Beyond, *Annu. Rev. Immunol.* 22, 129-156 (2004).

3. T. F. Tedder, D. A. Steeber, and P. Pizcueta, L-selectin-deficient mice have impaired leukocyte recruitment into inflammatory sites, *J. Exp. Med.* 181, 2259-2264 (1995).
4. B. Brenner, E. Gulbins, K. Schlottmann, U. Koppenhoefer, G. L. Busch, B. Walzog, M. Steinhausen, K. M. Coggeshall, O. Kinderkamp, and F. Lang, L-selectin activates the Ras pathway via the tyrosine kinase p56lck, *Proc. Natl. Acad. Sci. USA* 93, 15376-15381 (1996).
5. B. Brenner, S. Weinmann, H. Grassme, F. Lang, O. Linderkamp, and E. Gulbins, L-selectin activates JNK via src-like tyrosine kinases and the small G-protein Rac, *Immunology* 92, 214-219 (1997).
6. J. E. Smolen, T. K. Petersen, C. Koch, S. J. O'Keefe, W. A. Hanlon, S. Seo, D. Pearson, M. C. Fossett, and S. I. Simon, L-selectin signaling of neutrophil adhesion and degranulation involves p38 mitogen-activated protein kinase, *J. Biol. Chem.* 275, 15876-15884 (2000).
7. B. Brenner, E. Gulbins, G. L. Busch, U. Koppenhoefer, F. Lang, and O. Linderkamp, L-selectin regulates actin polymerization via activation of the small G-protein Rac2, *Biochem. Biophys. Res. Commun.* 231, 802-807 (1997).
8. C. Laudanna, G. Constantin, P. Baron, E. Scarlato, G. Cabrini, C. Dececchi, F. Rossi, M. A. Cassatella, and G. Berton, Sulfatides trigger increase of cytosolic free calcium and enhanced expression of tumor necrosis factor- α and interleukin-8 mRNA in human neutrophils: evidence for a role of L-selectin as a signaling molecule, *J. Biol. Chem.* 269, 4021-4026 (1994).
9. B. Brenner, H. U. C. Grassme, C. Muller, F. Lang, C. P. Speer, and E. Gulbins, L-selectin stimulates the neutral sphingomyelinase and induces release of ceramide, *Exp. Cell Res.* 243, 123-128 (1998).
10. J. M. Green, P. J. Noel, A. I. Sperling, T. L. Walunas, G. S. Gray, J. A. Bluestone, and C. B. Thompson, Absence of B7-dependent responses in CD28-deficient mice, *Immunity* 1, 501-508 (1994).
11. A. Shahinian, K. Pfeffer, K. P. Lee, T. M. Kundig, K. Kishihara, A. Wakeham, K. Kawai, P. S. Ohashi, C. B. Thompson, and T. W. Mak, Differential T cell costimulatory requirements in CD28-deficient mice, *Science* 261, 609-612 (1993).
12. V. V. R. Swarte, R. E. Mebius, D. H. Joziase, D. H. van den Eijnden, and G. Kraal, Lymphocyte triggering via L-selectin leads to enhanced galectin-3-mediated binding to dendritic cells, *Eur. J. Immunol.* 28, 2864-2871 (1998).
13. Y. Murakawa, Y. Minami, W. Strober, and S. P. James, Association of human lymph node homing receptor (Leu 8) with the TCR/CD3 complex, *J. Immunol.* 148, 1771-1776 (1992).
14. A. Varki, Selectin ligands, *Proc. Natl. Acad. Sci. USA* 91, 7390-7397 (1994).
15. D. L. Mueller, M. K. Jenkins, and R. H. Schwartz, Clonal expansion versus functional clonal inactivation: a costimulatory signaling pathway determines the outcome of T cell antigen receptor occupancy, *Annu. Rev. Immunol.* 7, 445-480 (1989).
16. Y. Yashiro, X.-G. Tai, and K. Toyo-oka, A fundamental difference in the capacity to induce proliferation of naive T cells between CD28 and other co-stimulatory molecules, *Eur. J. Immunol.* 28, 926-935 (1998).

17. V. A. Boussiotis, G. J. Freeman, P. A. Taylor, A. Berezovskaya, I. Grass, B. R. Blazar, and L. M. Nadler, p27^{kip1} functions as an anergy factor inhibiting interleukin 2 transcription and clonal expansion of alloreactive human and mouse helper T lymphocytes, *Nat. Med.* 6, 290-297 (2000).
18. P. E. Fields, T. F. Gajewski, and F. W. Fitch, Blocked Ras activation in anergic CD4⁺ T cells, *Science* 271, 1277-1278 (1996).
19. W. Li, C. D. Whaley, A. Mondino, and D. L. Mueller, Blocked signal transduction to the ERK and JNK protein kinases in anergic CD4⁺ T cells, *Science* 271, 1272-1276 (1996).
20. D. B. McKay, H. Y. Irie, G. Hollander, J. M. L. F. Ferrara, T. B. Strom, Y.-S. Li, and S. J. Burakoff, Antigen-induced unresponsiveness results in altered T cell signaling, *J. Immunol.* 163, 6455-6461 (1999).
21. M. D. Denton, C. S. Geehan, S. I. Alexander, M. Sayegh, and D. M. Briscoe, Endothelial cells modify the costimulatory capacity of transmigrating leukocytes and promote CD28-mediated CD4⁺ T cell alloactivation, *J. Exp. Med.* 190, 555-566 (1999).

TRANSCRIPTIONAL REGULATION OF THE α -FETOPROTEIN GENE IN HEPATOCYTES

Mikio Takahashi, Takeaki Dohda, Hidenori Kaneoka, Yoshitaka Sato, Yujin Inayoshi, Katsuhide Miyake, Masamichi Kamihira, and Shinji Iijima

Department of Biotechnology and Ecotopia Science Institute, Nagoya University, Furo-cho, Chikusa-ku, Nagoya 464-8603, Japan

Abstract: α -Fetoprotein (AFP) is a fetal serum protein enriched in fetal liver whose expression is downregulated during development. The proximal region of the AFP promoter contains two binding sites for CCAAT/enhancer-binding protein α (C/EBP α), two for hepatocyte nuclear factor-1 α (HNF1 α) and one for glucocorticoid receptor (GR) in addition to a nuclear factor-1 (NF-1) binding site, which partly overlaps with the distal C/EBP α binding site. Luciferase reporter assays showed that a combination of C/EBP α , HNF1 α , NF-1 and coactivator p300 gave the maximal activity. Mutation in either HNF1 α binding site diminished the expression completely but mutation in either or both of the C/EBP α binding sites did not severely reduce the expression level. Chromatin immunoprecipitation assays showed that GR, HNF1 α , C/EBP α , NF-1, and p300 bound to the AFP promoter in adult liver.

Key words: α -fetoprotein, HNF1 α , C/EBP α , Hepatocyte

1. INTRODUCTION

The albumin and α -fetoprotein (AFP) genes are known to be activated concurrently early in development in the hepatocytes, followed by a specific inactivation of the AFP gene expression after the birth.¹⁻³ Enhancers located in the -7kb upstream region of the AFP promoter control liver-specific expression of the gene.⁴⁻⁶ The promoter region also plays an important role in the liver-specific expression of the AFP gene.⁷ Furthermore, there is considerable similarity in the promoter structure between AFP and albumin, in particular, the presence and localization of CCAAT/enhancer-binding protein α (C/EBP α)-, and hepatocyte nuclear factor-1 α (HNF1 α)-binding sites.⁸ In the rat AFP promoter, two HNF1 α

binding sites at -65/-51 and -131/-117 bp, and two C/EBP α binding sites at -78/-69 and -115/-107 bp have been identified.⁷⁻¹⁰ Overlapping with the distal C/EBP α binding site, a nuclear factor-1 (NF-1) binding site exists.^{7,8}

The AFP gene is also regulated through glucocorticoid and the glucocorticoid receptor (GR) spanning -172 to -150 bp.^{11,12} It was reported that glucocorticoids reduced transcription of the AFP gene in neonatal rodents but promoted it in humans.^{11,12} These conflicting results remain to be explained.

In addition to these transcription factors, coactivators may be involved in the transcriptional control of the α -fetoprotein gene. In fact, it was recently reported that HNF1 α physically interacts with the coactivator p300/CBP,^{13,14} and GR and C/EBP α directly associate with SWI/SNF chromatin remodeling factors.^{15,16} In this study, we demonstrated that transcriptional coactivator p300/CBP bound to the AFP promoter region and activated the expression of this gene.

2. MATERIALS AND METHODS

2.1 Isolation and culture of rat hepatocytes

Adult rat hepatocytes were obtained from male Sprague-Dawley rats (6-7 weeks old; Japan SLC, Shizuoka) by the collagenase perfusion method.^{17,18} Williams' medium E (Invitrogen, San Diego, CA, USA), supplemented with 0.1 μ M CuSO₄·5H₂O, 25 nM Na₂SeO₃, 1.0 μ M ZnSO₄·7H₂O, 0.1 μ M insulin (Sigma-Aldrich, St. Louis, MO, USA), 1.0 μ M dexamethasone (Wako Pure Chemical Industries, Osaka), 20 ng/ml of epidermal growth factor (EGF) (Sigma), 48 μ g/ml of gentamicin sulfate (Sigma) and 100 μ g/ml of chloramphenicol (Wako) was used as the culture medium. Fetal hepatocytes were isolated from the fetus (17 embryonic days; E17) of Sprague-Dawley rats,^{3,19} and cultured in Williams' medium E containing 5% (v/v) fetal bovine serum. Cells were seeded onto collagen type I-coated plastic dishes (Iwaki Glass Works, Chiba) under a 5% CO₂ atmosphere.

2.2 Plasmids

To construct the AFP promoter-luciferase reporter plasmid, the AFP promoter region (-225/+13) was amplified from rat genomic DNA by PCR using a set of primers (forward primer; 5'-CCCCAAGCTTCATTTGCAGCATTGCAAG-3' and reverse primer;

5'-CCCCAAGCTTCTTCATGGTTGCTGGCTGC-3'; *Hind*III sites are underlined), and introduced into pGL3-basic vector (Promega, Madison, WI, USA).

2.3 Luciferase reporter gene assay

C33A cells and primary fetal hepatocytes were seeded in 24-well plates and transfected with expression and reporter plasmids using Lipofectamine 2000TM reagent (Invitrogen). One hundred nanogram of the luciferase reporter plasmid and 5 ng of the *Renilla* luciferase plasmid were introduced with or without 0.1 μ g of plasmid expressing C/EBP α , HNF1 α , GR, and p300. The amount of total DNA was kept constant by adding empty expression vector. Reporter gene assays were performed with a dual luciferase assay kit (Promega, Madison, WI, USA) according to the manufacturer's instructions. Luciferase activities were measured with a luminometer JNR II (Atto, Tokyo, Japan) and normalized to *Renilla* luciferase activity.

2.4 Chromatin immunoprecipitation (ChIP) assay

The ChIP assay was performed using salmon sperm DNA-conjugated protein A agarose (Upstate Cell Signaling Solutions, Charlottesville, VA, USA) according to the manufacturer's instructions. The immunoprecipitated DNA and the input DNA were analyzed by PCR using primers for the AFP promoter (direct primer; 5'-CTGAAGTGGTCTTTGTCCTTG-3' and reverse primer; 5'-ACTGTGAGCAGTAGCGCTG-3'). As a negative control, the coding region of the AFP gene was also amplified using primers (direct primer; 5'-TCTGTGTTTCTGGATGAAATTG-3' and reverse primer; 5'-ACATCGCCCTGTTTCTTGG-3').

3. RESULTS

3.1 Cooperative regulation of the AFP expression by transcription factors and coactivator

The binding sites for HNF1 α , C/EBP α and NF-1 have been identified in the AFP promoter (Fig. 1).

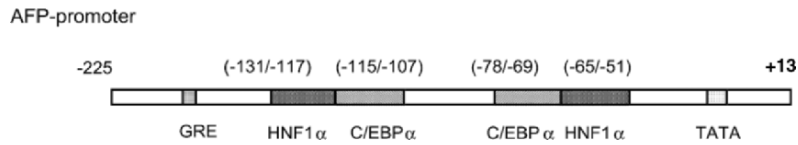


Figure 1. The structure of the promoter region of the rat AFP gene.

Furthermore, it is reported that HNF1 α physically interacts with the coactivator p300/CBP,^{13,14} and C/EBP α interacts with the ATPase subunit of chromatin remodeling complex, SWI/SNF.¹⁶ We therefore analyzed the effect of transcription factors HNF1 α , NF-1 and C/EBP α in combination with p300 by conducting reporter assays with C33A cells. The expression of C/EBP α , HNF1 α and p300 was not detected in C33A cells by Western blotting (data not shown). As shown in Fig. 2, a combination of transcription factors such as C/EBP α , HNF1 α , NF-1, and p300 caused an increase in the expression level. The coactivator p300 upregulated the gene expression with all combinations of these transcription factors. A similar result was observed in SW13 cells (data not shown).

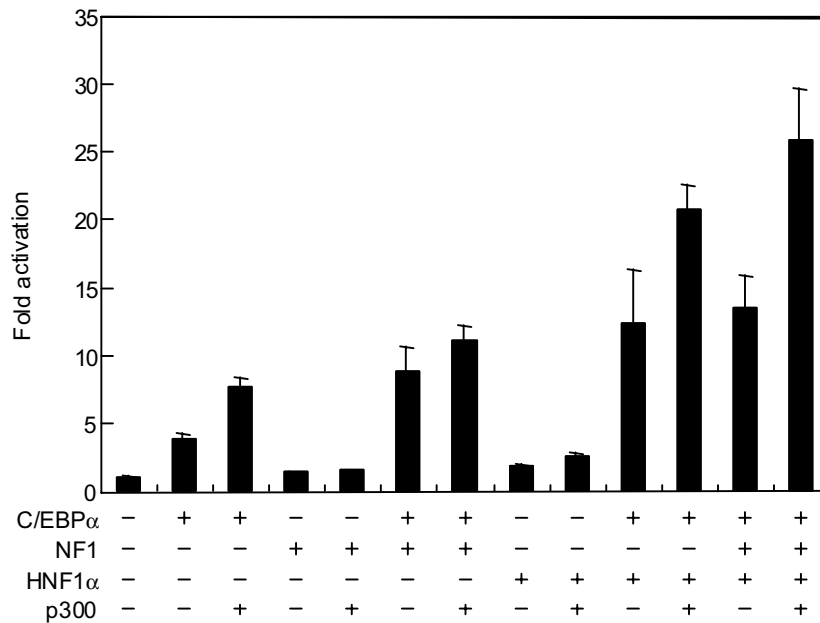


Figure 2. Cooperative effects of transcription factors and coactivator for the expression of the AFP gene in the C33A cells.

We next studied the effects of HNF1 α and C/EBP α binding more precisely using mutated proximal region. In a series of mutated promoter plasmids, either of two HNF1 α binding sites, or either or both of the C/EBP α sites were destroyed by replacing them with the *Eco*RI recognition sequence through PCR. As shown in Fig. 3, either mutants of the two HNF1 α binding sites completely lost transcriptional activity in primary fetal hepatocytes. C/EBP α binding site mutants that lacked either distal or proximal C/EBP α binding site also showed partial reduction of transcription (Fig. 3). On the other hand, the mutant defected in both C/EBP α sites showed weaker reduction comparing to the single C/EBP α mutation (Fig. 3).

These results mean that both HNF1 α binding sites are essential for transcription from the AFP promoter and that the presence of the C/EBP α binding sites may partly contribute to transcriptional repression as well as activation. C/EBP α may inhibit gene expression by recruiting a certain transcriptional inhibitor. Thus, C/EBP α seems to be bifunctional, and affects AFP expression differently depending on the situation. Since C/EBP α is possibly involved in the preinitiation complex (PIC) of RNA polymerase II, it is possible that the lack of C/EBP α sites blocks the formation of the PIC structure, but at the same time, hampers recruitment of some inhibitors, resulting in a partial activation of the AFP promoter.

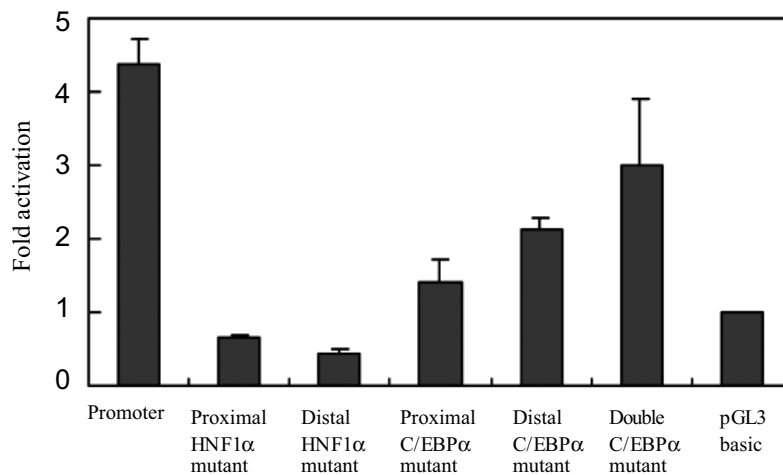


Figure 3. Mutation analysis of C/EBP α and HNF1 α binding sites for the AFP expression in primary fetal hepatocytes.

3.2 In vivo binding of transcription factors, coactivator to the proximal region of the AFP promoter

The binding of protein factors to the AFP promoter was then analyzed with the ChIP assay (Fig. 4). Both in fetal and adult hepatocytes, the binding of transcription factors, C/EBP α , NF-1 and GR to this region was observed, although the extent of the binding differed between these two cell types. And HNF1 α and p300 were also recruited to this region both in fetal and adult hepatocytes but the band of p300 was faint in adult hepatocytes. This result is consistent with the finding that the expression of p300 is weak in adult hepatocytes compared to the fetal cells.²⁰ Probably, this phenomenon is related to the fact that the expression of AFP is down-regulated at later stage of liver development.

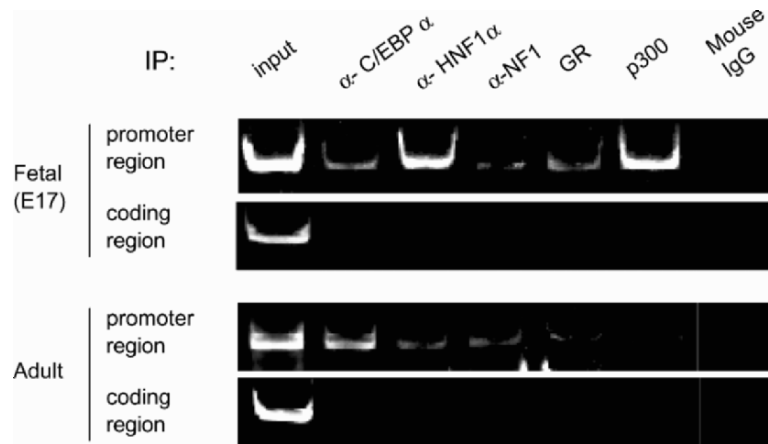


Figure 4. ChIP assay of the endogenous AFP gene of fetal and adult liver cells.

4. DISCUSSION

A ChIP assay of the endogenous AFP gene in both fetal and adult hepatocytes indicated that HNF1 α , C/EBP α , GR, NF-1 and p300 bind to the control region of the gene. The bindings of HNF1 α and p300 were decreased and that of C/EBP α was increased during liver development. Although it is not clear that the ChIP assay gave quantitative results under the conditions, it is possible that decreased binding of positive

regulators such as p300 and HNF1 α may play important roles in the repression of the AFP gene in the adult hepatocytes, in addition to the repression mediated by an inhibitor binding to an upstream control region as reported.²¹ This is consistent with the fact that p300/CBP is abundantly expressed in fetal hepatocytes.²⁰ Recently, we found that SWI/SNF repressed the AFP expression by luciferase reporter assays (Takahashi, unpublished result). Furthermore, SWI/SNF interacts with C/EBP α .¹⁶ Therefore, it is possible that decreased binding of transcriptional activators on the HNF1 α sites and increased binding of transcriptional inhibitors on the C/EBP α sites cause the reduction of AFP expression in adult hepatocytes. To clarify this point and to elucidate the mechanism of the repression, further study including that of the enhancer region is needed.

5. REFERENCES

1. Vacher, J. and Tilghman, S. M. (1990) Dominant negative regulation of the mouse α -fetoprotein gene in adult liver. *Science* 250, 1732-1735
2. Tilghman, S. M. and Belayew, A. (1982) Transcriptional control of the murine albumin/ α -fetoprotein locus during development. *Proc. Natl. Acad. Sci. USA* 79, 5254-5257
3. Hamamoto, R., Kamihira, M., and Iijima, S. (1999) Growth and differentiation of cultured fetal hepatocytes isolated from various developmental stages. *Biosci. Biotechnol. Biochem.* 63, 395-401
4. Group, E. R., Grawford N., and Locket, J. (1994) Characterization of the distal α -fetoprotein enhancer, a strong, long distance, liver-specific activator. *J. Biol. Chem.* 269, 22178-22187
5. Ramesh, T. M., Ellis, A. W., and Spear, B. T. (1995) Individual mouse α -fetoprotein enhancer elements exhibit different patterns of tissue-specific and hepatic position-dependent activities. *Mol. Cell Biol.* 15, 4947-4955
6. Watanabe, K., Saito, A., and Tamaoki, T. (1987) Cell-specific enhancer activity in a far upstream region of the human α -fetoprotein gene. *J. Biol. Chem.* 262, 4812-4818
7. Zhang, D-E., Hoyt, P. R., and Papaconstantinou, J. (1990) Localization of DNA protein-binding sites in the proximal and distal promoter regions of the mouse α -fetoprotein gene. *J. Biol. Chem.* 265, 3382-3391
8. Bernier, D., Thomassin, H., Allard, D., Guertin, M., Hamel, D., Blaquiére, M., Beauchemin, M., Larue, H., Estable-Puig, M., and Belanger, L. (1993) Functional analysis of developmentally regulated chromatin-hypersensitive domains carrying the α_1 -fetoprotein gene promoter and the albumin/ α_1 -fetoprotein intergenic enhancer. *Mol. Cell Biol.* 13, 1619-1633
9. Bois-Joyeux, B. and Danan, J. L. (1994) Members of the CCAAT/enhancer-binding protein, hepatocyte nuclear factor-1 and nuclear factor-1 families can differentially modulate the activities of the rat α -fetoprotein promoter and enhancer. *Biochem. J.* 301, 49-55
10. Zhang, D-E., Ge, X., Rabek, J. P., and Papaconstantinou, J. (1991) Functional analysis of the trans-acting factor binding sites of the mouse α -fetoprotein proximal promoter by site-directed mutagenesis. *J. Biol. Chem.* 266, 21179-21185

11. Rabek, J. P., Zhang, D-E., Torres-Ramos, C. A., and Papaconstantinou, J. (1994) Analysis of the mechanism of glucocorticoid-mediated down regulation of the mouse α -fetoprotein gene. *Biochim. Biophys. Acta* 1218, 136-144
12. Nakabayashi, H., Koyama, Y., Sakai, M., Li, H. M., Wong, N. C., and Nishi, S. (2001) Glucocorticoid stimulates primate but inhibits rodent alpha-fetoprotein gene promoter. *Biochem. Biophys. Res. Commun.* 287, 160-172
13. Soutoglou, E., Papafotiou, G., Katrakili, N., and Talianidis, I. (2000) Transcriptional activation by hepatocyte nuclear factor-1 requires synergism between multiple coactivator proteins. *J. Biol. Chem.* 275, 12515-12520
14. Soutoglou, E., Viollet, B., Vaxillaire, M., Yaniv, M., Pontoglio, M., and Talianidis, I. (2001) Transcription factor-dependent regulation of CBP and P/CAF histone acetyltransferase activity. *EMBO J.* 20, 1984-1992
15. Hsiao, P.-W., Fryer, C. J., Trotter, K. W., Wang, W., and Archer, T. K. (2003) BAF60a mediates critical interactions between nuclear receptors and the BRG1 chromatin-remodeling complex for transactivation. *Mol. Cell Biol.* 23, 6210-6220
16. Pedersen, T. A., Kowenz-Leutz, E., Leutz, A., and Nerlov, C. (2001) Cooperation between C/EBP α TBP/TFIIB and SWI/SNF recruiting domains is required for adipocyte differentiation. *Genes Dev.* 15, 3208-3216
17. Hamamoto, R., Yamada, K., Kamihira, M., and Iijima, S. (1998) Differentiation and proliferation of primary rat hepatocytes cultured as spheroids. *J. Biochem.* 124, 972- 979
18. Dohda, T., Nakamura, Y., Kamihira, M., and Iijima, S. (2004) Functional role of RhoA in growth regulation of primary hepatocytes. *J. Biochem.* 135, 631-637
19. Lorenzo, M., Roncero, C., and Benito, M. (1986) The role of prolactin and progesterone in the regulation of lipogenesis in maternal and foetal rat liver *in vivo* and in isolated hepatocytes during the last day of gestation. *Biochem. J.* 239, 135-139
20. Dohda, T., Kaneoka, H., Inayoshi, Y., Kamihira, M., Miyake, K., and Iijima, S. (2004) Transcriptional coactivators CBP and p300 cooperatively enhances HNF-1 α -mediated expression of albumin gene in hepatocytes. *J. Biochem.* 136, 313-319
21. Lee, K. C., Crowe, A. J., and Barton, M. C. (1999) p53-mediated repression of alpha-fetoprotein gene expression by specific DNA binding. *Mol. Cell. Biol.* 19, 1279-1288

MODULATION OF CYTOKINE AND IMMUNOGLOBULIN A RELEASE BY BETA-(1,3-1,6)-GLUCAN FROM *AUREOBASIDIUM PULLULANS* STRAIN 1A1

Takahiro Suzuki¹, Akira Hosono², Satoshi Hachimura³, Toshio Suzuki¹, and Shuichi Kaminogawa²

¹Research Laboratories, DAISO CO., LTD., Otakasu-cho, Amagasaki-shi, Hyogo, 660-0842, Japan. ²Department of Food Science and Technology, Nihon University. ³Department of Applied Biological Chemistry, The University of Tokyo

Abstract: Beta-glucan, derived from mushroom or yeast extracts, is well known for its various immunopharmacological effects such as anti-microbial properties and anti-tumor activities for host defense. We isolated β -glucans (DS- β G), secreted by the fungus body, from the culture medium of *Aureobasidium pullulans* strain 1A1. DS- β G form soluble microparticles and we prepared DS- β G to 85-95% purity. The structure of DS- β G is based on a backbone of β -(1,3)-linked β -D-glucopyranosyl units, with β -(1,6) linked side-chains of varying distribution. Their molecular weight range is 50,000-300,000, with the average estimated to be 100,000. In this study, we investigated the immunomodulatory effects of DS- β G, especially its *in vitro* and *in vivo* effects on the intestinal immune system. Peyer's patches (PP) cells from BALB/cA mice were cultured with DS- β G (0~200 μ g/ml) and IgA and cytokine levels in culture supernatant measured by ELISA. The addition of DS- β G induced IgA production in a dose-dependent manner. Both the levels of interleukin-5 (IL-5) and interleukin-6 (IL-6), cytokines known to enhance IgA production, were also elevated. Oral administration of DS- β G (400 μ g/mouse/day) for 7 consecutive days induced IgA production by PP cells. These results demonstrate that DS- β G acts on the gut immune system and increase IgA production that is vitally important for defense against infection.

Key words: β -(1,3-1,6)-glucan; *Aureobasidium pullulans*; immunomodulation

1. INTRODUCTION

Many kinds of fungi, yeasts and plants have immunomodulatory effects such as anti-microbial and anti-tumor activities important for host defense. These have been used clinically, as in the cases of lentinan (from *Lentinus edodes*), shizophyllan (from *Schizophyllum commune*) and Krestin (from *Coriolus versicolor*) for example (Adachi et al., 1994). Schizophyllan shows anti-tumor activity against sarcoma180, sarcoma37 etc (Hobbs, 1995). Lentinan significantly increased macrophage cytotoxicity *in vivo* when injected subcutaneously or intraperitoneally (Hamuro et al., 1980, Ladányi et al., 1993). β -glucan is known to be the major active constituent responsible for eliciting the immune responses of these molecules. It is an indigestive polysaccharide in humans. In light of these facts, it is speculated that β -glucans may modulate mucosal immunity in the intestinal tract.

Recent analysis of the response of leukocytes to β -glucan has shown that the integrin CR3 or dectin-1 receptor is required for its binding to cells (Xia et al., 1999, Brown et al., 2001, Thornton et al., 1996). β -glucans are known to act as immunostimulants, enhancing the activities of leukocytes, especially macrophages and natural killer cells (Konopski et al., 1991; Onderdonk et al., 1992). However, the mechanism of their immunomodulatory activities is not completely understood. The various physiological functions of different β -glucans have not been well clarified because of differences in their origin, the bonding pattern, the molecular weight and/or the size of the particles that contain the β -glucans (Janelle et al., 1999). In addition, the purification of β -glucan is difficult and few studies have investigated immune responses to purified β -glucan.

In this study, we isolated the original and purified β -glucan (DS- β G) from the culture of *Aureobasidium pullulans* strain 1A1 by fermentation methods, and determined the possibility to supplying them in large amounts (through Daiso, Osaka, Japan). DS- β G is a soluble microparticle glucan of low-molecular mass and with 50-80% (β -1,6/ β -1,3) branches. Additionally, we prepared DS- β G to around 85-95% purity. We investigated cellular immune responses to DS- β G, including cytokine and immunoglobulin A production in the mouse intestinal tract immune system.

2. MATERIALS AND METHODS

2.1 Beta-glucan

Beta-(1,3-1,6)-linked glucan (DS- β G) was received from DAISO CO., LTD. (Osaka, Japan). The β -glucan was prepared by Daiso Co., Ltd. as follows: The glucan was supplied as a soluble microparticle glucan obtained from the culture medium of *Aureobasidium pullulans* strain 1A1, grown in Czapek medium containing 3% sucrose as the sole carbon source and 0.3% ascorbic acid, sodium salt, under aerobic fermentation conditions for 3-7 days at 27°C. The highly purified β -glucan (85-95% in purity) was prepared by treatments that reduced viscosity by under-stirring with sodium hydrate (pH 12). The cell filtrate from the alkali-treated culture was filter pressed and low molecular weight substances and salts removed by ultrafiltration (UF membrane, NITTO DENKO CORPORATION). The ultrafiltered supernatant was adjusted to pH 3.5 with citric acid and filtered through a 0.8 μ m membrane. The resulting solution was used as the purified β -glucan sample. In some case, the β -glucan was precipitated with ethanol (more than 70%), freeze-dried, and dissolved in sterile saline.

The amount of total saccharide was measured via the phenol-sulfuric acid method (Hodge, J. E. et al. 1962). The amount of polysaccharide was determined after the recovery of polysaccharides by ethanol precipitation, as described above. The molecular weight was measured by gel filtration chromatography at pH 12 (TOYO PEARL HW-650; TOSOH CORPORATION, Tokyo, Japan), with pullulan (β -1,3-glucan) as a marker of molecular mass (5,900-1,600,000). The structure was determined by C-Hcosy-NMR spectra and the analysis of reaction products by β -1,3-glucanase (kitalase, K-I CHEMICAL INDUSTRY CO., LTD., Shizuoka, Japan) processing (Hamada et al. 1983). The size of the β -glucan microparticles was estimated by the measurement of particle size distribution by light scattering.

2.2 Animals

BALB/cA (6-8 weeks old) mice were obtained from Clea Japan (Tokyo, Japan) and housed in a room at 23-25°C in a humidified atmosphere with a 12 h light-dark cycle. Mice were fed ad libitum on a routine pelleted diet (MF, Oriental Yeast, Tokyo, Japan).

2.3 Cells and cell culture

PP and SPL cells were excised and isolated from BALB/cA mice. These immune tissue cells were prepared with Collagenase D (Roche, Mannheim, Germany) and Dnase I (Roche). Both cell types were cultured in RPMI 1640 medium (NISSUI Pharmaceutical CO., LTD., Tokyo, Japan) containing 5% heat-inactivated FBS (MP Biomedicals,

Inc, Irvine, CA), 100U/ml penicillin (BANYU Pharmaceutical CO., LTD., Tokyo, Japan), 100 μ g/ml streptomycin (MEIJI SEIKA KAISHA, LTD., Tokyo, Japan), 3mM L-glutamine, and 50 μ M 2-ME for the indicated times at 37 $^{\circ}$ C in a humidified atmosphere containing 5% CO₂.

2.4 Measurement of cytokine and IgA production *in vitro*

PP cells and splenocytes were prepared from 6-8 weeks old BALB/c mice. Mouse immune tissue cells (2.5 \times 10⁶cells/well in a total volume of 1ml) were cultured with 50-200 μ g/ml DS- β G, 20 μ g/ml Lipopolysaccharide (LPS; from *Esherichia coli* O55:B5) or 100 μ g/ml zymosan (Sigma, St. Louis, MO) in 48-well flat-bottomed plates. Control cultures were incubated in base medium alone. Culture supernatants were collected after 72 h and assayed for IL-5, IL-6, IL-12(p40/p70) and IFN- γ levels. At the same time, mouse immune tissue cells (2.0 \times 10⁵cells/well in a total volume of 200 μ l) were cultured with mitogens in 96-well flat-bottomed plates and supernatants collected after 1 week and assayed for IgA production. Cytokine and IgA levels were measured by sandwich ELISA.

2.5 Measurement of cell proliferation *in vitro*

PP cells and splenocytes (2.0 \times 10⁵cells/well in a total volume of 200 μ l) were cultured with 50-200 μ g/ml DS- β G, 20 μ g/ml LPS or 100 μ g/ml zymosan in 96-well flat-bottomed plates. Control cultures were incubated in base medium alone. After 40 h incubation, 20 μ l of CellTiter 96[®] AQueous One Solution Reagent (Promega Corporation, Madison, WI) was added to each well and the plate incubated for 3 h. Total cell count was measured by the absorbance of light at 490 nm via a microplate reader. Relative proliferation activity was quantified by comparison with control cultures.

2.6 Determination of cytokine and IgA levels by ELISA

Ninety-six-well plate (Immuno Plate; Nunc, Inter-Med, Denmark) were coated with relevant purified anti-mouse cytokine anti-bodies (BD Biosciences Pharmingen, San Jose, CA) or goat anti-mouse IgA (MP Biomedicals Inc., Irvine, CA) in 0.1M NaHCO₃ (pH 8.4) or 0.1M Na₂HPO₄ (pH 9.0) and incubated overnight at 4 $^{\circ}$ C. Wells were washed with phosphate buffered saline (PBS) buffer containing 0.05% Tween-20 (PBS-T). Uncoated binding sites in the wells were blocked with PBS containing 1% bovine serum albumin (Sigma) at room temperature for 2 h. Wells were washed with PBS-T and then either standard recombinant cytokines or IgA dilutions or culture supernatant samples in PBS-T were added to the wells and incubated overnight at 4 $^{\circ}$ C. Wells were then washed and relevant biotinylated anti-mouse cytokine antibodies (Pharmingen) or IgA antibody (Sigma) in PBS-T added and incubated at

room temperature for 2 h. Wells were washed and streptavidin-alkaline phosphatase (Invitrogen Corp., Carlsbad, CA) in PBS-T added and incubated at room temperature for 1 h. Plates were washed and the substrate solutions added (i.e. *p*-nitrophenyl phosphate) and incubated at 37°C for about 30 minutes. The absorbance of each well at 405 nm was measured using an automated spectrophotometer (microplate reader, BIO-RAD, Hercules, CA). Cytokines and IgA concentrations in culture supernatants were calculated from the standard curves produced by dilutions of the recombinant standard.

2.7 Statistical analyses

Results are expressed as means + S.E.M. and were compared using the Tukey test. Differences between control and stimulation groups were considered statistically significant at $p < 0.05^*$, $p < 0.01^{**}$ or $p < 0.001^{***}$.

3. RESULTS AND DISCUSSION

Beta-(1,3-1,6)-linked glucan (DS-βG) was prepared via specific treatments to reduce its viscosity, improve filtration and recovery. The molecular mass of DS-βG was determined to be between 5.0×10^4 and 3.0×10^5 by gel filtration chromatography, and the average mass approximately 1.0×10^5 . The structure consisted of a main chain of β-(1,3)-linked β-D-glucose with β-(1,6)-linked side-chains. The integral ratio of branches of β-1,6 for β-1,3 was estimated to be 50-80% from NMR and enzymatic analyses. Finally, DS-βG was prepared to 85 to 95% purity (Suzuki, T. 2005, Iizuka, M. 2002).

To investigate the effects of DS-βG on mouse immune tissue, cell proliferation, cytokine and IgA production were assessed *in vitro* following stimulation with 0-200μg/ml of DS-βG. As a positive control, LPS or zymosan were simultaneously added to the cultured immune cells. DS-βG stimulated cell proliferation of both PP cells and splenocytes in a dose-dependent manner (Table 1). DS-βG also stimulated IL-5 or IL-6 production by cultured PP cells in a dose-dependent manner (Table 2). A similar result was obtained for IgA production (Table 2). The culture supernatant from DS-βG-treated PP cells showed a significantly higher amount of IL-5, IL-6 and IgA comparable to those from zymosan-treated cultures at the same concentration (100μg/ml) (Table 2). As such, it appears that highly purified DS-βG causes a more effective immune response than zymosan. IL-12(p40/p70) and IFN-γ production were also stimulated by DS-βG (data not shown). These results clearly show that DS-βG stimulates PP

cells to produce cytokines or IgA *in vitro*. In addition, DS- β G stimulated IL-6 production by cultured splenocytes in a dose-dependent manner (data not shown).

We then postulated whether oral administration of DS- β G could stimulate IgA production in PP cells and splenocytes. IgA production was increased in PP cells from mice given DS- β G in comparison to the control group with results for both groups being almost the same (data not shown). IgA production by splenocytes from both groups was not significantly different (data not shown).

Table 1. Effects of DS- β G on cell proliferation by Peyer's patches cells and splenocytes of BALB/cA mice *in vitro*.

	(μg/ml)	Relative activities	
		PP	SPL
Control		1.000	1.000
DS- β G	50	1.523 ± 0.035***	1.243 ± 0.033**
DS- β G	100	1.636 ± 0.086***	1.373 ± 0.026***
DS- β G	200	1.784 ± 0.018***	1.652 ± 0.048***
LPS	20	2.396 ± 0.072***	1.795 ± 0.023***
Zymosan	100	0.889 ± 0.004	0.811 ± 0.027

PP cells and splenocytes were stimulated with DS- β G (50-200μg/ml), LPS (20μg/ml) or zymosan (100μg/ml). Control cultures were incubated in culture medium with sterile saline/diluent added. Cell proliferation levels show relative activity compared with control cultures as baseline. The results represent the mean ± S.E.M. of triplicate independent assays. Statistically significant differences are shown as $p < 0.01^{**}$, $p < 0.001^{***}$.

Table 2. Effects of DS- β G on IL-5, IL-6 and IgA productions by Peyer's patches cells from BALB/cA mice *in vitro*.

	(μg/ml)	Cytokine and IgA production (ng/ml)		
		IL-5	IL-6	IgA
Control		n.d. (+ / -)	+ / -	+ / -
DS- β G	50	n.d.	+	+
DS- β G	100	+	+	++
DS- β G	200	+	++	+++
LPS	20	n.d.	++	+
Zymosan	100	n.d.	-	-

PP cells were stimulated with DS- β G (50-200μg/ml), LPS (20μg/ml) or zymosan (100μg/ml). Control cultures were incubated in culture medium with sterile saline/diluent added. Supernatant cytokine and IgA levels were measured by ELISA. The results represent + / - (control), - (decreased), + (increased), ++ (increased, $p < 0.05$) and +++ (increased, $p < 0.01$). Statistically significant differences are shown as $p < 0.05^{*}$, $p < 0.01^{**}$.

In this study, we propose that DS- β G stimulates mucosal immune tissues, such as PP. IL-5 and IL-6 production was enhanced in PP cells

stimulated by DS- β G *in vitro*. IL-5 and IL-6 are known to further enhance IgA production. IgA production was enhanced in PP cells by DS- β G *in vitro*. Therefore, we suggest that DS- β G may prevent infection by pathogens through interactions with the intestinal immune system. In addition, IFN- γ production was enhanced in cultured PP cells by DS- β G. This result suggests that elimination of intracellular pathogens may also be effectively induced. We here suggest that DS- β G up-regulates intestinal immune responses and is available as a health food material.

4. REFERENCES

- Adachi, Y., Okazaki, M., Ohno, N., and Yadomae, T. (1994) Enhancement of cytokine production by macrophages stimulated with (1 \rightarrow 3)- β -D-glucan, grifolan (GRN), isolated from *Grifola frondosa*. Biol. Pharm. Bull. 12, 1554-1560.
- Brown, G.D. and Gordon, S. (2001) Immune recognition. A new receptor for beta-glucans. Nature 413, 36-37.
- Hamada, N., and Tsujisaka, Y. (1983) The structure of the carbohydrate moiety of an acidic polysaccharide produced by *Aureobasidium* sp. K-1. Agric. Biol. Chem. 47, 1167-1172.
- Hobbs, C. (1995) Medicinal mushrooms: an exploration of tradition, healing and culture. Botanica Press, Santa Cruz, Calif.
- Hodge, J. E. and Hofreiter, B. T. (1962) Method in Carbohydrate Chemistry 1, 338.
- Iizuka, M. (2002) Great Development of Microorganisms (Imanaka, T. ed.) pp. 1012-1020, NTS Inc., Tokyo.
- Janelle, A. C., Graham, E. K., and Alan, J. H. (1999) The effect of molecular weight and β -1,6-linkages on priming of macrophage function in mice by (1,3)- β -D-glucan. Immunol. Cell Biol. 77, 395-403.
- Konopski, Z., Rasmussen, L.T., Seljelid, R., and Eskeland, T. (1991) Phagocytosis of beta-1,3-D-glucan-derivatized microbeads by mouse peritoneal macrophages involves three different receptors. Scand. J. Immunol. 33, 297-306.
- Ladányi, A., T'már, J., Lapis, K. (1993) Effect of lentinan on macrophage cytotoxicity against metastatic tumor cells. Cancer Immunol. Immunother 36, 123-126.
- Onderdonk, A.B., Cisneros, R.L., Hinkson, P., and Ostroff, G. (1992) Anti-infective effect of poly-beta 1-6-glucotriosyl-beta 1-3-glucopyranose glucan *in vivo*. Infect. Immun. 60, 1642-1647.

- Suzuki, T. (2005) Food Style 21, vol.9, pp. 61-64, Food Chemicals Newspaper, Inc., Tokyo.
- Xia, Y., Vetvicka, V., Yan, J., Hanikyrova, M., Mayadas, T., and Ross, G.D. (1999) The beta-glucan-binding lectin site of mouse CR3 (CD11b/CD18) and its function in generating a primed state of the receptor that mediates cytotoxic activation in response to iC3b-opsionized target cells. *J. Immunol.* 162, 2281-2290.

INFLUENCE OF NATURAL REDUCED WATER ON RELEVANT TESTS PARAMETERS AND REACTIVE OXYGEN SPECIES CONCENTRATION IN BLOOD OF 320 DIABETES PATIENTS IN THE PROSPECTIVE OBSERVATION PROCEDURE

Z. Gadek¹, Y. Li² and S. Shirahata²

¹ Center for Holistic Medicine and Naturopathy, 57392 Nordenau, Germany; ² Department of Genetic Resources Technology, Faculty of Agriculture, Kyushu University, Fukuoka 812-8581, Japan

Abstract: The study examined changes in the relevant tests parameters of 320 diabetes patients (176 female, 144 male) drinking natural reduced water from the “Nordenau Spring” in Nordenau, Germany as well as the correlation of these changes with the fluctuation of the reactive oxygen species concentration in their blood. The average age of the test persons was 71.8 years old and the daily consumption of reduced water was as much as two liters. The average duration of stay in Nordenau lasted 6 days. The diagnostic parameters such as blood sugar, HbA1c, cholesterol, HDL, LDL, triglyceride and potassium were tested twice – at the beginning and at the end of the participants stay in Nordenau. Seventy-six of the test persons repeated the same procedure two or more times in the following months and years. Additionally a random sample of reactive oxygen species concentration in the blood of 50 patients had been taken in order to find out its possible causal connections to the diabetes relevant tests parameters.

Blood sugar and HbA1c had been considered as the substantial tests parameters in order to break down the whole group into responder and non-responder. Two hundred and thirty six tested persons that is to say (73.8%) had been assigned to the responder group and 84 (26.2%) to non-responder. Similar ratio of 37 responders (74%) and 13 non-responders (26%) respectively had been obtained in the random sample group with an additional free oxygen radicals test (FORT).

The survey pointed out the causal connections between the changes of blood sugar and HbA1c values and the fluctuation of reactive oxygen species concentration in the blood of the tested persons.

Furthermore we investigated the effect of Nordenau water on cytotoxicity of alloxan, a type-1 diabetes inducer, using hamster pancreatic β cells. Alloxan produces reactive oxygen species (ROS), which damage pancreatic β cells. Nordenau water scavenged alloxan-induced intracellular ROS and enhanced the glucose-stimulated elevation of intracellular ATP level and the release of insulin, protecting β cells from alloxan-induced cytotoxicity. Nordenau water also significantly suppressed the elevation of blood sugar level in alloxan-induced type 1 diabetes mouse.

These results suggest that natural reduced water such as Nordenau water may be effective in improving the deficient secretion of insulin from β cells in type 1- and 2-diabetes mellitus. In view of the fact that reduced water shows *in vitro* a stimulatory effect on the glucose uptake by muscle and fat cells, similar to that of insulin, which can be also reproduced in animal experiments - the results of this clinical trial seem to have sufficient correlation with the above mentioned results of basic researches to be worthy of serious consideration.

1. INTRODUCTION

Reactive oxygen species (ROS) are known to cause various diseases including diabetes mellitus. In the type II diabetes they cause reduction of glucose uptake by inhibiting the insulin-signaling pathway in muscle cells and adipocytes. The anti-oxidative waters (reduced waters) such as electrolyzed reduced water and several natural reduced waters e.g. Nordenau water in Germany, Hita Tenryosui water in Japan and Tracote water in Mexico scavenge ROS in insulin responsive L6 myotubes and mouse 3T3/L1 adipocytes and stimulate uptake of 1-deoxy-D-glucose into both L6 and 3T3/L1 cells in the presence or absence of insulin. This insulin-like activity is mediated by the activation of PI-3 kinase, resulting in stimulation of translocation of glucose transporter GLUT4 from microsome to plasma membrane (Oda et al.1999). Measurement of insulin secretion from beta cells of pancreas (HIT-T15 cell line derived from Syrian hamster) shown in the medium containing Nordenau reduced water 2.9 times higher concentration of insulin compared to control, respectively 2.2 for Hita Tenryosui water. Animal experiments using type II diabetes model mice (C57BL/Ks.J.Db+/Db+) exhibited the significant improved results in the sugar tolerance tests under administration of natural waters such as Nordenau water and Hita Tenryosui water (Shirahata et al. 2001). This prospective observation has been done to find out if an antioxidative operating mechanism of reduced water could really be in a position to suppress the concentration of reactive oxygen species in the blood of diabetes patients and by it to improve their diabetes relevant blood test parameters. Furthermore this study searched for if the results of clinical trials correlate with those of the basic researches and animal experiments.

2. MATERIAL AND METHOD

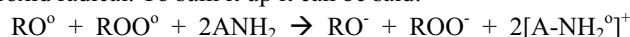
All the participants of the study were patients who had already been diagnosed by specialists and were receiving adequate medication as well as suitable diet guidelines. The inclusive criteria were defined only so far that all the tested persons were suffering by diabetes type II, no matter to age, sex, form of medication and diet. The test persons were particularly reminded to continue the medication prescribed by their specialists, to stick to their individual diet plans and not to alter any of their behavioral patterns. During their stay in Nordenau the patients drank two liters natural reduced water from "Nordenau spring" daily. We were looking after the patients diagnostically within the scope of what is known as "course control". The investigators strictly kept to the requirements of neutrality and didn't alter either regular medication of the tested persons or their diet instruction. The diagnostic parameters such as blood sugar, HbA1c, cholesterol, HDL, LDL, triglyceride and potassium were tested twice. Once at the beginning and once at the end of the participants stay in Nordenau. Parallel to that the random sample of reactive oxygen species concentration in the blood of 50 patients had been additionally taken to find out the possible causal connections between the alteration of diabetes relevant parameters and the changes of their blood ROS. Blood sugar and HbA1c had been considered as the substantial tests in order to break down the whole group of 320 patients into responder and non-responder. Seventy-six of the test persons repeated the same procedure two or more times during the following months and years.

The free oxygen radicals monitoring, which were applied, is based on so-called Haber-Weiss-reaction. This method is due to the fact that the peroxides, which come into being by lipid peroxydation as an interim product, create in the presence of free transition metals (not bound on proteins) high aggressive hydroxyl radicals. These products can be measured in the presence of N, N-diethyl-para-phenylendiamin on the photometric way. To go into detail it is possible with this method to measure the hydroperoxids level (ROOH), one of the group of reactive oxygen metabolites (ROMs) in the biologic samples e.g. blood. The test principal is based on the FENTON – reaction: $R\text{-OOH} + \text{Fe}^{2+} \rightarrow R\text{-O}^\bullet + \text{OH}^- + \text{Fe}^{3+}$

It means that the bivalent iron goes into reaction with hydroperoxid through which the trivalent iron and alkoxy radical (RO^\bullet) will be released:



The trivalent iron reacts with hydroperoxid and releases bivalent iron and peroxid radical. To sum it up it can be said:



In this connection 2ANH_2 stands for chromogen and $[\text{A-NH}_2^{\bullet}]^+$ for the cation radical of chromogen. The oxygen species level (ROS) in the blood had been stressed in FORT Units. Here 1 FORT Unit = 0.26 mg H_2O_2 /l blood. The values between 250 and 310 FORT Units are considered to be normal.

The statistical interpretation of this clinical data contains:

The descriptive statistics of the whole group and of both subgroups, a pairing-directed T-Test, a proportional evaluation of the entire group and of both subgroups, variance and co-variance analyses. The allowance for error probability was set at 5 %.

3. RESULTS AND DISCUSSION

The survey pointed out that in the first therapy period the percentage of responder (referring to blood sugar and HbA1c) of 73.8% or 236 patients is really very high considering such a short therapy time (in average 6 days).

The remaining 26.8% respectively 84 patients that did not respond to the active substance, didn't to all appearances stick to their diet plans or there are any other reasons for this state of affairs which are not discovered so far.

The reaction of the substantial parameters like blood sugar and HbA1c to consumption of reduced water was among the responder high significant positive. (*Figures 1 and 2*)

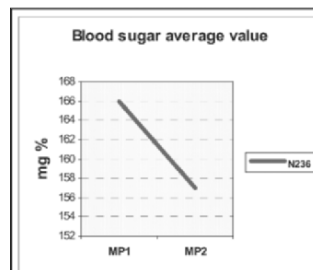


Figure 1. Suppressive effect of Nordenau water on blood sugar level in a short therapy period of 236 human diabetes patients-responder group, p-0, 000.

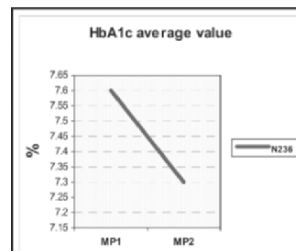


Figure 2. Suppressive effect of Nordenau water on HbA1c level of 236 human diabetes patients in a short therapy period-responder group, p-0, 000.

The random sample group of 50 patients with additional blood free oxygen radicals test (FORT) resulted in similar ratio of responder (74% or 37 patients) and non-responder 26% or 13 patients respectively. The comparison between decrease of the blood sugar and HbA1c average values with the downwards trend of reactive oxygen species concentration in the blood among responders pointed out causal connections between the changes of these substantial diabetes parameters and the fluctuation of reactive oxygen species in the blood of test persons. (Figures 3- 5)

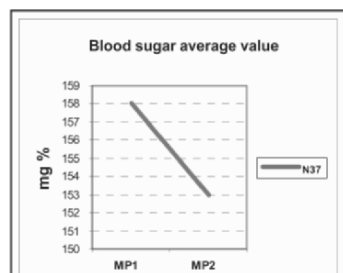


Figure 3. Decrease of the blood sugar average value of the 37 responder of the random sample group.

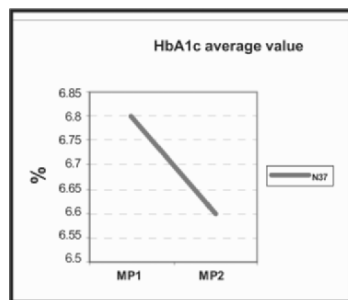


Figure 4. Decrease of the HbA1c average value of 37 responder of the random sample group.

On the other hand this clinical data can be considered as a hypothesis that the reduced water may be in a position to suppress the ROS concentration in the blood of diabetes patients and therefore to improve the diabetes relevant test parameters. Furthermore could be said that there are the causal connections between the variability of blood ROS level and the changes of diabetes relevant test parameters. Furthermore we investigated the effect of Nordenau water on cytotoxicity of alloxan, a type-1 diabetes inducer, using hamster pancreatic β cells. Alloxan produces reactive oxygen species (ROS), which damage

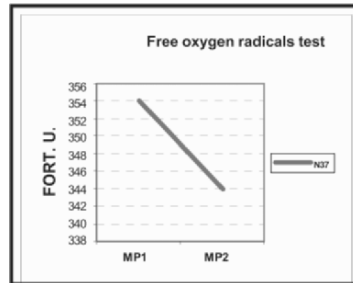


Figure 5. Decrease of free oxygen radicals concentration in blood of 37 responder of random sample group.

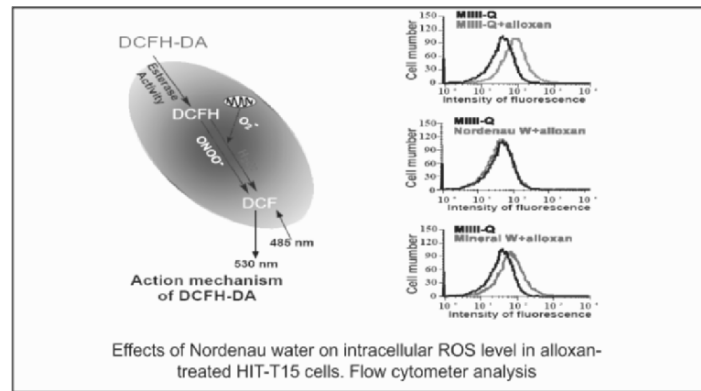


Figure 6.

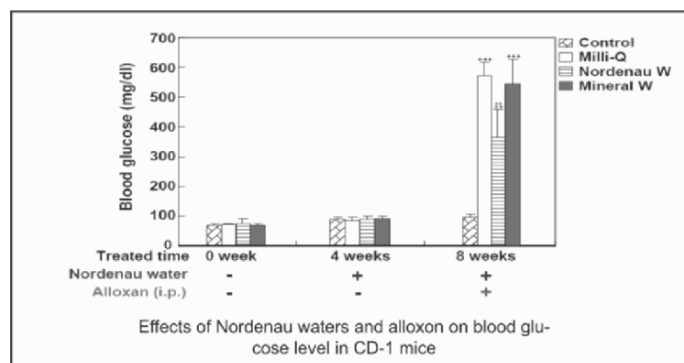


Figure 7.

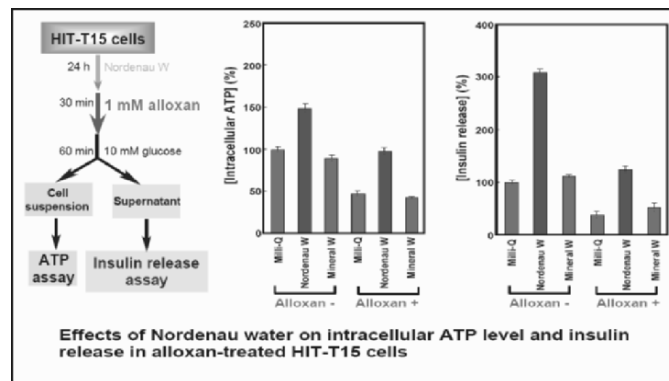


Figure 8.

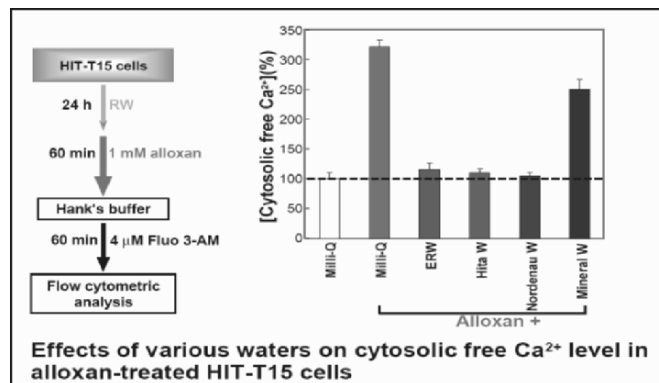


Figure 9.

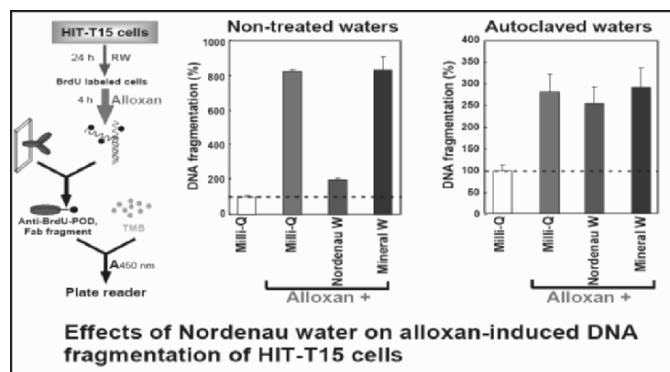


Figure 10.

pancreatic β cells. Nordenau water scavenged alloxan-induced intracellular ROS and enhanced the glucose-stimulated elevation of intracellular ATP level and the release of insulin, protecting β cells from alloxan-induced cytotoxicity. Nordenau water also significantly suppressed the elevation of blood sugar level in alloxan-induced type 1 diabetes mouse.

These results suggest that natural reduced water such as Nordenau water may be effective in improving the deficient secretion of insulin from β cells in type 1-and 2-diabetes mellitus. In view of the fact that reduced water shows *in vitro* a stimulatory effect on the glucose uptake by muscle and fat cells, similar to that of insulin, which can be also reproduced in animal experiments - the results of this clinical trial seem to have sufficient correlation with the above mentioned results of basic researches to be worthy of serious consideration.

4. CONCLUSION

RWs like ERW, Hita Tenryosui water and Nordenau water were all anti-oxidative waters that could scavenge intracellular ROS in hamster pancreatic β -cells, HIT-T15.

Alloxan induced lowering of viability, increase of cytosolic free Ca^{2+} , increase of DNA fragmentation, decrease of intracellular ATP, and decrease of glucose-stimulated insulin release. RW could inhibit all those cytotoxic effects of alloxan, increasing markedly the glucose-stimulated increase of ATP levels and insulin release.

The clinical trials pointed out the causal connections between the changes of blood sugar and HbA1c values and the fluctuation of reactive oxygen species concentration in the blood of the tested persons.

5. REFERENCES

- Borg LA, Eide SJ, Anderson A and Hellerstrom C (1979) Effect *in vitro* of alloxan on the glucose metabolism of mouse pancreatic β -cells. *Biochem J* 182: 797-802.
- Halliwell B and Gutteridge JMC (1990) Role of free radicals and catalytic metal ions in human disease: an overview. *Methods in Enzymol* 186: 1-85.
- Hanaoka K (2001) Antioxidant effects of reduced water produced by electrolysis of sodium chloride. *J Appl Electrochem* 31: 1307-1313.
- Kim H, Rho H, Park B, Park J, Kim J and Kim UH (1994) Role of Ca^{2+} in alloxan-induced pancreatic β -cell damage. *Biochim Biophys Acta* 1227: 87-91.
- LeBel CP, Ishiropoulos H and Bondy SC (1992) Evolution of the probe 2',7'-dichlorofluorescein as an indicator of reactive oxygen species formation and oxidative stress. *Chem Res Toxicol* 5: 227-231.
- Li Y., Nishimura T., Teruya K., Maki T., Komatsu T., Hamasaki T., Kashiwagi T., Kabayama S., Shim S.-Y., Katakura Y., Osada K., Kawahara T., Otsubo K., Morisawa S., Ishii Y., Gadek Z., Shirahata S. (2003) *Cytotechnology* 40: 139-149

- Malaisse WJ and Lea MA (1982) Alloxan toxicity to the pancreatic β -cell. A new hypothesis. *Biochem Pharmacol* 31: 3527-3534.
- Masumoto N, Tasaka K, Miyake A and Tanizawa O (1990) Superoxide anion increases intracellular free calcium in human myometrial cells. *J Biol Chem* 265: 22533-22536.
- Oda M, Kusumoto K, Teruya K, Hara T, Maki T, Kabayama Y, Katakura Y, Otsubo K, Morisawa S, Hayashi H, Ishii Y and Shirahata S (1999) Electrolyzed and natural reduced water exhibit insulin-like activity on glucose uptake into muscle cells and adipocytes. *Animal Cell Technology: Products from Cells, Cells as Products* (eds. Bernard A et al.), pp. 425-427, Kluwer Academic Publishers, the Netherlands.
- Rho H, Lee J, Kim H, Park B and Park J (2000) Protective mechanism of glucose against alloxan-induced β -cell damage: pivotal role of ATP. *Exp Mol Med* 32: 12-17.
- Shirahata S (2000) Regulation of functions of animal cells by reduced water and its medical application. *Nippon Nogei Kagaku Kaishi* 74: 994-998.
- Shirahata S (2002) Reduced water for prevention of diseases. *Animal Cell Technology: Basic & Applied Aspects*, Volume 12, pp. 25-30, Kluwer Academic Publishers, the Netherlands.
- Shirahata S, Kabayama S, Nakano M, Miura T, Kusumoto K, Gotoh M, Hayashi H, Otsubo K, Morisawa S and Katakura Y (1997) Electrolyzed-reduced water scavenge active oxygen species and protects DNA from oxidative damage. *Biochem Biophys Res Commun* 234:269-274.
- Shirahata S, Nishimura T, Kabayama S, Aki D, Teruya K, Otsubo K, Morisawa S, Ishii Y, Gadek Z and Katakura Y (2001) Anti-oxidative water improves diabetes. *Animal Cell Technology: From Target to Market* (eds. Linder-Olsson E et al.), pp. 574-577, Kluwer Academic Publishers, the Netherlands.
- Takasu N, Asawa T, Komiya I, Nagasawa Y and Yamada T (1991) Alloxan-induced DNA strand breaks in pancreatic islets: Evidence for H_2O_2 as an intermediate. *J Biol Chem* 266: 2112-2114.
- Tashiro H (1999) Clinical examination of alkaline ion water. Abstract book of Symposium "Electrolyzed functional water in therapy" in 25th Meeting of Japanese Medical Society. pp. 6-7.

PROTEOME ANALYSIS OF NEURITE DIFFERENTIATION OF PHYTOESTROGEN-TREATED PC12 CELLS: *Preliminary results*

Hiroko Isoda, Mariko Seki, Terence P. N. Talorete, Junkyu Han
Graduate School of Life and Environmental Sciences, University of Tsukuba, Japan

Abstract: A novel isoflavone, 7, 2', 4'-trihydroxyisoflavone-4'-O- β -D-glucopyranoside was isolated from the aerial part of *Crotalaria sessiliflora*. The isoflavone glucoside was found to enhance the proliferation of the MCF-7 human breast cancer cell line, which possesses estrogen receptors (ERs) and responds in culture to estrogen. The estrogenic property of the isoflavone glucoside was blocked by the known ER antagonist tamoxifen, indicating the involvement of the ER. Furthermore, the isoflavone was found to enhance the acetylcholinesterase (AChE) activity of the rat neuronal cell line PC12 treated with a low concentration (0.1 μ M) of nerve growth factor (NGF). In this study, it was shown that the phytoestrogen enhances AChE activity in PC12 cells by binding to the ER; the actual mechanism will be determined by proteome analysis.

Key words: Phytoestrogens, PC12, acetylcholinesterase

1. Introduction

Estrogenic compounds isolated from plants are commonly known as phytoestrogens and are known to exert a positive impact on human health (Knight and Eden 1996; Lamartiniere et al. 1995; Deodato et al. 1999). Although their chemical structures are relatively different from each other, they show some structural similarity: all contain a pharmacophore similar to that found in estradiol and diethylstilbestrol (Tham et al., 1998). Isoflavones are typical phytoestrogens that are found mostly in leguminous plants, particularly soybeans. Two major isoflavones found in soybeans are daidzein and genistein.

In the course of our study to find new antioxidative compounds from plants, we isolated a new isoflavone glucoside, 7,2',4'-trihydroxy isoflavone-4'-O- β -D-glucopyranoside from a BuOH soluble fraction obtained from the aerial part of *C. sessiliflora* (Leguminosae). Although this compound did not show antioxidative activity, its structure

resembled that of the phytoestrogen daidzein. Thus, we investigated the estrogenic activity of the compound by E-screen assay using the human breast cancer cell line MCF-7. This method is widely used as a rapid and straightforward assay to determine estrogenic activity of chemicals (Soto et al. 1995).

In a previous study, Isoda et al. (2002) reported that genistein and daidzein enhance the acetylcholinesterase (AChE) activity of the rat neuronal cell line PC12 at concentrations as low as 0.08 μM by binding to the estrogen receptor (ER). Results have shown that this enhancement was effectively blocked by the known estrogen receptor antagonist tamoxifen, indicating the involvement of the ER in AChE induction. That genistein and daidzein are estrogenic were confirmed in a cell proliferation assay using the human breast cancer cell line MCF7. This proliferation was also blocked by tamoxifen, again indicating the involvement of the ER. On the other hand, incubating the PC12 cells in increasing concentrations of 17 β -estradiol (E2) did not lead to enhanced AChE activity, even in the presence of genistein or daidzein. This suggests that mere binding of an estrogenic compound to the ER does not necessarily lead to enhanced AChE activity. Moreover, the effect of the phytoestrogens on AChE activity cannot be expressed in the presence of E2 since they either could not compete with the natural ligand in binding to the ER or that E2 downregulates its own receptor. The study clearly suggests that genistein and daidzein enhance AChE activity in PC12 cells by binding to the ER; however, the actual mechanism of enhancement is not known.

In this study, we also determined if the estrogenic activity of the isolated isoflavone was effectively blocked by the known ER antagonist tamoxifen to determine if the isoflavone glucoside can bind to the classical estrogen response element (ERE) and mediate gene transcription. We also provide preliminary results of an ongoing study of proteins from PC12 cells treated with daidzein using two-dimensional (2D) electrophoresis. Mass spectrometry of the protein spots of interest follows next. In 2D electrophoresis, the first dimension separates proteins according to their isoelectric point, while the second dimension separates them according to their molecular weight.

2. Materials and methods

2.1. Cell lines and maintenance

The cell lines used in this study and their maintenance were previously described (Isoda et al., 2002).

2.2 Acetylcholinesterase and cell proliferation assays

The acetylcholinesterase and cell proliferation assays were previously described (Isoda et al., 2002).

2.3. Proteome analysis

The cells were washed twice with tris-buffered sorbitol (10 mM Tris, 25 mM sorbitol pH 7), after which, one volume of the buffer was added, the cells then scraped and transferred to a polyallomer micro ultracentrifuge tube. Four volumes of lysis/extraction solution (7M urea, 2M thiourea, 4% CHAPS, 25 mM spermine base, 1mM EDTA, 50mM DTT, 4mM AEBSF) was immediately added and mixed by placing a piece of parafilm over the tube and inverting it several times. Extraction was carried out at room temperature for 60 min with occasional mixing. The sample was then centrifuged at 130,000 g for 1 h at 15°C. The protein-containing supernatant was kept and the protein concentration was determined using the 2D Quant Kit (Amersham). For first dimension, immobilized pH gradient (IPG) strips (Amersham) were rehydrated overnight with 350 µg of protein (in-gel rehydration) according to the manufacturer's instructions. Using a Multiphor II apparatus, the proteins were then separated according to their isoelectric point under conditions provided in the 2D protocol (Amersham) with some modifications. For second dimension, the isoelectrically focused IPG strips were then equilibrated with DTT and iodoacetamide following the Amersham protocol. Each strip was then applied onto a ready-made SDS 12-14 Excel Gel[®] (Amersham) and the proteins separated according to their molecular weight using SDS-PAGE. Immediately after electrophoresis, the gels were fixed overnight in 30% ethanol and 0.5% glacial acetic acid. The gels were then stained with Coomassie brilliant blue (CBB) using PhastGel[™] BlueR (Amersham). The stained gels were scanned using ImageScanner[™] (Amersham) and the spots analyzed using the ImageMaster[™] 2D software (Amersham).

3. Results and Discussion

Estrogen activity

Phytoestrogens or hormonally active agents can recognize the estrogen receptor and trigger cell proliferation in estrogen-responsive cells (Soto et al. 1991; White et al. 1994). Such compounds can also antagonize the effect of natural hormones, react directly or indirectly with the receptor, alter the pattern of synthesis of natural hormones, and even alter the hormone receptor level (Soto et al. 1995).

The estrogenic activities of isolated compounds were investigated by E-screen assay using the MCF-7 human breast cancer cell line. Daidzein and genistein, the best known naturally occurring nonsteroidal estrogens,

were used as positive controls. Cell proliferation was measured by a colorimetric MTT assay to estimate the number of cells as the end point (Mossman 1983).

Results in Figure 1 show that when the MCF-7 cells were incubated for 6 days in the presence of 7,2',4'-trihydroxy isoflavone-4'-*O*- β -D-glucopyranoside, there was a significant increase in cell proliferation compared to control ($P < 0.01$, *t* test). The proliferation of MCF-7 cells in the presence of this compound was found to be concentration-dependent. The isolated isoflavone glucoside at a low concentration resulted in lower cell proliferation activity than those in the presence of genistein and daidzein. Genistein at 0.3 μ M promoted cell proliferation by up to 1.99-fold over untreated cells (control), whereas the isoflavone glucoside at the same concentration caused the cells to proliferate by up to 1.14-fold compared with control. However, at 5 μ M, the isolated isoflavone glucoside increased cell proliferation by up to 1.74-fold over the control. This was nearly equal to that of genistein. Maximum cell proliferation was found to be in the presence of 5 μ M daidzein. In addition, the isolated isoflavone glucoside, like daidzein and genistein, did not exhibit cytotoxicity to the MCF-7 cell line up to 50 μ M (data not shown).

In this experiment, cell proliferation in the presence of daidzein was lower than that in the presence of genistein. This is in contrast to the results obtained by Han et al. (2002). It is known that the behavior and response of MCF-7 cells to 17 β -estradiol varies among different laboratories. The lack of a standard protocol, differences in conditions and MCF-7 strains in different laboratories may lead to significant inter-laboratory variability (Jones et al. 1998; Payne et al. 2000).

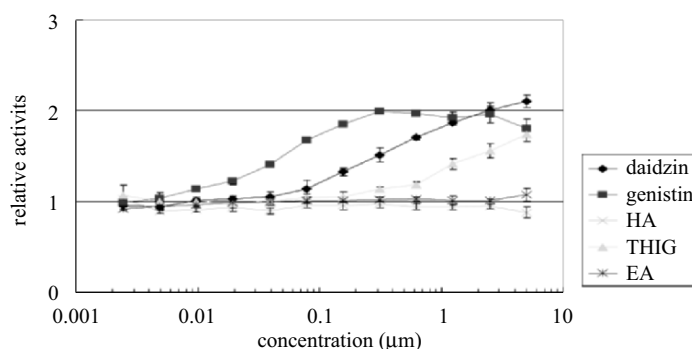


Figure 1. Estrogenic activity of phytoestrogens

To confirm whether the estrogenic activity of the new isoflavone glucoside was due to its binding to the ER, the cells were incubated with various concentrations of the tested compounds in the presence of 1.5

μM tamoxifen, an estrogen antagonist. Figure 2 shows the effect of the addition of tamoxifen on the estrogenic activity of the tested compounds. As shown in the result, cell proliferation in the presence of the tested compounds at all concentrations was blocked by tamoxifen.

Since cell proliferation in the presence of the isolated isoflavone glucoside was blocked by tamoxifen, it is suggested that the estrogenic activity was due to the binding of the isoflavone glucoside to the classical $\text{ER}\alpha$. In addition, the structural similarity between the isolated isoflavone glucoside and the soy isoflavones, genistein and daidzein, suggests that they may have identical mechanisms of action.

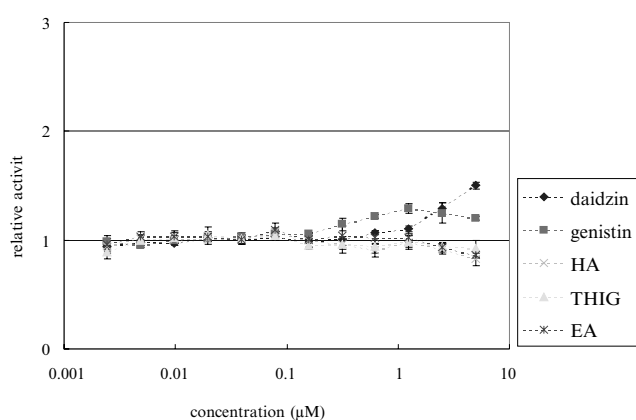


Figure 2. Inhibition of estrogenic activity by tamoxifen (ER antagonist)

Acetylcholinesterase activity

Acetylcholinesterase activity (AChE) is known as a marker of the neuronal differentiation in the rat pheochromocytoma cell line PC12. Results in Figure 3 show that $5 \mu\text{M}$ of isoflavone glucoside and daidzein significantly enhanced the AChE activity of PC12 cells in the presence of a low concentration of NGF ($<0.1 \mu\text{M}$). At higher NGF concentrations ($>20 \mu\text{M}$), the AChE activity was slightly enhanced by $5 \mu\text{M}$ of the isoflavone glucoside and daidzein. However, the AChE activity in the presence of genistein was similar to that of the control under 0 to $50 \mu\text{M}$ NGF treatment conditions. Results in Figure 1 clearly indicate that the three test compounds are estrogenic, as shown in the E-screen assay results. The results further show that this estrogenic property is attributable to the binding of the phytoestrogen to the ER, since the effect was effectively blocked by tamoxifen (Figure 2).

In a previous study, Isoda et al. (2002) determined whether the enhanced AChE activity of PC12 cells by phytoestrogen was due to the binding of estrogenic compounds to the ER. They incubated the cells with varying concentrations of 17 β -estradiol (E2) and E2 plus genistein and daidzein or tamoxifen. The results showed that there is no significant enhancement of AChE activity under these conditions. This suggests that binding of E2 to the ER does not enhance AChE activity, and that possibly the effect of genistein and daidzein on AChE activity cannot be expressed in the presence of E2, considering that it requires 1,000- to 10,000-fold molar excess of these phytoestrogens to compete with the ability of E2 to bind to the ER (Miksicek RJ, 1993). From these results, the authors hypothesize that the enhanced AChE activity of PC12 cells in the presence of 5 μ M of the novel isoflavone glucoside may possibly be due to tyrosine protein kinase inhibition.

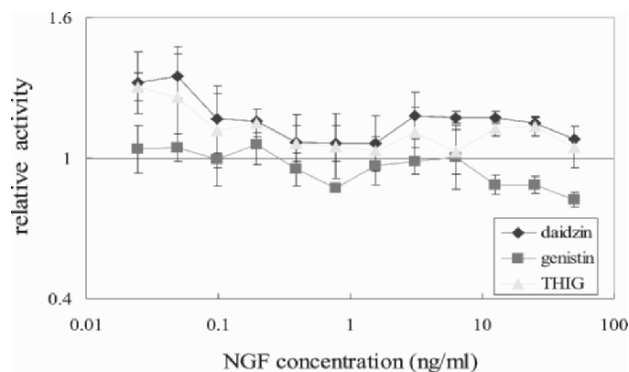


Figure 3. Sensitivity of PC12 cells to NGF

To examine possible mechanisms of action, proteome analysis was performed. Figure 4 shows a typical CBB-stained 2D gel showing the protein profile of NGF-differentiated PC12 cells treated with daidzein. Spots of interest from comparable 2D gels are shown. Spots D1, D2, D3 and D4 are overexpressed in daidzein-treated PC12 cells, while spots C1 and C2 are underexpressed in daidzein-treated cells. The next step in this ongoing study is the excision of the spots and their identification through mass spectrometry. Novel proteins whose expressions are affected by phytoestrogens are expected to be characterized and identified at the end of the study.

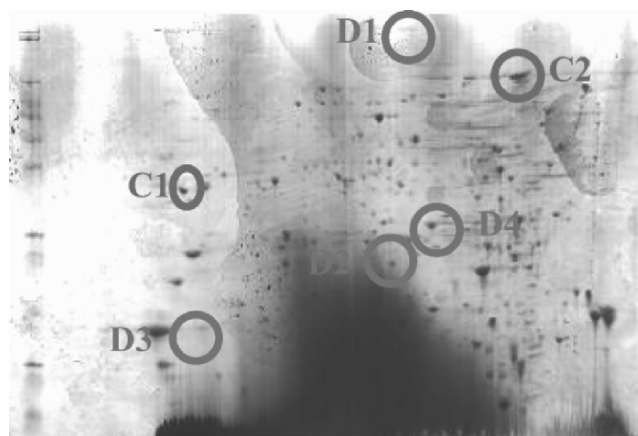


Figure 4. Protein profile of NGF-differentiated PC12 cells incubated with daidzein

4. References

- Deodato B, Altavilla D, Squadrito G, Campo GM, Arlotta M, Minutoli L, Saitta A, Cucinotta D, Calapai G, Caputi A P, Miano M & Squadrito F (1999) Cardioprotection by the phytoestrogen genistein in experimental myocardial ischaemia-reperfusion injury. *Br J Pharm* 128: 1683-1690.
- Han DH, Denison MS, Tachibana H & Yamada K (2002) Relationship between estrogen receptor-binding and estrogenic activities of environmental estrogens and suppression by flavonoids. *Biosci Biotechnol Biochem* 66:1479-1487.
- Isoda H, Talorete TPN, Kimura M, Maekawa T, Inamori Y, Nakajima N and Seki H (2002) Phytoestrogens genistein and daidzin enhance the acetylcholinesterase activity of the rat pheochromocytoma cell line PC12 by binding to the estrogen receptor. *Cytotechnology* 40: 117-123.
- Jones PA, Baker VA, Irwin AJE & Earl LK (1998) Interpretation of the *in vitro* proliferation response of MCF-7 cells to potential estrogens and non-estrogen substances. *Toxicol in Vitro* 12: 373-382.
- Knight DC & Eden JA (1996) A review of the clinical effect of phytoestrogens. *Obstet Gynecology* 87: 897-904.
- Lamartiniere CA, Moore JB, Brown NM, Thompson R, Hardin MJ & Barnes S (1995) Genistein suppresses mammary cancer in rats. *Carcinogenesis* 16: 2833-2840.
- Miksicek RJ (1993) Commonly occurring plant flavonoids have estrogenic activity. *Mol Pharmacol* 44: 37-43.
- Payne J, Jones C, Lakhani S & Kortenkamp A (2000) Improving the reproducibility of the MCF-7 cell proliferation assay for the detection of xenoestrogens. *Science Total Environ* 248: 51-62.
- Tham DM, Gardner CD & Haskell WL (1998) Potential health benefits of dietary phytoestrogens: A review of the clinical, epidemiological, and mechanistic evidence. *J Clin Endoc Metab* 83: 2223-2235.

- Soto AM, Justicia H, Wray JW & Sonnenschein C (1991) *p*-Nonyl-phenol: An estrogenic xenobiotic released from "modified" polystyrene. *Environ Health Perspect* 92: 167-173.
- Soto AM, Sonnenschein C, Chung KL, Fernandez MF, Olea N & Serrano FO (1995) The E-SRCEEN assay as a tool to identify estrogen: An update on estrogenic environmental pollutants. *Environ Health Perspect* 103: 113-122.
- White R, Jobing S, Hoare S A, Sumpter JP & Parker MG (1994) Environmentally persistent alkylphenolic compounds are estrogenic. *Endocrinology* 135: 175-182.

CAPSAICIN-ENHANCED RIBOSOMAL PROTEIN P2 EXPRESSION AND RECOVERY OF TIGHT JUNCTION PERMEABILITY IN HUMAN INTESTINAL Caco-2 CELLS

Junkyu Han, Mitsuaki Akutsu, Terence P. N. Talorete, Toshiyuki Tanaka and Hiroko Isoda

Graduate School of Life and Environmental Sciences, University of TsukubaTennodai 1-1-1, Tsukuba, Ibaraki 305-8572, Japan

Abstract: On the basis of transepithelial electrical resistance measurements, we found that capsaicin (100 μ M) treated-human intestinal Caco-2 cells show a momentary decrease in tight-junction (TJ) permeability followed by a complete recovery. We used proteome analysis to search for proteins that are associated with the recovery of TJ permeability in capsaicin-treated Caco-2 cells. A protein of relative molecular mass of 14 kDa was found to be expressed higher in capsaicin-treated cells than in nontreated cells. Mass spectrometry and sequence analysis revealed that the protein expressed significantly by capsaicin treatment was the ribosomal protein P2 and its cDNA sequence was identical to that found in the human genome database. An increase in amount of cellular filamentous actin (F-actin) was shown after 8 h of incubation with capsaicin. It is reported that ribosomal protein P2 can activate elongation factor 2, which stabilizes F-actin filaments, and that the depolymerization of F-actin was associated with the decrement in TJ permeability. Consequently, these results suggest that ribosomal protein P2 plays an important role in the recovery of the TJ permeability in capsaicin-treated human intestinal Caco-2 cells.

Key words: Caco-2 cells; capsaicin; ribosomal protein P2; TJ permeability

1. INTRODUCTION

Human intestinal Caco-2 cells have been widely used as *in vitro* models to evaluate the transport of absorbing water, ions, and nutrients across the intestinal epithelial barrier (Satsu *et al.*, 2003). Tight-junction (TJ) permeability increase in Caco-2 cells is regulated by various factors, such as food factors (capsaicin, capsiainoside, *etc.*) and chemicals (ealkylphenolic compounds, EDTA, *etc.*). Such factors can alter

epithelial transport and barrier function of human intestinal epithelial cells by various mechanisms (cytoskeletal reorganization, redistribution of ZO-1 and occludin, exertion of Rho A, Rac 1, and Cdc 42, *etc.*) (Han *et al.*, 2002; Nusrat *et al.*, 1995; Bruewere *et al.*, 2004).

In the previous studies (Han *et al.*, 2002; Isoda *et al.*, 2001), we showed that the TJ permeability increase (decrease in transepithelial electrical resistance (TER)) in capsaicin-treated (45 min) human intestinal Caco-2 cells is through binding of capsaicin to a capsaicin receptor-like protein. We also suggested that the increase in TJ permeability upon capsaicin treatment occurs due to a cytoskeletal reorganization of actin filaments, particularly due to the decrease in the amount of filamentous actin (F-actin) in Caco-2 cells. In addition, heat shock protein 47 (HSP47), which is activated during capsaicin treatment, plays an important role as a secondary messenger in the increase in TJ permeability by capsaicin treatment. A preliminary experiment indicated that Caco-2 cells treated with 100 μ M capsaicin longer than the time of previous studies, showed a decrease followed by a recovery of TER values. The recovery of TER values after capsaicin treatment, even without removal of capsaicin, was rapid. This suggests that some proteins, whose expressions are enhanced by capsaicin, facilitate the recovery of TER values after the momentary decrease.

Tools such as two-dimensional gel electrophoresis (2-DE) and mass spectrometry (MS) enable the study of cellular proteome analysis. Using these techniques, changes in protein expression profiles in capsaicin-treated human intestinal Caco-2 cells, particularly proteins related to the recovery of TJ permeability, can be determined.

In this study, we performed 2-DE and MS to determine the possible mechanism behind the recovery of TER after a momentary decrease in capsaicin-treated Caco-2 cells. We found that the expression of ribosomal protein P2 is enhanced by capsaicin treatment, and discussed its role in regulating the recovery of TJ permeability.

2. RESULTS AND DISCUSSION

TER measurement shows that the TJ permeability of the Caco-2 monolayer increased significantly ($p < 0.05$ vs control) upon treatment with capsaicin (100 μ M and 1 mM) (Figure 1). When treated with 100 μ M capsaicin, the TJ permeability recovered after 60 min, followed by the complete recovery after 90 min. However, by treatment with 1 mM capsaicin, the TJ permeability increased irreversibly (Figure 1). These results suggest that the barrier function was disrupted by the high

concentration of capsaicin (1 mM). However, treatment at low concentration (100 μ M) resulted in the recovery of the barrier function. It indicates that the permeability of the intestinal TJ can be regulated by the low concentration of capsaicin (100 μ M).

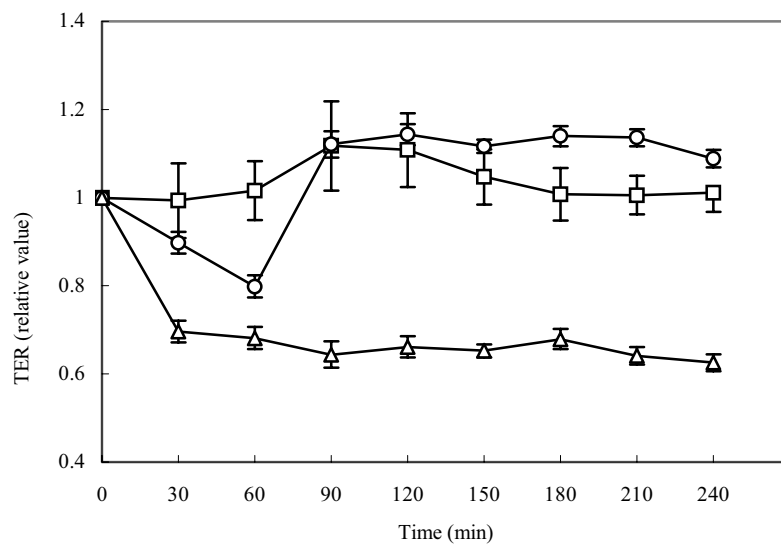


Figure 1. Effect of capsaicin on the TER. TER values are presented as relative to those values at time zero time. The concentrations of capsaicin are: (open circles) 0 μ M capsaicin; (filled boxes) 100 μ M capsaicin; and (open triangles) 1 mM capsaicin.

To elucidate the mechanism behind the recovery of the barrier function, we used 2-DE and MS. The extracted proteins were first subjected to 2-DE (Figure 2 A). A number of proteins were found to be expressed more markedly in the capsaicin-treated cells than in the nontreated cells (data not shown). In particular, the protein spot indicated by arrows in Figure 2 B shows the highest expression in capsaicin-treated cells. The isoelectric point of this protein is in the range of 3.8-4.3, and it has a relative molecular mass of 14 kDa. To identify this protein, the spot was subjected to tryptic digestion and MALDI-TOF MS analysis. The protein spot has a sequence closest to that of ribosomal protein P2; the matched peptides cover 72% (83/115 of amino acids) of ribosomal protein P2.

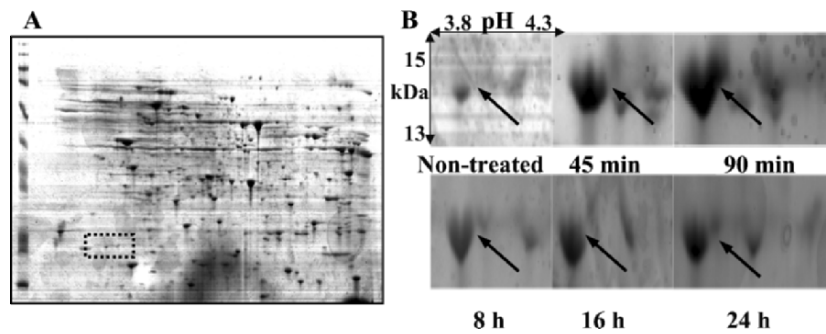


Figure 2. Two-dimensional 2D gel electrophoresis of nontreated-human intestinal Caco-2 cells (A), and time-dependent expression of a protein induced by capsaicin treatment (B). In panel (B), the encircled region in panel (A) and the corresponding region of the capsaicin-treated samples are magnified. The arrowed spot has an isoelectric point in the range of 3.8-4.3, and its molecular mass is approximately 14 kDa. 2-DE 2D gel electrophoresis was performed by the isoelectric focusing of proteins using immobilized pH 3-10 strips, followed by the second-dimensional separation on 12-14% polyacrylamide gels. The separated proteins were stained with Coomassie brilliant blue (CBB). The encircled arrowed spot has an isoelectric point in the range of present in the pH region 3.8-4.3 and its molecular mass is of 13-15 kDa.

By MS analysis, we were unable to get the complete amino acid sequence of the protein expressed by the capsaicin treatment. Therefore, we carried out the isolation and analysis of cDNA of ribosomal protein P2 from Caco-2 cells to examine whether there might be some discrepancy or diversity from the known nucleotide or amino acid sequence. The nucleotide and deduced amino acid sequences of the full-length cDNA clone of the ribosomal protein P2 from Caco-2 cell are shown in Figure 3. These sequences, and its 5'-upstream nucleotides sequence as well, are identical to those of the human ribosomal protein P2 deposited to the databases.

```

1  GTA GCC GTC TCT GCT GCC CCA GGC TCT GCA GCC CCT GCT GCT GGT TCT GCC CCT GCT GCA
61  GAG GAG AAG AAA GAT GAG AAG AAG GAG GAG TCT GAA GAG TCA GAT CCT TCC TTT TCC TCC
121  CTG TCG CCA CCG AGG TCG CAC GCG TGA GAC TTC TCC GCC GCA GAC GCC GCC GCG ATG GCG
      *
181  TAC GTC GCC TCC TAC CTG CTG GCT GCC CTA GGG GGC AAC TCC TCC CCC AGC GCC AAG GAC
      Y V A S Y L L A A L G G N S S P S A K D
241  ATC AAG AAG ATC TTG GAC AGC GTG GGT ATC GAG GCG GAC GAC GAC CCG CTC AAC AAG GTT
      I K K I L D S V G I E A D D D R L N K V
301  ATC AGT GAG CTG AAT GGA AAA AAC ATT GAA GAC GTC ATT GCC CAG GGT ATT GGC AAG CTT
      I S E L N G K N I E D V I A Q G I G K L
361  GCC AGT GTA CCT GCT GGT GGG GCT GTA GCC GTC TCT GCT GCC CCA GGC TCT GCA GCC CCT
      A S V P A G G A V A V S A A P G S A A P
421  GCT GCT GGT TCT GCC CCT GCT GCA GCA GAG GAG AAG AAA GAT GAG AAG AAG GAG GAG TCT
      A A G S A P A A A E E K K D E K K E E S
481  GAA GAG TCA GAT GAT GAC ATG GGA TTT GGC CTT TTT GAT TAA ATT CCT GCT CCC CTG CAA
      E E S D D D M G F G L P D *
541  ATA AAG CCT TTT TAC ACA GCA AAA AAA AAA AAA A

```

Figure 3. Nucleotide and deduced amino acid sequences of ribosomal protein P2. An asterisk indicates a stop codon. The peptide fragments determined by MS analysis (Table 2) are indicated by lines under the sequences.

What is the relation between the recovery of the barrier function and the significant expression of ribosomal protein P2. Ribosomal protein P2 is a member of the well-conserved acidic P (phosphor) protein family in the eukaryotic ribosome (Gonzalo *et al.*, 2002; Lavergne *et al.*, 1987). It plays an important role in the elongation step of protein synthesis and in the activation of elongation factor 2 (EF-2) (Vard *et al.*, 1997). It is reported that the EF-2 is activated by the homologous carboxy-terminal region of Ribosomal protein P2 (Furukawa *et al.*, 1992). EF-2 interacts with globular actin (G-actin), stabilizes filament structure, and causes lateral association of F-actin (Bektas *et al.*, 1994; Bektas *et al.*, 1998). F-actin is a ubiquitous intracellular protein, which in filamentous form constitutes a major component of the cytoskeleton, and plays an essential role in cell motility and mechanics (Holmes *et al.*, 1990; Dadabay *et al.*, 1991). Moreover, it has been suggested that the cytoskeletal reorganization of actin filaments mediates the increase in TJ permeability (Lim *et al.*, 2002). Therefore, it is possible that ribosomal protein P2, whose expression is enhanced by the capsaicin treatment, activates EF-2 to restore the F-actin in human intestinal Caco-2 cells followed by the prevention of the expressive TJ permeability. In the previous study (Isoda *et al.*, 2001), we examined whether the capsaicin-induced increase in TJ permeability is associated with the cytoskeletal reorganization of the actin filaments by determining the cellular F-actin amount in Caco-2 cells by 45 min treatment of capsaicin (0, 200, and 300

μM). The amount of cellular F-actin was found to decrease significantly in the capsaicin-treated Caco-2 cells. This reduction is probably due to the depolymerization of F-actin into G-actin as a form of cytoskeletal reorganization (Rayment *et al.*, 1993; Lim *et al.*, 2002). To confirm the hypothesis, we determined the amount of cellular F-actin in Caco-2 cells treated with 100 μM capsaicin with longer time scale (0, 8, 16, and 24 h), which is chosen to be comparable with the proteome analysis (Figure 2B). An increase in the amount of F-actin was shown in 8 h and continued till 24h of incubation (Figure 4). These and the previous results indicate that there is a close correlation between the amount of ribosomal protein P2 and that of F-actin.

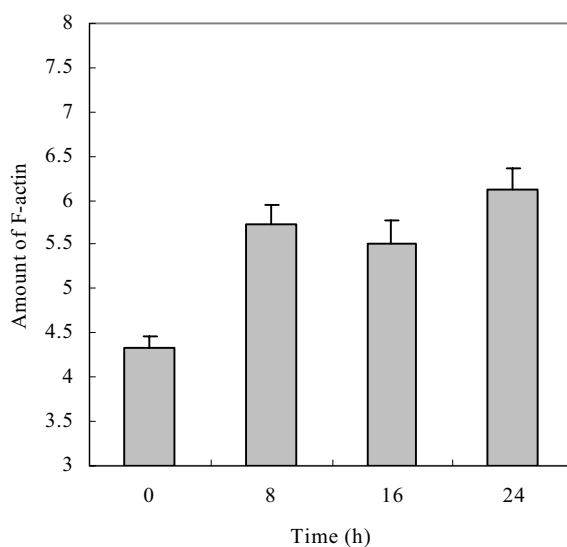


Figure 4. Effect of 100 μM capsaicin concentrations on the F-actin of Caco-2 cells. Standard deviation were <10%.

In summary, we have investigated the mechanism of the recovery of TJ permeability in capsaicin-treated human intestinal Caco-2 cells. The expression of ribosomal protein P2 was enhanced by the capsaicin-treatment, which is followed by the increment in the amount of F-actin and the recovery of TJ permeability. This result suggests that ribosomal protein P2 stabilizes F-actin and recover the TJ permeability through the activation of EF-2. This is the first report showing that the expression of ribosomal protein P2 is related to the recovery of TJ permeability in human intestinal Caco-2 cells.

3. REFERENCES

- Bektas, M.; Nurten, R.; Gurel, Z.; Sayers, Z.; Bermek, E. Interaction of eukaryotic elongation factor 2 with actin: a possible link between protein synthetic machinery and cytoskeleton. *FEBS Lett.* 1994, 356, 89-93.
- Bektas, M.; Nurten, R.; Gurel, Z.; Sayers, Z.; Bermek, E. Interaction of elongation factor 2 with the cytoskeleton and interference with DNase I binding to actin. *Eur. J. Biochem.* 1998, 256, 142-147.
- Bruewer, M.; Hopkins, A. M.; Hobert, M. E.; Nusrat, A.; Madara, J. L. RhoA, Rac1, and Cdc42 exert distinct effects on epithelial barrier via selective structural and biochemical modulation of junctional proteins and F-actin. *Am. J. Physiol. Cell Physiol.* 2004, 287, C327-C335.
- Dadabay, C. J.; Patton, E.; Cooper, J. A.; Pike, L. J. Lack of correlation between changes in polyphosphoinositide levels and actin/gelsolin complexes in A431 cells treated with epidermal growth factor. *J. Cell Biol.* 1991, 112, 1151-1156.
- Furukawa, T.; Uchiumi, T.; Tokunaga, R.; Taketani, S. Ribosomal pProtein P2, a nNovel iIron-bBinding pProtein. *Arch. Biochem. Biophys.* 1992, 298, 182-186.
- Gonzalo, P.; Lavergne, J. P.; Reboud, J. P. Pivotal rRole of P1 N-terminal dDomain in the aAssembly of the mMammalian rRibosomal sStalk and in the pProteosynthetic aActivity. *J. Biol. Chem.* 2002, 276, 19762-19769.
- Han, J. K.; Isoda, H.; Maekawa, T. Analysis of the mechanism of the tight junctional permeability increase by capsaicin treatment on the Caco-2 cells. *Cytotechnology* 2002, 40, 93-98.
- Hashimoto, K.; Kawagishi, H.; Nakayama, T.; Shimizu, M. Effect of capsianoside, a diterpene glycoside, on tight-junctional permeability. *Biochim. Biophys. Acta* 1997, 1323, 281-290.
- Holmes, K. C.; Popp, D.; Gebhard, W.; Kabsch, W. Atomic model of the actin filament. *Nature* 1990, 347, 44-49.
- Isoda, H.; Han, J. K.; Tominaga, M.; Maekawa, T. Effect of capsaicin on human intestinal cell line Caco-2. *Cytotechnology* 2001, 36, 155-161.
- Lavergne, J. P.; Conquet, F.; Reboud, J. P.; Reboud, A. M. Role of acidic phosphoprotein in the parartical reconstitution of the active 60 S ribosomal subunit. *FEBS Lett.* 1987, 216, 83-88.
- Lim, S. O.; Park, S. J.; Kim, W.; Park, S. G.; Kim, H. J.; Kim, Y. I.; Sohn, T. S.; Noh, J. H.; Jung, G. PProteome AAnalysis of HHepatocellular CCarcinoma. *Biochem. Biophys. Res. Commun.* 2002, 291, 1031-1037.
- Nusrat, A.; Giry, M.; Turner, J. R.; Colgan, S. P.; Parkos, C. A.; Carnes, D.; Lemichez, E.; Boquet, P.; Madara, J. L. Rho protein regulates tight junctions and perijunctional actin organization in polarized epithelia. *Proc. Natl. Acad. Sci. U.S.A.* 1995, 92, 10629-10633.
- Rayment, I.; Holden, H. M.; Whittaker, M.; Yohn, C. B.; Lorenz, M.; Holmes, K. C.; Milligan, R. A. Structure of the actin-myosin complex and its implications for muscle contraction. *Science* 1993, 261, 58-65.
- Satsu, H.; Yokoyama, T.; Ogawa, N.; Fujimura-Hatano, Y.; Shimizu, M. Effect of Neuronal PC12 Cells on the Functional Properties of Intestinal Epithelial Caco-2 Cells. *Biosci. Biotechnol. Biochim.* 2003, 67, 1312-1318.
- Vard, C.; Guillot, D.; Bargis, P.; Lavergne, J. -P.; Reboud, J. -P. A sSpecific rRole for the pPhosphorylation of mMammalian aAcidic rRibosomal pProtein P2. *J. Biol. Chem.* 1997, 272, 20259-20262.

METABOLIC RESPONSES OF EUKARYOTIC DRUG EFFICACY AND TOXICITY

D.B. Goodenowe, S. Ritchie, D. Heath

Phenomenome Discoveries Inc. 204-407 Downey Rd. Saskatoon, SK, Canada S7N 4L8.
www.phenomenome.com

Abstract: Identifying metabolic responses of cells to drugs can be highly informative for understanding mode of action and toxicity, and can provide value in the drug discovery process by complementing conventional pharmacokinetic/pharmacodynamic measurements. In many circumstances, drugs are known to impinge upon biochemical pathways comprising previously identified intermediates, of which there may be a necessity to assay during development. To address these concerns in the pharmaceutical industry, we have engineered a targeted analytical platform that can rapidly assay a predefined panel of metabolites. We are applying the technology to investigate the responses of predefined metabolites to several classical drugs in a eukaryotic cell model system. A simple and intuitive interface allows users to quickly associate aberrantly regulated pathways with specific drug activity.

Key words: targeted; analytical; metabolite; metabolome; LC/MS; GC/MS; primary metabolism; secondary metabolism; glycolysis; gluconeogenesis; PPP; TCA cycle; vitamin; carbohydrate; amino acid; nucleic acid; alkaloid; lipid; fatty acid; steroid.

1. TARGETED METHODS ANALYTICAL PLATFORM

Phenomenome Discoveries Inc. is developing a Targeted Methods analytical platform for the investigation of major primary and secondary metabolites.

Researchers can choose a combination of several preselected sets of primary and secondary metabolites in order to efficiently compare relevant biochemical levels in experimental samples. Our GC/MS and LC/MS analytical methods achieve excellent chromatographic separation of most metabolites, and by using SIM (single ion monitoring) and SRM (selected reaction monitoring) procedures combined with a retention time based database, most targeted metabolites are easily identified and quantitated with high specificity and sensitivity.

A wide variety of primary and secondary metabolic pathways have been considered for this targeted metabolite analysis platform in order to provide a wide coverage of the metabolome (see Tables 1-4).

As a result, this technology will be applicable to most metabolic research programs by allowing researchers to make informed discoveries.

Our predefined panels of metabolites (see Tables 1-4) will allow quantitation of specific metabolites of interest to each researcher, as well as give an opportunity to make unexpected discoveries about levels of metabolites that would not normally be analyzed.

Therefore, this Targeted Metabolite platform will provide both expected and novel information about system changes such as drug treatment.

Table 1. Targeted metabolites listed by analysis mode.

LC/MS - NESI AQUEOUS	LC/MS - NESI AQUEOUS	LC/MS - NESI AQUEOUS
Glycolysis/Gluconeogenesis/TCA/P PP: pyruvic acid	D-(+)-Cellotriose D-(+)-Glucosamine	Nucleic Acids: (-)-Adenosine 5'-monophosphate (cAMP) Adenosine 3',5'-cyclic monophosphate (CDP) Cytidine 5'-Diphosphate (CMP) Cytidine 5'-Monophosphate (cyclic CMP) Cytidine 2', 3'- cyclophosphate (FAD) Flavin adenine dinucleotide (PRPP) 5-Phosphorylribose 1-Pyrophosphate (UDP) Uridine 5'-diphosphate (UDP-glucose) Uridine 5'- diphosphoglucose (UMP) Uridine 5'-monophosphate 2'-Deoxyadenosine 2'-Deoxycytidine 2'-deoxyuridine 3'-Deoxyguanosine Acetoacetyl coenzyme A Acetyl coenzyme A (C2:0) Adenosine Adenosine 5' diphosphate Adenosine 5' triphosphate Adenosine 5'-diphosphoglucose Adenosine 5'-Diphosphoribose Coenzyme A CTP Cytidine dATP dCTP dGTP DL-3-hydroxy-3-methylglutaryl coenzyme A dTTP dUTP GTP Guanidineacetic Acid Guanosine Guanosine 5' Diphosphate Inosine 5' triphosphate Malonyl coenzyme A NAD NADP
lactic acid oxalacetic acid oxalic acid	D-(+)-Maltose D-(+)melezitose D-(+)raffinose	
methyl malonic acid malonic acid	D-Arabinose D-Erythrose 4-phosphate	
fumaric acid succinic acid	D-Fructose D-Galactose	
citric acid DL-isocitric acid maleic acid D-malic acid a-D-glucose-1-phosphate D-ribose-5-phosphate DL-Glyceraldehyde 3-phosphate D(-)3-Phosphoglyceric acid DL-isocitric acid D-gluconic acid 6-phosphogluconic acid D-fructose 1,6-diphosphate Dihydroxyacetone phosphate Glycerophosphate Phosphoenolpyruvic acid 2,3-diphospho-D-glyceric acid 2-Oxoglutaric acid	D-Glucose D-glucose 6-phosphate D-Glyceraldehyde D-Lyxose D-mannitol D-Myo-Inositol 4-monophosphate D-Ribose D-sorbitol D-Tagatose D-Trehalose dulcitol (galactitol) D-Xylose glycerol iso-erythritol isomaltotriose L-(-)-Arabitol L-(-)-Sorbitol L-(+)-Arabinose Lactose	
Plant Hormones:		
Indole-3-Acetic Acid 2-cis,4-trans-abscisic acid Zeatin (trans isomer)	L-gulonolactone L-Rhamnose maltitol maltoheptaose maltohexaose maltopentaose maltotetraose maltotriose Melibiose Myo-Inositol N-Acetyl-D-glucosamine N-Acetyl-D-Glucosamine 6- phosphate N-acetyl-D-mannosamine N-Acetylneuraminic acid ribitol (adonitol) Sedoheptulose stachyose Sucrose Sucrose-6'-monophosphate Xylitol	
Vitamins - Water Soluble: (PABA) p-aminobenzoic acid d-biotin folic acid d-pantothenic acid pyridoxal pyridoxamine		
pyridoxine riboflavin L-ascorbic acid (Vitamin C)		
Carbohydrates: D-(+)arabitol D-(+)-Cellobiose D-(+)-Cellopentaose D-(+)-Cellotetraose		

Table 2. Targeted metabolites listed by analysis mode.

LC/MS - NESI AQUEOUS	LC/MS - PESI AQUEOUS	LC/MS - PESI AQUEOUS
Shikimate Pathway:	Amino Acids and Derivatives:	(SAM) S-adenosyl-L-methionine
Chorismic acid	L-Alanine	Glutathione-oxidized
Prephenic acid	L-Arginine	L-Glutathione, reduced
(-)shikimic acid	L-Asparagine	L-Kynurenine
	L-Aspartic acid	L-Homocarnosine
	L-Cysteine	L-(+)-Cystathionine
		R-(-)-1-Amino
Other Acids:	L-Cystine	-2-Propanol
2,3-dimethylmaleic acid	L-Glutamic acid	L-carnosine
2-hydroxybutyrate	L-Glutamine	N-Acetylisatin
3,4-Dihydroxycinnamic acid	Glycine	L-DOPA
3-Hydroxybenzoic acid	L-Histidine	Beta-Alanine
4-Hydroxyphenylacetic acid	trans-4-hydroxy-L-Proline	Cys-Gly
4-Hydroxyphthalic acid	L-Isoleucine	
4-Methoxybenzoic acid	L-Leucine	Sulphates:
Acetylenedicarboxylic Acid	L-Lysine	thiogalactoside
benzoic acid	L-Methionine	
Cinnamic Acid	L-Phenylalanine	Nitrogenous bases:
cis-3-Chloroacrylic acid	L-Proline	Adenine
cis-Aconitic acid	L-Serine	Cytosine
D-Gluconic acid	L-Threonine	Guanine
D-Gluconic acid	L-Tryptophan	(-)-Inosine
Dimethyl Fumarate	L-Tyrosine	Hypoxanthine
D-tartaric acid	L-Valine	Uracil
Glutaric acid	L-Homoserine	Xanthine
Glycolic acid	L-Citrulline	
Glyoxylic acid	DL-Homocysteine	Amines and Amides:
Hippuric acid	Cadaverine	Pyridoxal 5-phosphate (PLP)
Itaconic acid	1,4-Diaminobutane (Putrescine)	6-Aminocaproic Acid
Mesaconic acid	L-Ornithine	Choline
Methylmalonic Acid	Tyramine	Acetylcholine
P-Coumaric Acid	3-Hydroxytyramine	Betaine (aka glycine betaine)
Phenylpyruvic acid	Taurine	Sanguinarine
Phosphonoacetic acid	N,N-Dimethylglycine	Berberine
phytic acid	5-hydroxy-L-tryptophan	Palmitate
quinic acid	Seleno-L-cystine	Tetrahydropalmitate
R-3-hydroxybutyric acid	Seleno-L-Methionine	R-(-)-epinephrine
Terephthalic acid	N-formyl-DL-phenylalanine	L-Noradrenaline
		3-Methoxy-4-
	O-acetyl-L-serine	hydroxyphenylethylamine
	L-carnitine	Nicotinic acid (aka niacin)
	Acetyl -L-carnitine	
	O-Succinyl-L-homoserine	nicotinamide (niacinamide)
	Creatine	thiamine
	Creatinine	Phenethylamine
	D-thyroxine	Tryptamine
	(GABA) 4-Aminobutyric acid	Serotonin
		(ACC) 1-aminocyclopropane-1-
	5-Aminolevulinic acid	carboxylic acid
	N-Acetyl-L-glutamic acid	
	S-(5'-Adenosyl)-L-Homocysteine	

Table 4. Targeted metabolites listed by analysis mode.

GC/MS - EI ORGANIC	GC/MS - EI ORGANIC	GC/MS - EI ORGANIC
Fatty Acids: continued	furfuryl hexanoate	Alpha-D-Glucose Pentaacetate
Cis-7,10,13,16,19-Docosapentaenoic acid methyl ester	furfuryl heptanoate	Beta-D-Galactose pentaacetate
Cis-8,11,14-Eicosatrienoic acid	furfuryl octanoate	Sinapyl alcohol
Decanoic acid	methyl butyrate	Coniferyl alcohol
Docosahexaenoic acid (22:6)	propyl butyrate	Scopoletin
Docosanoic acid	isopropyl butyrate	Methylglyoxal
Eicosanoic acid	hexyl butyrate	R-(-)-1,2-propanediol
Elaidic acid (18:1 trans)	allyl butyrate	Vanillic acid
Erucic acid (22:1)	benzyl butyrate	Homovanillic acid
Gamma linolenic acid	methyl tiglate	Protocatechuic Acid
Heptacosanoic acid	ethyl butyrate	Homoprotocatechuate
Heptadecanoic acid	propyl tiglate	4-Hydroxybenzoic acid
Heptanoic acid	isopropyl tiglate	Coumarin
Hexanoic acid	hexyl tiglate	Methyl 4-oxobutanoate
Lauric acid	allyl tiglate	Indole (aka 2,3-Benzopyrrole)
Linoleic acid (18:2)	benzyl tiglate	
Linoleic acid (18:2)	ethyl pentanoate (valerate)	Steroids, Lipids, Terpenoids:
Linolenic acid (18:3)	ethyl hexanoate	11 α -Hydroxyprogesterone
Linolenic acid (18:3)	ethyl heptanoate	3 β -Hydroxyandrost-5-en-17-one
Myristic acid	ethyl octanoate	5 α -Pregnane-3-20-dione-allo
Myristoleic acid	furfuryl propionate	5 α -Pregnane-3 α ,20 α -diol
Nervonic acid	furfuryl butyrate	Adrenosterone
Nervonic acid (24:1)	furfuryl pentanoate	Aldosterone
Nonadecanoic acid	2-Acetylpyrrole	Beta-estradiol
Nonanoic acid	2,4,5-Trimethylthiazole	Cholest-4-en-3-one
Octanoic acid	2-Isobutylthiazole	cholesterol
Oleic acid (18:1)	2-Ethoxythiazole	Cortisone
Palmitelaidic acid methyl ester	2-Methylpyrazine	Deoxycorticosterone
Palmitelaidic acid methyl ester	2,3-Dimethylpyrazine	Ergosterol
Palmitic acid (16:0)	2,5-Dimethylpyrazine	Estrinol
Palmitoleic acid (16:1)	2,6-Dimethylpyrazine	Estrone
Pentadecanoic acid	2,3,5-Trimethylpyrazine	Hydrocortisone
Petroselinic acid (18:1)	2,3,5,6-Tetramethylpyrazine	Lanosterol
Stearic acid	2-Ethylpyrazine	Prednisolone
Tetracosanoic acid	2-Acetylfuran	Pregnenolone
Tricosanoic acid	2,3-Diethylpyrazine	Progesterone
Tridecanoic acid	3-Ethyl-2-methylpyrazine	Prostaglandin B2
Undecanoic acid	2-Methoxy-pyrazine	Prostaglandin D2
	2-Methoxy-3-methylpyrazine	Prostaglandin F2A
Aldehydes:	2-Isobutyl-3-methoxy-pyrazine	stigmaterol
9-cis-retinal	2-Acetylthiophene	Leukotriene B4
	2-Acetylthiazole	Leukotriene C4
Phenolics:	2-Acetylpyridine	Thromboxane B2
2-methyl-1,4-naphthoquinone (PQQ) Pyrroloquinoline quinone	2-Acetylpyrazine	1-decene
	Thiazole	Aphidicolin
	4-Methylthiazole	Myrcene
Esters and Volatiles:	4,5-Dimethylthiazole	squalene
ethyl propionate		Vitamin K1

SUPPRESSIVE EFFECT OF FUCOIDAN DERIVED FROM *MOZUKU* ON *IN VITRO* INVASION OF HUMAN FIBROSARCOMA HT1080 CELLS

Jun Ye¹, Kiichiro Teruya¹, Yoshinori Katakura¹, Hiroshi Eto² and Sanetaka Shirahata¹

¹ Department of Genetic Resources Technology, Faculty of Agriculture, Kyushu University,
6-10-1 Hakozaki, Higashi-ku, Fukuoka 812-8581, Japan; ² Daiichi Sangyo Co. Ltd.,
Osaka 530-0037, Japan

Abstract: Fucoidan is a uniquely-structured sulfated polysaccharides that is found in the cell walls of several types of brown seaweed, but not of land plants. Recently, Fucoidan has clinically got a lot attention due to its anti-tumor metastasis potential. We report here that the enzyme-digested fucoidan extract derived from *Cladosiphon novae-caledoniae kylin*, which was called "mozuku" in the Kingdom of Tonga, inhibited *in vitro* invasion of human fibrosarcoma HT1080 cells. Flow cytometric analysis revealed that the enzyme-digested fucoidan extract effectively scavenged intracellular H₂O₂ of HT1080 cells. Both activities of MMP2 and 9 were decreased in a dose dependent manner by the fucoidan extract, suggesting that Fucoidan may inhibit the invasion of tumor cells via suppression of MMP2 and 9 activities.

Key words: fucoidan, antioxidation, MMPs, invasion, antitumor activity

1. INTRODUCTION

Metastasis is a major problem of cancer therapy. Matrix metallo-proteinase Fucoidan derived from *Cladosiphon novae-caledoniae kylin* that is called *mozuku* in the Kindom of Tonga, is a traditional food for local inhabitants. It is noteworthy that the cancer death rate in Okinawa is the lowest of all the prefectures in Japan, this phenomenon indicated a promising prospect of fucoidan as a dietary substance for preventing human from cancer attack. Untill now, fucoidan has been proved helpful in alleviating murine chronic colitis(1), acetic acid-

induced gastric ulcer in rats(2), and gastric mucosal protection(3). However, the effect of the fucoidan on tumor invasion have never been reported. In the study, we demonstrated that fucoidan derived from *Cladosiphon okamuranus Tokida* possesses antioxidative potential, suppressing *in vitro* invasion of HT1080 cells.

2. MATERIAL AND METHODS

2.1 Preparation of the enzyme-digested fucoidan extract and reagents

Fucoidan was obtained from the Daiichi Sangyo Corporation (Osaka, Japan) as healthy functional food (Power fucoidan). The undiluted solution was neutralized to PH7.0 by 1 M NaOH. The Precipitation was removed by Centrifuge at 3500rpm for 15min. The supernatant was then sterilized by 0.2µm pore filter (Millipore, MA, USA) and stored in 4°C. 2',7'-dichlorofluorescein diacetate (DCFH-DA) was obtained from Sigma (MO). WST-1[2-(4-Iodophenyl)-3-(4-nitrophenyl)-5-(2,4-disulfo-phenyl)-2H-tetrazolium, monosodium salt] was purchased from Kishida (Osaka, Japan). Matrigel was purchased from Funakoshi (Tokyo, JAPAN). Total and Phospho-p38 Mitogen-activated protein kinase (MAPK) antibody was obtained from Cell Signaling Technology (MA).

2.2 Cell culture and treatment

HT1080 was cultured in modified Eagle's medium (MEM) supplemented with 10% fetal bovine serum (FBS) (Biowest, France). Fucoidan solution was mixed with 10x MEM that was diluted with MilliQ water.

2.3 Cell viability assay

5x10⁵ cells/well HT1080 cells were cultured in 24-well microplate with MEM (10% FBS) at 5% CO₂, 37°C for 24 h, the culture medium was removed and MEM (10% FBS) containing fucoidan was added. The cells were challenged for another 24h. Then, the medium was removed and 500 µl WST-1 reagent was added to the wells at 37°C for 2h. 100µl reaction solution was added into 96-well microplate. The absorbance of the treated and untreated samples were measured using a microplate reader (Tecan spectra, Wako, Japan) at 450 nm.

2.4 Flow cytometric assessment of H₂O₂

HT1080 cells were pre-treated with MEM containing fucoidan liquid for 24 h, then incubated with 5 μ M DCFH-DA for 30 min at 37°C. The fluorescent intensity of DCFH was measured by a flow cytometer (EPICS XL system II, Beckman coulter).

2.5 Zymography

HT1080 cells were cultured in MEM supplemented with 10% FBS in 20mm dish overnight and subsequently treated with MEM (10 % FBS) containing fucoidan for 24 h. The culture medium was then removed and addition of 2ml MEM (serum free) was added for another 24h. The supernatant was collected and concentrated with centrifugal filter devices (Millipore, MA). Each 5 μ l samples of concentrated cell culture medium were mixed with 5 μ l of 2 x sample buffer (0.25 M Tris-HCl, pH6.0, 8.5% glycerol, 4% SDS, 0.01% bromophenol blue). The samples were then electrophoresed on gelatin containing gel (7.5% polyacrylamide gel containing 2mg/ml gelatin). After electrophoresis, the gel was three times washed for 10 min in 2.5% Triton X-100, and incubated with incubation buffer (50 mM Tris-HCl, pH 7.6; 10 mM CaCl₂; 50 mM NaCl; 0.05% Brij35) overnight at 37°C. After incubation, the gel was stained by CBB solution (0.25% Coomassie blue R250, 40% methanol and 10% acetic acid) for 1 h at room temperature, then destained with 40% methanol and 10% acetic acid until the bands became clear.

2.6 Matrigel invasion assay

A 24-well microplate was coated with 700 μ l of serum-free MEM containing 10 μ g of fibronectin. Eight- μ m chambers (Kurabo, Osaka, JAPAN) were then coated with 20 μ l matrigel on the upper parts and 10 μ l Collagen on the lower parts. The chambers were inserted into the 24-well microplate. HT1080 cells were pretreated with fucoidan liquid for 24 h, inoculated 1 x 10⁵ cells per well onto the chamber then incubated for 12 h at 37°C. The cells that invaded the lower surface of collagen were fixed and stained with Diff-Quik (Sysmex, IL). The invaded cells were counted three random fields under a light microscope.

3. RESULTS

3.1 Effect of the fucoidan extract on the cell viability of HT1080 cells

To examine the effect of power fucoidan on HT1080 cell viability, cells were treated with different concentrations of fucoidan solution (1-80%) for 2 days and cell proliferation was evaluated by WST-1 assay. As shown in Fig. 1, no significant effect was observed on viability of HT1080 cell when exposed 1-20% fucoidan solution. However, the cytotoxic effect of fucoidan happened in a dose-dependent when challenged by more than 20% fucoidan solution. To exclude toxic effect of fucoidan on the study, less than 20% fucoidan solution was used throughout the experiments.

3.2 The intracellular H_2O_2 -scavenging effect of fucoidan on HT1080 cells

Then, we checked to determine whether fucoidan could act as an H_2O_2 scavenger. DCFH-DA has been used as a substrate for measuring intracellular H_2O_2 production in HT1080 cells. DCFH-DA is hydrolyzed by esterases to dichlorofluorescein (DCFH), which is trapped within the cell. This nonfluorescent molecule is then oxidized to fluorescent dichlorofluorescein (DCF) by action of cellular H_2O_2 . HT1080 cells were pre-treated with MEM containing fucoidan for 24h, then incubated with 5 μ M DCFH-DA for 30 min at 37°C. As shown in Fig. 2, fucoidan proved to be effective in scavenging intracellular H_2O_2 in HT1080 cells in a dose-dependent manner.

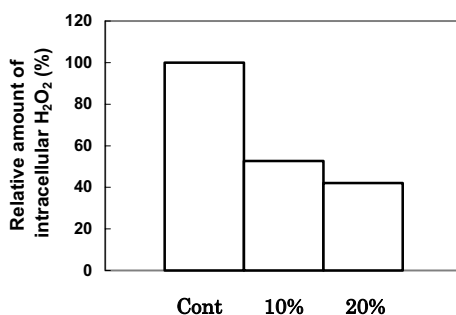


Figure 2. Fucoidan scavenges H_2O_2 in HT1080 cells. HT1080 cells were pre-treated with MEM (10% FBS) containing fucoidan for 24h, then incubated with 5 μ M DCFH-DA for 30 min at 37°C. The fluorescent intensity of DCFH was measured by a flow cytometer.

3.3 The fucoidan extract inhibits the *in vitro* invasion of HT1080 cells

MMP2 and 9 are the functional agents in tumor cells invasion and secreted in culture medium as soluble enzymes, we performed zymography to detect the level of the two enzymes in culture medium. Both activity of MMP-2 and 9 were decreased in a dose-dependent manner (data not shown). The invasive ability of the cells was analyzed by matrigel penetrating assay. As shown in Fig. 3, the number of cells penetrating the matrigel was also decreased in a dose-dependent manner, suggesting the effectiveness of fucoidan in inhibiting tumor cells invasion.

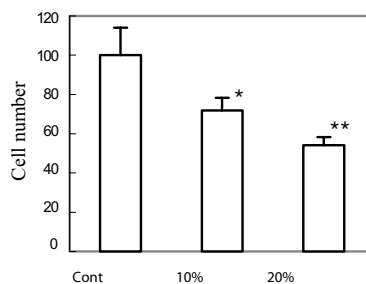


Figure 3. Fucoidan inhibits HT1080 cells invasion. HT1080 cells were pre-treated with MEM (10% FBS) containing fucoidan for 24h, 1×10^5 cells per well were seeded onto the chamber then incubated for 12 h at 37°C. The cells that invaded the lower surface of collagen were fixed and stained, the invaded cells were counted three random fields under a light microscope. Data are expressed as the mean \pm SD of three independent experiments. Results were statistically significant (* $P < 0.05$; $n = 3$) using the Student's *t* test.

4. DISCUSSION

Recently, a number of studies have documented the antioxidative effect of sulfated polysaccharides derivatives (4-7). Several fucoidan derivatives had been reported to inhibit tumor invasion through interfering the interaction between tumor cell and matrigel (8-9). Fucoidan derived from *Cladosiphon okamuranus Tokida* effectively decreased both intracellular and released extracellular H_2O_2 of HT1080 cells in a dose-dependent manner, though we did not know the exact mechanism, however, it is possible that, *in vivo*, fucoidan reduce reactive

oxygen species (ROS) by stimulating antioxidant enzymes, such as superoxide dismutase (SOD) and glutathione peroxidase (GSH-Px)(7). MMP-2, and 9 are key enzymes for tumor invasion, the inhibition of HT1080 cells invasion on matrigel was thought due to the reduced secretion of the two enzymes. In the other hand, MMP-2 and 9 gene expression were proved to be stimulated by oxidative stress (10-13). Therefore, the inhibitory effect of *Cladosiphon okamuranus Tokida* fucoidan on tumor invasion was, at least in part, due to the reduced expression of MMP-2 and 9 through scavenging intracellular H₂O₂.

In conclusion, we discovered that fucoidan derived from *Cladosiphon okamuranus Tokida* inhibited the invasion of HT1080 cells *in vitro* through reducing MMP2,9 expression. The inhibitory effect of *Cladosiphon* fucoidan was at least in part due to its antioxidative potential. *Cladosiphon okamuranus Tokida* fucoidan may be helpful as a dietary substance for preventing cancer in humans.

REFERENCES

1. Matsumoto S, Nagaoka M, Hara T, Kimura-Takagi I, Mistuyama K, Ueyama S. Fucoidan derived from *Cladosiphon okamuranus Tokida* ameliorates murine chronic colitis through the down-regulation of interleukin-6 production on colonic epithelial cells. *Clin Exp Immunol*. 2004 Jun; 136(3):432-9.
2. Shibata H, Nagaoka M, Takagi IK, Hashimoto S, Aiyama R, Yokokura T. Effect of oligofucose derivatives on acetic acid-induced gastric ulcer in rats. *Biomed Mater Eng*. 2001; 11(1):55-61.
3. Shibata H, Kimura-Takagi I, Nagaoka M, Hashimoto S, Aiyama R, Iha M, Ueyama S, Yokokura T. Properties of fucoidan from *Cladosiphon okamuranus tokida* in gastric mucosal protection. *Biofactors*. 2000; 11(4):235-45.
4. Xue C, Yu G, Hirata T, Terao J, Lin H. Antioxidative activities of several marine polysaccharides evaluated in a phosphatidylcholine liposomal suspension and organic solvents *Biosci Biotechnol Biochem*. 1998; 62(2):206-9.
5. Xue CH, Fang Y, Lin H, et al. Chemical characters and antioxidative properties of sulfated polysaccharides from *Laminaria japonica*. *JOURNAL OF APPLIED PSYCHOLOGY* 2001, 13(1):67-70.
6. Ruperez P, Ahrazem O, Leal JA. Potential antioxidant capacity of sulfated polysaccharides from the edible marine brown seaweed *Fucus vesiculosus*. *J Agric Food Chem*. 2002, 13; 50(4):840-5.
7. Zhang Q, Li N, Zhou G, Lu X, Xu Z, Li Z. *In vivo* antioxidant activity of polysaccharide fraction from *Porphyra haitanesis* (Rhodophyta) in aging mice *Pharmacol Res*. 2003 Aug; 48(2):151-5.

8. Soeda S, Ishida S, Shimeno H, Nagamatsu A. Inhibitory effect of oversulfated fucoidan on invasion through reconstituted basement membrane by murine Lewis lung carcinoma. *Jpn J Cancer Res.* 1994, 85(11):1144-50.
9. Haroun B F, Lindenmeyer F, Lu H, Soria C, Jozefonvicz J, Boisson VC. *In vitro* effects of fucans on MDA-MB231 tumor cell adhesion and invasion *ANTICANCER RESEARCH* 2002, 22 (4): 2285-2292.
10. Grote K, Flach I, Luchtefeld M, Akin E, Holland SM, Drexler H, Schieffer B. Mechanical stretch enhances mRNA expression and proenzyme release of matrix metalloproteinase-2 (MMP-2) via NAD(P)H oxidase-derived reactive oxygen species *Circ Res.* 92(2003):e80-6.
11. Belkhiri A, Richards C, Whaley W, McQueen SA, Orr FW. Increased expression of activated matrix metalloproteinase-2 by human endothelial cells after sublethal H₂O₂ exposure. *Lab Invest*, 77 (1997), 533-539.
12. Kolev K, Skopal J, Simon L, Csonka E, Machovich R, Nagy Z. Matrix metalloproteinase-9 expression in post-hypoxic human brain capillary endothelial cells: H₂O₂ as a trigger and NF-kappaB as a signal transducer *Thromb Haemost.* 2003, 90(3):528-37.
13. Gurjar MV, Deleon J, Sharma RV, Bhalla RC. Role of reactive oxygen species in IL-1 beta-stimulated sustained ERK activation and MMP-9 induction. *Am J Physiol Heart Circ Physiol.* 2001, 281(6):H2568-74.

INCREASED EXPRESSION, PURIFICATION AND CHARACTERIZATION OF THE WW DOMAIN OF CA150/FBP28

Yusuke Kato, Yoriko Sawano and Masaru Tanokura

Department of Applied Biological Chemistry, Graduate School of Agricultural and Life Sciences, University of Tokyo, 1-1-1 Yayoi, Bunkyo-ku, Tokyo 113-8657, Japan

Abstract: WW domain is well known protein module that mediates protein through protein interactions by binding to proline-containing ligands. Based on the ligand predilections, WW domains have been classified into three major groups, I, II/III and IV. Group-II/III WW domains have been reported to bind proline-rich ligands.

CA150/FBP28 is one of splicing factors, which enhances the efficiency of splicing and maturation of mRNA (Lin et al., 2004). The WW domain of CA150/FBP28 belongs to Group-II/III and was shown to have binding specificity to the –Pro-Pro-Leu-Pro– sequence. However, the binding is quite subtle and the quantitative analysis of the binding is required to confirm and evaluate the binding. Many WW domains showed relatively weak binding (Kato et al., 2004). Quantitative assay such as surface plasmon resonance or isothermal titration calorimetry needs large amount of protein samples (approximately tens of milligram per each sample) especially in the cases of the analysis in weak binding conditions.

The expression system of WW domains is mainly based on the GST-fusion system. However, the amount of the production was not enough with the conventional shaking cultivation. Thus, instead of shaking, we utilized an air pump to cultivate *E. coli* to produce more GST-fused WW domain. In the case of the WW domain of CA150/FBP28, apparently increased production of the fusion protein was observed with this method. In addition, the amount of culture liquid per one flask can be increased because the intense agitation is not needed.

The GST-fused WW domain was successfully purified using glutathione sepharose. Then, the fusion protein was digested with precession protease. GST forms dimer, which can interfere the accurate analysis of the binding property of the WW domain due to artificial avidity. The WW domain is isolated from GST with reverse-phase chromatography. The purity of the protein is over 95% with the analysis of mass spectrometry. The WW domain of CA150/FBP28 showed to have the activity to bind to its ligand

containing -Pro-Pro-Leu-Pro- sequence. The binding strength was approximately 1mM, which indicates avidity-free binding because the strength was rather weak compared with other WW domains.

This production system is easily applicable to other recombinant proteins including WW domains.

Key words: WW domain, surface plasmon resonance, protein expression

1. INTRODUCTION

CA150/FBP28 interacts with the PL motifs (-Pro-Pro-Leu-Pro-) or other Proline-rich sequences of other cytoplasmic proteins via its WW domains. The second WW domain of CA150/FBP28 was shown to bind the PL motif of formin¹. Recent report showed that the second and third WW domain of the CA150/FBP28 concern the activation of pre-mRNA splicing². CA150/FBP28 is dispensable in this process but activates and enhances the maturation of pre-mRNA to mRNA.

WW domain forms a quite small protein module that is constituted of approximately 30 amino acid residues. The domain is one of smallest protein modules that have no disulfide bonding or additional cofactors. Thus, the folding is ruled only the hydrogen bonding and Van del Waals force.

Despite such small molecular size, WW domains play roles in a diverse variety of cell processes, such as cell cycle regulation, ubiquitin ligation, transactivation and other cytoplasmic signal transduction. The genetic diseases that WW domains concern were demonstrated in Duchenne/Becker muscular dystrophy, Liddles syndrome, Huntingtin disease and Alzheimer's disease.

Former, the molecular configuration and other interaction study showed that WW domains were grouped into at least four groups. The Group I and IV identify the PY motif (-Pro-Pro-Xxx-Tyr-) and the pS/pT-P (-phospho Ser/phospho Thr-Pro- sequence), respectively³. Group II and III were considered to bind to the PL (-Pro-Pro-Leu-Pro-) and PR (Pro-rich sequence with Arg) motifs, respectively. But, the grouping of type II and III was confused due to its ambiguous ligand specificity. Thus, we have been demonstrating the nature of WW domains of this category. As a result we have proposed a new grouping method of WW domains, the three grouping model⁴. In this model, we do not distinguish the Group II and III because the WW domains of Group II and III can bind the ligands for both groups. The binding specificity of those WW domains has some predilection for those ligands but do not show any exclusiveness. In addition, the modeled structures of

Group II/III showed common surface structure, which is used to recognize those ligands.

At present, to elucidate detailed mechanism of ligand recognition of Group II/III is most pursued in terms of its characterization because the ligand-domain complex structure of this category has never been reported. Meanwhile, the importance of this category is progressively growing because the recent studies of Fe65 or FCA showed the indispensable role of WW domains in the regulation of transactivation or flowering timing control^{5,6}.

Thus, future aim of our present study is to obtain more robust evidence for the ligand recognition of Group II/III WW domains. For the breakthrough of this state of confusion, we need more detailed and exhaustive assay of WW domains such as structural, proteomic and quantitative analysis for the binding property of the category. Our present study shows the technical basis of our strategy, which is constituted of the efficient production and purification of WW domains and the quantitative assay of the binding.

2. MATERIALS AND METHODS

2.1 Plasmid construction and expression

The plasmid pGEX-6p3 (Amersham Bioscience) was ligated with the PCR-amplified DNA of the second WW domain of CA150/FBP28. The sequence of the DNA is artificially synthesized with multiple PCR process and several synthesized primers. Then the expression of the GST-fused WW domain was induced in *E. coli* BL21(DE3) (Novagen) cells in LB medium with 1mM IPTG at 37°C. The supply of air was tested in two ways, conventional shaking and bubbling air by a diaphragm pump for fish breeding (Nisso, Japan), the air-supplying capacity of which is 30 L/min. In the case of bubbling, small aliquot of silicon oil (1/10000 volume compared to the medium) was added to suppress excess growing of the foam from the medium. The sampling of the cell culture was carried out in every a few hours and the OD at 600nm was monitored. Then, the sample was collected and precipitated at max speed of centrifuge. Milli-Q water and SDS-PAGE sample buffer was added to the pellet and the *E. coli* cells were suspended and boiled for over 10 minutes to completely disrupt the cells.

2.2 Purification of WW domain

All the processes except the final reverse chromatography were carried out at 4°C. After the growth was saturated, the total LB medium was centrifuged to collect the cells. The cells were disrupted by sonifier (Branson) and again centrifuged to precipitate the needless cell debris. The supernatant was loaded onto glutathion sepharose (Amersham Bioscience) and washed and eluted as written in manufacturer's guide. The PreScission protease (Amersham Bioscience) was added into the eluted GST-WW domain and the solution was incubated at 4°C until the digestion was completed. The digested GST and WW domain was loaded to the Resource-RPC column (Amersham Bioscience) equilibrated by the solution composed of 0.1% TFA and 1% acetonitrile. The elution was carried out with gradual increase of acetonitrile concentration. The purified WW domain of CA150/FBP28 was analyzed by MALDI-TOF-MS on a Voyager mass spectrometer (PE) and the purity was also checked with SDS-PAGE.

2.3 Peptide synthesis

The ligand peptide with PL motif was synthesized by solid-phase peptide synthesis on a PSSM8 Peptide Synthesizer (Shimadzu, Kyoto). Rink amide AM resin (Novabiochem) and Fmoc-amino acids with protected side chains were used. Synthesized peptides were cleaved from the resin and deprotected in trifluoroacetate (TFA) in the presence of scavengers (5% water, 5% thioanisole, 3% ethylmethylsulfide, 2.5% ethandithiol, 2% thiophenol), and purified by reverse-phase chromatography with a preparative column ODS-AP303 (4.6 x 250 mm, YMC, Japan). Their molecular masses were also verified by MALDI-TOF-MS. The designed sequence of the ligand peptides was SPPAPPTPPPLPPP (from mouse formin).

2.4 Surface plasmon resonance binding assay

We measured surface plasmon resonance (SPR) on BIAcore 2000 (Biacore AB). The ligand peptide was immobilized on a flow cell of a sensor chip CM5 (Biacore AB) by the standard EDC/NHS method recommended by Biacore AB with a 1 mg/ml peptide solution dissolved in 25 mM NaHCO₃. For reference SPR signals, 25 mM NaHCO₃ was used instead of a peptide solution in the immobilization reaction. Remaining active carboxylates were inactivated with ethanolamine. The binding experiments were performed at 20°C with the GST-WW domains as analytes in 20 mM HEPES, pH 7.0, 100 mM NaCl and 0.5 mM EDTA. Regeneration of the flow cells was done with 100 mM

NaOH. The concentrations of the GST-WW domains were determined from the absorbance at 280 nm of the protein solutions. The dissociation constants (K_D) of the WW domains were determined by Scatchard plot analysis^{3,4}.

3. RESULTS

3.1 Expression of GST-CA150 WW domain

The system configuration for air bubbling is illustrated as in *Figure 1A*. The expression of GST-CA150 was monitored with sampling small aliquots of culture medium (*Figure 1B*). The increase in the production of GST-CA150 WW domain was saturated 2 hours after the induction in the case of shaking. But, the increase in the case of bubbling was saturated 5 hours after the induction. The total amount of production was approximately as much as 2-times of that of shaking. Monitored OD also showed the maximum value at this point, which was 3.5. This value was twice the value in the case of shaking. Thus, the increase in the amount of expression correlated with the total cell quantity of the culture.

3.2 Purification of CA150 WW domain

Purification of CA150 WW domain was successfully carried out using affinity chromatography and reverse phase chromatography. The final purity was over 95% (*Figure 1C*). The result of Mass spectrometry demonstrated the precise molecular weight of the product WW domain, which indicated that the GST-fused WW domain was successfully digested. The final production amount was 2.5 mg WW domain per 1 L culture medium with the bubbling method.

3.3 Surface plasmon resonance

The SPR assay was carried out to figure out the K_D value of the binding between the CA150 WW domain and the formin PL motif peptide. The K_D value was 1.88 ± 0.28 mM, which indicate remarkably weak strength of this binding. The binding showed no artificial avidity because the value was larger than any other K_D values of WW domain-mediated bindings published so far.

4. DISCUSSION

The production of GST-fused WW domain was increased in the bubbling method. Although the growth with this method was slower than

that of the shaking method, the final cell density apparently overwhelmed that of the conventional method. We can easily scale up the culture size using this method because more liter medium can be used per one flask in this method. For example in the case using 5 L flask, we can contain only up to 1.5L medium with shaking method, but with bubbling method 4 L medium can be contained. In addition the cost to introduce the bubbling pump was inexpensive because we do not need high power hydraulic pump to bubble the medium.

We also demonstrated the binding strength of the second WW domain of CA150/FBP28 to the ligand ever known. The binding strength was exceptionally weak, which suggests that this WW domain alone may not be able to bind tight to the ligand *in vivo*. CA150/FBP28 have two more WW domains and FF domains. Thus, these domains may play roles in a cooperative way to grasp its target proteins. Otherwise, CA150/FBP28 have to be expressed in a quite large amount in nuclear. Thus, quantitative binding assay can suggest the nature of cell process more precisely.

In addition, these binding assays or structural assay often need tens of mg of protein sample. Thus, the method for efficient protein expression is important to facilitate these assays.

5. REFERENCES

1. Chan D. C., Bedford M. T. and Leder P., Formin binding proteins bear WWP/WW domains that bind proline-rich peptides and functionally resemble SH3 domains. *EMBO J.* 15(5), 1045-1054 (1996).
2. Lin K. T., Lu R. M. and Tarn W. Y., The WW Domain-Containing Proteins Interact with the Early Spliceosome and Participate in Pre-mRNA Splicing *In Vivo*. *Mol. Cell. Biol.* 24(20), 9176-9185 (2004).
3. Kato Y., Ito M., Kawai K., Nagata K. and Tanokura M., Determinants of ligand specificity in groups I and IV WW domains as studied by surface plasmon resonance and model building. *J. Biol. Chem.* 277(12), 10173-10177 (2002).
4. Kato Y., Nagata K., Takahashi M., Lian L., Herrero J. J., Sudol M. and Tanokura M., Common mechanism of ligand recognition by group II/III WW domains: redefining their functional classification. *J. Biol. Chem.* 279(30), 31833-31841 (2004).
5. Cao X. and Sudhof T. C., A transcriptionally active complex of APP with Fe65 and histone acetyltransferase Tip60. *Science* 293(5527), 115-120 (2001).
6. Simpson G. G., Dijkwel P. P., Quesada V., Henderson I. and Dean C., FY is an RNA 3' end-processing factor that interacts with FCA to control the Arabidopsis floral transition. *Cell* 113(6), 777-787 (2003).

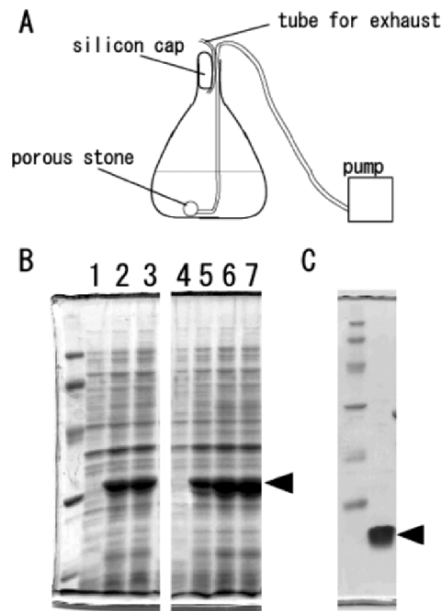


Figure 1. Expression and purification of GST-CA150 WW

A. System cartoon for air-bubbling cultivation. B. Time-dependent increase in the amount of GST-CA150 WW domain expression. Sizes of marker bands were 94, 67, 43, 30 and 20.1 from upper to bottom. The arrow indicates the band of the GST-CA150 WW domain. Lane 1 – 3, expression with shaking. Lane 4 – 8, expression with bubbling air. Lane 1 and 4, sampled culture at induction with 1 mM IPTG. Lane 2 and 5, 2 hours after the induction. Lane 3 and 6, 5 hours after the induction. Lane 7, 7.5 hours after the induction. Lane 8, 9 hours after the induction. C. Purity of WW domain of CA150. Sizes of marker bands were 94, 67, 43, 30, 20.1, 12.2 from upper to bottom. The arrow indicates the band of the CA150 WW domain.

IMPROVEMENT OF LIGATION-MEDIATED POLYMERASE CHAIN REACTION (LM-PCR) METHOD FOR GENOME WALKING WITH A SINGLE GENE-SPECIFIC PRIMER

Keina Kozono,¹ Ayako Aoki,² Masayoshi Tsukahara,¹ and Haruhiko Tsumura¹

¹CMC R&D Laboratories, KIRIN Brewery Co., Ltd., 100-1 Hagiwara, Takasaki, Gunma 370-0013, Japan; ²Pharmaceutical Research Laboratories, KIRIN Brewery Co., Ltd., 3 Miyahara, Takasaki, Gunma 370-1295, Japan

Abstract: We have devised an improved ligation-mediated polymerase chain reaction (LM-PCR) for genome walking to obtain unknown genomic DNA sequences located adjacent to known sequences. Dozens of PCR-based methods have been reported for genome walking; however, these methods are limited to the amplification of a particular region due to their relatively high non-specific background. To increase the specificity and efficiency, we designed a unique oligo-cassette consisting of two different length oligo-nucleotides, a 3'-end amino group modified short one and a hairpin-shaped longer one with the arbitrary gene-specific sequence. Using these oligo-cassettes, we can amplify the 2.3 kb of genomic region coding the α -1, 6-fucosyltransferase (*FUT8*) gene from Chinese hamster ovary (CHO) cells by one-round PCR with a single gene-specific primer.

Key words: ligation-mediated polymerase chain reaction; α -1, 6-fucosyltransferase (*FUT8*); Chinese hamster ovary (CHO) cell

1. INTRODUCTION

Chinese hamster ovary (CHO) cells are the most frequently used cell lines for recombinant therapeutic protein production; however, only a little

genomic DNA sequence information is available for these cells. To identify unknown regions flanking a known DNA sequence by the genome walking method, researchers typically screen a genomic library with known DNA as a probe. However, the preparation and screening of libraries to obtain the desired DNA fragment takes a good deal of time. Recently, the polymerase chain reaction (PCR)-based methods have become popular, since the method is efficient and fast, and there is no need to construct and screen libraries. The currently available methods, such as inverse PCR (1), vectorette PCR (2), capture PCR (3), and adaptor-specific PCR (4, 5, 6, 7, 8) are effective but these methods need two-round PCR with gene- and adaptor-specific nested primers to amplify the flanking regions and reduce the non-specific amplification (9, 10).

To improve the amplification specificity, we designed a unique oligo-cassette consisting of two different length oligo-nucleotides, a 3'-end amino group modified short one and a hairpin-shaped longer one with the arbitrary gene-specific sequence. In this study, we can obtain the 2.3-kb genomic region coding the α -1, 6-fucosyltransferase (*fut8*) gene from CHO cells by one-round PCR with a single gene-specific primer.

2. MATERIALS AND METHODS

2.1 PCR primers and oligo-cassette units

The primers and oligo-cassette units used in this study are listed in Table 1 and Table 2, respectively.

Table 1. Primer sequences


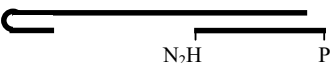
Name	Sequence (5' to 3')
fut8 P05	GCAGAGAGAAATCTCAGGGG
fut8 P10	ATACCTCCATCAGACTGGCC
fut8 P20	AGTTCCAGGACAGCTAGAGC
fut8 P23	TGGAAGGATGAAATCATTAGAAGGC
fut8 P30	TCTCAAAGTGGCTTGTCTC
fut8 P40	GTTTCCCTAGACTATTATGGACAAC
fut8 P50	GCTAAAATATAGAATGGGGGAGGGG
fut8 P60	ACCACACACGTTAGGGTTCTACCTG
OC-P1	AAGGAAAAAAGCGGCCGCA
OC-P2	TTCCTTTTTTCGCCGCGTTCGA
OC-P2PN	PO2-TTCCTTTTTTCGCCGCGTTCGA-NH2
OC-P3h	TTCCAGTGAAGGATGAAATCATTAGAAGCAAGGAAAAAAGCGGCCGCA

For the amplification of different size *fut8* fragments, eight primers (fut8 P05, fut8 P10, fut8 P20, fut8 P23, fut8 P30, fut8 P40, fut8 P50, and fut8 P60) in known *fut8* genomic sequence were synthesized, and they generated PCR fragments together with oligo-cassette-specific primers 0.5, 1.0, 2.0, 2.3, 3.0, 4.0, 5.0 and 6.0-kb, respectively.

For each conventional oligo-cassette unit, the annealing of the two primers OC-P1 and OC-P2 to form the unphosphorylated duplex oligo-cassette OC1 was performed by boiling 25 μ M of each primer solution, followed by slow cooling to room temperature.

For improved oligo-cassette units, a long primer, NHLPh10, was designed to have the same gene-specific sequences as *fut8* P23 and to form the 5' overhang and hairpin structure. A short primer, OC-P2PN, was made from the modification of the phosphorylate at the 5'-end and the amino group at the 3'-end of the OC-P2.

Table 2. Modification and expected structure of oligo-cassette units

Name	Oligomer	5'-P / 3'-N	Structure
OC1	OC-P1 OC-P2	- / -	
OC2	OC-P3h OC-P2PN	+ / +	

P: 5'-end phosphorylated, N: 3'-end modification of amino group

2.2 Construction of oligo-cassette library

Both oligo-cassette units have the *Hind*III site, which was only added as a TCGA overhang that can combine with *Hind*III digested ends to form a full *Hind*III site. To reduce the probability of self-ligation and possible ligation of the oligo-cassette units attached to both ends of the digested DNA fragment, we performed digestion with two restriction enzymes. Approximately 2 μ g of CHO-K1 genomic DNA was double digested at 37°C overnight using 10 units of *Hind*III and *Mun*I in a 50 μ l reaction. Then, inactivation of the enzyme was carried out by heating to 65°C for 20 min. For the construction of two oligo-cassette libraries, 4 μ l of *Hind*III and *Mun*I digested genomic DNA was ligated to each oligo-cassette unit, OC1 and OC2, in a final volume of 8 μ l containing 3 units of T4 DNA ligase. This ligation reaction was incubated at 16°C overnight (16 - 18 hr), and then inactivation of the enzyme was carried out by heating to 70°C for 5 min. Individual oligo-cassette libraries were diluted 10-fold with TE buffer, and

1 μ l these diluted reactions was used as a PCR template. We constructed an OC1 oligo-cassette library derived from plasmid DNA that contains the cloned *fut8* gene fragments isolated from genomic DNA, much like the construction of a genomic DNA library.

2.3 PCR amplifications

The amplification of the oligo-cassette libraries was performed with LA Taq DNA polymerase (TaKaRa) as recommended by the suppliers, in a GeneAmp PCR System 9700 (Applied Biosystems). In the case of the OC1 oligo-cassette library, 5 ng of the library was added to 25 μ l PCR amplification mixtures containing 1x LA Taq buffer (50 mM Tris-HCl, pH 9.3, 15 mM ammonium sulfate, and 2.5 mM MgCl₂), 0.2 μ M *fut8*-specific primer (*fut8* P05 - *fut8* P60), 0.2 μ M cassette-specific primer (OC-P1), 2.5 units of LA Taq DNA polymerase and 400 μ M each dNTP. In the case of the OC2 oligo-cassette library, 5 ng of the library was added to 25 μ l PCR amplification mixtures containing 1x LA Taq buffer (50 mM Tris-HCl, pH 9.3, 15 mM ammonium sulfate, and 2.5 mM MgCl₂), 0.4 μ M *fut8* P23 primer, 2.5 units of LA Taq DNA polymerase, and 200 μ M each dNTP. Standard PCR amplification was performed with the following temperature profile: after an initial denaturation step at 94°C for 5 min, 40 cycles of denaturation at 94°C for 30 s, annealing and extension at 62°C for 3 min, and final extension at 72°C for 7 min. On the other hand, gradient PCR amplification was set up at eight different annealing temperatures that ranged from 56 to 68°C in an iCycler (BIO-RAD), and the PCR temperature profile used was as follows: initial denaturation at 94°C for 4 min, 40 cycles of denaturation at 94°C for 30 s, annealing and extension at the desired temperature for 3 min, and final extension at 72°C for 7 min. The amplified products were separated in 0.8% agarose gel, stained with ethidium bromide, and visualized under UV light.

3. RESULTS AND DISCUSSION

3.1 Conventional oligo-cassette-ligated PCR

The basic outline of the oligo-cassette-mediated PCR, used in the present study to walk from a known sequences into flanking unknown sequences on the genomic DNA, is described in Fig. 1.

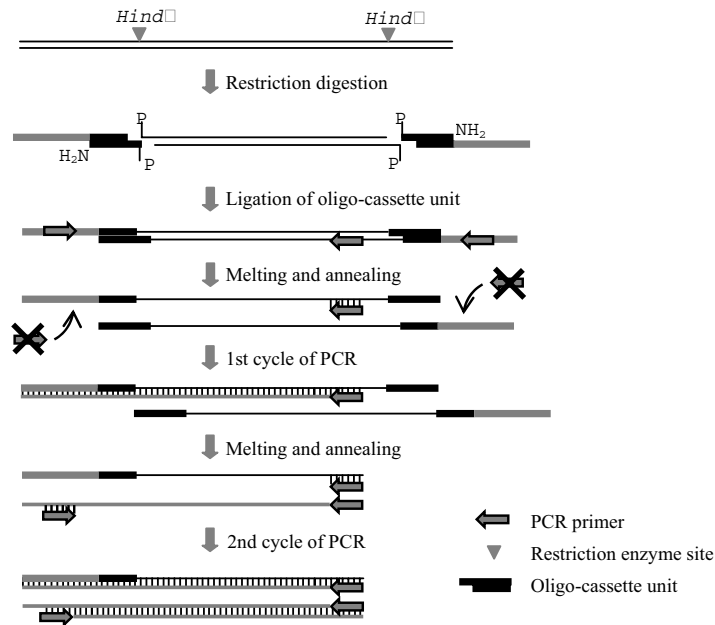


Figure 1. The scheme of oligo-cassette-ligated PCR for genome walking.

To examine the amplification efficiency of LM-PCR with a conventional oligo-cassette unit, we amplified both cloned *fut8* gene and genomic DNA libraries ligated with OC-1 by an oligo-cassette-specific primer (OC-P1, Table 1) and seven *fut8* gene-specific primers (*fut8* P05 - *fut8* P60, Table 1). Specific products were observed in all gene-specific primers from the cloned *fut8* gene library, even though non-specific bands appeared with primers for 5.0-kb and 6.0-kb fragments (Fig. 2a). On the other hand, no distinct products were observed in any primers from the genomic DNA library (Fig. 2b). In addition, there was no distinct PCR product from the oligo-cassette-ligated genomic DNA even if gene-specific primers were used (data not shown). This result suggests that the ligation of conventional design of oligo-cassette to genomic DNA decreases the specificity of PCR.

It has been reported that oligo-cassette-mediated PCR is an inefficient strategy because in most cases non-specific amplification accounts for the major proportion of the final PCR products. To resolve this problem, scientists have improved the process continually by employing different

adaptors and cassettes, and several improved LM-PCRs have been reported (11). However, none of the improved methods could eliminate this drawback completely.

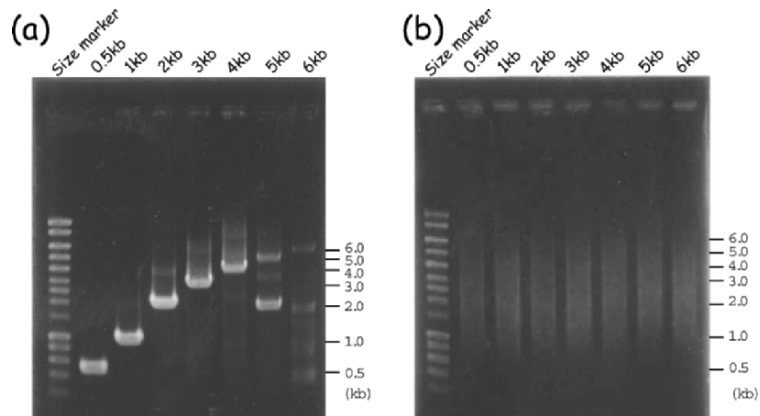


Figure 2. Comparison of target fragment sizes by oligo-cassette-mediated PCR using different templates; (a) plasmid DNA containing a *fut8* fragment and (b) CHO genomic DNA. Both templates were digested with *Hind III* and then ligated with an oligo-cassette.

3.2 Improved oligo-cassette-ligated PCR

To improve the amplification specificity, we designed an OC2 oligo-cassette that has three improved points. One is the adoption of the hairpin structure in the longer strand. This may reduce possible ligation artifacts in the library by preventing the extension of the 3'-end of the cassette-ligated genomic fragment. Second is the 5'-end phosphorylation of the shorter oligo, OC-P2PN. This may not be shed from the end of the genomic DNA fragment during the PCR procedure. This also may prevent the non-specific annealing with floating primers. Last is the presence of an amino group on the 3'-end of the shorter strand. This may block all the available 3'-ends of the restriction fragments, thereby preventing the synthesis of a

complementary strand on the longer 5' overhang end of the oligo-cassette and also preventing the creation of a gene-specific primer annealing site during PCR.

The improved 5' overhang oligo-cassette, OC2, library has the same sequence as the gene-specific primer, so no cassette-specific primer was required. This also may prevent non-specific amplification, because the complementary template can only be synthesized after the initial cycle of PCR is carried out by the gene-specific primer annealing to the target locus on template. Consequently, PCR amplification will not occur from the template when the oligo-cassette is attached to both ends of the genomic DNA fragment.

Using this improved oligo-cassette, we have successfully obtained a 2.3-kb fragment at an annealing temperature of 58.5°C in the PCR (Fig.3). DNA sequences of this amplicon were in agreement with the desired target.

In the present study, we have succeeded in improving the specificity of oligo-cassette-mediated PCR. We were able to obtain the target fragment with only a primary PCR. This improved PCR procedure is probably possible in any gene or organism for which there is only a little chromosomal information available.

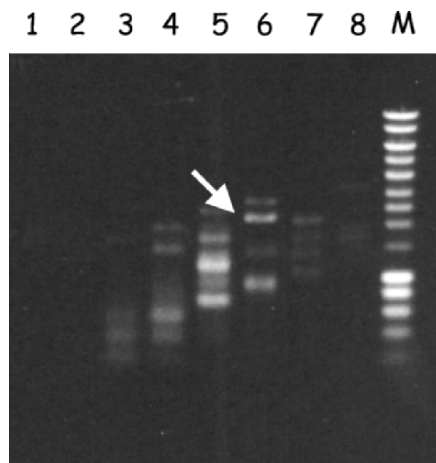


Figure 3. Improved oligo-cassette libraries amplified with a single fut8 P23 primer at different annealing temperatures (1. 68.0°C, 2. 67.3°C, 3. 65.9°C, 4. 63.7°C, 5. 60.6°C, 6. 58.5°C, 7. 57.0°C, 8. 56.0°C). The arrow indicates a band in lane 6 that is the desired 2.3-kb fragment that was confirmed by DNA sequences.

4. REFERENCES

1. Triglia, T., Peterson, M. G. and Kemp, D. J. (1988) A procedure for in vitro amplification of DNA segments that lie outside the boundaries of known sequences. *Nucl. Acids Res.* 16, 8186.
2. Rebecca, S. D., David, J. P., and Anthony, J. B. (1995) Splinkerettes-improved vectorettes for greater efficiency in PCR walking. *Nucl. Acids Res.* 23, 1644-1645.
3. Gilles, M., Martin, V., Leo, S., Jacques, C., Denise, L., Jan, V. E., and Allan, J. H. (1996) Sequence capture-PCR improves detection of mycobacterial DNA in clinical specimens. *J. Clin. Microbiol.* 34, 1209-1215.
4. Reddy, M. K., Nair, S., and Sopory, S. K. (2002) A new approach for efficient directional genome walking using polymerase chain reaction. *Anal. Biochem.* 306, 154-158.
5. Andre, R., Stephan, D., and Jones, C. (1990) Genomic walking and sequencing by oligo-cassette mediated polymerase chain reaction. *Nucl. Acids Res.* 18, 3095-3096.
6. Kilstrup, M., and Kristiansen, K. N. (2000) Rapid genome walking: a simplified oligo-cassette mediated polymerase chain reaction using a single genome-specific primer. *Nucl. Acids Res.* 28, e55.
7. Carolyn, A. F., Caroline, S. K., Maureen, D. M., Diana, J. S., Douglas, H. J., Nancy, B. S., Tammy, S., Matthew, R. H., Peter, C. N., Beverly, J. L., and Eric, F. R. (1997) Panhandle polymerase chain reaction amplifies MLL genomic translocation breakpoint involving unknown partner gene. *Blood* 90, 4679-4686.
8. Yuanxin, Y., Chengcai, A., Li, L., Jiayu, G., Guihong, T and Zhangliang, C. (2003) T-linker-specific ligation PCR (T-linker PCR): an advanced PCR technique for chromosome walking or for isolation of tagged DNA ends. *Nucl. Acids Res.* 31, e68.
9. Hui, E. K., Wang, P.C., and Lo, S. J. (1998) Strategies for cloning unknown cellular flanking DNA sequences from foreign integrates. *Cell Mol. Life Sci.* 54, 1403-1411.
10. Brown, A. J. H., Perry, S. J., Saunders, S. E., and Burke, J. F. (1999) Extender PCR: a method for the isolation of sequences regulating gene expression from genomic DNA. *Bio. Techniques* 26, 804-806.
11. Rishi, A.S., Nelson, N. D. and Goyal, A. (2004) Genome walking of large fragments: an improved method. *J. of Biotechnology* 111, 9-15.

Author Index

A

Ahmed S. 81, 87
Akutsu M. 395
Ali A. M. 67
Alloin C. 1
Amano Y. 143
Ando M. 353
Aoki A. 175, 425
Aoki M. 149

B

Balachandra K. 227, 255
Banu N. 87
Bassens C. 55
Bensellam M. 1
Blankaert D. 1
Boucher S. 285
Buddhirakku N. 227

D

Daley J. 285
de Sousa R. 1, 55
Dhepakson P. 227
Dohda T. 361
dos Santos Pedregal A. R. 1, 55

E

Esaka K. 309
Eto H. 409

F

Fujioka M. 93
Fujiwara A. 127, 135
Fukuda Y. 175

G

Gadek Z. 377
Goodenowe D.B. 21, 403
Gorfien S. F. 193
Gruber D. F. 193

H

Hachimura S. 93, 369
Hamano T. 255

Han J. 387, 395
Hara K. 185
Hayashi A. 353
Heath D. 403
Hendrick V. 1, 55
Heng C. K. 61
Hirayama K. 93
Hirose J. 317
Hisatsune T. 277
Hishiyama S. 277
Hitomi K. 339
Honda M. 255
Hosoi S. 149
Hosono A. 93, 101, 369
Hotta A. 293, 309
Hsu L.-W. 211
Hwang S.-M. 211

I

Iida S. 39
Iijima S. 293, 301, 309, 353, 361
Ikeda M. 317
Imai H. 39
Inayoshi Y. 361
Inoue Y. 219
Isoda H. 387, 395
Ito T. 325
Itoh K. 93
Iwaki M. 233

J

Jacobia S. J. 193
Jayme D. W. 193, 285
Jiang Y. 201
Joseph N. 1
Juurlink B. H. J. 21

K

Kagami H. 127, 135
Kakita S. 47
Kakitani M. 175
Kamihira M. 293, 301, 309, 353,
361
Kaminogawa S. 93, 101, 369

Kanda Y. 39
Kaneoka H. 361
Kao I.-T. 211
Kariya Y. 81
Katakura Y. 113, 409
Kato Y. 417
Kawabe Y. 309
Kenerson R. W. 193
Kimura M. 143
Kimura T. 101, 107
Kino-oka M. 155
Kinoshita Y. 353
Kittigul C. 227
Kobayashi K. 175
Koike M. 149
Kong Z.-L. 211
Konno Y. 149
Kotarsky K. 55
Kozono K. 175, 425
Kumagai I. 47
Kuni R. 39
Kurosawa H. 143

L

Leangaramgul P. 255
Lee Y. Y. 73
Li Y. 263, 377
Liesnard C. 1
Lowagie S. 1
Lyons I. 285

M

Maki M. 339
Maleki S. J. 9
Marique T. 1
Maseki Y. 175
Matsuda Y. 325
Matsuo K. 255
Matsuoka H. 121
Mekvichitsaeng P. 163, 169
Miki M. 107
Miyake K. 361
Miyamoto Y. 277
Mizutani M. 127
Mori K. 39
Morisawa S. 113
Morshed M. 301

Mosbeux C. 1
Munroe D. G. 193
Murakami Y. 317
Muramatsu D. 277
Mushika T. 135

N

Nagira T. 263
Nakamoto K. 47, 185
Nakamura K. 47
Nakamura N. 331
Nakamura R. 93
Nakanishi Y. 101
Nakano R. 39
Nakaya M. 239
Narita H. 317
Nishi K.. 339
Nishijima K. 293, 301, 309, 353
Nishikawa R. 113
Nissom P. M. 61, 73
Niwa R. 39
Noguchi T. 135

O

Ogawa A. 107
Okazaki A. 47
Okuizumi H. 135
Ono K. 309
Ono T. 127, 135
Otsubo K. 113

P

Parent D. 1
Poltawee K. 163
Poomputsa K. 163, 169
Prachasuphap A. 227
Price P. 285

R

Rigaux P. 55
Ritchie S. 201, 403

S

Saito Y. 271, 293
Sakamoto R. 233
Sano S. 301, 353
Sapsutthipas S. 255

Sasaki M. 107, 155
 Sato K. 55
 Sato S. 247
 Sato Y. 361
 Satoh M. 39
 Satsu H. 29
 Sawada R. 87, 325
 Sawano Y. 417
 Seki M. 387
 Shimizu M. 29
 Shinkawa T. 39
 Shirahata S. 113, 219, 377, 409
 Shitara K. 39, 47
 Shoji E. 47
 Shozushima M. 247
 Sotasan S. 169
 Sugahara T. 185
 Sugimoto Y. 219
 Sugimura Y. 339
 Sunthoranandh P. 227
 Suzuki T. 369

T
 Tachibana H. 233, 239
 Takagishi M. 149, 361
 Takasugi H. 149
 Takeda T. 121
 Takemura K. 347
 Takezawa T. 271
 Talorete T. P. N. 387, 395
 Tan W. S. 67
 Tanaka T. 395
 Tanokura M. 417
 Techkarnjanarak S. 163
 Terada S. 107, 155, 271, 347
 Teruya K. 113, 409
 Tescione L. D. 193
 Tey B. T. 67
 Tomizuka K. 175
 Toyosawa T. 155
 Tsuchiya T. 81, 87, 263, 325, 331
 Tsuda M. 93

Tsukahara M. 175, 425
 Tsumoto K. 47
 Tsumura H. 175, 425
 Tsutsumi R. 247

U

Uchida K. 39, 47

V

Van Vooren J. P. 1

W

Wakitani M. 47
 Wang C.K.D.C.F. 61
 Watanabe J. 121
 Werenne J. 1, 55
 Wong D. C. F. 61
 Wong K. 73
 Wong K. T. K. 61
 Wu M.-L. 211

X

Xu Q. 113

Y

Yamada H. 107, 155, 233, 239
 Yamaguchi A. 107
 Yamakawa N. 135
 Yamamoto J. 301
 Yamamoto K. 339
 Yamamoto Y. 135
 Yamane N. 39
 Yamano K. 39
 Yamashita T. 347
 Yamazaki Y. 21, 201
 Yao C.-L. 211
 Yap K. C. 67
 Yap M. G. S. 61, 73
 Ye J. 409
 Yoshida H. 175
 Yoshida N. 277

Subject Index

17 β -estradiol 239
2D-PAGE 163
8-hydroxy-2'-deoxyguanosine
149

A

acetylcholinesterase 387
active hydrogen 113
adhesion 1
 α -1, 6-fucosyltransferase (FUT8)
175, 425
 α -1,6-fucosylation 39
 α -fetoprotein 361
aggregation 155
alkaloid 403
allergen labeling 317
amino acid 403
analytical 403
anoikis-resistance 247
antibody 149
antibody dependent cell mediated
cytotoxicity 149
antibody production 219
antibody-dependent cellular
cytotoxicity 39,47
antioxidation 409
antitumor activity 409
astrocyte 331
Aureobasidium pullulans 369
avian 127, 135

B

β -(1,3-1,6)-glucan 369
Balb/c 3T3 cells 113
Bifidbacterium 101
Bifidbacterium 93
intestinal immune system 93
bioproduction 193
broccoli sprout 21
butyrate stimulation 55

C

C/EBP α 361
Caco-2 cells 395
capsaicin 395
carbohydrate 403
catalytic antibody 233
cathepsin 339
CD4+ T cells 101
cell culture 127, 135
cell proliferation 219
cell therapy 107
chemostat culture 121
chicken 301
chimeric antibodies 309
chinese hamster ovary (CHO) cell
1, 39, 55, 121, 149, 175, 425
chondrogenesis 87
CHO-S 193
CMV promoter 293
c-myc 325
coenzyme Q10 149
colon cancer 201
computer-controlled observation
system 155
costimulation 353
cytofluorimetry 55

D

Dengue virus 169
development 331
diabetes 107
differentiation 285
DNA methylation 301

E

EGFP 55
electrolyzed reduced water 113
endothelial cells 1
enzyme-linked immunosorbent
assay 317

epidermis 339
 estrogen receptor 239
 ex vivo expanded 211
 expansion 285

F

fatty acid 403
 fed-batch culture 39
 fermented milk 185
 fermenter 169
 fluorescence microscopy and
 photometry 55
 food allergy 317
 fructose 219
 fucoidan 409
 fusion protein 55
ET8 39

G

gap junction 263
 GC/MS 403
 gene targeting 175
 gene therapy. 293
 GJIC 81
 gluconeogenesis 403
 glucose 121
 glutamine 121
 glycolysis 403

H

HBV 227
 HEK 293 193
 HeLa 1, 55, 193
 hematopoietic stem cell 211
 hepatitis B surface antigen 227
 hepatocytes 361
 HIT-T15 cells 263
 hMSC 81, 325
 HNF1 α 361
 human articular cartilage 87
 human cell lines . 201
 hyaluronic acid 263
 hybridoma 155, 219
 Hz cell2D 163

I

IgA 101
 immunoglobulin M 239
 immunoglobulin production 185
 immunomodulation 369
 influenza virus 247
 insect cell culture 169
 insulin 107
 insulin secretion 263
 interferon-gamma 185
 internal ribosome entry site
 309
 intestinal immune systems 93
 invasion 409
 islet 107
 isothermal titration calorimetry
 47

K

Kaposi sarcoma 1
 keratinocyte 339
 knockout 39

L

LC/MS 403
 ligation-mediated polymerase
 chain reaction 425
 lipid 403
 L-selectin 353

M

MDCK 247
 mesenchymal stem cells 1
 metabolic engineering 121
 metabolite 403
 metabolome 403
 metalloproteinases 1
 migration 1, 155
 MMPs 409
 mobility 1
 monoclonal antibody 227, 317
 MPC coating 247
 murine stem cell virus (MSCV)
 293

N

natural killer cell 211
NHDF 81
non adhesive matrix 247
non-targeted LCMS profiling 201
NS0 149
nucleic acid 403
nucleostemin 325
nutrient optimization 285

O

optimization 193
ovalbumin 301
ovomucoid 317

P

passage effect 163
PC12 387
PER.C6® 193
peripheral blood lymphocytes 185
Peyer's patch 101
PGA 87
phage display 227
photinus luciferase reporter gene
55
Phytoestrogens 387
platinum nanoparticles 113
PLLA 331
pluripotent cells 127, 135
PPP 403
primary metabolism 403
proliferation 81, 155, 331
promoter 301
protein expression 417

Q

Q vector 293

R

reactive oxygen species 113
recombinant antibody 227
recombinant antibody production
39
recombinant monoclonal antibody
175

recombinant protein 169
retinoic acid 219
retroviral vector 293
ribosomal protein P2 395

S

scFv 227
secondary metabolism 403
secondary VJ recombination
233
sericin 107, 155
serum-free 155
serum-free culture 107, 285
silk 155
single use bioreactor 1
siRNA 39
splenocytes 239
stem cell 285
steroid 403
stroke-prone spontaneously
hypertensive rat 21
surface plasmon resonance 47,
417
suspension culture 247
SV40 replication origin 293

T

T cell receptor transgenic.TCR-
Tg. mice 93
T cells 353
targeted 403
TCA cycle 403
Th-HaNPV 163
Tin catalyst 87
TJ permeability 395
trace elements 193
transgenic chicken 309
transglutaminase . 339
tumorigenesis 325
two-stage cell transformation
113

U

ubiquinone Q₁₀ 149
umbilical cord blood 211

440

Subject Index

V

vesicular stomatitis virus G
 protein (VSV-G) 293
vitamin 403

W

Wnt-8B 325
WW domain 417

Y

YB2/0 149